

6 April 2007 | S10

Science



**Nothing in life is to be feared.
It is only to be understood.**

Marie Curie

Scientist (1867-1934)

We work to encourage vision and creativity that extends well beyond the short-term. Shimadzu believes in the value of science to transform society for the better. For more than a century, we have led the way in the development of cutting-edge technology to help measure, analyze, diagnose and solve problems. The solutions we develop find applications in areas ranging from life sciences and medicine to flat-panel displays. We have learned much in the past hundred years. Expect a lot more.

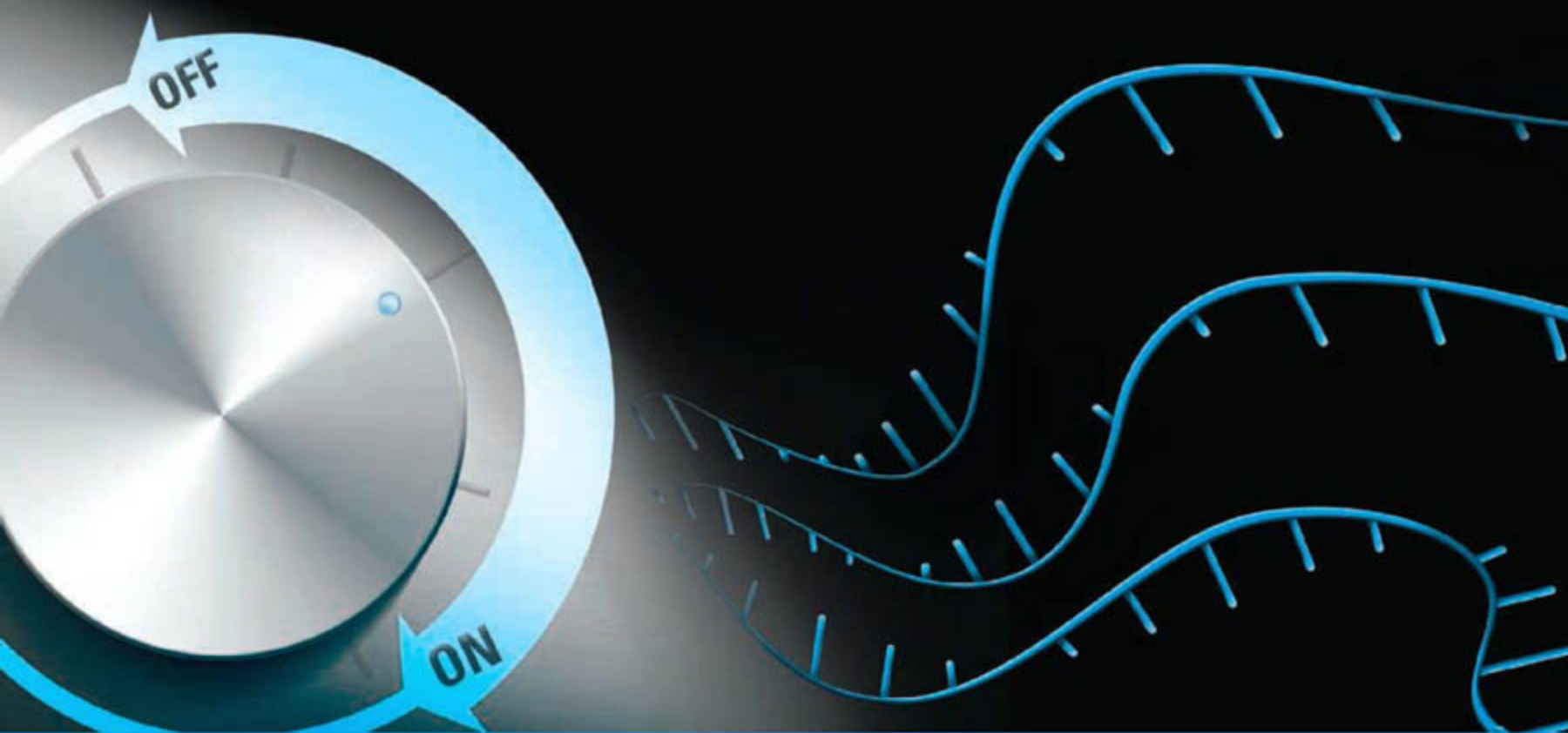
www.shimadzu.com



SHIMADZU

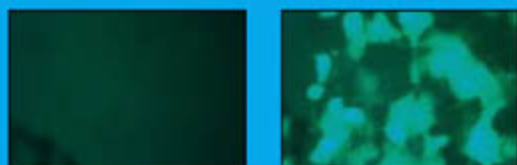
Inducible Expression Systems

Tet-On and Tet-Off Advanced

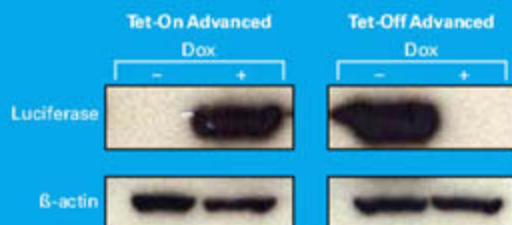


The Benchmark System Just Got Better

- *Highly Sensitive and Controllable*
- *Proven for Both Inducible RNAi and cDNA*
- *High Maximal Expression Levels*



HEK 293Tet-On Advanced cells transfected with pTRE-Tight-BI-AcGFP1, grown in the absence (left) and presence (right) of doxycycline (Dox), and observed by fluorescence microscopy (40x magnification).



Luciferase expression in HEK 293 Tet-On Advanced and HEK 293Tet-Off Advanced Cells transfected with pTRE-Tight-Luc grown in the presence and absence of Dox.

Visit our website today

www.clontech.com/tetsys
and plan for tomorrow!

Products for your research needs

Fluorescent & Luminescent Reporters
Gene Expression & Delivery
Gene Expression Profiling
Non-coding RNA Research & RNAi
Nucleic Acid Purification
Oligo Modification
PCR & RT-PCR Products
Protein Arrays
Protein Expression & Purification
Protein-Protein Interaction Systems
RNA

Clontech Laboratories, Inc.

A Takara Bio Company

www.clontech.com

United States/Canada: +1.800.662.2566 • Europe: +33.(0)1.3904.6880 • Asia Pacific: +1.650.919.7300 • Japan: +81.(0)77543.6116

For Research Use Only. Not for use in diagnostic or other specific procedures. Not for resale. Clontech, Clontech logo, and all other trademarks are the property of Clontech unless noted otherwise. ©2007 Clontech Laboratories, Inc.

AD732279



Bringing protein analysis to life with Ettan DIGE and Amersham ECL

When it comes to life sciences, GE Healthcare is setting the standard. Tens of thousands of scientists worldwide rely on our products and proven expertise in protein analysis and detection every day. But we're never content to stand still. We're constantly striving for innovations that boost accuracy and deliver quantitative data.

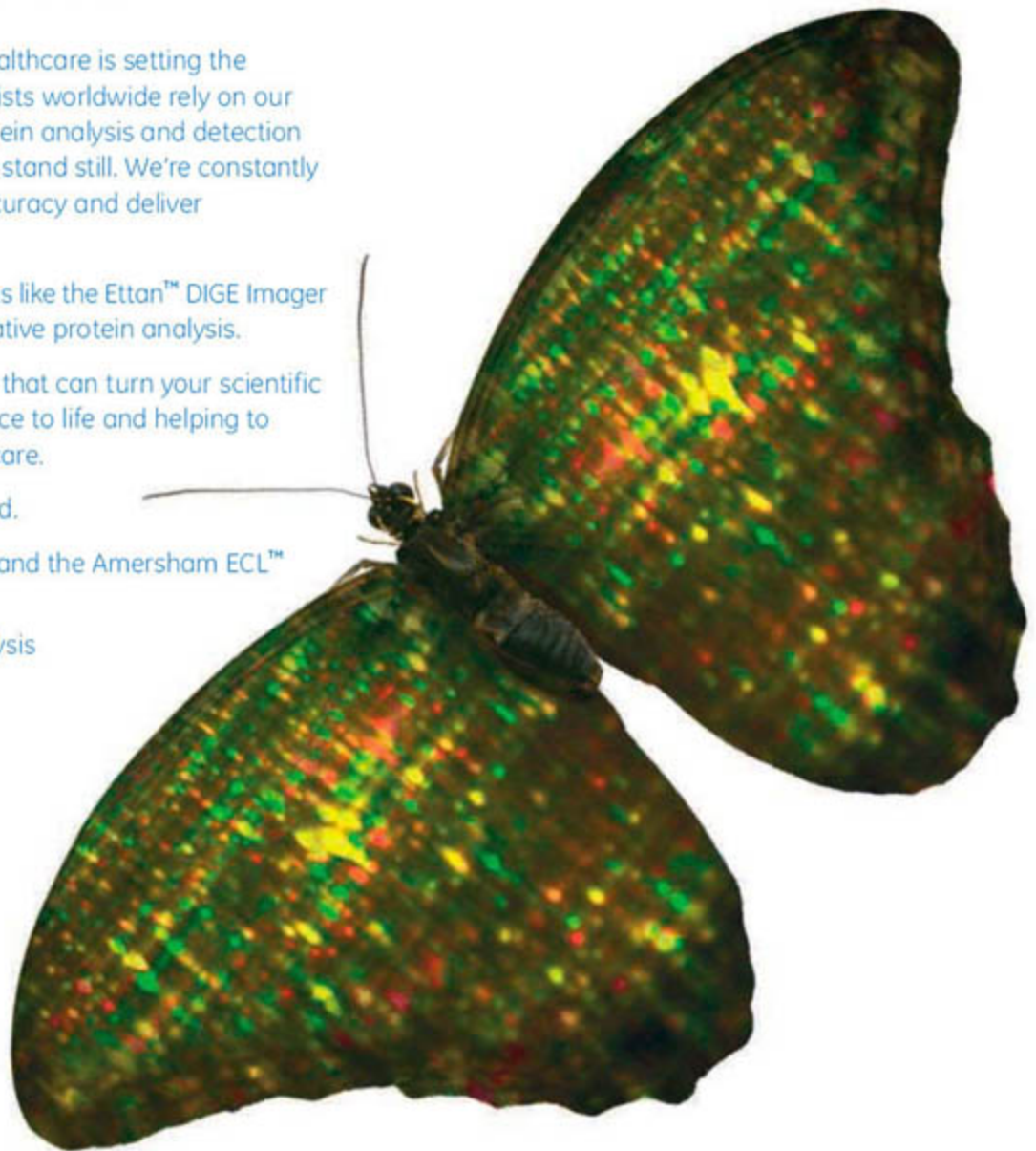
The result is new fluorescence platforms like the Ettan™ DIGE Imager and Amersham ECL Plex™ for quantitative protein analysis.

By continually developing technology that can turn your scientific ideas into reality, we're bringing science to life and helping to transform drug discovery and healthcare.

We call it Protein Analysis Re-imagined.

Discover the full power of Ettan DIGE and the Amersham ECL™ family of Western blotting systems.

www.gehealthcare.com/protein_analysis



imagination at work



COVER

A Chihuahua walking with a Great Dane more than 50 times its mass. The extreme diversity in body size among purebred dogs is greater than that of any other mammalian species. Researchers have identified a gene that helps explain this size diversity. See page 112.

Photo: Deanne Fitzmaurice

DEPARTMENTS

- 11 Science Online
- 13 This Week in Science
- 19 Editors' Choice
- 24 Contact Science
- 27 Random Samples
- 29 Newsmakers
- 129 Science Careers

EDITORIAL

- 17 A Two-Pronged Climate Strategy
by Rosina M. Bierbaum and Peter H. Raven

NEWS OF THE WEEK

- Turnover at the Top, but Problems Persist at the Smithsonian 30
- Design Flaw Could Delay Collider 31
- Attosecond Laser Pulses Illuminate Fleeting Dance of Electrons 33
- SCIENCE SCOPE** 33
- Hobbit's Status as a New Species Gets a Hand Up 34
- Chemistry Reports Warn of Eroding American Research Lead 35
- Indonesia to Share Flu Samples Under New Terms 37
- Appointee 'Reshaped' Science, Says Report 37

NEWS FOCUS

- An Asian Tiger's Bold Experiment 38
- Hard Data on Hard Drugs, Grabbed From the Environment 42
- The World Through a Chimp's Eyes 44
- American Physical Society Meeting 46
- Experimenters Agree: You Can Cross Off Flowing Crystals
- Ultrashort Laser Pulses See Inside the Body
- Pulling Strings to Untangle Catastrophe

LETTERS

- Making Articles Available for Flu Planning *M. Berger* 49
- Pneumococcal Vaccines and Flu Preparedness
K. P. Klugman and S. A. Madhi
- Timing of a Back-Migration into Africa
P. Forster and V. Romano
- Response *A. Olivieri et al.*
- Speeding Up the EPA Review Process *M. Peacock*

BOOKS ET AL.

- Charles Darwin and Victorian Visual Culture 54
J. Smith, reviewed by H. Ritvo
- Dr. Golem How to Think About Medicine 55
H. Collins and T. Pinch, reviewed by R. A. Ankeny

POLICY FORUM

- Framing Science 56
M. C. Nisbet and C. Mooney

PERSPECTIVES

- Rapid Consolidation 57
L. R. Squire
>> Research Article p. 76
- Processive Motor Movement 58
D. D. Hackney
>> Report p. 120
- Roots of Biosynthetic Diversity 60
D. W. Christianson
>> Research Article p. 73
- High Bond Orders in Metal-Metal Bonding 61
F. Weinhold and C. R. Landis
- So Small Yet Still Giant 63
I. V. Lerner
>> Report p. 99
- Searching for a Solid-State Terahertz Technology 64
M. Lee and M. C. Wanke



55



38

CONTENTS continued >>

Sample technologies by QIAGEN

Prepare for results

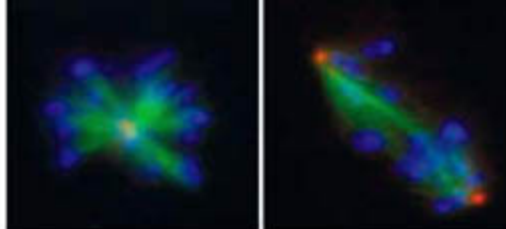


- Protein, RNA, and DNA purification
- Whole genome amplification
- Epigenetics
- Sample collection, stabilization, and preparation
- Plug and play automation with QIAcube

Contact QIAGEN today or visit www.qiagen.com/goto/SampleTech.



Sample & Assay Technologies



SCIENCE EXPRESS

www.scienceexpress.org

CELL BIOLOGY

Genes Required for Mitotic Spindle Assembly in *Drosophila* S2 Cells
G. Goshima et al.

A whole-genome screen identifies the 204 genes involved in assembling the mitotic spindle in flies and how they might contribute to cancer and other abnormalities.

10.1126/science.1141314

CLIMATE CHANGE

Model Projections of an Imminent Transition to a More Arid Climate in Southwestern North America

R. Seager et al.

A collection of 19 climate models predicts that southwest North America will dry significantly in the coming century, a transition that may already be under way.

10.1126/science.1139601

PHYSICS

Functional Quantum Nodes for Entanglement Distribution over Scalable Quantum Networks

C.-W. Chou et al.

Entanglement between atomic gas clouds 3 meters apart forms a quantum repeater, an essential tool for passing information in long-distance quantum communication.

10.1126/science.1140300

CELL BIOLOGY

Positive Regulation of Itk PH Domain Function by Soluble IP₄

Y. H. Huang et al.

A kinase phosphorylates the inositol pyrophosphate IP₃ to generate IP₄ and is necessary for cell signaling during positive selection of immune cells.

>> Reports pp. 106 and 109

10.1126/science.1138684

TECHNICAL COMMENT ABSTRACTS

ECOLOGY

Comment on "Divergent Induced Responses to an Invasive Predator in Marine Mussel Populations" 53

P. D. Rawson, P. O. Yund, S. M. Lindsay

full text at www.sciencemag.org/cgi/content/full/316/5821/53b

Response to Comment on "Divergent Induced Responses to an Invasive Predator in Marine Mussel Populations"

A. S. Freeman and J. E. Byers

full text at www.sciencemag.org/cgi/content/full/316/5821/53c

REVIEW

OCEAN SCIENCE

Atlantic Meridional Overturning Circulation During the Last Glacial Maximum 66

J. Lynch-Stieglitz et al.



102

BREVIA

ECOLOGY

Rapid and Recent Changes in Fungal Fruiting Patterns 71

A. C. Gange, E. G. Gange, T. H. Sparks, L. Boddy

The length of the autumn fruiting season for fungi in forest soil has increased for the past five decades, in parallel with temperature and rainfall increases in the United Kingdom.

RESEARCH ARTICLES

BIOCHEMISTRY

Chimeras of Two Isoprenoid Synthases Catalyze All Four Coupling Reactions in Isoprenoid Biosynthesis 73

H. V. Thulasiram, H. K. Erickson, C. D. Poulter

A synthetic protein made from the four enzymes that synthesize isoprenoids can effectively catalyze all four reactions, suggesting their origin from a common ancestor. >> Perspective p. 60

NEUROSCIENCE

Schemas and Memory Consolidation 76

D. Tse et al.

Rats learn to associate a place with a taste much more rapidly if they have already been given a chance to learn the spatial context of the new location. >> Perspective p. 57

REPORTS

MATERIALS SCIENCE

Nonstoichiometric Dislocation Cores in α -Alumina 82

N. Shibata et al.

Electron microscopy reveals that in aluminum oxide, nonstoichiometric dislocations form on adjacent planes and slip together during high-temperature deformation.

CHEMISTRY

Acid Catalysis in Basic Solution: A Supramolecular Host Promotes Orthoformate Hydrolysis 85

M. D. Pluth, R. G. Bergman, K. N. Raymond

The electrostatic environment within the cavity of a synthetic metal-ligand cluster enables acid catalysis in a basic solution.

CONTENTS continued >>

todaycouldbetheday.com

REPORTS CONTINUED...

CLIMATE CHANGE

The Deep Ocean During the Last Interglacial Period 89
J. C. Duplessy, D. M. Roche, M. Kageyama
 North Atlantic Deep Water was warmer during the last interglacial than it is today and probably warmed Antarctic waters, accelerating ice loss and raising sea levels.

PLANETARY SCIENCE

Subsurface Radar Sounding of the South Polar Layered Deposits of Mars 92
J. J. Plaut et al.
 Radar mapping of layered deposits at Mars' south pole shows that they are pure water ice, sitting on cratered terrain, with a volume equivalent to a global water layer 11 meters thick.

APPLIED PHYSICS

Synchronized Oscillation in Coupled Nanomechanical Oscillators 95
S.-B. Shim, M. Imboden, P. Mohanty
 A rich dynamic response, including synchronization and entrainment, is seen when two coupled nanomechanical beams are driven over a range of oscillating frequencies.

PHYSICS

Giant Fluctuations of Coulomb Drag in a Bilayer System 99
A. S. Price et al.
 Electrons flowing in one thin layer drag electrons in an underlying layer more than expected, implying that local electron properties are important in momentum exchange. >> *Perspective p. 63*

APPLIED PHYSICS

Direct-Current Nanogenerator Driven by Ultrasonic Waves 102
X. Wang, J. Song, J. Liu, Z. L. Wang
 Through their variable bending, which separates charge, a series of zinc oxide nanowires can convert sound waves to continuous electrical current to power nanoscale devices.

CELL BIOLOGY

A Conserved Family of Enzymes That Phosphorylate Inositol Hexakisphosphate 106
S. Mulugu et al.
 A yeast enzyme is regulated by pH and can both synthesize and metabolize the inositol pyrophosphate IP₆. >> *Science Express Report by Y. H. Huang et al.*

CELL BIOLOGY

Regulation of a Cyclin-CDK-CDK Inhibitor Complex by Inositol Pyrophosphates 109
Y.-S. Lee, S. Mulugu, J. D. York, E. K. O'Shea
 When yeast are starved for the nutrient phosphate, the inositol pyrophosphate IP₆ activates gene expression and a metabolic network for nutrient homeostasis. >> *Science Express Report by Y. H. Huang et al.*

GENETICS

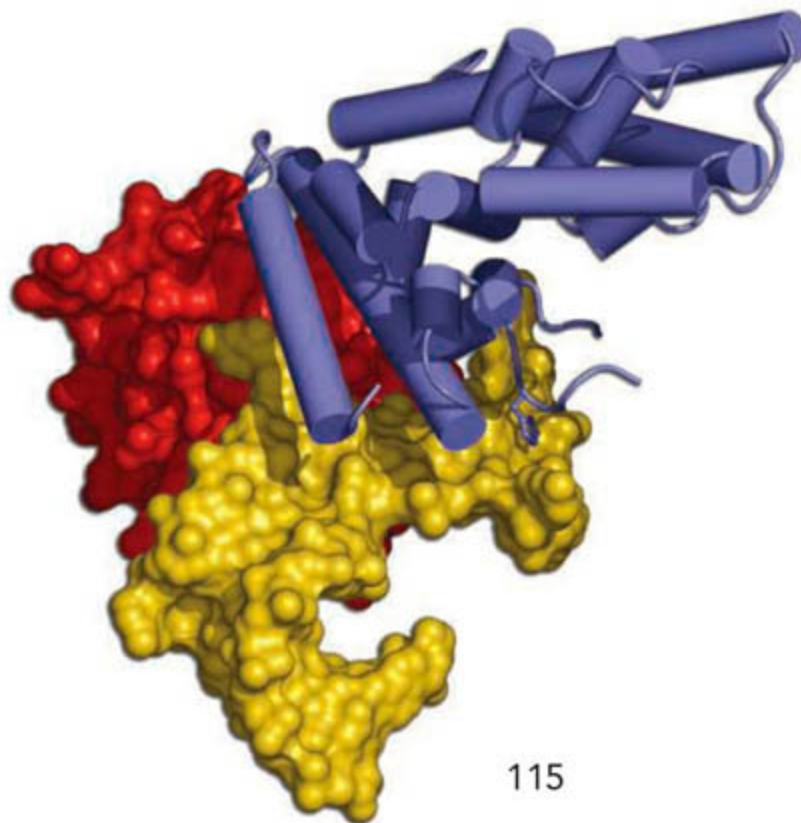
A Single *IGF1* Allele Is a Major Determinant of Small Size in Dogs 112
N. B. Sutter et al.
 Small dogs are small because they carry a particular allele of the gene encoding insulin-like growth factor 1.

BIOCHEMISTRY

Binding of the Human Prp31 Nop Domain to a Composite RNA-Protein Platform in U4 snRNP 115
S. Liu et al.
 A protein within the particle that assembles mature mRNAs has both RNA and protein binding surfaces, and it achieves binding specificity by acting as a molecular ruler.

BIOCHEMISTRY

An ATP Gate Controls Tubulin Binding by the Tethered Head of Kinesin-1 120
M. C. Alonso et al.
 The two-headed motor kinesin is gated by ATP independently of the microtubule along which it moves, contrary to current models of kinesin motion. >> *Perspective p. 58*



115

CREDIT: M. C. WAHL/MAX PLANCK INSTITUTE FOR BIOPHYSICAL CHEMISTRY, GÖTTINGEN, GERMANY



ADVANCING SCIENCE. SERVING SOCIETY

SCIENCE (ISSN 0036-8075) is published weekly on Friday, except the last week in December, by the American Association for the Advancement of Science, 1200 New York Avenue, NW, Washington, DC 20005. Periodicals Mail postage (publication No. 484460) paid at Washington, DC, and additional mailing offices. Copyright © 2007 by the American Association for the Advancement of Science. The title SCIENCE is a registered trademark of the AAAS. Domestic individual membership and subscription (51 issues): \$142 (\$74 allocated to subscription). Domestic institutional subscription (51 issues): \$710; Foreign postage extra: Mexico, Caribbean (surface mail) \$55; other countries (air assist delivery) \$85. First class, airmail, student, and emeritus rates on request. Canadian rates with GST available upon request, GST #1254 88122. Publications Mail Agreement Number 1069624. Printed in the U.S.A.

Change of address: Allow 4 weeks, giving old and new addresses and 8-digit account number. Postmaster: Send change of address to AAAS, P.O. Box 96178, Washington, DC 20090-6178. Single-copy sales: \$10.00 current issue, \$15.00 back issue prepaid includes surface postage; bulk rates on request. Authorization to photocopy material for internal or personal use under circumstances not falling within the fair use provisions of the Copyright Act is granted by AAAS to libraries and other users registered with the Copyright Clearance Center (CCC) Transactional Reporting Service, provided that \$18.00 per article is paid directly to CCC, 222 Rosewood Drive, Danvers, MA 01923. The identification code for Science is 0036-8075. Science is indexed in the Reader's Guide to Periodical Literature and in several specialized indexes.

CONTENTS continued >>

design>delivery>purification>assessment>detection

**New
siLentMer™
siRNA!**

Check out our
new validated and
pre-designed 27-mer
siRNA duplexes

Bio-Rad and RNAi. Come have a look.

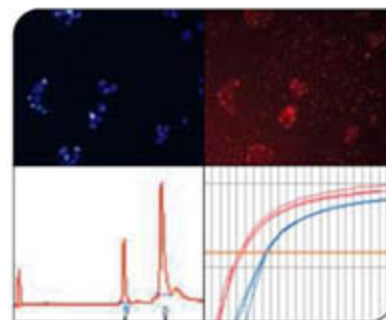
From design to detection, Bio-Rad supports your RNAi research.

With a broad range of proven delivery technologies, award-winning detection systems, and a suite of high-quality support products, it's clear that Bio-Rad has a vision for RNAi.

- High-performing potent siRNA for $\geq 85\%$ knockdown with as low as 5 nM siRNA
- Greatest choice of delivery technologies
- RNA and protein purification products
- Automated microfluidic RNA analysis
- Sensitive, optimized cDNA synthesis kits
- Systems for protein and mRNA detection

For a close look at Bio-Rad's tools for RNAi, visit us on the Web at www.bio-rad.com/rnai/

Practice of the polymerase chain reaction (PCR) may require a license.



MCF-7 cells transfected using siLentFect™ reagent. RNA purified and analyzed using the Aurum™ total RNA kit and Experion™ system. Real-time PCR detection performed using iScript™ cDNA synthesis kit.

Visit us on the Web at discover.bio-rad.com
Call toll free at 1-800-4BIORAD (1-800-424-6723);
outside the US, contact your local sales office.

BIO-RAD

SCIENCE NOW

www.sciencenow.org DAILY NEWS COVERAGE

Interspecies Tryst While Out of Africa?

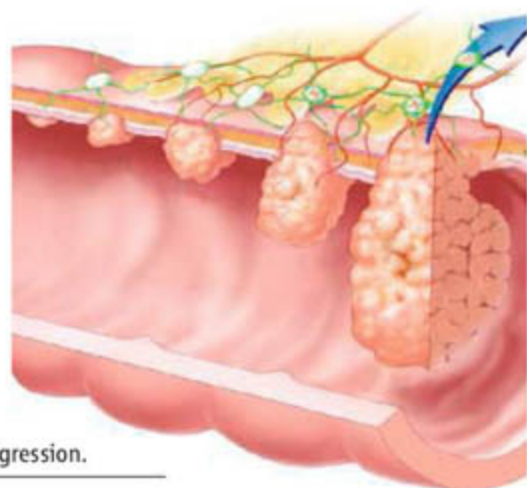
Other researchers question interpretation of oldest human skeleton found in China.

Not Your Type? Don't Sweat It

Enzymes convert type A and type B blood to type O.

Tatooine's Twin Suns Not So Farfetched

Planets may abound around double star systems.



Cancer progression.

SCIENCE'S STKE

www.stke.org SIGNAL TRANSDUCTION KNOWLEDGE ENVIRONMENT

EDITORIAL GUIDE: Focus Issue—Exploring New Avenues for Cancer Treatment

E. M. Adler and N. R. Gough

Recent research on cancer cell pathophysiology provides reasons to be hopeful about development of novel therapies.

MEETING REPORT: Tumor Biology—How Signaling Processes Translate to Therapy

K. Friedrich, O. Janssen, R. Hass

The most recent meeting of the Signal Transduction Society highlighted the translation of signaling research into advances in the cancer clinic (in Perspectives).

PERSPECTIVE: Metabolic Targeting as an Anticancer Strategy—Dawn of a New Era?

J. G. Pan and T. W. Mak

Could targeted therapies directed against aerobic metabolism represent a viable approach to treating cancer?

REVIEW: Sequestration and Segregation of Receptor Kinases in Epithelial Cells—Implications for ErbB2 Oncogenesis

C. A. C. Carraway and K. L. Carraway

Can oncogenesis occur by co-opting normal physiological responses to epithelial damage?



Scientific writing and publishing.

SCIENCE CAREERS

www.sciencecareers.org CAREER RESOURCES FOR SCIENTISTS

GLOBAL: Special Feature—Getting Published in Scientific Journals

E. Pain

Publications can make or break your career, but how can you improve your chance of success?

US: Tips for Publishing in Scientific Journals

K. Kelner

Science Deputy Editor Katrina Kelner offers advice on how to get your research published.

US: The Story's the Thing

R. Ness

One key to scientific writing is spinning a good (nonfiction) yarn.

EUROPE: Publishing for Non-Native Writers

E. Pain

When writing up their research for Western journals, non-native English speakers face extra challenges.

US: From the Archives—How to Write a Winning Résumé

P. Fiske

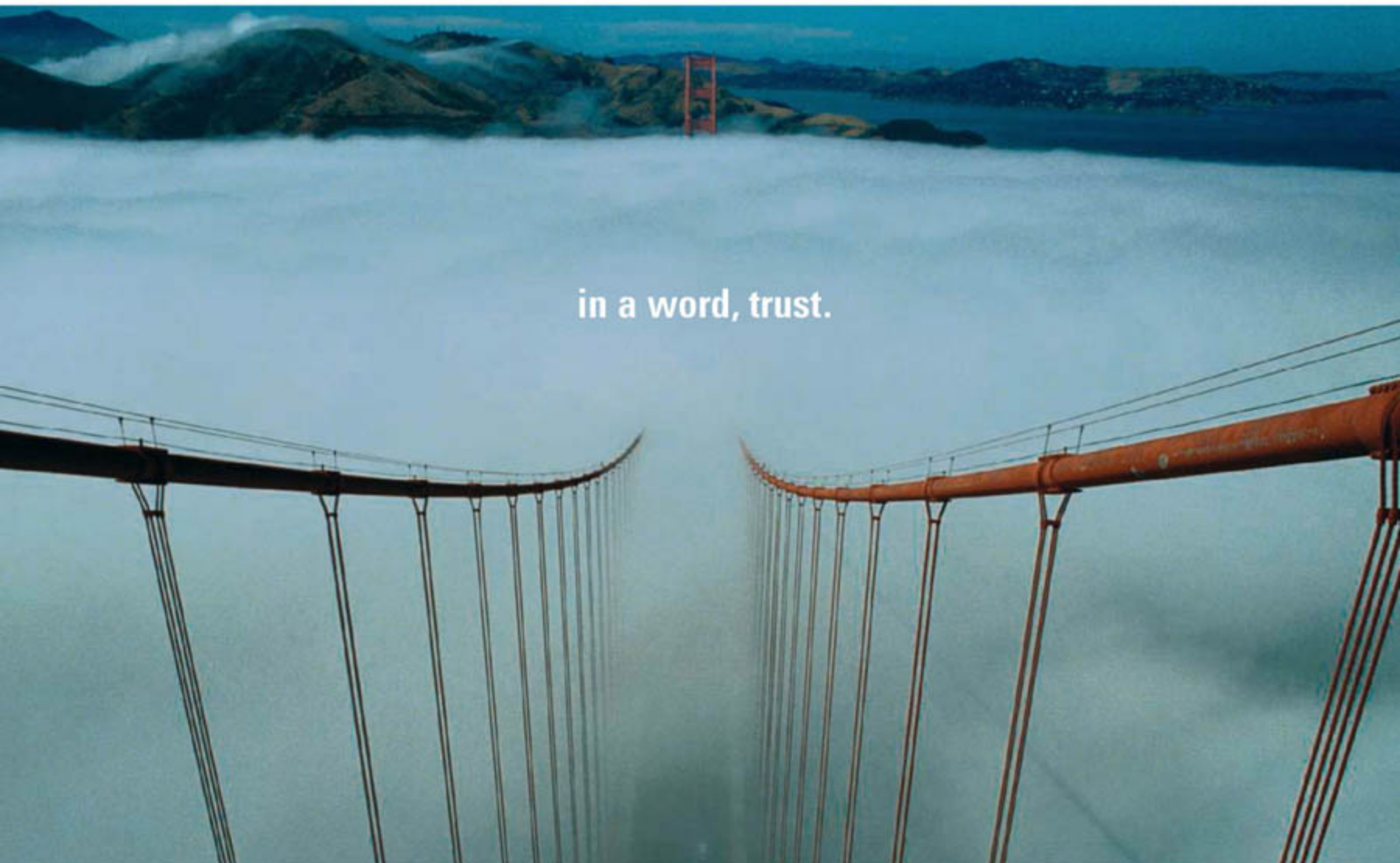
If your résumé isn't well honed, you may lose out to an inferior—but more polished—candidate.

GRANTSNET: April 2007 Funding News

GrantsNet Staff

Learn about the latest in research funding, scholarships, fellowships, and internships.

Separate individual or institutional subscriptions to these products may be required for full-text access.



in a word, trust.

T4 DNA Ligase from New England Biolabs

WHEN YOU NEED LIGASE, TURN TO THE INDUSTRY STANDARD

New England Biolabs is dedicated to providing our customers with guaranteed enzyme performance. Our recombinant T4 DNA Ligase is the most extensively used ligase for cloning experiments. It is available at exceptional value, and an even greater value when purchased in large quantities for high throughput technologies. For cohesive, blunt, simple or complex reactions, make T4 DNA Ligase from NEB your first choice.

■ T4 DNA Ligase*

Regular Concentration

For standard cloning reactions

M0202S/L

High Concentration

For large or difficult constructs

M0202T/M

■ Quick Ligation™ Kit*

For ligation of cohesive or blunt-end DNA fragments in 5 minutes at room temperature. See our website for more details.

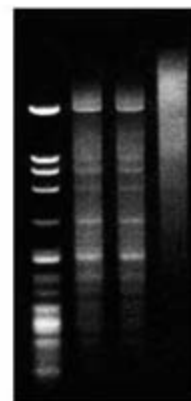
M2200S/L

Advantages:

- Quality – Highly pure enzyme with no lot-to-lot variation
- Convenience – Choose original T4 DNA Ligase or the Quick Ligation Kit to meet the demands of a variety of reaction conditions
- Flexibility – Active at room temperature or 16°C; reaction times run from 5 minutes to overnight
- Robustness – Active in a variety of reaction buffers

 = Recombinant

*NEB ligase products are BSA-free



0 0.1 0.2 1.0
T4 DNA Ligase (µl)
Ligation of blunt-ended HaeIII fragments of Lambda DNA using various amounts of T4 DNA Ligase (400,000 cohesive end units/ml) in a 20 µl reaction volume. Reactions were incubated for 30 minutes at 16°C.



0 10 20 30 60
Time (min)
Ligation of HindIII fragments (4-base overhang) of Lambda DNA using 1 cohesive end unit (1 µl of 1:400 dilution) of T4 DNA Ligase. Reactions were incubated at 25°C.

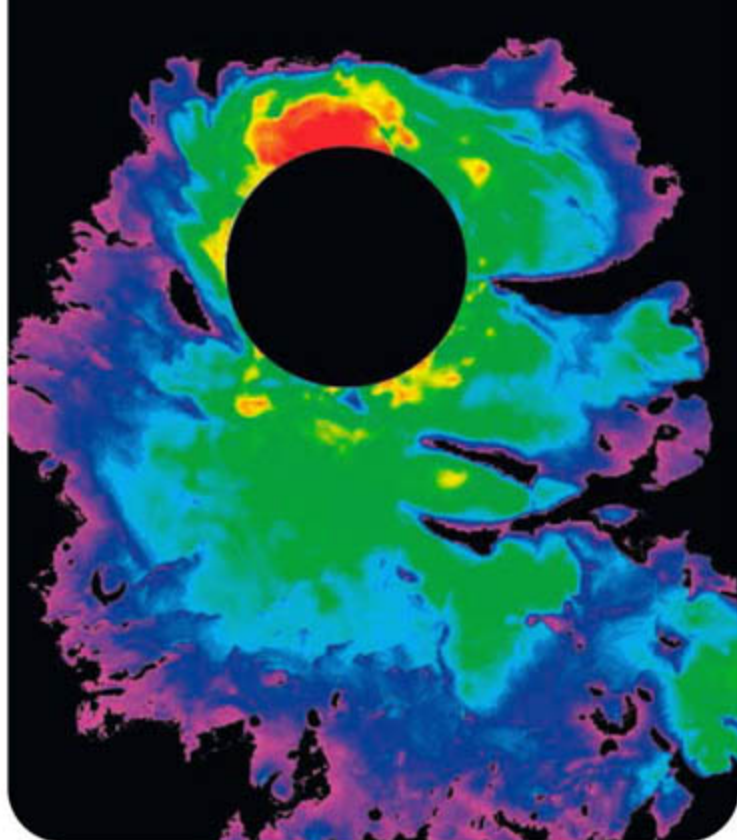
For more information and our international distribution network, please visit www.neb.com

New England Biolabs, Inc. is an ISO 9001 certified company

New England Biolabs Inc. 240 County Road, Ipswich, MA 01938 USA 1-800-NEB-LABS Tel. (978) 927-5054 Fax (978) 921-1350 info@neb.com

Canada Tel. (800) 387-1095 info@ca.neb.com • **China** Tel. 010-82378266 beijing@neb-china.com • **Germany** Tel. 0800/246 5227 info@de.neb.com

Japan Tel. +81 (0)3 5669 6191 info@neb-japan.com • **UK** Tel. (0800) 318486 info@uk.neb.com



Glaciers on Mars

Most of the water ice on the surface of Mars is locked up in the polar caps. The Mars Express orbiter has used its radar to penetrate to the base of the layered deposits on the north pole. Now **Plaut *et al.*** (p. 92, published online 15 March) have mapped the south polar-layered deposits. The radar penetrates 3.7 kilometers with little attenuation, which suggests that these deposits are almost pure water ice. The base of the deposits shows a set of buried depressions that may be past impact craters. The deposits themselves total 1.6×10^6 cubic kilometers, equivalent to a global water layer approximately 11 meters thick.

Ocean Conditions Past and Present

The formation of cold, dense water in the North Atlantic Ocean today helps drive meridional overturning circulation, in which warm water flows north over cold water flowing south, but conditions may have differed during the Last Glacial Maximum (LGM) 21,000 years ago.

Lynch-Stieglitz *et al.* (p. 66) review our understanding of this problem. The pace of deep Atlantic circulation during the LGM was nearly as vigorous as it is now, but patterns of sea surface temperatures and the distribution of water masses were different, indicating that different mechanisms drove circulation then. Furthermore, during the last interglacial, around 125,000 years ago, land and sea surface temperatures at high latitudes were higher than they are today, and sea level was 4 to 6 meters higher. Did deep ocean conditions contribute to melting of the Greenland and Antarctic ice sheets? **Duplessy *et al.*** (p. 89) analyzed cores from the Atlantic and Southern oceans and show that North Atlantic Deep Water was warmer during the last interglacial than it is today. Using two models, they infer that extra heat would have been transferred to Circumpolar Deep Water in the Southern Hemisphere, which would have melted more of the Antarctic Ice Sheet.

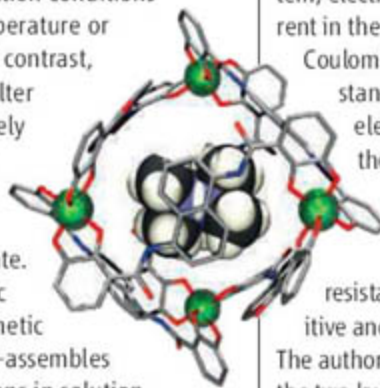
Dissecting Oxide Dislocations

Imbalances in stoichiometry in layered oxides, such as at grain boundaries, can affect their electrical and mechanical properties. Less is

known about the structure of dislocations, which are defects in the crystalline ordering, and the role they may play. **Shibata *et al.*** (p. 82) use high-resolution electron microscopy to study dislocations in aluminum oxide. Two nonstoichiometric partial defects form close to each other, and at high temperatures, the motion of the partial defects occurs with those on adjacent planes.

Acid Buried in Base

Chemists often tailor reaction conditions by manipulating the temperature or acidity of the medium. In contrast, enzymes cannot grossly alter their surroundings, and rely instead on internal cavities that tune the molecular environment of an individual docked substrate. **Pluth *et al.*** (p. 85) mimic this strategy using a synthetic cage-like cluster that self-assembles from ligands and metal ions in solution. The electrostatic environment inside the cluster stabilizes cations, and so favors protonation of guest molecules. The cage can function as an acidic enclave in a basic solution and be used to perform acid-catalyzed orthoformate hydrolysis in a surrounding basic medium.



In Sync Several Times

An organism or cell can synchronize its oscillatory behavior with that of its neighbors, as in the blinking of fireflies or the beating of cardiac cells. **Shim *et al.*** (p. 95) studied the behavior of two coupled nanomechanical beams, a concep-

tually simple system that nonetheless shows rich dynamic behavior. The beams are driven at a wide range of frequencies. Frequency-locking or entrainment occurred in a number of regions in which the two beams synchronize to a single resonance. These resonators may be of use in signal processing and communication.

Electrons Feel the Drag

When current flows in one layer of a bilayer system, electron-electron interactions can drag current in the other layer. Measurements of this Coulomb drag effect are important for understanding coupled electronic and correlated electron systems. **Price *et al.*** (p. 99; see the Perspective by **Lerner**) report on the observation of giant fluctuations, four orders of magnitude greater than that expected, of the Coulomb drag resistance, which result in an alternating positive and negative frictional force on electrons. The authors propose a model in which electrons in the two layers interact in the ballistic regime, characterized by large momentum transfers, where the local electron properties become important.

Engineering Isoprenoid Builders

Isoprenoids, a diverse family of natural products, are built from five-carbon building blocks using four coupling reactions. Enzymes that catalyze chain elongation and cyclopropanation have been identified, however, enzymes that catalyze

Continued on page 15

Bibliographies made Xtra easy.



For over two decades, EndNote® has been the industry standard software tool for creating and managing bibliographies. Now with EndNote X and EndNote® Web, we are creating a new standard for ease-of-use. And that has students, researchers, writers and librarians jumping for joy.

EndNote X connects seamlessly to our newest service, EndNote Web, so you can organize your research and collaborate with colleagues and students—anywhere, anytime. With EndNote X you can move references to and from your Web library with ease and cite references from both locations in a single paper. And, EndNote Web provides unique integration with ISI Web of KnowledgeSM giving you one-click access to a wealth of content such as dynamic links to times cited detail, related records and more.

EndNote X and EndNote Web are not only Xtra easy to use, but also Xtra easy to work with throughout your organization—and all over the world.

Advance Your Scholarly Publishing Today!
www.endnote.com • www.endnoteweb.com

EndNote®
...Bibliographies Made Easy™

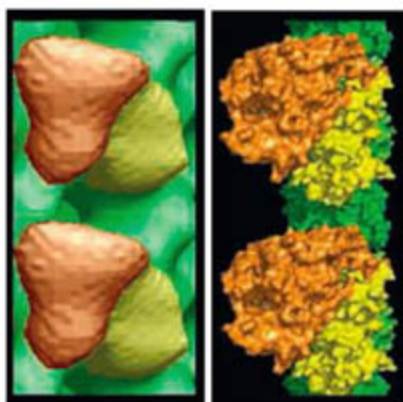
Thomson ResearchSoft
800-722-1227 • 760-438-5526
www.researchsoft.com • rs.info@thomson.com

Continued from page 13

branching and cyclobutanation have not. **Thulasiram et al.** (p. 73; see the Perspective by **Christianson**) show that all four reactions can be catalyzed by engineered enzymes that are chimeras of a chain elongation enzyme and a cyclopropanation enzyme. The products have the same stereochemistry as the natural products, suggesting that enzymes catalyzing the four reactions evolved from a common ancestor.

The More You Know, the More You Learn

The ability to remember complex new information often depends on prior knowledge of the topic. This is because we have already formed a relevant mental schema as a framework. **Tse et al.** (p. 76; see the Perspective by **Squire**) used rats to study the effects of prior learning of schemas on the ability to acquire new episodic associations. These associations were acquired faster when the animals were first trained on a consistent set of associations than when they occurred in the context of a novel set of associations. The acquisition of novel associations was dependent on the hippocampus. However, within 48 hours the associations were independent of the hippocampus, which is substantially faster than typical memory consolidation. Thus, animals—like people—can bring activated mental schemas to bear during learning.



Motor Mechanics

Kinesin-1 is a two-headed molecular motor that takes 8-nm steps along microtubules. At each step, one molecule of adenosine triphosphate (ATP) is hydrolyzed and between steps kinesin pauses until another molecule of ATP binds. Now **Alonso et al.** (p. 120; see the Perspective by **Hackney**) show that kinesin-1 interacts with free tubulin heterodimers in solution and that this system too is gated by ATP. The observed behavior would not be predicted by current models for the motor mechanism that include a role for the microtubule lattice in the gating mechanism.

Understanding Inositol Pyrophosphates

Inositol pyrophosphates are relatively poorly understood, highly phosphorylated members of the inositol polyphosphate family. Two studies describe related advances in signaling involving inositol pyrophosphates. **Mulugu et al.** (p. 106) purified an inositol pyrophosphate synthase from yeast that has two catalytic domains. The enzyme, called Vip1, appears to act as a switch, with its catalytic activity determined by the local pH. **Lee et al.** (p. 109) purified a molecule that regulates the yeast Pho80-Pho85-Pho81 complex, a protein complex containing a cyclin, a cyclin-dependent kinase (CDK), and a CDK inhibitor. The active molecule turned out to be myo-D-inositol heptakisphosphate (IP7), which is synthesized through the kinase activity of Vip1.

Sizing Up Man's Best Friend

In contrast to most mammalian species, *Canis familiaris* (the domestic dog) shows extreme diversity in body size. **Sutter et al.** (p. 112, cover) show that a single allele of the gene encoding insulin-like growth factor-1 (IGF-1) is shared by all small dog breeds but is nearly absent from giant dog breeds, implying that sequence variation in the *IGF-1* gene plays a causal role in dog size. Discovery of the *IGF-1* gene was facilitated by its localization within a genomic signature, or haplotype block, that probably arose as a result of centuries of dog breeding by humans.

Spliceosome Assembly

Human Prp31 is a protein in the spliceosome that is essential for pre-mRNA splicing. It is assembled onto the spliceosome after 15.5K protein binds to an RNA component, U4 small nuclear (sn)RNA. **Liu et al.** (p. 115) present structural and biochemical data of hPrp31-15.5K-U4 snRNA complexes that give insight into this hierarchical assembly. hPrp31 presents both RNA and protein binding surfaces, making it a true ribonucleoprotein (RNP) binding protein. Binding occurs through the nucleolar protein (Nop) domain, which may act as a molecular ruler that measures the length of an RNA stem to achieve RNP binding specificity.

CREDIT: ALONSO ET AL.

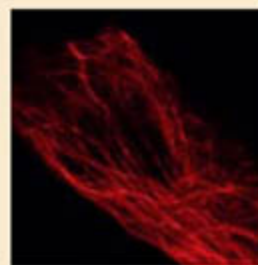
FOUR COLORS



FOR PROTEIN LABELING

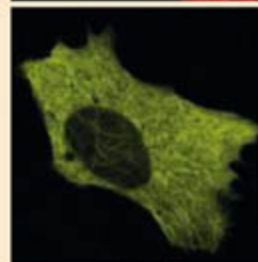
New generation of bright monomeric fluorescent proteins

for research and commercial use



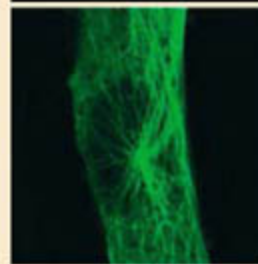
TagRFP

excitation
555 nm
emission
583 nm



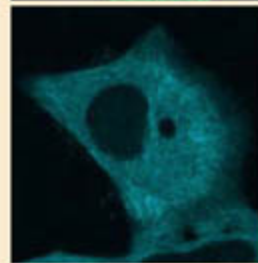
TagYFP

excitation
508 nm
emission
524 nm



TagGFP

excitation
482 nm
emission
505 nm



TagCFP

excitation
458 nm
emission
480 nm

Tubulin filaments visualization
using Evrogen TagFPs
(confocal images of mammalian cells)

Evrogen JSC, Moscow, Russia
Tel: +7(495) 336 6388
Fax: +7(495) 429 8520
E-mail: evrogen@evrogen.com

www.evrogen.com
EVROGEN

The National Institutes of Health invites applications for the inaugural



NIH DIRECTOR'S **NEW INNOVATOR** AWARD

Announced in early 2007, the NIH Director's New Innovator Award will support research by new investigators who propose highly innovative projects with the potential for exceptionally great impact on biomedical or behavioral science.

NIH expects to make at least 14 awards in September 2007. Each grant will be for 5 years and up to a total of \$1.5 million in direct costs plus applicable facilities and administrative costs.

Women and members of groups that are underrepresented in biomedical or behavioral research are especially encouraged to apply.

Open to New Investigators Who

Have not yet obtained an NIH R01 or similar grant

Hold an independent research position at an institution in the United States

Received a doctoral degree or completed medical internship and residency in 1997 or later

Propose research in any scientific area relevant to the NIH mission

Apply Electronically

Get instructions at <http://grants.nih.gov/grants/guide/rfa-files/RFA-RM-07-009.html>

Prepare the short application; preliminary data allowed, but not required

Submit the application through Grants.gov between April 25 and May 22, 2007

More Information

See http://grants.nih.gov/grants/new_investigators/innovator_award/

E-mail questions to newinnovator@nih.gov or call 301-594-4469





Rosina M. Bierbaum is co-chair (with Peter H. Raven) of the SEG on Climate Change and Global Development, and professor and dean of the School of Natural Resources and Environment, University of Michigan. rbierbau@umich.edu



Peter H. Raven is co-chair (with Rosina M. Bierbaum) of the SEG on Climate Change and Global Development, and president of the Missouri Botanical Garden. praven@nas.edu

A Two-Pronged Climate Strategy

A SENSIBLE STRATEGY TO MINIMIZE THE DAMAGES FROM ANTHROPOGENIC CLIMATE change has two objectives: mitigate the pace and ultimate magnitude of the changes that occur and adapt to the changes that cannot be avoided. To underline this two-pronged approach, the recent report *Confronting Climate Change*, prepared for the United Nations (UN) by an international panel we co-chaired, was subtitled *Avoiding the Unmanageable and Managing the Unavoidable* (www.unfoundation.org/SEG/). On 27 February 2007, we presented UN Secretary-General Ban Ki-moon with this urgent call for new levels of commitment and coordination by the UN and its member states to avoid the worst climate-change dangers while there is still time.

The Scientific Expert Group (SEG) on Climate Change and Sustainable Development was organized by the scientific research society Sigma Xi and the UN Foundation at the request of the UN Department on Economic and Social Affairs. Our 18 expert members come from 11 countries and a wide range of disciplines and institutions. Unlike the Intergovernmental Panel on Climate Change (IPCC), which may not make recommendations for action, the SEG was invited to tell the UN what it should do to address the climate-change challenge, and after over 2 years of work, it did.

The group's unanimous recommendations focus equally on mitigation and adaptation. The SEG concludes that unmanageable changes in the future are avoidable only if the world community acts now. Global carbon dioxide emissions must level off by 2015 or 2020 at little more than their current level and then decline to no more than a third of that level by 2100. Emissions of methane and black soot must also be controlled. This can be done with a mix of existing and new technologies, with many subsidiary benefits. We recommend several urgent goals: improved efficiency in the transportation sector and in the energy efficiency of buildings; expanded use of biofuels; and, very important, the design and deployment of coal-fired power plants capable of environmentally sound retrofits for carbon capture.

Equally important is our capacity to adapt to unavoidable change by improving preparedness and response strategies to meet the needs of the world's poor, who will bear the heaviest burden of climate change. The summary of the new IPCC report on *Impacts, Adaptation and Vulnerability*, expected this week, makes it clear that the future will be very different from the past and that changes under way challenge our land management regimes and our ability to maintain ecosystem services. Climate-resilient energy-efficient cities must become the norm, and institutions must be strengthened to cope with weather-related disasters and climate-change refugees, whose numbers may reach tens of millions in the future. Building on land less than 3 feet above sea level is certainly not sustainable. Preserving a major proportion of the poorly known biological diversity of the world requires curbing the rates of climate change but also needs enhanced and innovative efforts to save surviving species.

Global climate has already changed noticeably, with more than half of the increase in temperature since preindustrial times occurring since 1970. Heat waves; ice melt; shifting ranges of plants and animals; sea-level rise; and droughts, floods, and wildfires are increasing, as expected. Even if emissions were completely halted today, the total temperature increase from greenhouse gases already in the atmosphere would be approximately 1.5°C globally. Unless we can keep global average temperature from exceeding 2° to 2.5°C above preindustrial levels, we may reach tipping points that could produce intolerable human impacts. Business as usual could have us 3° to 5°C above preindustrial temperatures by 2100—a temperature jump equaling that from the height of the last ice age to the present warm period. Unless the world acts now, we will fail miserably to meet the UN Millennium Development Goals, fail to improve the fate of the poor, and fail to achieve global sustainability. The human race, now numbering 6.5 billion people, has never faced a greater challenge, and there is no time for further delay.

— Rosina M. Bierbaum and Peter H. Raven

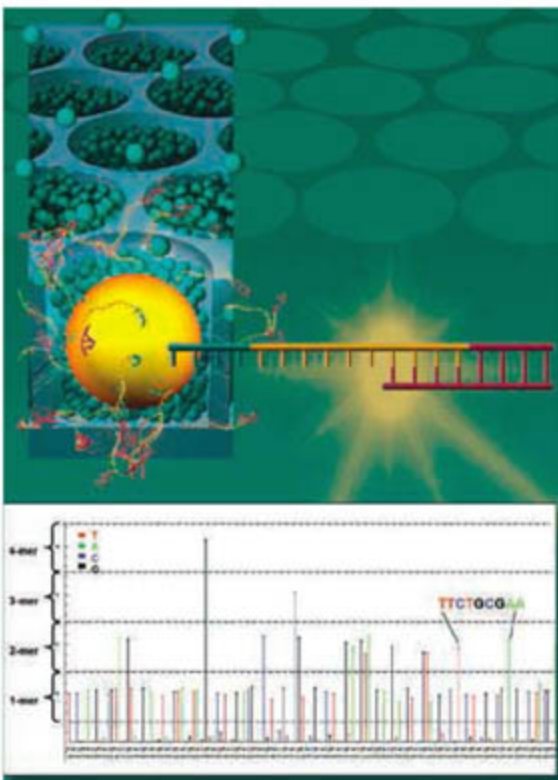




www.roche-applied-science.com

Introducing Our Second Generation Genome Sequencing System

Genome Sequencer FLX



Be First to the Finish with...

- Increased read lengths averaging 200 to 300 bases per read
- Throughput of more than 400,000 reads per run
- High single-read accuracy greater than 99.5% over 200 bases
- Consensus-read accuracy greater than 99.99%

...more Flexibility and more Applications.

Visit www.genome-sequencing.com to learn about the expanding number of peer-reviewed publications appearing weekly.

454 LIFE SCIENCES



Diagnostics



Central California
grasslands.

ECOLOGY/EVOLUTION

Perennial Infection

Although grazing and fire have been proposed as explanations for the remarkable success of exotic annual grasses in California, where they have established themselves among the native perennials over wide swathes of the landscape despite being inferior competitors for resources, active management based on these factors has failed to stem the invasions. It is known that disease can alter the competitive balance between species in ecological communities, and Borer *et al.* have developed a model showing quantitatively how invasion has been mediated by viral disease (barley and cereal yellow dwarf viruses, which are a major pathogen in crops, including wheat, barley, and oats). They find that the key to the success of the annual grasses is that virus is horizontally transmitted by aphids, rather than vertically via seeds; hence, seed survival is unaffected, and each generation suffers infection anew. In contrast, perennial grasses serve as long-term reservoirs for the virus and experience deleterious effects on survival and on lifetime seed production, thus facilitating the invasion by annuals. — AMS

Proc. Natl. Acad. Sci. U.S.A. **104**, 5473 (2007).

PHYSICS

Probing Quantum Memories

Can't quite place a name to the face, or associate a singer with a song? You know, or at least hope, that the information lies intact somewhere in your head, needing only the correct memory trick or stimulus to retrieve it. For quantum communications, where information is transmitted along quantum channels and stored in quantum memories, it is necessary that the stored information be robust and retrievable. However, quantum memories are known to decay because of decoherence, and physicists therefore have to develop their own set of tricks to probe and measure how reliable these memories are. Staudt *et al.* look at quantum information stored in an optical memory, where the information is encoded in the coherent transfer of the phase and amplitudes of light pulses onto a suitable solid-state medium. They use a photon-echo technique whereby a sequence of pulses initializes the memory cell, encodes the data onto it, and uses a read pulse to generate a stimulated echo pulse which replicates the stored information. The advantage of this scheme is that, though memories may be lost, if they are recalled they remain undistorted. — ISO

Phys. Rev. Lett. **98**, 113601 (2007).

BIOCHEMISTRY

Step by Step

Recent exponential growth in databases as a consequence of big-science projects such as genome sequencing and structural genomics

has, in some environments, credentialed bioinformatic analysts and relegated experimental work to the back-benchers. Nevertheless, the significance of mutations can be hard to predict without actually making the proteins and assessing their behavior.

Kona *et al.* have taken this approach in trying to understand the role of a Cd^{2+} -binding cysteine in the *Escherichia coli* enzyme KDO8P synthase in comparison to an asparagine in the *Aquifex aeolicus* version of the same enzyme. The reaction they catalyze is an aldol condensation of phosphoenolpyruvate and arabinose 5-phosphate. This enzymatic step is a critical one in the bacterial biosynthetic pathway leading to lipopolysaccharides and hence is a potential drug target. A comparison of the structures enabled them to make a series of mutations bridging the metallo- and nonmetallo-KDO8P synthases; follow-up kinetic and structural analyses yielded several insights. The cysteine-coordinated metal fulfills the same function as the asparagine carboxamide in binding and orienting a water molecule for attack on the *si* side at C2. Even though the metallo- and nonmetallo-KDO8P synthases produce the same chemical intermediate, probably via the same reaction pathway, the binding constants of the

substrates and products differ, which may reflect an evolutionary adaptation to changes in metabolite concentrations. — GJC

Biochemistry **46**, 10.1021/bi6024879 (2007).

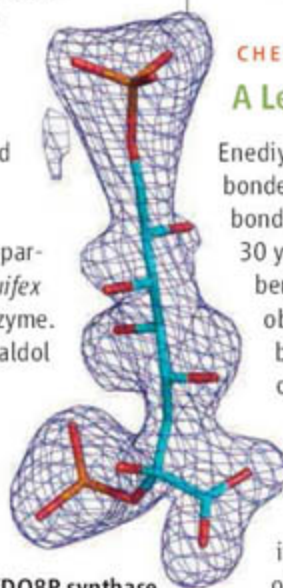
CHEMISTRY

A Less Radical Pathway

Eneidyne molecules, in which two doubly bonded carbons tether two sets of triply bonded carbons, have been known for over 30 years to cyclize to the intriguing *para*-benzyne biradical. This species has been observed in many cases to behave as a benzene ring with two diametrically opposed trivalent carbons, which each react rapidly with hydrogen or halogen atom sources.

Perrin *et al.* have observed a surprisingly different mode of reactivity, which is more consistent with nucleophilic attack at one of the unsaturated carbons than with radical atom abstraction. Their studies show that slight heating of an eneidyne in the presence of lithium halide salts and acid results in a halide and proton adding to opposite ends of the resultant benzene ring. Isotopic labeling reveals that even as weak an acid as dimethylsulfoxide can serve as the proton donor, implicating a highly basic phenyl anion intermediate formed after halide attack. The reaction is high-yielding for chloride, bromide, and iodide salts, and shows kinetics consistent with *p*-benzyne formation as the rate-

Continued on page 21



KDO8P synthase
intermediate.



“The Digital Library”

Vinton G. Cerf
Vice President and Chief Internet Evangelist
Google



“Online Books and Courses”

Amy Wu
Computer Science Student
Stanford University



“Publications”

Benjamin Mako Hill
Research Assistant
MIT Media Laboratory



“Conferences”

Maria Klawe
President
Harvey Mudd College

ACM: KNOWLEDGE, COLLABORATION & INNOVATION IN COMPUTING

Uniting the world's computing professionals, researchers and educators to inspire dialogue, share resources and address the computing field's challenges in the 21st Century.



Association for Computing Machinery
Advancing Computing as a Science & Profession
www.acm.org/learnmore

Continued from page 19

limiting step. These findings offer a compelling rationale for the puzzling isolation from marine sources of monochlorinated cyanosporaside isomers whose structures were inconsistent with established radical or electrophilic chlorination pathways. — JSY

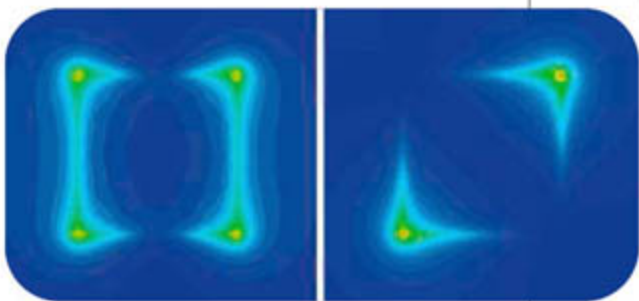
J. Am. Chem. Soc. **129**, 10.1021/ja070023e (2007).

CHEMISTRY

SERS from Sharp Silver

Surface-enhanced Raman scattering (SERS) is observed on a variety of silver and gold surfaces where nanoscale roughness creates high local fields, and giant enhancements have been observed in "hot spots" created between two nanoparticles. However, even single nanoparticles can create fields large enough to enable single-molecule detection.

To better understand the origin of this effect, McLellan *et al.* have deposited silver nanoparticles of various shapes on silicon substrates that have registration marks. Scanning electron microscopy was used to determine the orienta-



Field amplitudes around a silver cube.

tion of the particles so that the effect of laser polarization on SERS spectra could be studied. For nanocubes, the SERS intensity of adsorbed 1,4-benzenedithiol varied greatly with the direction of polarization, and the spectra were more

intense when the field cut across the cube's corners; more rounded truncated cubes showed little variation with polarization direction. Similar effects were seen in simulations of the local fields for these particles. — PDS

Nano Lett. **7**, 10.1021/nl070157q (2007).

MOLECULAR BIOLOGY

The Evolution of Origins

Prokaryote genomes are generally organized as a single circular chromosome with a single origin of DNA replication; most eukaryotes, on the other hand, have multiple chromosomes, each with multiple replication origins. This latter feature has recently been found in a number of archaea, including *Sulfolobus* species, which have several origins on a single chromosome. Might these have arisen simply by duplication?

Robinson and Bell show that origins that are conserved across *Sulfolobus* species share the gene *copG*, encoding a plasmid copy-number control protein, as well as a number of stress response genes. Furthermore, one of the two origins in the archaeal *Aeropyrum pernix* bears a striking resemblance to two origins found in a distantly related *Sulfolobus* species; several genes and evidence of a putative prokaryotic viral integration site are conserved. Among the genes is a protein that is similar to RepA, a bacterial plasmid initiator protein, as well as the yeast replication initiation protein Cdt1.

Altogether, this evidence points to a captured extrachromosomal element, possibly a virus/plasmid hybrid, as the source of the supernumerary origins. A hybrid phage/eukaryotic replication initiation site on the yeast 2 μ plasmid hints at a similar genesis for the multiple origins on eukaryotic chromosomes. — GR

Proc. Natl. Acad. Sci. U.S.A. **104**, 5806 (2007).



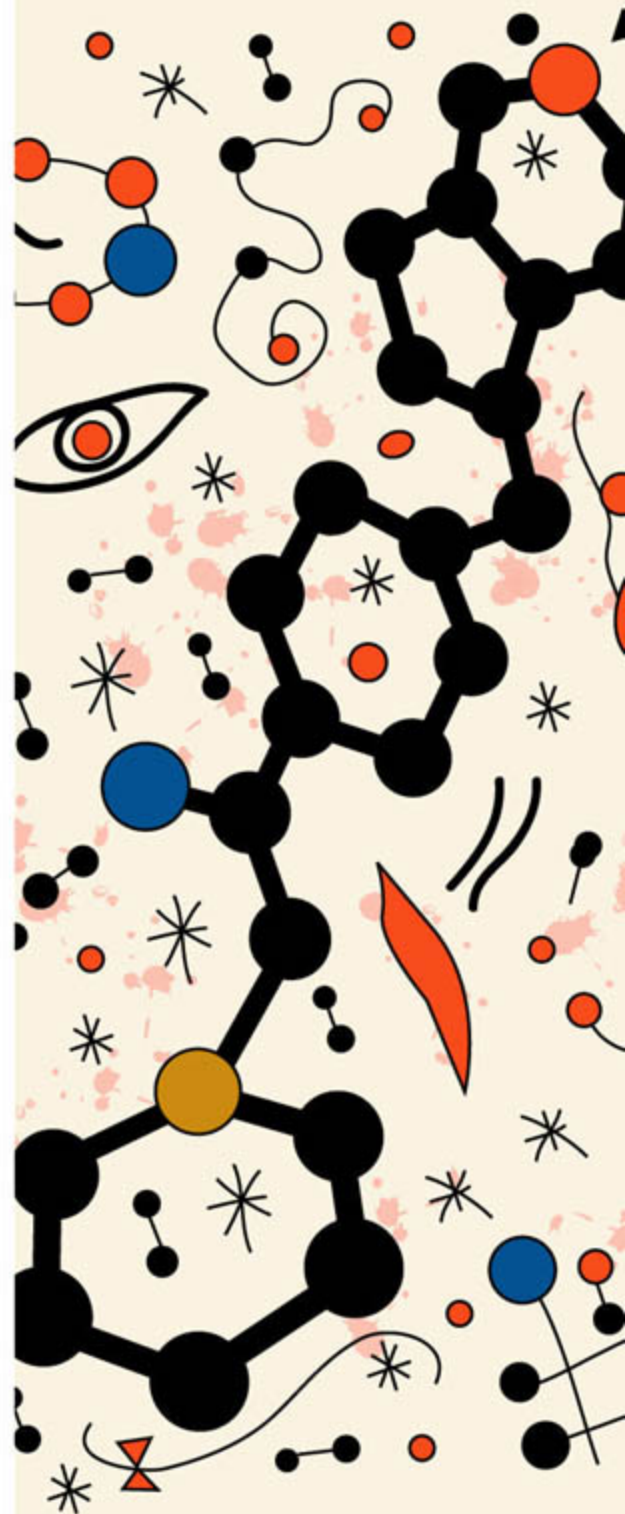
www.stke.org

<< Better Bones Without Bax

At about age 50, the depletion of ovarian follicles through apoptosis leads to the loss of cyclic ovarian function in women. Although aging female mice do not undergo menopause, they do suffer a depletion of ovarian follicles and health complications similar to those of postmenopausal women. After their earlier finding that oocyte loss was mitigated in mice lacking the proapoptotic protein Bax, Perez *et al.* investigated aging *Bax*-deficient female mice and found them to be leaner and more active than their wild-type counterparts. They retained more of their hair, developed fewer cataracts, experienced less wrinkling of the skin, and had stronger bones. Although older *Bax* knockout mice failed to become pregnant, they did ovulate in response to gonadotropin, and when their ovarian tissue was grafted into young wild-type females, the oocytes produced viable pups. Finally, behavioral analyses indicated that the knockouts were less anxious and more attentive than wild-type mice. — EMA

Proc. Natl. Acad. Sci. U.S.A. **104**, 5229 (2007).

The Art of Global Discovery Chemistry



CHEMBRIDGE CORPORATION IS THE WORLD'S LARGEST GLOBAL DISCOVERY CHEMISTRY CRO AND PREMIER PROVIDER OF ADVANCED SCREENING LIBRARIES FOR SMALL MOLECULE DRUG DISCOVERY.

PLEASE VISIT WWW.CHEMBRIDGE.COM



Does your next career step
need direction?



*For a career in science,
I turn to Science*

*I have a great new research idea.
Where can I find more grant options?*



ScienceCa


We know science



*You know, ScienceCareers.org
is part of the non-profit AAAS*



*That means they're putting
something back into science*



*With thousands of job postings,
it's a lot easier to track down a
career that suits me*

*I got the offer I've been
dreaming of.*

Now what?

careers.org



*I want a career,
not just a job*

There's only one place to go for career advice if you value the expertise of *Science* and the long experience of AAAS in supporting career advancement - ScienceCareers.org. The pages of *Science* and our website ScienceCareers.org offer:

- Thousands of job postings
- Career advice articles and tools
- Funding information
- Networking opportunities

www.sciencecareers.org



New! BigDye®
XTerminator™ Kit.
Game over blobs.

Find out more @
[appliedbiosystems.com/
gameoverblobs](http://appliedbiosystems.com/gameoverblobs)

25 years of delivering next-generation systems

Accelerate your time to publish

Human disease researchers bridge diverse research areas to advance the medical field, moving forward in small but steady strides. Your road requires perseverance and demands commitment. Over the past 25 years, Applied Biosystems has helped to pave the way with cutting-edge technology for genetic analysis. AB offers reagents, instruments, and software for applications including DNA sequencing, fragment analysis, and genotyping—accelerating scientific research.

To find out more, visit: info.appliedbiosystems.com/hdr



AB Applied
Biosystems

For Research Use Only. Not for use in diagnostic procedures. This instrument is authorized for use in DNA sequencing and fragment analysis under process claims of U.S. Patent Nos. 5,821,058 and 5,332,666 and under all process claims for DNA sequence and fragment analysis of U.S. and foreign counterpart patents owned or licensable by Applied Biosystems. The Applied Biosystems 3130/3130x Genetic Analyzers include patented technology licensed from Hitachi, Ltd., as part of a strategic partnership between Applied Biosystems and Hitachi, Ltd., as well as patented technology of Applied Biosystems. Applied Biosystems and AB (Design) are registered trademarks and Applied is a trademark of the Applied Biosystems Corporation or its subsidiaries in the US and/or certain other countries. ©2007 Applied Biosystems. All rights reserved.

New
instrument!

More Flexible LCM



Molecular Devices introduces Arcturus^{XT}, the only open, modular microdissection instrument to combine Laser Capture Microdissection (LCM) with UV laser cutting. Arcturus^{XT} is the ideal solution for researchers who require more flexibility and system ease of use.

- ⊕ Unique IR-enabled LCM—never lose contact with the sample!
- ⊕ Nikon® TE2000U base—research-grade microscope with high-quality optics
- ⊕ Fully upgradable and extendable platform
- ⊕ Optional UV Laser Cutting and Epi-Fluorescence
- ⊕ Phase contrast and DIC options—ideal for live-cell applications
- ⊕ Ergonomic touch-screen monitor and trackball-controlled stage
- ⊕ Full range of objective offerings—2x to 100x
- ⊕ Compatible with glass or membrane slides

By combining gentle LCM and rapid UV laser cutting, you have more choices in the isolation of pure cell populations to fit any research application. The new Arcturus^{XT} system, along with our Arcturus[®] microgenomics reagents and GenePix[®] microarray scanners and software, provide a more complete solution for microarray research. Visit www.moleculardevices.com/LCM for more information.

Expect more. We'll do our very best to exceed your expectations.

See us in Montréal at the Society for Biomolecular Sciences 13th Annual Conference & Exhibition, April 15–19, Booth #401 and in Los Angeles at the American Association for Cancer Research Annual Meeting, April 14–18, Booth #1856.

 **Molecular Devices**

tel. +1-800-635-5577 | www.moleculardevices.com

LIFE SCIENCE TECHNOLOGIES

CELL SIGNALING

IN THIS ISSUE:

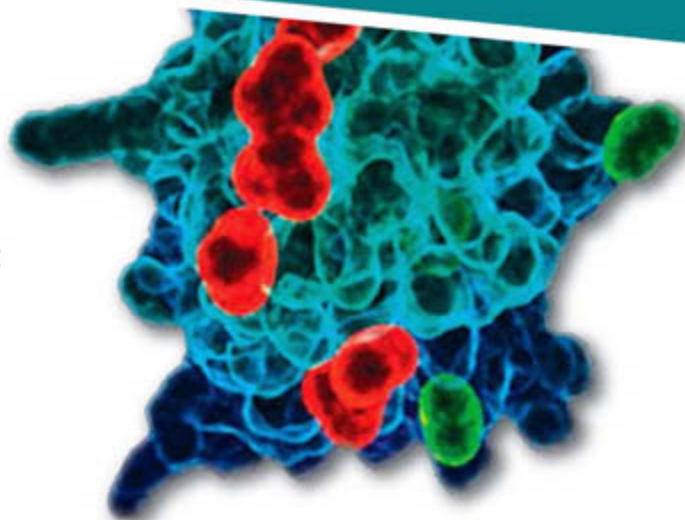
Phosphorylation reactions catalyzed by cellular kinases are ubiquitous in signaling cascades, making them important players in cell function and dysfunction. Read about new technologies for detecting, characterizing, and quantitating kinase activity in the **Cell Signaling** feature on **page 125** of this issue.

UPCOMING FEATURES:

April 20— Stem Cells

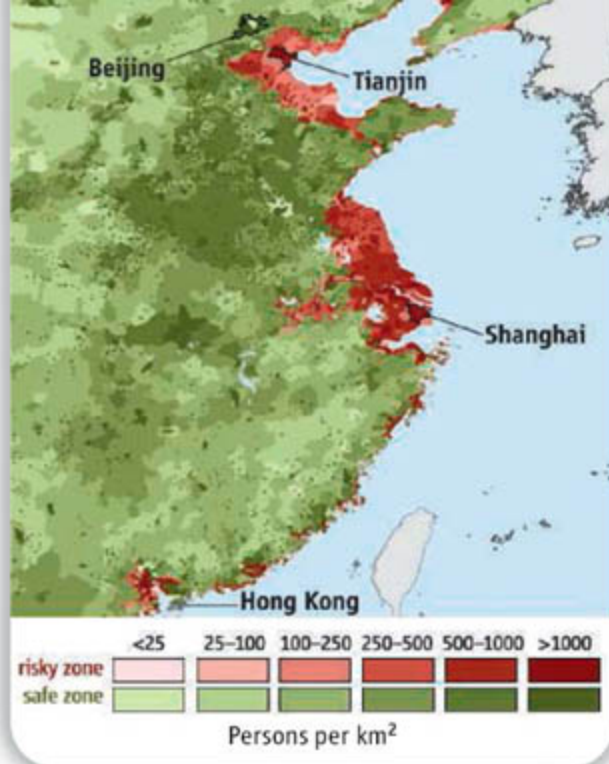
June 1— RNAi

June 22— Cell Signaling 2



Also available at www.sciencemag.org/products/articles.dtl





Going Under

Two-thirds of all cities with populations exceeding 5 million are “especially vulnerable to risks resulting from climate change,” according to a study from Columbia University and the International Institute for Environment and Development in London. A team of geographers defined danger zones as areas within 10 meters above sea level, the places most vulnerable to weather oscillations combined with the 25- to 60-cm sea-level rise forecast by 2100. China (see map) is in the lead, with 144 million people, or 11% of its population, at or below the 10-meter level. The world’s poor are the most imperiled, with some 247 million at risk in least developed nations. Numbers will climb with continued urbanization, note the authors, who say nations should develop policies to encourage inland growth.

Ins and Outs of Carbon

NET WATCH

Some parts of the world pump more carbon dioxide into the atmosphere than they remove, whereas other regions are net absorbers. A new site for charting the ups and downs of the greenhouse gas is CarbonTracker from the U.S. National Oceanic and Atmospheric Administration in Boulder, Colorado.

CarbonTracker incorporates CO₂ measurements from some 60 locations around the world to provide a broad picture of carbon uptake and release for North America, the globe, and the oceans between 2000 and 2005. Visitors can also check out the “carbon weather” to see how storms alter levels of the gas. The researchers hope other labs will contribute data that could help make CarbonTracker an objective tool for gauging whether carbon emission targets are being met. >>

www.esrl.noaa.gov/gmd/ccgg/carbontracker

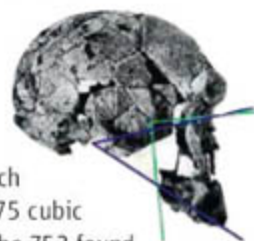
New Face for Kenya Hominid?

Homo rudolfensis, a 1.9-million-year-old skull from Kenya, may not be a *Homo* after all, says a scientist who has done a computer reconstruction of the skull.

The skull fragments—found in 1972 near Lake Turkana and put together by Richard Leakey—have sparked much debate, because their owner seemed to have had a much larger brain than other hominids of similar age.

Now Timothy Bromage, a paleoanthropologist and expert on facial bone development at New York University, claims to have sorted out

the puzzle. In a virtual reconstruction, he followed a rule that he says applies to all primates: The angle created by drawing a line from the eye socket to the ear and then to the top back molar is always 45°. Shifting the skull bones to conform to the rule pushes out the lower face and leads to a much smaller brain: about 575 cubic centimeters instead of the 752 found by Columbia University anthropologist Ralph Holloway. That downsizing along with the newly prognathous profile just about edge the skull out of the *Homo* ballpark,



Bromage told a meeting of the International Association for Dental Research last week in New Orleans, Louisiana.

Holloway says he’s sticking to his own estimate. “I sincerely doubt that these fragments can be so radically reconstructed,” he says. “Maybe with a computer, but not by a trained anatomist’s hand.” But paleoneurologist Dean Falk of Florida State University in Tallahassee says she thinks Bromage’s method for hafting faces onto crania is “really exciting. ... We’re exploring applying it ourselves.”

Before and after.

neurologist Dean Falk of Florida State University in Tallahassee says she thinks Bromage’s method for hafting faces onto crania is “really exciting. ... We’re exploring applying it ourselves.”

A Discriminating Parasite >>

Toxoplasma gondii is a parasite that requires two hosts. It’s born in a cat’s intestines, develops in another animal—such as a rat—and must return to a cat to reproduce. To boost its chances of making that return trip, researchers at Oxford University have shown, *Toxoplasma* makes rodents less afraid of cats. Now a Stanford University team led by Ajai Vyas has found that rats carrying the parasite don’t mellow out across the board; they just lose their fear of the smell of cats.

In the lab, infected rats showed much less aversion than normal ones to bobcat urine. But they reacted normally when the researchers probed other types of fear responses. That means *Toxoplasma* has a “remarkably specific” behavioral effect, says co-author Robert Sapolsky. He says most parasites control behavior in much cruder ways—for example, by destroying muscle metabolism so an organism can’t evade a predator. In the 2 April online *Proceedings of the National Academy of Sciences*, the scientists report that *Toxoplasma* cysts form preferentially on the rat amygdala, which Sapolsky calls “ground zero” for fear in the brain.

“I always found it incredible that the parasite would be able to alter a response, cat aversion, that is so ingrained in the rat’s psyche,” says Oxford veterinary scientist Manuel Berdoy, an author of the earlier work. He says the new research shows that the parasite may have the “astonishing” ability to zero in on the neural pathways for processing cat odors.



IMMUNODEFICIENT MODELS AND XENOGRRAFT STUDIES



Nude Mice

Nude Rats

SCID Mice

**NOD SCID
Mice**

**Custom
Xenograft
Studies**

We offer excellent availability of nine immunodeficient rodent models. Our Preclinical Services group also provides xenograft and other oncology-based services.

US: 1.877.CRIVER.1
Europe: info@eu.crl.com
WWW.CRIVER.COM


**CHARLES RIVER
LABORATORIES**
Research Models and Services

Preclinical Research Resources

Biological and Reference Reagents
available from the National Cancer Institute



New Reagents Available

Rabbit Antisera to NF κ B Signaling Proteins
Recombinant Human IL-6
Immunocytokine Hu 14.18-IL2

Bulk Cytokines Available: *Murine* – Fc-endostatin; *Human* – IL-1 α , IL-2, FGF (basic), and VEGF are available free to investigators with peer-reviewed financial support at not-for-profit institutions.

Monoclonal Antibodies Available: HeFi-1 (anti-human CD30), B72.3 (anti-human TAG-72), R24 (anti-GD3), 3ZD (anti-human IL-1 β), and 11B.11 (anti-mouse IL-4) are available to investigators with peer-reviewed financial support at institutions or commercial establishments.

Other Reagents: Hynic-rh-Annexin V.

Reference Reagents for Murine and Human Cytokines

The Biological Resources Branch (NCI), the Division of Microbiology and Infectious Diseases (NIAID), and the National Institute for Biological Standards and Control (UK) have made available reference reagents for use in the calibration of *in vitro* bioassays and in-house standards. They are not to be used for experimental purposes. Distribution is limited to the USA. To obtain Reference Reagents outside the USA, contact NIBSC at www.nibsc.ac.uk.

Please visit our Web site for a complete list of our murine and human cytokines.

For questions contact: Dr. Rosemarie Aurigemma

NCI-Frederick

Fax: 301-846-5429

e-mail: raurigemma@ncicrf.gov



Investigators wishing to obtain any of these materials should visit the BRB Repository Web site at web.ncicrf.gov/research/brb/site/preclinRepo.asp

Complimentary Pre-Conference Workshop on:

Raising Money for Antibody Development

Funding Each Stage of the Scale-Up Process

Chaired by Patrick Huddie, Ph.D.
from Evergreen Capital, LLC

Sunday, April 22 from 4:00-6:30 PM

The 12th Annual

Waterside Conference

*Scale-Up and Production of
Recombinant and Monoclonal Antibodies*

April 23-25, 2007 • San Juan, Puerto Rico

Topics Include:

- Purification
- Assay Development
- Single-Use Components
- Cell Culture Scale-Up
- Product - Single Characterization
- Regulatory Issues

*WilBio's
Conferences are
consistently rated
the best for:*

**Content
Networking
Format
Cost
Food
Entertainment
Accommodations**



*The Most Trusted
Source of BioProcessing
Technology*

P.O. Box 1229
Virginia Beach, VA 23451 USA
757.423.8823
Fax 757.423.2065
www.wilbio.com
info@wilbio.com

Featuring Presentations from:

- Alois Jungbauer, Ph.D. - Austrian Center of Biopharmaceutical Technology
- Joy Adiletta - Amgen
- Oscar Salas-Solano, Ph.D. - Genentech, Inc.
- Robert DuBridg, Ph.D. - PDL BioPharma, Inc.
- Jonida Basha - Merck & Co., Inc.
- Dorothee Ambrosius - Boehringer-Ingelheim Pharma GmbH & Co.
- Jeanne Novak, Ph.D. - CBR International Corp.
- Gerald Carson - Abbott Laboratories
- Stephen Notarnicola, Ph.D. - Biogen Idec MA, Inc.
- Richard Root, M.Sc. - Roche Diagnostics Corp.
- Tongtong Wang, Ph.D. - Eli Lilly & Company
- Shujun Sun - Wyeth Biotech
- Missag Parseghian, Ph.D. - Peregrine Pharmaceuticals
- NingNing Ma, Ph.D. - Pfizer, Inc.
- Shue-Yuan Wang - Abbott Laboratories
- Peter Gagnon - Validated Biosystems, Inc.
- Xing Wang, Ph.D. - Pfizer, Inc.
- Cori Gorman, Ph.D. - Selexis USA



MOVERS

PARTING WAYS. Claire Fraser-Liggett is leaving the DNA research institute founded by her former husband, J. Craig Venter, after running it for nearly a decade.

Fraser-Liggett's decision to step down as president of The Institute for Genomic



Research (TIGR) in Rockville, Maryland, comes 5 months after a board chaired by Venter stripped TIGR of its independent status and made it a division of the J. Craig Venter Institute (JCVI), also located in Rockville. A JCVI spokesperson says, "We will be making

some announcements in the very near future about additional changes."

Fraser-Liggett has led a team of pioneering microbial DNA scientists at TIGR since Venter launched it in 1992 with proceeds from a DNA-sequencing deal (*Science*,

14 June 2002, p. 1957). Fraser-Liggett is now weighing an appointment at a major academic medical center that will link her lab research more directly to clinical work, and the speculation is that she and several TIGR staffers are being recruited by the University of Maryland.

MONEY MATTERS

HELP WANTED. The province of Alberta, Canada, is offering \$17 million packages for a few rising stars in biomedical research who like the idea of making their name on the Canadian plains. "We're looking to attract people who could be really big players 5 to 10 years down the road," says Kevin Keough, president of the Alberta Heritage Foundation for Medical Research. "The idea is to provide

them with the wherewithal to really build something here."

The new, 10-year Polaris Investigator Awards are for a total of three faculty spots at the universities of Alberta, Calgary, and Lethbridge, which are sharing the cost of the awards in a quest to make a bigger mark on the biomedical research frontier. The recipient "creates critical mass," says University of Alberta President Indira Samarasekera, "and becomes a global magnet for talent in that particular field."

The awards are an offshoot of an economic boom in the province fueled by spiraling oil prices. And the foundation has sweetened the deal by excusing the winners from any administrative duties for the first 5 years of their contracts. Applicants should contact one of the universities. The West is calling.

Three Q's >>

Thailand's new science minister, **Yongyuth Yuthavong**, brings a deep understanding of science to a post traditionally headed by bureaucrats. A biochemist who along with colleagues deciphered the structure of a key enzyme of the malaria parasite, Yongyuth, 62, is lobbying the National Assembly to approve a several-fold increase in R&D spending over the next 3 years. *Science* caught up with him recently.

Q: What is the motivation for your draft science law?

We want a system for science policy development, with the science minister as the chief scientific adviser to the government. The science ministry has always been a "grade C" ministry. I want it to be "grade A."

Q: How will the legislation help rank-and-file scientists?

The law designates a level of support for R&D—not less than 3% of the budget. Even if I get 2%, it will be three or four times the present level. [But] we'll have to lobby.

Q: What are your chances of success?

My first name means "keep on fighting," and my surname means "fighting family." And [he laughs] I have friends on the assembly's science and technology committee.



They Said It

"None of us is running for president, so I think we can get away with plagiarism."

—Representative Vernon Ehlers (R-MI), at a 28 March meeting of the House Science and Technology Committee, after committee chair Bart Gordon (D-TN) confessed to "plagiarizing" the recommendations of a 2005 National Academies report in a bill to improve math and science education (H.R. 362) that the committee then passed unanimously.

Got a tip for this page? E-mail people@aaas.org



Ultrafast getaway captured

33



Hobbit's archaic wrist

34

MUSEUM MANAGEMENT

Turnover at the Top, but Problems Persist at the Smithsonian

When Lawrence Small abruptly resigned as secretary of the Smithsonian Institution last week, you could almost hear the staff's collective sigh of relief. Although Small shored up the Smithsonian's sagging finances during his 7-year term, his departure signaled an end to the internal audits, the harsh press coverage, and congressional outrage over high executive salaries and exorbitant personal expenses—such as first-class tickets for a Hawaiian vacation.

The turnover also hinted at better times for the Smithsonian's 500 researchers in locations from Panama to Massachusetts. Many think science didn't fully benefit from Small's fundraising, which focused on "bricks and mortar" improvements. They are encouraged that scientists have been made interim leaders.

The Board of Regents, which oversees the Smithsonian's activities, picked the 41-year-old director of the Smithsonian National Museum of Natural History, biologist Cristián Samper, as acting secretary. This move is fueling hopes that Samper, or someone with a research background, might take charge long term. In another big change, David Evans, who oversaw Smithsonian science for 4 years under Small, also resigned last week. Ira Rubinoff, director of the Smithsonian Tropical Research Institute in Panama, has stepped in as his temporary replacement. Paul Risser, a botanist and chair of the University of Oklahoma Research Cabinet, will be the new acting director of the natural history museum.

Although it's too soon to tell what this will mean for the institution's programs, the new leaders are speaking in a way that's bound to please scientists. In the past, "the whole issue of infrastructure and facilities has received a

WHO'S IN

WHO'S OUT

SMITHSONIAN SECRETARY



UNDERSECRETARY



Yellow ties take charge. At the Smithsonian, Cristián Samper (*top, left*) has replaced Secretary Lawrence Small (*top, right*); Ira Rubinoff (*lower, left*) has stepped in for David Evans as undersecretary for science.

lot of attention," Samper said in an interview. "I want to strengthen the programmatic side—the scholarship and science." Rubinoff says his goal is to get "more balance" among the institution's priorities, suggesting a closer look at research objectives and not a single-minded emphasis on refurbishing museums. Among the staff, "there were a lot of smiling faces this week," says William Fitzhugh, a Smithsonian archaeobiologist.

Unfinished business

Although the new leaders may be more in tune with research, it will be difficult for them—or anyone—to launch programs while maintaining the Smithsonian's sprawling conglomeration of 19 museums and galleries, the National Zoo, and nine research facilities.

The U.S. Congress foots about 70% of the Smithsonian's bills, but increases in this federal allocation have not kept up with costs, in particular the demand for finishing new museums and repairing old ones. Small helped bring in a lot of private money—about \$1 billion during his term—for this quasi-federal institution. But most of it was not for science. Scientists have looked elsewhere for research support, with mixed success.

The harsh reality is that money is still tight, and the Smithsonian is groaning under the weight of its obligations. "Our biggest need is still facilities," says Roger Sant, chair of the board of the Summit Foundation in Washington, D.C., and a member of the Smithsonian's Board of Regents. "When your backlog [of obligations] is \$2.3 billion, it's hard to say anything is going to get a greater amount of attention."

The bricks-and-mortar problem dates back to the 1980s when then-Smithsonian Secretary Sidney Dillon Ripley built eight museums and set up seven new research programs, few of which were fully funded by Congress. When Small came on board, the Smithsonian's finances were in a shambles, and construction projects were underfunded. "The place really did need fixing," says Sant. In addition to raising money, Small, a well-connected banker, got the National Museum of the American Indian and a new branch of the National Air and Space Museum up and running; he also began repairing bad heating systems and solving other infrastructure problems. But "he seemed to lose sight of the important research role of the institution," says Peter Raven, head of the Missouri Botanical Garden in St. Louis.

Belt-tightening measures did away with an internal grants program and research fellowships. An ever-larger percentage of congressional funding—which remained flat—had to cover mandatory expenses, such as salaries and shortfalls in the infrastructure budget. At the Smithsonian Astrophysical Observatory (SAO), based in Cambridge, Massachusetts, 2-year delays affected both a new spectrograph and a new infrared camera for the Multiple Mirror Telescope—both deemed key improvements by the scientific community.

Early in his tenure, Small angered scientists when he called for a reorganization that would have separated the exhibits from the research programs and closed a ▶



conservation research center in Front Royal, Virginia, and a materials research lab in Suitland, Maryland (*Science*, 13 July 2001, p. 194). The fuss prompted the Board of Regents to appoint an 18-member commission that in 2003 presented Small and Evans with almost 100 recommendations for changes. Since then, "the Smithsonian has made a huge amount of progress," says Jeremy Sabloff, the University of Pennsylvania anthropologist who chaired that commission.

The threatened research centers survived and appear to be on firm ground. There is now money for fellowships and new blood in charge at the zoo, the natural history museum, the Smithsonian Environmental Research Center (SERC) in Edgewater, Maryland, and the SAO.

Samper has turned the natural history museum around since he took over in 2003, hiring young curators to replace about a dozen retirement-age staff members who had stayed in place to help out their departments. Botany, for example, brought in new people for the first time since the early 1990s.

The natural history museum has received some \$70 million in outside funds in the past 4 years, most for exhibits but some for research. There are now two endowed chairs, one in ocean sciences and one in human origins. Furthermore, "we've had a great infusion of attention to the mechanics of doing good science here now," says Fitzhugh.

Nonetheless, problems persist. "A lot of the scientists, like myself, think we have a long way to go," says Warren Wagner, a botanist at the natural history museum. Small did not push for a major research initiative during his tenure; it's been more than a decade since the Smithsonian budget included one. SAO, for example, is looking for \$60 million as its contribution to the Giant Magellan Telescope but has yet to even get the request on the funding wish list the Smithsonian sends to the White House. The one science initiative in many years to become part of the institution's budget proposal—for a global environmental observatory focused on forests in 2008—was nixed last year by the White House Office of Management and Budget.

SERC has made up for a decline in direct support from the Smithsonian's federal budget over the past 10 years by seeking grants from the National Oceanic and Atmospheric

Administration and other agencies. But these sources could dry up. It's becoming increasingly difficult to maintain the long-term studies so crucial to distinguishing climate change from normal variation in the environment, notes SERC Director Anson Hines.

Researchers say what the Smithsonian really needs is a spokesperson who will lobby Congress and the White House more strongly. "We must articulate very well why our science is important," says Samper. It's not enough to win backing for individual projects; the research enterprise needs a champion, says

Smithsonian paleontologist Douglas Erwin: "There are some things you can [easily] raise money for ... exhibits and flashy research, but not for the preservative in jars of fish." He and others think a scientist, or at least a scholar of some sort, needs to be in charge.

But Board of Regents members are wary. "In the best of all worlds, you want a great scholar," says philanthropist Eli Broad. "But you want someone also [who] can rally the troops and can get the resources over and above what the government provides. It's a tough job."

—ELIZABETH PENNISI

HIGH-ENERGY PHYSICS

Design Flaw Could Delay Collider

A magnet for the Large Hadron Collider (LHC) failed during a key test at the European particle physics laboratory CERN last week. Physicists and engineers will have to repair the damaged magnet and retrofit others to correct the underlying design flaw, which could delay the start-up of the mammoth subterranean machine near Geneva, Switzerland, from November until the spring of 2008. That would eliminate a 1-month "engineering run" with which physicists had hoped to shake the bugs out of the machine before shutting down for the winter, when power becomes prohibitively expensive.

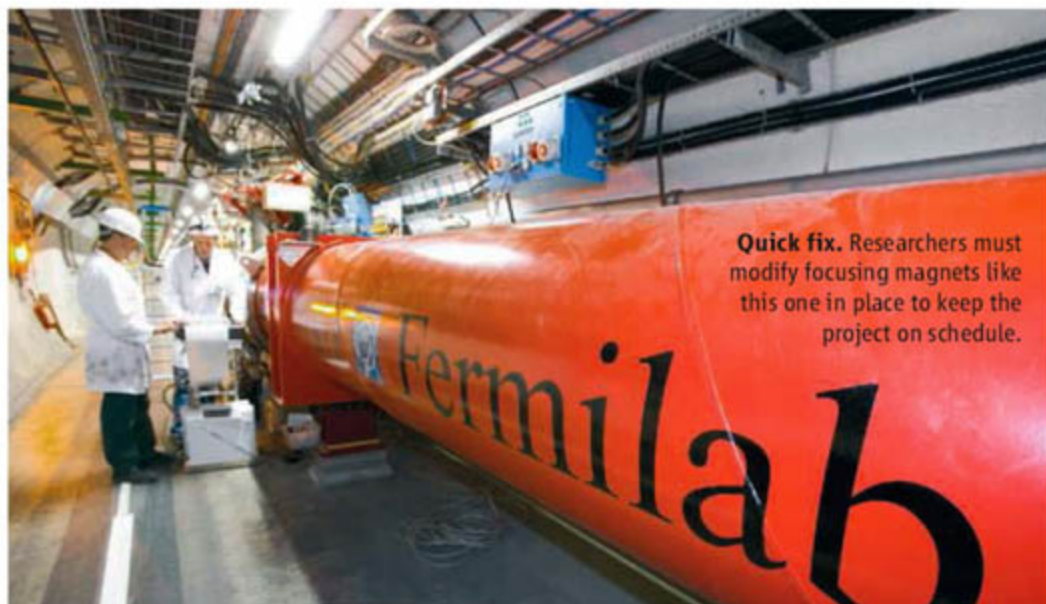
Laboratory officials aren't giving up hope just yet, however. "We are pretty well along on finding a fix that can be implemented in

the tunnel without having to bring [the magnets] up to the surface," says CERN's Lyndon Evans, who leads the construction of the accelerator. Only the damaged magnet will have to come out of the tunnel, he says.

The faulty magnets are designed to focus the LHC's beams of protons just before they collide. The beams will run through three such quadrupoles on either side of each of four collision points spaced around the 27-kilometer ring. The LHC's four massive particle detectors will sit at the collision points.

Designed and built at Fermi National Accelerator Laboratory (Fermilab) in Batavia, Illinois, the magnet failed when

Continued on page 34 ▶



Quick fix. Researchers must modify focusing magnets like this one in place to keep the project on schedule.

Predicting the Future of mRNA Capping

mScript™ mRNA will
boost your *in vivo*
protein expression
成功

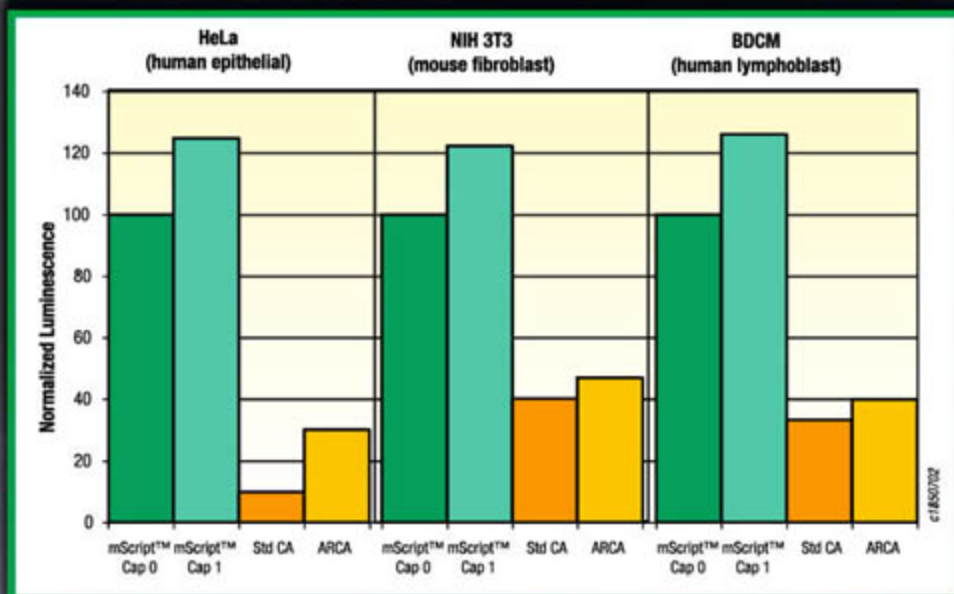
EPICENTRE's mScript™ mRNA Production System combines the ScriptCap™ Capping enzymes with our transcription and poly(A) tailing technology to provide an optimized solution for mRNA production.

- **100% capped mRNA transcripts**—versus 40% to 80% effective capping in co-transcriptional cap analog systems.
- **Cap 1 structure**—Cap 1 boosts *in vivo* translation by at least 20 to 50%.
- **Saves time and money**—Superior mRNAs and higher yields all in less time and at a lower cost.



To save a fortune on your mRNA,
go to www.EpiBio.com
and enter QuickInfo code: **MSA14**

mScript™ mRNA provides better *in vivo* translation



mScript™ mRNA produces more Luciferase activity than co-transcriptionally capped mRNA. Equal amounts of mScript, standard cap (Std CA), and ARCA capped and tailed mRNA were transfected into various mammalian cell lines. *In vivo* protein expression was measured by determining the RLU per μg of total protein 24 hours post-transfection.

P-702MS-A

PHYSICS

Attosecond Laser Pulses Illuminate Fleeting Dance of Electrons

Like a prisoner trapped behind the wall of a fortress, an electron faces a huge barrier in escaping the confines of an atom. Yet when hit by a burst of intense light, it can set itself free in just a few hundred attoseconds (10^{-18} s), thanks to a quantum-mechanical phenomenon known as tunneling. In essence, it seeps through the barrier—the binding energy that normally holds it in place. Now, for the first time, scientists have seen this blindingly fast escape act happen in real time.

This week in *Nature*, Ferenc Krausz of the Max Planck Institute of Quantum Optics in Garching, Germany, along with researchers in Austria and the Netherlands, reports watching electrons in neon atoms burrowing their way to freedom. The team says the findings—made possible by the use of 250-attosecond pulses of ultraviolet (UV) radiation—confirm theoretical predictions about the tunneling process.

The researchers also report using tunneling itself to image the acrobatics of electrons jumping from one orbital to another in neon and xenon atoms that have been excited by light. The work shows how “the powerful tools of attosecond science” can be used to understand atomic-level phenomena, says Paul Corkum, a physicist at the Steacie Institute for Molecular Sciences in Ottawa, Canada, who did not take part in the work.

To produce attosecond UV pulses, researchers bombard a cloud of neon atoms with a short burst of laser light that wrenches an electron out from deep inside the atom and smashes it back toward the atomic core. The most energetic photons emitted in this process are filtered out to yield a UV burst lasting a few hundred attoseconds.

In their experiment, Krausz and his colleagues trained an attosecond pulse as well as the laser wave used to generate it toward a second chamber of neon atoms. First, the attosecond pulse yanked electrons out from the atoms' inner shells to their outer edges, preparing the atoms for ionization and the electrons for escape. The laser

wave then took them the rest of the way.

When the laser's oscillating electric field reached its peak, it suppressed the atom's binding potential—in effect, thinning the



Looking in. In the Garching experiments, atoms in the cylindrical chamber were blasted with attosecond pulses and laser waves.

wall holding the electron in. At precisely those points in the laser's oscillation cycle, which lasted several hundred attoseconds, the researchers saw a marked increase in the number of ionized atoms in the chamber as the outer electrons tunneled their way through the lowered binding potential.

In other experiments, the researchers used tunneling to probe the intra-atomic dynamics of neon and xenon atoms. In the xenon study, they blasted atoms with an attosecond pulse powerful enough to knock an electron out of the element's innermost shell, causing electrons in the outer shells to rearrange themselves in an adjustment known as Auger decay. By targeting the atoms with the laser wave and noting how the number of ions created by tunneling changed over time, the team was able to trace the details of the Auger decay.

Researchers say the ability to control atomic-scale motion of electrons would have numerous applications. “Even simple-seeming processes such as laser surgery have attosecond phenomena at their core that have never been resolved,” says Corkum. In the longer term, Krausz says, such work could lead to better compact x-ray light sources for biological imaging and radiation therapies.

—YUDHIJIT BHATTACHARJEE

Going Against the Flow

Notwithstanding the laws of gravity, construction money this year at the National Science Foundation (NSF) is flowing from the bottom of the ocean to the top of a 5-km mountain. NSF has shifted \$15 million from the budgets of its fledgling oceans and ecological observatories networks to the Atacama Large Millimeter Array in the Chilean Andes, in tune with ALMA's rising costs and the agency's continued tinkering with the two networks.

The changes have touched a nerve in NSF's oversight body, the National Science Board. Speaking up at last week's board meeting, several members said that the long time between approval and the start of a project has left them feeling out of the loop. “We're just asking NSF to explain how things have changed and whether the science still justifies that level of support,” says Mark Abbott of Oregon State University in Corvallis, noting that NSF now plans to spend \$20 million less during the first 2 years of the ocean observatories initiative than when the board gave it the green light in 2002, for example, whereas ALMA is costing \$125 million more than originally planned. The board has asked NSF Director Arden Bement for more frequent updates on the \$240-million-a-year account and better estimates of the lifetime costs of operating each facility. —JEFFREY MERVIS

Pathology Institute Gets Lifeline

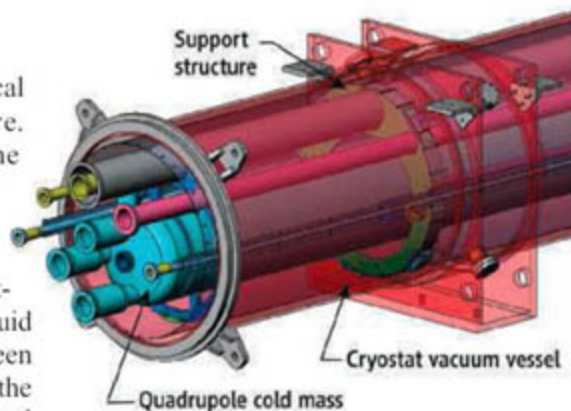
Congressional supporters of the U.S. Armed Forces Institute of Pathology (AFIP), which the Defense Department is planning to “de-establish,” are making a last-ditch attempt to salvage its functions. Last week, the Senate voted to delay the move until after the department has responded to a pending report on the impact of AFIP's closing. Last month, the House voted to prevent the use of federal funds for the planned closing of Walter Reed Army Medical Center, where AFIP resides, in its version of the bill, which funds military operations in Iraq and Afghanistan.

“This gives AFIP some breathing room,” says a Senate staffer about legislation that President George W. Bush has promised to veto because of the inclusion of nonmilitary items. Pathology groups oppose the dispersal of AFIP's functions, particularly the possible mothballing of its renowned tissue repository (*Science*, 20 May 2005, p. 1101), and Senator Edward Kennedy (D-MA) is also hoping to slow the current outflow of talent. Advocates want to move the repository to the Uniformed Services University of the Health Sciences in nearby Bethesda, Maryland. —CONSTANCE HOLDEN

Continued from page 31

researchers tried to pressurize its cylindrical casing to 25 times atmospheric pressure. The test was supposed to simulate the buildup of helium gas during a "quench," an event in which the superconducting wire in the magnet temporarily loses its superconducting properties and starts acting like a giant heating coil, boiling the liquid helium coolant that fills the volume between magnet and casing. The pressure pushed the innards of the magnet through the cylindrical container like a piston as a key support broke. The support was not designed to take a lengthwise push, says Stephen Holmes, an accelerator physicist at Fermilab.

"It's better to catch it now than a year



from now when the LHC has its first quench," Holmes says. But, he adds, "we should have caught this before we got this far." Researchers at Fermilab and CERN already have ideas for modifying the mag-

Overlooked. Faulty support was not designed to resist a force pushing the magnet's innards through its casing.

nets and will meet at CERN at the end of the month to finalize the plan and start the fix.

The schedule for starting the LHC in November was already extremely tight. Workers have lowered all but a handful of the LHC's 1624 main magnets into the tunnel and are busy connecting the equipment. Even so, they are currently about 5 weeks behind schedule and pushing to catch up, Evans says. "If it goes into 2008, then there is no question of having an engineering run and 3-month shutdown," Evans says. "We'll have to do without it."

—ADRIAN CHO

PALEOANTHROPOLOGY

Hobbit's Status as a New Species Gets a Hand Up

PHILADELPHIA, PENNSYLVANIA—The diminutive human who lived on the Indonesian island of Flores 18,000 years ago has been called many things: a pygmy, a diseased *Homo sapiens*, a hobbit. Now, in a report that was the talk of the Paleoanthropology Society's annual meeting here last week, a postdoctoral researcher claimed that the shapes of the fossil's wrist bones are so primitive that it cannot be *H. sapiens*. "It is definitely not a modern human. It's not even close," paleoanthropologist Matthew Tocheri of the Smithsonian Institution in Washington, D.C., said in his talk. Although

some critics still think the bones could be those of a diseased *H. sapiens*, others who heard Tocheri's report were persuaded. "It's the most convincing evidence so far that it really is something different," says paleoanthropologist Carol Ward of the University of Missouri, Columbia.

The roughly 1-meter-tall skeleton has sparked heated debate. Its discoverers claim it as a new species of human called *H. floresiensis*, whereas critics argue that the tiny skull belonged to a modern human suffering from a disease such as microcephaly, which leads to a small head.

When Tocheri first saw casts of the hand bones at a lecture last fall, he was struck immediately by their primitive shape. In his Ph.D. dissertation from Arizona State University in Tempe—which he is defending this week—he used three-dimensional imaging to analyze an innovation in the modern human hand. Living people and our most recent ancestors possess a complex of five bones that mesh together to ease stress on the wrist when the hand is used forcefully, for example in pounding large tools or in precision work. Neandertals had this derived shock-absorber complex, too; it is first seen in the hand of an 800,000-year-old human ancestor, *H. antecessor*, from Atapuerca, Spain.

But the bony complex is not found in apes or earlier human ancestors, including *H. habilis*, which lived 1.75 million years ago in Africa. That species did use tools, but the shape of its hand bones does not distribute force away from the base of the thumb and across the wrist as efficiently as in modern humans.

Tocheri got permission to study high-quality casts of the Flores bones, which were made for Stony Brook University biological anthropologist William Jungers. What Tocheri saw confirmed his impression that three bones in the wrist closely resembled those of an ancient hominid, not modern humans.

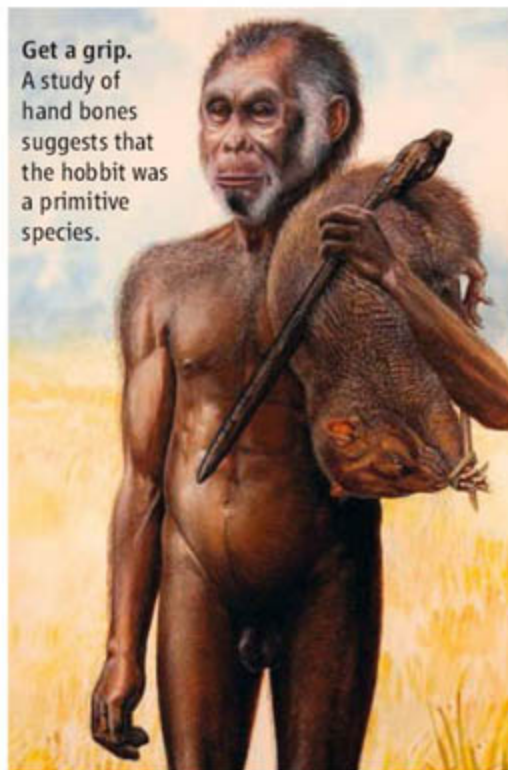
Tocheri ruled out that the primitive hand bones were altered by disease because their distinctive shape develops in the first trimester, long before deformation from most diseases begins later in pregnancy or after birth. He also says known diseases do not reproduce the primitive bone shapes. "This is not pathological," Tocheri said. That fits with emerging evidence from the long limb bones, which show no pathology either, says Jungers (*Science*, 19 May 2006, p. 983). "The sick-hobbit scenario is wrong," he says.

But until the hobbit bones can be compared with a wrist of a microcephalic human, some remain unconvinced. "The wrist bones don't look like those of a normal modern human, but how can we rule out that it's a pathological modern human until we get comparative evidence?" asks paleoanthropologist Robert Martin of the Field Museum in Chicago, Illinois.

Although much work has focused on the fossil's chimp-sized skull (*Science*, 2 February, p. 583), the new skeletal data are proving convincing to many. Says lower-limb expert Henry McHenry of the University of California, Davis: "It clinches it for me that [the Flores fossil] was not modern."

—ANN GIBBONS

Get a grip. A study of hand bones suggests that the hobbit was a primitive species.



U.S. COMPETITIVENESS

Chemistry Reports Warn of Eroding American Research Lead

CHICAGO, ILLINOIS—The outlook for United States scientific leadership remains cloudy with a chance of showers. That's the gist of two new reports* the National Research Council released last week on the future of U.S. research in chemistry and chemical engineering, both of which were detailed here for the first time at the semiannual meeting of the American Chemical Society.

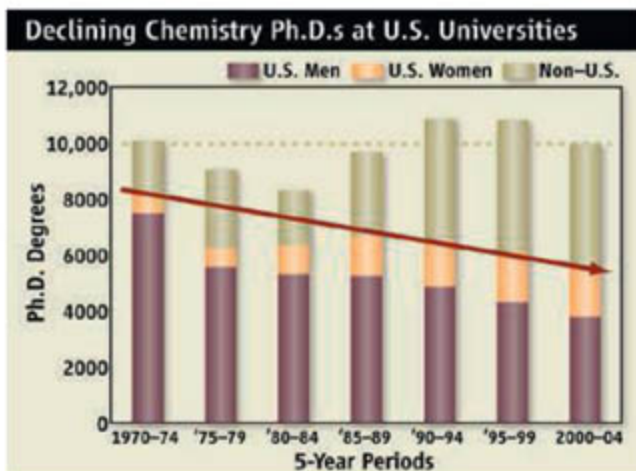
The first report warned that American preeminence in chemistry research is slipping away as the country grapples with declining numbers of homegrown doctoral degrees in chemistry and the rise of competition from Western Europe and Asia. The second predicted sunnier skies for U.S. leadership in broad areas of chemical engineering research, although it warned that the heavy emphasis on biology, nanotechnology, and other hot fields in research spending threatens to undermine less-sexy areas of the discipline.

The new reports are the latest in a series of disturbing forecasts for U.S. scientific leadership. The strongest warning came from a 2005 report from the National Academies that claimed the United States faced a "gathering storm" of dwindling educational performance and lackluster federal commitment to basic research, particularly in the physical sciences (*Science*, 21 October 2005, p. 423).

Although the United States remains the single strongest country in a variety of measures of chemistry research, the trends are largely pointing in the wrong direction, says Charles Casey, a chemist at the University of Wisconsin, Madison, who chaired the chemistry report. Today, for example, U.S. researchers publish only 18% of the papers in the field, down from 23% a decade ago. Over that same period, the output from Asian countries other than Japan tripled and is now on par with the U.S. output.

* *Benchmarking the Research Competitiveness of the United States in Chemistry; Benchmarking the Research Competitiveness of the United States in Chemical Engineering.*

In education, the clouds appear even darker. According to panel member Sylvia Ceyer, a chemist at the Massachusetts Institute of Technology in Cambridge, the number of chemistry Ph.D.s awarded to native-born students has sunk roughly 25% since 1970. Universities have made up the difference with foreign students, who now earn nearly half of all chemistry Ph.D.s awarded by U.S. universities. But Ceyer warned that as industry jobs continue to move overseas and visas remain tight in the wake of the 11 September 2001 attacks, the percentage of foreign-born Ph.D. chemists who have



Brain drain. Falling numbers of homegrown Ph.D.s are one of several signs that U.S. preeminence in chemistry research is threatened.

chosen to stay in the United States has declined slowly but steadily over the past 5 years. The upshot: "The U.S. will remain a leader in chemistry for the next 5 years," Ceyer says. "But the U.S. lead will continue to shrink as the chemistry world becomes flatter and more competitive."

Mark Wrighton, chancellor of Washington University in St. Louis, Missouri, says that although such trends are cause for concern, the situation isn't yet dire. "I think it would be a mistake to read too much into these trends," Wrighton says. "We need to keep in mind that the United States is still the world leader." Although the new reports didn't offer solutions, Casey says the Bush Administration's competitiveness initiative, which aims to double U.S. physical sciences research over 10 years, is a step in the right direction. "From the chemistry perspective, it will help tremendously," Casey says.

—ROBERT F. SERVICE

Russian Academy Fights Plan

MOSCOW—The Russian government appears to be backing away from its bid to strip the autonomy of the Russian Academy of Sciences (RAS) after members of the centuries-old institution rejected plans last week to change how its money is spent and properties are used. The Ministry of Education and Science suggested last month that RAS alter its charter to create a supervisory council that would have the final word in managing the academy's 450 research institutes. Composed of three academicians, three government officials, two legislators, and a Kremlin representative, such a council would relegate scientists largely to research.

But in a rare act of defiance, RAS's general assembly voted almost unanimously to reject the council proposal. The plan "goes against the spirit of science and the traditions of science," says Yuri Osipov, academy president. The ministry appears willing to drop the idea if further negotiations yield a version of the charter acceptable to the cabinet, which must approve the document. "I do not believe that we must strongly insist upon [the council]," said Andrei Fursenko, education and science minister.

—BRYON MACWILLIAMS

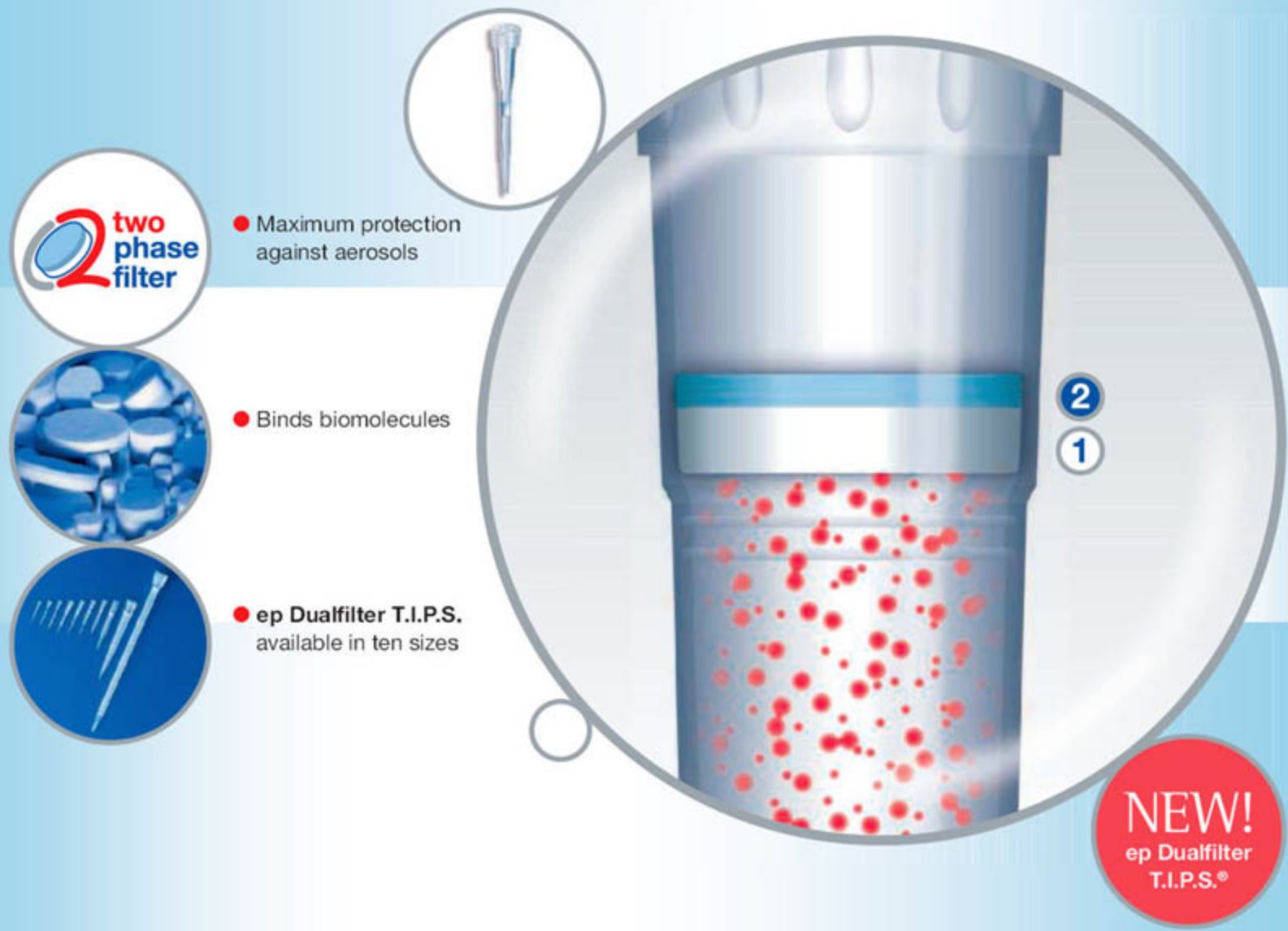
India Court Halts Quota Rise

NEW DELHI—The Indian Supreme Court has blocked a plan to more than double the number of university slots reserved for disadvantaged students, saying that the government is relying on outdated statistics. The plan, adopted by Parliament, triggered protests last year by students from privileged castes, who worried that it would hinder their entry into some of the country's most elite institutions.

To overcome the evils of the caste system, which relegates several groups to menial jobs and subjects them to overt discrimination, India has long had an affirmative action plan that guarantees those groups 22.5% of public-sector jobs and slots at many universities. The new law would boost that figure to 49.5%. But last week, the court said the government was basing its argument on data collected as far back as 1931 and demanded fresher facts.

Pavagada Venkata Indiresan, former director of the Indian Institute of Technology in Chennai, called the ruling "a defeat for cynical politicians who tried to replace an essential service by unwarranted draconian regulation." The government is weighing its options before a final verdict is issued in August.

—PALLAVA BAGLA



Stop aerosols!

Unique two-phase filter protection with ep Dualfilter T.I.P.S.®

The new Eppendorf ep Dualfilter T.I.P.S., with their unique two-phase filter, provide the perfect shield against contamination.

The filter consists of two visible phases, each with a different pore size. This two-phase filter protection ensures ultimate absorption of aerosols ❶ and biomolecules ❷, outmatching all conventional filters. Rely on it.

For more information go to www.eppendorf.com/dualfilter

Features of the ep Dualfilter T.I.P.S.

Double protection provided by the two phase filter

- Provides maximum protection for both pipette and sample
- Ultimate absorption of aerosols and biomolecules
- Free from PCR inhibitor additives
- Patent pending two phase filter technology
- Supplied sterile, Eppendorf PCR clean and pyrogen-free
- IvD conformity
- Batch-related certificates available



AVIAN INFLUENZA

Indonesia to Share Flu Samples Under New Terms

Indonesia has agreed to resume sharing samples of the H5N1 avian influenza virus with the World Health Organization in return for a promised rewrite of WHO's rules governing the use of donated viral samples. The new "Terms of Reference" for handling viral samples, which will be hammered out over the next several months, may include a clause giving countries that provide flu samples more control over how and whether WHO can pass the virus on to third parties, such as companies making vaccines. Indonesia had halted sharing its samples over concerns that it would not have access to any H5N1 vaccine ultimately produced (*Science*, 23 February, p. 1065).

Although health officials and scientists are happy that Indonesia will once again provide flu samples, some worry about a possible new precedent. "My concern is that if this rule [takes effect], some country may in the future refuse to share the viruses or vaccine seed virus strain outside" the WHO network, jeopardizing vaccine production, says Masato Tashiro, director of the WHO Collaborative Center for Influenza Surveillance and Research in Tokyo.

For more than 50 years, the WHO Global Influenza Surveillance Network has collected seasonal flu viruses and provided vaccine seed viruses to drug companies. Virtually all the vaccines produced have been used in advanced countries in temperate zones to fight seasonal flu.

WHO took the same approach in dealing with H5N1, which so far has primarily affected developing countries in tropical and subtropical Asia. Indonesia, which has the highest number of human H5N1 fatalities—at least 63 so far—ceased sharing its samples of the virus with WHO in January. Indonesian officials said they feared the country would not be able to afford a vaccine or get a share of limited supplies in the event of a pandemic. At a meeting in Jakarta organized by WHO to resolve the impasse on 26 and 27 March, Siti Fadilah Supari, Indonesia's minister of health, called the current scheme "more dangerous than the threat of an H5N1 pandemic itself."

Under an interim agreement, Indonesia will again provide samples, which WHO's



Shots for tots. Indonesia's Health Minister Siti Fadilah Supari (left) wants vaccines to protect citizens against bird flu in return for sharing H5N1 samples.

reference labs watch for mutations that might suggest the virus is mutating into a form more easily transmitted among humans. In return, WHO will request

advance purchase agreement. The initiative, he hopes, will "provide the reassurance developing countries need to continue sharing viruses." —DENNIS NORMILE

ENDANGERED SPECIES ACT

Appointee 'Reshaped' Science, Says Report

Environmental groups have long vilified Julie MacDonald, the Bush Administration's point person at the Interior Department on endangered species. Last week, their complaints got some support from the agency's in-house watchdog, who has concluded that the political appointee played fast and loose with research.

A report by the inspector general's (IG's) office found that MacDonald not only has been "heavily involved" in editing scientific documents by the U.S. Fish and Wildlife Service (FWS) but also leaked some of that confidential material to industry groups. Next month, Congress will hold hearings on her actions.

MacDonald is a civil engineer who previously worked on endangered species issues for the California state government. Since 2004, she has been deputy assistant secretary for fish and wildlife and parks. The IG's report was sent last week to Representative Nick Rahall (D-WV), now chair of the House Natural Resources Committee, who had received an anonymous tip that MacDonald had "bullied, insulted, and harassed" FWS scientists to alter biological reports about endangered species. The findings, which haven't been publicly released, were first reported by the *New York Times*.

The report documents, for example, how MacDonald told agency scientists to lower the

status of tiger salamanders in California from endangered to threatened (*Science*, 10 September 2004, p. 1554)—a decision that was later tossed out by the courts. It also quotes the former director of the FWS Endangered Species Program saying that "MacDonald regularly bypassed managers to speak directly with field staff, often intimidating and bullying them into producing documents that had the desired effect."

Although the IG found nothing illegal in MacDonald's actions, the report says she violated the federal code in two ways. She leaked internal agency documents to lobbyists for the California Farm Bureau Federation and other groups. And she appeared to give those lobbyists preferential treatment—a charge that MacDonald denied to the investigators. (The Interior Department declined to comment on the report, calling it a personnel matter, and MacDonald has not made any public statements.)

Rahall says that next month's hearing will be "a sweeping review on whether politics is infiltrating decisions" about endangered species. The issue may also come up during the Senate confirmation hearing of Lyle Laverly, director of Colorado's Division of Parks and Outdoor Recreation, whom the White House on 23 March proposed to be MacDonald's boss. The job has been vacant since November 2005. —ERIK STOKSTAD

An Asian Tiger's Bold Experiment

As Singapore embarks on a billion-dollar second phase of its makeover as a research hub, critics wonder whether the island nation is really getting its money's worth

SINGAPORE—From the crest of a low hill in a southern corner of this island state, Philip Yeo makes a sweeping gesture toward a scientific Emerald City: nine gleaming new research buildings teeming with more than 1000 biomedical scientists. “We’ve gone from nothing to this in 5 years,” says Yeo, chair of Singapore’s Agency for Science, Technology, and Research (A*STAR), a government agency that runs Biopolis, as the campus is known.

Thanks in no small measure to Yeo’s wizardry at winning government support and wooing overseas talent, Biopolis has put this tiny Southeast Asian nation on the biomedical research map. As one indicator of success, the number of papers produced at the flagship Institute of Molecular and Cell Biology (IMCB) zoomed from 82 in 2000 to 165 in 2006, according to Thomson Scientific. Citation rates rival those of institutions with longer histories. Other Biopolis centers are still coming up to speed. But in building up a research capacity from scratch, boasts Yeo, “no other country has ever moved so fast.”

That claim has a number of prominent backers. What’s happened in Singapore in just 5 or 6 years “is pretty darn remarkable,” says Edward Holmes, formerly dean of the School of Medicine at the University of California, San Diego (UCSD). By comparison, says Holmes, deputy chair of Singapore’s Biomedical Research Council, it took San Diego 40 years to become a biomedical hub. The research enterprise has progressed “beyond my wildest expectations,” adds molecular oncologist Edison Liu, director of the Genome Institute of Singapore.

But some now question whether A*STAR

is heading in the right direction. Late last year, in an opinion piece in the influential *Straits Times* newspaper, Lee Wei Ling, head of Singapore’s National Neuroscience Institute, wrote that “if the present approach is followed without modification, a coherent body of research and success in a series of related fields is unlikely to develop.” Among other things, Lee is skeptical of the reliance on imported scientific talent and believes the overall effort lacks a coherent focus. Her article triggered a rare spectacle in this prim city-state: a public debate over research and development (R&D) policy waged in dueling editorials and opinion pieces.

Yeo brushes off the criticism. “I’m not very good at listening,” he admits. “My forte is getting things done.” But the debate has raised questions about when Singapore can expect to receive an economic payoff from the 2 billion Singapore dollars (\$1.3 billion) spent so far on building and staffing Yeo’s field of dreams. And A*STAR can expect closer scrutiny as it embarks on the \$1.3 billion second phase of its biomedical initiative: another batch of institutes with links to hospitals to extend the research to patients.

Whale hunting

In June 2000, Singapore unveiled a National Biomedical Science Strategy to make this research area a central pillar of a knowledge-driven economy (*Science*, 30 August 2002,

p. 1470). The first phase called for creating a public research infrastructure that would generate discoveries, train personnel for big pharma R&D, spin off start-up firms, and generally build up local expertise in biomedical sciences.



Getting things done. Biopolis visionary Philip Yeo says he is too busy to listen to critics of Singapore’s biomedical strategy.



Sustainable? Some Singaporeans are asking how a massive investment in biomedical talent and facilities will play out.

Tapped to implement the strategy was Yeo, an engineer with a Harvard University MBA who was named chair of the National Science and Technology Board, which became A*STAR. A career civil servant, Yeo is credited with having led Singapore’s drive into semiconductors and specialty chemicals while chair of the Economic Development Board. A colleague describes Yeo’s lifestyle as “ascetic” and giving new meaning to the word “workaholic.” He is relentlessly cheerful, peppering facts and numbers with wisecracks.

When the biomedical strategy was launched, Singapore had a single life sciences institute, IMCB, affiliated at the time with the National University of Singapore, plus a center on pharmaceutical technologies under the Economic Development Board. A*STAR took charge of both and created three more institutes, building Biopolis to house them. To staff the labs, Yeo started luring scientific stars from abroad, in some cases spending years to fill a strategic post.

A big catch early on was Liu, imported in 2001 from the U.S. National Cancer Institute in Bethesda, Maryland, to head Singapore’s newly minted Genome Institute. Researchers there quickly made their mark, becoming the first in the world to sequence the SARS virus at the height of that crisis in 2003.

Since then, Liu has been joined by an array of world-class scientists. For example, David



Lane, renowned for his work on the *p53* tumor suppressor gene, is on a sabbatical from the University of Dundee, U.K., to head IMCB. In addition to an international standing, Lane brought to the job wide-ranging contacts and industrial acumen—in 1996, he founded Cyclacel Pharmaceuticals, which is developing novel cancer drugs. Lane says the contacts are important for an institute so distant from established research centers of the United States and Europe. And his Cyclacel experience helps when exploring interactions with pharma executives.

Yeo lured others to Singapore by dangling irresistible research opportunities. Nancy Jenkins and Neal Copeland, a wife-husband team of mouse geneticists, say they opted for Singapore to escape tightening budgets and restrictions on consulting work at the U.S. National Institutes of Health. In the United States, says Copeland, “there wasn’t a lot of new money to do new things.” At IMCB, he says, they are assured of generous funding for their work developing mouse models for human cancers, and they’re encouraged to interact with companies.

Yeo has also imported heavyweight administrators to run institutes and develop policy. The roster includes the husband-wife team of UCSD’s Holmes and Judith Swain, who was the university’s dean of translational medicine; Philippe Kourilsky, former president of the Pasteur Institute in Paris; and

George Radda, former chief of the U.K.’s Medical Research Council.

Yeo calls these senior figures “whales” who have schools of ambitious young researchers—“guppies”—trailing in their wakes. So far, roughly 75% of the 500 or so Ph.D.-level Biopolis researchers are foreigners. Aiming for a 50–50 balance among A*STAR’s institutes, Singapore plans to send abroad and fund some 1000 students to earn undergraduate to Ph.D. degrees at top foreign universities by 2015. The full ride costs more than 900,000 Singapore dollars (\$590,000)—his “million-dollar kids,” Yeo says. The presence of senior scientists in Singapore, Lane adds, ensures that scholarship students “will continue to have outstanding mentoring when they come back here.”

Building a research effort from scratch has made it easy to create institutions with complementary aims, says Lane. “In most countries, the rivalries between institutions can hold them back from working together in a successful way,” he says. Another Singaporean strength is a small, pragmatic government to oversee the initiative, argues Yeo, who professes disdain for bigger and messier dem-

ocratic systems. “Look at how the guys in California are fighting [over plans for] stem cells,” Yeo says. “Nothing is moving!”

A*STAR claims to be nearing its economic goals of generating 25 billion Singapore dollars (\$16.4 billion) in biomedical manufacturing and 15,000 jobs in the sector by 2015. Last year, manufacturing output hit S\$23 billion, having almost quadrupled in the past 6 years. Biomedical employment grew 3.9% to reach

10,571. The agency figures that investment commitments in 2006 will add 1800 jobs when facilities come online. And private spending on biomedical R&D in 2005 reached 35% of the nation’s total

R&D spending, up from 28.5% in 2001.

“If the present approach is followed, ... a coherent body of research and success in a series of related fields is unlikely to develop.”

—Lee Wei Ling, Biopolis critic

A voice in the wilderness

Not everyone buys that rosy picture. Lee’s broadside in *The Straits Times* last November questioned the strategy of hiring “foreign stars and then letting them decide for themselves what areas of research to engage.” She criticized the initiative as lacking coordination and called for a lead agency to take control and identify niches in which Singapore could excel. Examples she gave included hepatitis B, liver and stomach cancer,

INTERNATIONAL SCIENCE & ENGINEERING
VISUALIZATION CHALLENGE

COMPETITION DEADLINE
APPROACHING

ENTRY DEADLINE: MAY 31, 2007

SCIENCE AND ENGINEERING'S MOST POWERFUL STATEMENTS
ARE NOT MADE FROM WORDS ALONE



When the left brain collaborates with the right brain, science emerges with art to enhance communication and understanding of research results—illustrating concepts, depicting phenomena and drawing conclusions.

The National Science Foundation (NSF) and the journal *Science*, published by the American Association for the Advancement of Science, invite you to participate in the fifth annual Science and Engineering Visualization Challenge. The competition recognizes scientists, engineers, visualization specialists and artists for producing or commissioning innovative work in visual communication.

Winners in each category will be published in the September 28, 2007 issue of *Science* and *Science Online*, and will be displayed on the NSF Web site.

Award Categories

- Illustration
- Informational Graphics
- Interactive Media
- Non-Interactive Media
- Photographs

COMPLETE ENTRY INFORMATION:
WWW.NSF.GOV/NEWS/SPECIAL_REPORTS/SCIVIS



autoimmune diseases, and head injury. "Smaller countries with limited resources have to be more focused on how those resources are used," Lee wrote.

The critique carried particular weight in Singapore, given Lee's membership in what one researcher refers to as Singapore's "ruling family." She's the daughter of Lee Kuan Yew, Singapore's revered first prime minister.

Lee's piece "created a stir in the entire A*STAR community," says IMCB's Copeland. But neither A*STAR nor Yeo made a formal response. So a week before A*STAR held its annual press briefing on the biomedical initiative on 6 February, Lee repeated her claims in an interview with Reuters. Not surprisingly, questions about Lee's comments dominated the briefing. At the time, Yeo said that he intended to "just ignore" criticism from "one voice in the wilderness." And he mocked Lee's recommendations. Childhood vaccinations have vanquished hepatitis B among Singaporeans, Yeo says. And rather than spend money on head-injury research, he told *Science*, "it would be cheaper to give every child a crash helmet."

Lee declined to comment further, writing in an e-mail to *Science*, "The points have been put across to the small number of individuals I was targeting." Her views have gotten oblique support from Ting Choon Meng, a physician and founder of medical device maker HealthSTATS. In a January *Straits Times* article, Ting argued that Singapore's researchers are "putting the cart before the horse" by overlooking the practical payoffs of research. "As a nation and as individuals, we have begun to showcase our innovations. But we may still end up not fully reaping the rewards of our IP ideas," he wrote.

Yeo may have little time for critics. But his star scientists, perhaps more used to defending science policies, are keen to make the case that research in Singapore can be both globally significant and locally relevant. "Everybody agrees, it's a small place and you need to focus," says Copeland. But "people are focusing," he says. Cancer is one target, and a majority of Yeo's recruits work on themes related to cancer. Swain adds that as translational medicine extends to work with patients, it is imperative to align with local needs. One example is gastric cancer, which for genetic and dietary reasons is prevalent in Asia.

Whether the initiative is giving the economy the desired kick is trickier to assess. Singapore had big pharma investment before the

initiative: Production at drug company plants reached S\$6.4 billion in 2000. And most observers agree that pharma investment would have continued to grow even in the absence of the biomedical strategy. A*STAR officials counter that their bootstrapping efforts have boosted the value of the manufacturing, moving from simple molecules to biologics: drugs cultured from living cells. And they maintain that the growing pool of trained researchers is attracting additional interest from big pharma. Within the last few weeks, GlaxoSmithKline opened a \$13 million medicinal chemistry outfit at Biopolis that will double the firm's research corps in Singapore to 60; and Eli Lilly announced a 5-year, \$150 million plan to boost its drug-discovery efforts in Singapore in part by tripling its R&D staff to 150.

Last November, the World Bank published a report examining how six Asian cities—

Foreign, senior scientists ensure that Singaporeans returning from training abroad "will continue to have outstanding mentoring when they come back here."

—David Lane, Institute of Molecular and Cell Biology



Bangkok, Beijing, Seoul, Shanghai, Singapore, and Tokyo—are seeking new strategies for economic growth. World Bank economist Shahid Yusuf says that he and co-author Kaoru Nabeshima are impressed at how quickly Singapore has put together an infrastructure resembling that of San Diego and other hot spots. But he notes that research budgets are rising across Asia, and other rivals have biotech strategies. "When all of them get into this business, how will that affect the others' prospects?" he asks. As for Singapore, which has invested more heavily than others in biotech, Yusuf says, the questions are: "How much longer do they need to wait, and will [the returns] be large enough to provide a major engine of growth for Singapore?"

Yeo dismisses the report. "I don't believe World Bank people are competent to make recommendations to Singapore," he says.

Safe for now

In the wake of the debate touched off by Lee's article, Singapore's leaders have signaled their confidence in the National Biomedical Science Strategy. Most recently, in a 14 February speech unveiling the fiscal 2007 budget, Second

Finance Minister Tharman Shanmugaratnam said, "It is too early to evaluate the results of our R&D initiatives. But from [the Ministry of Finance's] perspective, I am satisfied that this is a good use of public funds."

That's A*STAR's reading as well. It's forging ahead full-speed with phase two. A pair of new centers, the Institute for Clinical Sciences and the Singapore Immunology Network, will link bench researchers and staff at local hospitals to pursue clinical studies. The Ministry of Health is developing programs to enable clinicians to devote part of their time to research. And it plans a new medical school in cooperation with Duke University.

Swain, head of the Institute for Clinical Sciences, believes Singapore's unique mix of Indians, Malays, and Chinese "could be a competitive advantage" for studies of how different ethnicities respond to drugs. One disadvantage, however, is a small population size. Alan Colman, CEO of ES Cell International, says his firm is likely to go to the United States or Europe with their cardio stem cell therapy when it is ready for trials.

Whether Singapore can sustain its rapid development in biomedical science is another open question. Much may depend on the success of Biopolis managers in keeping senior scientists rooted to the island. Lane says he will move back to Dundee at the end of 2007, although he plans to spend "considerable time" in Singapore for research and to advise A*STAR.

One looming uncertainty is whether Biopolis can continue on its present trajectory without the energy of Yeo, who stepped down as A*STAR's chair on 1 April. Yeo is not going far, however. He will chair an arm of the Ministry of Trade and Industry that promotes small and medium-sized businesses. He will also serve as a policy adviser to the prime minister.

Striding across the hill near Biopolis, Yeo doesn't sound as though his interest in biomedicine is waning. He points to two just-completed Biopolis buildings now being fitted out for new labs. Nearby, several low-rise buildings will soon be demolished to make way for a Biopolis daycare center. A bit farther, cranes are topping out the two towers of Fusionopolis, a S\$550 million Biopolis clone in which A*STAR is gathering six institutes that work on information and communications technologies. Yeo can't contain his enthusiasm. "Come back in another few years and see what's here," he says.

—DENNIS NORMILE



◀ **Hot money.** Researchers are gathering currency across Europe and testing its cocaine content.

Follow the money

Money has a peculiar life of its own. When not folded into a wallet or crumpled in a pocket, the typical €20 bill can pass between hundreds of hands for about a year before getting recycled at a bank. In this time, it moves through every part of society, from the wealthy to the unemployed. But where most scientists see a symbolic unit driving social phenomena, Sörgel sees a cotton-paper filter ideal for sponging up chemicals. And because of the way that electrons are strung on cocaine's carbon frame, he says, it "binds perfectly to the fibers."

One explanation for the widespread contamination of paper currency is that cocaine is often snorted up the nose through rolled-up bills, and that sorting machines in banks cause cross-contamination. "We really don't know for sure yet," says Sörgel, but the evidence so far supports this story. In a typical sample of bills from European banks these days, he finds that the majority of euros carry detectable amounts of cocaine. Among the contaminated bills, about 1 in 20 is typically loaded with around 10 micrograms of cocaine, while the rest usually have a hundredth of that. (These amounts are minuscule compared with the typical 100-milligram line that goes up a nose.)

For 7 years, Sörgel has been playing the part of the annoying tourist, buying bottles of water with €100 bills in every European country, building a continent-wide map of cocaine use. There have been some close shaves on this trip, such as when Jakob was suspected of shoplifting because of a suspicious lump under her shirt—which was the money. (Sörgel managed to talk his way out of that one.)

Banks have at times been suspicious when Sörgel asks to exchange wads of bills for his "study of cocaine," but they also have been extremely helpful. The entire project would have been a nonstarter if a German bank had not agreed to redeem the entire €30,000 after laboratory testing. The cocaine is detected using a device called a mass spectrometer, but the first step is a methanol bath to extract the chemical residues. That makes the bills look crisp and clean at the end, but it also loosens the metallic foil used to check against counterfeit money. Sörgel exchanges the bills for crisp new money, and the bank recycles the treated bills.

Although Sörgel's study of money is the biggest and longest-running, it is not the only one. Parallel projects are under way elsewhere

PUBLIC HEALTH

Hard Data on Hard Drugs, Grabbed From the Environment

Fieldwork in new and fast-growing areas of epidemiology requires wads of cash and a familiarity with sewer lines

BARCELONA—It's almost midnight when Fritz Sörgel and Verena Jakob walk into a chic cocktail bar. Still on the early side, the place is barely beginning to fill with the typical clientele of young, hip Spaniards. Installing themselves on low couches, the pair scan the drinks menu. "What I really want is a piña colada," says Sörgel with feeling. Returning from the bar, he looks defeated. "Only daiquiris."

You probably wouldn't guess that Sörgel and Jakob, environmental chemists who have been working since dawn, are still on the job. Indeed, despite the tragic absence of piña coladas, Sörgel gets what he's really after: Spanish bills in exchange for a crisp German €100 note. Jakob carefully squirrels away the change in a plastic tube. With the final sampling of the day done, they breathe a sigh of relief.

"It's so stressful always having to worry about the money," says Sörgel, director of the Institute for Biomedical and Pharmaceutical Research in Nuremberg, Germany. He's referring to the brick of new German bills worth €30,000 (\$40,000) that Jakob, his Ph.D. student, has been carrying in a secret pocket under her shirt since they arrived in Spain a few days ago. (If it goes missing, the institute is out of luck, says Sörgel.) In a few days, they will have exchanged all of the

German euros for Spanish ones. Back at the lab in Germany, they'll extract the chemical residues that have adsorbed to each bill—a process that destroys the money, but more on that later. Among the thousands of compounds that can be detected, Sörgel is looking for one: methylbenzoyllecgonine, better known as cocaine.

It's been known since the mid-1980s that cocaine residue contaminates paper currencies, but Sörgel and others are taking advantage of a natural experiment that began in 2000 with the simultaneous introduction of the euro currency across Europe. Each country's circulating stock of bills is becoming contaminated with cocaine at a different rate.

Measuring cocaine on the money is part of a new effort to study the phenomenon of illicit drug use by turning to the environment. Epidemiologists have struggled to get a quantitative view of drug use for decades. But the traditional data—tons of drugs seized, the number of people seeking treatment for addiction, drug-related mortality, and responses to drug-use questionnaires—are biased and patchy, says Roberto Fanelli, a toxicologist at the Mario Negri Institute for Pharmacological Research in Milan, Italy. By interrogating the environment rather than the people, he says, "you can obtain data in real time" that are not only objective but also "rather affordable."

in Europe, and the collective data are adding up to a worrying picture. In Ireland, for example, "people have been in denial that there's a cocaine problem," says Jonathan Bones, an environmental chemist at Dublin City University (DCU). But he and fellow DCU chemist Brett Paull have been finding some of the highest levels of cocaine contamination on euros from Dublin's banks. In one case, 100% of a sample of 45 bills was coated in cocaine. They have recently analyzed a sample of 75 bills and again found them all to be contaminated.

The main advantage of using money is that it's quick and dirty: Instead of running around an entire country to get data, "the money does it for us," says Sörgel. Paull is confident that his data are at least a "warning light" that Ireland has a serious drug problem, but he says that many unknowns make it difficult to translate the data into quantitative statements about drug use. He and Bones are trying to nail some of them down. For example, to put a rate on the natural degradation of cocaine on money, Paull and Bones are spiking euro bills with varying amounts of pure cocaine and incubating them under controlled conditions.

One encouraging fact is that the rank of average amounts of cocaine found on euros from different countries roughly matches the ranking of national drug problems by the E.U.'s traditional survey-based statistics. Spain is in the lead, followed closely by Italy, with Ireland now catching up.

But tracking contaminated money is only one part of the epidemiology story. After cocaine enters the nostril of a drug user and messes with the brain's chemistry for about an hour, it is modified by enzymes in the liver and washed out of the blood by the kidneys. You can guess where it ends up next.

The sewers don't lie

One morning last month, Sörgel and Jakob went high up on a narrow, winding road in the Sierra Nevada mountains, dodging villagers and wood-hauling donkeys to reach the pristine, presumably cocaine-free snowmelt streams that feed the Spanish city Granada to the south. At a small bridge over a glassy brook, they dangled a plastic-lined net into the water, bringing up two samples that Jakob sealed in bottles and labeled. From there they sampled their way back down to Granada, following the Genil River as it wends through suburban sprawl, arcs

through the city center, and there meets the two municipal wastewater treatment plants. For their final samples, Sörgel dipped right into the output of one of these plants, a trickle in a scummy gully.

Sörgel aims to administer a drug test to the entire city. The metabolic byproduct of cocaine, benzoylecgonine, is chemically unique in the environment and breaks down slowly. Using the mountain stream water as his baseline, he can estimate the amount of cocaine that passes through the entire population. Repeating the procedure at intervals should reveal drug consumption in a fixed

Check the source. Researchers in Spain aim to drug-test an entire city.



geographic area in full detail, from seasonal dips to weekend spikes.

Fanelli pioneered this technique in a 2005 study of water from the Po River near Milan. His group was studying the persistence of legal pharmaceuticals in the aquatic environment, he says, "but then we realized that we could detect other drugs as well." It is "completely proven" that cocaine can be detected in the environment, he says, and now the more difficult task is "how to use these data for drug epidemiology." Translating a minute and fluctuating signal in the environment to its ultimate source requires many assumptions, he says, "such as the percentage of the cocaine that is metabolized in the body and the amount that is degraded before it reaches the sampling site."

European researchers say they are putting the technique on firm experimental ground. Sörgel notes that about a ton of cocaine is seized annually in Germany, a country thought to have a "moderate" drug problem compared to others in Europe. Based on his sampling from rivers and wastewater at 29 locations across Germany, he estimates that Germans now consume on the order of 20 tons of cocaine per year. Sörgel's data suggest an upward trend, and indeed, the country's traditional indicators of drug abuse have all increased in recent years. "The methods are working," he says.

Fanelli has now hunted for cocaine residues in the wastewaters of London and of Lugano, Switzerland, a popular party destination for Italian tourists. He estimates that London's daily cocaine consumption is on the order of 1 kilogram for every 1 million people. He says this "reasonably translates" to cocaine use among 4% of Londoners 15 to 30 years old. Official estimates put that figure at 2%. "So we know we're close to the real figure," he says. Fanelli's team found similar per capita cocaine loads in Lugano's wastewater, but there they also extended the sampling over several months, revealing the variation by day of the week. Monday was consistently the low point of cocaine consumption, says Fanelli, whereas weekends were typically 30% to 40% higher than the weekday average, and sometimes double that.

U.S.-based researchers are hot on the trail as well, but some are running into barriers. Jörg Rieckermann, an environmental chemist at San Diego State University in California, has won a research grant from the Swiss National Science Foundation to survey cocaine contamination in wastewater. He selected San Diego for his analysis, but the city has forbidden him from taking samples.

Controversy has been brewing since September 2006, when city politicians learned that a representative of the White House's Office of National Drug Control Policy (ONDCP) wanted samples of San Diego's wastewater. ONDCP press secretary Jennifer de Vallance said that the study started about a year ago and is costing the office about \$20,000. Samples have been collected from about 100 participating wastewater facilities across the United States, she says, generating about 500 samples, which are being analyzed at the Office of the Armed Forces Medical Examiner in Rockville,

Maryland. Others have heard about ONDCP's project. "People from the White House contacted me soon after my 2005 study of the Po River," says Fanelli. "They plan to sample wastewater from 100 sites and publish a report."

If public concerns can be overcome and these methods can be scaled up to monitor "several thousand" wastewater treatment plants across a country, says Fanelli, "sewer epidemiology" will become a field in its own right. But several technical hurdles must first be cleared. For one, researchers use slightly different methods. Whereas Sörgel uses upstream river water for control samples, Fanelli uses sterile, deionized water. "Those differences can have significant effects on the results," says Sörgel, so "standardizing the methods is critical."

Beyond the lab, sewer epidemiologists will need the help of social scientists to draw meaningful conclusions from their data. Computer models already track shifts in crime patterns, income, and pollution in large urban centers—as well as the daily flow of water through pipes and sewers. Plugging in environmental drug data could allow researchers to "score" communities in terms of "drug-abuse levels," says Barbara Tempalski, a social geographer at the Center for Drug Use and HIV Research in New York City. And hunting for correlations between drug load and other social, public health, and economic factors may reveal useful risk predictors that so far have been obscured by the noise in the available data. "Finding the hot spots of drug consumption can let us focus resources in

the right places," says Fanelli.

"I have no doubt that these data are meaningful," says Norbert Frost, chief drug epidemiologist at the European Monitoring Centre for Drugs and Drug Addiction in Lisbon, Portugal, "but we must bring this to the next level, where the techniques are standardized and producing peer-reviewed reports."

The first formal opportunity to compare notes will come later this month. Frost is gathering a small group of international drug-abuse researchers from various fields in Lisbon on 16 April to discuss environmental drug monitoring, the first meeting of its kind. It will be "an open discussion," says Frost, covering everything from analytical techniques to integration with the social sciences.

—JOHN BOHANNON

ANIMAL BEHAVIOR

The World Through a Chimp's Eyes

A novel meeting assembled the world's leading thinkers about chimp culture, tools, cooperation, reasoning, and other heady topics

CHICAGO, ILLINOIS—It's not every day that a scientific meeting opens with a roomful of eminent researchers pant-hooting like chimpanzees, but then "The Mind of the Chimpanzee" conference held here at the Lincoln Park Zoo last week marked a rare occasion in itself. For only the third time in 20 years, the zoo hosted a meeting that brought together researchers who study chimpanzees in the wild and in the labora-

tory. And surprisingly, it was the first one to focus solely on the cognitive abilities of our nearest animal relatives. "It's amazing," said pioneering field researcher Jane Goodall, one of approximately 300 participants at the meeting. "We're talking about things now that I couldn't talk about in the '60s. We couldn't even talk about the chimpanzee mind because chimpanzees didn't have one."

The meeting, held from 23 to 25 March, covered a broad range of topics from cooperation and communication to tool use and culture, experimental design, and conservation of this endangered species. "It's a whole different quality of science from the exciting cowboy era of maybe 2 decades ago," said Richard Wrangham, an anthropologist at Harvard University who for 20 years has studied wild chimps in Uganda's Kibale Forest. "It's a sign of a maturing field. You have technical brilliance and tremendous innovation in a wide range of areas."

The cumulative effect of the talks—many of which included videos that few people had seen—powerfully demonstrated that new insights are continuing to redraw the dividing line between "us" and "them." And one clear theme emerged from the blending of laboratory and field studies: More effort than ever is being made to perceive the world the way that chimpanzees do, as opposed to simply asking how closely their behavior mirrors our own.

Beyond compare

After the zoo's Elizabeth Lonsdorf, a conference co-organizer, kicked off the meeting by having the participants give each other a "proper chimp greeting," she introduced Kyoto University's Tetsuro Matsuzawa, one of the few researchers who studies both wild and captive chimpanzees. Matsuzawa's talk kept the audience participation level high, eliciting loud "oohs," "ahhs," and guffaws. Matsuzawa described the numerical skills of a chimpanzee named Ai and her son Ayumu, who live at the university's Primate Research Institute in Kyoto. Building on work he first reported in *Nature* 7 years ago, he showed videos of Ayumu using a touch-screen monitor to select the randomly displayed numbers 0 through 9,



Testing, 1, 2, 3. Tetsuro Matsuzawa taught the chimp Ayumu to touch numbers in sequence.

CREDIT: TETSURO MATSUZAWA/KYOTO UNIVERSITY

in ascending order. He then repeatedly performed a more difficult variation on this task, in which the numbers were masked with white blocks shortly after they were flashed on the screen. "No one can do this," he said, proving the point with a hilarious clip of his graduate students failing the exercise with only four masked numbers. "Our common ancestors might have had immediate memory, but in the course of evolution, they lost this and acquired languagelike skills," posited Matsuzawa.

As difficult as it is to assess a chimpanzee's memory, researchers similarly have a shaky handle on how they communicate with each other. "There could be a whole 'nother level of chimp communication that we don't have the capability of understanding," said psychologist Lisa Parr, who studies chimpanzee facial expressions at Yerkes National Primate Research Center at Emory University in Atlanta, Georgia.

Parr described an objective metric she has helped develop called the Chimp Facial Action Coding System to understand better what they are saying to each other with their expressions. "People have only looked at peak-intensity expressions," says Parr, such as the bared teeth that have been compared to the human smile. "Expressions are graded in intensity and force. No one has looked at whether those have meaning."

In a similar vein, Katie Slocombe of the University of St. Andrews in Fife, U.K., has begun parsing chimpanzee vocalizations to see whether they have meanings that we have yet to recognize. "It's a very neglected area of chimpanzee cognition," said Slocombe. "Up until now, everyone's been so dismissive. They say, 'It's stimulus-response; it's hardwired; it's boring.' I don't think that's the case."

As Slocombe and Klaus Zuberbühler reported in the February 2005 *Journal of Comparative Psychology*, they analyzed vocalizations she recorded during aggressive interactions between 14 chimpanzees at the Budongo Forest Reserve in Uganda. They found that aggressors and victims gave distinct screams. Slocombe is now planning to do what she said will be the first ever "playback" experiments in the wild of recorded screams. Similar studies in monkeys have revealed that they use calls to identify specific predators. "Vocalizations can tell us a lot more than we currently think," said Slocombe.

Cultural sensitivities

In chimpanzee research circles, incendiary debates revolve around the degree to which the animals cooperate, reason, teach, imitate, and have culture. The debates burn on because there are no firm answers, but pre-

senters at the meeting offered intriguing clues to some of these riddles—and urged their colleagues to keep a chimp-centric view when designing experiments.

Kyoto University's Satoshi Hirata showed videos of a cooperation test he designed with captive chimps. He placed fruit in a hole in the ground, and then covered it with large stones.



Do as I do. Two chimps in Bossou, Guinea, watch an elder crack nuts, a skill that appears to pass from generation to generation by observation rather than teaching—and is considered part of their "culture."

Chimps failed to work together to move the stones, but when he placed himself in the experiment, a chimp solicited his help—possibly because it knew he would not compete for the food. In a different test that required two chimps to pull ropes cooperatively and move a plank holding food close enough for them to reach, they would cooperate but never solicit help. When he stood in the room, one of the chimps came and took his hand, again soliciting his help. "Experimental arrangements should be considered very carefully," he said.

Many researchers have long assumed that chimpanzees in the wild cooperate when they hunt for red colobus monkeys, one of their favorite meats. Harvard University's Ian Gilby said think again—and see it through chimp eyes. In a study he conducted at Kibale Forest, he found that "impact" males that were good hunters attracted other males. "Is it collaboration or byproduct mutualism taking advantage of key hunters?" asked Gilby. "Impact males may act as a catalyst for hunting."

Researchers face equally vexing conundrums when they try to tease out cultural (that's what others in the community do) versus ecological (that's what the environment dictates) determinants of tool use. Matsuzawa and Tatanya Humle famously reported in 2002 that chimps in Bossou, Guinea, used sticks of different lengths to dip for ants based on the risk of being bitten—suggesting ecological rather than cultural roots. Now there's a deluge of new observations of unique tool use at recently

developed field sites that are sure to trigger yet more investigations into cultural versus ecologically determined behaviors.

Crickette Sanz of the Max Planck Institute for Evolutionary Anthropology in Leipzig, Germany, described three different large communities of chimpanzees she has extensively studied with her husband, David Morgan, in the

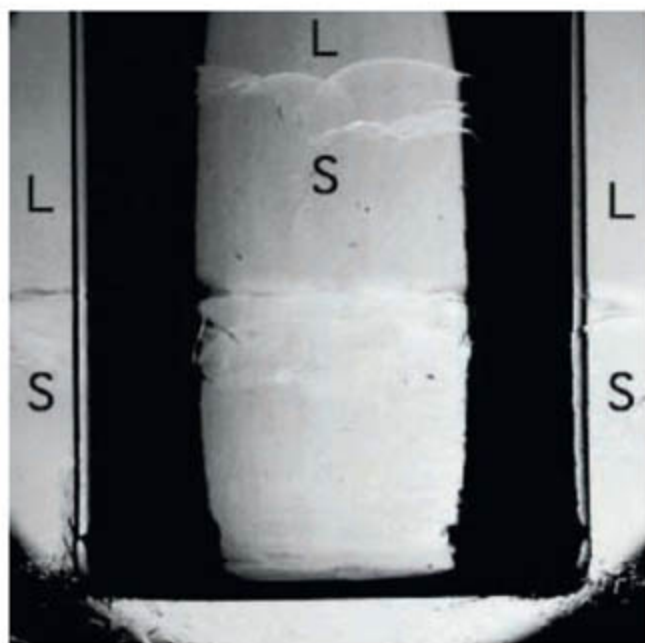
Goualougo Triangle in the Republic of Congo. Aided by 18 remote video cameras, Sanz and Morgan have documented 22 different tool uses since 1999, including various types of honey gathering, termite fishing, and leaf-sponging for water. "Crickette has done a marvelous job of looking at tool use in a systematic way," said Jill Pruetz, an anthropologist at the University of Iowa, Ames, who recently received much attention for describing chimpanzees' use of spears to trap bush babies at a site she has developed in Fongoli, Senegal (*Science*, 23 February, p. 1063).

Goualougo and Fongoli are two recently developed field sites that Andrew Whiten, an evolutionary psychologist at the University of St. Andrews, included in an update of what's known as the Collaborative Chimpanzee Cultures Project. In 1999, Whiten, Goodall, Wrangham, and colleagues published a landmark paper in *Nature*, "Culture in Chimpanzees," that focused on six field sites, documenting 39 different behaviors (most of which were tool use) not due to ecological forces. Since then, said Whiten, the number of sites has doubled, and researchers have documented 571 potentially unique behaviors. "Fifty years ago, we knew nothing about wild chimpanzees," said Whiten, praising the "richness and complexity" of the data at the meeting. "Look at us now." No one vocalized in response, but the human facial actions—smiles and nods—spoke volumes.

—JON COHEN

Experimenters Agree: You Can Cross Off Flowing Crystals

It was exciting while it lasted, but the claim that crystalline solid helium can flow like the thinnest liquid has seeped away. Such bizarre “supersolidity” would have been perhaps the strangest manifestation of quantum mechanics among things bigger than atoms and molecules. Alas, experimenters now agree that crystalline helium itself does not budge. Instead, the resistance-free “superfluid” flow emerges as helium atoms wend along faults and defects in the crystal.



Frozen. Eliminate defects such as the grain boundaries visible in this photo, and solid helium won't flow.

“The hypothesis that fits all the experiments is that the crystal does not support superfluidity and that any experiment that shows flow can be explained by remnant disorder” in the crystal, says John Reppy, a physicist at Cornell University.

Flowing helium crystals have been on shaky ground for a while. The first signs of the element's supersolidity emerged in 2004 when Moses Chan of Pennsylvania State University in State College and Eunseong Kim, now at the Korea Advanced Institute of Science and Technology in Daejeon, set a small can of solid helium twisting back and forth on the end of a thin shaft (*Science*, 1 July 2005, p. 38). Below a certain temperature—a few ten-thousandths of a degree above absolute zero—the frequency of twist-

ing suddenly increased, indicating that some helium atoms had let go of their brethren and were standing stock-still. That could happen only if they slipped through the crystal without any resistance.

Some theorists quickly argued that such flow was simply impossible in an orderly crystal. Instead, they said, it likely arose from more-conventional superfluid liquid helium percolating through defects in the crystal. That interpretation was bolstered last year when Reppy and Cornell's Ann Sophie Rittner reproduced the effect but found that it went away if they gently heated the crystal to eliminate defects, a process called annealing (*Science*, 24 March 2006, p. 1693). However, Chan and colleagues countered that they saw no evidence that annealing stanching the flow.

Now, Chan and colleague Anthony Clark, Reppy and Rittner, and Keiya Shirahama and colleagues at Keio University in Yokohama, Japan, all have managed to shrink the apparent flow by annealing their crystals. What's more, all reported that they can increase the signal by freezing helium quickly to make defect-laden crystals consisting of many tiny grains. In fact, Reppy and Rittner found that up to 20% of the atoms can flow in such a helium snowball.

The concordance of results shows that defects are the key ingredient. “It will probably change the direction of research,” Chan says. Norbert Mulders of the University of Delaware in Newark says experimenters can expect a little gloating from their theorist colleagues. “They will absolutely love it,” Mulders says. “They can run around for a couple of years saying ‘We told you so!’”

Precisely how the disordered solid flows remains unclear. Theorists Lode Pollet and Matthias Troyer of the Swiss Federal Institute of Technology in Zurich presented simulations confirming that atoms can glide along the boundaries between grains without resistance. But some experimenters argue that flow along grain boundaries cannot account

for the streaming of 20% of the atoms.

The bigger question may be, will researchers continue to pursue the phenomenon? “Clearly, this is a real effect,” says Sébastien Balibar, an experimenter at the École Normale Supérieure in Paris. “This is really very new physics, even if it isn't the spectacular idea originally proposed.” But the messy details of defects may not generate as much excitement as the prospect of an oh-so-cool flowing crystal.

Ultrashort Laser Pulses See Inside the Body

Energetic x-rays zip through flesh and set the standard for quickly seeing inside the body, but flashes of gentler visible and near-infrared light can also reveal what lies under the skin. Using laser pulses a few millionths of a nanosecond long, Warren Warren, a chemist at Duke University in Durham, North Carolina, and colleagues can trace biomolecules such as melanin within tissue to make a three-dimensional image of their microscopic distribution. The new technique might be used to detect without biopsy a type of skin cancer called melanoma.

“This is absolutely first-rate work,” says David Jonas, a chemist at the University of Colorado, Boulder. “The very small level of signal they can detect is very impressive, and that seems to be the key to making this useful for medical applications.”

Red and near-infrared light can pass through flesh, which is why your fingers glow luridly when you hold them over a flashlight. You cannot make out the insides of your fingers, however, because the light scatters off inhomogeneities in flesh, obscuring the details. To get around that problem, Warren and his team used light pulses a few femtoseconds long and exploited subtle interactions between the light and material that vary in a nonlinear way with the intensity of the light.

Researchers can trace a fluorescent substance by scanning a sample with tightly focused femtosecond pulses whose wavelengths are two times too long to trigger the fluorescence. Because of the mismatch, a target molecule fluoresces only when it is tickled simultaneously by two photons, which will happen only where the light is most intense. By monitoring the fluorescence while moving the laser's focal spot through the sample,

Pulling Strings to Untangle Catastrophe

About the simplest experiment imaginable may yield insights into calamitous events such as the sudden failure of cables on a suspension bridge. Taking a break from work on liquid crystals, physicist Peter Palffy-Muhoray and graduate student Jake Fontana of Kent State University in Ohio spent a few months tugging on string to see how the force required to break it varied with its length. Their preliminary results fit a model based on a gambling puzzle that stumped Daniel Bernoulli and other mathematicians in the early 18th century.

"Rare events are by their very nature hard to find but also extremely important because they can lead to catastrophe," says Mark Warner, a theorist at the University of Cambridge in the U.K. "You have to find a system in which you can explore a large range of [length] scales, and a long string seems to be just the thing." Size plays a key role in failure: A big rock is typically weaker than a small one because it has longer cracks.

The string experiment embodies the tricky mathematics of the Petersburg paradox, a game in which a gambler's winnings inevitably fall far short of his reasonable expectations. After paying an entry fee, the player flips a coin until it comes up heads. If he tosses tails once before that happens, he gets \$2. If he tosses tails twice, he gets \$4. With every additional tails, the payout doubles. In principle the average winnings are infinite, so a gambler ought to pay any amount to play. In reality, however, the game never pays out more than a few dollars.

That's because the average is inflated by extremely rare events. For example, although the chances of flipping 25 tails in a row are just 1 in 33,554,432, the payout for such a run is also a whopping \$33,554,432, which still drives the average winnings up. The paradox can be avoided by recognizing that, in any finite number of tosses, such runs are so improbable they should be ignored. If the game is repeated until the coin has been



Snap judgment. Jake Fontana took his string-pulling rig outdoors to gain insight into catastrophic failure.

tossed 100 times, there probably won't be a run of more than six tails, and even that would pay out only \$64.

To apply this scheme of ignoring exceedingly improbable events to string, Palffy-Muhoray and Fontana assumed that the string would break wherever unspecified defects accumulated. These accumulations corresponded to runs of tails in the coin tossing, and on average, they should make any long

stretch of string infinitely weak. Discounting the improbable accumulations, however, shows that a finite string has a strength that decreases in a particular way as its length increases—namely, with the logarithm of the length.

To test this model, the researchers pulled on strands of thread and fishing line ranging from a millimeter to a kilometer long—stretching the longer lengths along a bike path. Their logarithmic prediction fit the data better than two other well-studied models: one that treats the string as a chain and assumes an exponentially decreasing distribution for the weakness of the links, and another that focuses on how stress is shared by fibers in a multifiber line.

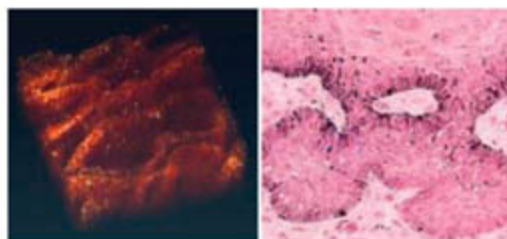
Others have probed how strength varies with length for the short fibers used in composite material, but few have examined extremely long ones, says William Curtin, who studies theoretical mechanics at Brown University. "It's a nice data set," he says. Curtin cautions that the relation should depend on the specific microscopic structure of the line. "There's not a universal form" for the length-strength relation, he says.

Fontana says he enjoyed the chance to work outdoors, but the experiment still had its trials. "The most stressful part was trying to keep people on the path from hitting the string, trying to be as polite as possible," he says. The researchers hope to pull even longer strings, perhaps using pulleys to wrap them back on themselves.

—A.C.

researchers can map the target substance. A commercial system already images skin using such two-photo fluorescence.

But the fluorescence technique has drawbacks, Warren says. Many biomolecules, such as melanin, fluoresce only weakly, and light from the fluorescence itself scatters within the flesh. So Warren and his team instead measure the amount of light absorbed by specific substances. For example, they apply pulses of two different colors chosen so that when a melanin molecule absorbs a photon of the first color, it will more readily absorb a photon of the second color as well.



Flashy. A new laser technique (*left*) reveals details of melanoma ordinarily seen with biopsy.

The amount of absorption is still tiny, however, and to see it, the researchers employ another trick. They make the intensity of the first color's pulses oscillate up and down and check whether this causes the absorption from the second beam to vary in a similar way. That technique enables them to convert a tiny intensity variation into a much clearer frequency signal. To make the conversion, they

track the pulses of the second color as they are reflected from the sample. They break the entire train of pulses into its component frequencies. The tiny oscillation then shows up as an additional frequency.

The technique lets researchers detect absorption of as little as one 10-millionth of the original pulses. "We're trying to look at processes where there's just barely enough signal so that you can access them using less average power than a laser pointer," Warren says. Jonas says that "by being able to detect such small effects, you're able to get the power down enough that you'd feel safe having this done to you."

Warren presented an image of a melanoma removed from human skin that showed the telltale streaks and clumps of accumulating melanin. As a step toward clinical applications, he and his colleagues have proposed a trial in which they will analyze irregular moles in patients that doctors intend to remove shortly anyway.

—ADRIAN CHO



Register before
10 May to avoid
last-minute
surcharge



4th IAS Conference

ON HIV PATHOGENESIS, TREATMENT AND PREVENTION

22-25 July 2007, Sydney, Australia



International
AIDS Society

Stronger Together

in partnership with



ashm

Australasian Society for HIV Medicine Inc

www.ias2007.org

Exhibit at IAS 2007 to reach 5,000 HIV clinicians, researchers and experts
For more information: exhibitions@ias2007.org

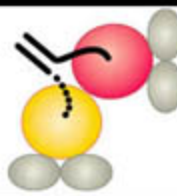
Thinking about
medicine

55



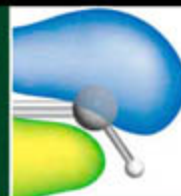
Molecular motoring

58



Understanding bonding

61



LETTERS | BOOKS | POLICY FORUM | EDUCATION FORUM | PERSPECTIVES

LETTERS

edited by Etta Kavanagh

Making Articles Available for Flu Planning



RECENT DISCUSSION ABOUT THE SHARING OF H5N1 SAMPLES BY THE Indonesian government with the World Health Organization highlights the importance of intellectual property issues in vaccine development ["Indonesia, WHO patch up," M. Enserink, *ScienceScope*, 23 Feb., p. 1065; (1)]. It is also worth noting the barriers to collaboration and information sharing represented by another form of intellectual property: copyrighted articles about avian flu and pandemic flu preparedness contained within medical and scientific publications.

It is disappointing that, at a time when many political and governmental officials are emphasizing the importance of collaboration, information sharing, and community involvement in pandemic flu planning and preparedness, interested professionals and members of the public are compelled to pay high fees or wait for weeks for an inter-library loan request to be filled when articles from medical and scientific journals are readily available online and could be easily shared with a broad audience.

Articles from major scientific publications are available, but in many cases, there is a cost. For instance, to read an interesting article about the utility of blood transfusions from the *Journal of the American Medical Association* costs \$15 (2). It costs \$10 to access relevant articles in *Science* online (3), while *Nature* charges \$30 (4). A recent discussion of the 1918 influenza pandemic co-authored by a high-ranking U.S. government official costs \$15 for 24-hour access (5). To their credit, some journals do occasionally make relevant articles available for free upon initial publication or at other times. Others can be found on various blogs and Web sites (e.g., Flu Wiki). However, this information is often difficult to access for those not affiliated with the large academic institutions, corporations, or governmental entities that can

afford to subscribe to certain scientific journals and databases.

The more we can do to reduce artificial and unnecessary barriers to information sharing and collaboration—

at every level—the better off all of us will be in the long term as we collectively prepare for a worldwide flu epidemic, and other potential public health emergencies. Enhanced access to scientific journals will help better ensure that community planning and preparedness efforts reflect the latest and most authoritative and substantive scientific knowledge and insights. It also will help broaden involvement in discussions about critical and often unresolved scientific, medical, regulatory, and ethical questions.

Researchers and publishers should do their part to help make sure that important information about this public health threat reaches professionals and members of the public in a timely manner (6). Allowing unrestricted access to relevant articles, letters, and correspondence about avian influenza and pandemic flu preparedness would be an excellent start.

MITCHELL BERGER*

Public Health Planner, DiPiero Center, Camden County Department of Health and Human Services, 512 Lakeland Road, 2nd floor, Blackwood, NJ 08012, USA.

*The opinions expressed in this article are solely those of the author and should not be imputed to any public or private entity.

References and Notes

1. D. G. McNeil Jr., "Indonesia may sell, not give, bird flu virus to scientists," *N.Y. Times*, 7 Feb. 2007, p. A6.
2. T. Hampton, *JAMA* **296**, 1827 (2006).
3. For instance, M. Enserink, *Science* **313**, 1555 (2006).
4. D. Butler, J. Ruttimann, *Nature* **441**, 137 (2006).
5. D. Morens, A. Fauci, *J. Infect. Dis.* **195**, 1018 (2007).
6. One free service, funded through unrestricted grants by several pharmaceutical companies, already collects and distributes to subscribers on a weekly basis journal abstracts about influenza and other topics. Perhaps this or a similar site also could provide relevant articles about pandemic influenza (see <http://www.amedeo.com/>).

Pneumococcal Vaccines and Flu Preparedness

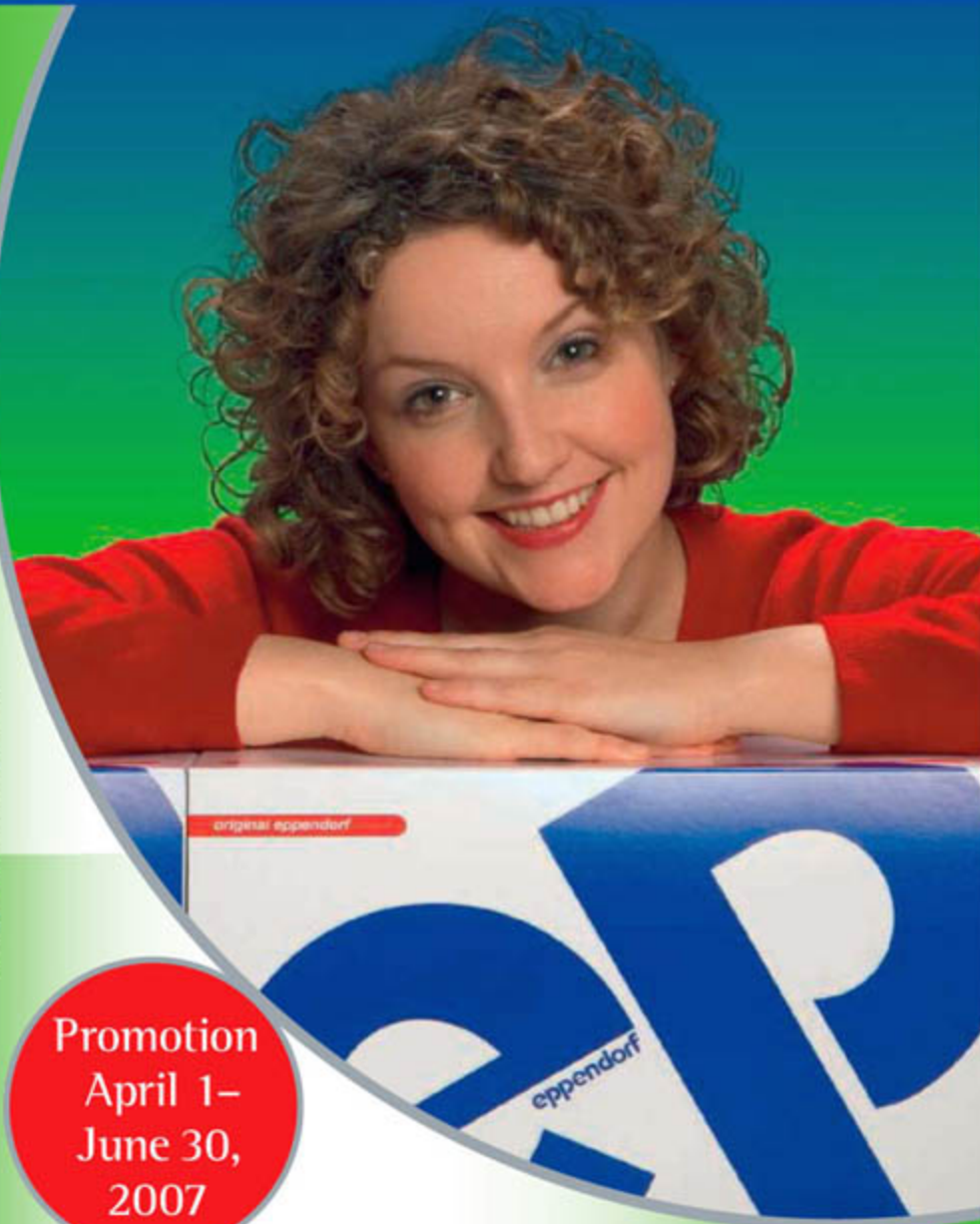
INFLUENZA-ASSOCIATED MORTALITY IN THE next five decades is likely to exceed that of any other global catastrophe (1, 2). The role of secondary bacterial infections and the need for bacterial vaccines are not mentioned in the U.S. Department of Health and Human Services Pandemic Influenza Plan (2). The evidence that pneumococcal infec-

tion played a major role in the 1918 influenza pandemic is substantial, but seems to have been forgotten (3). In two studies, culturable pneumococci could be found in the peripheral blood of 50 of 105 living soldiers with influenza, during the pandemic in the United States and the UK (4, 5), and from 55 of 89 heart blood cultures taken from U.S. soldier influenza victims immediately after death (6, 7). Roughly 1/3 of deaths during the 1918 pandemic occurred more than 2 weeks after the onset of symp-

oms (8). Blood culture and time of death both suggest a role for the pneumococcus in a substantial fraction of the deaths of these young soldiers.

The role of conjugate pneumococcal vaccine in reducing influenza-associated morbidity has recently been demonstrated (9). Children who received the vaccine and then developed laboratory-confirmed influenza were at 45% less risk of hospitalization due to the influenza-associated pneumonia than were children who had not received the

eppendorf® is a registered trademark.



Promotion
April 1–
June 30,
2007

Gentle & Easy!

With **Eppendorf Advantage** offers it is now easier than ever to add Eppendorf premium quality centrifuges to your lab.

Gentle & Easy: Centrifuge 5702/5702 R Bonus Packs

The Eppendorf 5702 family of centrifuges offers an outstanding combination of gentle treatment of sensitive clinical samples and ease-of-use.

Take advantage now!

From April 1–June 30, 2007, Centrifuge 5702 and Centrifuge 5702 R are available as attractive Bonus Packs at special prices that are too good to miss*.

Our exciting offers are just a few clicks away!

For more details visit www.eppendorf.com/advantage

*Offers may vary by country.

vaccine in a prospective double-blind randomized trial (9). These data suggest that conjugate vaccine given to infants may greatly reduce influenza-associated morbidity, but also, coupled with data on herd immunity of conjugate pneumococcal vaccine in the United States (10), suggest that immunization of children may protect adults as well.

The reasons for increased pneumococcal morbidity and mortality after influenza have been reviewed recently (11). Practical measures to be taken to prevent and treat secondary bacterial infections include antibiotic stockpiling; the enhancement of conjugate pneumococcal vaccine coverage of children to ensure optimal protection for them and high levels of herd immunity among adults; and provision to adults of 23 valent pneumococcal vaccine to prevent pneumococcal bacteremias. Research studies evaluating the impact of conjugate pneumococcal vaccine introduction on influenza-associated morbidity in adults and children in the United States and other countries contemplating the introduction of these vaccines are needed as well.

KEITH P. KLUGMAN¹ AND SHABIR A. MADHI²

¹William H. Foege Professor of Global Health, Rollins School of Public Health and Professor of Infectious Diseases, School of Medicine, Emory University, Atlanta, GA 30322, USA. E-mail: keith.klugman@emory.edu. ²Associate Professor, Respiratory and Meningeal Pathogens Research Unit, Medical Research Council and University of the Witwatersrand, Johannesburg 2000, South Africa.

References

1. V. Smil, *Pop. Dev. Rev.* **31**, 201 (2005).
2. *HHS Pandemic Influenza Plan* (U.S. Department of Health and Human Sciences, Washington, DC, 2005).
3. J. F. Brundage, *Lancet Infect. Dis.* **6**, 303 (2006).
4. R. Muir, G. H. Wilson, *Br. Med. J.* **1**, 3 (1919).
5. E. F. Hirsch, M. McKinney, *JAMA* **71**, 1735 (1918).
6. L. H. Spooner, L. H. Scott, E. H. Heath, *JAMA* **72**, 155 (1919).
7. J. N. Hall, M. C. Stone, J. C. Simpson, *JAMA* **71**, 1986 (1918).
8. C. E. Mills, J. M. Robbins, M. Lipsitch, *Nature* **432**, 904 (2004), supplementary fig 2.
9. S. A. Madhi, K. P. Klugman, Vaccine Trialist Group, *Nat. Med.* **10**, 811 (2004).
10. CDC, *Morb. Mortal. Wkly. Rep.* **54**, 893 (2005).
11. J. A. McCullers, *Clin. Microbiol. Rev.* **19**, 571 (2006).

Timing of a Back-Migration into Africa

INDIGENOUS NORTH AFRICANS ARE GENETICALLY quite distinct from sub-Saharan Africans (1), and this difference is reflected in their lighter skin and European/Middle Eastern physical features. We have previously suggested, on the basis of the distribution of mtDNA type M1, that North Africans are largely descended from a back-

migration into Africa within the last 2000 to 15,000 years, resettling the temporarily lush Sahara and spreading the Afro-Asiatic language family (2). In their Report "The mtDNA legacy of the Levantine early Upper Palaeolithic in Africa" (15 Dec. 2006, p. 1767), A. Olivieri and colleagues used high-resolution mtDNA data to propose that the migration from Asia back to North Africa happened much earlier, and they link the settlement of North Africa with the settlement of Europe 40,000 to 45,000 years ago.

Three points lead us to believe that our younger chronology for the back-migration into northern Africa still merits consideration. First, the mtDNA trees reconstructed by Olivieri and colleagues are less than conclusive because they consist of phylogeographically mixed branches, which cause uncertainty in identifying the relevant founder



Neolithic cave art from the central Sahara Desert. This example is from the Sefar site in Algeria. [Image after (3)]

nodes for genetic dating. Second, in our view the fact that the North African mtDNA marker types still correspond so closely with the Afro-Asiatic language zone argues against the existence of that correlation for tens of thousands of years. Third, cave art in the Sahara shows that in Neolithic times (around 5000 B.C.), the population of the Sahara was still of sub-Saharan African ancestry (see figure), whereas "Europoid" figures documenting the arrival of west Eurasians appear later in the cave art record (3).

Within the framework of our younger chronology, the occurrence of low frequencies of M1 types in the European Mediterranean can be explained by diffusion from the Middle East and North Africa during and since the Neolithic. The Sardinian M1 mtDNA founder date of 7700 ± 3100 years years calculated by Olivieri and

colleagues would conveniently fit with the arrival of farming in the European Mediterranean.

In conclusion, we suggest that more recent influx from Asia, possibly since the Last Glacial Maximum 20,000 years ago, may better explain some of the major genetic and linguistic patterns in North Africa and adjacent areas [cf. (4, 5)]. We nevertheless believe that future archaeogenetic research on Ice Age Africa and subsequent periods will benefit greatly from the complete mtDNA sequencing approach taken by Olivieri and colleagues.

PETER FORSTER¹* AND VALENTINO ROMANO²

¹Department of Forensic Science and Chemistry, Anglia Ruskin University, Cambridge CB1 1PT, UK, and New Hall, University of Cambridge, Cambridge CB3 0DF, UK.

²Dipartimento di Oncologia Sperimentale e Applicazioni Cliniche Università di Palermo, Palermo, Italy, and Associazione OASI Maria SS. (I.R.C.C.S.), Troina, Italy.

*To whom correspondence should be addressed. E-mail: pf223@cam.ac.uk

References

1. L.-L. Cavalli-Sforza, P. Menozzi, A. Piazza, *The History and Geography of Human Genes* (Princeton Univ. Press, Princeton, NJ), 1994.
2. P. Forster, *Philos. Trans. R. Soc. London Ser. B* **39**, 255 (2004).
3. A. Muzzolini, *L'Art Rupestre Préhistorique des Massifs Centraux Sahariens* (BAR, Oxford, 1986).
4. C. Renfrew, *Camb. Archaeol. J.* **1**, 3 (1991).
5. I. Diakonoff, *J. Semit. Stud.* **43**, 209 (1998).

Response

THE PRINCIPAL PROBLEM WITH GREAT SYNTHESISSES of languages, genes, and figurines (or pots) is that they lump together different migrational and cultural processes and especially overstretch recent events of the Holocene, thereby downplaying or swamping the genetic signals that point to much earlier events of the Pleistocene (1, 2).

Forster and Romano propose a recent arrival—within the last 2000 to 15,000 years—of haplogroup M1 in North Africa from western Asia, linked to the spread of Afro-Asiatic languages. This would entail a Near Eastern origin of the Afro-Asiatic language family and thus would be in agreement with Bellwood (3), provided that one subscribes to such a tight link between genes and languages. Afro-Asiatic scholarship (4), as well as the coalescence times of both M1a and M1b and the diverse basal distribution of M1a lineages especially in East Africa, however, militate against this interpretation. As we proposed in our Report, the arrival of M1 in Africa is most likely contemporary with that of U6, but if one alternatively hypothesized that only M1a originally went into the Northeast African Mediterranean coast, then 25,000 to 30,000 years ago

eppendorf
advantage ✓



5702/5702 R Bonus Packs

Centrifuge
+ swing-bucket rotor
+ 4 round buckets
in one package!



Promotion
April 1–
June 30,
2007

Your additional bonus

Each Centrifuge 5702/5702 R Bonus Pack comes standard with:

- an extra 100 ep-points* registration bonus
- the chance to win one of 50 gift certificates (e.g., Amazon, American Express, or equivalent) to the amount of approx. 50 Euro each
- one unique Eppendorf pipette pen

More product details and contact information at

www.eppendorf.com/advantage

eppendorf
In touch with life

*Offers may vary by country. ep-points are not available in all countries. For details see www.ep-points.com

would be the realistic time frame.

The latter hypothesis is valid when one assumes the less parsimonious scenario that only haplogroup U6 was involved 40,000 to 45,000 years ago in the early Upper Palaeolithic diffusion of Levantine populations into North Africa and that a diffusion of M1a lineages marked a new phase in the Nile Valley Complex, 25,000 to 30,000 years ago (5). It is then also more plausible to see the development and emergence of proto-Afro-Asiatic languages there, in the Nile Valley (6, 7). Later migrations and gene flow, which undoubtedly took place, have certainly complicated phylogeographic patterns. For instance, one may also envision some mutual contacts between the Levantine Natufian culture and contemporary autochthonous cultures of the Lower Nile Valley (~15,000 years ago). Later Neolithic influence then brought a whole package of Near Eastern mtDNA lineages into all of North Africa, as attested, for instance, by the relatively high frequency of mtDNA haplogroups H, J, and T in modern North African populations (8, 9).

The cave art argument adduced by Forster

and Romano has no impact on the issue of the late Near Eastern influx because haplogroup U6 very clearly testifies to an early presence in North Africa of Near Eastern lineages, which must have proceeded to as far as Northwest Africa with the ancestors of the Iberomaurusians before the Late Glacial Maximum (8). The anthropological evidence from North Africa, pointing to the autochthonous Mechta-Afalou physical type, with continuity well into the Capsian of the mid-Holocene, gives clear support to the ancient presence of Upper Palaeolithic people in North Africa (5). Moreover, the presence of figurines of sub-Saharan type in the cave art of the Sahara may simply be indicative of resettlement of the region by groups from the south, already adapted to savannah ecology, after the early Holocene arrival of monsoon rains changed the Sahara into a habitable region (10). Thus, the argument is not informative on the antiquity of a "Euro-roid" settlement in North Africa.

ANNA OLIVIERI,¹ ALESSANDRO ACHILLI,¹
 MARIA PALA,¹ VINCENZA BATTAGLIA,¹
 SIMONA FORNARINO,¹ NADIA AL-ZAHERY,^{1,2}
 ROSARIA SCOZZARI,³ FULVIO CRUCIANI,³

DORON M. BEHAR,⁴
 JEAN-MICHEL DUGOUJON,⁵ CLOTILDE COUDRAY,⁵
 A. SILVANA SANTACHIARA-BENERECETTI,¹
 ORNELLA SEMINO,¹ HANS-JÜRGEN BANDELT,⁶
 ANTONIO TORRONI^{1*}

¹Dipartimento di Genetica e Microbiologia, Università di Pavia, Via Ferrata 1, 27100 Pavia, Italy. ²Department of Biotechnology, College of Science, University of Baghdad, Iraq. ³Dipartimento di Genetica e Biologia Molecolare, Università "La Sapienza," Piazzale Aldo Moro 5, 00185 Rome, Italy. ⁴Molecular Medicine Laboratory, Rambam Health Care Campus, Efron 9 street, Bat Galim, 31096 Haifa, Israel. ⁵Centre d'Anthropologie, FRE 2960 CNRS, Université Paul Sabatier, Toulouse III, 37, allées Jules Guesde, 31073 Toulouse Cedex, France. ⁶Department of Mathematics, University of Hamburg, Bundesstrasse 55, 20146 Hamburg, Germany.

*To whom correspondence should be addressed. E-mail: torroni@ipvgen.unipv.it

References

1. H.-J. Bandelt, V. Macaulay, M. Richards, in *Examining the Farming/Language Dispersal Hypothesis*, P. Bellwood, C. Renfrew, Eds. (McDonald Institute Monographs, McDonald Institute for Archaeological Research, Cambridge, 2003), pp. 99–111.
2. M. Richards, *Annu. Rev. Anthropol.* **32**, 135 (2003).
3. P. Bellwood, *Science* **306**, 1681 (2004).
4. C. Ehret, S. O. Y. Keita, P. Newman, *Science* **306**, 1680 (2004).
5. D. W. Phillipson, *African Archaeology* (Cambridge Univ. Press, Cambridge, ed. 3, 2005).

FOCUS ON CAREERS

Careers in Cancer Research

IN THIS ISSUE:

Many different roads can lead to a career in cancer research. Which path will you take? Find some direction in the latest **Careers in Cancer Research** feature in this issue, **page 131**.

UPCOMING FEATURES:

April 20— Postdoctoral Careers: Transferable Skills
 April 27 — Biotech and Pharma
 May 4 — Interdisciplinary Research



Also available online at www.sciencecareers.org/businessfeatures



6. C. Ehret, *A Reconstruction of Proto-Afroasiatic (Proto-Afrasian): Vowels, Tone, Consonants and Vocabulary* (Univ. of California Press, Berkeley/Los Angeles/London, 1995).
7. M. Brett, E. Fentress, *The Berbers: the Peoples of Africa* (Blackwell, Oxford, 1996).
8. J. C. Rando et al., *Ann. Hum. Genet.* **62**, 531 (1998).
9. V. Macaulay et al., *Am. J. Hum. Genet.* **64**, 232 (1999).
10. R. Kuper, S. Kröpelin, *Science* **313**, 803 (2006).

Speeding Up the EPA Review Process

AS ERIK STOKSTAD'S ARTICLE "EPA DRAWS FIRE OVER AIR-REVIEW REVISIONS" (News of the Week, 15 Dec. 2006, p. 1672) notes, everyone agrees that the U.S. Environmental Protection Agency's (EPA) process for developing ambient air quality standards is slow and cumbersome. Steve Johnson, the first career scientist ever to head the EPA, has also found that this process doesn't deliver up-to-date science and could be more transparent to the public. The revisions to this process will result in more timely and transparent reviews that do deliver up-to-date research.

The article states that these improve-

ments will apply immediately to the review of the ozone standard. This is not the case. The ozone review is pretty far down the pipeline, and the EPA concluded some time ago that any significant changes to this review would likely delay getting this standard completed.

MARCUS PEACOCK

Deputy Administrator, U.S. Environmental Protection Agency, Washington, DC 20460, USA.

TECHNICAL COMMENT ABSTRACTS

COMMENT ON "Divergent Induced Responses to an Invasive Predator in Marine Mussel Populations"

Paul D. Rawson, Phillip O. Yund, Sara M. Lindsay

Freeman and Byers (Reports, 11 August 2006, p. 831) presented evidence for the rapid evolution of antipredator defenses in the mussel *Mytilus edulis*. However, their analysis is confounded by three issues. Samples from some sites are likely to have included a second species, *M. trossulus*; their manipulation of chemical cues does not preclude other interpretations; and they failed to establish an adaptive significance to shell thickening.

Full text at www.sciencemag.org/cgi/content/full/316/5821/53b

RESPONSE TO COMMENT ON "Divergent Induced Responses to an Invasive Predator in Marine Mussel Populations"

Aaren S. Freeman and James E. Byers

Preliminary DNA analysis indicates that only a few *Mytilus trossulus* mussels were present in our study of *M. edulis*. Excluding these *M. trossulus* did not influence the outcome of our analyses. Our study provides essential evidence that populations of *M. edulis* respond differently to the two crab predators, and the adaptive significance of shell thickening in mollusks is well established.

Full text at www.sciencemag.org/cgi/content/full/316/5821/53c

Letters to the Editor

Letters (~300 words) discuss material published in *Science* in the previous 3 months or issues of general interest. They can be submitted through the Web (www.submit2science.org) or by regular mail (1200 New York Ave., NW, Washington, DC 20005, USA). Letters are not acknowledged upon receipt, nor are authors generally consulted before publication. Whether published in full or in part, letters are subject to editing for clarity and space.



JPT Peptide Technologies – for Peptide Arrays!

Off-The-Shelf Peptide Microarrays

Kinase Peptide Microarrays

- > 5 000 annotated kinase substrate peptides on glass slides

PhosphoSite Detector

- Peptide scans through > 70 kinase substrate proteins on glass slides

Protease Peptide Microarrays

- > 2 000 fluorescent peptides from annotated protease cleavage sites

Phosphatase Peptide Microarrays

- > 2 000 phosphopeptides on glass slides derived from annotated phosphosites

Customized Peptide Arrays

PepSpot™

- Peptide scans or collections of peptides on cellulose membranes
- **Fast** (≤ 2 weeks turnaround)
- **Affordable** (< \$ 5/peptide)
- **Flexible** (≤ 5 000 PepSpots/membrane)

PepStar™

- Economical access to identical peptide microarrays on glass slides
- **Fast** (≤ 3 weeks turnaround)
- **Affordable** (from < \$ 200/chip)
- **Flexible** (≤ 5 000 peptides/slide)

Applications

- Systematic study of protein-protein interactions
- Antibody epitope mapping, mapping of immunodominant regions
- Identification of substrates for kinases, proteases, and phosphatases
- Profiling of substrate specificities
- Testing of inhibitors and many more



HISTORY OF SCIENCE

Seeing Is Believing?

Harriet Ritvo

As Jonathan Smith notes at the beginning of *Charles Darwin and Victorian Visual Culture*, Darwin's most famous book is almost completely devoid of illustration. There is only one illustration in *On the Origin of Species*, a powerfully abstract diagram of branching evolutionary descent. In this, as in much else, the *Origin* was unusual. Illustration was a highly valued feature of 19th-century work in zoology, botany, and geology, whether it was intended for specialists or for a broader public. Most naturalists (although not Darwin) were adept draftsmen, and there was a ready market even for expensive volumes with lavishly produced plates. Like most of his contemporaries, Darwin understood that images could function as argument as well as description. It is well known that he considered the *Origin* to be a mere abstract of the much longer and more fully substantiated treatise that he would have written if he had not feared being scooped by Alfred Russel Wallace. In his more leisurely and typical works, Darwin made frequent and subtle use of visual images.

Smith (a professor of English at the University of Michigan, Dearborn) examines many of these illustrations in detail, discussing them both in relation to the written texts they accompanied and in relation to the larger scientific and popular visual cultures from which they were drawn. He argues persuasively that Darwin's images should not be considered merely as adornment, or even as illustration in the rhetorical sense, but as a thoroughly integrated component of the work in which they appear. He thus refers to Darwin's works as "imagetexts" (he did not coin this rather ponderous neologism).

Perhaps as a way of emphasizing the persistence of Darwin's concern with the visual dimension of his books, Smith devotes most of his attention to the beginning and the end of Darwin's career. Of the series of works in which Darwin elaborated the schematic arguments of the *Origin*, only two receive much attention: *The Expression of the Emotions in Man and Animals*, which is extensively discussed in the two chapters on faces, and *The Descent of Man*, which figures in recurrent considerations of the aesthetic implications of

sexual selection. Otherwise, Smith focuses on Darwin's early monograph on barnacles, his late experimental works on plants, and his final volume on worms.

The chapter titles (all of the same form: "Darwin's Barnacles," "Darwin's Birds," etc.) belie the complexity and richness of Smith's interpretation. Smith anchors each chapter in the explication of specific images. He does a very good job of explaining their significance, strongly supported by the generous design of the book: not only are there plenty of illustrations, but most of them are large enough for their details to be discernable. Smith's explanations require him to integrate many separate threads of scholarship, including the history of the book, art history, and the history of science, as well as Victorian literary and cultural studies. For example, the chapter on barnacles begins by comparing the illustrations in Darwin's



"Grotesque realism." Darwin used three engravings from photographs to support his argument that worms pass large quantities of castings.

monograph to other contemporary scientific work on the Cirripedia and concludes by comparing them to the illustrations in books that inspired and sustained the mid-Victorian craze for aquaria and tide pool naturalizing.

Perhaps the most interesting chapter is the final one, which analyzes the images in *The Formation of Vegetable Mould Through the Action of Worms*, published the year before Darwin's death. In it, Darwin returned to his early fascination with geology, combining the epochal and the domestic scales as

he described the role of earthworms in producing soil and burying the evidences of human civilization. The book contained no earthworm portrait and only one diagram of the annelid digestive system. According to Smith, this omission highlights the functional or utilitarian emphasis of Darwin's argument: what is interesting about the worms is that by passing earth through their digestive system they

transform the landscape—both by turning it over and by enriching it with their castings (excrement). Several of the illustrations are rather monumental representations of worm castings, which itself gave offense to those committed to a more rarefied ideal of the art of natural history. The rest are of objects—whether monuments like Stonehenge or more modest efforts like Roman villas or random stones in cultivated fields—gradually being submerged under the slowly accumulated by-products of earthworm metabolism.

Carefully considered, none of these images would have given much comfort to the cultural critics (of whom John Ruskin was the most prominent) who had long complained about what they considered the degrading influence of the materialist aesthetic implicit in Darwin's work. In particular, his arguments about sexual selection suggested that the human sense of beauty was shared by animals (or at least that it was very similar to a faculty that animals also possessed) and that it had developed in response to the exigencies of reproductive competition rather than as a reflection of some higher mode of perception. Perhaps still more disturbing to Victorian convention, Darwin suggested that in many cases the definitive aesthetic judgment of strutting males was exercised by females (although he endorsed other conventional ideas about human gender).

One of the many strengths of the book is that, in addition to placing Darwin's use of imagery in several contemporary contexts, Smith traces Darwin's impact on the popular

Charles Darwin and Victorian Visual Culture

by Jonathan Smith

Cambridge University Press, Cambridge, 2006.

374 pp. \$100, £60.

ISBN 9780521856904.

Cambridge Studies in Nineteenth-Century Literature and Culture.

The reviewer is at the Department of History, Massachusetts Institute of Technology, Cambridge, MA 02139, USA. E-mail: ritvo@mit.edu

visual culture of his time. Of course this impact increased dramatically after 1859. Its most conspicuous products were not the heartfelt laments of the artistic elite, but several still-familiar stock caricatures or cartoons such as the ape or monkey with a human face (in the early days the face often bore Darwin's own easily recognizable features) and the staggered evolutionary transformation from a monkey (or, sometimes, from a fish or lizard) to an ape to a caveman to a modern human. The fact that these images continue to provoke a range of reactions very similar to those they raised a century and a half ago illustrates the importance of studies like Smith's, which can help us to understand our own time as well as Darwin's.

10.1126/science.1141442

MEDICINE

Placebo or Protector?

Rachel A. Ankeny

The traditional Jewish myth of the golem centers on a human-like creature created by humans out of clay and water. It will follow orders and is very powerful yet also is a bit stupid and clumsy and hence dangerous. The golem has become a familiar trope in popular culture, making appearances in literary novels such as Umberto Eco's *Foucault's Pendulum* (1) and even in the Pokémon games. It serves as an especially appropriate framing metaphor for the series of books focused on science and technology by the sociologists and science studies scholars Harry Collins (Cardiff University) and Trevor Pinch (Cornell University) (2, 3). In this latest installment, *Dr. Golem*, we are taken on a tour of the "messiness" that characterizes medicine in order to reflect on the complexities inherent in medical science and practice and on how we should make medical choices given these uncertainties.

To illustrate medicine's recognized fallibility, the authors present a series of case studies that popularize existing scholarly accounts. These range from familiar debates over the definition of death and contested disease categories such as chronic fatigue and fibromyalgia to more mundane interactions with the

medical establishment such as uncertainties over the diagnosis of tonsillitis. It is likely that our perceptions of medicine, unlike most other branches of science and technology, already include some knowledge of its successes and failures and of the gaps in its existing theories. Nonetheless, documenting examples of these failures and gaps is a useful exercise, in part as an antidote to increasing public confidence that cures and answers are just around the corner. This has been evident in much of the hype surrounding genetic, stem cell, and cancer research.

The book explores eight topics, beginning with the placebo effect. Collins and Pinch describe it as "the hole in the heart of medicine" as it encapsulates the problematic nature of nonscientific aspects of medicine and their impact on any attempts to scientize medicine. A provocative chapter covers the dubious acceptance of cardiopulmonary resuscitation (CPR). They note that critics have argued that CPR at best is nothing more than a "passing ritual" (whose primary use is to allow families more time with a dying loved one) and at worst is dangerous and a substantial waste of resources in terms of training and equipment.

A less successful chapter on "alternative medicine" focuses on the early-1970s controversy that surrounded Linus Pauling's championing of large doses of vitamin C as a cure for cancer. This case study fails to do justice to the original scholarly research on which it is based. Nor does it provide an adequate examination of the complex issues associated with

today's complementary and alternative medical theories and practices (which are only briefly touched within the placebo chapter).

Collins and Pinch also integrate some of their own experiences with medicine into their narrative. Although these personal threads may sometimes annoy a more scholarly-minded reader, they do help illustrate disagreements between the authors (for instance, about measles, mumps, and rubella vaccination). The authors emphasize that this book forced them to consider not only what to think but also what to do—what choices to make when faced with difficult medical decisions.



The claim that medicine is golem-like is far from novel, and as the authors put it: "The really hard question that remains is, 'Knowing medicine is fallible, what should we do?'"

Although *Dr. Golem* indeed may lead readers to reflect on their experiences with medicine and its limitations (particularly with regard to prognosis and therapy), it unfortunately fails to provide much guidance about what in fact patients should do in light of this knowledge. For example—perhaps because the book arose implicitly in parallel to considerations of science and technology—there is little engagement with issues of personal values and ethics in relation to medical decision-making

or with the political, social, and economic contexts within which medicine (particularly in underdeveloped countries) is practiced. Nor do the authors examine the art or craft of medicine in any detail. Hence they ignore long-standing debates in the philosophy of medicine over the other skills (such as communication and diagnostic talent) that are clearly central to good medical practice. In fact, they set up an odd dichotomy between medicine as science and medicine as "succor," which implicitly denies that nonscientific forms of knowledge might play important roles beyond providing comfort when science cannot cure—a striking omission for scholars quick to recognize alternative forms of expertise in other settings. They leave underexplored the hybrid nature of medicine as a pragmatic, scientific, artistic, and social undertaking.

In a sense, Collins and Pinch appear to have used *Dr. Golem* to confront their own personal demons: faced with the need to make personal, life-and-death decisions, they seem to want to hold medicine to higher standards than we might hold other forms of science. The problem is that when viewed in this limited and idealized way, medicine falls so far short that it is unclear how we should understand the implications of these case studies for any medical choices with which we might be faced.

References

1. U. Eco, *Foucault's Pendulum* (Secker and Warburg, London, 1989).
2. H. Collins, T. Pinch, *The Golem: What Everyone Should Know About Science* (Cambridge Univ. Press, Cambridge, 1993); reviewed by U. Segerstråle, *Science* 263, 837 (1994).
3. H. Collins, T. Pinch, *The Golem at Large: What You Should Know About Technology* (Cambridge Univ. Press, Cambridge, 1998).

10.1126/science.1124931

Dr. Golem
How to Think About
Medicine

by Harry Collins and
Trevor Pinch

University of Chicago
Press, Chicago, 2005.
258 pp. \$25, £17.50.
ISBN 9780226113661.

The reviewer is at the School of History and Politics, University of Adelaide, Adelaide, SA 5005, Australia. E-mail: rachel.ankeney@adelaide.edu.au

SCIENCE AND SOCIETY

Framing Science

Matthew C. Nisbet¹* and Chris Mooney²

Issues at the intersection of science and politics, such as climate change, evolution, and embryonic stem cell research, receive considerable public attention, which is likely to grow, especially in the United States as the 2008 presidential election heats up. Without misrepresenting scientific information on highly contested issues, scientists must learn to actively “frame” information to make it relevant to different audiences. Some in the scientific community have been receptive to this message (1). However, many scientists retain the well-intentioned belief that, if laypeople better understood technical complexities from news coverage, their viewpoints would be more like scientists’, and controversy would subside.

In reality, citizens do not use the news media as scientists assume. Research shows that people are rarely well enough informed or motivated to weigh competing ideas and arguments. Faced with a daily torrent of news, citizens use their value predispositions (such as political or religious beliefs) as perceptual screens, selecting news outlets and Web sites whose outlooks match their own (2). Such screening reduces the choices of what to pay attention to and accept as valid (3).

Frames organize central ideas, defining a controversy to resonate with core values and assumptions. Frames pare down complex issues by giving some aspects greater emphasis. They allow citizens to rapidly identify why an issue matters, who might be responsible, and what should be done (4, 5).

Consider global climate change. With its successive assessment reports summarizing the scientific literature, the United Nations’ Intergovernmental Panel on Climate Change has steadily increased its confidence that human-induced greenhouse gas emissions are causing global warming. So if science alone drove public responses, we would expect increasing public confidence in the validity of the science, and decreasing political gridlock.

Despite recent media attention, however, many surveys show major partisan differences on the issue. A Pew survey conducted in January found that 23% of college-educated Republicans think global warming

is attributable to human activity, compared with 75% of Democrats (6). Regardless of party affiliation, most Americans rank global warming as less important than over a dozen other issues (6). Much of this reflects the efforts of political operatives

and some Republican leaders who have emphasized the frames of either “scientific uncertainty” or “unfair economic burden” (7). In a counter-strategy, environmentalists and some Democratic leaders have framed global warming as a “Pandora’s box” of catastrophe; this and news images of polar bears on shrinking ice floes and hurricane devastation have evoked charges of “alarmism” and further battles.

Recently, a coalition of Evangelical leaders have adopted a different strategy, framing the problem of climate change as a matter of religious morality. The business pages tout the economic opportunities from developing innovative technologies for climate change. Complaints about the Bush Administration’s interference with communication of climate science have led to a “public accountability” frame that has helped move the issue away from uncertainty to political wrongdoing.

As another example, the scientific theory of evolution has been accepted within the research community for decades. Yet as a debate over “intelligent design” was launched, antievolutionists promoted “scientific uncertainty” and “teach-the-controversy” frames, which scientists countered with science-intensive responses. However, much of the public likely tunes out these technical messages. Instead, frames of “public accountability” that focus on the misuse of tax dollars, “economic development” that highlight the negative repercussions for communities embroiled in evolution battles, and “social progress” that define evolution as a building block for medical advances, are likely to engage broader support.

The evolution issue also highlights another point: Messages must be positive and respect diversity. As the film *Flock of Dodos* painfully

To engage diverse publics, scientists must focus on ways to make complex topics personally relevant.

demonstrates, many scientists not only fail to think strategically about how to communicate on evolution, but belittle and insult others’ religious beliefs (8).

On the embryonic stem cell issue, by comparison, patient advocates have delivered a

focused message to the public, using “social progress” and “economic competitiveness” frames to argue that the research offers hope for millions of Americans. These messages have helped to drive up public support for funding between 2001 and 2005 (9, 10). However, opponents of increased government

funding continue to frame the debate around the moral implications of research, arguing that scientists are “playing God” and destroying human life. Ideology and religion can screen out even dominant positive narratives about science, and reaching some segments of the public will remain a challenge (11).

Some readers may consider our proposals too Orwellian, preferring to safely stick to the facts. Yet scientists must realize that facts will be repeatedly misapplied and twisted in direct proportion to their relevance to the political debate and decision-making. In short, as unnatural as it might feel, in many cases, scientists should strategically avoid emphasizing the technical details of science when trying to defend it.



References

1. T. M. Beardsley, *Bioscience* **56**, 7 (2006). www.aibs.org/bioscience-editorials/editorial_2006_07.html.
2. S. L. Popkin, *The Reasoning Voter* (Univ. of Chicago Press, Chicago, IL, 1991).
3. J. Zaller, *Nature and Origins of Mass Opinion* (Cambridge Univ. Press, New York, 1992).
4. W. A. Gamson, A. Modigliani, *Am. J. Sociol.* **95**, 1 (1989).
5. V. Price, et al., *Public Opin. Q.* **69**, 179 (2005).
6. Pew Center for the People and the Press (2007); <http://pewresearch.org/pubs/282/global-warming-a-divide-on-causes-and-solutions>.
7. A. M. McCright, R. E. Dunlap, *Soc. Probl.* **50**, 3 (2003).
8. Film promotion, www.flockofdodos.com/
9. Virginia Commonwealth University Life Sciences Survey (2006); www.vcu.edu/lifesci/images2/lis_survey_2006_report.pdf
10. Pew Center for the People and the Press (2006); <http://peoplepress.org/reports/display.php3?ReportID=283>.
11. M. C. Nisbet, *Int. J. Public Opin. Res.* **17** (1), 90 (2005).

¹School of Communication, American University, Washington, DC 20016, USA. ²Washington correspondent, *Seed Magazine* (seedmagazine.com).

*Author for correspondence. E-mail: nisbet@american.edu

NEUROSCIENCE

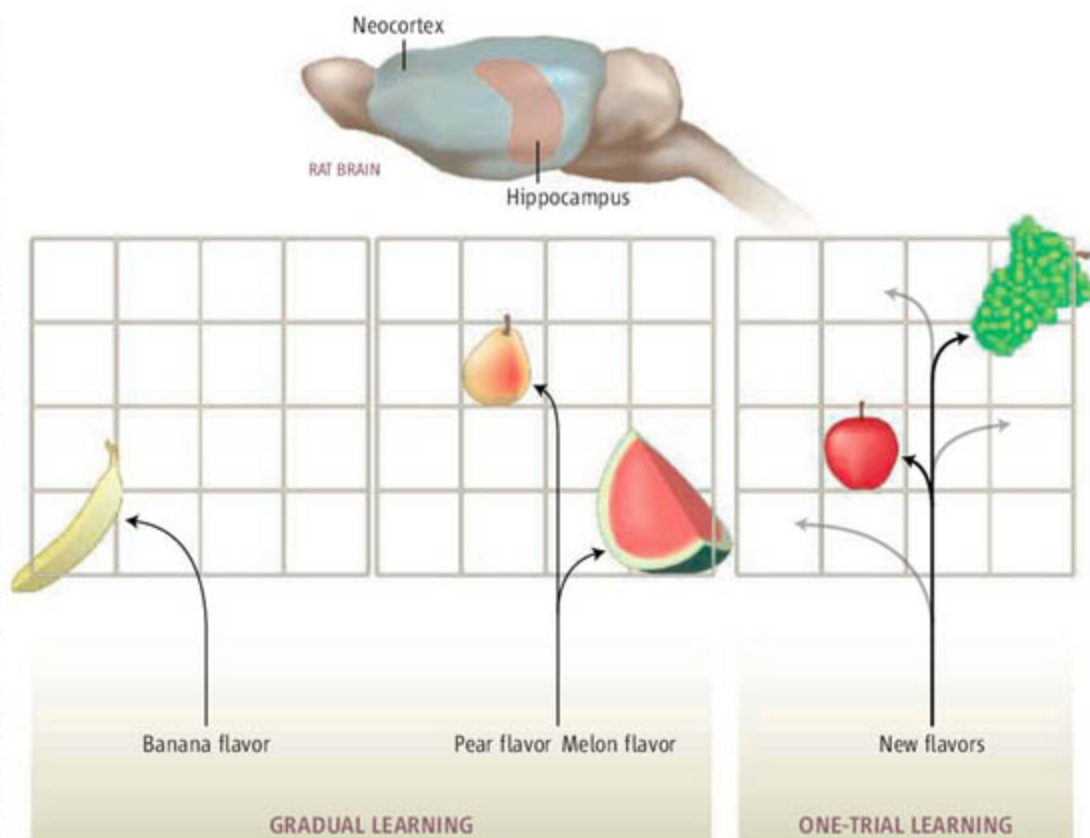
Rapid Consolidation

Larry R. Squire

We learn and remember better when new material can be related to what we already know. Professional athletes can remember details of particular plays that occurred in a long match. Experienced poker players can reconstruct the card distribution and betting sequence that occurred in previous hands. This is possible because these individuals have a rich background of relevant experience and therefore can organize new material into meaningful and orderly patterns. On page 76 of this issue, Tse *et al.* (1) make use of these ideas to explain their new findings in rats.

In his classic 1932 monograph on remembering (2), British psychologist Frederic Bartlett developed the concept of “schemas” to refer to preexisting knowledge structures into which newly acquired information can be incorporated. Although the schema concept is fundamental to the psychological science of human memory, it has been difficult to bring the concept to biology and especially to studies with experimental animals. Tse *et al.* show in rats how the schema concept is relevant to the phenomenon of memory consolidation. Memory consolidation refers to the gradual process of reorganization by which new memories become remote memories (3, 4). Initially, the learning of facts and events (declarative memory) depends on the hippocampus, a structure deep in the temporal lobe of the mammalian brain. As time passes after learning, the importance of the hippocampus gradually diminishes and a more permanent memory is established in distributed regions of the neocortex. This process typically takes a few years in humans and at least a month in rodents. According to one influential model (5), the process is slow because if changes were made rapidly, they would interfere with the preexisting framework of structured knowledge that has been built up from other experiences.

In the Tse *et al.* study, rats learned to associate six flavors with six places in a familiar testing arena. A rat was first cued with a particular flavor (a 0.5-g morsel of flavored food) in one of four start boxes and then could receive more of the same food by going to the



Good schemas wanted. When a rat learns associations between flavors and spatial locations, as studied by Tse *et al.* (1), the associations are initially learned as individual facts (left). With extended training, the animal develops an organized structure or schema for flavors and places (middle). This organized knowledge structure (bold lines) can then support rapid learning of new associations in a single trial and the rapid consolidation of information into the neocortex (right).

correct location in the arena. Animals learned the six flavor-place associations gradually across 6 weeks of training; each flavor-place pair was presented once per session for training and three sessions were scheduled each week. Not surprisingly, animals with hippocampal lesions failed to learn the associations.

Evidence that flavor-place training afforded the development of a schema came from finding that animals were subsequently able to learn new flavor-place associations in a single trial and could remember the new associations for at least 2 weeks (see the figure). The extended training had helped because in a similar task in which rats were trained on a new flavor-place association each day (6), memory was only weakly established and persisted for less than a day. Tse *et al.* also tested other rats that learned six flavor-place associations in one arena (the consistent arena) and concurrently learned six different flavor-place associations in another arena but with the fla-

We may be able to learn new things very quickly, and incorporate them into memories, if representations of related information have already been stabilized in the brain.

vor-place combinations rearranged every two sessions (the inconsistent arena). In the consistent arena, animals could then learn new flavor-place associations in a single trial, as before. By contrast, in the inconsistent arena, animals failed at one-trial learning, presumably because they had not established a stable schema that could guide rapid learning.

The most surprising finding by Tse *et al.*, and what connected the schema concept to memory consolidation, was that removal of the entire hippocampus as early as 48 hours after the rapid learning of two new flavor-place associations fully spared memory of the associations (these animals had first been given extensive training on six other flavor-place associations, thus establishing a schema). It was not the case that memory of the new associations was never dependent on the hippocampus, nor that memory was somehow formed directly in the neocortex, because hippocampal lesions made 3 hours after learning abolished memory of the new associations. In

short, the neocortex was able to incorporate new information rapidly. This is unexpectedly rapid for a process that, on the basis of as many as 20 studies in experimental animals, ordinarily takes at least a month (7).

It is tempting to suppose that memory consolidation proceeded rapidly because new information was fully compatible with what had already been learned—in other words, a good schema was available. If so, questions naturally arise about the minimum requirements for an effective schema. Perhaps continued training with two new flavor-place pairs every day would be sufficient (not just extended training with the same set of pairs, as was done by Tse *et al.*). Although new associations trained in this way ordinarily persist for less than a day (6), with extended experience they might persist much longer and also become rapidly independent of the hippocampus. And what might happen if animals simply explored the same arena day after day? Would merely having strong familiarity with a consistent environment support the rapid learning

and rapid consolidation of new associations? Answers to these questions would help sharpen the notion of schema and clarify the conditions under which rapid memory consolidation occurs.

The study also casts fresh light on an issue of long-standing interest. As the authors point out, the fact that storage and recall of spatial memory can occur independently of the hippocampus runs counter to the proposal that the hippocampus forms and stores cognitive maps (8). Thus, the new findings, as well as other work (9), give no special emphasis to spatial cognition and suggest instead that the hippocampus is a general-purpose learner of new facts and events, both spatial and nonspatial.

The larger question concerns the nature of memory consolidation itself. Recent studies of brain metabolism and activity-related genes in mice describe the decreasing importance of the hippocampus as time passes after learning and the increasing importance of several cortical regions, including the prefrontal, temporal, and anterior cingulate cortex (4). The idea is

not that memory is literally transferred from hippocampus to neocortex, but rather that the hippocampus guides gradual changes in the neocortex that increase the complexity, distribution, and interconnectivity of memory storage sites. This new study is the first to show that this process can occur rapidly.

References

1. D. Tse *et al.*, *Science* **316**, 76 (2007).
2. F. C. Bartlett, *Remembering* (Cambridge Univ. Press, Cambridge, 1932).
3. L. R. Squire, P. Alvarez, *Curr. Opin. Neurobiol.* **5**, 169 (1995).
4. P. W. Frankland, B. Bontempi, *Nat. Rev. Neurosci.* **6**, 119 (2005).
5. J. L. McClelland, B. L. McNaughton, R. C. O'Reilly, *Psychol. Rev.* **102**, 419 (1995).
6. M. Day, R. Langston, R. G. M. Morris, *Nature* **424**, 205 (2003).
7. L. R. Squire, R. E. Clark, P. J. Bayley, in *The Cognitive Neurosciences III*, M. Gazzaniga, Ed. (MIT Press, Cambridge, MA, 2004).
8. J. O'Keefe, L. Nadel, *The Hippocampus as a Cognitive Map* (Oxford Univ. Press, Oxford, 1978).
9. L. R. Squire, P. J. Bayley, *Curr. Opin. Neurobiol.*, in press.

10.1126/science.1141812

BIOCHEMISTRY

Processive Motor Movement

David D. Hackney

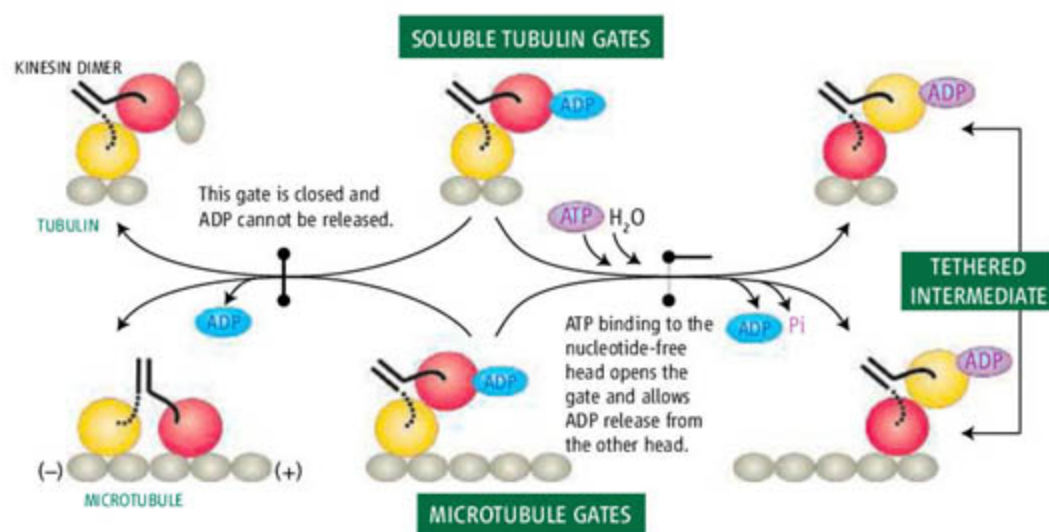
Permeating throughout a eukaryotic cell is a lattice of filamentous tracks called microtubules, upon which molecular motors travel, moving cargo about. In this transport system, the molecular motor kinesin-1 carries relatively large loads (molecular complexes, membranous vesicles, and organelles), its motion powered by the energy liberated from hydrolyzing adenosine triphosphate (ATP) (1). In fact, kinesin-1 can move processively for long distances (over a micrometer) along a microtubule without falling off. This feat requires coordinating the two motor domains ("heads") of kinesin so that one head is always attached to the microtubule while the other is detached and moving further along the track, in the direction of movement. The proposed molecular mechanism underlying this processive motion has been highly debated. One controversial point has been how an operation called "gating" proceeds, that is, how the ATPase cycle of a kinesin head is stalled until a specific binding or conformational change needed for

motility occurs. On page 120 of this issue, Alonso *et al.* (2) show that a microtubule track is not necessary for such gating to occur. This throws a surprising wrench into existing models of kinesin movement and suggests that the track is not required to pro-

A mechanism that controls the stepwise movement of a molecular motor along a filamentous microtubule track in the cell does not seem to require the track itself.

duce the nonequivalence of the heads that is needed for processive movement.

The first indication of a gate with either a monomer or dimer of kinesin (one or two heads, respectively) was that steady-state ATP hydrolysis rates are low unless microtubules



Kinesin's gates. Kinesin has two motor domains (heads; red and yellow) joined by a coiled coil. A tethered intermediate of kinesin (shown in one possible conformation) is gated if release of ADP from one head is blocked. ATP can bind and trigger interchange of heads that bind to a microtubule track. This is coupled to release of ADP, hydrolysis of ATP, and release of phosphate (Pi). Alonso *et al.* find that soluble tubulin also has a gate that blocks binding of another tubulin molecule and release of the second ADP. This gate can also be opened by ATP.

The author is in the Department of Biological Science, Carnegie Mellon University, Pittsburgh, PA 15213, USA. E-mail: ddh@andrew.cmu.edu

are present (3). This gate, much like a checkpoint, occurs because adenosine diphosphate (ADP) release from kinesin is very slow (gate closed) until binding of a microtubule to the kinesin-ADP complex opens the gate (4). Alonso *et al.* show that this gate can also be opened by soluble tubulin heterodimers, the protein constituent of microtubules.

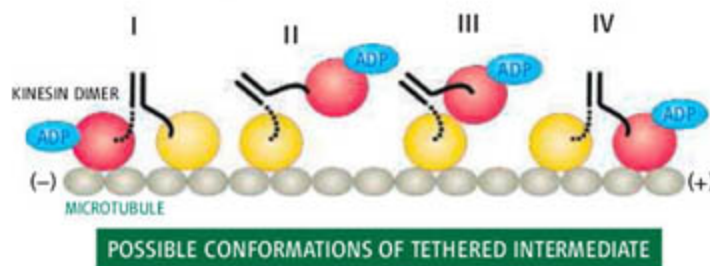
Another gate coordinates the actions of both heads. When kinesin, with ADP bound to each head, associates with a microtubule, only half the ADP is released (5) and a “tethered intermediate” forms, with one head attached tightly to the microtubule in the nucleotide-free form and the other head retaining its bound ADP. This gate prevents further progress until ATP binds to the nucleotide-free head and allows ADP release from the tethered head to occur—a so-called “ATP waiting state” (see the first figure). ATP hydrolysis returns the dimer to the same ATP waiting state, but with the roles of the heads reversed and with net movement of one binding site in the direction of movement (toward the plus end of the polarized microtubule track).

A reasonable explanation for the failure of the tethered intermediate to release the second ADP is that constraints of kinesin’s dimer interface prevent the tethered head from also interacting productively with the microtubule to induce rapid ADP release. But Alonso *et al.* show that even soluble tubulin heterodimers that are freely available for binding (not restricted within a track structure) cannot open this gate. However, the gate can still be opened by the addition of ATP or a nonhydrolyzable ATP analog.

These new results bear on unresolved issues about the conformation of the tethered intermediate and the mechanism that controls the gate. Four possible conformations for the tethered intermediate can be considered (see the second figure). All have one nucleotide-free head tightly associated with the microtubule but differ in the position of the tethered head, which contains ADP and is free or weakly bound to the microtubule. In two cases, the tethered head with ADP is held off the surface of the microtubule, with either considerable diffusional freedom (state II) or docked against the other head that is attached to the track (state III). In both cases, the microtubule should not stimulate release of ADP from the tethered head because there is no contact between them.

Reasons for proposing why the two other possible conformations cannot release ADP must be more subtle because the tethered head is actually in contact with the microtubule,

albeit weakly and reversibly, permitting rapid dissociation if not tethered to the microtubule by the strongly attached head. Rice *et al.* (6) reported that the position of the neck linker region that joins the head to the coiled coil dimerization region of kinesin is coupled to nucleotide binding. In that analysis, the lead head (closest to the plus end of the microtubule) can release ADP because its neck linker is directed backward. The trailing head cannot release ADP because its neck linker is directed forward (state I). A less likely conformation (state IV) orients the neck linkers in opposite direction. Gating occurs in this model because the head in the trailing position is forced to have its neck linker directed toward the plus end of the track, and this ori-



In waiting. Shown are four possible conformations for the tethered intermediate of kinesin. Each state awaits binding to ATP.

entation is unfavorable for ADP release. Alonso *et al.* suggest this cannot be the mechanism because the gate is still present with soluble tubulin, which could bind to both heads without forcing the neck linker of either one into a conformation that is unfavorable for ADP release. Rather, the authors favor the conformation in which the tethered head, bound to ADP, does not contact the microtubule but is docked against the other head (state III). In this conformation, they ascribe the failure of kinesin to bind two soluble tubulin molecules to either a conformational change in the tethered head or to a steric conflict that prevents binding two tubulins in the absence of nucleotide on both heads.

The analysis of Alonso *et al.* is heavily influenced by electron microscopy of kinesin bound to microtubules in which density observed off the microtubule surface is attributed to the tethered head (state II) (7, 8). Others, however, report that both heads bind to a microtubule (states I or IV) and that any extra density off the microtubule surface is due to binding of a second layer of kinesin (9, 10). Evidence specifically for state I or IV also comes from the observed alternation of 16- and 0-nm “steps” that a head makes along a microtubule (11). This is consistent with state I or IV but not with state III, which would have more steps of similar length.

Additionally, gate-limiting ADP release does not apply to ATP synthesis. The tethered intermediate synthesizes ATP from ADP and inorganic phosphate at a rate that is 20 times as fast as that of a monomer (12). ATP synthesis requires microtubule contact, and the more rapid synthesis by dimers argues against an intermediate state in which a tethered head with ADP is not in contact with a microtubule for at least part of the time in the presence of phosphate. This favors state I, because the Rice *et al.* (6) model is consistent with more facile ATP synthesis when the neck linker is directed forward.

The experiments underlying these conflicting conclusions regarding the conformation of the tethered dimer each have their limitations. Fluorescence polarization experiments (13) favor state I, or IV during processive movement at saturating ATP concentrations, but the conformation of the ATP waiting state may be different. Measurements by fluorescence resonance energy transfer are consistent with state I (14), but do not exclude states II or III. Structural studies by electron microscopy require that the microtubule lattice be fully saturated with kinesin heads. However, heads often bind cooperatively (9, 15). Thus, the conformation of an isolated dimer on a bare tubulin lattice may be different from that in a localized region of interacting dimers packed together on the lattice. Clearly, kinesin has more stories to tell, and further work will be required to fully distinguish between the different possible intermediary states.

References

1. C. J. Lawrence *et al.*, *J. Cell Biol.* **167**, 19 (2004).
2. M. C. Alonso *et al.*, *Science* **316**, 120 (2007).
3. S. A. Kuznetsov, V. I. Gelfand, *Proc. Natl. Acad. Sci. U.S.A.* **83**, 8530 (1986).
4. D. D. Hackney, *Proc. Natl. Acad. Sci. U.S.A.* **85**, 6314 (1988).
5. D. D. Hackney, *Proc. Natl. Acad. Sci. U.S.A.* **91**, 6865 (1994).
6. S. Rice *et al.*, *Nature* **402**, 778 (1999).
7. K. Hirose, J. Lowe, M. Alonso, R. A. Cross, L. A. Amos, *Mol. Biol. Cell* **10**, 2063 (1999).
8. I. Arnal, R. H. Wade, *Structure* **6**, 33 (1998).
9. A. Hoenger *et al.*, *J. Mol. Biol.* **297**, 1087 (2000).
10. A. Hoenger *et al.*, *Biol. Chem.* **381**, 1001 (2000).
11. A. Yildiz, M. Tomishige, R. D. Vale, P. R. Selvin, *Science* **303**, 676 (2004).
12. D. D. Hackney, *Proc. Natl. Acad. Sci. U.S.A.* **102**, 18338 (2005).
13. A. B. Asenjo, N. Krohn, H. Sosa, *Nat. Struct. Mol. Biol.* **10**, 836 (2003).
14. M. Tomishige, N. Stuurman, R. D. Vale, *Nat. Struct. Mol. Biol.* **13**, 887 (2006).
15. A. Vilfan *et al.*, *J. Mol. Biol.* **312**, 1011 (2001).

CHEMISTRY

Roots of Biosynthetic Diversity

David W. Christianson

With more than 50,000 compounds serving myriad functions in all forms of life, the terpenoids or isoprenoids are the most structurally and stereochemically diverse family of natural products found on Earth (1). Despite the complexity and magnitude of this chemical library—referred to as the terpenome—all terpenoid compounds ultimately derive from one or both of two simple precursors: isopentenyl diphosphate (IPP) and dimethylallyl diphosphate (DMAPP) (see the first figure) (2). These molecules can be linked together in head-to-tail fashion by enzymes that catalyze chain-elongation reactions, or in a more irregular fashion by enzymes that catalyze cyclopropanation, branching, or cyclobutane reactions. On page 73 of this issue, Thulasiram and co-workers provide compelling evidence that the metal-dependent synthases that catalyze these fundamental coupling reactions diverged from a common ancestor early in the evolution of terpenoid biosynthesis (3).

The authors created a series of “chimeric” proteins—artificial enzymes constructed by replacing segments of a synthase involved in chain elongation with corresponding segments from another synthase involved in cyclopropanation. The synthases in question are farnesyl diphosphate synthase (FPPase), which catalyzes the chain-elongation reaction with IPP and DMAPP, and chrysanthemyl diphosphate synthase (CPPase), which catalyzes the cyclopropanation reaction between two DMAPP molecules (see the first figure).

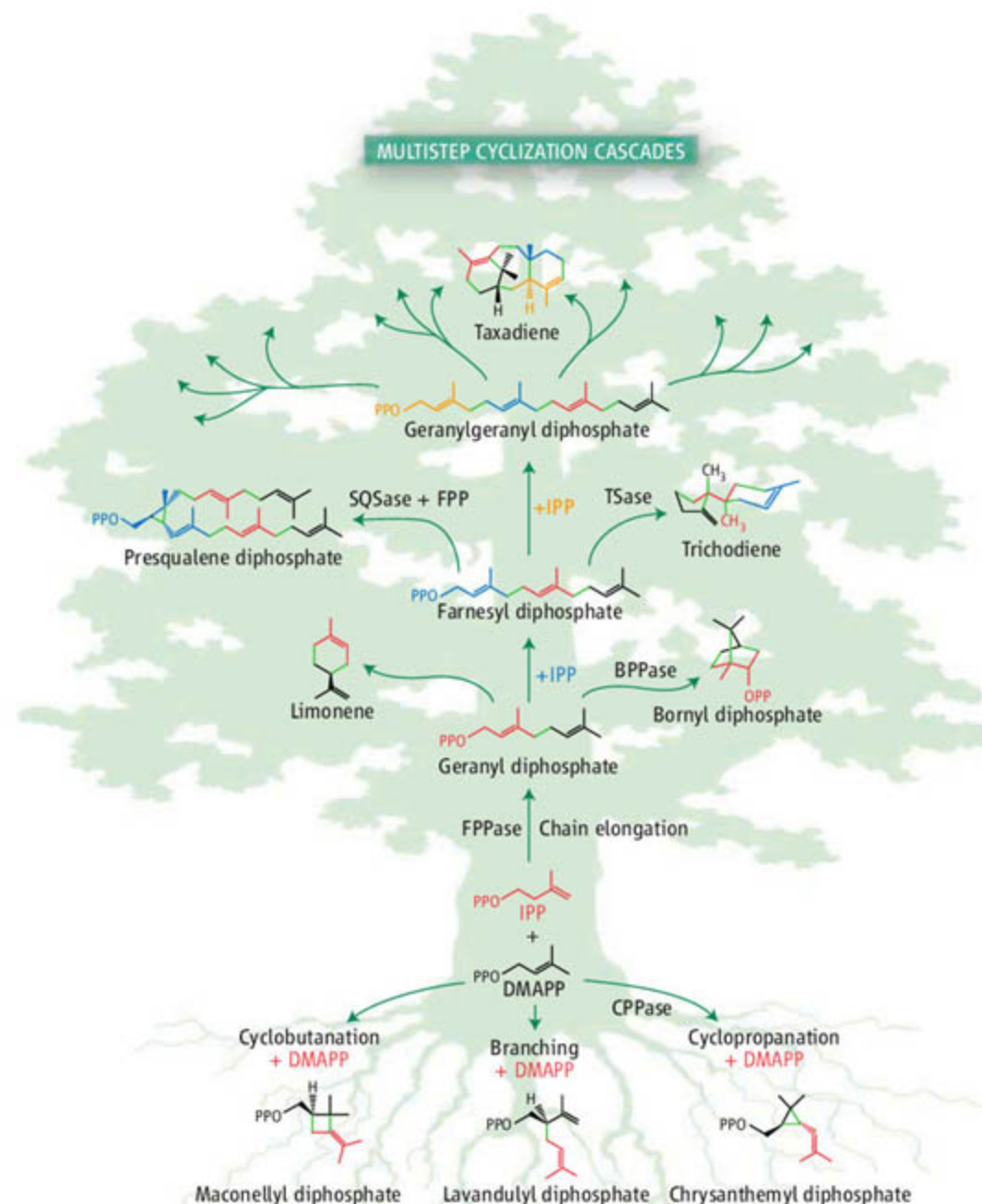
The structures of FPPases shed light on how terpenoid synthases are able to generate and manipulate highly reactive carbocation intermediates in catalysis. The first structure, of avian FPPase, showed that this distinctive chemistry is facilitated in a hydrophobic active-site cleft nested within an α -helical fold (4). Further insight into the mechanism of chain elongation has been gained from the structure of *Escherichia coli* FPPase complexed with IPP and an unreactive DMAPP analog, showing that the active-site contour is a template that binds the flexible isoprenoid reactants with the proper orientation and conformation for catalysis (5). The α -helical fold of CPPase from snowfield sagebrush shows

75% sequence identity to that of FPPase from the same species, yet catalyzes a different chemical reaction.

The CPPase-FPPase chimeras exhibit remarkable trends in biosynthetic versatility. For example, as the chimeras become increasingly CPPase-like and are incubated with IPP and DMAPP, chain-elongation activity shifts from

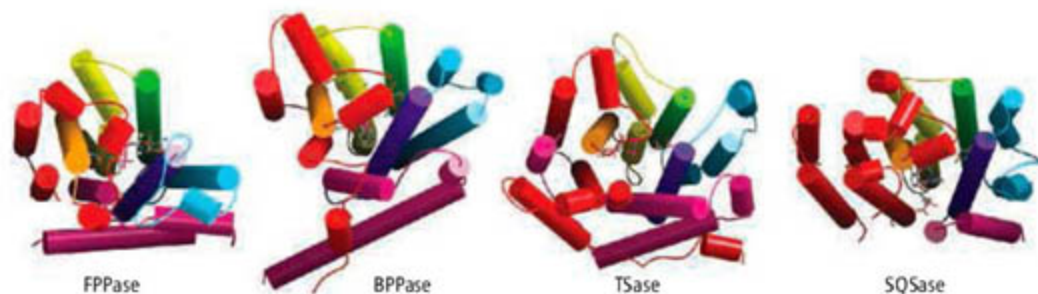
Terpenoid synthases generate an extraordinarily diverse set of natural products. Evolution of these enzymes from a common α -helical ancestor has resulted in profound changes in activity.

the generation of 15-carbon to 10-carbon products, and chimeras that are predominantly CPPase-like generate 10-carbon cyclopropanation and branching products. When incubated solely with DMAPP, cyclobutane products are generated by chimeras that are predominantly FPPase-like, a cyclopropanation product is generated by chimeras that are predomi-



Complexity from simple roots. Family tree of terpenomic diversity (2), showing examples of 10-, 15-, 20-, and 30-carbon natural products generated by terpenoid synthases that share the FPPase fold. Isoprene groups are colored to trace their biosynthetic fates; newly formed carbon-carbon bonds are in green. Thulasiram and co-workers show that the α -helical FPPase fold can be mutated in CPPase-FPPase chimeras to catalyze all four coupling reactions at the base of the tree. BPPase, bornyl diphosphate synthase; PPO, diphosphate; SQSase, squalene synthase; and TSase, trichodiene synthase.

The author is in the Roy and Diana Vagelos Laboratories, Department of Chemistry, University of Pennsylvania, Philadelphia, PA 19104, USA. E-mail: chris@sas.upenn.edu



A shared fold. FPPase from *E. coli* (5) is colored violet-red, representing the successively larger domains of CPPase substituted for FPPase in the sagebrush CPPase-FPPase chimeras reported by Thulasiram *et al.* For example, the c69f chimera contains the violet domain of CPPase and the blue-red domains of FPPase, and so on. The α -helical fold of FPPase is also shared by terpenoid synthases that generate larger and more complex products (6–9). The chemistry (3) and structural biology (6–9) of these synthases suggest divergence from a common α -helical ancestor in the evolution of terpenoid biosynthesis.

nantly CPPase-like, and a branching product is generated by all CPPase-FPPase chimeras.

The CPPase-FPPase chimeras are biosynthetically more promiscuous than either native CPPase or FPPase as a result of a reshaped template for substrate binding, which permits alternative trajectories for intermolecular carbon-carbon bond formation. Such promiscuity portends evolution: Given that the FPPase fold is readily evolvable to catalyze all four of the fundamental isoprenoid coupling reactions, native synthases catalyzing these reactions such as squalene synthase (SQSase, see the figures) (6) likely diverged from an FPPase-like ancestor.

A family of terpenoid cyclases that generate cyclic and polycyclic compounds also shares the FPPase fold (see the second figure) (7–9). These enzymes bind a flexible isoprenoid diphosphate substrate with the proper conformation for an intramolecular cycliza-

tion cascade that typically proceeds through multiple carbocation intermediates. Some terpenoid cyclases are high-fidelity templates that chaperone reactive substrate and intermediate conformations to generate a single product, but others tolerate a surprising degree of biosynthetic promiscuity and thereby reflect significant evolutionary potential. For example, γ -humulene synthase generates 52 different products from substrate farnesyl diphosphate (10). However, mutation of different groups of three to five active-site residues reshapes the template, thereby decreasing the overall number of products and altering the main product formed (11). The products of other sesquiterpene cyclases can also be changed through active-site mutations (12).

Thus, a recurring theme among the greater family of terpenoid synthases is that only a few amino acid substitutions are sufficient to

reshape the active-site template and change the resulting reaction product or products. Moreover, the promiscuous activities of terpenoid synthases introduced by nature (10) or by design (3, 11, 12) should enable further evolution—both in the test tube and in nature—of an ever-expanding array of natural products, with virtually limitless potential in chemistry, biology, and medicine.

References and Notes

1. D. E. Cane, Ed., *Isoprenoids, Including Carotenoids and Steroids*, vol. 2, *Comprehensive Natural Products Chemistry*, D. H. R. Barton, K. Nakanishi, O. Meth-Cohn, Eds. (Elsevier, Oxford, 1999).
2. J. C. Sacchettini, C. D. Poulter, *Science* **277**, 1788 (1997).
3. H. V. Thulasiram, H. K. Erickson, C. D. Poulter, *Science* **316**, 73 (2007).
4. L. C. Tarshis, M. Yan, C. D. Poulter, J. C. Sacchettini, *Biochemistry* **33**, 10871 (1994).
5. D. J. Hosfield *et al.*, *J. Biol. Chem.* **279**, 8526 (2004).
6. J. Pandit *et al.*, *J. Biol. Chem.* **275**, 30610 (2000).
7. D. W. Christianson, *Chem. Rev.* **106**, 3412 (2006).
8. D. A. Whittington *et al.*, *Proc. Natl. Acad. Sci. U.S.A.* **99**, 15375 (2002).
9. M. J. Rynkiewicz, D. E. Cane, D. W. Christianson, *Proc. Natl. Acad. Sci. U.S.A.* **99**, 13543 (2001).
10. C. L. Steele, J. Crock, J. Bohlmann, R. Croteau, *J. Biol. Chem.* **273**, 2078 (1998).
11. Y. Yoshikuni, T. E. Ferrin, J. D. Keasling, *Nature* **440**, 1078 (2006).
12. B. T. Greenhagen, P. E. O'Maille, J. P. Noel, J. Chappell, *Proc. Natl. Acad. Sci. U.S.A.* **103**, 9826 (2006).
13. I thank the NIH (grant GM56838) and the Biotechnology and Biological Sciences Research Council (UK) for the Underwood Fellowship supporting my study at the University of Cambridge. I am grateful to D. E. Cane and T. Blundell for stimulating scientific discussions and to L. Di Costanzo, H. A. Gennadios, E. Y. Shishova, L. S. Vedula, and T. Zakharian for assistance with the figures.

10.1126/science.1141630

CHEMISTRY

High Bond Orders in Metal-Metal Bonding

Frank Weinhold and Clark R. Landis

What is a chemical bond, and how many bonds can be made between any two atoms? Each generation of chemists readdresses and refines such questions in the framework of its best current experimental and theoretical methods. Recent synthetic and computational advances in metal-metal bonding seem to extend the concept of bond order to surprising new levels. Such expansion of chemical valency is fueling a reconsideration of fundamental bonding

principles articulated by G. N. Lewis more than 90 years ago.

The advances in question are the quintuple bond of a recently synthesized dichromium species (1) and the hexuple bond proposed for W_2 (2). As was the case following Cotton's report in 1973 of the first metal-metal quadruple bond and West's synthesis in 1981 of the first Si-Si double bond, these species challenge anew our understanding of the meaning and limits of chemical valency and bond order. To chemists this is no minor matter. In Shaik's words, the chemical bond is a fundamental territory of chemistry, "the element from which an entire chemical universe is constructed" (3).

The recent discovery of high-order bonds between metal atoms raises fundamental questions about the nature of chemical bonding.

At a superficial level, bonding might describe anything that holds atoms together. However, chemists generally reject this term for weak or nonspecific atom-atom attractions (such as those resulting from gravitational or dispersion forces) that cannot withstand the jostlings of ambient thermal collisions or that do not exhibit the regularity of atomic valency patterns of the periodic table. "Putting grams in a bottle" is no longer a must for a chemically bonded species, but chemists generally demand sufficient robustness to permit characterization of its chemical and electronic structure. In Cotton's words, bond order is "how many electron pairs . . . play a signifi-

The authors are in the Department of Chemistry, University of Wisconsin, Madison, WI 53706, USA. E-mail: weinhold@chem.wisc.edu, landis@chem.wisc.edu

cant role in holding the atoms together" (4).

The notions of chemical valency and structural bonding were first developed by Kekulé and others in the 19th century. In 1916, these developments culminated in Lewis's formulation of his remarkable "shared electron pair" concept (5). Empirical data at the time indicated that two atoms may share up to six electrons to form single, double, or triple bonds. This concept was further enriched by Robinson, Ingold, and others with the introduction of two or more Lewis structures that "resonate" to describe a single molecular structure. A famous example is the dual-Kekulé representation of benzene as two resonating "cyclohexatriene" bond patterns with net 1.5 carbon-carbon bond order.

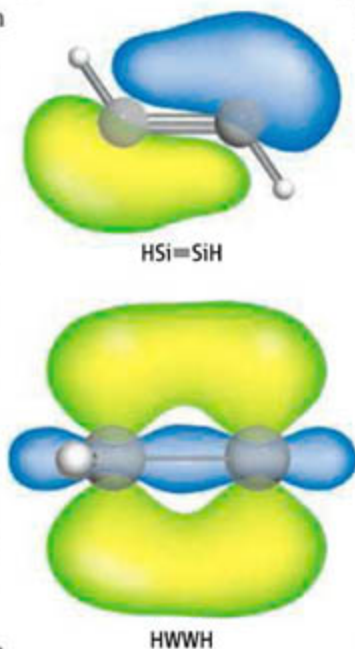
In the 1920s, Schrödinger's discovery of the wave equation and its application by Heitler and London to the H_2 molecule laid the basis for a rational theory of chemical bonding and associated phenomena. Yet despite these theoretical triumphs, the connection between quantum wave functions and the "pairing" and "sharing" of electrons that underlie Lewis-like chemical bonding were not immediately resolved.

Pauling initially combined the rather inaccurate Heitler-London ansatz with Lewis structure diagrams to create the valence bond (VB) method. In VB theory, two atoms share electron pairs in localized wave functions that are constructed from atomic valence orbitals, or combinations ("hybrids") of atomic orbitals. Thus, a connection between the Lewis and quantum viewpoints was forged. The directional features of orbitals limit the maximum number of bonds; although the carbon atom has four valence electrons and four valence orbitals, the directional qualities of the orbitals that lead to the strongest electron pair bond prevent a quadruple bond in dicarbon.

As numerical accuracy improved in the 1970s, the VB wave functions were found (6) to be inferior (except for H_2) to delocalized molecular orbital wave functions that appear to abandon the localized chemical bonding concept. As two leading practitioners expressed it, "The more accurate the calculations become, the more the concepts tend to vanish into thin air" (7), and "the supercomputer has dissolved the chemical bond" (8). Early bond-order metrics were devised to extract chemical meaning from computations,

but they were often plagued with nonorthogonality artifacts and unphysical limiting behavior. In some cases, bond order was simply a surrogate for bond length—an assumption based on a presumed mathematical relation between bond order and bond length derived from a few molecules (such as ethane, ethene, or ethyne). In this extreme, the bond-order concept ceases to have independent meaning, limits, or intellectual content.

More general and powerful tools of analysis were required to successfully recover chemical bonding and bond-order concepts from modern delocalized ab initio wave functions. The density matrix techniques pioneered by Löwdin (9) provided a rigorous basis



High-order bonding. Bonding orbital surfaces for the unusual "slipped" π bond of trans-bent $HSi=SiH$ (top) and the side-on δ bond of trans-bent, quintuply bonded $HWWH$ (bottom). These bonds exemplify unconventional orbital shapes that result from competition between forming the strongest σ bonds and retaining optimal orbital directionality for the higher-order bond components.

for expressing any wave function (including, in principle, exact solutions of Schrödinger's equation) in terms of intrinsic "natural" orbitals. (Natural orbitals are optimized combinations of basis set functions that provide maximum parsimony and minimal dependence on the details of numerical basis set selection in constructing molecular wave functions.) In addition, Pople and Lennard-Jones (10) demonstrated how one could rigorously transform the confusing delocalized molecular orbitals into equivalent localized molecular orbitals that recover the expected Lewis bond pattern.

In the 1980s, the more general natural bond orbital (NBO) (11) and natural resonance theory (NRT) (12) methods were developed for extracting the optimal Lewis structure(s) and quantifying the density error in this (or any chosen alternative) bonding pattern. For a wide range of organic and inorganic species, NRT bond orders are found to be in excellent agreement with expected empirical values, including the near-integer total valency values associated with periodic table assignments.

Assigned bond orders conjure up powerful imagery in the minds of chemists. For example, the formula $HX\equiv XH$ (where X is a group 14 element such as carbon or silicon) strongly

suggests a linear geometry, unusually strong XH bonds, and high reactivity of the "unsaturated" triple bond. No wonder the consternation when the first stable $Si\equiv Si$ species was reported to adopt a planar, but nonlinear, trans-bent geometry (13)! Is this a true triple bond? Theoretical studies (14) support the notion that three pairs of electrons contribute significantly to holding the atoms together. Rather than form one σ bond and two equivalent π bonds as in carbon-carbon triple bonds, the high preference for p-atomic orbital character in the Si-Si σ bond leads to one normal π bond, one "slipped" π bond, and a trans-bent geometry (see the figure, top panel).

Transition metals, which have six valence atomic orbitals (one s and five d), offer greater opportunities for electron pair sharing.

The HMMH bimetallic hydrides (where M = Cr, Mo, or W) were theoretically predicted (15) to exhibit quintuple bonding and strong trans-bent geometry, as was later found in the synthesized chromium derivative (1).

From the 14 total valence electrons of HMMH, five shared electron pairs hold the two metals together and the remaining two pairs make the M-H bond. The quintuple bond comprises familiar σ , 2π , and δ bond orbitals. The final bond is constructed from a side-on bonded pair of sd-hybridized orbitals (see the figure, bottom panel). Again, the σ -skeletal requirements enforce the trans-bent geometry and significant barriers to rigid rotation about the M-M bond.

Is there a limit to how many electron pairs may hold two atoms together? For the transition metals, the limit seems to be six as a result of the dominance of the s and d atomic orbitals in bonding interactions. In principle, actinide elements might use a larger set of s, d, and f valence atomic orbitals, suggesting as many as 13 possible bonds. However, Roos *et al.* (2) find that weak bonding interactions and promotion effects limit the effective bond orders (which maximize at diatomic Pa_2) to five or less. Poor matches in the radial extents of the s, d, and f orbitals make use of all actinide valence orbitals in the formation of bonds unfavorable. It seems safe to say, at least until new experiments or improved calculations prove otherwise, that six is the maximum number of electron pairs that hold two atoms together.

The discovery of new high-order metal-metal bond motifs signals a landmark in synthetic methodology and a renaissance of

Lewis-like structural concepts in inorganic chemistry. Future synthetic and computational explorations should be guided by closer attention to the maximally matched donor-acceptor interactions that lead to favorable Lewis-like bonding patterns.

References

1. T. Nguyen *et al.*, *Science* **310**, 844 (2005).

2. B. O. Roos, A. C. Borin, L. Gagliardi, *Angew. Chem. Int. Ed.* **46**, 1469 (2007).

3. S. Shaik, *J. Comput. Chem.* **28**, 51 (2007).

4. F. A. Cotton, in *Multiple Bonds Between Metal Atoms*, F. A. Cotton, C. A. Muttillio, R. A. Walton, Eds. (Springer, New York, 2005), pp. 707–795.

5. G. N. Lewis, *J. Am. Chem. Soc.* **38**, 762 (1916).

6. J. M. Norbeck, G. A. Gallup, *J. Am. Chem. Soc.* **96**, 3386 (1974).

7. R. S. Mulliken, *J. Chem. Phys.* **43**, 52 (1965).

8. B. Sutcliffe, *Int. J. Quantum Chem.* **58**, 645 (1998).

9. P.-O. Löwdin, *Phys. Rev.* **97**, 1474 (1955).

10. J. A. Pople, J. Lennard-Jones, *Proc. R. Soc. London Ser. A* **202**, 166 (1950).

11. A. E. Reed, L. A. Curtiss, F. Weinhold, *Chem. Rev.* **88**, 899

(1988).

12. E. D. Glendening, J. K. Badenhoop, F. Weinhold, *J. Comput. Chem.* **19**, 628 (1998).

13. A. Sekiguchi, R. Kinjo, M. Ichinohe, *Science* **305**, 1755 (2004).

14. C. R. Landis, F. Weinhold, *J. Am. Chem. Soc.* **128**, 7335 (2006).

15. F. Weinhold, C. R. Landis, *Valency and Bonding* (Cambridge Univ. Press, Cambridge, 2005), pp. 555–559.

10.1126/science.1140756

PHYSICS

So Small Yet Still Giant

Igor V. Lerner

Although electronic devices keep shrinking toward the nanometer scale of atoms, physicists still deal with many-particle systems in which tracing the paths of individual particles is beyond the reach of theory and experiment. Because of this, we have to rely on a statistical approach. Conventional wisdom, inherited from 19th-century statistical physics, says that physical measurements on a given sample are well described by averaging over an ensemble of identical samples.

This notion became obsolete more than two decades ago, however, with the prediction of reproducible conductance fluctuations (i.e., variations from sample to sample) in “mesoscopic” structures with dimensions intermediate between atoms and bulk matter (1, 2). These fluctuations do not decrease with sample size (as they should in classical physics) but still remain much smaller than the average conductance. On page 99 of this issue, Price *et al.* (3) report the observation of the Coulomb drag (4) in a bilayer system at very low temperatures where the reproducible fluctuations of the drag turn out to be much larger than its average value. Thus, the authors have discovered mesoscopic fluctuations that, in contrast to the conductance fluctuations, fully govern the effect rather than give corrections to it—a very unusual situation in statistical physics. In carrying out this work, they have developed a new tool for studying the wave-like behavior of electrons in solids.

Mesoscopic fluctuations exist because quantum mechanics reigns not only at microscopic scales, as had always been expected, but at the much larger mesoscopic scale, de-

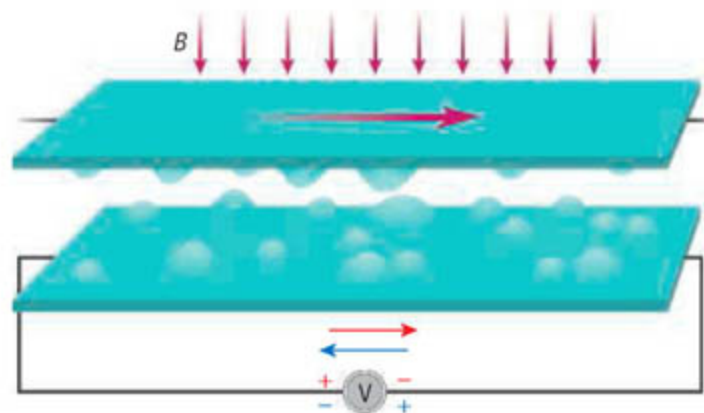
fining as the scale over which the phase coherence of electron quantum waves is maintained. This scale increases as the temperature T decreases, reaching hundreds of nanometers at $T \sim 1$ K. For these temperatures, the wave nature of electrons reveals itself in the interference between waves going along different paths as a result of scattering from impurities. This leads to an irregularly oscillating but reproducible dependence of the sample conductance on magnetic field or electron concentration.

In metallic materials, these conductance fluctuations are always very small. Price *et al.* have made an experimental breakthrough by measuring the Coulomb drag at a temperature so low that this effect is suppressed on average and is governed by the fluctuations. The dominant role of the fluctuations in the Coulomb drag at very low temperatures was recently predicted theoretically (5); however, the observed effect turns out to be four orders of magnitude higher than the prediction. Thus, these fluctuations can truly be called giant, although they are still an order of magnitude smaller than the intralayer conductance fluctuations.

The Coulomb drag effect studied by Price *et al.* occurs between two close but spatially separated layers of electrons, when an electrical current flowing through the “active” layer induces a voltage in the second “passive” layer. It works via Coulomb friction: Electrons

An analysis of currents confined to layers in a semiconductor structure reveals information about electron-electron interactions.

in the active layer scatter from electrons in the passive layer, transferring momentum to them and thus dragging them in the same direction until the resulting intralayer electrostatic force equals the dragging force. Much experimental effort has been spent to study it under different conditions, although up to now these studies



Coulomb drag and its fluctuations. An electric current in the upper layer drags electrons and holes in the bottom layer, resulting in the electron and hole currents in opposite directions. The net flow, which is due to the electron-hole asymmetry, is detected by a voltmeter V . At low temperatures, the main reason for the asymmetry is the wave nature of electrons revealed in random interference patterns in the local densities of states due to scattering in both layers. This makes the direction of the drag force unpredictable, leading to its random but reproducible fluctuations in an external magnetic field B that changes the electron interference pattern in both layers.

were largely limited to the drag effect at relatively high T where its fluctuations were unobservable.

The first experimental observations of Coulomb drag (6–8) took place more than 10 years after it had been theoretically predicted three decades ago (9). One of the reasons for such a long delay is that the drag effect is very small. Partly, this is due to a very weak Coulomb coupling between the layers: Momentum transfer between the layers is very inefficient. But quantum mechanics is the

main culprit and takes the blame for the suppression of the effect.

The reason is that electrons are fermions, and the Pauli exclusion principle at the heart of quantum mechanics tells us that two identical fermions cannot coexist. At zero temperature, therefore, each state can either hold one electron or remain empty; because lower-energy states are filled up first, all the states are occupied up to a certain level, the Fermi energy ϵ_F , while the states above this level remain empty. Thus, the drag effect is possible only at a finite temperature T , when in both layers the states around ϵ_F become only partially occupied (that is, electrons are kicked out by thermal energy and can be scattered among the states). Furthermore, charge carriers in the active layer from both positively charged holes below ϵ_F and negatively charged electrons above ϵ_F in the passive layer, dragging both in the same direction. Had the electron and hole states been totally symmetric, positive and negative flows would exactly cancel each other, resulting in no drag effect whatsoever.

Thus, the drag effect exists only as a result of the electron-hole asymmetry. On average, the asymmetry is due to a slightly different energy distance of the electron and hole states from the bottom of the Fermi sea. Thus, the asymmetry is small and so is the Coulomb drag. The sign of the effect is positive with the net flow of charge carriers in the passive layer

being in the same direction as the current in the active layer.

However, the density of states (the number of energy levels per unit of energy) also fluctuates in the mesoscopic regime (10). This led to the suggestion (5) that at low enough temperatures the Coulomb drag force could become random, governed by the electron-hole asymmetry due to the fluctuations. The net sign of the effect then becomes random (see the figure). This was expected to be observable only for quite small samples with considerable disorder, where the magnitude of the fluctuations in conductance and density of states within one layer approaches the average.

Price *et al.* courageously ventured to measure the effect in a relatively large and relatively clean sample where the intralayer fluctuations are tiny. The random drag resistance measured by Price *et al.* is small, but it is still four orders of magnitude higher than predicted. The authors have proposed a plausible qualitative explanation for such a dramatic enhancement. In their samples, the electron mean free path for impurity scattering in each layer is much larger than the separation between the layers, so that only large momentum transfer from the active to the passive layer is effective for the drag. As a result, the electron-hole asymmetry is contributed only by fluctuations in the local density of states known to be much bigger (11) than those in the density of states of aver-

aged over the entire sample. The drag temperature dependence is very specific for such a mechanism, and the authors show that it is in a good agreement with the measurements.

The fluctuational Coulomb drag effect results from the interplay of the interlayer electron-electron interactions and the interlayer quantum coherence effects. This phenomenon is a sensitive tool to help us learn more about the electron-electron interactions in different materials and structures. Without doubt, the first observation of this effect by Price *et al.* opens a new direction in studying the fundamental properties of electrons in solids at very low temperatures.

References and Notes

1. B. L. Altshuler, *JETP Lett.* **41**, 648 (1985).
2. P. A. Lee, A. D. Stone, *Phys. Rev. Lett.* **55**, 1622 (1985).
3. A. S. Price *et al.*, *Science* **316**, 99 (2007).
4. This effect is so-named because it refers to a current of electrons in one layer "dragging" a current in the other layer through electrical (Coulomb) forces.
5. B. N. Narozhny, I. L. Aleiner, *Phys. Rev. Lett.* **84**, 5383 (2000).
6. P. M. Solomon, P. J. Price, D. J. Frank, D. C. La Tulipe, *Phys. Rev. Lett.* **63**, 2508 (1989).
7. T. J. Gramila, J. P. Eisenstein, A. H. MacDonald, L. N. Pfeiffer, K. W. West, *Phys. Rev. Lett.* **66**, 1216 (1991).
8. U. Sivan, P. M. Solomon, H. Shtrikman, *Phys. Rev. Lett.* **68**, 1196 (1992).
9. M. B. Pogrebinskii, *Sov. Phys. Semicond.* **11**, 372 (1977).
10. B. L. Altshuler, B. I. Shklovskii, *Sov. Phys. JETP* **64**, 127 (1986).
11. I. V. Lerner, *Phys. Lett. A* **133**, 253 (1988).

10.1126/science.1141972

APPLIED PHYSICS

Searching for a Solid-State Terahertz Technology

Mark Lee and Michael C. Wanke

The range of frequencies around 1 terahertz (THz = 10^{12} cycles per second) is like the neglected middle child in the electromagnetic spectrum. Both microwaves (<0.1 THz) and infrared radiation (>20 THz) are used widely, thanks to the combination of high technical performance and mass-produced solid-state microelectronics. Caught in between, the THz spectrum has yet to be used in a mature solid-state device. The pace of recent advances gives hope, however, for a viable THz technology that would permit such applications as sen-

sors for fast, high-specificity chemical detection and new modes of biological and medical imaging.

Microwave electronics ultimately fail at higher frequencies because of fundamental electron velocity limits, causing transistor performance to degrade rapidly above ~0.1 THz. At the other end of the spectrum, infrared photonics cannot be extended down to frequencies less than about 20 THz. Perversely, atmospheric attenuation of THz radiation is also much stronger than for microwave or infrared, leading to far more stringent requirements on signal-to-noise performance in this THz technology gap.

Nevertheless, the impetus to develop a technically practical and economically feasi-

Advances in device fabrication are facilitating production and detection of electromagnetic radiation at terahertz frequencies.

ble THz technology infrastructure has arguably never been stronger than it is now. As reviewed by Borak (1), the characteristic interactions of THz radiation with various forms of matter can lead to new applications. Laboratories worldwide have carried out proof-of-principle demonstrations to show how THz can be used in rapid-but-precise hazardous chemical sensing, concealed weapon detection, noninvasive medical and biological diagnostics, and high-speed telecommunications. To get such THz applications out of the laboratory and into common use will require elevating the THz microelectronic technology base to be on a par with microwave electronics and infrared photonics.

The authors are at Sandia National Laboratories, Albuquerque, NM 87185-1082. E-mail: mcwanke@sandia.gov

A generic THz application requires two main components: a coherent THz source and a THz detector. This THz source/detector combination must provide sufficient signal-to-noise and speed performance to detect, usually at "real-time" rates (100 Hz to 1 kHz), a signal that has propagated through the atmosphere. As a result, the primary goals of solid-state THz source and detector device research are increasing average source power and decreasing detector noise.

Solid-state THz detector devices have proven to be quite capable in many regards. If one is willing to operate at temperatures near liquid helium (~4 K), several types of superconductor and semiconductor detectors have been developed for research situations. However, the need for such cooling is generally seen as an insurmountable obstacle to broad acceptance outside the research lab. For this reason, researchers are keen to develop THz detectors that operate at or closer to room temperature.

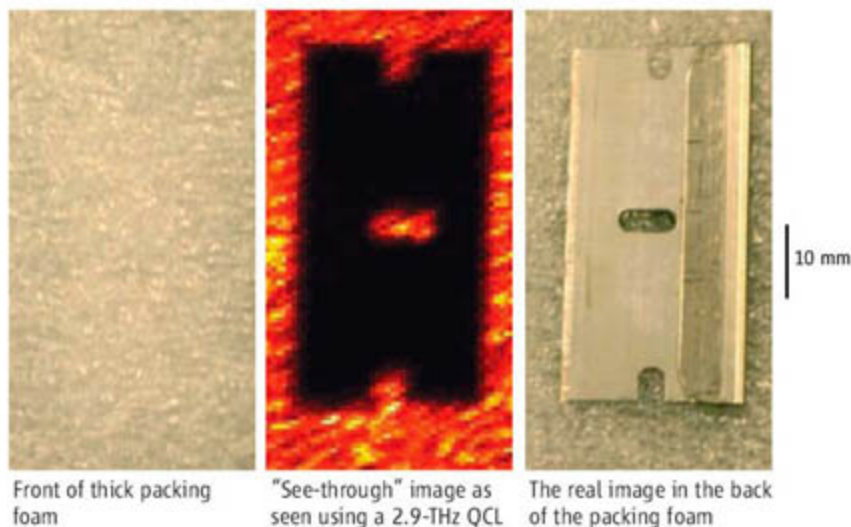
For example, current work in high electron mobility transistors has sought to circumvent electron speed limits by using collective charge-density

oscillations, known as plasmons, instead of individual electrons as the charge carriers. Plasmon wave velocities in a semiconductor channel can be 10 times as high as electron velocities, similar to how water waves travel much faster than the water molecules in the wave. THz response has recently been observed in various forms of plasmonic transistors up to room temperature in submicrometer channel length devices and near liquid nitrogen temperature (77 K) in millimeter-length devices (2, 3).

In another example, NASA's Jet Propulsion Laboratory applied modern nanolithography methods to a classic microwave device, the metal-semiconductor Schottky diode, to fabricate mixers (which can be used to measure power spectra around a reference frequency) that operate to at least 3 THz (4). These receivers operate at ambient temperature, have low enough noise for most conceivable applications, and have proven robust enough to travel onboard NASA's Earth-observing Aura satellite. The chief drawback is that these devices

require 5 to 10 mW from a THz source to function optimally.

This milliwatt power requirement lies at the heart of the THz solid-state technology problem. Realistic estimates of the THz source power needed to deliver acceptable signal-to-noise ratios outside a controlled research environment usually lead to the conclusion that tens of milliwatts are desired. Until 2002, the only coherent THz oscillators capable of average power much greater than 1 mW were vacuum tube-based or accelerator sources, such as molecular gas lasers and backward-wave oscillators that are large, finicky, and expensive.



Cutting-edge imaging. Terahertz imaging could be used for detecting concealed weapons, among other applications. (Left) Front of packing foam. (Middle) Image of hidden razor blade taken with 2.7-THz quantum cascade laser operating at a few milliwatts. (Right) Back of foam with concealed object.

A revolutionary advance in THz solid-state source technology came in 2002 when Kohler *et al.* reported successful operation of a quantum cascade laser (QCL) at THz frequencies (5). The QCL evades semiconductor band-gap limitations on photonic devices by using sophisticated semiconductor heterostructure engineering and fabrication methods to create synthetic electron energy gaps at frequencies much smaller than those that nature provides. Since 2002, THz QCLs have progressed rapidly in frequency coverage, increased power output, and increased operating temperature. Currently, they are the only solid-state source capable of generating >10 mW of coherent average power above 1 THz, with record continuous wave power of 138 mW near 4.4 THz and an operation temperature of 10 K (6, 7). The output power of QCLs drops as the temperature increases, but milliwatts can still be obtained at liquid nitrogen temperature, and submilliwatt laser operation has been achieved up to 164 K. To date, THz QCLs have spanned the frequency range between 1.5 and 4.5 THz.

Competing all-solid-state THz sources cannot currently meet the several milliwatt average power threshold but may exhibit other useful features. Frequency multipliers for use with high-power microwave sources are a mature and compact technology that operates at room temperature and can be easily tuned over wide frequency ranges from roughly 0.1 to 1 THz. However, intrinsic conversion losses for large frequency multiplication factors and difficulties in handling large input powers cause a multiplier's power output to drop rapidly with increasing output frequencies, so that only about 10 μ W are available near 1 THz (8). Similarly, obtaining lower frequencies by mixing two solid-state near-infrared lasers on a photoconductive semiconductor switch at room temperature produces very broadly tunable power up to a few THz but currently exhibits only microwatts or less of average power above 1 THz (9). Recently, a record peak pulse power of 100 W was demonstrated in a p-doped germanium (p-Ge) laser near 2.7 THz. Unfortunately, current p-Ge lasers typically require large magnetic fields, temperatures below 15 K, and a very low duty cycle to operate (10).

Current research in solid-state THz technology emphasizes individual component development.

The present focus is on improving detector sensitivity, source power, and operating temperature with microelectronic materials and methods that are ultimately amenable to large-scale production. Should this work progress at its current pace, this part of the spectrum will become as useful as the microwave and infrared frequency bands are today.

References and Notes

1. A. Borak, *Science* **308**, 638 (2005).
2. E. A. Shaner *et al.*, *IEEE Photonics Tech. Lett.* **18**, 1925 (2006).
3. R. Tauk *et al.*, *Appl. Phys. Lett.* **89**, 253511 (2006).
4. P. H. Siegel *et al.*, *IEEE Trans. Microwave Theory Tech.* **47**, 596 (1999).
5. R. Köhler *et al.*, *Nature* **417**, 156 (2002).
6. B. S. Williams *et al.*, *Elec. Lett.* **42**, 89 (2006).
7. B. S. Williams *et al.*, *Optics Express*, **13**, 3111 (2005).
8. See, for example, www.virginiaiodides.com/multipliers.htm.
9. J. E. Bjarnason *et al.*, *Appl. Phys. Lett.* **85**, 3983 (2004).
10. R. E. Peale *et al.*, *J. Nanoelectron. Optoelectron.* **2**, 1 (2007).
11. Sandia is operated by Sandia Corporation, a Lockheed Martin Company, for the U.S. Department of Energy's National Nuclear Security Administration under contract DE-AC04-94AL85000.

10.1126/science.1141012

Atlantic Meridional Overturning Circulation During the Last Glacial Maximum

Jean Lynch-Stieglitz,^{1*} Jess F. Adkins,² William B. Curry,³ Trond Dokken,⁴ Ian R. Hall,⁵ Juan Carlos Herguera,⁶ Joël J.-M. Hirschi,⁷ Elena V. Ivanova,⁸ Catherine Kissel,⁹ Olivier Marchal,³ Thomas M. Marchitto,¹⁰ I. Nicholas McCave,¹¹ Jerry F. McManus,³ Stefan Mulitza,¹² Ulysses Ninnemann,¹³ Frank Peeters,¹⁴ Ein-Fen Yu,¹⁵ Rainer Zahn¹⁶

The circulation of the deep Atlantic Ocean during the height of the last ice age appears to have been quite different from today. We review observations implying that Atlantic meridional overturning circulation during the Last Glacial Maximum was neither extremely sluggish nor an enhanced version of present-day circulation. The distribution of the decay products of uranium in sediments is consistent with a residence time for deep waters in the Atlantic only slightly greater than today. However, evidence from multiple water-mass tracers supports a different distribution of deep-water properties, including density, which is dynamically linked to circulation.

In today's Atlantic Ocean, water more shallow than about 1 km flows northward while deeper water flows south, forming what is called a meridional overturning circulation (MOC) (Fig. 1A). The northward-flowing surface and intermediate waters lose buoyancy in the North Atlantic, where they are transformed into the southward-flowing North Atlantic Deep Water (NADW). This meridional circulation is considered an important element of the climate because of its attendant meridional heat flux; the northward-flowing surface waters are warm, whereas the southward-flowing deep waters are cold, so the MOC is accompanied by a net northward transport of heat in the Atlantic. The possibility that this overturning circulation could change in the future motivates us to understand how it may have differed in the past. The Last Glacial Maximum (LGM), a time interval centered at about 21,000 years ago and with a duration of a few millennia [e.g., (1)], was a

period during which the factors controlling the structure of the Atlantic MOC (e.g., freshwater budgets and atmospheric circulation in the northern and southern high latitudes) appear to have differed from today.

In the 1980s, a prominent community effort in the emerging field of paleoceanography provided evidence suggesting that this Atlantic overturning circulation may not have existed in its current form during the LGM. The nutrient-poor NADW seemed to have been replaced by higher-nutrient waters like those formed in the Southern Ocean today (2–5). Both theoretical studies (6) and ocean general circulation model experiments (7) suggested that the MOC may have multiple equilibria and that transitions between the equilibria may be triggered by anomalies in the freshwater fluxes at the sea surface.

A new generation of coupled ocean-atmosphere general circulation models has since been developed. When forced with estimated LGM atmospheric CO₂ concentration and continental ice sheets, these models produce widely different Atlantic circulation scenarios. Some show a stronger overturning cell associated with NADW formation either extending slightly deeper (8) or unchanged in vertical extent (9); others show a weaker and shallower overturning cell associated with NADW production (10, 11). Only when perturbed with enhanced freshwater fluxes to the North Atlantic, as presumably occurred in the past during brief periods of accelerated decay of the continental ice sheets, do the coupled models produce a shutdown of NADW (12, 13). The large freshwater fluxes capable of shutting down the Atlantic MOC in these models would not have been sustainable for the entire LGM. It is of more than academic interest to determine which models (if any) show the correct response to ice age conditions, as these are the same models that are used to predict

future changes in the Atlantic MOC resulting from increasing levels of carbon dioxide in the atmosphere. Here we review the currently available paleoceanographic data for the LGM and find support for an active circulation in the deep Atlantic, but not for the strong, deep MOC involving enhanced production of NADW in the northern North Atlantic.

Density Gradients in the Main Thermocline and Below

The tilt of the surfaces of equal seawater density between the western and eastern sides of the basin provides tangible evidence for a meridional overturning in the Atlantic Ocean today [e.g., (14)] (Fig. 2A). The very fact that these surfaces are not strictly horizontal suggests the existence of a vertical shear in the average meridional flow in the basin: For a fluid on a rotating planet, a zonal density contrast must be balanced by a vertical shear in the meridional motion to lowest order (the “thermal wind relationship”). The shear reflects a northward flow near the surface and southward flow below (i.e., a MOC) (15).

Seawater density depends on temperature, salinity, and pressure. Density at a given depth on either side of the Atlantic Basin in the past can be estimated from the ratio of oxygen isotopes, ¹⁸O/¹⁶O, in the fossil carbonate tests of benthic foraminifera, bottom-dwelling protists (16). This ratio reflects both the temperature and the ¹⁸O/¹⁶O ratio (which generally covaries with salinity in the upper ocean) of the seawater in which the foraminifera calcify (16, 17).

The density contrast across the width of the entire ocean basin reflects the vertical shear in the integrated meridional flow across the basin (18–20). In the South Atlantic at 30°S, density is higher along the eastern margin in the upper 2 km, reflecting the vertical shear in mass transport associated with the MOC (Fig. 2A). The benthic foraminifera from surface sediments reflect this contrast, with higher ¹⁸O/¹⁶O on the higher-density eastern margin (Fig. 2B). During the LGM, however, the cross-basin gradient in the oxygen isotopes of the foraminifera was reduced and perhaps even reversed (21) (Fig. 2C). The circulation that we see today (flow to the north above 1 km and to the south below this depth), or a similar overturning circulation with a shallower southward flow of NADW as in some of the model simulations for the LGM (10, 11), would require higher densities along the eastern margin than along the western margin in the upper 2 km of the South Atlantic. If the LGM relationship between the oxygen isotope ratio in the foraminifera and density was similar on both sides of the South Atlantic Basin (as it is today), these scenarios would be incompatible with the oxygen isotope data. Water masses with very different temperatures, salinities, and oxygen isotope ratios occupying the same density horizon on either side of the ocean basin could potentially cause a change in the oxygen isotope ratios

¹Georgia Institute of Technology, Atlanta, GA 30332, USA. ²California Institute of Technology, Pasadena, CA 91125, USA. ³Woods Hole Oceanographic Institution, Woods Hole, MA 02543, USA. ⁴Bjerknes Centre for Climate Research, 5007 Bergen, Norway. ⁵Cardiff University, Cardiff CF10 3YE, UK. ⁶CICESE, Oceanologia, 22860 Ensenada, Baja California, Mexico. ⁷National Oceanography Centre, University of Southampton, Southampton SO14 3ZH, UK. ⁸Shirshov Institute of Oceanology, Russian Academy of Sciences, Moscow 117997, Russia. ⁹Laboratoire des Sciences du Climat et de l'Environnement, CEA/CNRS/UVSQ, 91198 Gif-sur-Yvette Cedex, France. ¹⁰University of Colorado, Boulder, CO 80309, USA. ¹¹University of Cambridge, Cambridge CB2 3EQ, UK. ¹²Forschungszentrum Ozeanränder/MARUM, Universität Bremen, 28334 Bremen, Germany. ¹³Bjerknes Centre for Climate Research, University of Bergen, 5007 Bergen, Norway. ¹⁴Vrije Universiteit, 1081HV Amsterdam, Netherlands. ¹⁵National Taiwan Normal University, Taipei 116, Taiwan, Republic of China. ¹⁶Institució Catalana de Recerca i Estudis Avançats, Universitat Autònoma de Barcelona, E-08193 Bellaterra (Cerdanyola), Spain.

*To whom correspondence should be addressed. E-mail: jean@eas.gatech.edu

across the South Atlantic without a change in density contrast. These properties need to be better constrained before any circulation scenarios can be ruled out on the basis of the oxygen isotope data alone (21, 22).

Deep-Water Nutrient Properties

Surface waters sinking in the Greenland, Iceland, Norwegian, and Labrador seas collectively form the NADW, which is readily identifiable as a tongue of nutrient-poor water extending to great depths in the Atlantic and eventually reaching the Southern Ocean (Fig. 1A). Some high-nutrient water from the Southern Ocean (Antarctic Bottom Water, AABW) can be seen penetrating northward beneath the NADW. The nutrient distributions for times in the past are reconstructed by measuring the carbon isotopic composition ($^{13}\text{C}/^{12}\text{C}$) of fossil shells of benthic foraminifera buried in the sediments. Primary producers in the surface ocean take up both nutrients and carbon, discriminating against the heavy isotope of carbon as they do so, leading to high $^{13}\text{C}/^{12}\text{C}$ ratios in surface waters and low-nutrient water masses (e.g., NADW). Higher nutrient concentrations and lower $^{13}\text{C}/^{12}\text{C}$ in AABW reflect the longer time these waters have spent away from the surface, collecting nutrients and ^{13}C -poor carbon from the decay of organic matter transported to depth in particulate and dissolved forms. Past nutrient distributions have also been reconstructed from the ratio of cadmium to calcium in tests of benthic foraminifera. Like the major nutrients, Cd is taken up by organisms at the sea surface and released at depth as the organic material is decomposed. Both of these nutrient proxies ($^{13}\text{C}/^{12}\text{C}$ and Cd/Ca) show that during the LGM there was a low-nutrient water mass above a depth of about 2 km (often referred to as Glacial North Atlantic Intermediate Water, GNAIW) and high-nutrient waters below 2 km (23–27) (Fig. 1, B and C). There are multiple factors (air-sea exchange of carbon, carbonate saturation state, oxidation of organic matter in sediments) controlling the isotopic and chemical compositions of the foraminifera tests that can potentially decouple the nutrient proxies from nutrient distributions in

the open ocean (28). Nonetheless, the agreement between the reconstructions based on these two water-mass tracers provides increased confidence in the overall picture.

be rich in zinc, which supports the idea that some of this water mass comes from the Southern Ocean (29). However, the deep (>2 km) water mass does show higher $^{13}\text{C}/^{12}\text{C}$ and lower

Cd in the deep North Atlantic than in the deep South Atlantic; this finding suggests that waters originating in the North Atlantic also contributed to the deep (>2 km) water mass in the LGM Atlantic. This contribution may be simply the result of mixing between GNAIW—which may form as far south as the Labrador Sea or the subpolar open North Atlantic—and the deeper water mass originating in the south, or it may consist of the addition of small amounts of a distinct, denser water mass forming in the far North Atlantic (30).

Although the nutrient tracers provide a coherent picture of the distribution of water masses, they provide little information about the absolute rates of flow in the deep ocean. A fundamental reason is that the remineralization of organic matter has a relatively small effect on the nutrient concentration of deep waters in the Atlantic (at least today) and is relatively poorly understood.

Deep-Water Radiocarbon Activities

The rate of radioactive decay of ^{14}C is well understood and, in principle, could provide a measure of the rate of deep-water renewal or ventilation. Two approaches have been developed to correct past ^{14}C ages from carbonate that grew in the deep ocean for the time since their deposition. Radiocarbon measurements on benthic foraminifera can be corrected using ages of contemporaneous planktonic (surface-dwelling) foraminifera (31–33), and radiocarbon measurements on deep-sea corals can be adjusted using independent ages derived from uranium and thorium isotopes (34–36). Today, the radiocarbon distribution in the deep Atlantic mostly reflects the relative contributions of water from the north with high ^{14}C activity and water from the south with low ^{14}C activity, with only a small decrease in ^{14}C activity due

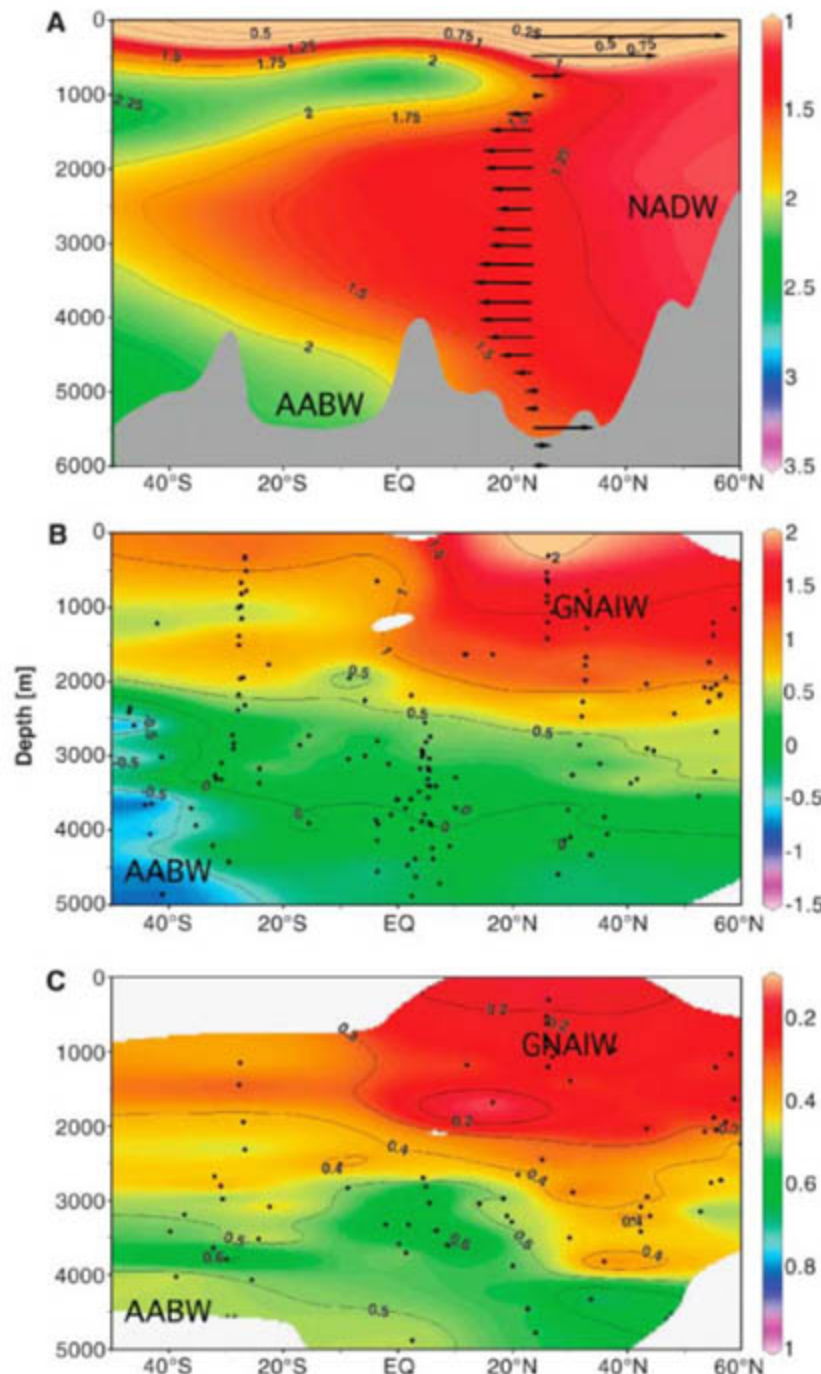


Fig. 1. (A) The modern distribution of dissolved phosphate ($\mu\text{mol liter}^{-1}$)—a biological nutrient—in the western Atlantic (61). Also indicated is the southward flow of North Atlantic Deep Water (NADW), which is compensated by the northward flow of warmer waters above 1 km, and the Antarctic Bottom Water (AABW) below. (B) The distribution of the carbon isotopic composition ($^{13}\text{C}/^{12}\text{C}$, expressed as $\delta^{13}\text{C}$, Vienna Pee Dee belemnite standard) of the shells of benthic foraminifera in the western and central Atlantic during the LGM (23, 24). Data from different longitudes are collapsed in the same meridional plane. (C) Estimates of the Cd (nmol kg^{-1}) concentration for LGM from the ratio of Cd/Ca in the shells of benthic foraminifera from (25). Today, the isotopic composition of dissolved inorganic carbon and the concentration of dissolved Cd in seawater both show “nutrient”-type distributions similar to that of PO_4 .

The LGM configuration is often interpreted as a shoaling of NADW and a northward extension of AABW in the Atlantic Ocean. The high-nutrient water below 2 km also appeared to

to in situ decay within the deep North Atlantic. Similar to its use in the modern ocean, past ^{14}C could be combined with other water-mass tracers to account for this overprint of water-mass

mixing and thereby estimate the contribution due to radiocarbon decay within the Atlantic (37). To use radiocarbon to directly constrain the LGM circulation in the Atlantic would require a large number of precise measurements (38, 39).

However, the existing measurements of ^{14}C activity in benthic foraminifera suggest a water-mass structure in the LGM Atlantic that is consistent with the nutrient proxies, with ^{14}C -rich waters indicating recent exchange with the atmosphere above 2 km depth and ^{14}C -poor waters below this depth (40). The interpretation of the ^{14}C is complicated by assumptions about the surface-ocean radiocarbon activity and the mixing of shells of different ages by organisms living within the sediments, so the agreement between the reconstructions based on ^{14}C and the nutrient tracers gives us further confidence in the overall picture of the deep-water masses in the LGM Atlantic.

Radioisotopes of Protactinium and Thorium

The contrasting chemical behavior of uranium decay-series nuclides provides a means for assessing the rate of deep circulation. Uranium is highly soluble in seawater and thus has a residence time of several hundred thousand years in the ocean. Because this is far longer than the overall oceanic mixing time (a millennium or two), uranium is approximately evenly distributed throughout the ocean. This means that the radioactive decay of U isotopes, and hence the production of its daughter isotopes, is spatially uniform to a good approximation. By contrast, these radioactive-decay products, thorium and protactinium, are extremely particle-reactive (41) and are rapidly removed from seawater by settling particles and subsequently buried on the sea floor. The resulting oceanic residence times are on the order of decades for ^{230}Th and

centuries for ^{231}Pa . Because the residence time of deep waters in the Atlantic is also on the order of centuries, most of the ^{230}Th produced in the Atlantic is buried in Atlantic Ocean sediments, whereas some of the ^{231}Pa is exported to the Southern Ocean. This leaves the modern $^{231}\text{Pa}/^{230}\text{Th}$ ratio in Atlantic sediments below the ratio at which these isotopes are produced by the decay of U (42). A longer residence time of water in the Atlantic should cause the $^{231}\text{Pa}/^{230}\text{Th}$ ratio in the underlying sediments to increase, but there was no significant difference in the mean $^{231}\text{Pa}/^{230}\text{Th}$ of Atlantic sediments deposited during the LGM relative to those laid down more recently (42). These data could be consistent with a range of past circulation states, from a slight increase in the MOC to a decrease of up to 30% (43). More recently, with detailed downcore records, slightly higher ratios were found for the LGM sediments relative to the Holocene at a water depth of 4.5 km near Bermuda (44), consistent with an overall small increase in the residence time of overlying deep waters (GNAIW and AABW). Lower ratios were found at 1.7 km depth in the northern North Atlantic (45) and 3.4 km depth on the Iberian margin (46), allowing for the possibility of vigorous renewal of GNAIW. Because variations in particle flux (47) and composition (48) can also influence sedimentary $^{231}\text{Pa}/^{230}\text{Th}$, a better understanding of these factors will strengthen our ability to quantify past ocean circulation with the use of these nuclides.

Glacial Circulation of the Atlantic

At this point, the most robust observations that can help to constrain scenarios of past variability in the Atlantic MOC are as follows: (i) There was a water-mass divide in the LGM Atlantic, with a

nutrient-poor, radiocarbon-rich water mass (GNAIW) dominant above 2 km and more nutrient-rich, radiocarbon-poor water below 2 km (perhaps a glacial analog of AABW). The maintenance of these two distinct water masses in the face of mixing processes similar to those in the modern ocean that would tend to erase these boundaries requires one or both water masses to be renewed fairly rapidly (24). (ii) $^{231}\text{Pa}/^{230}\text{Th}$ ratios in deep-ocean sediments deposited during the LGM are comparable to those deposited under modern conditions. This also argues against a much slower circulation for both deep-water masses in the Atlantic. (iii) The cross-basin contrast in oxygen isotopes in benthic foraminifera in the South Atlantic collapsed during the LGM. This would argue against a strong MOC that imports surface and intermediate waters to the Atlantic compensated by the export of deeper waters. Hence, we have good evidence for a circulation of deep waters in the LGM Atlantic that was not completely sluggish. The data also do not support a MOC with the same extent and structure as today. Sea surface temperature reconstructions in the North Atlantic (49, 50) also appear inconsistent with a stronger version of today's overturning cell characterized by surface water inflow compensating deep-water export from the polar seas of the North Atlantic. These observations seem to rule out at least some of the more extreme circulation states produced by climate models for the LGM.

Outlook

What would be required to provide a reliable observational estimate of the Atlantic MOC during the LGM? Paleoceanographic methods inherently are associated with larger errors and have a sparser geographic coverage than modern oceanographic measurements, and using this type of data to produce a conclusive quantitative reconstruction of past ocean circulation is a challenge. It will almost certainly require a combination of different paleoceanographic proxies such as those discussed here (38, 51). Ocean margin density reconstructions and $^{231}\text{Pa}/^{230}\text{Th}$ measurements may be particularly useful, as they may integrate the effects of circulation in the ocean interior where paleoceanographic measurements are not possible; measurements of ^{14}C may also be useful as a direct measure of elapsed time. But work remains to be done in order to (i) better understand the processes by which Pa and Th are removed from the water column; (ii) better assess past ocean temperatures and salinities for paleodensity reconstructions, possibly by using the elemental chemistry of

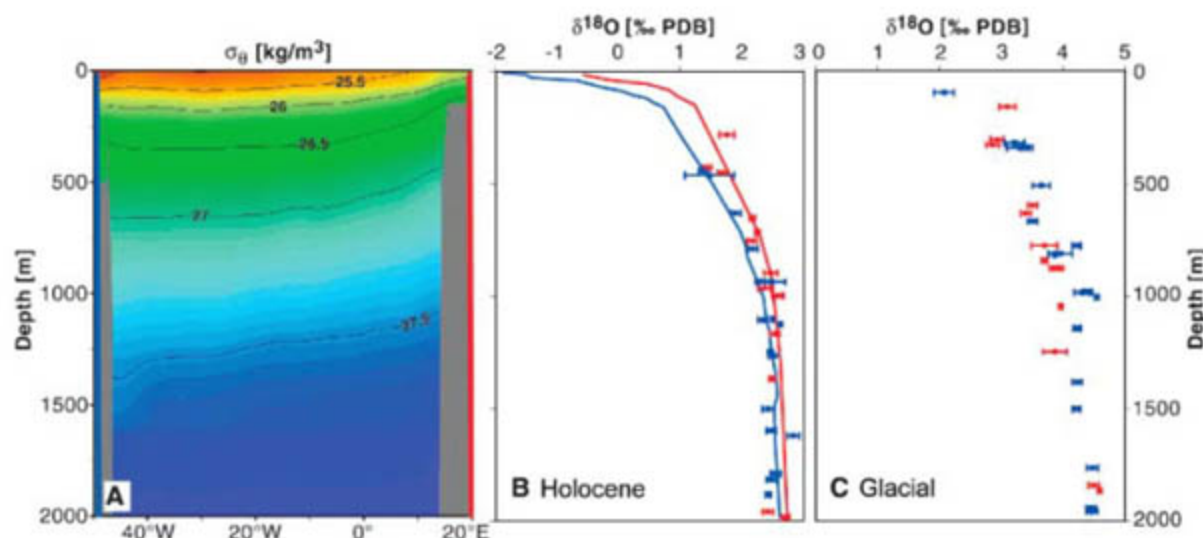


Fig. 2. (A) Density (σ_θ) of seawater across the South Atlantic at 30°S (61). The waters are denser on the eastern side of the basin, reflecting the presence of the meridional overturning circulation. (B) Oxygen isotopic composition of the shells of benthic foraminifera ($\delta^{18}\text{O}$) in recent sediments on the eastern (red symbols) and western (blue symbols) side of the basin, reflecting the density contrast across the basin today, with higher $\delta^{18}\text{O}$ for the higher-density waters on the eastern side. The solid lines are the predicted $\delta^{18}\text{O}$ values based on modern hydrographic data (21). (C) Oxygen isotopic composition of the shells of benthic foraminifera for the LGM suggest that the modern density contrast in the upper 2 km was absent or reversed (21).

the shells (52) and paleosalinity estimates from measurements of chloride in pore waters (53); and (iii) better constrain water-mass properties for accurate use of the ^{14}C clock. Other approaches that show promise are the quantitative analysis of the grain size population in the terrigenous sediment fine fraction that provides a proxy for near-bottom flow speed, which has the advantage of having a direct physical connection to flow and an immediate response to any changes in flow speed (54). New water-mass tracers that are independent of nutrient cycling, such as the Nd isotopic composition of metallic precipitates in deep-sea sediments, are also being developed and successfully applied on a number of time scales [e.g., (55)], and magnetic properties have been used to reconstruct the flow path of bottom waters (56). Although challenges remain before we arrive at a well-constrained quantitative estimate of the glacial circulation, much will be gained in the coming years by the combined use of the tools currently at our disposal. It is worth recalling that the basic structure of the modern Atlantic MOC was largely described by the 1950s on the basis of a few measurements of water-mass properties and the thermal wind relationship, whereas quantitative estimates of the modern MOC based on inverse methods have only been possible in the past two decades or so (57).

Different circulation scenarios are consistent with the currently available data for the LGM, but certain hypotheses regarding the glacial circulation in the Atlantic already are testable. In particular, general circulation models provide a set of circulation hypotheses that are physically consistent (given the assumptions used in constructing the models) with the ice sheets and CO_2 concentration of the last ice age. We can already say with some confidence that the data can rule out some of the more extreme scenarios produced by the models. To compare the less extreme model scenarios directly with the data, we need to account for the multiple physical, chemical, and biological controls on the paleoceanographic observations. A better representation in the models of the full complexity of these processes that lead to the record left behind in the sediments and the explicit prediction of the values of the paleoceanographic proxies will allow for a more direct comparison between model output and data [e.g., (58, 59)].

Reconstructing ocean circulation during the LGM is a critical first step, but there is already a strong community focus on generating the time-series data that will allow for the reconstruction

of a detailed history of ocean circulation over the abrupt climate changes that punctuated the cooler climates of the past. Changes in the Atlantic MOC play a critical role in many of the hypotheses put forth to explain these abrupt climate transitions, and there is already compelling evidence to support this link, at least for the most recent of these abrupt climate change events (44, 60). The quantitative reconstruction of these circulation changes remains a challenge that, if tackled successfully, will further our understanding of the relationship between ocean circulation and climate, enabling us to better constrain the scenarios for the future.

References and Notes

1. A. C. Mix, E. Bard, R. Schneider, *Quat. Sci. Rev.* **20**, 627 (2001).
2. J. C. Duplessy, J. Moyes, C. Pujol, *Nature* **286**, 479 (1980).
3. S. S. Streeper, N. J. Shackleton, *Science* **203**, 168 (1979).
4. E. A. Boyle, L. D. Keigwin, *Science* **218**, 784 (1982).
5. W. B. Curry, G. P. Lohmann, *Quat. Res.* **18**, 218 (1982).
6. H. Stommel, *Tellus* **13**, 224 (1961).
7. S. Manabe, R. J. Stouffer, *J. Clim.* **1**, 841 (1988).
8. A. Kitoh, S. Murakami, H. Koide, *Geophys. Res. Lett.* **28**, 2221 (2001).
9. C. D. Hewitt, R. J. Stouffer, A. J. Broccoli, J. F. B. Mitchell, P. J. Valdes, *Clim. Dyn.* **20**, 203 (2003).
10. B. L. Otto-Blieneser et al., *J. Clim.* **19**, 2526 (2006).
11. S. I. Shin et al., *Clim. Dyn.* **20**, 127 (2003).
12. M. Vellinga, R. A. Wood, *Clim. Change* **54**, 251 (2002).
13. R. Zhang, T. L. Delworth, *J. Clim.* **18**, 1853 (2005).
14. M. M. Hall, H. L. Bryden, *Deep Sea Res.* **29**, 339 (1982).
15. D. Roemmich, C. Wunsch, *Deep Sea Res.* **32**, 619 (1985).
16. J. Lynch-Stieglitz, W. B. Curry, N. Slowey, *Paleoceanography* **14**, 360 (1999).
17. C. Emiliani, *J. Geol.* **63**, 538 (1955).
18. J. Hirschi, J. Lynch-Stieglitz, *Geochem. Geophys. Geosyst.* **7**, Q10N04 (2006).
19. J. Lynch-Stieglitz, *Geochem. Geophys. Geosyst.* **2**, 10.1029/2001GC000208 (2001).
20. J. Marotzke et al., *J. Geophys. Res.* **104**, 29529 (1999).
21. J. Lynch-Stieglitz et al., *Geochem. Geophys. Geosyst.* **7**, Q10N03 (2006).
22. G. Gebbie, P. Huybers, *Geochem. Geophys. Geosyst.* **7**, Q11N07 (2006).
23. T. Bickert, A. Mackensen, in *The South Atlantic in the Late Quaternary: Reconstruction of Material Budget and Current Systems*, G. Wefer, S. Mulitza, V. Ratmeyer, Eds. (Springer-Verlag, Berlin, 2004), pp. 671–693.
24. W. B. Curry, D. W. Oppo, *Paleoceanography* **20**, PA1017 (2005).
25. T. M. Marchitto, W. S. Broecker, *Geochem. Geophys. Geosyst.* **7**, Q12003 (2006).
26. J.-C. Duplessy et al., *Paleoceanography* **3**, 343 (1988).
27. M. Sarnthein et al., *Paleoceanography* **9**, 209 (1994).
28. J. Lynch-Stieglitz, in *The Oceans and Marine Geochemistry*, H. Elderfield, Ed., vol. 6 of *Treatise on Geochemistry* (Elsevier, Oxford, 2003), pp. 433–451.
29. T. M. Marchitto, W. B. Curry, D. W. Oppo, *Paleoceanography* **15**, 299 (2000).
30. K. Matsumoto, J. Lynch-Stieglitz, *Paleoceanography* **14**, 149 (1999).
31. W. S. Broecker et al., *Radiocarbon* **30**, 261 (1988).

32. J. C. Duplessy et al., *Radiocarbon* **31**, 493 (1989).
33. N. J. Shackleton et al., *Nature* **335**, 708 (1988).
34. J. F. Adkins, E. A. Boyle, L. Keigwin, E. Cortijo, *Nature* **390**, 154 (1997).
35. A. Mangini et al., *Nature* **392**, 347 (1998).
36. L. F. Robinson et al., *Science* **310**, 1469 (2005); published online 3 November 2005 (10.1126/science.1114832).
37. J. F. Adkins, E. A. Boyle, in *Reconstructing Ocean History: A Window into the Future*, F. Abrantes, A. C. Mix, Eds. (Kluwer Academic, New York, 1999), pp. 103–120.
38. P. Huybers, G. Gebbie, O. Marchal, *J. Phys. Oceanogr.* **37**, 394 (2007).
39. C. Wunsch, *Quat. Sci. Rev.* **22**, 371 (2003).
40. L. D. Keigwin, *Paleoceanography* **19**, PA4012 (2004).
41. M. P. Bacon, R. F. Anderson, *J. Geophys. Res.* **87**, 2045 (1982).
42. E. F. Yu, R. Francois, M. P. Bacon, *Nature* **379**, 689 (1996).
43. O. Marchal, R. Francois, T. F. Stocker, F. Joos, *Paleoceanography* **15**, 625 (2000).
44. J. F. McManus, R. Francois, J. M. Gherardi, L. D. Keigwin, S. Brown-Leger, *Nature* **428**, 834 (2004).
45. I. R. Hall et al., *Geophys. Res. Lett.* **33**, L16616 (2006).
46. J. M. Gherardi et al., *Earth Planet. Sci. Lett.* **240**, 710 (2005).
47. N. Kumar, R. Gwiazda, R. F. Anderson, P. N. Froelich, *Nature* **362**, 45 (1993).
48. Z. Chase, R. F. Anderson, M. Q. Fleisher, P. W. Kubik, *Earth Planet. Sci. Lett.* **204**, 215 (2002).
49. M. Kucera et al., *Quaternary Sci. Rev.* **24**, 951 (2005).
50. A. Paul, C. Schafer-Neth, *Paleoceanography* **18**, 1058 (2003).
51. P. Legrand, C. Wunsch, *Paleoceanography* **10**, 1011 (1995).
52. H. Elderfield, J. Yu, P. Anand, T. Kiefer, B. Nyland, *Earth Planet. Sci. Lett.* **250**, 633 (2006).
53. J. F. Adkins, D. P. Schrag, *Earth Planet. Sci. Lett.* **216**, 109 (2003).
54. I. N. McCave, I. R. Hall, *Geochem. Geophys. Geosyst.* **7**, Q10N05 (2006).
55. A. M. Piotrowski, S. L. Goldstein, S. R. Hemming, R. G. Fairbanks, *Science* **307**, 1933 (2005).
56. C. Kissel et al., *Earth Planet. Sci. Lett.* **171**, 489 (1999).
57. A. Ganachaud, C. Wunsch, *Nature* **408**, 453 (2000).
58. A. N. LeGrande et al., *Proc. Natl. Acad. Sci. U.S.A.* **103**, 837 (2006).
59. A. Schmittner, A. Oschlies, X. Giraud, M. Eby, H. L. Simmons, *Global Biogeochem. Cycles* **19**, GB3004 (2005).
60. P. U. Clark, N. G. Pisias, T. F. Stocker, A. J. Weaver, *Nature* **415**, 863 (2002).
61. M. E. Conkright et al., *World Ocean Atlas 2001: Objective Analyses, Data Statistics, and Figures, CD-ROM Documentation* (National Oceanographic Data Center, Silver Spring, MD, 2002).
62. We thank the Scientific Committee on Ocean Research, IMAGES, and NSF for their support of the Working Group on Past Ocean Circulation and the workshop that was held on this topic in March 2005 at Georgia Tech. We also thank the scientists who contributed their ideas to this review through their participation in that workshop and the ORMEN/VAMOC Workshop on LGM ocean circulation in Amsterdam in October 2005. We thank T. Bickert for providing data for Fig. 1.

10.1126/science.1137127

Discover the
leading resource in
the life sciences ...

Encyclopedia of

 **Life
Sciences**

www.els.net

Spanning the entire spectrum of life science research, the *Encyclopedia of Life Sciences* features thousands of specially commissioned and peer-reviewed articles, most of which are accompanied by colour images and tables.



- Available in print and online
- Over 3,500 original articles
- Contributions from 5,000 of the world's leading scientists
- Introductory, advanced and keynote articles
- More than 9,000 illustrations and figures

Original 20 Volume
print set

Hardcover

978-0-470-01617-6
£3150 / \$5670 / €4899

NEW 6

Supplementary
print volumes

Hardcover

978-0-470-06141-1
£795 / \$1435 / €1249, valid until 30 June
2007 - thereafter £995 / \$1795 / €1549

26 Volume print set (20 Volumes + 6
Supplementary volumes)

Hardcover

978-0-470-06651-5
£3550 / \$6390 / €5499, valid until
30 June 2007 - thereafter
£4145 / \$7465 / €6449



10107

HOW TO ORDER

EUROPE, MIDDLE EAST,
ASIA & AFRICA

John Wiley & Sons Ltd
Tel: +44 (0)1243 843294
Fax: +44 (0)1243 843296

E-mail:
cs-books@wiley.co.uk
www.wiley.com

NORTH, CENTRAL &
SOUTH AMERICA

John Wiley & Sons Inc
Tel: 877 762 2974
Fax: 800 597 3299
E-mail: custserv@wiley.com
www.wiley.com

GERMANY, SWITZERLAND
& AUSTRIA

Wiley-VCH Verlag GmbH
Tel: +49 6201 606 400
Fax: +49 6201 606 184
E-mail: service@wiley-vch.de
www.wiley-vch.de



Science

MAGAZINE'S

STATE
OF THE
PLANET

2006-2007



DONALD KENNEDY
and the Editors of *Science*

AAAS

Science Magazine's State of the Planet 2006-2007

Donald Kennedy, Editor-in-Chief,
and the Editors of *Science*

The American Association for
the Advancement of Science

The most authoritative voice in science,
Science magazine, brings you current
knowledge on the most pressing
environmental challenges, from population
growth to biodiversity loss.

COMPREHENSIVE • CLEAR • ACCESSIBLE



ISLANDPRESS

Science

AAAS

islandpress.org

Rapid and Recent Changes in Fungal Fruiting Patterns

A. C. Gange,^{1*} E. G. Gange,² T. H. Sparks,³ L. Boddy⁴

Many studies have demonstrated recent phenological responses to climate change, but these largely involved higher organisms, such as plants, insects, or birds, and were restricted to events in spring (1). Autumnal events have received far less attention, even though the end of the growing season has seen significant delays (2). Fungi provide vital ecosystem services through decomposition, nutrient cycling, and soil aggregation, yet they are missing from previous considerations of ecosystem responses to global change (3). In this study, we analyzed a data set consisting of over 52,000 individual fungal fruiting records, from nearly 1400 localities, collected in southern England over the period 1950–2005. We extracted information on a total of 315 autumnal fruiting species, each of which had been recorded in more than 20 years (4).

The first fruiting date averaged across all species has become significantly earlier, whereas average last fruiting date has become significantly later (Fig. 1A). The increase in the overall fruiting period is dramatic; in the 1950s, the average (\pm SE) was 33.2 ± 1.6 days, but this has more than doubled to 74.8 ± 7.6 days in the current decade. For the species that show significantly earlier first fruiting dates ($n = 85$), the average advancement is 8.6 ± 0.6 days decade⁻¹, whereas for species showing significantly later last fruiting dates ($n = 105$), the delay is 7.5 ± 0.5 days decade⁻¹,

both of which are greater than equivalent spring data previously reported for higher organisms (5).

The alteration in fungal fruiting mirrors changes in British temperatures that have occurred since 1975 (6). To substantiate this, we examined relations between fruiting dates of each species and monthly records of local temperature and rainfall (4). Over the past 56 years, August temperatures have increased ($F_{1,54} = 11.4$, $P < 0.01$), as has October rainfall ($F_{1,54} = 5.8$, $P < 0.05$). The increase in late summer temperatures and autumnal rains has caused early season species to fruit earlier and late season species to continue fruiting later. Seventy-eight (91%) of the species showing an advanced fruiting date have a significant relation between first fruiting date and August temperature, whereas 92 (88%) of the species showing later last dates could be explained by positive relations between August temperature and October rainfall.

We noticed that 47 (59%) of the deciduous mycorrhizal species showed a delay in last fruiting date, whereas no coniferous mycorrhizal species were delayed. To examine this further, we studied the 11 mycorrhizal species that were recorded beneath both coniferous and deciduous hosts. Average fruiting date in each year was calculated and regressed against time (56 years). Eight of the species showed a significantly larger regression coefficient when

growing beneath deciduous hosts (Fig. 1B). Therefore, the fruiting season of these species has changed in a habitat-dependent manner. If these responses were due to microclimatic differences beneath deciduous and coniferous trees, then there would likely be similar differences in fruiting patterns of nonmycorrhizal forest-floor fungi. To examine this possibility, we compared regression coefficients of seven nonmycorrhizal leaf litter-decay species and a further seven wood-decay fungi that occurred in both forest types. In no case did the regression coefficient differ (all $P > 0.05$); thus, microclimatic effects can be discounted. These data suggest that changes in the temporal allocation of nutrients to roots have occurred in deciduous forests but not in coniferous woods, where there is no single large loss of leaf material. Nutrients are intercepted by the mycorrhizal species and used for fruit body production (7).

Furthermore, climate warming seems to have caused significant numbers of species to begin fruiting in spring as well as autumn (fig. S1). Given that active mycelial growth is required before sporophore production, this is strong evidence that the mycelium of certain species must be active in late winter and early spring as well as late summer and autumn, suggesting increases in decay rates in forests.

References and Notes

1. C. Parmesan, G. Yohe, *Nature* **421**, 37 (2003).
2. A. Menzel, P. Fabian, *Nature* **397**, 659 (1999).
3. D. Schröter *et al.*, *Science* **310**, 1333 (2005); published online 27 October 2005 (10.1126/science.1115233).
4. Materials and methods are available as supporting material on Science Online.
5. T. L. Root *et al.*, *Nature* **421**, 57 (2003).
6. A. H. Fitter, R. S. R. Fitter, *Science* **296**, 1689 (2002).
7. F. T. Last, J. Pelham, P. A. Mason, K. Ingleby, *Nature* **280**, 168 (1979).
8. We are extremely grateful to all those who collected fungi, especially I. Gange, the late J. Hindley, A. McKee, W. Freemantle, R. Nicholls, and R. Chapman.

Supporting Online Material

www.sciencemag.org/cgi/content/full/316/5821/71/DC1

Materials and Methods

Fig. S1

References

13 November 2006; accepted 8 January 2007
10.1126/science.1137489

¹School of Biological Sciences, Royal Holloway, University of London, Egham, Surrey TW20 0EX, UK. ²Belvedere, Southampton Road, Whaddon, Salisbury, Wilts SP5 3DZ, UK. ³Natural Environment Research Council Centre for Ecology and Hydrology, Monks Wood, Cambridgeshire PE28 2LS, UK. ⁴Cardiff School of Biosciences, Cardiff University, Main Building, Museum Avenue, Cardiff CF10 3TL, UK.

*To whom correspondence should be addressed. E-mail: a.gange@rhul.ac.uk

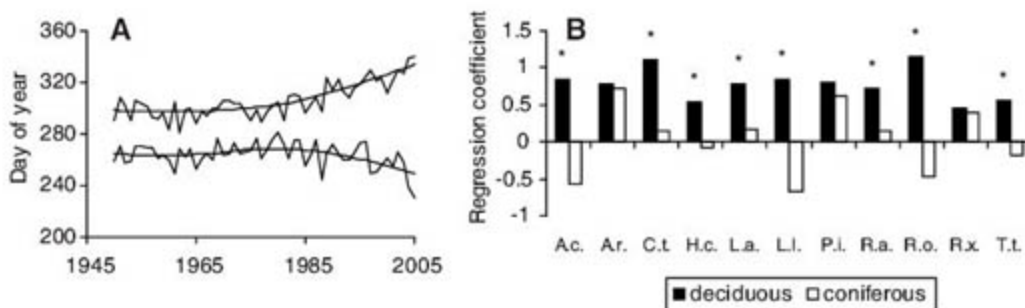


Fig. 1. (A) Average first fruiting date (lower line) and average last fruiting date (upper line) of 315 fungal species over 56 years. The underlying pattern is represented by lowess (locally weighted scatter plot smoother) lines. (B) Regression coefficients for mean fruiting date versus years for 11 mycorrhizal fungal species when growing under coniferous or deciduous trees. A.c. represents *Amanita citrina*; A.r., *A. rubescens*; C.t., *Cantherellus tubaeformis*; H.c., *Hebeloma crustuliniforme*; L.a., *Laccaria amethystina*; L.l., *L. laccata*; P.i., *Paxillus involutus*; R.a., *Russula atropurpurea*; R.o., *R. ochroleuca*; R.x., *R. xerampelina*; and T.t., *Tricholoma terreum*. Asterisks above bars indicate a significant difference in coefficients between the host types at $P = 0.05$.

Looking for solid ground in the ever-changing landscape of science & technology policy and budget issues?

Join the nation's top S&T experts at the 32nd Annual AAAS Forum on Science & Technology Policy
3-4 May 2007 • Washington DC
International Trade Center in the
Ronald Reagan Building



The AAAS Forum on Science and Technology Policy provides a setting for discussion and debate about the federal budget and other policy issues facing the science, engineering, and higher education communities. Initiated in 1976 as the AAAS R&D Colloquium with about 100 participants, the Forum has emerged as the major public meeting in the U.S. devoted to science and technology policy issues. It annually draws upwards of 500 of the nation's top S&T policy experts.

- Get a full analysis of the President's federal R&D funding proposals.
 - Have an opportunity to meet directly with key S&T policymakers.
 - Learn how the changes in Congress are affecting S&T policy issues.
 - Network with colleagues, including top decisionmakers in science and technology policy from all sectors.
 - Learn about broader national and international developments that will affect strategic planning in universities, industries, and government.
- Registrants will receive, at the Forum, *AAAS Report XXXII: Research and Development, FY 2008*, a comprehensive analysis of the proposals for the FY 2008 budget, prepared by AAAS and a group of its affiliated scientific, engineering, and higher education associations.

For more complete details on the program, hotel registration and on-line registration, please visit the website: www.aaas.org/forum.



www.aaas.org/forum

Chimeras of Two Isoprenoid Synthases Catalyze All Four Coupling Reactions in Isoprenoid Biosynthesis

Hirekodathakallu V. Thulasiram,* Hans K. Erickson,† C. Dale Poulter‡

The carbon skeletons of over 55,000 naturally occurring isoprenoid compounds are constructed from four fundamental coupling reactions: chain elongation, cyclopropanation, branching, and cyclobutanation. Enzymes that catalyze chain elongation and cyclopropanation are well studied, whereas those that catalyze branching and cyclobutanation are unknown. We have catalyzed the four reactions with chimeric proteins generated by replacing segments of a chain-elongation enzyme with corresponding sequences from a cyclopropanation enzyme. Stereochemical and mechanistic considerations suggest that the four coupling enzymes could have evolved from a common ancestor through relatively small changes in the catalytic site.

Isoprenoid metabolism is the most chemically diverse of nature's biosynthetic pathways. Over 55,000 naturally occurring isoprenoid molecules have been discovered, with a large number of new structures reported each year. Isoprenoid compounds play crucial metabolic and structural roles in cells, and the pathway is found in all forms of life. Among the better-known classes of isoprenoids are sterols (hormones and membrane components), carotenoids (visual pigments and photoprotective agents), prenylated proteins (membrane structure and cell signaling), dolichols (glycoprotein synthesis and bacterial cell wall synthesis), monoterpenes (insect sex pheromones and fragrances), and sesquiterpenes (plant defensive agents). The carbon skeletons of isoprenoid compounds are constructed from 3-methyl-1-butyl units, which are joined in one of nine different patterns (Fig. 1) (1–3). In four of these structures, C1' of one unit (red) is joined to a single carbon of the other unit (black) (1'-1, 1'-2, 1'-3, and 1'-4). In one case, C1' is inserted between atoms in the other unit (2-1'-3), and in three cases, C1' is joined to the other unit in a cyclic structure (c1'-1-2, c1'-2-3, and c1'-2-3-2'). The example that does not involve C1' is the 4'-4 pattern seen in membrane lipids from Archaea (3).

Except for the 4'-4 attachment, the isoprenoid skeletons in Fig. 1 are formed early in the isoprenoid pathway, before the modification reactions that are required to synthesize specific natural products. Four of the basic isoprenoid structures (1'-2, 1'-4, c1'-2-3, and c1'-2-3-2') are synthesized by joining simpler units, whereas

the other four (1'-1, 1'-3, 2-1'-3, and c1'-1-2) are produced by rearrangement of 1'-2-3 structures (4, 5). The basic building reaction in the pathway is chain elongation, where the growing isoprenoid chain of an isoprenoid allylic diphosphate is added to the double bond in isopentenyl diphosphate (IPP) (Fig. 2). This reaction occurs in all organisms. The 1'-4 linkage is by far the most common that is seen in isoprenoid compounds, and compounds with this attachment between isoprene units are called head-to-tail or regular terpenes. Other attachment patterns are designated as non-head-to-tail or irregular. The cyclopropanation reaction is the first pathway-specific step in the biosynthesis of sterols (6) and carotenoids (7) to give metabolites widely distributed in Eukarya, Archaea, and some Bacteria. Branching is only found in a limited number of plants (1, 8). The only documented compounds from cyclobutanation are mealybug mating pheromones (2, 9).

The enzymes that catalyze chain elongation can be divided into two convergently evolved families based on the stereochemistry, *E* or *Z*, of the double bond in the newly added isoprene unit (10). Members of the *E* family typically synthesize shorter-chain isoprenoid diphosphates found early in the pathway, whereas those in the *Z* family synthesize longer-chain diphosphates. Farnesyl diphosphate synthase (FPPase) is the prototypal representative of the *E* family. FPPase catalyzes two reactions: the sequential condensation of dimethylallyl diphosphate (DMAPP, C₅) and geranyl diphosphate (GPP, C₁₀) with IPP to give farnesyl diphosphate (FPP, C₁₅). Structural studies and phylogenetic comparisons indicate that the α -helical "isoprenoid fold" originally discovered in avian FPPase is found in all of the *E*-family chain-elongation enzymes (11) and in more distant relatives that catalyze the cyclopropanation reactions in sterol biosynthesis (12) and terpenoid cyclization reactions (13). An ancestral FPPase or a closely related relative is a

likely candidate for the protein from which these other enzymes evolved.

We recently isolated the genes for chrysanthemyl diphosphate synthase (CPPase), an enzyme with cyclopropanation activity, from *Chrysanthemum cinerariaefolium* (chrysanthemum) (14) and *Artemisia tridentata* ssp. *spiciformis* (snowfield sagebrush) (15). The encoded sagebrush FPPase and CPPase proteins have similar sequences (75% identity and 96% similarity), suggesting that they share a recent common ancestor. Because FPPases are universally distributed, whereas CPPases are confined to members of a closely related family of higher plants, it is apparent that the cyclopropanation activity evolved from the chain-elongation activity of a parental FPPase. In contrast, the cyclopropanation enzymes squalene (13) and phytoene (16) synthase have no discernable sequence similarity with chain-elongation enzymes, suggesting an independent divergence of chain-elongation and cyclopropanation activities at a much earlier time, probably at the very beginning of cellular life.

On closer examination, we discovered that CPPase also synthesized lesser amounts of the 1'-2 branched product lavandulyl diphosphate (LPP) and the chain-elongation product GPP. In preliminary experiments with a series of chimeric proteins constructed by replacing amino acids of sagebrush FPPase with corresponding sequences from sagebrush CPPase, we found a transition in activities from chain elongation to branching and finally to cyclopropanation (17). Studies with a full set of chimeric proteins demonstrate that they catalyze all four of the fundamental isoprenoid-coupling reactions and that the absolute stereochemistries of the chiral products are identical to their naturally evolved counterparts.

Synthesis and expression of chimeric enzymes. By means of procedures reported previously, a common set of specific restriction

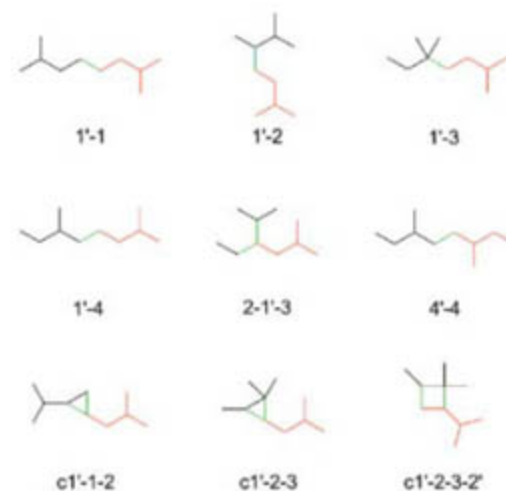


Fig. 1. Patterns found in nature for connecting isoprene units. Colors indicate isoprene units (red and black) and bonds joining the isoprene units (green).

Department of Chemistry, University of Utah, 315 South 1400 East, Room 2020, Salt Lake City, UT 84112, USA.

*Present address: Division of Organic Chemistry, National Chemical Laboratory, Pune 411008, India.

†Present address: ImmunoGen Incorporated, 128 Sidney Street, Cambridge, MA 02139, USA.

‡To whom correspondence should be addressed. E-mail: poulter@chemistry.utah.edu

sites at identical locations was introduced into the open reading frames (ORFs) for FPPase and CPPase (fig. S1) (18). The kinetic constants for the modified (M) proteins, FPPase-M and CPPase-M, were similar to those of the wild-type (WT) enzymes (table S1). Eleven chimeras were constructed from FPPase-M and CPPase-M by fusing fragments of the two proteins at the common restriction sites. In six of the constructs, amino acids in FPPase-M, beginning at the N terminus, were replaced with increasingly longer segments from CPPase-M. A complementary set of six constructs was prepared in a similar manner by replacing amino acids in CPPase-M, again beginning at the N terminus, with the corresponding segments from FPPase-M. The chimeras were named by designating the site of the junction and the origin of the amino acids, either FPPase-M or CPPase-M, on either side of the junction. For example, the "C69F" chimera (where C indicates CPPase and F indicates FPPase) has a junction site constructed at the common BseR I restriction sites in the ORFs for FPPase-M and CPPase-M where the first 69 amino acids (FPPase-M numbering) are from CPPase-M and the remaining amino acids are from FPPase-M. The chimeric proteins were obtained for 11 of the 12 constructs (only F243C failed to give protein) and were purified (>95%) by Ni²⁺-affinity chromatography. Removing the His₆ tag in FPPase-M and CPPase-M did not alter their activity, and the histidine tags were not removed from the parental enzymes or chimeric enzymes used in this study.

A screen for chain-elongation and "irregular" products. FPPase-M, CPPase-M, and 11 chimeric proteins were screened for synthesis of chain-elongation and irregular products (Fig. 3). The screen for chain elongation involved incubation of the proteins with [¹⁴C]IPP and either DMAPP or GPP. Products and substrates

were separated by thin-layer chromatography (TLC) and analyzed by phosphor autoradiography (fig. S2). The screen for irregular monoterpene synthesis involved incubation with [¹⁴C]DMAPP. Incubation of FPPase-M with [¹⁴C]IPP and DMAPP gave products that comigrated with C₁₀ (GPP) and C₁₅ (FPP) isoprenoid diphosphates. No products were seen when the enzyme was incubated with [¹⁴C]DMAPP. Incubation of CPPase-M with [¹⁴C]DMAPP gave products that comigrated with chrysanthemyl diphosphate (CPP). However, the enzyme also gave products characteristic of a C₁₀ diphosphate when incubated with [¹⁴C]IPP and DMAPP in the chain-elongation assay. TLC traces for the series of chimeras from C69F to C243F reflect a gradual transition from the C₁₀ and C₁₅ chain-elongation products typically synthesized by FPPase to the irregular products synthesized by CPPase. Between C69F and C178F, chain-elongation activity gradually shifted from predominant synthesis of C₁₅ FPP to exclusive synthesis of C₁₀ GPP. Activity in the [¹⁴C]DMAPP assay was readily detected for the C219F chimera and became progressively greater for C243F and CPPase. The F219C protein was inactive in both assays. Activity for irregular products was low in all of the chimeras in the F → C series. Trace amounts of materials were seen in all of the TLC traces, with the F178C chimera giving somewhat more C₁₀ product than the others.

Product analysis. The TLC radioassay did not resolve individual components within each group of C₅, C₁₀, and C₁₅ diphosphates. Gas chromatographic (GC) and GC mass spectrometric analysis of alcohols obtained after hydrolysis of the diphosphates with alkaline phosphatase showed that C₁₀ and C₁₅ chain-elongation alcohols were the exclusive products from FPPase-M with selective, but not exclusive, formation of the *E* double-bond iso-

mers when the enzyme was incubated with IPP and DMAPP (Fig. 4 and table S2) (18). A similar incubation with CPPase-M gave four C₁₀ products: chrysanthemol (COH) (15) from cyclopropanation, lavandulol (LOH) (17) from branching, and geraniol and nerol (19) from chain elongation. In the series C69F → C243F, irregular monoterpenes were first detected as minor products with the C98F chimera, which gave LOH and an unexpected isomer, maconelliol (MOH) (2), from a cyclobutanation reaction. Synthesis of irregular monoterpenes became the dominant reaction for the C243F chimera, where LOH was favored over COH by a ratio of ~3:1. For CPPase-M, the major product was COH, which was only favored over LOH by a ratio of ~2:1. In the F69C → F178C series, irregular products (LOH and COH) were only detected for the F69C chimera (table S2). The proportion of chain-elongation products to irregular products increased as the concentration of IPP increased relative to that of the allylic substrate, reflecting competition between the isomeric substrates for binding.

Except for CPPase-M and the C243F and F69C chimeras, reactions proceeded slowly when DMAPP was the sole substrate. In addition to COH, LOH, and MOH, small amounts of planococcol (POH) (9), an isomer of MOH, were detected in extracts from incubations with the C98F and C147F chimeras, indicating that these two enzymes also synthesized planococcol diphosphate (PPP) (Fig. 4 and table S3). Thus, most of the proteins that we studied synthesized irregular monoterpenes. The exceptions were FPPase-M and C178F, which only catalyzed chain elongation, and F219C, which was inactive in all of the assays. Several of the enzymes synthesized at least one compound generated by the cyclopropanation, branching, and cyclobutanation reactions in addition to chain-elongation products. The WT *A. tridentata* ssp. *spiciformis* CPPase was

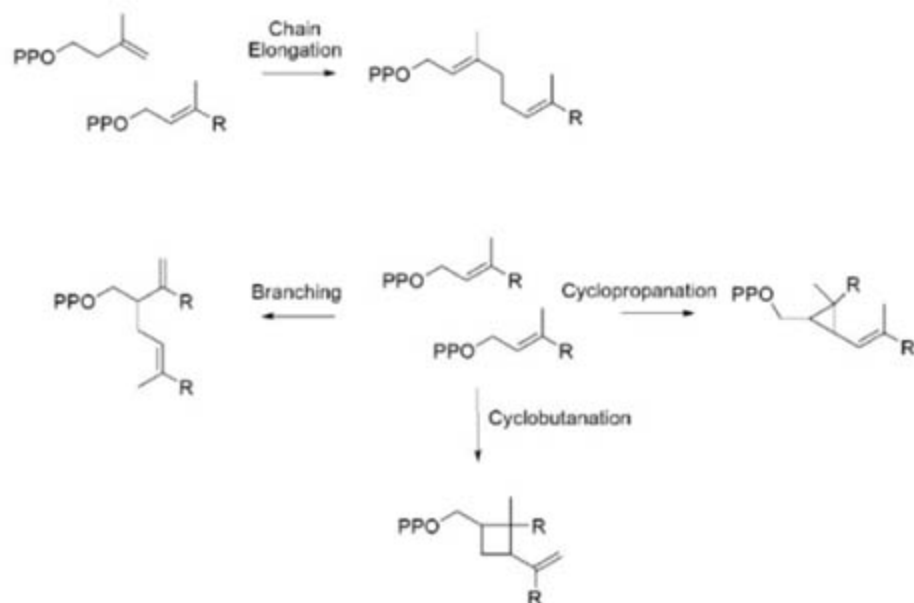


Fig. 2. Building reactions in the isoprenoid biosynthetic pathway. PPO, diphosphate; R, CH₂(CH₂CH=C(CH₃)CH₂)_nH, where n = 0, 1, 2, 3, and so forth.

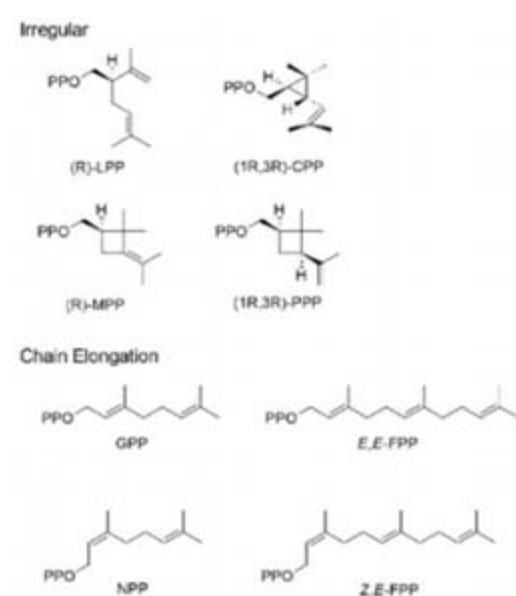


Fig. 3. Products from incubations with IPP and DMAPP. NPP, neryl diphosphate.

slightly more selective for CPP than CPPase-M. The WT CPPase from *C. cinerariaefolium* was slightly more selective for cyclopropanation relative to branching and chain elongation than the sagebrush enzymes.

Stereochemistry. The absolute stereochemistries of the irregular products from the enzyme catalyzed reactions were established by hydrolyzing the isoprenoid diphosphates to the corresponding alcohols and comparing their GC retention times by coinjection with authentic samples on a chiral column (figs. S3 and S4). In each case, a single enantiomer [(1*R*,3*R*)-COH (19), (*R*)-LOH (20), (*R*)-MOH (2), and (1*R*,3*R*)-POH (9)] was found. The absolute stereochemistries of the alcohols isolated from our enzyme-catalyzed reactions were identical to those of the corresponding alcohols isolated from natural sources.

Overview. The isoprenoid pathway uses only four different coupling reactions to build the carbon skeletons of its metabolites from the fundamental five-carbon building blocks IPP and DMAPP. Metabolites built by chain elongation and cyclopropanation are broadly distributed in nature, and the enzymes that catalyze the

coupling reactions have been identified and characterized. Metabolites from branching and cyclobutanation are narrowly distributed, and the biosynthetic enzymes and the corresponding genes have not been identified.

CPPase and the FPPase/CPPase chimeras synthesize single enantiomers of CPP, LPP, maconelliyl diphosphate (MPP), and PPP. The absolute stereochemistries of the cyclopropane ring in CPP, the chiral center in LPP, and cyclobutane rings in MPP and PPP require that C1 of the dimethylallyl unit destined to alkylate the C2-C3 double bond of the other dimethylallyl unit is located on the *Re* face of the C2-C3 double bond. If one assumes that formation of PPP proceeds through a "least motion" reaction coordinate, the absolute configuration of the C3 cyclobutane carbon dictates that the enzymes bind the two molecules of DMAPP in an "endo" orientation (fig. S5).

Thus far, only a single set of enantiomers has been reported for the naturally occurring irregular isoprenoid compounds formed by branching, cyclopropanation, and cyclobutanation reactions. The absolute stereochemistries of the alcohols obtained by hydrolysis of CPP, LPP, MPP, and PPP in our studies are identical to those of COH, MOH, and POH isolated from natural sources. Likewise, the topologically related 1*R*,2*R*,3*R* enantiomers of presqualene diphosphate (21) and prephytoene diphosphate (22) are the only known naturally occurring

stereoisomers of these two important metabolites. Work with recombinant squalene synthase indicates that the relative orientation of the two molecules of FPP, which are condensed to form presqualene diphosphate, is identical to the "endo" orientation predicted for DMAPP (4). The stereochemical similarities between the compounds synthesized by the chimeric proteins and those synthesized by their respective WT enzymes in nature are consistent with a scenario in which the naturally occurring enzymes evolved from a common ancestor that provided the original template for the orientation of the bound substrates. Genes for the cyclopropanation enzymes evolved twice, presumably from an *E*-selective chain-elongation template: once at the very beginning of cellular evolution for biosynthesis of squalene and phytoene, and subsequently much later for biosynthesis of CPP.

The rather conservative changes that we made in the catalytic site suggest that the elongation and irregular isoprenoid products are formed by a similar chemical mechanism with branches leading to the individual products. A comprehensive mechanism for the four coupling steps during biosynthesis of irregular isoprenoid compounds, based on what is known about the stereochemistries of chain elongation, cyclopropanation, branching, and cyclobutanation and the mechanism of chain-elongation reaction, is shown in Fig. 5. The chain-elongation reactions catalyzed by FPPase proceed by a

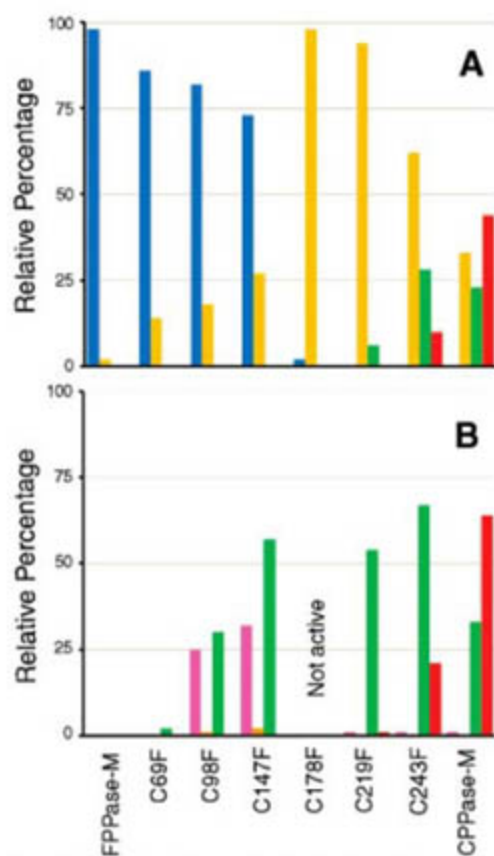


Fig. 4. Relative percentage of products from incubations with FPPase-M, CPPase-M, and the C → F series of chimeras. FPP, blue; GPP, gold; LPP, green; CPP, red; MPP, pink; PPP, orange. Diphosphate products were hydrolyzed by treatment with alkaline phosphatase, and the relative percentages of the corresponding alcohols were determined by GC. (A) Incubation for 2 hours at 30°C with IPP (200 μM) and DMAPP (200 μM). (B) Incubation for 12 hours at 30°C with DMAPP (3 mM).

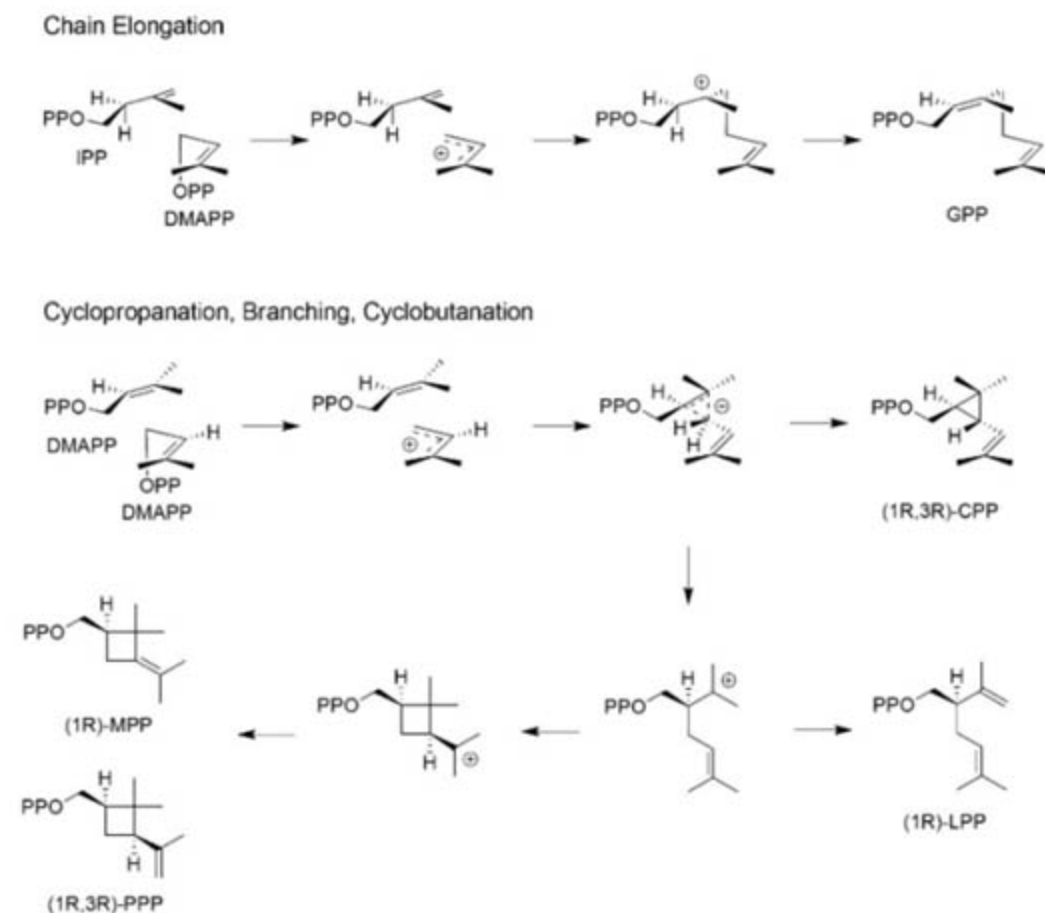


Fig. 5. A dissociative electrophilic alkylation mechanism for chain elongation, cyclopropanation, branching, and cyclobutanation.

dissociative electrophilic alkylation of the double bond in IPP by the allylic cations generated from DMAPP or GPP (23). By analogy, for biosynthesis of irregular monoterpenes, we suggest that a related dissociative electrophilic alkylation of the double bond in DMAPP by the dimethylallyl cation results in a protonated cyclopropane intermediate. This species can be deprotonated to give CPP or rearrange to a tertiary cation, which can in turn be deprotonated to give LPP. Alternatively, the tertiary cation can cyclize to give a cyclobutylcarbinyl cation that can then be deprotonated to give MPP or LPP. Formation of any specific product would be controlled by the ability of the enzyme to stabilize a specific intermediate along the reaction coordinate through dipolar and electrostatic interactions and to facilitate the selective removal of protons. The stereochemistries of the products result from the conformations of the two bound substrate molecules before the reaction. Only minor changes in the relative positions of the substrates are required to accommodate the formation of the different products.

This scenario provides an attractive mechanism for the evolution of the isoprenoid pathway through gene duplication and random mutagenesis of the duplicate genes to give new proteins, one of which is constrained to retain its original function, whereas the other is free to acquire a new activity. The isoprenoid fold first seen in the *E*-selective chain-elongation en-

zyme avian FPPase (12) has also been found in the cyclopropanation enzyme squalene synthase (13) (sterol biosynthesis) and several different terpenoid cyclases (14) along with aspartate-rich motifs involved in binding allylic diphosphate substrates, indicating that the enzymes evolved from a common ancestor. Phylogenetic correlations suggest that the cyclopropanation enzyme phytoene synthase (carotenoid biosynthesis) also has an isoprenoid fold. Our discovery that chimeric enzymes from FPPase and CPPase catalyze branching and cyclobutanation reactions suggests that WT enzymes with these activities also share this common ancestor.

References and Notes

1. K. Gunawardena, S. B. Rivera, W. W. Epstein, *Phytochemistry* **59**, 197 (2002).
2. A. Zhang *et al.*, *Proc. Natl. Acad. Sci. U.S.A.* **101**, 9601 (2004).
3. C. H. Heathcock, B. L. Finkelstein, T. Aoki, C. D. Poulter, *Science* **229**, 862 (1985).
4. M. B. Jarstfer, D. L. Zhang, C. D. Poulter, *J. Am. Chem. Soc.* **124**, 8834 (2002).
5. B. S. J. Blagg, M. B. Jarstfer, D. H. Rogers, C. D. Poulter, *J. Am. Chem. Soc.* **124**, 8846 (2002).
6. H. C. Rilling, W. W. Epstein, *J. Am. Chem. Soc.* **91**, 1041 (1969).
7. L. J. Altman *et al.*, *J. Am. Chem. Soc.* **94**, 3257 (1972).
8. J. D. Berkowitz, J.-L. Giner, T. Andersson, *J. Nat. Prod.* **63**, 267 (2000).
9. B. A. Bierl-Leonhardt, D. S. Moreno, M. Schwarz, J. Fargerlund, J. R. Plimmer, *Tetrahedron Lett.* **22**, 389 (1981).

10. C. D. Poulter, *Phytochem. Rev.* **5**, 17 (2006).
11. L. C. Tarshis, M. Yan, C. D. Poulter, J. C. Sacchetti, *Biochemistry* **33**, 10871 (1994).
12. J. Pandit *et al.*, *J. Biol. Chem.* **275**, 30610 (2000).
13. D. W. Christianson, *Chem. Rev.* **106**, 3412 (2006).
14. S. B. Rivera *et al.*, *Proc. Natl. Acad. Sci. U.S.A.* **98**, 4373 (2001).
15. A. Hemmerlin, S. B. Rivera, H. K. Erickson, C. D. Poulter, *J. Biol. Chem.* **278**, 32132 (2003).
16. D. Iwata-Reuyl, S. K. Math, S. B. Desai, C. D. Poulter, *Biochemistry* **42**, 3359 (2003).
17. H. K. Erickson, C. D. Poulter, *J. Am. Chem. Soc.* **125**, 6886 (2003).
18. H. V. Thulasiram, C. D. Poulter, *J. Am. Chem. Soc.* **128**, 15819 (2006).
19. K. Alexander, W. W. Epstein, *J. Org. Chem.* **40**, 2576 (1975).
20. M. Soucek, L. Dolejs, *Collect. Czech. Chem. Commun.* **24**, 3802 (1959).
21. G. Popjak, J. Edmond, S.-M. Wong, *J. Am. Chem. Soc.* **95**, 2713 (1973).
22. L. J. Altman, R. C. Kowerski, D. R. Laungani, *J. Am. Chem. Soc.* **100**, 6174 (1978).
23. J. M. Dolence, C. D. Poulter, in *Comprehensive Natural Products Chemistry*, O. Meth-Cohn, Ed. (Elsevier, Oxford, UK, 1999), vol. 5, pp. 18473–18500.
24. We thank A. Zhang for providing a sample of (*R*)-MOH. This work was supported by NIH grant GM 21328.

Supporting Online Material

www.sciencemag.org/cgi/content/full/316/5821/73/DC1

Materials and Methods

Figs. S1 to S5

Tables S1 to S3

Electron Impact (EI) Mass Spectra

Chemical Ionization (CI) Mass Spectra

References

20 November 2006; accepted 16 February 2007

10.1126/science.1137786

Schemas and Memory Consolidation

Dorothy Tse,^{1*} Rosamund F. Langston,^{1*} Masaki Kakeyama,² Ingrid Bethus,¹ Patrick A. Spooner,¹ Emma R. Wood,¹ Menno P. Witter,³ Richard G. M. Morris^{1†}

Memory encoding occurs rapidly, but the consolidation of memory in the neocortex has long been held to be a more gradual process. We now report, however, that systems consolidation can occur extremely quickly if an associative “schema” into which new information is incorporated has previously been created. In experiments using a hippocampal-dependent paired-associate task for rats, the memory of flavor-place associations became persistent over time as a putative neocortical schema gradually developed. New traces, trained for only one trial, then became assimilated and rapidly hippocampal-independent. Schemas also played a causal role in the creation of lasting associative memory representations during one-trial learning. The concept of neocortical schemas may unite psychological accounts of knowledge structures with neurobiological theories of systems memory consolidation.

The concepts of “mental schema” and “mental models” as frameworks of knowledge are now well established (1, 2), with implications for story recall, deductive inference, and education (3, 4). For example, the memory of grammatically correct but semantically unusual prose passages is substantially better when subjects have an activated and relevant mental framework with which to understand them (5). An everyday experience for working scientists is remembering complex new information in an academic seminar. Our ability to do so depends as much on our possession of an appropriate mental schema as on the communi-

cative skill of the speaker in logically conveying his or her message. In the absence of such mental frameworks, we are unable to follow scientific inferences in a talk and have the phenomenological experience of being functionally amnesic for its content a surprisingly short time later.

Curiously, this fundamental idea about memory has had little impact in neuroscience. Selective activation of a specific region within the posterior parietal cortex occurs in human subjects when, having been given relevant pictorial information earlier, they correctly interpret unusual textual information that would otherwise be incomprehensible (6). Animal studies have rarely

considered the issue of what the animal itself brings in the way of knowledge to a learning situation, with the exception of studies of spatial and relational memory (7–9). This is partly because most experiments are conducted with “experimentally naïve” animals, and also because the creation of a mental schema is difficult to map precisely onto concrete neuroscience concepts such as anatomical connectivity or synaptic plasticity. The present experiments test the idea that the schema concept is directly relevant to the neural mechanisms of systems memory consolidation (10–12).

Experiments on schema learning. We trained rats to learn several flavor-place associations concurrently, using different flavors of food (flavor cues) and sand wells (place cues) located within a familiar testing environment called an “event arena” (13). The task was to learn which

¹Laboratory for Cognitive Neuroscience, Centre for Cognitive and Neural Systems, and Centre for Neuroscience Research, University of Edinburgh, 1 George Square, Edinburgh EH8 9JZ, Scotland, UK. ²Division of Environmental Health Sciences, Center for Disease Biology and Integrative Medicine, Graduate School and Faculty of Medicine, University of Tokyo, Faculty of Medicine Building 1, 7-3-1 Hongo, Bunkyo-ku, Tokyo 113-0033, Japan. ³Centre for the Biology of Memory, Medical-Technical Research Centre, NO-7489 Trondheim, Norway.

*These authors contributed equally to this work.

†To whom correspondence should be addressed. E-mail: r.g.m.morris@ed.ac.uk

flavor was in which location such that, when cued with a specific flavor in start boxes at the side of the arena, the animals would be rewarded for going to the correct location by receiving more of that same food (i.e., “cued recall”). They should be able to recall that banana-flavored food is at one location, bacon-flavored food at another, and so on (Fig. 1, A and B). Such paired-associate learning is likely to be mediated by the hippocampus initially (14–16), with long-term storage of paired-associate memory traces eventually consolidated in the neocortex (17, 18). This makes this paradigm ideal for looking at the temporal dynamics of systems memory consolidation (10, 12, 19, 20), a process widely held to be quite slow. Additionally, the use of location as one member of each paired associate allowed the animals to learn each association as either an isolated declarative “fact,” in which spatial information is generally considered as no different from other kinds of information (10), or as some kind of mapping of flavors to arena locations, resulting in the formation of a spatial or relational framework (7, 21).

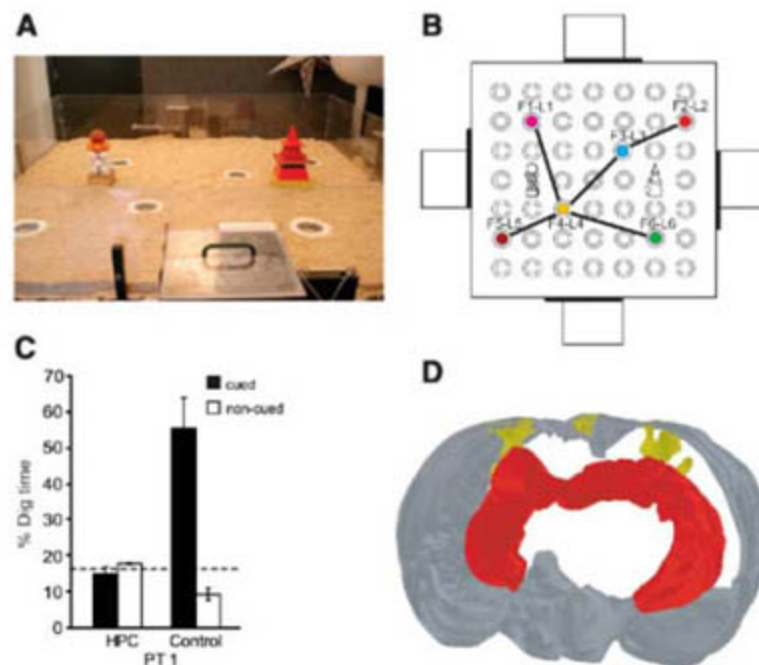
After habituation, the animals were started from one start box of the arena (at north, south, east, or west) on all six trials of a session. A different start box was used for each session. A trial began when the rat was given a cue flavor in the start box. Upon entering the arena, the animal was confronted by six sand wells (Fig. 1, A and B) of which only one contained flavored food—the same flavor given as a cue in the start box (22). The animals visited and sometimes dug at incorrect sand wells, which did not contain food on that particular trial, until they found the correct one. On each trial, the animals would retrieve the first of three buried food pellets, return to the start box to eat it, and then run back to the correct sand well to collect and transport the second and third pellets. One hour later, the second trial began with a different cue flavor in the start box and a different sand well baited. There were six trials per session, with the next session run 48 hours later (23).

We began by examining the impact of neurotoxic hippocampal lesions made before training (experiment 1). After 13 sessions, sham-lesioned animals were digging less frequently at incorrect sand wells before going to the correct one, whereas the hippocampal-lesioned animals did not improve. A single nonrewarded probe trial was then scheduled, which started with the provision of a cue flavor in the start box. The sham-lesioned animals spent significantly more time digging at the cued location than at the other five incorrect sand wells, whereas the hippocampal-lesioned animals were at chance (Fig. 1C; see tables S1 and S2 and figs. S1 to S3 for the lesions and full experimental design). The lesions were extensive, leaving minimal residual tissue throughout the longitudinal axis of the hippocampus (Fig. 1D).

To investigate the properties of paired-associate learning and its consolidation in more detail (experiment 2), we trained normal animals in a

similar way. Probe tests, other controls, and novel context training were scheduled at various stages before and after making sham or hippocampal lesions (fig. S4). Using the same paired-associate layout as in experiment 1, we examined acquisition of sand-well choice behavior during training. A “performance index” was calculated, and this index improved monotonically across sessions (Fig. 2A). In nonrewarded probe trials, preferential digging at the correct location rather than the other five locations increased from chance levels at the outset of training to a highly significant preference for the cued location (Fig. 2B). To exclude the possibility that an olfactory cue in the correct sand well guided choice performance on training days, we conducted a single session of six trials in which the daily protocol was unchanged, except that no cue flavors were offered in the start box. Choice performance fell to chance (Fig. 2A, session 18), returning to above chance on the next normal session. The possibility of cryptic olfactory guidance by cues on the arena near the correct sand well was also ruled out in a later session by physically rotating the arena through 90° after the third trial of a session and back to its normal orientation after the third trial of a second session on the next day. The sand wells and intramaze cues were re-located such that their places relative to the distal room cues remained the same. Arena rotation had no effect (fig. S4, A3). With a different start box used in each session, it would appear that the animals can visually perceive their own location relative to the intra- and extramaze landmarks and use allocentric memory representations to identify the correct goal location among the six available sand wells.

Fig. 1. Paradigm for hippocampal-dependent paired-associate (PA) learning. (A) The large event arena (1.6 m by 1.6 m) contains a 7 × 7 grid of locations at which sand wells can be made available and four surrounding start boxes. After being given a cue flavor in a start box, the animals recall the spatial location with which it is associated, and run into the arena to that location to secure more of that flavor of food. (B) The spatial arrangement of the six PAs and the “schema” this constitutes (F, flavor; L, location). (C) Preferential digging during a nonrewarded probe test [probe trial 1 (PT1)] by sham-lesioned but not hippocampal (HPC)-lesioned animals ($n_s = 6$). Groups $t = 5.25$, $df = 10$, $P < 0.001$; sham versus chance, $t = 5.01$, $df = 5$, $P < 0.005$; HPC versus chance, not significant (n.s.). (D) A three-dimensional reconstruction of the volume of hippocampus lesioned in a representative rat (red), together with typical overlying cortical damage (yellow). The gray region represents the transparent volume of the rat brain.



If the animals develop a neocortical associative schema for this task, and if this is activated when the animals enter the apparatus, it might aid the encoding of new paired associates and their rapid assimilation into the schema. A single training session of six trials was given (Fig. 2A, session 21) in which paired associates (PAs) 1 and 6 were replaced by two new PAs, 7 and 8, hidden at two nearby locations; PAs 2 to 5 were trained normally. Note that PAs 7 and 8 received only one rewarded trial each. The inset of Fig. 2C shows how the new PAs were located near those of the now-closed sand wells. A nonrewarded probe trial was given 24 hours later to test memory for the new associates. Preferential digging was observed at the correct cued location in the arena relative to the new noncued location (i.e., less digging at location 8 for those animals on a PA7 trial, and vice versa) and to any of the original locations (PAs 2 to 5; Fig. 2D). The rapid acquisition of new PAs in a single trial, and their retention over 24 hours, are indications that the prior learning of an associative schema may aid the encoding, storage, and/or consolidation of new PAs. In contrast, animals trained on a similar one-trial task, but with novel PAs each day, showed consistent forgetting over 90 min (13).

Time course of memory consolidation. Hippocampal or sham lesions were then made 24 hours later—a much shorter time after training of the new flavors (48 hours) than is usually thought necessary for systems consolidation to be completed (24–27), and shorter than the usual time scale of differential changes in the patterns of glucose use or immediate early gene activation between hippocampus and neocortex after learning (19, 28). After recovery from surgery, a series of nonrewarded probe tests (with

interpolated training days using the original flavor-place pairs) was given to examine memory for the original schema and the two new PAs. These consisted of separate tests of the original PAs 2 to 5 and new PAs 7 and 8, each repeated once across a series of four sessions to enable both PA7 and PA8 to be tested in all animals. The hippocampal-lesioned group not only could successfully recall the original PAs learned over the previous month (Fig. 2D) but also, remarkably, could remember the newly acquired pairs PA7 and PA8. Because the lesions were near-complete (~90%; see Fig. 1D and fig. S2B), these two findings imply that (i) the memory traces for these PAs must be stored outside the hippocampus, probably in the neocortex; and (ii) consolidation of new associates whose acquisition is mediated by the hippocampus takes place within 48 hours.

To be more confident of these claims, it was essential to establish that the learning of further new PAs still required the integrity of the hippocampus in these same animals. Accordingly, immediately after this series of postoperative probe tests, we conducted a single six-trial training session with PAs 2 to 5 of the original schema, but with PAs 7 and 8 now replaced by sand wells containing two new flavors in nearby locations in the arena (PAs 9 and 10; Fig. 2E). The probe test conducted 24 hours later showed that sham-lesioned animals could readily learn and recall these new pairs, whereas the hippocampal-lesioned group could not. Thus, the one-trial acquisition of new PAs in this paradigm in experienced animals was still blocked by hippocampal lesions. Hence, it is unlikely that any relearning took place after the hippocampal lesions during the earlier series of four probe tests that had examined remote memory (the interpolated training was restricted to the well-trained PAs 2 to 5). The effective cued recall of the new PAs 7 and 8 introduced before the lesion must therefore reflect rapid, successful systems consolidation.

Although the animals appear to have acquired an associative schema reflecting the mapping of flavors to places in the arena, an alternative might be a response-based "win-stay, lose-shift" inference strategy in the manner of a learning set (29). It is not entirely clear how such a procedural strategy could be applied in this context, with six choice locations and only one trial per day to each cued location. However, as procedural strategies are generally context-independent, this account would predict that the learning of an entirely new set of six PAs in a new context would occur very quickly. In contrast, the schema hypothesis requires that a new schema be gradually learned. The same animals of experiment 2 were first trained on a new set of PAs in the same event arena (fig. S7) and then in a novel event arena in a different room with new intra- and extramaze landmarks, new flavors, and a distinct spatial geometry to the new set of sand wells (Fig. 3, A and B). Acquisition again took

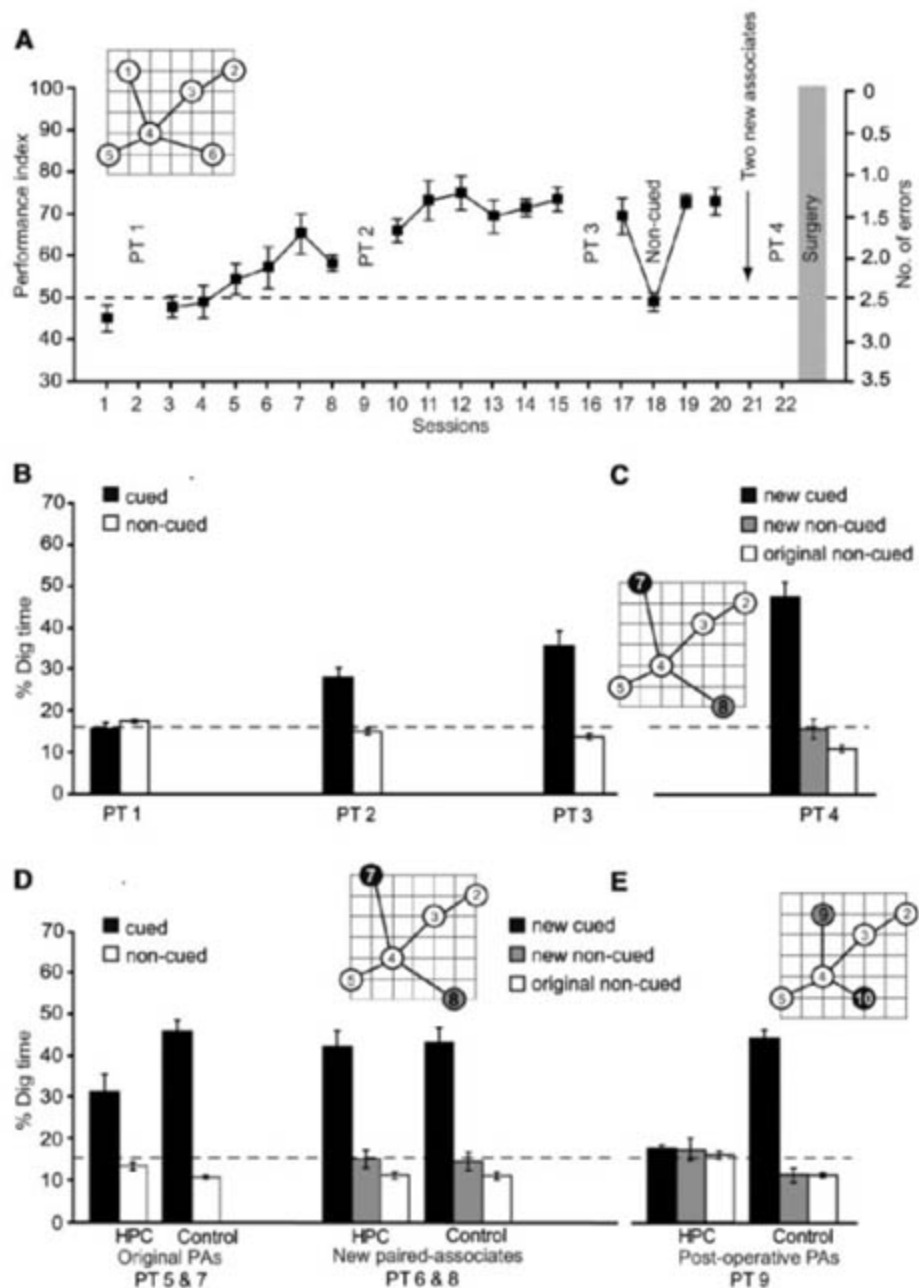


Fig. 2. Acquisition of an associative schema and its role in new learning and consolidation. (A) Acquisition of PAs. The animals ($n = 18$) made fewer choice errors over training ($F = 18.24$, $df = 5.7/97.5$, $P < 0.001$; Greenhouse-Geisser correction, including degrees of freedom) such that the performance index, computed as $100 - [100 \times (\text{errors}/5)]$, was significantly above chance from session 10 onward ($t_s > 5.08$, $df = 1/17$, $P_s < 0.001$). Removing cue flavors from the start box on session 18 resulted in performance dropping to chance and then returning to 70% correct on a succeeding normal session (session 19). (B) Cued-recall probe trials. Nonrewarded probe tests revealed a graded learning of the original PAs (cued flavor = solid bars) across sessions 2, 9, and 16 ($F = 16.24$, $df = 1.54/26.22$, $P < 0.001$; above chance in PTs 2 and 3; $t_s = 3.94$ and 6.17 , $df = 17$, $P < 0.005$ and $P < 0.001$, respectively). (C) Effective recall in PT4 of the location of the cued new PA (solid bar), coupled with avoidance of the noncued new PA (gray bar) and the remaining original associates (open bar) 24 hours after a single session of training with only one trial of each new PA (repeated-measures $F = 65.28$, $df = 1.7/29.1$, $P < 0.001$; cued location above chance, $t = 10.29$, $df = 17$, $P < 0.001$; noncued versus original, n.s.). (D) Postoperative retention. Both sham-lesioned ($n = 8$) and HPC-lesioned ($n = 10$) animals could effectively remember both original PAs (PTs 5 and 7) and new PAs introduced for a single trial 2 days before surgery (PTs 6 and 8). Both groups dug at the sand wells of the original associates (flavors 2 to 5) significantly more than chance (HPC $t = 3.60$, $df = 9$, $P < 0.01$; sham $t = 12.89$, $df = 7$, $P < 0.001$; sham versus HPC group, $t = 2.86$, $df = 16$, $P < 0.05$). Both groups also dug equally at the cued locations of the new associates relative to the noncued locations (Group \times Location $F < 1$, n.s.), and at these cued locations better than chance ($t_s > 8.07$, $df = 9$ and 7 , $P < 0.001$). (E) Postoperative new training. Hippocampal lesions prevented the learning of new PAs (PAs 9 and 10; Group \times Location $F = 60.23$, $df = 1.64/26.17$, $P < 0.001$). Digging at the cued new location in PT9 was significantly above chance only in the sham group ($t = 17.07$, $df = 7$, $P < 0.001$) and significantly lower in the HPC group than in the sham group ($t = 13.78$, $df = 16$, $P < 0.001$).

place gradually, such that the learning curve of the now experienced sham-lesioned animals did not differ from the original rate of learning

of the normal animals in the first event arena. The hippocampal-lesioned animals did not learn the new spatial schema despite repeated trials. Probe

test performance early in training followed the same gradual pattern in the sham group, resulting in effective probe test performance only by session 67 (Fig. 3C). These findings argue against a response-based strategy, such as a learning set, because learning was no faster in the new room with new flavor-place geometry.

Completion of training in the second room offered the opportunity of returning the animals to the first arena to examine their now remote memory of the original set of PAs first learned 4 to 5 months earlier. Remarkably, the hippocampal-lesioned animals were above chance in cued spatial recall (session 68, Fig. 3D) and even showed a nonsignificant trend toward better performance than did sham-lesioned controls in a probe test as early as session 2. The sham-lesioned animals may have sustained some associative interference arising from their successful training on other sand-well arrangements in this and the other contexts, but after as few as six sessions of retraining, both groups showed effective cued recall of the original PAs (Fig. 3E). Thus, the failure to learn new PAs in a new context after a hippocampal lesion did not affect the ability to remember, after several months, information acquired before the lesion—a pattern exactly like that shown by patient E.P. in his knowledge of current and past hometown topography (30).

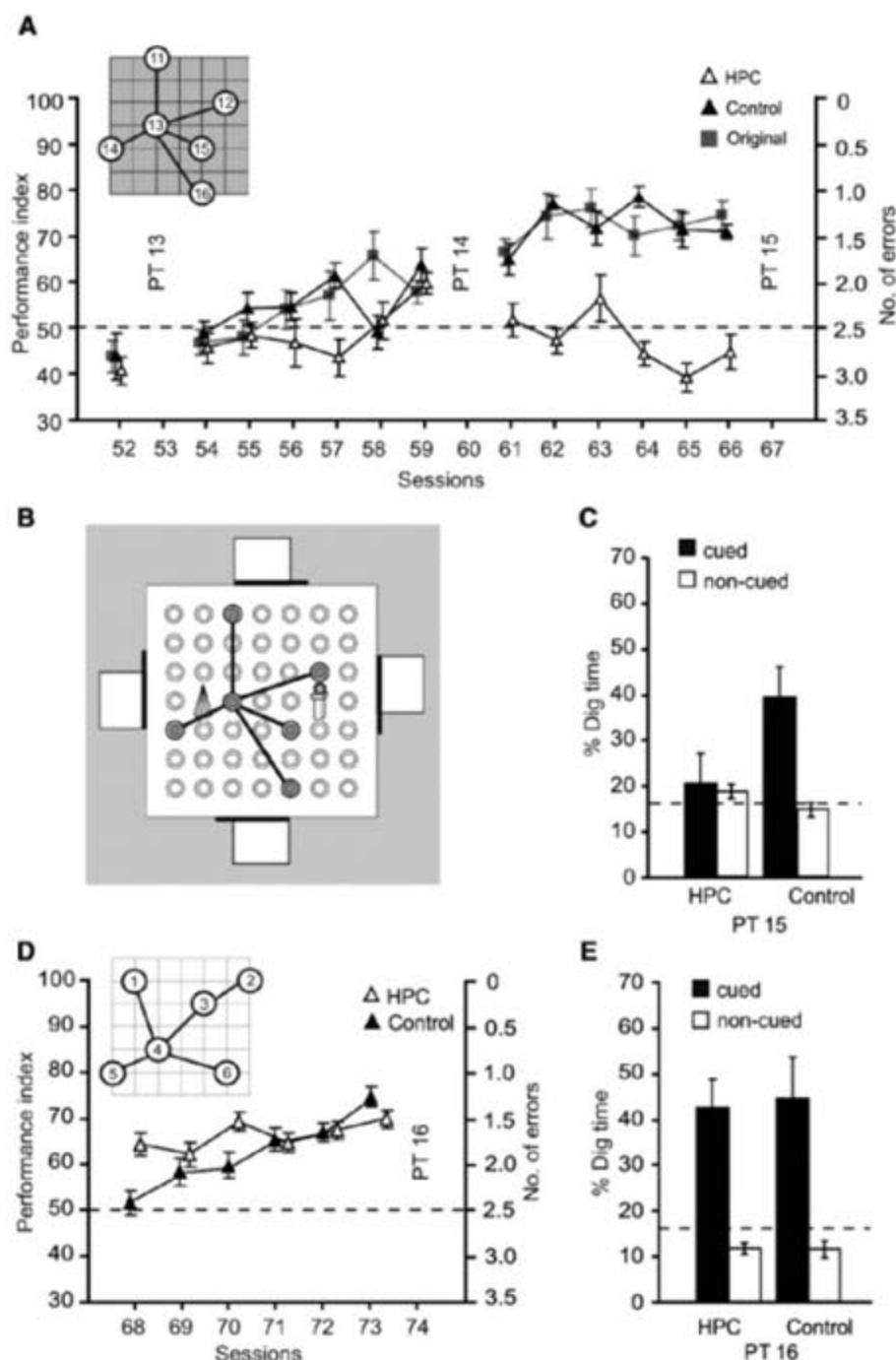


Fig. 3. Gradual acquisition of new PAs in a new context by experienced animals. (A) Acquisition of PAs. The now experienced sham group ($n = 8$) learned a new set of six PAs in the second event arena at a comparable rate to that shown by normal animals in the first event arena (Group \times Session $F = 1.97$, $df = 6.9/116.9$, $0.10 > P > 0.05$, treating Group as a between-subjects factor). Relative to the sham-lesioned group, the HPC-lesioned group ($n = 10$) failed to learn (Group $F = 128.63$, $df = 1/15$, $P < 0.001$; Group \times Session $F = 7.42$, $df = 5.9/89.3$, $P < 0.001$). (B) Spatial arrangement of the new PAs (PAs 11 to 16) in the new event arena. (C) Cued-recall probe trial. Proportion of digging at the cued location relative to the noncued locations by sham- and HPC-lesioned animals (PT15, session 67). The sham group was above chance ($t = 2.38$, $df = 7$, $P < 0.05$); the HPC group was not ($t < 1$). However, the difference between groups showed only a trend toward significance ($t = 1.83$, $df = 15$, $0.10 > P > 0.05$). (D) Return to the original event arena and flavors (flavors 1 to 6). Inset indicates transition to the original schema acquired before surgery. The HPC group is above chance at the outset ($t = 3.9$, $P < 0.005$; session 68), but neither Group nor Group \times Session effects were significant for the performance index ($P_s > 0.05$). After six sessions of retraining, the sham group caught up, and both groups were well above chance ($t_s = 8.7$ and 8.9 , $P_s < 0.001$). (E) Performance in the probe test (PT16) indicated that both HPC and sham groups were consistently above chance in preferentially digging at the cued location ($t = 4.37$, $df = 8$, $P < 0.005$; $t = 3.19$, $df = 7$, $P < 0.025$, respectively) and did not differ from each other ($t < 1$, $n.s.$).

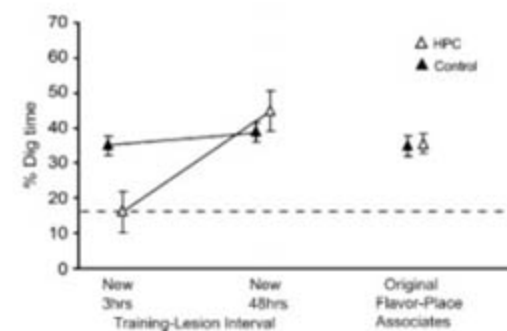


Fig. 4. Identifying the interval between training and hippocampal lesions for consolidation. A striking temporal gradient of retrograde amnesia is observed in this paradigm. HPC lesions made 3 hours after training ($n = 7$) on the novel flavor tested 14 days later prevented consolidation, whereas consolidation was complete when HPC lesions ($n = 6$) were made after 48 hours (Group \times Delay $F = 15.77$, $df = 1/13$, $P < 0.005$). The HPC and control 48-hour groups did not differ ($t < 1$). The performance of the HPC 48-hour group was significantly higher than that of the HPC 3-hour group ($t = 4.82$, $df = 11$, $P < 0.001$), but the corresponding two control groups ($n_s = 9$) did not differ ($t < 1$). The control groups were above chance at both training-lesion intervals ($t_s > 5.1$, $df = 8$, $P < 0.001$); the HPC 3-hour group did not differ from chance ($t < 1$), whereas the HPC 48-hour group was above chance ($t = 4.90$, $df = 5$, $P < 0.005$). Separate analyses of the postsurgery memory for the original PAs learned over 14 sessions showed above-chance performance for both the HPC and sham groups (HPC $t = 5.80$, $df = 12$, $P < 0.001$; sham $t = 9.85$, $df = 17$, $P < 0.001$).

If systems consolidation within the neocortex can take place in as little as 48 hours, it becomes of interest to find out the minimal time required for it to occur. Some theoretical models suppose that a memory trace stored in the hippocampus, serving as an "index" or "pointer" to cortically encoded information, must last sufficiently long to guide the slower systems-level consolidation process that is thought to take place in sleep, requires sharp-wave activity, and has previously been shown to involve hippocampal-neocortical interactions over time (31–35). The prediction is that hippocampal lesions made 3 hours after training to animals that do not sleep during this short training-surgery interval should prevent neocortical consolidation. In experiment 3 (using a new set of 18 rats that acquired the basic schema of PAs 1 to 6 over 14 sessions as before), we compared the impact of hippocampal lesions given 3 or 48 hours after the training of two new PAs in single trials (PAs 7 and 8). This experiment used a "reverse" day-night cycle (with all testing during the animal's night) to minimize, in the case of the 3-hour interval, the likelihood of sleep episodes between the end of training and the time of the lesion. A partial within-subjects design was also used (fig. S8), with some animals having hippocampal lesions at appropriate time points soon after novel PAs 7 and 8, and others that were only anesthetized in this first phase given hippocampal or sham lesions after the later

introduction of PAs 9 and 10. Cued recall was examined for the new associates shortly before surgery and was found to be effective for all animals. After surgery, cued recall for the new one-trial PAs was at chance for those animals subject to hippocampal lesions 3 hours after acquisition, but—replicating the results of experiment 2—it was effective when lesions were made 48 hours after training (Fig. 4). This is a strikingly steep upward temporal gradient of remote memory.

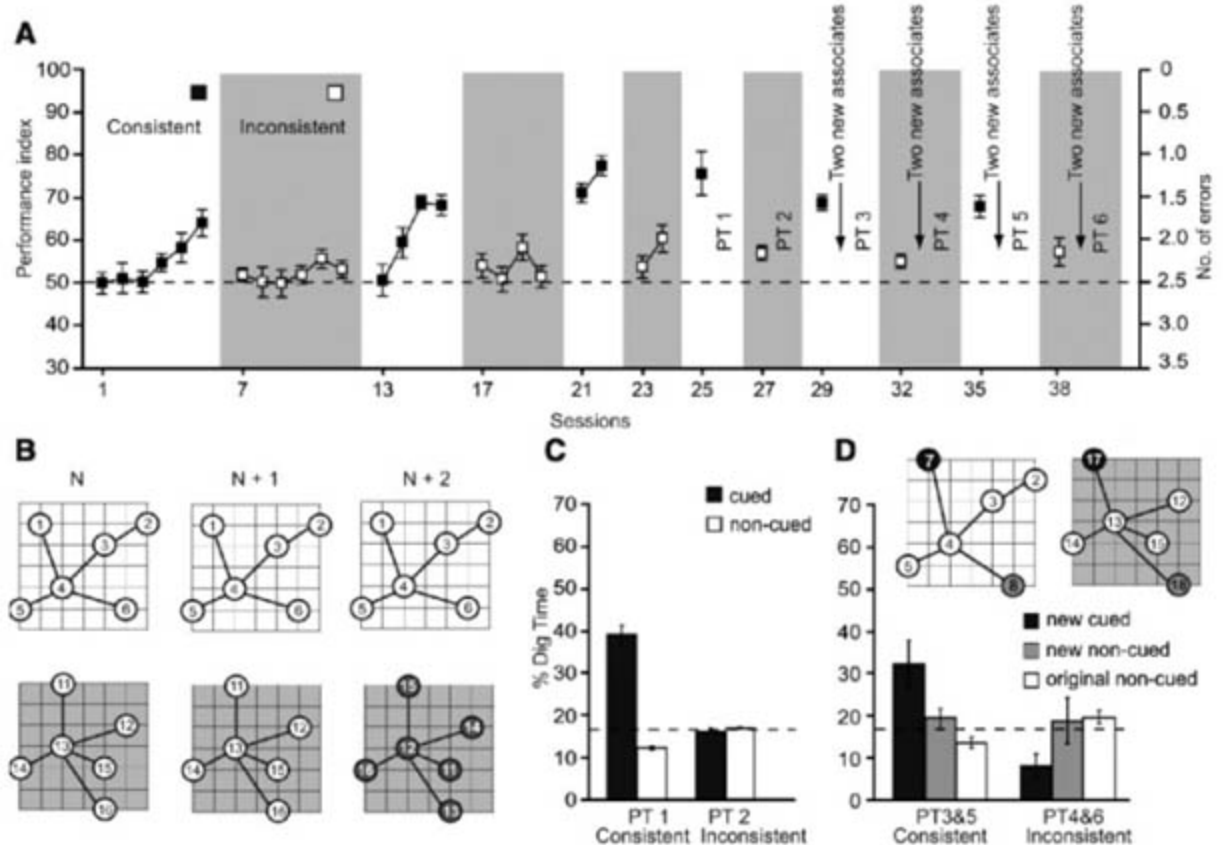
Causal role for schemas in learning. The final issue to consider is whether an activated schema is causally necessary for rapid memory consolidation (5). An alternative account of these experiments could be that the animals find it increasingly easier over the course of training to encode, store, and/or consolidate individual PAs as a result of increasing familiarity with the context of learning, with the "schema" concept being superfluous. To contrast these alternatives, we trained normal animals in two event arenas concurrently (experiment 4). In one room, they were trained on a "consistent" schema in which flavors 1 to 6 were always placed consistently at locations 1 to 6, respectively (schema 1 = PAs 1 to 6; Fig. 5B). In the other room, the animals were trained on "inconsistent" schema in which a single set of six locations (locations 11 to 16) and a set of six flavors (flavors 11 to 16) were used, but the mapping of flavors to locations was

changed every two sessions (Fig. 5B). The scheduled inconsistency was therefore in the relational pairing of the items rather than the identity of the flavors or the locations of the sand wells. Moreover, a change only every two sessions did not preclude the animals attempting to learn these PAs across sessions, but would have precluded the creation of a context-specific schema. Choice performance gradually improved in the consistent schema room but not in the inconsistent room (Fig. 5A); nonrewarded probe tests also established that the animals dug preferentially in the cued location in the arena of a start-box flavor in the consistent but not the inconsistent context (Fig. 5C). This difference between the two contexts is not in itself surprising and would occur even if the animals were still trying to learn individual PAs in the inconsistent room. However, this differential rate of learning sets the stage for a last and crucial test of the schema concept.

This test involved the learning of new PAs. If animals learn PAs as isolated "facts," and if they do so ever more quickly because of context familiarity as training in this protocol proceeds, the rate of learning in the two contexts should be the same. However, if the animals bring something like "activated schema" to bear on the process of learning, a difference between the two contexts might be observed. The "consistent schema" would only be activated in its appropriate context. Procedurally, the comparison in the rate of

Fig. 5. A consistent activated schema promotes effective memory.

(A) Differential acquisition of consistent and inconsistent schemata. Effective acquisition by normal rats ($n = 9$) occurred when mapping of flavors to places remained consistent, with six, four, two, and then single sessions (sessions 1 to 40; white background). Above-chance performance was consistent from session 15 onward ($P < 0.025$ for each comparison with chance). The same animals failed to learn a series of inconsistent schemas in the second event arena (selected days are above chance, e.g., session 27, but performance never rose above 60% correct; gray background). (B) With the consistent schema, the mapping of flavors to places is consistent across sessions; inconsistent schema used a common set of six flavors and locations that were associated for two sessions but then changed every third session (see $N + 2$, shaded gray). (C) Preferential digging in the probe trials at the cued locations for the consistent



schema (PT1: $t = 10.9$, $df = 8$, $P < 0.001$) but not for the inconsistent schema (PT2: $t < 1$). (D) New PA probes. Performance 24 hours after exposure to the two new cue flavors and their locations when the animals would be encoding information using a consistent activated schema (PTs 3 and 5) was consistently good to the cued new location, whereas performance after use of an inconsistent

schema was not (PTs 4 and 6; Group \times Location $F = 13.92$, $df = 1.64/26.30$, $P < 0.001$). Approach latencies from the start box to the correct sand well during these probe trials were equivalent in the consistent (20.9 ± 1.9 s) and inconsistent (20.0 ± 2.5 s) contexts, indicating comparable motivation to perform each task.

learning new information had to be done in a manner that ensured an identical behavioral protocol in the consistent and inconsistent rooms. In this phase, beginning at session 29, the animals were therefore trained on four successive sequences of three training sessions beginning as follows: session 29, further consistent-context training of flavors 1 to 6; session 30, two new PAs trained in a session consisting of only two trials (PAs 7 and 8); session 31, a nonrewarded probe test for these novel associates. This three-session sequence was then repeated in the inconsistent context (sessions 32 to 34) using flavors 11 to 16, then PAs 17 and 18 followed by a nonrewarded probe test; and again in the consistent and then the inconsistent context with PAs 9 and 10 and PAs 19 and 20, respectively. The sequence ended with PT6 on session 40 (Fig. 5). The use of only two rewarded trials instead of the usual six trials per day on session 2 of this three-session sequence ensured that both the behavioral procedure and the memory-encoding demands on the animals were identical in the two training contexts on session 2. Figure 5D shows successful acquisition and 24-hour retention of these new PAs only when encoding occurred in the consistent-schema context. The apparent motivation of the animals to perform these two learning tasks was equivalent, as indexed by equivalent approach latencies to the target sand well in both the consistent and inconsistent contexts (Fig. 5D).

These findings indicate that animals—no less than people—can bring activated mental schemas to bear in a PA learning task and thereby encode, assimilate, and rapidly consolidate relevant new information after a single trial. The capacity of animals to make deductive inferences on the basis of their “mental models” of the world is, of course, far more limited than that of humans (4), but the principle that associative schemas can be useful in memory is not unique to humans.

In experiment 1, animals used hippocampal-dependent learning to acquire several PAs concurrently, of which one member of each pair was a spatial location in a familiar environment. This enabled the animals to treat these several associates as a connected spatial set, rather than as individual “facts,” and so build up a framework in which similar new information could be stored. The construction of this “schema” took about a month—approximately the same period that several studies of retrograde amnesia have suggested is always required after learning for effective systems consolidation to occur. We observed, however, that if the several weeks of schema building was completed before new learning, the assimilation and consolidation of novel information within these neocortical schemata could be very rapid (experiments 2 and 3). We also established that the possession of an activated schema is causally important in the acquisition of new information (experiment 4). The use of rigorous control protocols (e.g., the noncued memory test, arena rotation) established that performance is mediated by PA memory rather than by cryptic

uncontrolled olfactory cues. Similarly, the use of two new PAs exploring associative assimilation into a schema, rather than a single PA, ensured that the effective recall in probe trials was not an artifact of stimulus novelty.

Discussion. These findings have implications for a number of key issues in the neurobiology of learning and memory. First, they indicate that the rate at which systems consolidation occurs in the neocortex can be influenced by what is already known. In contrast, in the complementary learning systems approach (36, 37), the hippocampus is said to be “specialized for rapidly memorizing specific events” (37) and the neocortex for “slowly learning the statistical regularities of the environment.” Consolidation of memory traces in the neocortex is held to be a largely time-dependent process determined by the specific patterns of information representation, anatomical connectivity, and synaptic plasticity expression rules that it can support. Broadly speaking, this is a fair characterization of a large body of data (27), but it does not quite capture the potential that the neocortex has for rapid consolidation when newly acquired information is compatible with previously acquired knowledge. Given our observation that the neocortex can sometimes consolidate very rapidly, it follows that it must also be able to encode associative memory traces very rapidly—perhaps even “on-line” within sensory-perceptual systems. The widely held supposition that the neocortex is a slow learner therefore needs to be reappraised. The distinct temporal dynamics of these memory processes may contribute to the usual finding that the cortex does learn more slowly than subcortical structures—a generality that extends to conditional-associative motor learning (38)—but that this may not always occur.

A second finding is that the storage and recall of allocentric spatial memory can occur outside the hippocampus in the rat, even for information that has been acquired in a single trial as a consequence of hippocampal-dependent processing. This conflicts with both the cognitive-map theory and the multiple-trace theory of memory consolidation (7, 39, 40). Spatial memory has been shown previously in rats with hippocampal lesions, but the information was either acquired postoperatively and inflexibly over very extended training (41, 42) or “semanticized” over many months before the lesion (43). The long-sought upward gradient of remote spatial memory in rats when varying intervals of time are systematically scheduled before making hippocampal lesions (44–47) is now definitively shown using a cued-recall protocol for information acquired in one trial. The temporal gradient is much steeper than might have been expected on the basis of prior work using a within-subjects design for contextual fear conditioning (26). Moreover, the effective remote spatial memory in hippocampal-lesioned animals upon their return to the first event arena, learned as young animals, is strikingly similar to that displayed by patient E.P.

(30). It is unclear why effective remote spatial memory is found here but not in the water maze (48). One possibility is that the water maze is more “recall-like” in character (10), requiring an animal to generate its own reminder cues. The PA paradigm used here could allow apparent cued recall to be mediated in part by cued recognition based on proximal intramaze cues.

Third, the failure of animals with near-complete hippocampal lesions to acquire PAs over many trials of training (experiments 1 and 2) calls into question the capacity for effective “semantic-like” learning in the absence of functional hippocampal tissue. This idea emerged particularly in studies of developmental amnesia (49), but it has proved difficult to distinguish whether the intriguing dissociations between impaired episodic and intact semantic memory in such patients are due to intact neocortical learning of semantic information (50), to functional reorganization in the developing brain, or to islands of residual hippocampal function in these amnesic patients. When the medial temporal lesions are large, as in patient E.P., essentially no declarative fact learning occurs (51). Our findings suggest that, in animals in which it is possible to make selective 90% lesions of the hippocampus as adults, the acquisition of new flavor-place PAs is also consistently blocked and not rescued by multiple training trials. The generality of this observation beyond the spatial domain should be followed up in young animals, including primates, in order to model the situation in developmental amnesia more closely.

That the acquisition of a schema took about a month points to the possibility of it involving some kind of neuroanatomical growth process in the neocortex that creates an associative “space” in which new PAs can be rapidly stored without interference—analogue to “phase sequences” (52). Intercortical synaptic connections may be created or unmasked within a functional network that has only silent or baseline synaptic strengths. These could then be rapidly potentiated by relevant information when the network is in an “active” state (an activated schema). The initial growth process would necessarily take a period of days or weeks—the very time period that has hitherto been thought to mediate systems consolidation and to occur only after learning (20). Thus, an intriguing speculation to emerge from the present data, with conceptual similarities to the principles of synaptic tagging and capture (53, 54), is that an associative space into which new information can be assimilated can be constructed before the exposure to that information. However, this construction of associative interconnections can be noncommittal or “experience-expectant” in character (55).

The findings bring to neuroscience a set of ideas hitherto largely discussed in the context of psychological studies of human memory. The concept of “activated schemas” has been discussed only in relation to humans (3), as it implies a conscious awareness that rats are unlikely

to possess. However, even if they are implicit, schemas are an economical way to characterize the gradual acquisition of an organized framework of associative “semantic-like” information from “episodic-like” events that, once acquired, allows relevant new information to be assimilated and stored rapidly. Given that animals have daily activities such as finding food and water, it is important for them to retain an organized body of knowledge about where these may be found and to be able to update such a framework rapidly, within one trial. This inferential flexibility of rodent cognition is now established in several domains (9).

References and Notes

1. F. C. Bartlett, *Remembering* (Cambridge Univ. Press, Cambridge, 1932).
2. K. Craik, *The Nature of Explanation* (Cambridge Univ. Press, Cambridge, 1943).
3. J. D. Bransford, *Human Cognition: Learning, Understanding and Remembering* (Wadsworth, Belmont, CA, 1979).
4. P. N. Johnson-Laird, *Mental Models: Towards a Cognitive Science of Language, Inference, and Consciousness* (Cambridge Univ. Press, Cambridge, 1983).
5. J. D. Bransford, M. K. Johnson, *J. Verb. Learn. Verb. Behav.* **11**, 717 (1972).
6. E. A. Maguire, C. D. Frith, R. G. M. Morris, *Brain* **122**, 1839 (1999).
7. J. O'Keefe, L. Nadel, *The Hippocampus as a Cognitive Map* (Clarendon, Oxford, 1978).
8. B. O. McGonigle, M. Chalmers, *Nature* **267**, 694 (1977).
9. H. Eichenbaum, *Neuron* **44**, 109 (2004).
10. L. R. Squire, *Psychol. Rev.* **99**, 195 (1992).
11. Y. Dudai, R. G. M. Morris, in *Brain, Perception and Memory: Advances in Cognitive Sciences*, J. Bolhuis, Ed. (Oxford Univ. Press, Oxford, 2001), pp. 147–162.
12. J. L. McClelland, B. L. McNaughton, R. C. O'Reilly, *Psychol. Rev.* **102**, 419 (1995).
13. M. Day, R. F. Langston, R. G. M. Morris, *Nature* **424**, 205 (2003).
14. M. Bunsey, H. Eichenbaum, *Nature* **379**, 255 (1996).
15. R. P. Kesner, M. R. Hunsaker, P. E. Gilbert, *Behav. Neurosci.* **119**, 781 (2005).
16. S. Wirth *et al.*, *Science* **300**, 1578 (2003).
17. K. Sakai, Y. Miyashita, *Nature* **354**, 152 (1991).
18. Y. Miyashita, *Science* **306**, 435 (2004).
19. B. Bontempi, C. Laurent-Demir, C. DeStrade, R. Jaffard, *Nature* **400**, 671 (1999).
20. P. W. Frankland, B. Bontempi, *Nat. Rev. Neurosci.* **6**, 119 (2005).
21. H. Eichenbaum, P. Dudchenko, E. Wood, M. Shapiro, H. Tanila, *Neuron* **23**, 209 (1999).
22. The food used as one member of each PA (diet pellets manufactured in a range of different flavors) was hidden in a sand mixture that had been adulterated by ground-up pellets consisting of 1% of each of the six flavors used on any daily session (6% total). This and other procedures masked any olfactory cue that might have guided the animals to the correct sand well. The animals were shown to use recall of spatial location exclusively in making their sand-well choices. No food pellets were present in the sand mixture during nonrewarded probe tests.
23. See supporting material on Science Online.
24. S. M. Zola-Morgan, L. R. Squire, *Science* **250**, 288 (1990).
25. J. J. Kim, M. S. Fanselow, *Science* **256**, 675 (1992).
26. S. G. Anagnostaras, S. Maren, M. S. Fanselow, *J. Neurosci.* **19**, 1106 (1999).
27. P. J. Bayley, J. J. Gold, R. O. Hopkins, L. R. Squire, *Neuron* **46**, 799 (2005).
28. T. Maviel, T. P. Durkin, F. Menzaghi, B. Bontempi, *Science* **305**, 96 (2004).
29. H. F. Harlow, *Psychol. Rev.* **56**, 51 (1949).
30. E. Teng, L. R. Squire, *Nature* **400**, 675 (1999).
31. T. J. Teyler, P. DiScenna, *Behav. Neurosci.* **100**, 147 (1986).
32. G. Buzsaki, *Neuroscience* **31**, 551 (1989).
33. A. G. Siapas, M. A. Wilson, *Neuron* **21**, 1123 (1998).
34. B. L. McNaughton *et al.*, in *Sleep and Synaptic Plasticity*, C. Smith, P. Maquet, Eds. (Oxford Univ. Press, New York, 2003), pp. 225–246.
35. R. G. Morris, *Eur. J. Neurosci.* **23**, 2829 (2006).
36. R. C. O'Reilly, J. W. Rudy, *Psychol. Rev.* **108**, 311 (2001).
37. K. A. Norman, R. C. O'Reilly, *Psychol. Rev.* **110**, 611 (2003).
38. A. Pasupathy, E. K. Miller, *Nature* **433**, 873 (2005).
39. R. S. Rosenbaum, G. Winocur, M. Moscovitch, *Behav. Brain Res.* **127**, 183 (2001).
40. M. Moscovitch, L. Nadel, G. Winocur, A. Gilboa, R. S. Rosenbaum, *Curr. Opin. Neurobiol.* **16**, 179 (2006).
41. R. G. M. Morris, F. Schenk, F. Tweedie, L. E. Jarrard, *Eur. J. Neurosci.* **2**, 1016 (1990).
42. H. Eichenbaum, C. Stewart, R. G. M. Morris, *J. Neurosci.* **10**, 3531 (1990).
43. G. Winocur, M. Moscovitch, S. Fogel, R. S. Rosenbaum, M. Sekeres, *Nat. Neurosci.* **8**, 273 (2005).
44. J. J. Bolhuis, C. A. Stewart, E. M. Forrest, *Q. J. Exp. Psychol. B* **47**, 129 (1994).
45. R. J. Sutherland *et al.*, *Hippocampus* **11**, 27 (2001).
46. R. E. Clark, N. J. Broadbent, L. R. Squire, *Hippocampus* **15**, 260 (2005).
47. S. J. Martin, L. de Hoz, R. G. M. Morris, *Neuropsychologia* **43**, 609 (2005).
48. R. G. M. Morris, P. Garrud, J. N. Rawlins, J. O'Keefe, *Nature* **297**, 681 (1982).
49. F. Vargha-Khadem *et al.*, *Science* **277**, 376 (1997).
50. M. Mishkin, W. A. Suzuki, D. G. Gadian, F. Vargha-Khadem, *Philos. Trans. R. Soc. London Ser. B* **352**, 1461 (1997).
51. P. J. Bayley, L. R. Squire, *J. Neurosci.* **22**, 5741 (2002).
52. D. O. Hebb, *The Organization of Behaviour* (Wiley, New York, 1949).
53. U. Frey, R. G. M. Morris, *Nature* **385**, 533 (1997).
54. A. Govindarajan, R. J. Kelleher, S. Tonegawa, *Nat. Rev. Neurosci.* **7**, 575 (2006).
55. W. T. Greenough, J. E. Black, in *Developmental Behavioral Neuroscience*, M. R. Gunnar, C. A. Nelson, Eds., vol. 24 of *Minnesota Symposia on Child Psychology* Erlbaum, Hillsdale, NJ, 1992; pp. 155–200.
56. Supported by a UK Medical Research Council program grant (R.G.M.M.), a UK Biotechnology and Biological Sciences Research Council studentship award (R.F.L.), and a Fondation pour la Recherche Médicale fellowship (I.B.). We thank J. Tulloch for assistance with the histology.

Supporting Online Material

www.sciencemag.org/cgi/content/full/316/5821/76/DC1

Materials and Methods

Figs. S1 to S8

Tables S1 and S2

References

5 October 2006; accepted 23 February 2007

10.1126/science.1135935

REPORTS

Nonstoichiometric Dislocation Cores in α -Alumina

N. Shibata,^{1*} M. F. Chisholm,² A. Nakamura,³ S. J. Pennycook,² T. Yamamoto,⁴ Y. Ikuhara¹

Little is known about dislocation core structures in oxides, despite their central importance in controlling electrical, optical, and mechanical properties. It has often been assumed, on the basis of charge considerations, that a nonstoichiometric core structure could not exist. We report atomic-resolution images that directly resolve the cation and anion sublattices in alumina (α -Al₂O₃). A dissociated basal edge dislocation is seen to consist of two cores; an aluminum column terminates one partial, and an oxygen column terminates the second partial. Each partial core is locally nonstoichiometric due to the excess of aluminum or oxygen at the core. The implication for mechanical properties is that the mobile high-temperature dislocation core structure consists of two closely spaced partial dislocations. For basal slip to occur, synchronized motion of the partials on adjacent planes is required.

The core structures of dislocations are critical to the electronic, optical, and mechanical properties of a wide range of materials. For most simple monometallic crys-

tals, dislocation core termination can be determined; however, in complex crystals such as oxides, either cation or anion columns (or both) can be the terminating atomic columns even

with the same dislocation character (i.e., characteristic displacement vectors called Burgers vectors, **b**). The possibility of nonstoichiometric cores also arises but has usually been rejected because it suggests the possibility of charged dislocations (1, 2) and the presence of long-range Coulomb fields with a high associated electrostatic energy. This has been suggested to be the reason why the close-packed {111} crystal plane in alkali halides cannot be an easy slip system (2, 3). Detailed knowledge of dislocation core structures and compositions is critical to understand dislocations in ionic crystals.

¹Institute of Engineering Innovation, University of Tokyo, 2-11-16, Yayoi, Bunkyo, Tokyo 113-8656, Japan. ²Materials Science and Technology Division, Oak Ridge National Laboratory, Oak Ridge, TN 37831-6030, USA. ³Department of Intelligent Materials Engineering, Osaka City University, 3-3-138, Sugimoto, Sumiyoshi-ku, Osaka, 558-8585, Japan. ⁴Department of Advanced Materials Science, University of Tokyo, 5-1-5, Kashiwanoha, Kashiwa, Chiba 277-8561, Japan.

*To whom correspondence should be addressed. E-mail: shibata@sigma.t.u-tokyo.ac.jp

The inherent structural complication of alpha alumina ($\alpha\text{-Al}_2\text{O}_3$) and, indeed, other complex compounds has led to conflicting models for dislocation glide (4–6). Alumina is widely used in many industrial areas because of its superior mechanical, thermal, and chemical stability at high temperatures. Slip on the $\{0001\}$ basal plane is reported to be the dominant deformation system at elevated temperatures (7), and thus important for understanding the high-temperature mechanical behavior. Kronberg (4) first proposed a basal dislocation slip model based on structurally related hexagonal metals. Slip was assumed to occur between Al and O basal-plane layers. To maintain the nor-

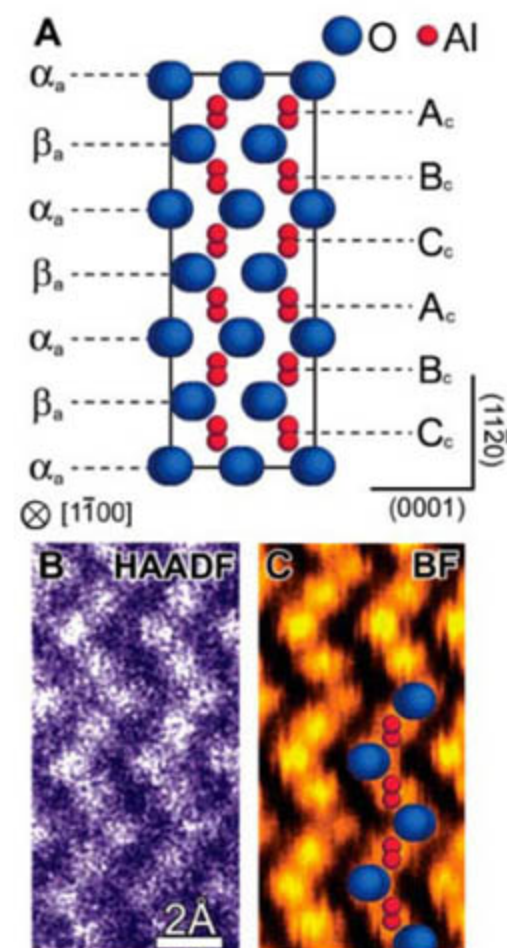


Fig. 1. Crystal structure and simultaneous atomic-resolution high-angle annular dark-field (HAADF) and bright-field (BF) STEM images of $\alpha\text{-Al}_2\text{O}_3$. (A) Unit structure of $\alpha\text{-Al}_2\text{O}_3$ viewed from the $\langle 1\bar{1}00 \rangle$ direction. The structure of $\alpha\text{-Al}_2\text{O}_3$ consists of alternating Al and O planes along the $\langle 0001 \rangle$ direction, whose stacking sequence is $\cdots\alpha_a A_c \beta_a B_c \alpha_a C_c \beta_a A_c B_c \beta_a C_c \alpha_a \cdots$. From the $\langle 1\bar{1}00 \rangle$ projection, we can distinguish individual Al and O columns. (B and C) Simultaneous HAADF (B) and bright-field (C) STEM images of $\alpha\text{-Al}_2\text{O}_3$ viewed from the $\langle 1\bar{1}00 \rangle$ direction. Comparison of the images shows that the bright spots in the bright-field image directly correspond to the positions of atomic columns under the conditions used to obtain the images (11). As seen in the images, bright-field STEM can distinguish Al and O atomic columns in this projection.

mal octahedral coordination of the oxygen to aluminum sites, Kronberg proposed the synchroshear mechanism, whereby two shears operate in different directions on adjacent atomic planes. This mechanism has been shown to operate in the Laves phase compound HfCr_2 (8). Later, Bilde-Sørensen *et al.* (5) argued that the slip between Al and O planes would require charge transport. Alternatively, they proposed that dislocation slip would occur along the midplane on the puckered Al (cation) layer. They argued that this choice of the slip plane allows the moving dislocations to carry no net charge.

Figure 1A shows a ball-and-stick model of $\alpha\text{-Al}_2\text{O}_3$ in the $\langle 1\bar{1}00 \rangle$ projection. From this viewing direction, Al- and O-atom sites are arranged as distinct columns. The stacking sequence of $\alpha\text{-Al}_2\text{O}_3$ along the $\langle 0001 \rangle$ direction

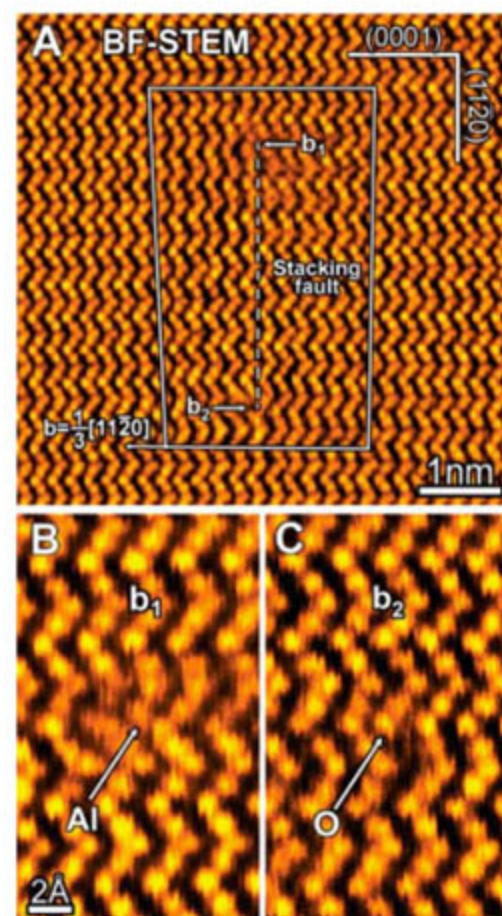


Fig. 2. Atomic-resolution bright-field STEM image of a basal edge dislocation core in $\alpha\text{-Al}_2\text{O}_3$. (A) Typical core structure of a basal dislocation observed from the $\langle 1\bar{1}00 \rangle$ direction. The dislocation core is dissociated with two partials ($\frac{1}{2}\langle 10\bar{1}0 \rangle$ and $\frac{1}{2}\langle 01\bar{1}0 \rangle$) connected by a $\{1\bar{1}20\}$ stacking fault. (B and C) Bright-field STEM images of the upper and lower partial dislocation cores, respectively. The upper partial core is terminated by an Al column, whereas the lower partial core is terminated by an O column. Both core terminations lie in between the Al and O atomic planes. Each partial core is non-stoichiometric due to the excess of Al or O, but the total basal dislocation chemically preserves Al_2O_3 stoichiometry.

consists of 12 alternating cation and anion basal layers. The cation layers are slightly puckered along the $\langle 0001 \rangle$ direction. Bilde-Sørensen *et al.* proposed that basal slip occurs between these shifted Al sites (5).

The core structure of a basal edge dislocation in $\alpha\text{-Al}_2\text{O}_3$ is observed by scanning transmission electron microscopy (STEM). Now, sub-angstrom resolution can be achieved with this technique (9). Figure 1, B and C, show simultaneous high-angle annular dark-field (HAADF) and bright-field STEM images of $\alpha\text{-Al}_2\text{O}_3$ viewed along the $\langle 1\bar{1}00 \rangle$

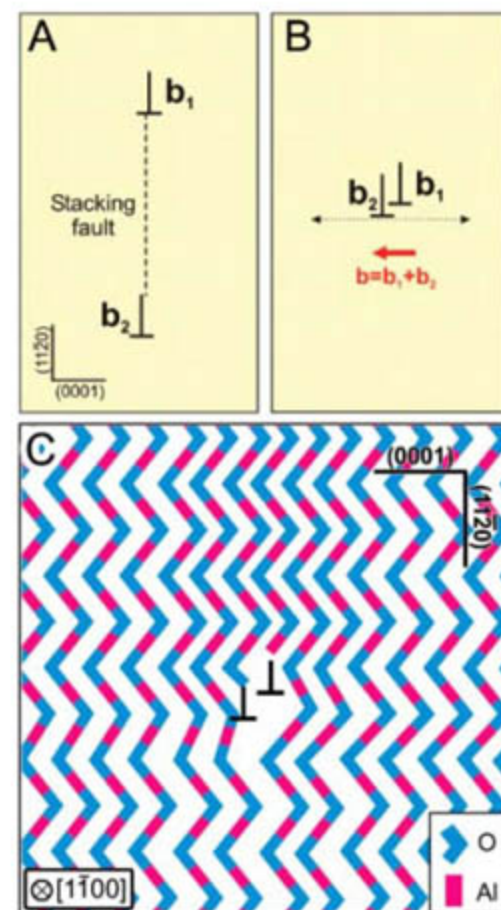


Fig. 3. Schematics of basal edge dislocation core structures observed at low temperatures and the mobile core at high temperatures. (A) Schematic illustration of basal edge dislocation core structure observed in this study. The perfect basal edge dislocation dissociates into two partial dislocations perpendicular to the slip plane with the formation of a $\{1\bar{1}20\}$ stacking fault in between. (B) Schematic illustration of mobile basal edge dislocation core model at high temperatures. Two partials move very close together without forming a $\{1\bar{1}20\}$ stacking fault in between. (C) Proposed atomic structure model ($\langle 1\bar{1}00 \rangle$ projection) of mobile perfect basal edge dislocation at high temperatures, based on the present low-temperature observations. Blue and red segments in the figure correspond to the O and Al atomic columns, respectively. In this model, the two dissociated partials observed at low temperature are located on adjacent basal planes in the mobile high-temperature dislocation.

direction. The Z-contrast image obtained with the HAADF detector is an incoherent image (10); it is essentially a map of the scattering power of the specimen. There is a direct correspondence between the features in the specimen and their image. In contrast, the phase-contrast image obtained with a small bright-field detector has coherent image characteristics, which is comparable to the parallel beam high-resolution TEM. The contrast is influenced by the focus of the objective lens and specimen thickness, orientation, and scattering power. This makes phase-contrast images of unknown structures difficult to directly interpret. However, this sensitivity can be exploited to provide much greater contrast variations than can be obtained from the Z-contrast images of low-atomic number elements (such as Al and O). The simultaneously recorded Z- and phase-contrast images (Fig. 1, B and C) of the $\langle 1\bar{1}00 \rangle$ projection of $\alpha\text{-Al}_2\text{O}_3$ reveal parallel kinked lines of spots that reflect the arrangement of alternating O and Al columns along the $\langle 0001 \rangle$ direction. Under the conditions used to obtain these two images, the bright features of the Z-contrast image are seen to correspond to the bright features in the bright-field image. These bright features identify the positions of the two O columns and the puckered Al column in each segment of the kinked lines seen in this projection (11).

Figure 2A shows a typical bright-field STEM image of a basal dislocation core in $\alpha\text{-Al}_2\text{O}_3$. The line direction of the dislocation is parallel to the observing direction, so that the core structure is set at an "edge-on" condition. In this condition, bright spots in the image correspond to the positions of atomic columns as determined from the simultaneous

Z-contrast image. It is apparent that at room temperature, this dislocation is not a single perfect dislocation ($\mathbf{b} = \frac{1}{2}\langle 1\bar{1}\bar{2}0 \rangle$), but has an extended structure with partials ($\mathbf{b} = \frac{1}{2}\langle 10\bar{1}0 \rangle$ and $\mathbf{b} = \frac{1}{2}\langle 01\bar{1}0 \rangle$) connected by a $\{11\bar{2}0\}$ stacking fault, consistent with the previous reports of dislocation observations after basal slip deformation (12–14). The dissociation is considered to be driven by the reduction of strain energy and suppressed by increasing stacking-fault energy. Dissociation occurs on the $\{11\bar{2}0\}$ plane by self-climb (14). No evidence for dissociation on the $\{0001\}$ basal plane is observed. Our low-temperature observations show that the cores are separated in the $\langle 11\bar{2}0 \rangle$ direction by only 0.24 nm. This observation is consistent with stacking-fault energy calculations that show that the $\{0001\}$ fault has higher energy than the $\{11\bar{2}0\}$ fault at low temperatures (15).

The bright-field STEM images of each dissociated partial core are shown in Fig. 2, B and C. The arrows in the images indicate the respective position of an extra half-plane termination of the two partials. The images reveal that the upper core is terminated between vertices of the kinked line of atoms at an Al-column position, whereas the lower core is terminated at a vertex of the kinked line of atoms at an O-column position. These observations clearly show both dislocation core terminations and, thus, indicate that the slip planes of the dislocations are located between the Al and O atomic planes. Moreover, the partials terminated by Al or O column indicate that the partial cores are locally not stoichiometric. Contrary to the common assumption, nonstoichiometric core structures actually exist in an ionic crystal. Although each partial dislocation core is nonstoichiometric,

the total dislocation preserves Al_2O_3 stoichiometry.

Because the dissociation occurs in the direction normal to the $\{0001\}$ slip plane, as in Fig. 3A, glide of the dissociated dislocations on the $\{0001\}$ planes would require continuous structural rearrangements as the stacking fault between the partials is moved. In this case, dislocation motion would require atomic diffusion and would be very sluggish at low temperatures. It is thus expected that the dislocations that are mobile at high temperatures are not dissociated with a $\{11\bar{2}0\}$ stacking fault (13, 14), as schematically shown in Fig. 3B. That is, the mobile dislocation core at high temperature should consist of two closely spaced partial dislocations. At the most basic level, dislocation glide occurs by the successive slip of terminating atomic columns on the stationary atomic planes. In $\alpha\text{-Al}_2\text{O}_3$, the relative motions of $\{0001\}$ O layers and the sandwiched Al layer are considered to be involved in the basal dislocation glide. The difference in core termination results in two slightly different slip processes. If the dislocation is O terminated, the moving O plane slips over an Al plane. If, instead, the dislocation is Al terminated, the moving Al plane slips over an O plane. On the basis of our low-temperature observations, we propose that the slip planes of moving partials are located not on the same atomic plane, but on adjacent Al and O $\{0001\}$ planes. Figure 3C shows the possible perfect basal edge dislocation core structure mobile at high temperatures. We assume that the two dissociated partials observed at low temperature are located on adjacent basal planes in the mobile high-temperature dislocation. Although other reconstructions are possible, our observations show that these Al- and O-terminated partials exist, and when the dislocation glide stops, this model can dissociate by climb to form partial dislocation core structures consistent with our experimental observation. Thus, we propose that the atomic-scale basal slip processes are based on the simple core model shown in Fig. 3C. Because the schematic is viewed in a $\langle 1\bar{1}00 \rangle$ projection, the vector component normal to the schematic is not shown. However, it should be stated that the two partials have equal and opposite vector components normal to the schematic.

Figure 4, A to C, shows the slip sequence of the core model shown in Fig. 3C. The partial dislocations ($\mathbf{b} = \frac{1}{2}\langle 10\bar{1}0 \rangle$ and $\mathbf{b} = \frac{1}{2}\langle 01\bar{1}0 \rangle$) combine to produce a unit dislocation ($\mathbf{b} = \frac{1}{2}\langle 1\bar{1}\bar{2}0 \rangle$). Again, only the slip components perpendicular to the $\langle 1\bar{1}00 \rangle$ projection are shown in this schematic. The successive slip of the two partials on adjacent planes (slip planes 1 and 2) recovers the perfect stacking sequence on the Al sublattice (11). However, in sapphire, there is a slight deviation from the perfect close-packed structure seen in the oxygen

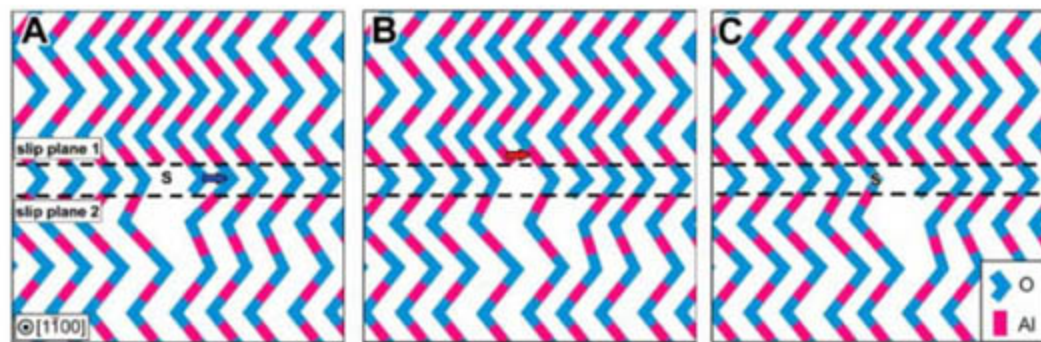


Fig. 4. Schematics of the mobile high-temperature basal edge dislocation core structure in cross section ($\langle 1\bar{1}00 \rangle$ projection). Blue and red segments in the figure correspond to the O and Al atomic columns, respectively. (A) The dislocation, consisting of adjacent partial dislocations with O and Al termination. The slip planes of the two partials are on adjacent atomic planes (slip planes 1 and 2). "s" indicates the initial position of the dislocation. In these schematics, only the vector components perpendicular to the viewing direction are shown, but the two partials actually have equal and opposite vector components perpendicular to the schematic. (B) The first partial (O-terminated) slipping on a fixed Al plane. (C) The passage of the second partial (Al-terminated) slipping on an O plane. It is expected that (B) and (C) occur simultaneously, and during the process, slight relaxation in the O plane in between the slip planes 1 and 2 is required to preserve the perfect stacking sequence in O layers. The plain-view schematics of the present basal dislocation motion show that the proposed dislocation motion preserves a perfect stacking sequence in Al layers (11).

sublattice that is correlated with the stacking of adjacent Al layers (16). This slight deviation in oxygen positions can be schematically seen in the projected structure model of Fig. 1A. If these deviations were a spatially fixed part of the structure, the motion of a single partial would result in a stacking fault in the oxygen sublattice. In the present slip model, the O plane in between slip planes 1 and 2 is sheared by only one partial, and thus a stacking fault on the O sublattice would be produced if we assume rigid O layers. However, the deviations are related to the positions of the Al atoms, neighboring O, atoms and vacant sites sandwiched between the O layers. Because the perfect Al stacking is preserved after the dislocation motion, the O sublattice can also preserve a perfect stacking sequence by an appropriate small modification in the O atom positions. It is important to note that these two partial motions are not independent in our proposed model. Both partials move simultaneously on adjacent {0001} basal planes to complete the perfect dislocation slip. A total basal dislocation is thus considered to possess two atomic slip planes. This core structure is expected to dissociate after the dislocation stops moving and form two partials, consistent with our observations in Fig. 2.

We propose that basal slip in α -Al₂O₃ is controlled by the partial dislocations that dissociate from the perfect $\frac{1}{2}(11\bar{2}0)$ dis-

location. The structure of these partials is based on our low-temperature observations, in which each partial core is terminated by Al and O columns, respectively, but the total dislocation preserves Al₂O₃ stoichiometry. Bilde-Sørensen *et al.* (5) also proposed a stoichiometric core model, but the slip plane (located at the midplane on the puckered Al layer) is not consistent with our images. Our images clearly show that the termination of both partials is located in between the Al and O layers at low temperature. Our results represent a definitive starting point for realistic atomic-level modeling of slip processes, dislocation generation, and their effects on the mechanical properties of α -Al₂O₃. Also, the present results will provide a crucial check for future theoretical calculations of dislocations in complex oxides.

We have provided experimental evidence that locally nonstoichiometric structures are allowed in crystals with strong ionic character. Simultaneous HAADF and bright-field STEM imaging with aberration correction is a powerful tool for observing such localized defect structures, even in very complex crystals. The possibility for atomic-scale characterization of dislocation core structures will assist our understanding of dislocation activity and its effects on the electrical, optical, and mechanical properties of complex, multicomponent materials.

References and Notes

1. J. P. Hirth, J. Lothe, *Theory of Dislocations* (Krieger, Malabar, FL, ed. 2, 1992).
2. R. W. Whitworth, *Adv. Phys.* **24**, 203 (1975).
3. J. J. Gilman, *Acta Metall.* **7**, 608 (1959).
4. M. L. Kronberg, *Acta Metall.* **5**, 507 (1957).
5. J. B. Bilde-Sørensen *et al.*, *Acta Mater.* **44**, 2145 (1996).
6. D. E. Luzzi, G. Rao, T. A. Dobbins, D. P. Pope, *Acta Mater.* **46**, 2913 (1998).
7. K. P. D. Lagerlöf, A. H. Heuer, J. Castaing, J. P. Rivière, T. E. Mitchell, *J. Am. Ceram. Soc.* **77**, 385 (1994).
8. M. F. Chisholm, S. Kumar, P. Hazledine, *Science* **307**, 701 (2005).
9. P. D. Nellist *et al.*, *Science* **305**, 1741 (2004).
10. S. J. Pennycook, D. E. Jesson, *Phys. Rev. Lett.* **64**, 938 (1990).
11. Materials and Methods are available as supporting material on Science Online.
12. T. E. Mitchell, B. J. Pletka, D. S. Phillips, A. H. Heuer, *Philos. Mag.* **34**, 441 (1976).
13. A. Nakamura, T. Yamamoto, Y. Ikuhara, *Acta Mater.* **50**, 101 (2002).
14. K. P. D. Lagerlöf *et al.*, *Acta Metall.* **32**, 97 (1984).
15. P. R. Kenway, *Philos. Mag. B* **68**, 171 (1993).
16. S. Geschwind, J. P. Remeika, *Phys. Rev.* **122**, 757 (1961).
17. We thank K. P. D. Lagerlöf for valuable discussions. This research was supported by the Japan Society for the Promotion of Science and the Division of Materials Sciences and Engineering, Office of Basic Energy Sciences, U.S. Department of Energy.

Supporting Online Material

www.sciencemag.org/cgi/content/full/316/5821/82/DC1

Materials and Methods

Figs. S1 and S2

References

11 October 2006; accepted 14 February 2007

10.1126/science.1136155

Acid Catalysis in Basic Solution: A Supramolecular Host Promotes Orthoformate Hydrolysis

Michael D. Pluth, Robert G. Bergman,* Kenneth N. Raymond*

Although many enzymes can promote chemical reactions by tuning substrate properties purely through the electrostatic environment of a docking cavity, this strategy has proven challenging to mimic in synthetic host-guest systems. Here, we report a highly charged, water-soluble, metal-ligand assembly with a hydrophobic interior cavity that thermodynamically stabilizes protonated substrates and consequently catalyzes the normally acidic hydrolysis of orthoformates in basic solution, with rate accelerations of up to 890-fold. The catalysis reaction obeys Michaelis-Menten kinetics and exhibits competitive inhibition, and the substrate scope displays size selectivity, consistent with the constrained binding environment of the molecular host.

Synthetic chemists have long endeavored to design host molecules capable of selectively binding slow-reacting substrates and catalyzing their chemical reactions. Whereas synthetic catalysts are often site-specific

and require certain properties of the substrate to insure catalysis, enzymes are often able to modify basic properties of the bound substrate such as pK_a (where K_a is the acid dissociation constant) in order to enhance reactivity. Two common motifs used by nature to activate otherwise unreactive compounds are the precise arrangement of hydrogen-bonding networks and electrostatic interactions between the substrate and adjacent residues of the protein (1). Precise arrangement of hydro-

gen bonding networks near the active sites of proteins can lead to well-tuned pK_a matching (2) and can result in pK_a shifts of up to eight units, as shown in bacteriorhodopsin (3). Similarly, purely electrostatic interactions can greatly favor charged states and have been responsible for pK_a shifts of up to five units for acetoacetate decarboxylase (4). Attempts have been made to isolate the contributions of electrostatic versus covalent interactions to such pK_a shifts; however, this remains a difficult challenge experimentally. This challenge emphasizes the importance of synthesizing host molecules that, like enzyme cavities, can enhance binding of small molecular guests and, in a few cases, catalyze chemical reactions (5–9).

Supramolecular assemblies with available functional groups have been used to generate solution-state pK_a shifts of up to two pK_a units (10–13) and to catalyze chemical reactions (14, 15). Synthetic hosts often rely on hydrogen bonding or ion-dipole interactions for guest inclusion, and numerous studies have investigated the effects of charge on guest binding affinities in supramolecular host-guest systems (16, 17). We report here a synthetic supramolecular host assembly that relies exclusively on electrostatic and hydrophobic interactions for thermodynamic stabilization of protonated

Department of Chemistry, University of California, Berkeley, Berkeley, CA 94720, USA.

*To whom correspondence should be addressed. E-mail: rbergman@berkeley.edu (R.G.B.); raymond@socrates.berkeley.edu (K.N.R.)

substrates. As nature has exploited pK_a shifts to activate otherwise unreactive substrates toward catalysis, this stabilization is exploited to promote acid-catalyzed hydrolyses in strongly basic solution.

During the past decade, the Raymond group has reported the formation and guest-hosting properties of supramolecular assemblies of the stoichiometry M_4L_6 [M is Ga^{III} (**1**), Al^{III} , In^{III} , Fe^{III} , Ti^{IV} , or Ge^{IV} ; L is N,N' -bis(2,3-dihydroxybenzoyl)-1,5-diaminonaphthalene] (18, 19). These components self-assemble in solution to form tetrahedral clusters with chiral metal ions at the vertices and bridging ligands spanning each edge (Fig. 1). The strong mechanical coupling of the ligands transfers chirality from one metal vertex to the others, thereby leading exclusively to $\Delta\Delta\Delta\Delta$ or $\Lambda\Lambda\Lambda\Lambda$ configurations with respect to the vertices. These enantiomers are stable, noninterconverting, and resolvable (20). The metal-ligand assembly **1** is able to encapsulate a wide variety of small monocationic guests in a 300 to 500 \AA^3 cavity protected from the bulk solution. The naphthalene walls render the interior hydrophobic, whereas the tetra-anionic ligands in combination with the trivalent metal centers confer a 12^- overall charge to the assembly. As a host, **1** stoichiometrically mediates (21, 22) as well as catalyzes (5, 23) several important organic and organometallic reactions. In addition, it stabilizes reactive guests, such as the tropylium cation (24), phosphine-acetone adducts (25), and iminium cations (26), all of which rapidly decompose in water and are only stable under anhydrous or extremely acidic conditions.

The binding strength of monocationic guests prompted our investigation into the ability of **1** to thermodynamically drive the monoprotection of guest molecules within the cavity. Neutral guests could then be either stoichiometrically or transiently protonated to promote acid-catalyzed reaction on encapsulation. To test our hypothesis, we added a variety of amines and phosphines to solutions of **1** in D_2O . Upon addition of N,N,N',N' -tetramethyl-1,4-diaminobutane (**2**) or N,N,N',N' -tetraethyl-1,2-diaminoethane (**3**), upfield nuclear magnetic resonance (NMR) resonances characteristic of encapsulation were observed, corresponding to a 1:1 host-guest complex. Similarly, two-dimensional 1H nuclear overhauser effect spectroscopy (NOESY) (fig. S1) shows strong through-space correlation between the naphthalene protons of the assembly and the encapsulated guest (27).

In order to confirm that these weakly basic compounds were being encapsulated in their conjugate acid forms, we added an isostructural phosphine, 1,2-bis(dimethylphosphino)methane (**4**) to **1** and probed by using ^{31}P NMR spectroscopy. As with both amines, new upfield resonances corresponding to $[4-H^+ \subset 1]^{11-}$ (\subset denotes encapsulation) were observed in both the 1H NMR and the ^{31}P NMR spectra. In D_2O , the proton-decoupled phosphorus ($^{31}P\{^1H\}$) NMR

spectrum showed a 1:1:1 triplet with spin-spin H-P coupling constant ($^1J_{DP}$) = 75 Hz. In H_2O , the uncoupled ^{31}P NMR spectrum showed a doublet ($^1J_{HP}$ = 490 Hz) corresponding to a one-bond P-H coupling that definitively establishes binding of a proton to phosphorus. Because similarly substituted amines and phosphines exhibit analogous base strengths, by

inference the encapsulated amines must be protonated as well, even at high pH.

For the amines encapsulated in **1**, the magnitude of the effective shift in basicity was investigated by monitoring 1:1 host-guest complexes as a function of pH. In order to confirm that the encapsulated amines were exchanging with the amines in free solution and that **1** was

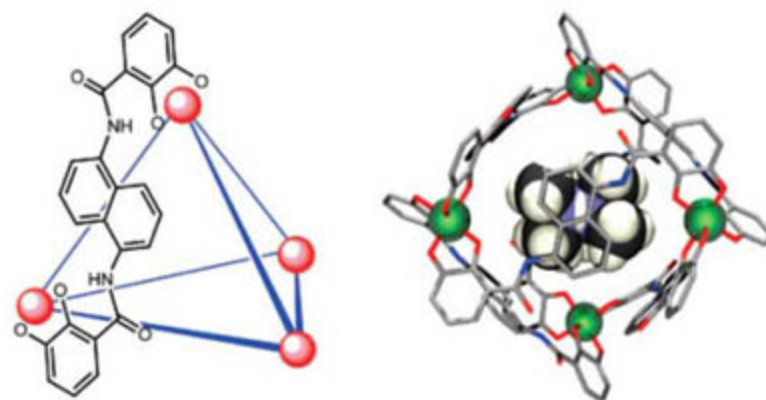


Fig. 1. (Left) A schematic representation of the host M_4L_6 assembly. Only one ligand is shown for clarity. (Right) A model of $[2-H^+ \subset 1]^{11-}$; hydrogen atoms on the host assembly are omitted for clarity.

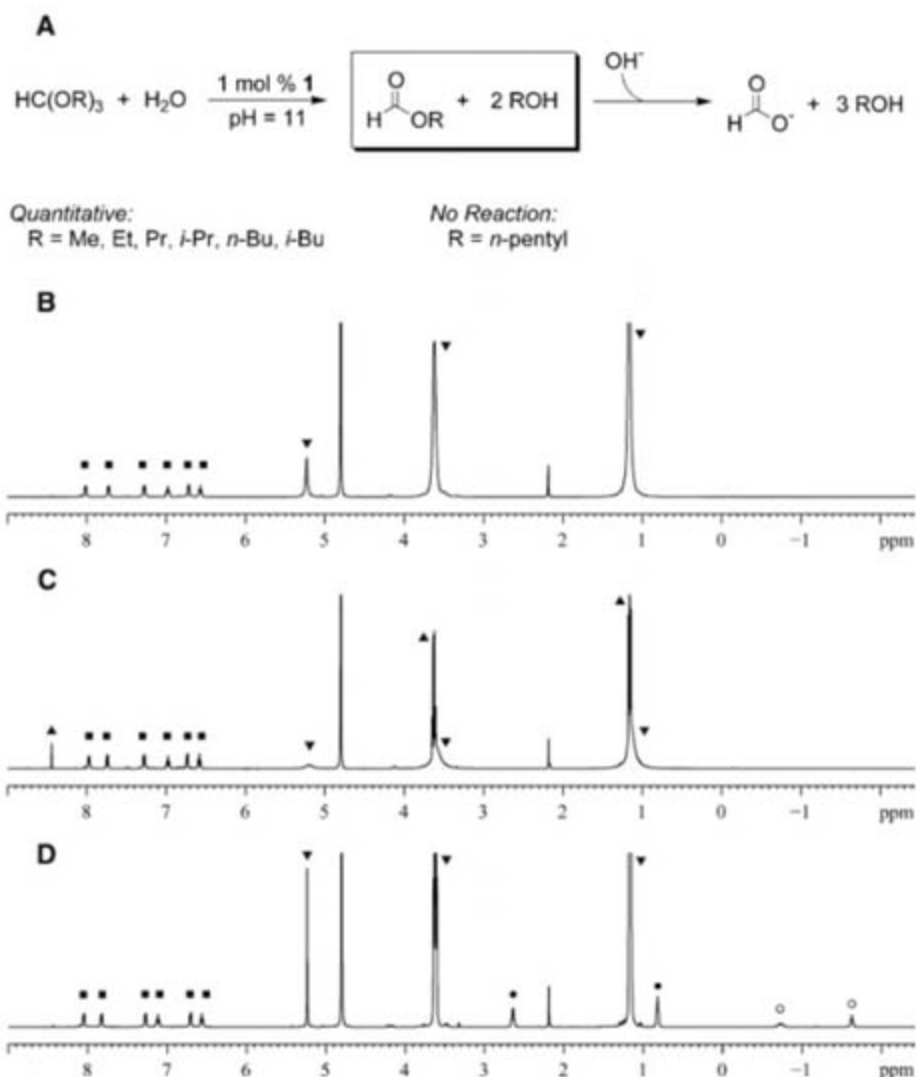


Fig. 2. (A) Reaction and substrate scope for orthoformate hydrolysis in the presence of catalytic **1**. Bu, butyl; Me, methyl; Pr, propyl. (B to D) All spectra taken with 50 equivalents (equiv.) of triethyl orthoformate with respect to **1** at $pD = 11.0$, 100 mM K_2CO_3 , $22^\circ C$, in D_2O . (B) Initial spectrum. (C) Spectrum after 60 min. (D) Spectrum of **1** with 2 equiv. NEt_4^+ after 60 min. Molecule **1** represented by \blacksquare ; $HC(OEt)_3$, \blacktriangledown ; NEt_4^+ , \bullet for exterior and \circ for interior, and product HCO_2H , \blacktriangle .

not acting as a kinetic trap, we measured the guest self-exchange rates of the encapsulated amines (28) by using the selective inversion recovery (SIR) method (29) and found the amines to be exchanging on the NMR time scale [for **2**, $k_{320\text{K}} = 0.24(3) \text{ s}^{-1}$; for **3**, $k_{320\text{K}} = 0.13(2) \text{ s}^{-1}$] (30). We carried out the SIR experiments at five different temperatures from 300 K to 340 K to extract the activation parameters (fig. S3). The activation parameters for guest exchange for **2** were ΔG_{298}^\ddagger (standard Gibbs energy of activation) = 19(2) kcal mol⁻¹, ΔH^\ddagger (standard enthalpy of activation) = 10.8(9) kcal mol⁻¹, and ΔS^\ddagger (standard entropy of activation) = -28(4) entropy units (e.u.) and for **3** were $\Delta G_{298}^\ddagger = 19.9(8) \text{ kcal mol}^{-1}$, $\Delta H^\ddagger = 16.7(6) \text{ kcal mol}^{-1}$, and $\Delta S^\ddagger = -10.9(6) \text{ e.u.}$ These values are consistent with those for the self-exchange activation parameters of tetraalkylammonium cations encapsulated in **1**, suggesting that the same exchange mechanism is present (31). Upon monitoring 1:1 host-guest solutions of $[\mathbf{2}\text{-H}^+ \subset \mathbf{1}]^{11-}$ and $[\mathbf{3}\text{-H}^+ \subset \mathbf{1}]^{11-}$ at different pHs, the free energies of binding ($-\Delta G^\circ$) for the amines were

found to be 5.2(5) kcal mol⁻¹ and 4.8(4) kcal mol⁻¹, respectively. Heating the host-guest complexes to 75°C for 24 hours and returning the sample to room temperature did not change the ratio of encapsulated to free guest, confirming that the thermodynamic equilibrium had been reached. Although the $\text{p}K_a$ of **3**-H⁺ is 10.8 in free solution, stabilization of the protonated form by **1**, which can be calculated as the product of the $\text{p}K_a$ and the binding constant of the protonated amine, shifts the effective basicity to 14.3 (32). This dramatic shift highlights the substantial stabilization of the protonated species over the neutral species upon encapsulation in the highly charged cavity (33).

We next sought to apply this host-induced shift in effective basicity to promote reaction chemistry. We focused on the hydrolysis of orthoformates, HC(OR)₃ (where R is an alkyl or aryl group), a class of molecules responsible for much of the formulation of the Brønsted theory of acids almost a century ago (34). Although orthoformates are readily hydrolyzed in acidic solution, they are exceedingly stable in neutral

or basic solution (35). However, we found that in the presence of a catalytic amount of **1** in basic solution, triethyl orthoformate is quickly hydrolyzed ($t_{1/2} \sim 12 \text{ min}$, pH = 11.0, 22°C) to the corresponding formate ester, HC(O)(OR), and finally to formate, HCO₂⁻ (36). We monitored the reaction by ¹H NMR spectroscopy and observed that the resonances of host **1** shifted upon substrate addition, suggesting that **1** is intimately involved in the reaction. The substrate C-H resonance broadens to $\nu_{1/2} = 14.3 \text{ Hz}$ compared with the nonencapsulated $\nu_{1/2} = 3.2 \text{ Hz}$, which is suggestive of fast guest exchange. Increasing the concentration of **1** to 80 mM makes the encapsulated substrate observable (fig. S3). With a limited volume in the cavity of **1**, substantial size selectivity was observed in the orthoformate hydrolysis, with orthoformates smaller than triethyl orthoformate being readily hydrolyzed with 1 mole percent of **1** (Fig. 2).

To further establish that the interior cavity of **1** was catalyzing the hydrolysis, we explored the propensity of a strongly binding guest, NEt₄⁺ (where Et is ethyl) [$-\Delta G^\circ = 6.20(8) \text{ kcal mol}^{-1}$], to inhibit substrate binding. As expected, addition of NEt₄⁺ to the solution completely inhibited the hydrolysis of orthoformates. In the presence of NEt₄⁺, the orthoformate methine resonances sharpened to $\nu_{1/2} = 3.4 \text{ Hz}$, confirming lack of encapsulation.

We probed the reaction mechanism by using triethyl orthoformate as the substrate at pH = 11.0 and 50°C. First-order substrate consumption was observed under stoichiometric conditions (fig. S4). Working under saturation conditions (see below), kinetic studies revealed that the reaction is also first-order in proton concentration and first-order in the concentration of **1** while being 0th-order in substrate (fig. S4). When combined, these mechanistic studies establish that the rate law for this catalytic hydrolysis of orthoformates by host **1** obeys the overall termolecular rate law: $\text{rate} = k[\text{H}^+][\text{Substrate}][\mathbf{1}]$ but under saturation conditions reduces to $\text{rate} = k'[\text{H}^+][\mathbf{1}]$.

We conclude that the neutral substrate enters **1** to form a host-guest complex, leading to the observed substrate saturation. We considered the possibility that saturation is due to complete protonation of substrate outside of the assembly; however, it would not be possible to attain saturation at pH = 11, because protonated orthoformates have estimated $\text{p}K_a$ values of about -5 (30). Similarly, we considered that protonation of the interior of the assembly was the first step in the mechanism; however, this mechanism would require a binding constant of H⁺ in the assembly to be greater than 10¹⁰, which is not attainable. In the next step of the cycle, the encapsulated substrate is protonated, presumably by deprotonation of water, and undergoes two successive hydrolysis steps in the cavity, liberating two equivalents of the corresponding alcohol.

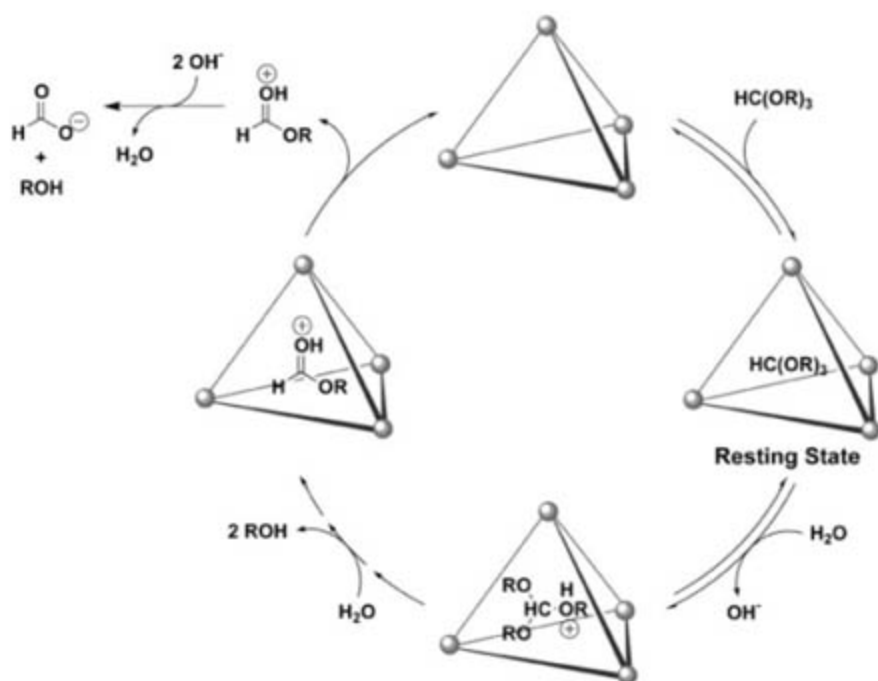
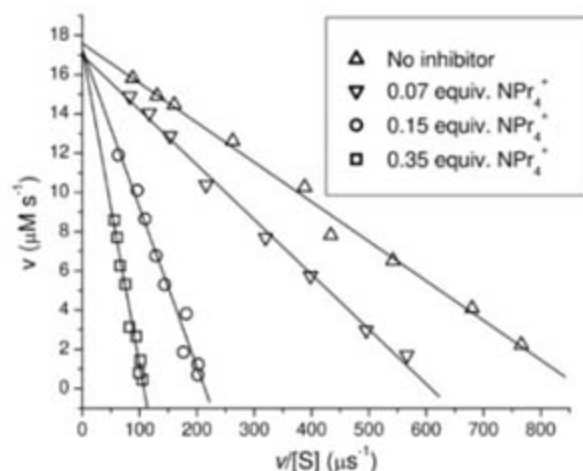


Fig. 3. Mechanism for catalytic orthoformate hydrolysis in the presence of catalytic **1**.

Fig. 4. Eadie-Hofstee plot showing competitive inhibition of the hydrolysis of HC(OEt)₃ by NPr₄⁺ in H₂O, pH = 11.0, 50°C, and 4.0 mM **1**.



Lastly, the protonated formate ester is ejected from **1** and further hydrolyzed by base in solution (Fig. 3) (37).

The reaction mechanism in Fig. 3 shows direct parallels to enzymatic pathways that obey Michaelis-Menten kinetics because of an initial pre-equilibrium followed by a first-order rate-limiting step. Lineweaver-Burk analysis (fig. S5) using the substrate saturation curves affords the corresponding Michaelis-Menten kinetic parameters of the reaction. Representative Michaelis-Menten parameters for triethyl orthoformate ($V_{\max} = 1.79 \times 10^{-5} \text{ M s}^{-1}$, $K_M = 21.5 \text{ mM}$, and $k_{\text{cat}} = 8.06 \times 10^{-3} \text{ s}^{-1}$, where V_{\max} is the maximum velocity of the reaction, K_M is the Michaelis constant, and k_{cat} is the turnover rate of the bound substrate) and triisopropyl orthoformate ($V_{\max} = 9.22 \times 10^{-6} \text{ M s}^{-1}$, $K_M = 7.69 \text{ mM}$, and $k_{\text{cat}} = 3.86 \times 10^{-3} \text{ s}^{-1}$) show substantial rate acceleration over the background reaction. When compared to the background hydrolysis reactions under the same reaction conditions (triethyl orthoformate $k_{\text{uncat}} = 1.44 \times 10^{-5} \text{ s}^{-1}$ and triisopropyl orthoformate $k_{\text{uncat}} = 4.34 \times 10^{-6} \text{ s}^{-1}$), the rate accelerations ($k_{\text{cat}}/k_{\text{uncat}}$) for triethyl orthoformate and triisopropyl orthoformate are 560 and 890, respectively. Further analysis of the Michaelis-Menten kinetic parameters yielded additional information about the catalytic reaction. Assuming a fast pre-equilibrium with respect to k_{cat} , K_M is essentially the dissociation constant of the encapsulated neutral substrate. In order to compare how efficiently **1** catalyzes the hydrolysis of different substrates, the specificity factor (k_{cat}/K_M) can be examined. This parameter corresponds to the second-order proportionality constant for the rate of conversion of preformed enzyme-substrate complex, in this case [orthoformate \subset **1**] $^{12-}$, to product, thus providing a measure of the effectiveness with which two substrates can compete for the same site. Triethyl orthoformate and triisopropyl orthoformate have specificity constants of $0.37 \text{ M}^{-1} \text{ s}^{-1}$ and $0.50 \text{ M}^{-1} \text{ s}^{-1}$, respectively, showing that triisopropyl orthoformate is more efficiently hydrolyzed by **1**.

Also characteristic of enzymes that obey Michaelis-Menten kinetics is that suitable inhibitors can compete with the substrate for the enzyme active site, thus leading to inhibition. The binding of an inhibitor to the enzyme active site prevents the substrate from entering and impedes the reaction. If the inhibitor binds reversibly to the enzyme active site, then the substrate can compete for the substrate and at suitably high concentrations will completely displace the inhibitor, leading to competitive inhibition. In order to test for competitive inhibition for the hydrolysis of orthoformates with **1**, we measured the rates of hydrolysis of triethyl orthoformate in the presence of a varying amount of the strongly binding inhibitor NPr_4^+ [$-\Delta G^\circ = 2.7(2) \text{ kcal mol}^{-1}$]. The lower binding constant of NPr_4^+ with respect

to NEt_4^+ facilitates the competitive binding experiments by allowing for the weakly binding substrate, HC(OEt)_3 , to more readily compete for the binding cavity of **1**. By varying the concentration of substrate for each amount of inhibitor, we compared the saturation curves with use of an Eadie-Hofstee plot (Fig. 4) (38, 39). The saturation curves intersect on the y axis, signifying that at infinite substrate concentration the maximum reaction velocity is independent of the amount of inhibitor, confirming competitive inhibition. If NPr_4^+ were competing for a different site than the active site of **1** responsible for the catalytic hydrolysis, such as an exterior ion-pairing site, then the saturation curves in the Eadie-Hofstee plot would be parallel. Back calculation of the binding constant of the NPr_4^+ inhibitor affords $-\Delta G^\circ = 2.8(1) \text{ kcal mol}^{-1}$, which is consistent with the known affinity of this guest.

Using synthetic hosts to modify the chemical properties of encapsulated substrates was used to greatly enhance the reactivity of orthoformates and promote the acid catalyzed hydrolysis in basic solution. Similar strategies could be used to hydrolyze other acid-sensitive molecules in which the charged transition state of the reaction can be stabilized by a molecular host. The size selectivity in synthetic molecular hosts is a property often used by nature but rarely incorporated into standard homogeneous or heterogeneous catalysis. This type of selectivity could be used to differentiate reactive sites of a substrate which would otherwise exhibit equivalent reactivity toward standard organic, organometallic, or inorganic catalysts. Such strategies would be synthetically useful for common organic protecting groups such as acetals or ketals and could also be applied to more biologically relevant substrates such as amides or phosphate esters, furthering the analogy to enzymatic systems.

References and Notes

- N.-C. Ha, M.-S. Kim, W. Lee, K. Y. Choi, B.-H. Oh, *J. Biol. Chem.* **275**, 41100 (2000).
- W. W. Cleland, P. A. Frey, J. A. Certl, *J. Biol. Chem.* **273**, 25529 (1998).
- S. Szaraz, D. Oesterhelt, P. Ormos, *Biophys. J.* **67**, 1706 (1994).
- F. H. Westheimer, *Tetrahedron* **51**, 3 (1995).
- D. Fiedler, R. G. Bergman, K. N. Raymond, *Angew. Chem. Int. Ed.* **43**, 6748 (2004).
- M. Yoshizawa, M. Tamura, M. Fujita, *Science* **312**, 251 (2006).
- J. Kang, J. Rebek Jr., *Nature* **385**, 50 (1997).
- K. R. Rao, Y. V. D. Nageswar, N. S. Krishnaveni, K. Surendra, *Adv. Org. Syn.* **1**, 301 (2005).
- J. K. M. Sanders, *Chem. Eur. J.* **4**, 1378 (1998).
- C. Marquez, W. M. Nau, *Angew. Chem. Int. Ed.* **40**, 3155 (2001).
- X. Zhang, G. Gramlich, X. Wang, W. M. Nau, *J. Am. Chem. Soc.* **124**, 254 (2002).
- J. Mohanty, A. C. Bhasikuttan, W. M. Nau, H. Pal, *J. Phys. Chem. B* **110**, 5132 (2006).
- H. Bakirci, A. L. Koner, T. Schwarzlose, W. M. Nau, *Chem. Eur. J.* **12**, 4799 (2006).
- F. Ortega-Caballero, C. Rousseau, B. Christensen, T. E. Petersen, M. Bols, *J. Am. Chem. Soc.* **127**, 3238 (2005).

- H. H. Zepik, S. A. Benner, *J. Org. Chem.* **64**, 8080 (1999).
- S. Shinkai, K. Araki, O. Manabe, *J. Chem. Soc. Chem. Commun.* **3**, 187 (1988).
- C. H. Haas, S. M. Biros, J. Rebek Jr., *J. Chem. Soc. Chem. Commun.* **48**, 6044 (2005).
- D. L. Caulder, K. N. Raymond, *J. Chem. Soc. Dalton Trans.* **8**, 1185 (1999).
- D. L. Caulder, K. N. Raymond, *Acc. Chem. Res.* **32**, 975 (1999).
- A. J. Terpin, M. Ziegler, D. W. Johnson, K. N. Raymond, *Angew. Chem. Int. Ed.* **40**, 157 (2001).
- D. H. Leung, D. Fiedler, R. G. Bergman, K. N. Raymond, *Angew. Chem. Int. Ed.* **43**, 963 (2004).
- D. H. Leung, R. G. Bergman, K. N. Raymond, *J. Am. Chem. Soc.* **128**, 9781 (2006).
- D. Fiedler, H. van Halbeek, R. G. Bergman, K. N. Raymond, *J. Am. Chem. Soc.* **128**, 10240 (2006).
- J. L. Brumaghim, M. Michels, D. Pagliero, K. N. Raymond, *Eur. J. Org. Chem.* **22**, 5115 (2004).
- J. L. Brumaghim, M. Michels, K. N. Raymond, *Eur. J. Org. Chem.* **24**, 4552 (2004).
- V. M. Dong, D. Fiedler, B. Carl, R. G. Bergman, K. N. Raymond, *J. Am. Chem. Soc.* **128**, 14464 (2006).
- The ^{23}Na NMR spectrum of encapsulated **2** in the presence of $\text{Na}_{12}\text{Ga}_4\text{L}_6$ showed only a singlet at 1.0 parts per million, corresponding to free solvated sodium ions and suggesting that a $\text{Na-N,N,N,N-tetramethyl-1,2-diaminoethane}$ adduct was not the encapsulated guest.
- The exchange rates were measured at $\text{pD} = 13.0$ and 500 mM KCl to ensure uniform ionic strength.
- A. D. Bain, J. A. Cramer, *J. Magn. Reson. A* **118**, 21 (1996).
- The error notation used throughout this paper, for example, $k = 0.24(3)$, means that for the value of $k = 0.24$ there is a standard uncertainty of 0.03.
- A. V. Davis et al., *J. Am. Chem. Soc.* **128**, 1324 (2006).
- Formally, this is a shift in the pK_a of the amine, but because we are unable to observe the neutral amine guest inside of **1**, this is more accurately referred to as an effective shift in basicity.
- Examination of crystal structures of **1** with various guests shows that the catechol oxygens are not accessible to a bound guest, thus removing the possibility that hydrogen bonding between **1** and the guest is taking place. Furthermore, examination of NOEs between **1** and the guest reveals strong through-space interactions between the guest and naphthyl protons but not between the guest and catechol protons (fig. S1).
- J. N. Brønsted, W. F. K. Wynne-Jones, *Trans. Faraday Soc.* **25**, 59 (1929).
- E. H. Cordes, H. G. Bull, *Chem. Rev.* **74**, 581 (1974).
- At high pH, the formate ester product is quickly hydrolyzed by OH^- to formate ion (HCO_2^-). However, at lower pH, the formate ester product is stable and is the exclusive product.
- After the initial catalyzed step inside of **1**, any of the intermediates can be hydrolyzed by either acid or base; however, we have not observed any intermediates free in solution.
- G. S. Eadie, *J. Biol. Chem.* **146**, 85 (1942).
- B. H. J. Hofstee, *Science* **116**, 329 (1952).
- We gratefully acknowledge financial support from the Director of the Office of Energy Research, Office of Basic Energy Sciences, Chemical Sciences Division (U.S. Department of Energy) under contract DE-AC02-05CH11231 and an NSF predoctoral fellowship to M.D.P. The authors thank D. Leung, G. Lalic, M. Seitz, and C. Hastings for helpful discussions and H. van Halbeek and R. Nunlist for assistance with NMR experiments.

Supporting Online Material

www.sciencemag.org/cgi/content/full/316/5821/85/DC1
Materials and Methods
Figs. S1 to S5
References

12 December 2006; accepted 5 March 2007
10.1126/science.1138748

The Deep Ocean During the Last Interglacial Period

J. C. Duplessy,^{1*} D. M. Roche,² M. Kageyama³

Oxygen isotope analysis of benthic foraminifera in deep sea cores from the Atlantic and Southern Oceans shows that during the last interglacial period, North Atlantic Deep Water (NADW) was $0.4^\circ \pm 0.2^\circ\text{C}$ warmer than today, whereas Antarctic Bottom Water temperatures were unchanged. Model simulations show that this distribution of deep water temperatures can be explained as a response of the ocean to forcing by high-latitude insolation. The warming of NADW was transferred to the Circumpolar Deep Water, providing additional heat around Antarctica, which may have been responsible for partial melting of the West Antarctic Ice Sheet.

The climate of the last interglacial (LIG) period, from 129,000 to 118,000 years ago (1, 2), was slightly warmer than today's and is often viewed as an analog of the climate expected during the next few centuries. Recent assessments of the LIG climate have provided strong evidence that sea level was 4 to 6 m above the present level, due to partial melting of both Greenland and the West Antarctic Ice Sheet (WAIS) (3, 4). At peak interglacial conditions, summer temperatures were 2° to 5°C warmer than today in the North Atlantic (5) over Greenland (6) and the Arctic (7). The Norwegian-Greenland Sea experienced large variability, but during the warmest period, the Arctic oceanic front was located west of its present location (8). Consequently, the Arctic climate was warm enough to explain the shrinking of the Greenland Ice Sheet during the LIG (9).

In the Southern Hemisphere, an $\sim 2^\circ\text{C}$ warming occurred over the Antarctic Plateau during the LIG (10), but it could not have resulted in any melting because local air temperature was still extremely cold ($\sim -50^\circ\text{C}$). In the Southern Ocean, summer sea surface temperatures were about 2°C higher than during the Holocene (11, 12). Over New Zealand and Tasmania, the LIG warming was between 0° and 2°C (13, 14). Such increases in surface water or air temperature seem too small to have resulted in substantial melting of the WAIS (15).

However, the WAIS is sensitive to deep ocean temperatures (16). Indeed, the volume of this ice sheet is related to the efficiency of ice shelves in blocking the ice flow from the central part of the ice sheet outward, and ice shelves are themselves sensitive to deep ocean temperatures. Under

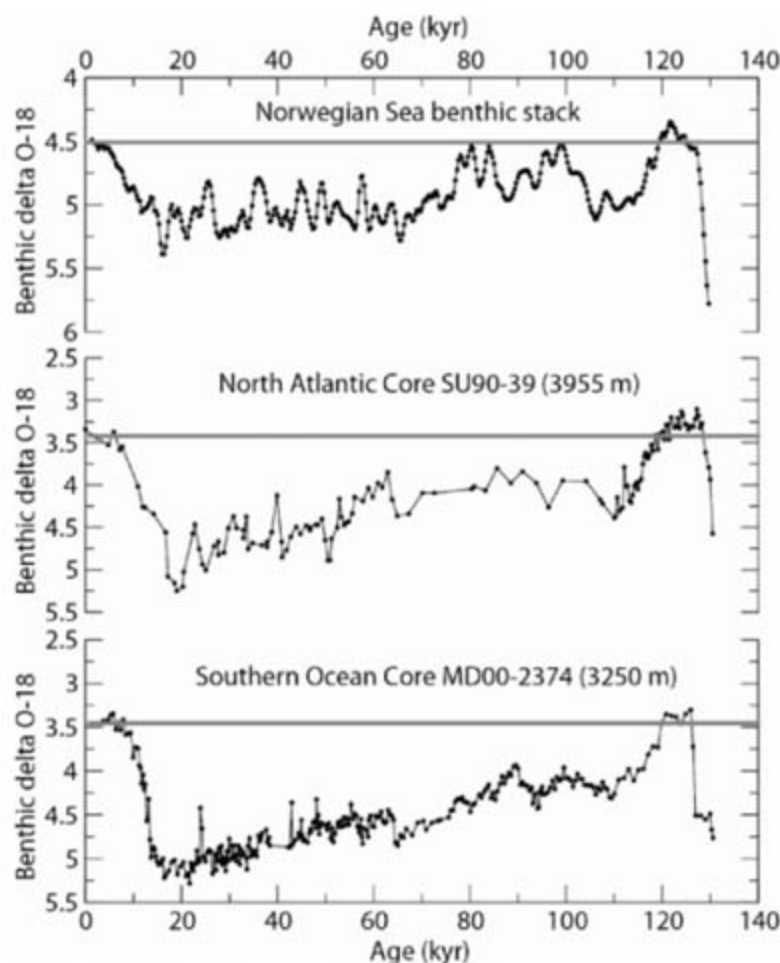
modern conditions, the meridional overturning circulation carries warm surface waters northward in the Atlantic, replacing the export of the relatively cold North Atlantic Deep Water (NADW). However, NADW is warmer than the cold bottom water formed around Antarctica. NADW therefore carries heat to the Southern Ocean. It mixes with recirculated deep water from the Indian and Pacific Oceans, forming a relatively warm deep water mass, the Circumpolar Deep Water (CDW), characterized by a temperature maximum of $\sim +2^\circ\text{C}$ around 600 m depth and overlying the cold Antarctic Bottom Water. CDW floods the floor of the Amundsen and Bellinghousen Sea continental shelves and reaches the undersides of ice shelves flowing from the WAIS. This heat

flow, which originates from the Northern Hemisphere, results in ice-shelf bottom melting near grounding lines (17). This melting process substantially contributes to decreasing the stability of the ice shelves that drain the grounded part of the WAIS (18).

To investigate whether the LIG ocean could have helped to destabilize the West Antarctic ice shelves and ice sheet, we examined the oxygen isotopic composition ($\delta^{18}\text{O}$) of benthic foraminifera. This quantity is a function of both temperature and seawater $\delta^{18}\text{O}$. On the one hand, the isotopic composition directly reflects isotopic variations in the ambient water (δ_w). On the other, the fractionation between the carbonate shell and the water increases by about 0.25 per mil (‰) for each degree that the water is cooled. Because the global ocean circulation during the LIG period was very similar to the present circulation (19), $\delta^{18}\text{O}$ differences between benthic foraminifera from the LIG period and from the Holocene in a core reflect both the temperature and $\delta^{18}\text{O}$ differences experienced by the same deep water mass as the one that is present today at the core location.

The LIG $\delta^{18}\text{O}$ records are characterized by quasi-constant values forming a plateau, in agreement with coral reef data showing that the LIG high-sea-level period lasted at least 7000 years (1, 2, 20). In all cores, the LIG plateau exhibits $\delta^{18}\text{O}$ values that are significantly lighter than those of the Holocene (Fig. 1). To accurately determine the $\delta^{18}\text{O}$ difference between these two

Fig. 1. Comparison of three $\delta^{18}\text{O}$ benthic foraminifer records for the past 135,000 years, obtained from deep-sea cores raised from the major water masses found in the Atlantic and Southern Oceans. The upper panel shows a Norwegian Sea benthic stack record (36), the middle panel is core SU 90-39 ($52^\circ 32'\text{N}$, $21^\circ 56'\text{W}$, depth 3955 m) from the North Atlantic, and the lower panel is core MD 00-2374 ($46^\circ 04'\text{S}$, $96^\circ 48'\text{E}$, depth 3250 m) from the Southern Ocean. All records encompass the LIG (135,000 to 110,000 years ago) and the present interglaciation (since 8000 years ago), together with the last glacial period. The gray line in each panel shows the mean Holocene $\delta^{18}\text{O}$ value. kyr, thousand years.



¹Laboratoire des Sciences du Climat et de l'Environnement/ Institut Pierre Simon Laplace (LSCE/IPSU), Laboratoire Commissariat à l'Énergie Atomique/CNRS/Université de Versailles Saint Quentin (CEA/CNRS/UVSQ), Parc du CNRS, 91198 Gif sur Yvette, France. ²Department of Paleoclimatology and Geomorphology, Vrije Universiteit Amsterdam, De Boelelaan 1085, NL-1081 HV Amsterdam, Netherlands. ³Laboratoire des Sciences du Climat et de l'Environnement, LSCE/IPSU, Laboratoire CEA/CNRS/UVSQ, CE Saclay, l'Orme des Merisiers, 91191 Gif-sur-Yvette Cedex, France.

*To whom correspondence should be addressed. E-mail: Jean-Claude.Duplessy@lsce.cnrs-gif.fr

interglacial periods, we compared the records of benthic foraminifera from the same species in 42 cores (table S1). The mean $\delta^{18}\text{O}$ value of LIG benthic foraminifera in these cores is $0.11 \pm 0.01\text{‰}$ lighter than during the Holocene, but with significant regional variations: The $\delta^{18}\text{O}$ difference between the LIG period and the Holocene varies from $0.15 \pm 0.02\text{‰}$ in the Norwegian Sea to $0.11 \pm 0.01\text{‰}$ in the Atlantic Ocean and to only $0.04 \pm 0.03\text{‰}$ in the Southern Ocean (table S2).

Light $\delta^{18}\text{O}$ values of LIG benthic foraminifera are partly explained by partial melting of both Greenland and the WAIS, which injected isotopically light meltwater into the ocean. To estimate the seawater $\delta^{18}\text{O}$ variation associated with LIG sea level, which was 4 to 6 m above the present level, we note that between the last glacial maximum and today, the sea level rose by 130 ± 10 m (21) and seawater $\delta^{18}\text{O}$ decreased by $1.05 \pm 0.20\text{‰}$ (22, 23). This implies that seawater $\delta^{18}\text{O}$ decreases by $0.008 \pm 0.002\text{‰}$ per meter of

global sea-level rise. This rate is likely to be an upper estimate for interglacial conditions, because ice melting at the end of the glaciation originated from snow deposited at low temperature and highly depleted in ^{18}O . In contrast, ice melting during an interglacial climate would originate from snow deposited at temperatures higher than those of glacial climate and less depleted in ^{18}O . We conclude that the 4- to 6-m LIG sea-level rise would have resulted in a seawater $\delta^{18}\text{O}$ decrease of 0.03 to 0.06‰. This change was uniform in all water masses, because the turnover of the ocean (about 1500 years) is much shorter than the LIG duration. Therefore it should be recorded in all benthic foraminiferal $\delta^{18}\text{O}$ values. We then computed a local $\delta^{18}\text{O}$ anomaly as the difference between the measured foraminiferal $\delta^{18}\text{O}$ value and that owing to the input of meltwater. This local $\delta^{18}\text{O}$ anomaly is only due to changes in deep water $\delta^{18}\text{O}$ and temperature. For the deep Southern Ocean (1900 to 3500 m), the anomaly is not statistically different from zero. This result implies that during the LIG, bottom water formed on the Antarctic continental shelf at the freezing point, as it does today. In the Norwegian Sea and the Atlantic Ocean, the anomaly is significantly different from zero at the 1σ level (-0.15 and -0.11‰ , respectively). However, it is small and can be considered to be a minor departure from modern conditions. Such small changes in the physical properties of water masses tend to develop at almost constant density, as observed in hydrographic data

Fig. 2. Calcite $\delta^{18}\text{O}$ anomaly (LIG – modern) simulated by CLIMBER-2 (in per mil) in the Atlantic Ocean (computed between the averages over the last 100 years of the simulations). Calcite $\delta^{18}\text{O}$ is computed as $\delta^{18}\text{O}_c = 21.9 - 0.27 + \delta^{18}\text{O}_w - \sqrt{310.61 + 10T}$ where T is the oceanic temperature (37). The global $\delta^{18}\text{O}$ change in seawater composition of -0.045‰ due to sea-level change at the LIG is taken into account.

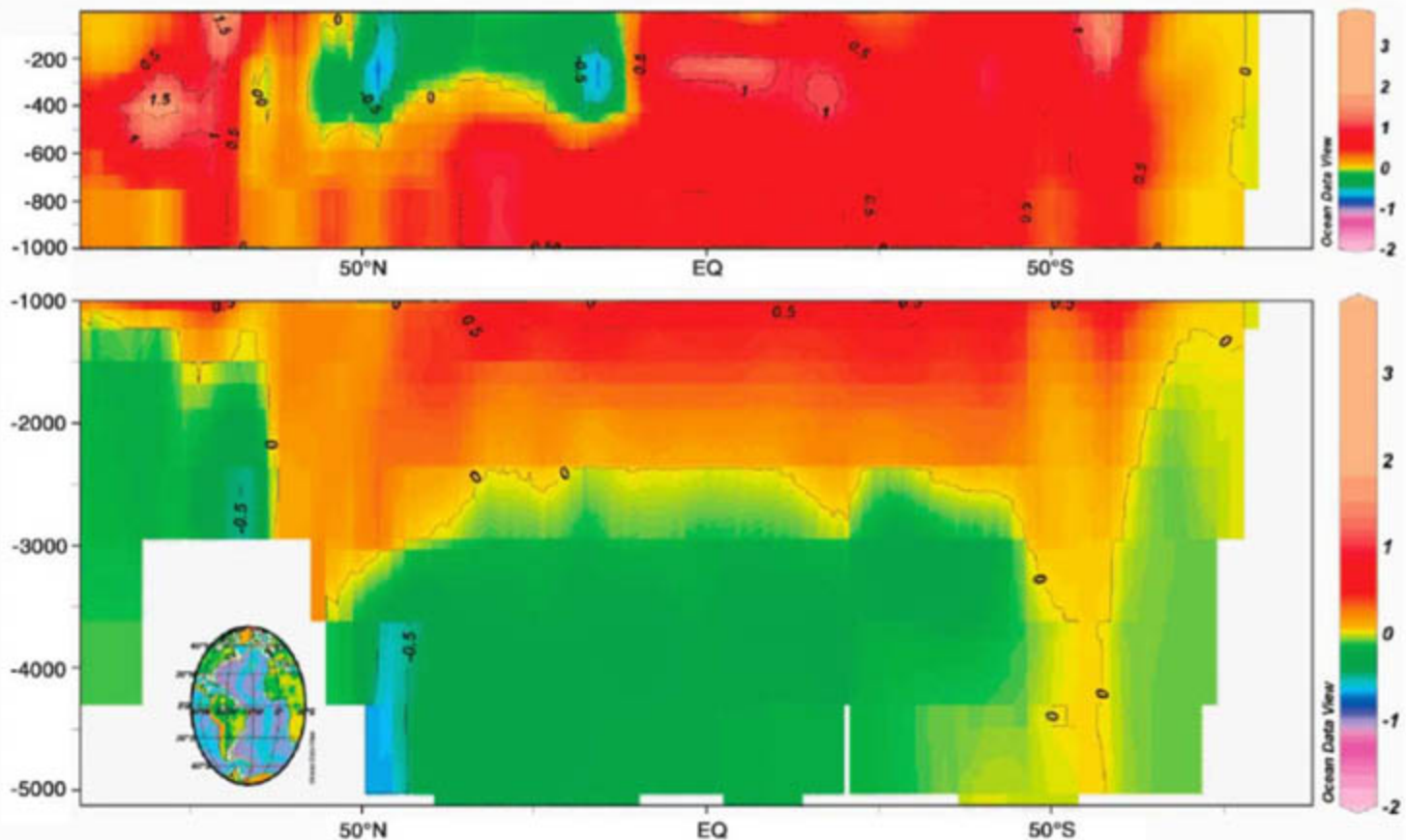
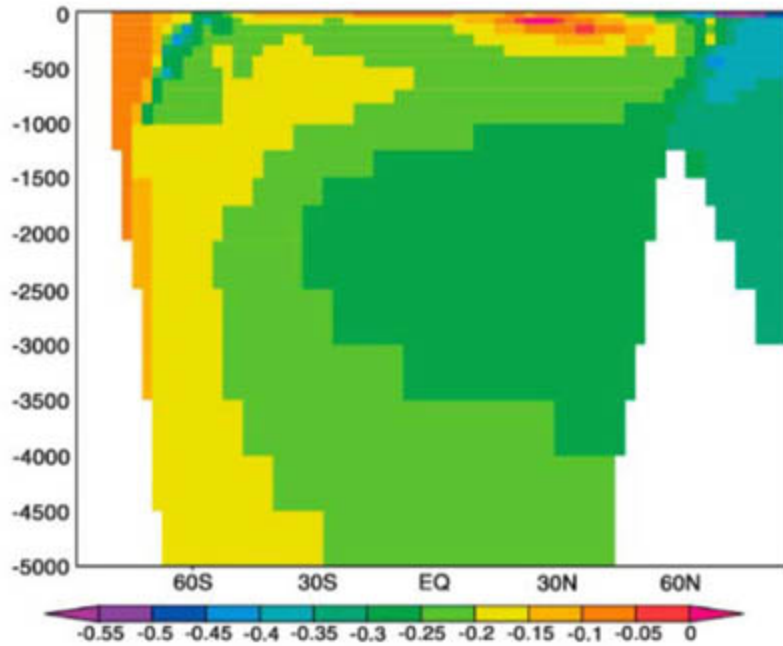


Fig. 3. Annual mean temperature anomalies (LIG – modern) simulated by LOVECLIM (in °C) along the western boundary of the Atlantic Ocean. The field is averaged over the last 100 years of the simulation. The inset map shows the path chosen for the section.

collected during the past 50 years (24, 25). At present, the temperature and salinity of NADW are close to 3°C and 34.96 practical salinity units (psu). To maintain a constant density, salinity must increase by 0.12 psu for each degree that the water is warmed. Thus, we can compute that the $\delta^{18}\text{O}$ anomalies measured in LIG benthic foraminifera result from a $0.37^\circ \pm 0.20^\circ\text{C}$ warming of NADW, compensated for by a 0.04 increase in salinity. Similarly, a $0.57^\circ \pm 0.2^\circ\text{C}$ warming compensated for by a salinity increase of 0.07 psu occurred in the Norwegian Sea (table S2).

Among the factors responsible for a LIG warmer than today, insolation changes are the best candidates. Indeed, Earth's orbital parameters during the LIG favored warm Northern Hemisphere summers as compared to the present. LIG atmospheric greenhouse gas concentrations were not significantly different from preindustrial values. To simulate the LIG atmosphere/ocean state, we therefore forced our climate models with the insolation values for 126,000 years before the present (supporting online text). We used two Earth System models of intermediate complexity: CLIMBER-2 (26) and LOVECLIM (27). In CLIMBER-2, the ocean is represented by three latitude/depth basins, and the computed calcite $\delta^{18}\text{O}$ can be directly compared with measurements. LOVECLIM includes a full-ocean general circulation model but no oceanic oxygen isotope calculation.

The CLIMBER-2 model simulates negative calcite $\delta^{18}\text{O}$ anomalies (LIG-control) in all ocean basins (Fig. 2). The magnitude of these anomalies decreases from the Nordic Seas (-0.16%), through the Atlantic (-0.12%), into the Southern Ocean (-0.06%). There is good agreement with data (table S2), in particular for the Atlantic Ocean, where the reconstructions are the most robust. Furthermore, both models simulate sea surface temperature changes consistent with reconstructions and numerical studies for the LIG (9, 28–30) (supporting online text). Sea surface temperatures increase at nearly all latitudes, with a maximum increase at high northern latitudes and a secondary maximum in the Southern Ocean. Maxima occur at high latitudes because of reduced sea-ice cover. The increased summer boreal insolation is responsible for a significant melting of the northern sea ice, which translates into a year-round warming of the ocean due to its large thermal inertia. As a consequence of these higher sea surface temperatures, ocean evaporation increases. This increase is not compensated for by an increase in precipitation. Consequently, salinity increases, which agrees with the paleoceanographic reconstructions (5). Hence, the model results are in broad agreement with the surface hydrographical reconstructions and the benthic $\delta^{18}\text{O}$ data, the latter being simply interpreted as the response of the ocean to the LIG insolation values.

Simulated density is quasi-constant because the impacts of the temperature and salinity

changes compensate for each other (table S2). Both models therefore confirm the hypothesis at the basis of our interpretation of the benthic $\delta^{18}\text{O}$ data. Furthermore, a nearly constant density explains why the deep oceanic circulation is little affected by the insolation changes at 126,000 years before the present. Nordic Sea surface waters, fed by warmer and saltier North Atlantic surface waters, form a deep water mass, also slightly warmer and saltier than today [change in temperature (ΔT) = 0.6°C and change in salinity (ΔS) = 0.04 psu for the CLIMBER-2 model; ΔT = 0.5°C and ΔS = 0.06 psu for the LOVECLIM model, see table S2]. This water invades the North Atlantic as a large NADW mass (Fig. 3), which then flows to the Southern Ocean.

As a result, the Antarctic Circumpolar Waters are slightly warmer than today. Our LIG simulations show a -0.1° to 0.5°C warming in the upper 500 m of the Southern Ocean close to the Antarctic coast (Fig. 3 and fig. S2). This value is similar to the 0.5°C warming simulated by the National Center for Atmospheric Research model for the upper 200 m of the Southern Ocean (3). Although apparently modest, this warming should not be underestimated. Recent results obtained with satellite radar interferometry reveal that bottom melting near an ice-shelf grounding line is strongly influenced by the temperature of the surrounding seawater, and that the melting rate at the base of ice shelves increases by 1 m per year for each 0.1°C rise in ocean temperature (16). Thus, in addition to the higher sea level resulting from the partial melting of the Greenland ice sheet, the 0.1° to 0.5°C warming that we have estimated for LIG NADW and CDW may have affected vulnerable WAIS grounding lines and further weakened the ice shelves by causing thinning from below.

Our data show that changes in climate in the high-latitude North Atlantic could have triggered some ice sheet melting in Antarctica, but they provide no information on the speed at which the WAIS shrank during the LIG. Although it is not our goal to predict the future of the WAIS, we note that recent ocean temperatures directly seaward of Antarctica's continental shelf have already increased by $\sim 0.2^\circ\text{C}$ (31), a warming comparable to that of the LIG period. Consequently, the future evolution of the WAIS might be a key component of sea-level change resulting from anthropogenic warming, as Mercer warmed more than 25 years ago (32).

References and Notes

- J. H. Chen, H. A. Curran, R. White, G. J. Wasserburg, *Geol. Soc. Am. Bull.* **103**, 82 (1991).
- C. H. Stirling, T. M. Esat, K. Lambeck, M. T. McCulloch, *Earth Planet. Sci. Lett.* **160**, 745 (1998).
- J. T. Overpeck *et al.*, *Science* **311**, 1747 (2006).
- A WAIS contribution to the high sea level of the LIG is supported by diatoms and ^{10}Be data collected from sediments below the ice-stream region of the Ross Embayment, indicating that the central WAIS was probably smaller during the Pleistocene (33). The LIG and not an earlier interglaciation is the most likely

candidate for an associated sea-level rise of the needed magnitude (34, 35).

- E. Cortijo *et al.*, *Paleoceanography* **14**, 23 (1999).
- North Greenland Ice Core Project Members, *Nature* **431**, 147 (2004).
- A. V. Lozhkin, P. M. Anderson, *Quat. Res.* **43**, 147 (1995).
- T. Fronval, E. Jansen, H. Hafliðason, H. P. Sejrup, *Quat. Sci. Rev.* **17**, 963 (1998).
- B. L. Otto-Bliesner, S. J. Marshall, J. T. Overpeck, G. H. Miller, A. Hu, *Science* **311**, 1751 (2006).
- F. Vimeux, K. M. Cuffey, J. Jouzel, *Earth Planet. Sci. Lett.* **203**, 829 (2002).
- L. Labeyrie *et al.*, *Paleoceanography* **11**, 57 (1996).
- K. Pahnke, R. Zahn, H. Elderfield, M. Schulz, *Science* **301**, 948 (2003).
- E. A. Colhoun, J. S. Pola, C. E. Barton, H. Heijnis, *Quat. Int.* **57/58**, 5 (1999).
- M. J. Vandergoes *et al.*, *Nature* **436**, 242 (2005).
- M. Oppenheimer, *Nature* **393**, 325 (1998).
- E. Rignot, S. S. Jacobs, *Science* **296**, 2020 (2002).
- S. S. Jacobs, H. H. Hellmer, A. Jenkins, *Geophys. Res. Lett.* **23**, 657 (1996).
- A. Shepherd, D. Wingham, E. Rignot, *Geophys. Res. Lett.* **31**, L23402 (2004).
- J. C. Duplessy *et al.*, *Quat. Res.* **21**, 225 (1984).
- C. Israelson, B. Wohlfarth, *Quat. Res.* **51**, 306 (1999).
- K. Lambeck, J. Chappell, *Science* **292**, 679 (2001).
- J. C. Duplessy, L. Labeyrie, C. Waelbroeck, *Quat. Sci. Rev.* **21**, 315 (2002).
- D. P. Schrag *et al.*, *Quat. Sci. Rev.* **21**, 331 (2002).
- R. Dickson *et al.*, *Science* **416**, 832 (2002).
- R. Curry, C. Mauritzen, *Science* **308**, 1772 (2005).
- D. Roche, D. Paillard, A. Ganopolski, G. Hoffmann, *Earth Planet. Sci. Lett.* **218**, 317 (2004).
- E. Driesschaert, thesis, Université Catholique de Louvain-la-Neuve, Belgium (2005).
- N. Groll, M. Widmann, J. Jones, F. Kaspar, S. J. Lorenz, *J. Clim.* **18**, 4032 (2005).
- F. Kaspar, N. Kuhl, U. Cubasch, T. Litt, *Geophys. Res. Lett.* **32**, L11703 (2005).
- C. Kubatzki, M. Montoya, S. Rahmstorf, A. Ganopolski, M. Claussen, *Clim. Dyn.* **16**, 799 (2000).
- S. S. Jacobs, C. F. Giulivi, P. A. Mele, *Science* **297**, 386 (2002).
- J. H. Mercer, *Nature* **271**, 321 (1978).
- R. P. Scherer *et al.*, *Science* **281**, 82 (1998).
- A. W. Droxler, R. Z. Poore, L. H. Burckle, Eds., *AGU Monogr.* **137**, 240 (2003).
- D. Q. Bowen, *Eos* **87** (fall meeting suppl.), abstr. PP51B-1139 (2006).
- L. D. Labeyrie, J. C. Duplessy, P. L. Blanc, *Nature* **327**, 477 (1987).
- N. J. Shackleton, in *Les Methodes Quantitatives d'Etude des Variations du Climat au Cours du Pleistocène* (CNRS, Gif sur Yvette, France, 1974), pp. 203–209.
- D.M.R. is supported by the Netherlands Organization for Scientific Research (NWO). J.-C.D. and M.K. are funded by CNRS, CEA, Institut Polaire, the European Union Pole-Ocean-Pole (EVK-2000-00089) project, the Impairs project of the Institut des Sciences de l'Univers and the "Intégration des contraintes Paléoclimatiques: réduire les Incertitudes sur l'évolution du Climat des périodes Chaudes (PICC)" project of the Agence Nationale de la Recherche. The authors thank the Potsdam Institute for Climate Impact Research for providing the CLIMBER-2 model and Hugues Goosse at the Université Catholique de Louvain-la-Neuve for technical assistance with the LOVECLIM model, A. Friend and J. Overpeck for their reviews of an early version of the manuscript, and two anonymous reviewers for their suggestions.

Supporting Online Material

www.sciencemag.org/cgi/content/full/316/5821/89/DC1
SOM Text

Figs. S1 and S2
Tables S1 and S2
References

8 December 2006; accepted 5 March 2007
10.1126/science.1138582

Subsurface Radar Sounding of the South Polar Layered Deposits of Mars

Jeffrey J. Plaut,¹ Giovanni Picardi,² Ali Safaeinili,¹ Anton B. Ivanov,¹ Sarah M. Milkovich,¹ Andrea Cicchetti,² Wlodek Kofman,³ Jérémie Mouginot,³ William M. Farrell,⁴ Roger J. Phillips,⁵ Stephen M. Clifford,⁶ Alessandro Frigeri,⁷ Roberto Orosei,⁸ Costanzo Federico,⁷ Iwan P. Williams,⁹ Donald A. Gurnett,¹⁰ Erling Nielsen,¹¹ Tor Hagfors,¹¹ Essam Heggy,⁶ Ellen R. Stofan,¹² Dirk Plettmeier,¹³ Thomas R. Watters,¹⁴ Carlton J. Leuschen,¹⁵ Peter Edenhofer¹⁶

The ice-rich south polar layered deposits of Mars were probed with the Mars Advanced Radar for Subsurface and Ionospheric Sounding on the Mars Express orbiter. The radar signals penetrate deep into the deposits (more than 3.7 kilometers). For most of the area, a reflection is detected at a time delay that is consistent with an interface between the deposits and the substrate. The reflected power from this interface indicates minimal attenuation of the signal, suggesting a composition of nearly pure water ice. Maps were generated of the topography of the basal interface and the thickness of the layered deposits. A set of buried depressions is seen within 300 kilometers of the pole. The thickness map shows an asymmetric distribution of the deposits and regions of anomalous thickness. The total volume is estimated to be 1.6×10^6 cubic kilometers, which is equivalent to a global water layer approximately 11 meters thick.

The polar regions of Mars are covered with extensive finely layered deposits that contain a record of climate variations of an unknown time span (1). Although the precise composition of the deposits is unknown, it is believed that they are predominantly water ice and that they represent the largest known reservoir of H₂O on the planet (2). We applied a technique commonly used to study the interior of ice sheets and glaciers on Earth—radar echo sounding—to study the south polar layered deposits (SPLD) of Mars. We report here on observations of the SPLDs by the Mars Advanced Radar for Subsurface and Ionospheric Sounding (MARSIS) instrument on the Mars Express orbiter. The data were used to characterize the electrical properties of the deposits in order to understand their composition, map the topography of the bed of the deposits, and measure the total volume of the SPLD.

Martian PLD were first identified in orbital images obtained by the Mariner and Viking spacecraft (3–6). They were noted to consist of dozens of layers of contrasting albedo, with thicknesses down to the resolution of the available images (about 10 m). Higher-resolution images acquired by the Mars Orbiter Camera on Mars Global Surveyor (MGS) indicated that the scale of layering extends down to the resolution of that camera; that is, a few meters (7). Topographic data obtained by the Mars Orbiter Laser Altimeter (MOLA) on MGS showed that the north PLD (NPLD) and the SPLD are similar in gross morphology and thickness (2). Both the NPLD and SPLD units are roughly domical in shape and about 1000 km across, with maximum relief relative to the surrounding terrain of about 3.5 km. MOLA data were used to estimate the volume of the PLD, which is equivalent to a global layer 16 to 22 m thick (2). Although the relationship of the layering to climate variations is not well understood, it is believed that the rhythmic nature of the deposits is related to oscillations in Mars' orbital parameters (8). The albedo variations among layers are thought to be caused by varying mixtures of ice and dust. The mixing ratio of ice and dust cannot be precisely measured from optical data, but it has been shown that only a small fraction (<10%) of dust is needed to lower the albedo of pure ice to the observed levels (9).

MARSIS is a multifrequency synthetic-aperture orbital sounding radar (10). In its subsurface modes, MARSIS operates in frequency bands between 1.3 and 5.5 MHz, with a 1-MHz instantaneous bandwidth that provides free-space range resolution of approximately 150 m. Lateral spatial resolution is 10 to 30 km in the cross-track direction; and the along-track footprint, narrowed by onboard synthetic-aperture processing, is 5 to 10 km. Processing includes a correction for phase distortion and delay in the ionosphere (11). We

report here on data collected during the southern hemisphere nightside campaign of Mars Express between November 2005 and April 2006. Data were collected during more than 300 orbits, with MARSIS primarily operating in a two-frequency mode using bands centered on 3.0, 4.0, or 5.0 MHz.

The NPLD were observed previously by MARSIS during two orbits in June 2005 (11). The MARSIS signals appeared to penetrate to the base of the deposit, which was estimated to be 1.8 km deep in the thickest area observed, near the periphery of the deposits. The very low attenuation of the MARSIS signals in the NPLD materials suggests that they contain only a few percent dust mixed with pure water ice. The basal interface was seen to remain essentially horizontal beneath the NPLD, showing that flexural downwarping due to the load does not exceed the estimated detection limit of several hundred meters and implying a thick lithosphere in that region of the planet (11).

In a typical MARSIS observation over the SPLD (Fig. 1), the echo from the surface splits into two continuous traces as the spacecraft passes over the margin of the deposits. The surface trace follows a profile expected from MOLA topography. The bright lower trace occurs at a time delay consistent with a continuation of the surrounding surface topography beneath the SPLD, assuming a nominal value of the refractive index of water ice. The lower interface is interpreted as the boundary between the base of the ice-rich SPLD materials and the predominantly lithic substrate. The interface is detected beneath most of the SPLD, although in places it becomes discontinuous, indistinct, or absent. It is generally lower in backscatter intensity than the surface above it, but in places it appears equivalent to or brighter than the surface echo. Propagation of the signal in the SPLD medium can be described with a simple two-layer homogeneous model, using reflection and absorption coefficients that are appropriate for materials expected on Mars. As in the case of the NPLD (11), the strong return from the basal interface indicates very low attenuation values within the SPLD. If the material is assumed to be "dirty" water ice overlying a basaltic substrate, effective loss tangent values between 0.001 and 0.005 are obtained for the SPLD material (12). This corresponds to water ice with a dust contamination of 0 to 10% (13). The general behavior of the surface and subsurface echoes over most of the SPLD is consistent with a composition of water ice that is relatively free of impurities, overlying a typical Martian regolith and crust.

An extended area of unexpectedly bright basal reflections occurs in an area between the thickest part of the SPLD (~3.7 km) and the nearby SPLD margin, from 310° to 0° east longitude (Fig. 1). The returns are often brighter than the surface return, which is not expected for propagation through a lossy medium. Although a strong contrast in dielectric constant at the base

¹Jet Propulsion Laboratory, California Institute of Technology, Pasadena, CA 91109, USA. ²Infocom Department, "La Sapienza" University of Rome, 00184 Rome, Italy. ³Laboratoire de Planetologie de Grenoble, 38041 Grenoble Cedex, France. ⁴NASA/Goddard Space Flight Center, Greenbelt, MD 20771, USA. ⁵Department of Earth and Planetary Sciences, Washington University, St. Louis, MO 63130, USA. ⁶Lunar and Planetary Institute, Houston, TX 77058, USA. ⁷Dipartimento di Scienze della Terra, Università degli Studi di Perugia, 06123 Perugia, Italy. ⁸Istituto di Fisica dello Spazio Interplanetario, Istituto Nazionale di Astrofisica, 00133 Rome, Italy. ⁹Astronomy Unit, School of Mathematical Sciences, Queen Mary University of London, Mile End Road, London E1 4NS, UK. ¹⁰Department of Physics and Astronomy, University of Iowa, Iowa City, IA 52242, USA. ¹¹Max Planck Institute for Solar System Research, 37191 Katlenburg-Lindau, Germany. ¹²Proxemy Research, Laytonsville, MD 20882, USA. ¹³Fakultät fuer Elektrotechnik und Informationstechnik, Technische Universität Dresden, D-01062 Dresden, Germany. ¹⁴Center for Earth and Planetary Studies, National Air and Space Museum, Smithsonian Institution, Washington, DC 20560, USA. ¹⁵Center for Remote Sensing of Ice Sheets, University of Kansas, Lawrence, KS 66045, USA. ¹⁶Fakultät fuer Elektrotechnik und Informationstechnik Ruhr-Universität Bochum, D-44780 Bochum, Germany.

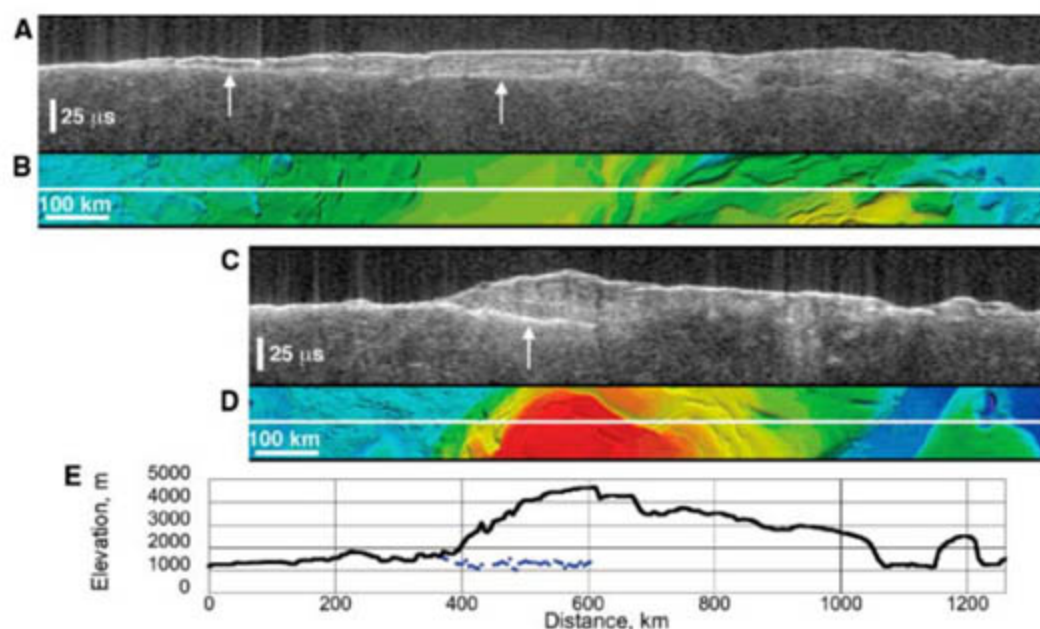
may be responsible, we deem it highly unlikely that liquid water [from basal melting (14)] causes the bright return, because it occurs below thin (as well as thick) sections of the SPLD that are among the coldest places on the surface of Mars. The low attenuation is consistent with very low temperatures throughout

the ice, further arguing against basal melting. Nevertheless, we cannot completely rule out unusual geothermal conditions or an exotic composition of the substrate in these anomalously bright areas.

A pattern of banding commonly occurs between the surface and basal interface traces in

MARSIS radargrams of the SPLD (Fig. 1). The banding consists of bright continuous reflectors, sometimes hundreds of kilometers long, alternating with lower-backscatter bands. The banding is certainly related to the layered structure of the SPLD, possibly due to contrasts in dust content or density, but the precise mechanism that

Fig. 1. (A) MARSIS data from orbit 2753, showing typical features of the SPLD. (B) MOLA topography along the ground track. The lower echo trace (arrows) is interpreted as the SPLD basal interface with the substrate. The basal reflector becomes indistinct at the right of center. The central area shows multiple continuous bands internal to the SPLD, where the estimated SPLD thickness is 1.6 km. (C) MARSIS data from orbit 2682, showing a bright basal reflector (arrow). (D) MOLA topography along the ground track. The reflector extends from the margin of the SPLD (left of center) to below a 3.5-km-thick section of the SPLD. The basal reflector abruptly disappears for unknown reasons. (E) MOLA surface elevations (black line) and MARSIS measured basal elevations (blue symbols), assuming a refractive index of ice. The basal reflector is at a fairly constant elevation between 1000 and 1500 m. The apparent curvature of the reflector in (C) is an artifact of the time representation of the data. The vertical dimension in (A) and (C) is round-trip travel time. See Fig. 2 for the location of ground tracks and the MOLA elevation scale.



(A) and (C) is round-trip travel time. See Fig. 2 for the location of ground tracks and the MOLA elevation scale.

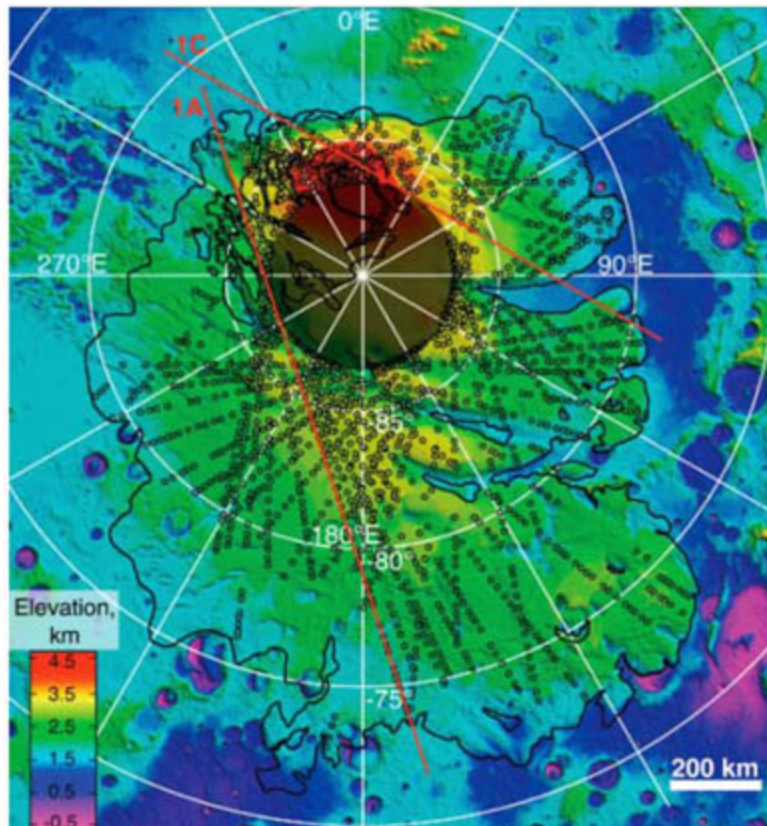
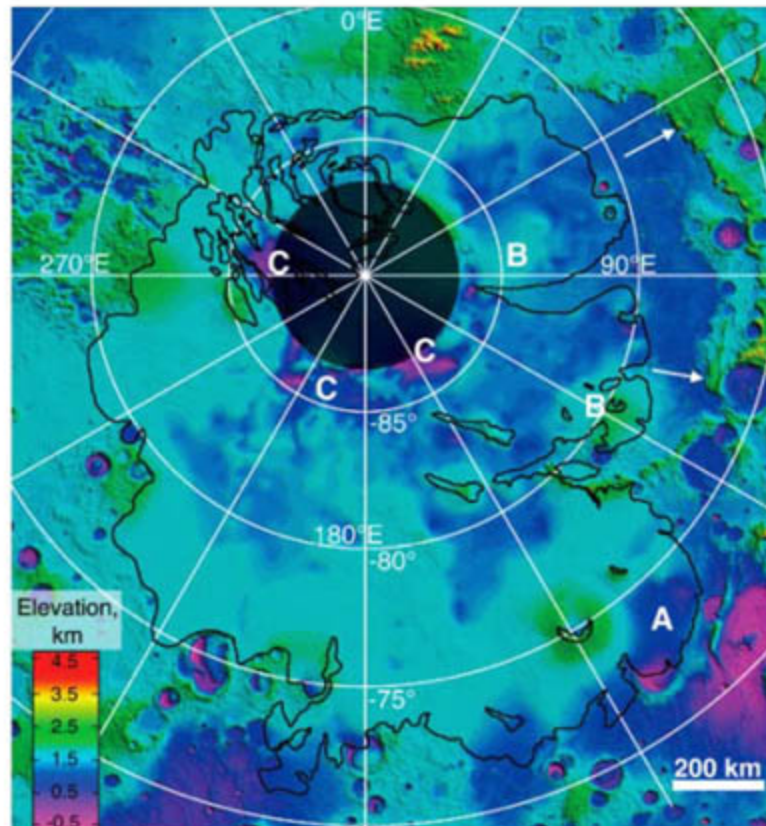


Fig. 2. (left). Topography of the south polar region of Mars from MGS MOLA data, with locations of MARSIS measurements of the SPLD thickness shown as open circles. The SPLD unit as mapped by (15) is outlined in black. Red lines indicate ground tracks of the orbits in Fig. 1. Apparent gaps in coverage are due to the lack of a discernible basal interface, and not to gaps in observations. No MARSIS data are available poleward of



87°S (dark circle in upper center). **Fig. 3** (right). Same as Fig. 2, with topography at the SPLD basal interface shown, based on MARSIS measurements of SPLD thickness. A indicates a depression below a distal SPLD lobe. B indicates relative highs within the remnant Prometheus basin (the basin rim is indicated with arrows). C indicates depressions in the near-polar region.

creates the bands is unknown. The position and brightness of the bands sometimes vary with the frequency of the MARSIS observation, suggesting that the bands may be due to interference effects that depend on the relative scales of the radar wavelength and the internal layering of the SPLD.

Detection of the basal interface below most of the SPLD allows us to generate a map of the topography of this interface and to provide new estimates of the thickness and volume of the SPLD. The methodology used is as follows: The time delay was measured between the peak of the surface reflection and the peak of the last bright continuous reflector, which is assumed to be the basal interface. Over 1800 points from 60 high-quality MARSIS orbits were used. The orbits were chosen to provide coverage that was sufficiently dense to generate medium-resolution maps of basal topography and SPLD thickness. Data from two frequencies were evaluated for most points. All points were verified to be actual subsurface reflectors and not surface "clutter," using simulations of surface echoes based on MOLA topography (11). The vertical resolution of the data used was about 100 m in ice, with an estimated uncertainty on a given measurement less than 200 m. To convert time delay to depth, we used the refractive index of pure ice with a real dielectric constant of 3. We could reasonably expect this estimate to be off by ± 0.5 , which translates into an additional error in our depth estimate of somewhat less than 10%. Figure 2 shows a map of the locations of the measured points.

To obtain a map of the basal interface, the MARSIS measured elevations of the interface

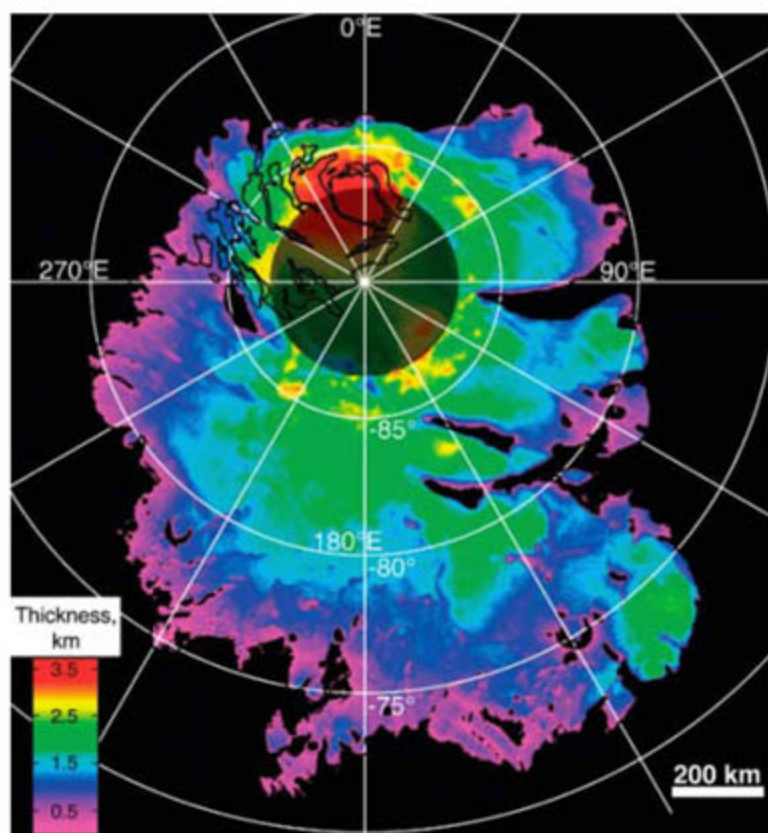
were combined with MOLA elevations along the margin of the SPLD unit as mapped by (15), where the thickness of the unit is considered to be zero. The results of a "natural-neighbor" interpolation (16, 17) of these data are shown in Fig. 3. The map of the sub-SPLD topography is generally consistent with that expected from simple interpolation of MOLA data from the margins of the unit (18). The surface is typically low in relief, with broad areas of higher and lower topography. A pronounced low area is seen near the SPLD margin around 72° to 74° S, 130° to 145° E, and elevated regions within the remnant Prometheus impact basin are seen to continue below the SPLD at 78° to 82° S, 100° to 130° E, and from 70° to 90° E poleward of about 83° S. An unexpected feature of the basal topography is a series of depressions at the highest latitudes (84° to 87° S). These occur discontinuously from longitudes 95° to 295° E. The depressions range in width from 50 to 200 km and reach a depth as much as 1 km below the surrounding sub-SPLD topography. The basal reflection within the depressions is typically dimmer than under the rest of the SPLD. This fact and the position of the depressions in the near-polar areas suggest that there may be processes unique to this sub-SPLD area. The depressions may be the result of differential compaction of megaregolith in response to the SPLD load. Alternatively, they may be a group of buried impact craters or other preexisting topography such as the ~ 1 -km-deep pits ("Cavi") in the nearby plains. On a regional scale, the basal interface is relatively flat. The lack of evidence of regional downwarping in response to the SPLD load suggests that the

elastic lithosphere in the south polar region is very thick (>150 km), as was inferred for the north polar region (11).

A thickness map of the SPLD was generated by subtracting the elevations of the interpolated basal topography from the high-resolution MOLA surface topography (Fig. 4). The distribution of SPLD thickness reflects the asymmetry of the south polar geology, with the thickest portions offset from the pole near 0° E longitude and the much more areally extensive but thinner portion centered near 180° E. The newly discovered near-polar depressions show clearly as anomalously thick areas, as do several of the distal lobes. The maximum measured thickness is 3.7 ± 0.4 km, under the highest elevations of the SPLD near 0° E. Our estimate of the integrated volume of the entire SPLD is $1.6 \pm 0.2 \times 10^6$ km³ (19). This translates to an equivalent global water layer thickness of 11 ± 1.4 m (assuming an SPLD composition of nearly pure ice) and is within the range estimated by previous workers using MOLA data alone (2, 18, 20). Knowledge of the basal topography now allows us to estimate the volume with a much smaller range of uncertainty.

MARSIS data do not allow us to distinguish a component of CO₂ ice in the SPLD material, but there is no corroborative evidence for such a component. Spectral and albedo observations of the surface of the SPLD indicate an optically thick lag of dust or rocky material, but this layer is "optically" thin at MARSIS wavelengths. Similarly, MARSIS detects no difference in surface or subsurface echoes from areas covered by the residual ("perennial") CO₂-rich ice unit, which is consistent with recent analyses indicating that it is a deposit no more than a few tens of meters thick (21, 22).

Fig. 4. Map of the SPLD thickness, based on MARSIS measurements and MOLA surface topography. An anomalous thick section appears at lower right (see A in Fig. 3). The thickest areas occur beneath the highest elevations of the SPLD (red areas near the top) and in association with the near-polar depressions (see C in Fig. 3).



References and Notes

1. P. C. Thomas, K. Herkenhoff, A. Howard, B. Murray, in *Mars*, H. H. Kieffer et al., Eds. (Univ. of Arizona Press, Tucson, AZ, 1992), pp. 767–795.
2. D. E. Smith et al., *J. Geophys. Res.* **106**, 23689 (2001).
3. B. C. Murray et al., *Icarus* **17**, 328 (1972).
4. J. A. Cutts, *J. Geophys. Res.* **78**, 4231 (1973).
5. K. R. Blasius, J. A. Cutts, A. D. Howard, *Icarus* **50**, 140 (1982).
6. A. D. Howard, J. A. Cutts, K. R. Blasius, *Icarus* **50**, 161 (1982).
7. M. C. Malin, K. S. Edgett, *J. Geophys. Res.* **106**, 23429 (2001).
8. O. B. Toon, J. B. Pollack, W. Ward, J. A. Burns, K. Bilski, *Icarus* **44**, 552 (1980).
9. H. H. Kieffer, *J. Geophys. Res.* **95**, 1481 (1990).
10. G. Picardi et al., in *Mars Express: A European Mission to the Red Planet* [SP-1240, European Space Agency (ESA) Publications Division, European Space Research and Technology Centre, Noordwijk, Netherlands, 2004], pp. 51–69.
11. G. Picardi et al., *Science* **310**, 1925 (2005).
12. Loss tangent in this context is defined as (ϵ''/ϵ') where ϵ'' and ϵ' are the imaginary and real parts, respectively, of the complex dielectric permittivity.
13. E. Heggy et al., in *4th International Conference on Mars Polar Science and Exploration* (Lunar and Planetary Institute, Houston, TX, 2006), abstr. 8105.
14. S. M. Clifford, *J. Geophys. Res.* **92**, 9135 (1987).

15. K. Tanaka, E. Kolb, *U.S. Geol. Surv. Open-File Rep.* 2005-1271 (2005).
16. R. Sibson, in *Interpolating Multivariate Data* (Wiley, New York, 1981), pp. 21–36.
17. We used the natural-neighbor interpolation as implemented in the ArcMap GIS software from ESRI (Redlands, CA). The interpolation applies a weighted moving average and is a preferred method for irregularly distributed data sets (16).
18. C. Davies, B. A. Murray, J. Byrne, *Eos* **85**, Fall Meeting Supplement, abstr. P13A-0971 (2004).
19. The error on this estimate includes a 10% uncertainty in refractive index and an additional factor due to gaps in coverage and detectability of the basal interface.
20. P. M. Schenk, J. M. Moore, *J. Geophys. Res.* **105**, 24529 (2000).
21. S. Byrne, A. P. Ingersoll, *Science* **299**, 1051 (2003).
22. J.-P. Bibring *et al.*, *Nature* **428**, 627 (2004).
23. The authors acknowledge the support of the space agencies of Italy (Agenzia Spaziale Italiana), the United States (NASA), and Europe (European Space

Agency) for the operations of MARSIS and Mars Express. We thank Y. Gim for clutter simulation. Some of the research described in this publication was carried out at the Jet Propulsion Laboratory, California Institute of Technology.

8 January 2007; accepted 27 February 2007
Published online 15 March 2007;
10.1126/science.1139672
Include this information when citing this paper.

Synchronized Oscillation in Coupled Nanomechanical Oscillators

Seung-Bo Shim,* Matthias Imboden, Pritiraj Mohanty†

We report measurements of synchronization in two nanomechanical beam oscillators coupled by a mechanical element. We charted multiple regions of frequency entrainment or synchronization by their corresponding Arnold's tongue diagrams as the oscillator was driven at subharmonic and rational commensurate frequencies. Demonstration of multiple synchronized regions could be fundamentally important to neurocomputing with mechanical oscillator networks and nanomechanical signal processing for microwave communication.

The concept of synchronized oscillation in coupled systems is pervasive in both nature (1) and human physiology (2). Examples of synchronization include rhythmic blinking of fireflies (3), the activity of pacemaker cells in the sinoatrial node of a human heart (4), and the spin-orbit resonance of the planet Mercury (5). In physical systems, synchronization has been studied for over three centuries, starting

with Huygens' discovery of the phenomenon in two coupled pendulum clocks (6) and leading to modern-day experiments on coherent radiation in coupled spin-torque nano-oscillators (7, 8) and parametric resonance in mechanical oscillators (9, 10).

Frequency entrainment, a class of synchronization, of coupled micro- and nanomechanical oscillators is of fundamental and technical

interest. A two-oscillator system demonstrates inherently rich linear and nonlinear dynamics, which contrast with its deceptive simplicity (1, 11). After the historical observation of synchronization of two pendulum clocks by Huygens, Appleton (12) and van der Pol (13) showed that the frequency of a triode generator can be entrained, or synchronized, to an external drive; their work was motivated by the potential application in radio communication. The first systematic studies of synchronization in biological systems (and, in particular, human physiology) started with Peskin's attempt to model self-synchronization of cardiac pacemaker cells to understand the generation of a heartbeat (4). In biological neurocomputing, neural networks show rhythmic behavior, exemplified in many

Department of Physics, Boston University, 590 Commonwealth Avenue, Boston, MA 02215, USA.

*Present address: Center for Strongly Correlated Materials Research and School of Physics and Astronomy, Seoul National University, Seoul, South Korea.

†To whom correspondence should be addressed. E-mail: mohanty@physics.bu.edu

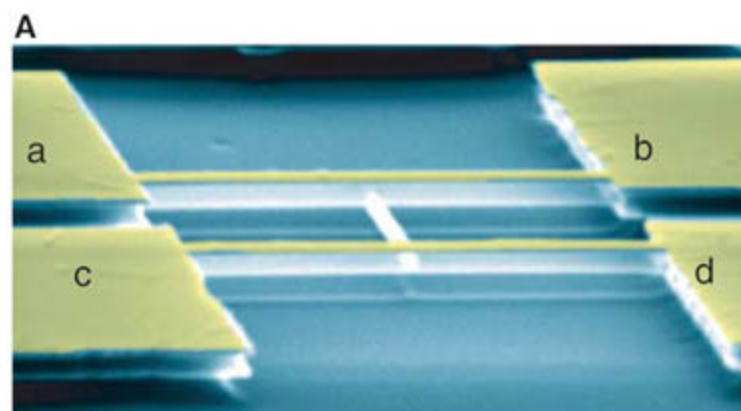
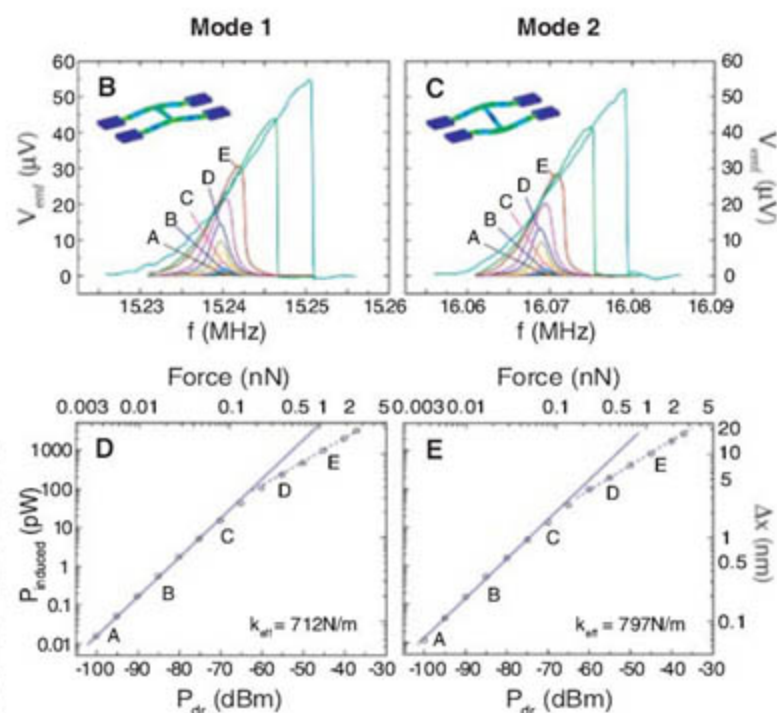


Fig. 1. Device micrograph, magnetomotive characterization, and mode shape. (A) Scanning electron micrograph of the coupled nanomechanical oscillator. Two main beams, each 10 μm in length, are doubly clamped to contact pads a and b and to c and d, respectively. The main beams are mechanically coupled near the center by a 5- μm -long beam. The beams are 500 nm wide and thick. The electrical leads (colored yellow) are selectively deposited such that contacts a and b are electrically isolated from contacts c and d. We observe two separate modes in the coupled nanomechanical resonator, labeled below as mode 1 and mode 2 with resonance frequencies of 15.241 and 16.071 MHz, respectively. (B) Linear and nonlinear response of the device structure in mode 1. The response has Lorentzian shape in the linear regime. Asymmetric responses and hysteresis occur when P_{drive} is greater than -60 dBm (trace D). The inset shows the mode shape from finite element simulation. V_{emf} is the voltage measured by the network analyzer. (C) Linear and nonlinear response of the device structure in mode 2. Nonlinearity commences at similar powers as in the mode 1. (D and E)



Plots of induced power (P_{induced}) as a response of P_{drive} at 5 T. P_{induced} is a measure of the resonant displacement, and P_{drive} corresponds to the driving force. From the log-log plot of driving force versus displacement, we calculate the effective linear-response spring constants $k_{\text{eff}} = 712$ and 797 N/m for modes 1 and 2, respectively. Δx , the central displacement of the beam. See SOM for technical details.

brain subsystems, in which the pattern recognition properties are similar to those of oscillator networks. Therefore, with the use of networks of nanomechanical oscillators, it might be possible to build a neurocomputer with associative memory in which the network can store and retrieve complex oscillatory patterns as synchronized states (14).

Synchronized states are often represented by Arnold's tongues, which are regions of frequency locking in the parameter space. In mathematical models, these regions appear (11, 15) whenever the drive frequency f_d is a rational fraction of the resonance frequency f_0 , such that $f_d = (m/n)f_0$, where m and n are respective integer winding numbers of two oscillators. As the coupling increases, the frequency-locking regimes widen, which give the appearance of a tongue shape. In another graphical representation, the Devil's staircase depicts the winding number of the synchronized regions as a function of f_d . This monotonic increase contains plateaus where the response frequency is locked to a given winding number. In general, the simplest fractions have the largest frequency-locked synchronized regions (16).

Another representation of synchronization is frequency entrainment, where two or many different frequencies of the oscillators, upon coupling, entrain or lock to a single frequency, determined by either the dynamics of the oscillator network or an external drive. In our experiment, we study entrainment of a given oscillator mode f_0 by observing its response as another part of the structure is driven at a fractional frequency, $f_d = (m/n)f_0$.

Our coupled oscillator consists of two electrically independent doubly clamped beams (10 μm long by 500 nm wide by 500 nm thick), which are coupled by a 5- μm -long beam of the same width and thickness that is attached to the centers of the main beams (Fig. 1A). Selectively evaporated gold electrodes on each beam serve as electrical connections for measurements. Because the beams are electrically isolated, the coupling between the beams is purely mechanical. The device is fabricated from single-crystal silicon by electron-beam lithography and a combination of dry and wet etch processes. For all experimental data, the sample is cooled to 280 mK with a ^3He cryostat and placed at the center of a 5 T in-plane magnetic

field. The structure is driven magnetomotively (17) with alternating current along the beam length and perpendicular to magnetic field B . Using a network analyzer, we identify two resonances at 15.241 MHz (mode 1) and 16.071 MHz (mode 2). Corresponding mode shapes are analyzed by means of finite element simulation. Each mode has a well-defined linear and nonlinear response (Fig. 1, B and C), as well as the expected B^2 dependence (18). Low driving power P_{drive} measurements in the linear regime result in effective spring constants k_{eff} of 712 and 797 N/m for modes 1 and 2, respectively. From a simple point particle and spring-coupled oscillator model, the k_{eff} value of the coupling beam is estimated to be 39 N/m [see the supporting online material (SOM) for more technical details].

To observe the frequency entrainment, we drove one of the beams with a frequency generator, and the response of the second beam was measured with a spectrum analyzer at the first resonant mode [characterized by the resonant frequency of 15.241 MHz and full width at half maximum (FWHM) of 1.5 kHz]. Figure 2 shows the response at f_0 when driving the beam at sub-

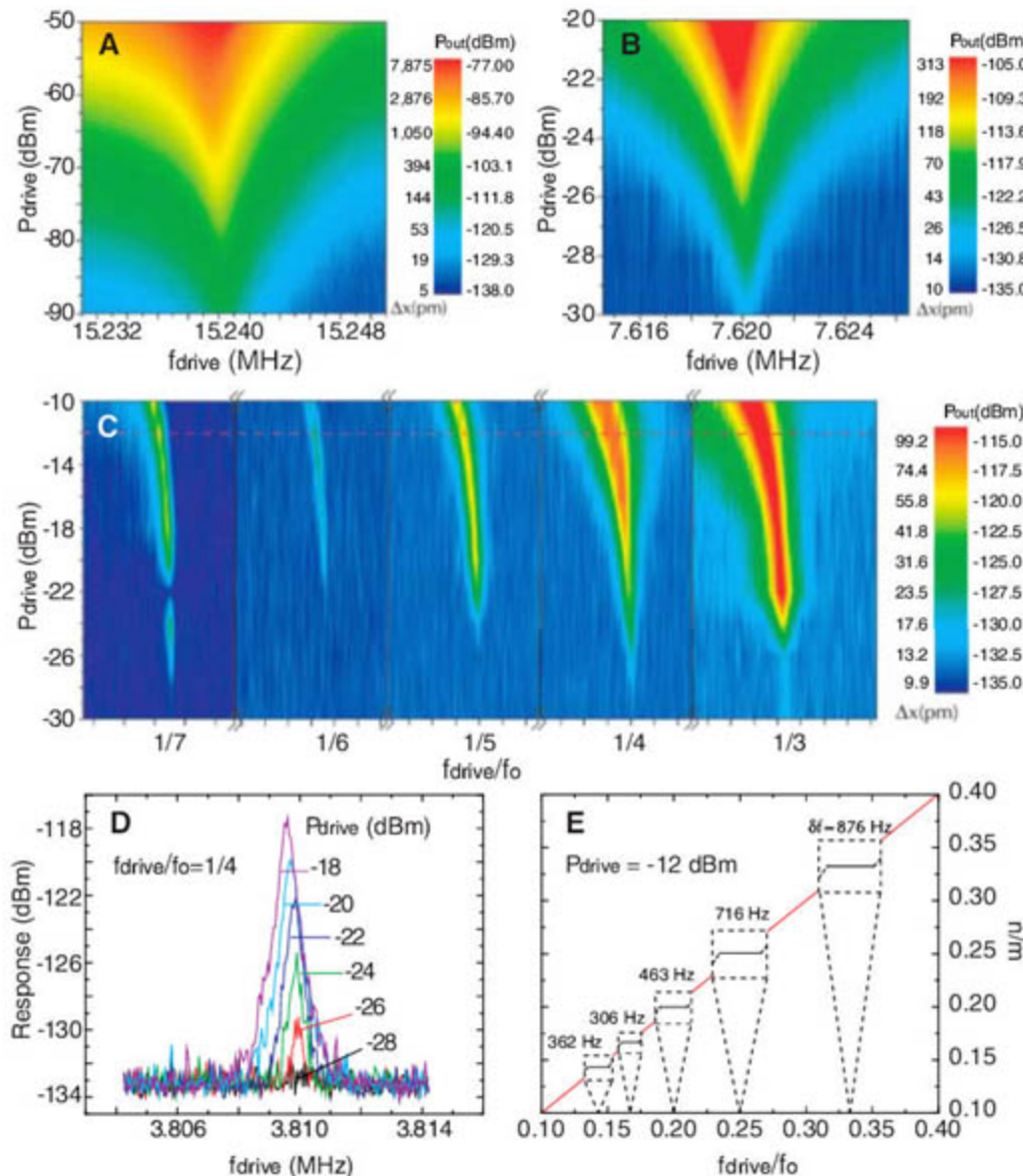


Fig. 2. Synchronization at subharmonic driving. Frequency-power sweep with subharmonic f_d (f_0/n , $n = 1, 2, \dots, 7$). A signal generator drives one beam, and the response of the second beam is measured with a spectrum analyzer. The contours represent the response in dBm. The synchronized regions become visible in the contour plots when the response exceeds the noise level of -136 dBm. We drive one of the beams at a frequency f_0/n and record the response of the second beam at the fundamental frequency f_0 . The coupling is purely mechanical as a result of the center beam (Fig. 1A). (A) Frequency-power sweep at resonant frequency $n/m = 1$. P_{out} , power output. (B) Synchronization with $f_d = f_0/2$. (C) Frequency-power sweep for subharmonic excitations (f_0/n , $n = 3, 4, 5, 6, 7$). For these measurements, a minimum of 200-dB isolation is ensured so that the higher harmonic outputs from the RF source no longer contribute. (D) Response extracted from contour plot for $f_d = f_0/4$. Each plot has Lorentzian shape and shows a linear increase with P_{drive} . (E) Devil's staircase plot depicting the width of the Lorentzian of each synchronized region. For clarity, the plateaus are greatly magnified. We measure FWHM (δf) of the Lorentzian peaks at $P_{\text{drive}} = -12$ dBm [dashed line in (C)]. The y axis (n/m) represents the winding number between driving frequency and fundamental frequency.

harmonic frequencies. The observed Arnold's tongues appear at all subharmonic drive frequencies $f_d = (1/n)f_0$ with n ranging from 1 (resonance) to 7, which means that, when the actuation frequency is an integer fraction of f_0 of the first mode, this mode of the structure starts to oscillate.

Figure 2A shows the Arnold's tongue $m/n = 1/1$ for which f_d sweeps over f_0 . This is essentially the same plot as the linear part of Fig. 1B. In a typical measurement, the drive-frequency resolution is 40 Hz, and P_{drive} is increased in 2-dBm steps, which provides 10,521 averaged measurements taken over 12 hours. For the remaining Arnold's tongues (Fig. 2, B and C), low-pass filters with high isolation are used to ensure that there is no higher harmonic output from the frequency generator, because it would drive the structure on resonance. Because we do not measure the phase of the response, synchronization is detected purely through frequency locking. The term "frequency locking" is used

here rather loosely, as a synonym for resonant actuation, in which the response is measured at mode 1 and not at a single frequency; the use of the term "locked" is justified because the response frequency is correlated to a respective f_d . Resonant actuation is not observed when the drive frequency is not in the proximity of $f_d = f_0/n$ or other well-defined drive frequencies as is seen below. The Arnold's tongues only appear with high P_{drive} where the structure is known to have nonlinear response when driven at the resonant frequency (Fig. 1).

Figure 2E displays the Devil's staircase plot, which maps the widths of the Arnold's tongues, defined as the FWHM for a given P_{drive} . Essentially, this is a slice for a given power level out of the Arnold's tongue contour plots. The actual width of frequency locking is much greater than the FWHM of the fundamental resonant mode; however, the electronic noise floor prevents detection far from the center of the Lorentzian. The x axis indicates f_d , and the y axis

represents the approximate winding number. The plateaus, representing the region of synchronization, vary in size. They tend to be larger for drive frequencies closer to f_0 . However, for $f_d = f_0/7$, the synchronized regime is larger than the regime for $f_d = f_0/6$. This is not unexpected because, in a Devil's staircase, the plateau sizes do not grow monotonously.

The maximum responses in Arnold's tongues shift to lower drive frequencies for higher driving powers. Within a frequency-locked regime, the locked frequency, observed close to resonance, shifts upward with increasing f_d over a 10- to 20-kHz range. In idealized systems, Arnold's tongues are expected for every rational number m/n , where small m and n values are preferred. For this structure, drive frequencies such as $f_d = (2/3)f_0$, $(3/4)f_0$, $(3/2)f_0$, and similar fractions could not be detected within the experimental limitations. It is possible that the missing Arnold's tongues are present but are either too weak in amplitude (below the noise floor of -136 dBm)

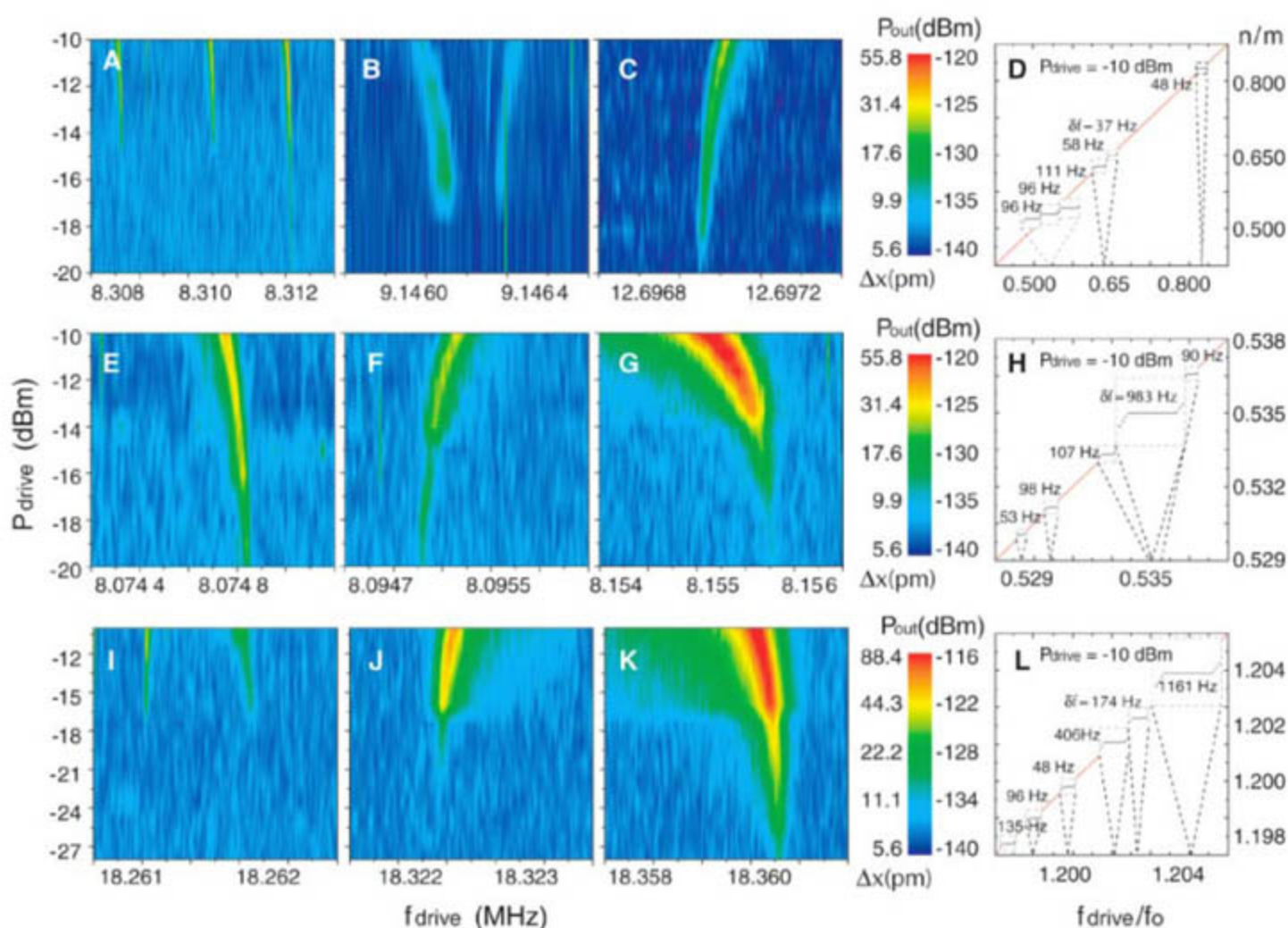


Fig. 3. Synchronization at non-subharmonic driving frequency. Synchronization regions other than f_0/n were discovered for a large range of frequencies by means of the same experimental procedure as in Fig. 2. In most cases [(A to C), (E) and (F), and (I) and (J)], these regions are narrow with a small response. However, two synchronization regions [(G) and (K)] were discovered to have a very prominent response, which is comparable to the $f_0/3$ result. (G) shows subharmonic synchronization at $f_d = 8.155$ MHz, and (K) indicates superharmonic synchronization at $f_d = 18.360$ MHz. No obvious integer fractions can be associated with these frequencies. (D), (H),

and (L) are staircase plots indicating the widths of 16 synchronization regions. As in Fig. 2E, the plateaus have been magnified for clarity. There are two classes of synchronization regions that are characterized by their behavior when sweeping P_{drive} . In some cases, the synchronization regions appear at lower frequencies as P_{drive} increases [(A) and (B)], (E), (G), (I), and (K)] (i.e., the tongues bend to the left). However, there is also a substantial number of regions with the opposite behavior: the f_d at which frequency locking occurs increases with increasing P_{drive} [(B) and (C)], (F), and (J)] (i.e., the tongues bend to the right).

or too narrow in frequency span to be detected with our setup. Alternatively, they simply may not exist in this non-idealized setup.

In addition to the Arnold's tongues shown in Fig. 2, synchronized regions are also found at frequencies with no obvious commensurate relation to f_0 . These are depicted in Fig. 3. A drive-frequency range of 370 kHz starting at 8.01 MHz, well above the $f_d = f_0/2$ frequency, reveals 34 Arnold's tongues, with the possibility of more, where the limitations are given by the frequency resolution and preamplifier noise. A smaller drive span of 180 kHz starting at 18.24 MHz (well above f_0) reveals a similar Arnold's tongue count of 24. Not only is resonant actuation observed, but some of these frequency-locking regimes (Fig. 3, G and K) are also larger than the synchronized regimes illustrated in Fig. 2. For both sub- and superharmonic drive frequencies, some Arnold's tongues bend down (maximum response is observed at decreasing f_d) (Fig. 3, A, E, G, I, and K) and some Arnold's tongues bend up (maximum response is observed at increasing f_d) (Fig. 3, C, F, and J) for growing P_{drive} . It is not clear whether there is a pattern that can be established in the data. The response frequency (i.e., the frequency at which mode 1 is observed) actually decreases as f_d increases for the Arnold's tongues that bend up. This effect is the opposite of that for the Arnold's tongues that bend down as P_{drive} increases. It is noteworthy that the bending of Arnold's tongues is also observed in mathematical simulations of phase-locked oscil-

lators as discussed in the SOM. The Devil's staircase is also plotted for these off-harmonic Arnold's tongues. The sizes of the frequency-locked regimes appear to fluctuate randomly, and no pattern could be established. A large number of frequency-locked regimes would be essential to the realization of neural computers based on oscillator networks.

Another notable aspect of nonresonant excitation is parametric amplification, which enables the enhancement of small signals in individual oscillator modes in a network. In our structure, on-chip amplification of small mechanical signals can be performed by parametric down-conversion in which the small signal generated in one beam can be amplified by coupling it to a second beam that provides the necessary pumping for signal amplification. In mechanical structures, parametric down-conversion or amplification has been studied in optical setups with cantilever (19), torsional (20), and disk resonators (21). Here, we report parametric amplification of mechanical signals in a nanometer-scale mechanical resonator with a distinct two-oscillator or two-beam structure. Parametric amplification is defined by a gain in the mechanical response on resonance (frequency f_0) when modulating a parameter of the oscillator such as the spring constant, for instance, by adding parametric modulation (pumping) at twice the resonance frequency (pump frequency $2f_0$). Because the two beams on each side of the structure are electrically isolated, we can drive the structure

through one beam and pump on the other beam. This enables us to explore purely mechanical amplification effects. In our experiment, we modulate the spring constant of the structure by applying a high-amplitude pump signal at twice the resonance frequency. We apply a pump signal ($f_{\text{pump}} = 2f_0$) on one beam (c to d, Fig. 1A) while driving at f_0 through the other beam (a to b, Fig. 1A). Two referenced signal generators are used for the drive and pump signals. The pre-amplified induced voltage is detected with an RF lock-in amplifier. A Lorentzian fit to the data is used to extract f_0 and the amplitude A .

We observe that f_0 shifts down by 1.7 kHz with an -8 -dBm pump signal (Fig. 4A), possibly as a result of the applied strain from the pump. This corresponds to a 0.4% change in k_{eff} . Here, the gain is defined as the ratio of the response with and without pumping: $G = \frac{A_{\text{pump-on}}}{A_{\text{pump-off}}}$. Figure 4A illustrates an example of two Lorentzian responses with the pump on and off ($A_{\text{pump-on}} = 95.6$ nV and $A_{\text{pump-off}} = 33.1$ nV), yielding a gain of 2.9. In this coupled oscillator structure, the maximum phase-sensitive gain (19, 22) is found to be 3.3 at a relative phase of 0° . At a relative phase of 90° , parametric attenuation is observed as expected (Fig. 4B). In the experimental setup, the phase between the drive and pump signals can be locked because they represent f and its harmonic $2f$. The phase locking between the two signals is monitored with the use of an oscilloscope. Figure 4C shows the measured phase and amplitude relationship between the two signals.

The mechanically coupled two-oscillator structure demonstrates a large number of frequency synchronization regions, as illustrated by Arnold's tongues. Furthermore, we demonstrate phase-sensitive mechanical parametric amplification of small signals. Future work would involve an array of mechanically coupled nanomechanical oscillators with the ability to self-oscillate. Even though synchronization resulting from reactive coupling and nonlinear frequency pulling has been studied in a model of a large array (23), a comprehensive study of two coupled nanomechanical oscillators will elucidate further aspects of the data in our experiments.

Demonstration of a large number of synchronization regions provides exciting opportunities for practical realization of pattern recognition with the use of oscillator networks. Storage and retrieval of complex patterns through the corresponding synchronized states will enable the feasibility of constructing nanomechanical neurocomputers. Small size, high speed, and low power consumption in these structures further add to the fundamental benefit of an on-chip nanomechanical oscillator network with distributed on-chip signal processing at microwave frequencies (24). The advantage of such a device would be its scalable architecture, based on standard lithography and semiconductor processing techniques. Beyond neural network models, nanomechanical oscillator networks capable of individual-oscillator addressing and global cou-

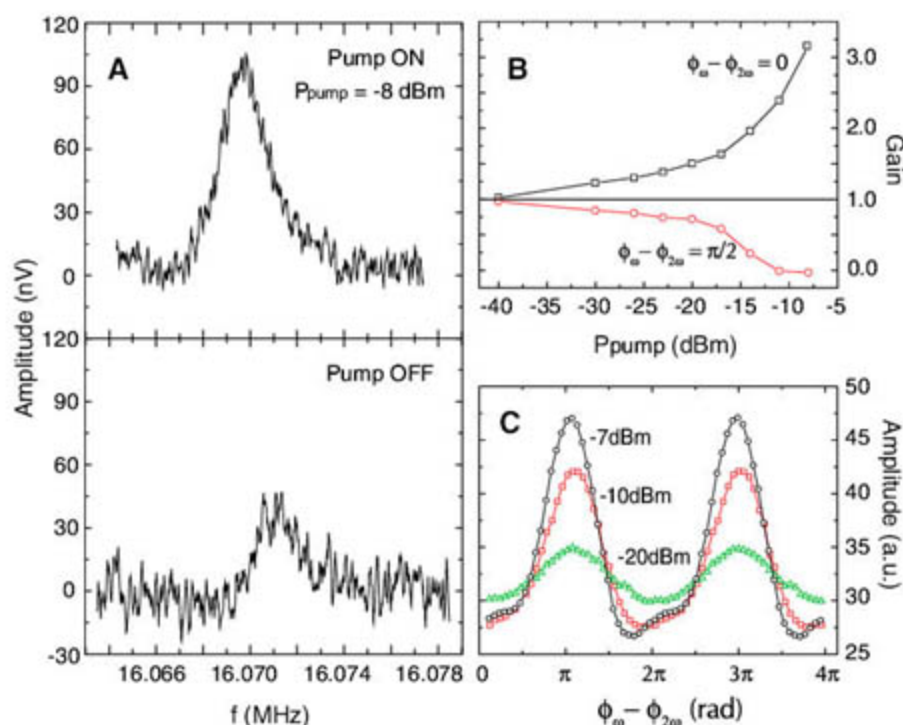


Fig. 4. Parametric amplification. (A) Response of the device structure with (top) and without (bottom) pumping. P_{pump} , pumping power. (B) Dependence of gain for varying P_{pump} . At a relative phase of 0° between driving and pumping signals, we measure parametric amplification, and, at a relative phase of 90° , we observe parametric attenuation. The maximum gain observed is 3.3 with possible indication of oscillation death. $\phi_\omega - \phi_{2\omega}$ is the phase difference between the pump and drive signals. (C) Response as relative phase varies between the drive and the pump signal (monitored with an RF oscilloscope) for three different pumping powers. We observe a notable change in response as the two signals sweep from in phase to out of phase. a.u., arbitrary units.

pling could provide paradigms by enabling experimental realization of physical models that show phase transition, glassy states, and other collective behavior. If two coupled oscillators demonstrate such rich collective behaviors, a network of nanomechanical oscillators could possibly realize the complexity and intelligence, if not of the human brain subsystems, then at least those of pacemaker cells of a human heart or the rhythmic blinking of a congregation of fireflies.

References and Notes

1. A. T. Winfree, *The Geometry of Biological Time* (Springer-Verlag, New York, 1980).
2. S. Strogatz, *Sync: The Emerging Science of Spontaneous Order* (Hyperion, New York, 2003).
3. J. Buck, E. Buck, *Science* **159**, 1319 (1968).
4. C. S. Peskin, *Mathematical Aspects of Heart Physiology* (Courant Institute of Mathematical Sciences, New York University, New York, 1975).
5. S. F. Dermott, *Nature* **429**, 814 (2004).
6. C. Huygens, *Horologium Oscillatorium [The Pendulum Clock]* (Apud F. Muguet, Paris, 1673) [R. J. Blackwell, Transl. (Iowa State Univ. Press, Ames, IA, 1986)].
7. F. B. Mancoff, N. D. Rizzo, B. N. Engel, S. Tehrani, *Nature* **437**, 393 (2005).
8. S. Kaka *et al.*, *Nature* **437**, 389 (2005).
9. M. Zhalutdinov *et al.*, *Appl. Phys. Lett.* **78**, 3142 (2001).
10. K. L. Turner *et al.*, *Nature* **396**, 149 (1998).
11. V. I. Arnold, *Mathematical Methods of Classical Mechanics*, K. Vogtmann, A. Weinstein, Transl. (Springer-Verlag, New York, ed. 2, 1989).
12. E. V. Appleton, *Proc. Cambridge Philos. Soc.* **21**, 231 (1922).
13. B. van der Pol, *Philos. Mag.* **3**, 65 (1927).
14. E. M. Izhikevich, F. C. Hoppensteadt, *SIAM J. Appl. Math.* **63**, 1935 (2003).
15. C. Hayashi, *Nonlinear Oscillations in Physical Systems* (Princeton Univ. Press, Princeton, 1985).
16. A. Pikovsky, M. Rosenblum, J. Kurths, *Synchronization: A Universal Concept in Nonlinear Sciences* (Cambridge Univ. Press, Cambridge, 2001).
17. A. Gaidarzh, G. Zolfagharkhani, R. L. Badzey, P. Mohanty, *Phys. Rev. Lett.* **94**, 030402 (2005).
18. A. N. Cleland, M. L. Roukes, *Appl. Phys. Lett.* **69**, 2653 (1996).
19. D. Rugar, P. Grutter, *Phys. Rev. Lett.* **67**, 699 (1991).
20. D. W. Carr, S. Evoy, L. Sekaric, H. G. Craighead, J. M. Parpia, *Appl. Phys. Lett.* **77**, 1545 (2000).
21. M. Zhalutdinov *et al.*, *Appl. Phys. Lett.* **79**, 695 (2001).
22. A. N. Cleland, *New J. Phys.* **7**, 235 (2005).
23. M. C. Cross, A. Zumedeck, A. Lifshitz, J. L. Rogers, *Phys. Rev. Lett.* **93**, 224101 (2004).
24. R. L. Badzey, P. Mohanty, *Nature* **437**, 995 (2005).
25. This work was supported by NSF under grant number CCF-0432089 and partially under grant number DMR-0449670. We thank N. Kopel, Y. D. Park, J. Wei, and M. Grifoni for their valuable comments.

Supporting Online Material

www.sciencemag.org/cgi/content/full/316/5821/95/DC1
Materials and Methods

SOM Text

Figs. S1 to S5

References

8 November 2006; accepted 14 February 2007
10.1126/science.1137307

Giant Fluctuations of Coulomb Drag in a Bilayer System

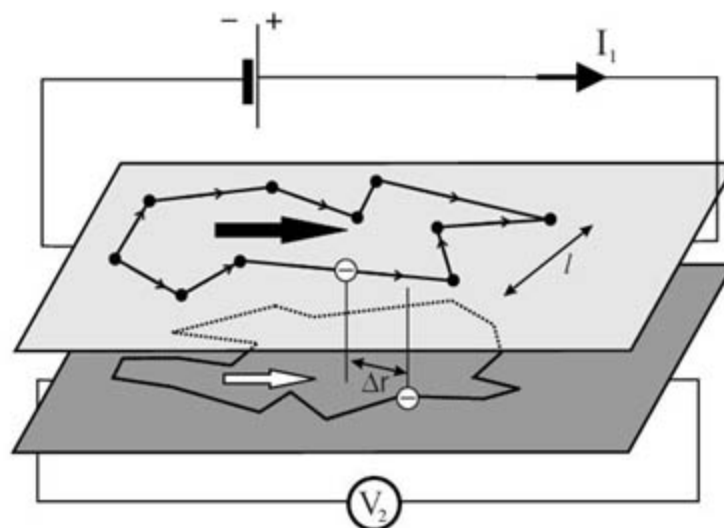
A. S. Price,¹ A. K. Savchenko,^{1*} B. N. Narozhny,² G. Allison,¹ D. A. Ritchie³

The Coulomb drag in a system of two parallel layers is the result of electron-electron interaction between the layers. We have observed reproducible fluctuations of the drag, both as a function of magnetic field and electron concentration, which are a manifestation of quantum interference of electrons in the layers. At low temperatures the fluctuations exceed the average drag, giving rise to random changes of the sign of the drag. The fluctuations are found to be much larger than previously expected, and we propose a model that explains their enhancement by considering fluctuations of local electron properties.

In conventional measurements of the resistance of a two-dimensional (2D) layer, an electrical current is driven through the layer and the voltage drop along the layer is measured. In contrast, Coulomb drag studies are performed on two closely spaced but electrically isolated layers, where a current I_1 is driven through one of the layers (active layer) and the voltage drop V_2 is measured along the other (passive) layer (Fig. 1). The origin of this voltage is electron-electron ($e-e$) interaction between the layers, which creates a “frictional” force that drags electrons in the second layer. The ratio of this voltage to the driving current $R_D = -V_2/I_1$ (the drag resistance) is a measure of $e-e$ interaction between the layers. The measurement of Coulomb drag in systems of parallel layers was first proposed in (1, 2) and later realized in a number of experiments (3–7) [for a review, see (8)].

Because Coulomb drag originates from $e-e$ interactions, it has become a sensitive tool for their study in many problems of contemporary condensed-matter physics. For example, Coulomb drag has been used in the search for Bose-condensation of interlayer excitons (9), the metal-insulator transition in 2D layers (10), and Wigner crystal formation in quantum wires (11).

Fig. 1. Schematic showing the origin of the drag signal V_2 induced by the current I_1 . The fluctuations of the drag arise from the interference of electron waves in each layer, before the two electrons take part in the interlayer interaction.



¹School of Physics, University of Exeter, Stocker Road, Exeter EX4 4QL, UK. ²The Abdus Salam International Centre for Theoretical Physics, Strada Costiera 11, Trieste I-34100, Italy. ³Cavendish Laboratory, University of Cambridge, Madingley Road, Cambridge CB3 0HE, UK.

*To whom correspondence should be addressed. E-mail: a.k.savchenko@ex.ac.uk

after collisions with impurities, over the characteristic area $\sim L_\phi^2$, where L_ϕ is the coherence length (Fig. 1). This interference is very important for the conductive properties of electron waves. For example, the interference pattern is changed when the phase of electron waves is varied by a small magnetic field, producing universal conductance fluctuations (UCF) seen in small samples with size $L \sim L_\phi$. There is, however, an important difference between UCF and the fluctuations of the drag resistance. The former are only a small correction to the average value of the conductance: In our experiment, the single-layer resistance fluctuates by ~ 200 milliohm around an average resistance of ~ 500 ohm. In contrast, the drag fluctuations, although small in absolute magnitude (~ 20 milliohm), are able to change randomly but reproducibly the sign of the Coulomb drag between positive and negative. Surprisingly, we have found that these fluctuations of the Coulomb drag, observed at temperatures below 1 K, are four orders of magnitude larger than predicted in (12).

Our explanation of the giant drag fluctuations takes into account that, unlike the UCF, the drag fluctuations are not only an interference effect but also fundamentally an interaction effect. In conventional drag structures, the electron mean free path l is much larger than the separation d between the layers, and therefore large momentum transfers $\hbar q$ between electrons in the layers become essential. According to the quantum mechanical uncertainty principle, $\Delta r \Delta q \sim 1$, electrons interact over small distances $\Delta r \ll l$ when exchanging large values of momentum (Fig. 1). As a result the local properties of the layers, such as the local density of electron states (LDOS), become important in the interlayer e - e interaction. These local properties at the scale $\Delta r \ll l$ exhibit strong fluctuations (14) that directly manifest themselves in the fluctuations of the Coulomb drag.

The samples used in this work are AlGaAs-GaAs double-layer structures, in which the carrier concentration of each layer can be independently controlled by gate voltage. The two GaAs quantum wells of the structure, 200 Å in thickness, are separated by an $\text{Al}_{0.33}\text{Ga}_{0.67}\text{As}$ layer of thickness 300 Å. Each layer has a Hall-bar geometry, 60 μm in width and with a distance between the voltage probes of 60 μm (15).

Figure 2 shows the appearance of the fluctuations in the drag resistivity, ρ_D , at low temperatures. At higher temperatures, the drag resistance changes monotonically with both T and n ; the insets to Fig. 2 show that ρ_D increases with increasing temperature as T^2 and decreases with increasing passive-layer carrier concentration as n_2^{-b} , where $b \approx -1.5$. These results are consistent with existing experimental work on the average Coulomb drag (4, 16).

Figure 3A shows a magnified view of the reproducible fluctuations as a function of n_2 . These fluctuations result in an alternating sign of

the drag, which is demonstrated in the inset to Fig. 3 where the temperature dependence of the drag is shown at two different values of n_2 . The drag is seen first to decrease as the temperature is decreased, but then become either increasingly positive or increasingly negative, dependent upon n_2 . The reproducible fluctuations of the drag resistivity have also been observed as a function of magnetic field (Fig. 3B). For a fixed temperature, the magnitude of the drag fluctuations as a function of n_2 is roughly the same as that as a function of B .

The theory of (12) calculates the variance of drag fluctuations in the so-called diffusive regime, $l < d$. In this case the drag is determined by global properties of the layers, averaged over a region $\Delta r \gg l$. The expected variance of

drag fluctuations (at low T , when the fluctuations exceed the average) in the diffusive regime is

$$\langle \Delta \sigma_D^2 \rangle \approx A \frac{e^4 E_T(L) \tau_\phi \ln \kappa d}{h^2 g^4 h(\kappa d)^3} \quad (1)$$

where $\sigma_D \approx \rho_D / (\rho_1 \rho_2)$, and ρ_1 and ρ_2 are the active- and passive-layer resistivities, respectively; $E_T(L)$ is the Thouless energy, $E_T(L) = \hbar D / L^2$, where D is the diffusion coefficient; τ_ϕ is the decoherence time; κ is the inverse screening length; $A = 4.9 \times 10^{-3}$; and $g = \hbar / (e^2 \rho)$ is the dimensionless conductivity of the layers. When the parameters of our system are used, this

Fig. 2. Drag resistivity as a function of passive-layer carrier concentration for different temperatures: $T = 5, 4, 3, 2, 1, 0.4$, and 0.24 K, from top to bottom. Inset (A): ρ_D as a function of T^2 . Inset (B): ρ_D as a function of n_2 , with $n_1 = 1.1 \times 10^{11} \text{ cm}^{-2}$; dashed line is a $n_2^{-1.5}$ fit.

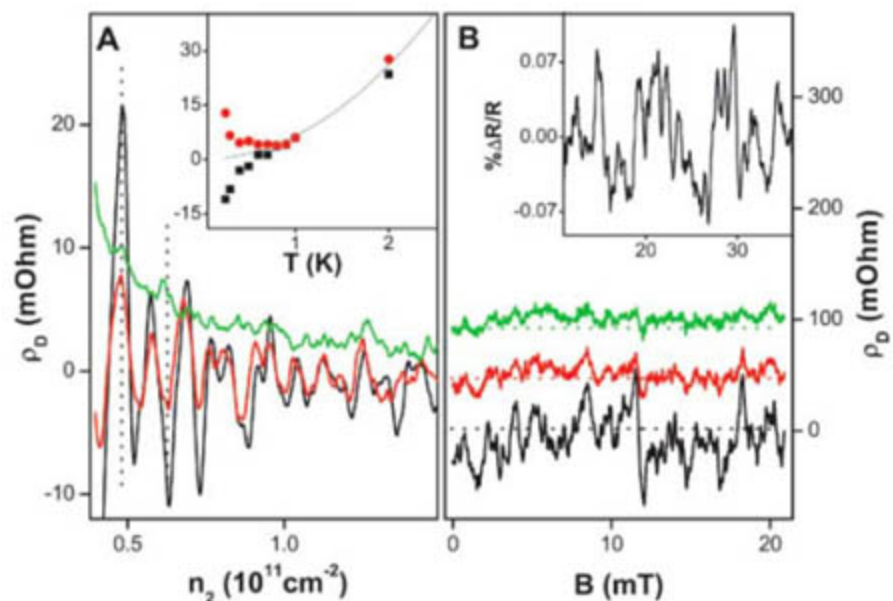
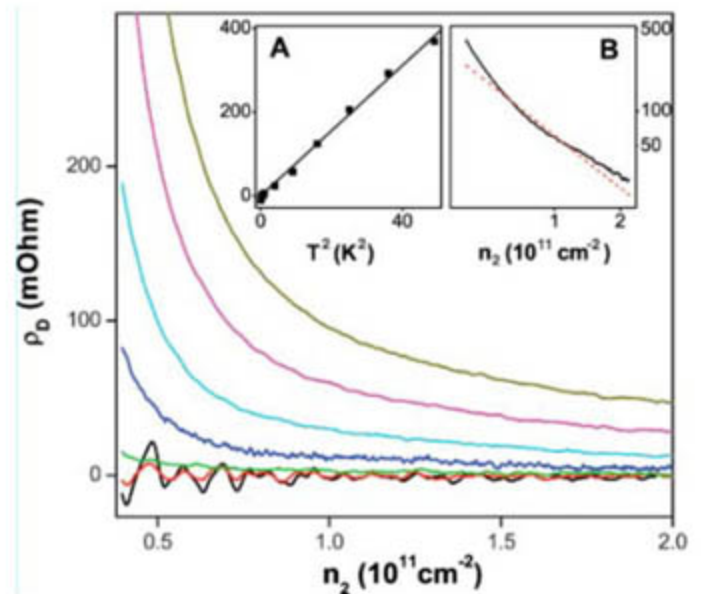


Fig. 3. (A) Drag resistance measured at low temperatures as a function of passive-layer concentration; $T = 1, 0.4$, and 0.24 K, from top to bottom. (Inset) ρ_D as a function of T for two values of n_2 denoted by the dotted lines in Fig. 3A; solid line is the expected T^2 dependence of the average drag. (B) ρ_D as a function of B ; $T = 0.4, 0.35$, and 0.24 K, from top to bottom. (Graphs for higher T are vertically offset for clarity.) Single-layer concentration for each layer is $5.8 \times 10^{10} \text{ cm}^{-2}$. (Inset) The UCF of the single layer, with an average background resistance of 500 ohm subtracted.

expression gives a variance of $\sim 6 \times 10^{-11} \mu\text{S}^2$, which is approximately eight orders of magnitude smaller than the variance of the observed drag fluctuations. The fluctuations in ρ_D have been measured in two different samples, and their variance is seen to be similar in magnitude and T dependence, confirming the discrepancy with the theoretical prediction (12).

The expected fluctuations of the drag conductivity share the same origin as the UCF in the conventional conductivity: coherent electron transport over L_ϕ in the layers before e - e interaction between the layers (Fig. 1). Therefore, we have compared the drag fluctuations with the fluctuations seen in the single-layer resistivity of the same structure (Fig. 3B, inset), which have shown the usual behavior (17). We estimate the expected variance of the single-layer conductance fluctuations using the relation $\langle \Delta\sigma_{xx}^2 \rangle = (e^2/h)^2 (L_T/L)^2$, where $L_T = \sqrt{\hbar D/k_B T}$ is the thermal length (17). This expression produces a value of $0.8 \mu\text{S}^2$, which is in good agreement with the measured value of $0.6 \mu\text{S}^2$. The typical "period" of the drag fluctuations (the correlation field, ΔB_c) is similar to that of the UCF (15), indicating that both depend upon the same L_ϕ and have the same quantum origin.

To address the question of the discrepancy between the magnitude of drag fluctuations in theory (12) and our observations, we stress that the theoretical prediction for the variance, Eq. 1, was obtained under the assumption of diffusive motion of interacting electrons, with small interlayer momentum transfers, $q \ll 1/l$. Because the layers are separated by a distance d , the e - e interactions are screened at distances $\Delta r > d$. Therefore, in all regimes the maximum momentum transfers are limited by $q < 1/d$. In the diffusive regime, $l < d$, this relation also means that $q < 1/l$, that is, interlayer e - e interactions occur at distances $\Delta r > l$ and involve scattering by many impurities in the individual layers. In the opposite situation, $l \gg d$, the transferred momenta will include both small and large

q -values: $q < 1/l$ and $1/l < q < 1/d$. We have seen that small q values cannot explain the large fluctuations of the drag (12), and so argue that it is large momentum transfers with $q > 1/l$ that give rise to the observed effect. In this case the two electrons interact at a distance Δr that is smaller than the average impurity separation and, therefore, it is the local electron properties of the layers that determine e - e interaction. In (14), it is shown that the fluctuations of the local properties are larger compared to those of the global properties that are responsible for the drag in the diffusive case.

A theoretical expression for the drag conductivity is obtained by means of a Kubo formula analysis (18–21) (see detailed description in the supporting text). For a qualitative estimate, three factors have to be taken into account: (i) the interlayer matrix elements of the Coulomb interaction D_{ij} ; (ii) the phase space (the number of electron states available for scattering); and (iii) the electron-hole (e - h) asymmetry in both layers. Point (iii) takes into account that in a quantum system, the current is carried by both electron-like (above the Fermi surface) and hole-like (below the Fermi surface) excitations. If they were completely symmetric with respect to each other, then the current-carrying state of the active layer would have zero total momentum, and thus no drag effect would be possible. The physical quantity that measures the degree of e - h asymmetry is the nonlinear susceptibility Γ of the 2D layer. Theoretically, the drag conductivity is represented in terms of the nonlinear susceptibilities of each layer and dynamically screened interlayer Coulomb interaction $D_{ij}(\omega)$ as $\sigma_D \propto \int d\omega D_{12}(\omega) \Gamma_2(\omega) D_{21}(\omega) \Gamma_1(\omega)$ (indices 1 and 2 correspond to the two layers) (18, 12). The e - h asymmetry appears in Γ as a derivative of the density of states ν and the diffusion coefficient D : $\Gamma \propto \partial(\nu D)/\partial\mu$, and it is this quantity that allows drag fluctuations to exceed the average. Because $D\nu \sim g$ and the typical energy of electrons is the Fermi energy, E_F , we have $\partial(\nu D)/\partial\mu \sim g/E_F$ for the average drag. The typical energy scale for the

interfering electrons, however, is $E_T(L_\phi)$ (17), which is much smaller than E_F , and therefore in a mesoscopic system e - h asymmetry produces a larger effect.

Under the condition of large momentum transfer between the layers, fluctuations in Γ are enhanced by a factor of g compared with (12), similarly to the fluctuations of the LDOS, which can be estimated as $\delta v^2 \sim (v^2/g) \ln[\max(L_\phi, L_T)/l]$ (14). Also, the interaction in the ballistic regime can be assumed to be constant, $D_{ij} \approx -1/\nu\kappa d$, because q is limited by $q \leq 1/d$. Finally, to average fluctuations of the drag over the sample with size L , we should divide it into coherent patches of size L_ϕ that fluctuate independently and thus decrease the total variance: $\langle \Delta\sigma_D^2 \rangle = \langle \Delta\sigma_D^2(L_\phi) \rangle (L_\phi/L)^2$. If $k_B T > E_T(L_\phi)$, fluctuations are further averaged on the scale of $\sim k_B T$, and therefore the variance is suppressed by an additional factor of $E_T(L_\phi)/k_B T$. Combining the above arguments we find

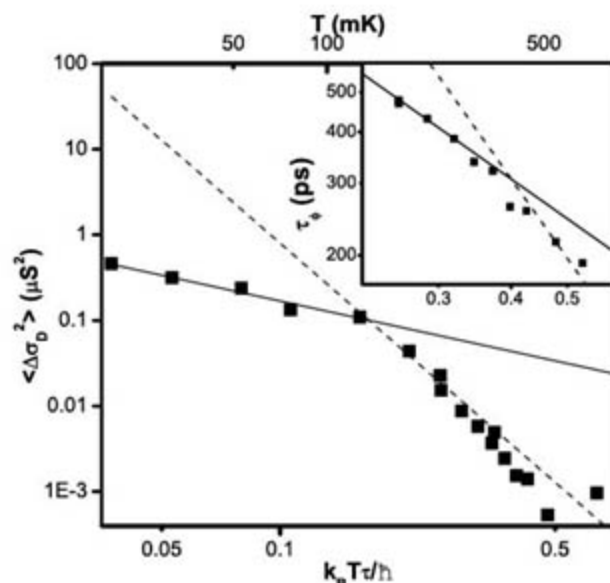
$$\langle \Delta\sigma_D^2 \rangle = N \frac{e^4}{g^2 \hbar^2 (\kappa d)^4} \frac{(k_B T)^2 l^4 L_\phi^2}{E_T^2(L_\phi) d^4 L^2}, \quad (2)$$

where N is a numerical coefficient.

Compared to the diffusive situation (Eq. 1), the fluctuations described by our model are greatly enhanced. Equations 2 and 1 differ because in the ballistic regime, electrons are not scattered by impurities between events of e - e scattering. Large momentum transfers correspond to short distances, and thus in the ballistic regime, drag measurements explore the local (as opposed to averaged over the whole sample) nonlinear susceptibility. This leads to the appearance of three extra factors in Eq. 2: (i) the factor l^4/d^4 [which is also present in the average drag in the ballistic regime (18)]; (ii) the phase space factor T/E_T (which appears because the interaction parameters D_{ij} become energy independent); and (iii) the extra factor g^2 due to fluctuations of the local nonlinear susceptibility. Local fluctuations are enhanced because the random quantity Γ becomes averaged over a small part of the ensemble, allowing one to detect rare impurity configurations.

Our model not only explains the large magnitude of the fluctuations but also predicts a nontrivial temperature dependence of their magnitude. The latter comes from the change in the temperature dependence of L_ϕ (22): At low temperatures, $k_B T \tau / \hbar \ll 1$, the usual result is $L_\phi \propto T^{-1/2}$, whereas for $k_B T \tau / \hbar > 1$, the temperature dependence changes to $L_\phi \propto T^{-1}$ (23). Consequently, the temperature dependence of the variance of the drag fluctuations is expected to change from T^{-1} at low T to T^{-4} at high T . This temperature dependence is very different from the T dependence of drag fluctuations in the diffusive regime, $\langle \Delta\sigma_D^2 \rangle \propto T^{-1}$. To test the prediction of Eq. 2, we have analyzed the T dependence of $\langle \Delta\sigma_D^2 \rangle$ (Fig. 4). The variance is

Fig. 4. The variance of the drag conductivity fluctuations (squares) plotted against temperature. The solid and dashed lines are calculated from Eq. 2 with the diffusive and ballistic asymptotes of τ_ϕ , respectively. (Inset) τ_ϕ extracted from the correlation magnetic field of the single-layer fluctuations, plotted against temperature.



calculated in the limits of both the diffusive τ_ϕ (solid line, $\tau_\phi^{-1} \propto T$) and ballistic τ_ϕ (dashed line, $\tau_\phi^{-1} \propto T^2$), with $N \cong 10^{-4}$. In fitting the drag variance, we have found τ_ϕ to agree with theory to within a factor of 2 (15), which is typical of the agreement found in other experiments on determining τ_ϕ (24). (The single-layer values of τ_ϕ found from our analysis of the UCF agree with theory to within a factor of 1.5.) Thus, the temperature dependence of the observed drag fluctuations strongly supports the validity of our explanation.

We have observed reproducible fluctuations of the Coulomb drag and demonstrated that they are an informative tool for studying wave properties of electrons in disordered materials, and the local properties in particular. Contrary to UCF, which originate from quantum interference, fluctuations of drag result from an interplay of the interference and e - e interactions. More theoretical and experimental work is required to study their manifestation in different situations. For instance, similarly to the previous extensive studies of the evolution of UCF with increasing magnetic field, such experiments can be performed on the fluctuations of

drag. One of the important developments in the field of Coulomb drag fluctuations can be their study in quantizing magnetic fields, including the regimes of integer and fractional quantum-Hall effects.

References and Notes

- M. B. Pogrebinskii, *Sov. Phys. Semicond.* **11**, 372 (1977).
- P. J. Price, *Physica* **117B**, 750 (1983).
- P. M. Solomon, P. J. Price, D. J. Frank, D. C. La Tulipe, *Phys. Rev. Lett.* **63**, 2508 (1989).
- T. J. Gramila, J. P. Eisenstein, A. H. MacDonald, L. N. Pfeiffer, K. W. West, *Phys. Rev. Lett.* **66**, 1216 (1991).
- U. Sivan, P. M. Solomon, H. Shtrikman, *Phys. Rev. Lett.* **68**, 1196 (1992).
- M. P. Lilly, J. P. Eisenstein, L. N. Pfeiffer, K. W. West, *Phys. Rev. Lett.* **80**, 1714 (1998).
- J. G. S. Lok et al., *Phys. Rev. B* **63**, 041305 (2001).
- A. G. Rojo, *J. Phys. Condens. Matter* **11**, R31 (1999).
- D. Snoke, *Science* **298**, 1368 (2002).
- R. Pillarisetty et al., *Phys. Rev. B* **71**, 115307 (2005).
- M. Yamamoto, M. Stopa, Y. Tokura, Y. Hirayama, S. Tarucha, *Science* **313**, 204 (2006).
- B. N. Narozhny, I. L. Aleiner, *Phys. Rev. Lett.* **84**, 5383 (2000).
- N. A. Mortensen, K. Flensberg, A.-P. Jauho, *Phys. Rev. B* **65**, 085317 (2002).
- I. V. Lerner, *Phys. Lett. A* **133**, 253 (1988).

- The details of the structures, measurements, and the model are available as supporting material on Science Online.
- M. Kellogg, J. P. Eisenstein, L. N. Pfeiffer, K. W. West, *Solid State Commun.* **123**, 515 (2002).
- B. L. Al'tshuler, P. A. Lee, R. A. Webb, Eds., *Mesoscopic Phenomena in Solids* (North-Holland, New York, 1991).
- A. Kamenev, Y. Oreg, *Phys. Rev. B* **52**, 7516 (1995).
- L. Zheng, A. H. MacDonald, *Phys. Rev. B* **48**, 8203 (1993).
- A.-P. Jauho, H. Smith, *Phys. Rev. B* **47**, 4420 (1993).
- K. Flensberg, B. Y.-K. Hu, A.-P. Jauho, J. M. Kinaret, *Phys. Rev. B* **52**, 14761 (1995).
- B. N. Narozhny, G. Zala, I. L. Aleiner, *Phys. Rev. B* **65**, 180202 (2002).
- B. L. Al'tshuler, A. G. Aronov, *Electron-Electron Interactions in Disordered Systems*, A. L. Efros, M. Pollak, Eds. (North-Holland, Amsterdam, 1985).
- C. W. J. Beenakker, H. van Houten, in *Solid State Physics*, H. Ehrenreich, D. Turnbull, Eds. (Academic Press, San Diego, 1991).
- We thank I. L. Aleiner, M. Entin, I. L. Lerner, A. Kamenev, and A. Stern for numerous helpful discussions.

Supporting Online Material

www.sciencemag.org/cgi/content/full/316/5821/99/DC1
Materials and Methods

SOM Text

Figs. S1 to S3

References

22 December 2006; accepted 6 March 2007

10.1126/science.1139227

Direct-Current Nanogenerator Driven by Ultrasonic Waves

Xudong Wang, Jinhui Song, Jin Liu, Zhong Lin Wang*

We have developed a nanowire nanogenerator that is driven by an ultrasonic wave to produce continuous direct-current output. The nanogenerator was fabricated with vertically aligned zinc oxide nanowire arrays that were placed beneath a zigzag metal electrode with a small gap. The wave drives the electrode up and down to bend and/or vibrate the nanowires. A piezoelectric-semiconducting coupling process converts mechanical energy into electricity. The zigzag electrode acts as an array of parallel integrated metal tips that simultaneously and continuously create, collect, and output electricity from all of the nanowires. The approach presents an adaptable, mobile, and cost-effective technology for harvesting energy from the environment, and it offers a potential solution for powering nanodevices and nanosystems.

The operation of nanodevices fabricated with one-dimensional nanostructures [such as nanowires, nanotubes, and nanobelts (1-8)] usually requires very low power (9-11), which is provided by an external source, such as a battery that may have to be replaced or recharged regularly. The reliance on an external power source may present a limitation for these systems. Various approaches have been developed for energy scavenging with applications in wireless electronics, such as thermoelectric, piezoelectric thin-film, and vibrational cantilevers (12). We have recently demonstrated an innovative approach for converting nanoscale

mechanical energy into electric energy by piezoelectric zinc oxide (ZnO) nanowire (NW) arrays (13). By deflecting the aligned NWs with a conductive atomic force microscopy (AFM) tip in contact mode, the mechanical energy created by the deflection force was converted into electricity with the use of the piezoelectric properties of the NWs. To improve the power generation capabilities of the system, it is necessary to replace the AFM tip with a simpler source of mechanical energy that can actuate all the NWs simultaneously and continuously. We solved these problems by using ultrasonic waves to drive the motion of the NWs, leading to the production of a continuous current.

The experimental setup is schematically shown in Fig. 1A. An array of aligned ZnO NWs was covered by a zigzag Si electrode coated with Pt. The Pt coating not only

enhanced the conductivity of the electrode, but also created a Schottky contact at the interface with ZnO. The NWs were grown on either GaN substrates (Fig. 1B) or sapphire substrates that were covered by a thin layer of ZnO film (14, 15), which served as a common electrode for directly connecting the NWs with an external circuit. The density of the NWs was $\sim 10/\mu\text{m}^2$, and the height and diameter were $\sim 1.0 \mu\text{m}$ and $\sim 40 \text{ nm}$, respectively. The top electrode was composed of parallel zigzag trenches fabricated on a (001) orientated Si wafer (16) and coated with a thin layer of Pt (200 nm in thickness) (Fig. 1C). The electrode was placed above the NW arrays and manipulated by a probe station under an optical microscope to achieve precise positioning; the spacing was controlled by soft-polymer stripes between the electrode and the NWs at the four sides. The resistance of the nanogenerator was monitored during the assembly process to ensure a reasonable contact between the NWs and the electrode by tuning the thickness of the polymer film. Then the assembled device was sealed at the edges to prevent the penetration of liquid. A cross-sectional image of the packaged NW arrays is shown in Fig. 1D; it displays a "lip/teeth" relationship between the NWs and the electrode. Some NWs are in direct contact with the top electrode, but some are located between the teeth of the electrode. The inclined NWs in the scanning electron microscopy (SEM) image were primarily caused by the cross sectioning of the packaged device. The packaged device was supported by a metal plate that was direct in contact with water contained in the cavity of an ultrasonic generator. The operation

School of Materials Science and Engineering, Georgia Institute of Technology, Atlanta, GA 30332-0245, USA

*To whom correspondence should be addressed. E-mail: zhong.wang@mse.gatech.edu

frequency of the ultrasonic wave was ~ 41 kHz. The output current and voltage were measured by an external circuit at room temperature.

The experimental design relies on a unique coupling between piezoelectric and semiconducting properties of the aligned ZnO NWs (13, 17, 18). The asymmetric piezoelectric potential across the width of a ZnO NW and the Schottky contact between the metal electrode and the NW are the two key processes for creating, separating, preserving, accumulating, and outputting the charges [see figure 3 in (13)]. A top electrode is designed to achieve the coupling process and to replace the role played by the AFM tip, and its zigzag trenches act as an array of aligned AFM tips (fig. S2 and Fig. 2A). When subject to the excitation of an ultrasonic wave, the zigzag electrode can move down and push the NW, which leads to lateral deflection of NW I. This, in turn, creates a strain field across the width of NW I, with the NW's outer surface being in tensile strain and its inner surface in compressive strain. The inversion of strain across the NW results in an inversion of piezoelectric field E_z along the NW (fig. S1), which produces a piezoelectric-potential inversion from V^- (negative) to V^+ (positive) across the NW (Fig. 2B). When the electrode makes contact with the stretched surface of the NW, which has a positive piezoelectric potential, the Pt metal–ZnO semiconductor interface is a reversely biased Schottky barrier, resulting in little current flowing across the interface. This is the process of creating, separating, preserving, and accumulating charges (13). With further pushing by the electrode, the bent NW I will reach the other side of the adjacent tooth of the zigzag electrode (Fig. 2C). In such a case, the electrode is also in contact with the compressed side of the NW, where the metal/semiconductor interface is a forward-biased Schottky barrier, resulting in a sudden increase in the output electric current flowing from the top electrode into the NW. This is the discharge process.

Figure 2, A to C, shows four possible configurations of contact between a NW and the zigzag electrode. Analogous to the situation described for NW I, the same processes apply to the charge output from NW II. NW III is chosen to elaborate on the vibration/resonance induced by an ultrasonic wave. When the compressive side of NW III is in contact with the electrode, the same discharge process as that for NW I occurs, resulting in the flow of current from the electrode into the NW (Fig. 2C). NW IV, which is short in height, is forced (without bending) into compressive strain by the electrode. In such a case, the piezoelectric voltage created at the top of the NW is negative [see figure 4 in (13)]. Thus, across the electrode–ZnO interface, a positively biased Schottky barrier is formed; hence, the electrons can flow freely across the interface. As a result, electrons flow from the grounded substrate electrode into the NW and then into the top zigzag electrode as the

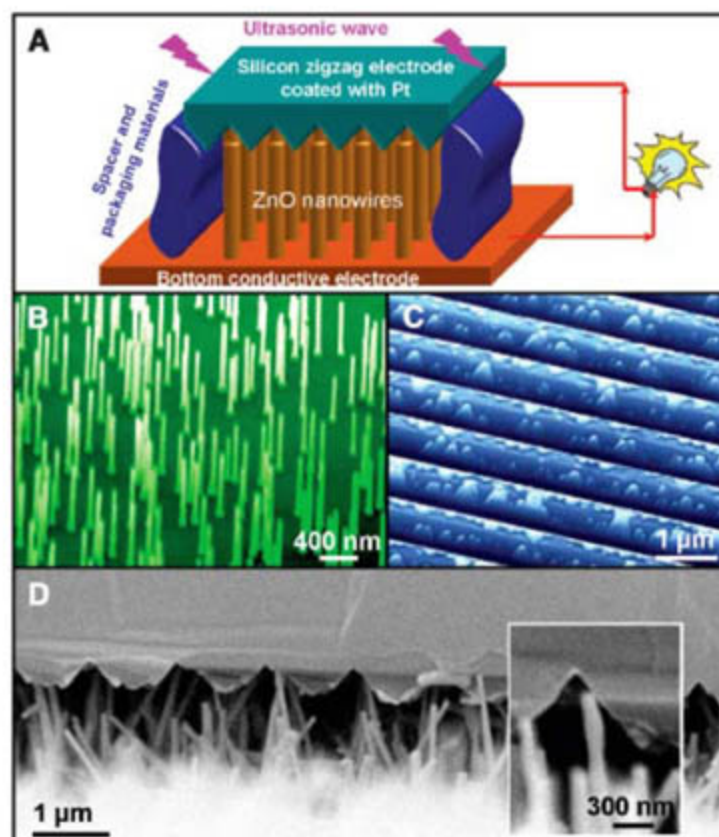
deformation occurs. This discharging process, if substantial, may also contribute to the measured current. In each of the four cases described in Fig. 2, A to C, all of the currents are added up in the same phase.

An equivalent electric circuit is shown in Fig. 2D to illustrate the measurements and outputs of the nanogenerator. The NWs producing current in the nanogenerator are equivalent to a voltage source V_s plus an inner resistance R_i that also contains the contact resistance between the active NWs and the electrode. On the other hand, there are a lot of NWs that are in contact with the electrode but cannot be bent or move freely; thus, they do not actively participate in the current generation, but they do provide a path for conducting current. These NWs are simply represented by a resistance R_w that is parallel to the portion that generates power. A resistance R_c is introduced to represent the contact resistance between the electrode and the external measurement circuit. The capacitance in the system is ignored in the circuit in order to simplify the discussion about dc measurement.

The current and voltage outputs of the nanogenerator are shown in Fig. 2, E and F, respectively, with the ultrasonic wave being turned on and off regularly. A jump of ~ 0.15 nA was observed when the ultrasonic wave was turned on, and the current immediately fell back to the baseline once the ultrasonic wave was turned off. Correspondingly, the voltage signal exhibited a similar on and off trend but with a negative output of ~ 0.7 mV. The negative sign

of the voltage is consistent with the mechanism presented in Fig. 2C. The signal-to-noise ratio of the current is substantially better than that of the output voltage for the following reasons: Because the resistance of the current meter (ideally, zero) plus R_c (20 to 30 ohms) was only $\sim 1/1000$ of R_w when the current was measured, the current generated by the nanogenerator can be safely assumed to be bypassing R_w ; the current path is indicated by a solid blue curve in Fig. 2D, so the measured current is $I_A \approx V_s/(R_c + R_i)$. However, because R_w was very much smaller than the inner resistance of a voltage meter (ideally, infinity) when the voltage was measured, a loop was formed between the power-generating portion of the system and R_w , as shown by a solid pink curve in Fig. 2D. In this case, the current is I_V and the measured voltage V is that across the power-generating portion, $V \approx -I_V R_w/(R_i + R_w)$. During the ultrasonic vibration, for the unstable contacts between the NWs and the electrodes, I_A is affected by the instability of V_s and R_i (but mainly by V_s because R_c is a constant), and V is affected by the instability of V_s , R_i , and R_w . As a result, V has about two times the noise level of I_A , consistent with the observations displayed in Fig. 2, E and F. On the other hand, because the voltages created by all of the NWs are in parallel, the output voltage is effectively the voltage created by one NW; thus, it appears relatively unstable and with a larger noise level than that of I_A (Fig. 2F). Furthermore, the output voltage is naturally smaller than that created by deflecting a NW by AFM, because it is limited

Fig. 1. Nanogenerators driven by an ultrasonic wave. (A) Schematic diagram showing the design and structure of the nanogenerator. Aligned ZnO NWs grown on a solid/polymer substrate are covered by a zigzag electrode. The substrate and the electrode are directly connected to an external load. (B) Aligned ZnO NWs grown on a GaN substrate. The gold catalyst particles used for the growth had been mostly vaporized; thus, the final NWs were purely ZnO with flat top ends. (C) Zigzag trenched electrode fabricated by the standard etching technique after being coated with 200 nm of Pt. The surface features are due to nonuniform etching. (D) Cross-sectional SEM image of the nanogenerator, which is composed of aligned NWs and the zigzag electrode. (Inset) A typical NW that is forced by the electrode to bend.



by the smaller degree of deflection amplitude of the NW, as induced by an ultrasonic wave in comparison to that induced by the AFM tip (13). Finally, the output current is a sum of the currents produced by many NWs. Therefore, the current signal is more stable and continuous, and it has been used to characterize the performance of the dc nanogenerator in this study. The resistance of the entire nanogenerator was also measured with and without turning on the ultrasonic wave (Fig. 2G). The resistance remained very stable at $R = 3.560 \pm 0.005$ kilohms. This measurement indicates that the jump in current could not be due to the variation in resistance, as caused by the vibration of the NWs (19), suggesting that the current signal presented in Fig. 2E was created by the nanogenerator.

The output electricity of the nanogenerator is continuous and reasonably stable. A continuous output current is generated when the ultrasonic wave is turned on, and the current disappears when the wave is turned off (Fig. 3A). The output current is in the nanoampere range. The current signal shows no direct coupling with the frequency of the ultrasonic wave, because the wave frequency is ~ 80 times smaller than the resonance frequency of the NWs (~ 3 MHz) (20). The size of the nanogenerator is ~ 2 mm² in effective substrate surface area. The number of NWs that were actively contributing to the observed output current is estimated to be 250 to 1000 in the current experimental design. The nanogenerator worked continuously for an extended period of time of beyond 1 hour (Fig. 3B).

The experimental design [as presented in (Fig. 1)] has been tested in comparison to the experiments conducted using different materials or configurations. Using the design shown in Fig. 1A, simply by replacing a ZnO NW array with an array of carbon nanotubes (CNTs), no jump in current was observed when the ultrasonic wave was turned on (Fig. 4A). This is because the CNTs are not piezoelectric. In a system with a ZnO NW array but in which the top electrode was replaced with a flat, thin Pt film that totally covered the tips of the NWs (Fig. 4B), no jump in output current was observed. This is because the design does not follow the mechanism of the nanogenerator (fig. S1) (13). A clear jump was observed only when the top electrode was in a zigzag shape and when ZnO NWs were present (Fig. 4C). These experiments may rule out possible contributions from electronic noise and/or measurement error or artifacts in producing the output current, and they consistently support the process proposed in Fig. 2, A to C, for piezoelectric NWs.

In comparison to our previous work (13), our current work has achieved three major objectives: (i) We have replaced the expensive and sophisticated AFM tip with ultrasonic waves/vibrations to induce the elastic deformation and vibration of the NWs, and we have demon-

strated a cost-effective prototype technology for fabricating the nanogenerator. (ii) We have integrated an array of tips into a zigzag electrode for the simultaneous creation, collection, and output of electricity generated by many NWs, establishing the principle for raising the output power. (iii) We have achieved a continuous and fairly stable dc output with this system. The principle demonstrated here has set a platform for harvesting energy from the environment to power in vivo biosensors, wireless and remote sensors, and nanorobots, and it has also established the basis for building zero-power force/pressure sensors.

The number of NWs that was effective for producing output electricity can be estimated

from the output power of the nanogenerator. From our previous study [see supporting online material for (13)], the NW deformed by AFM produced an electric energy of $\Delta E_{AFM} \sim 0.01$ fJ for each cycle of discharge, which lasted for 0.1 ms; thus, the power generated by one NW was $\Delta W_{AFM} \sim 0.1$ pW. In the current experimental design, the vibrational amplitude of the NW was much smaller than that of the NW directly deflected by an AFM tip; thus, the output voltage was ~ 1 mV, which is about 5 to 10 times smaller than that received when AFM was used as the deformation tool (13). In this case, the output power of a NW, as driven by ultrasonic wave, would be $\Delta W_{wave} = 1$ to 4 fW. The output-power volume density per NW is ~ 1 to

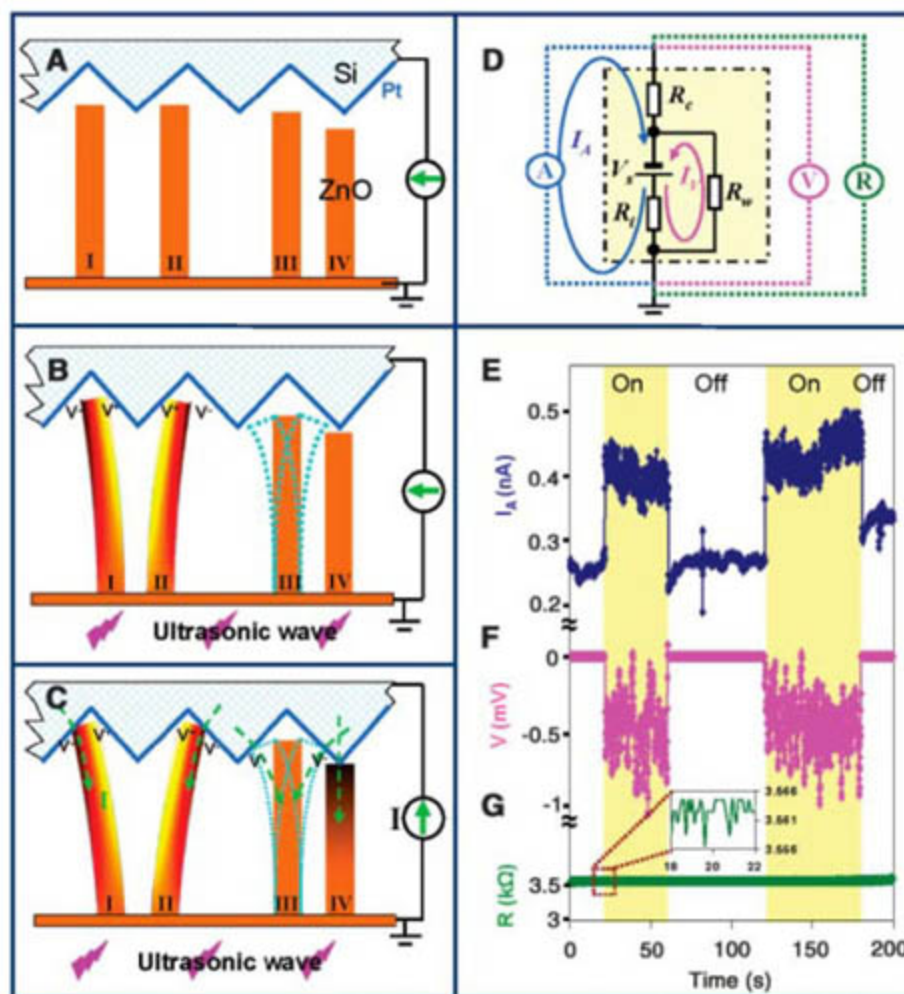


Fig. 2. The mechanism of the nanogenerator driven by an ultrasonic wave. (A) Schematic illustration of the zigzag electrode and the four types of NW configurations. (B) Piezoelectric potential created across NWs I and II under the push or deflection of the electrode, as driven by the ultrasonic wave, but without the flow of current because of the reversely biased Schottky barrier at the electrode/NW interface. NW III is in vibration under the stimulation of the ultrasonic wave. NW IV is in compressive strain without bending. (C) Once the NWs touch the surface of the adjacent teeth, the Schottky barrier at the electrode/NW interface becomes forward-biased, and piezoelectric discharge occurs, resulting in the observation of current flow in the external circuit. (D) Equivalent circuit of the nanogenerator and the setup for measuring the output current I , output voltage V , and resistance R . (E to G) I , V , and R measured with the connections shown in (D), respectively, when the ultrasonic wave was turned on and off purposely. The baseline of the current signal was produced by the electronic measurement system and the interference from the ultrasonic-wave source. Because the voltages created by all of the NWs are in parallel, the output voltage is effectively the voltage created by one NW; thus, it appears to be relatively unstable and with a larger noise level than that of I_A . A pixel averaging was applied for (F). The inset in (G) is an enlargement of the resistance before and after the wave was turned on.

4 W/cm^3 , which is more than two orders of magnitude higher than that produced by a vibrational microgenerator (21). The output power of the nanogenerator fabricated with a substrate of area $= 2 \text{ mm}^2$ is $W_{\text{wave}} = I_{\Delta} V \approx 1 \text{ pW}$ (Fig. 2, C and D). Therefore, the number of NWs that was active for producing electricity in Fig. 2E was $N = W_{\text{wave}}/\Delta W_{\text{wave}} \approx 250$ to 1000 NWs. As limited by the multiple contacts between the NWs and the electrode in the present design (Fig. 1D), the large majority of the NWs did not produce electricity because of their nonuniformity in height and distri-

bution on the substrate surface; thus, the output current was rather small in the present design. In addition, some of the NWs directly pushed the electrode at the top edges/apexes of the zigzag trenches, preventing the other NWs from reaching and contacting the electrode to produce electricity. These technical difficulties could be overcome by an optimized design to improve nanogenerator efficiency. For example, nanogenerator efficiency could be improved with the use of patterned-tip arrays as the electrode, the designed and patterned growth of high-quality uniform NW

arrays matching the design of the electrode (fig. S2), and an improved packaging technology to keep a precise control on the spacing and alignment between the electrode and the NW arrays. If the area taken by each metal tip is $0.5 \text{ by } 0.5 \mu\text{m}$ (fig. S2), the grown density of the NWs is $\sim 10^9/\text{cm}^2$. If one NW produces 10 fW of power by optimizing its size and shape, the output power per unit of area could be $10 \mu\text{W}/\text{cm}^2$. The power used to operate a device fabricated with one NW or nanotube is $\sim 10 \text{ nW}$ (9–11); thus, the nanogenerator built with the NWs grown on an area of 1 cm^2 could operate up to 1000 of such nanodevices, based on our current study. We anticipate that the performance will be improved by two to three orders of magnitude with improved design and optimization of the nanogenerator (22–23).

Fig. 3. Continuous dc output of the nanogenerator, as characterized by the current signal. (A) Reproducible and highly repeatable current output of the nanogenerator when the ultrasonic wave was turned on and off. (B) Continuous current output of the nanogenerator for an extended period of time. The data are displayed after they were corrected for the background introduced by electronic drift. The baseline of the current signal was produced by the electronic measurement system and the interference from the ultrasonic-wave source. The size of the nanogenerator is $\sim 2 \text{ mm}^2$ in effective substrate surface area.

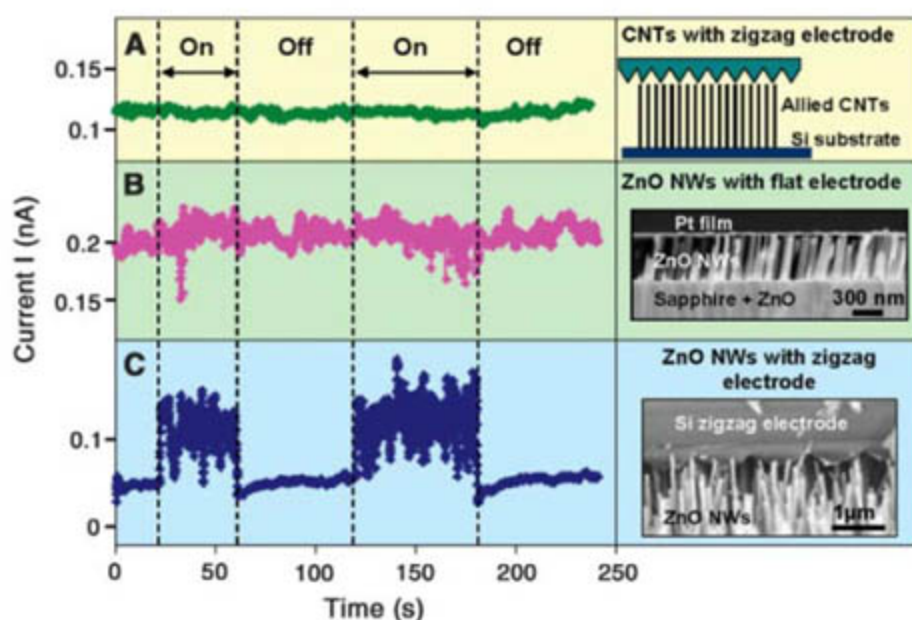
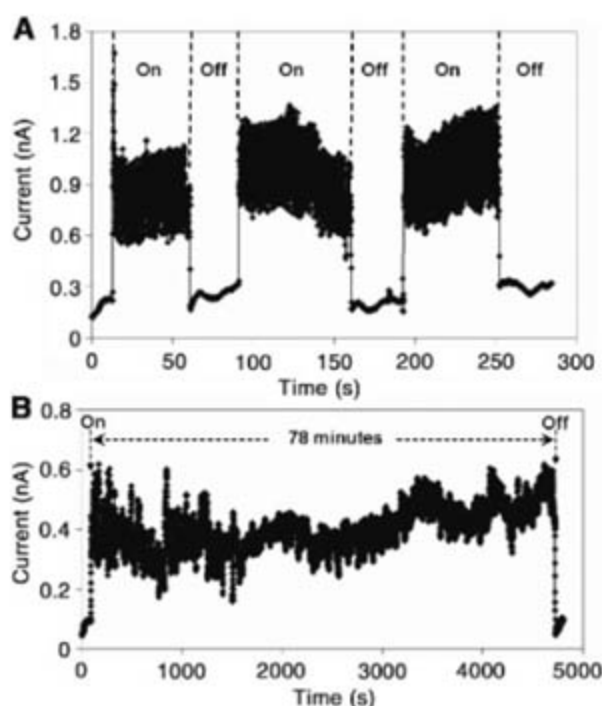


Fig. 4. Output of the nanogenerator with different materials and design configurations. The designs and true-device SEM images are shown on the right-hand side, and the corresponding current curve is on the left-hand side. (A) Nanogenerator based on arrays of CNTs with a zigzag top electrode, showing no jump in current when the ultrasonic wave was turned on. (B) Nanogenerator based on arrays of ZnO NWs but with a flat top electrode, showing no jump in current while stimulated by an ultrasonic wave. (C) Nanogenerator based on arrays of ZnO NWs with a zigzag top electrode, showing a large jump in current when the ultrasonic wave was turned on. The baseline in the current signal was produced by the measurement electronics.

References and Notes

1. F. Patolsky *et al.*, *Science* **313**, 1100 (2006).
2. Y. Li, F. Qian, J. Xiang, C. M. Lieber, *Mater. Today* **9**, 18 (2006).
3. F. Patolsky, C. M. Lieber, *Mater. Today* **8**, 20 (2005).
4. P. Pauzauskis, P. Yang, *Mater. Today* **9**, 36 (2006).
5. A. Javey, J. Guo, Q. Wang, M. Lundstrom, H. J. Dai, *Nature* **424**, 654 (2003).
6. J. W. R. Hsu *et al.*, *Nano Lett.* **5**, 83 (2005).
7. Z. R. Tian *et al.*, *Nat. Mater.* **2**, 821 (2003).
8. Z. W. Pan, Z. R. Dai, Z. L. Wang, *Science* **291**, 1947 (2001).
9. Y. Huang *et al.*, *Science* **294**, 1313 (2001).
10. A. Bachtold, P. Hadley, T. Nakanishi, C. Dekker, *Science* **294**, 1317 (2001).
11. J. Chen *et al.*, *Science* **310**, 1171 (2005).
12. J. A. Paradiso, T. Starner, *IEEE Pervasive Comput.* **4**, 18 (2005).
13. Z. L. Wang, J. Song, *Science* **312**, 242 (2006).
14. X. D. Wang *et al.*, *J. Am. Chem. Soc.* **127**, 7920 (2005).
15. X. D. Wang, C. J. Summers, Z. L. Wang, *Nano Lett.* **4**, 423 (2004).
16. J. Frühauf, S. Krönert, *Microsyst. Technol.* **11**, 1287 (2005).
17. J. H. Song, J. Zhou, J. Liu, Z. L. Wang, *Nano Lett.* **6**, 1656 (2006).
18. X. D. Wang *et al.*, *Nano Lett.* **6**, 2768 (2006).
19. Among the 200,000 NWs on the substrate surface, less than 0.5% were actively creating current. A large percentage of the NWs were serving as current paths between the top and bottom electrodes (Fig. 1D). The resistance introduced by the active NWs was less than 2% of the total resistance, when considering the NWs that were not in contact with the electrodes; thus, it could not produce the large jump in current as observed experimentally.
20. X. D. Bai, P. X. Gao, Z. L. Wang, E. G. Wang, *Appl. Phys. Lett.* **82**, 4806 (2003).
21. P. D. Mitcheson *et al.*, *J. Microelectromech. Syst.* **13**, 429 (2004).
22. P. X. Gao, J. H. Song, J. Liu, Z. L. Wang, *Adv. Mater.* **19**, 67 (2007).
23. Z. L. Wang, *MRS Bull.* **32**, 109 (2007).
24. We thank the Emory Georgia Tech Center of Cancer Nanotechnology Excellence funded by NIH, the Defense Advanced Research Projects Agency, and NSF (grant DMR 9733160) for support. We also thank C. M. Lieber and P. Gao for many stimulating discussions.

Supporting Online Material

www.sciencemag.org/cgi/content/full/316/5821/102/DC1
SOM Text
Figs. S1 and S2

28 December 2006; accepted 1 March 2007
10.1126/science.1139366

A Conserved Family of Enzymes That Phosphorylate Inositol Hexakisphosphate

Sashidhar Mulugu,^{1*} Wenli Bai,¹ Peter C. Fridy,¹ Robert J. Bastidas,¹ James C. Otto,¹ D. Eric Dollins,¹ Timothy A. Haystead,² Anthony A. Ribeiro,³ John D. York^{1†}

Inositol pyrophosphates are a diverse group of high-energy signaling molecules whose cellular roles remain an active area of study. We report a previously uncharacterized class of inositol pyrophosphate synthase and find it is identical to yeast Vip1 and Asp1 proteins, regulators of actin-related protein-2/3 (ARP 2/3) complexes. Vip1 and Asp1 acted as enzymes that encode inositol hexakisphosphate (IP₆) and inositol heptakisphosphate (IP₇) kinase activities. Alterations in kinase activity led to defects in cell growth, morphology, and interactions with ARP complex members. The functionality of Asp1 and Vip1 may provide cells with increased signaling capacity through metabolism of IP₆.

Activation of phosphoinositide-specific phospholipase C (PLC) generates an ensemble of intracellular inositol phosphate (IP) second messengers involved in diverse cellular processes (1–3). Among these is inositol 1,4,5-trisphosphate, which functions as a regulator of calcium release (4) and as a precursor to more highly phosphorylated IP molecules, including inositol tetrakis- (IP₄), pentakis- (IP₅), hexakis- (IP₆), and inositol pyrophosphates (PP-IPs) (5). The PP-IPs have more phosphates than IP₆ (6, 7) and were chemically identified as diphosphoryl inositol species (7, 8). Cloning of the inositol pyrophosphate synthase designated IP₆ kinase (IP6K in metazoans and Kcs1 in budding yeast) (9, 10) provided a molecular basis for the synthesis of PP-IP₅ (also known as IP₇ or InsP₇) through the coupled activities of PLC and inositol phosphate kinases (IPKs) (11–13). Loss of IP6K results in pleiotropic cellular defects including aberrant DNA recombination, vacuolar morphology, gene expression, chemotaxis, osmotic stress, protein phosphorylation, and telomere length (5, 14). Cells also have a second IP₆ kinase detected in *kes1* deficient cells whose molecular identity has yet to be reported (15, 16).

We used a biochemical approach to purify and clone the remaining IP₆ kinase activity. To reduce interference by contaminating IP₆ kinase and PP-IP pyrophosphatase activities, initial protein extracts were prepared from *kes1Δ ddp1Δ*-deficient cells and then fractionated on a series of ion-exchange chromatography columns (tables S1 and S2). IP₆ kinase activity was

enriched by a factor of more than 3000. Partially purified peak fractions were separated by SDS-polyacrylamide gel electrophoresis, and individual protein bands were excised and subjected to microsequence analysis. Numerous proteins were identified, so we obtained and purified individual candidate proteins from the tandem-affinity purification (TAP)-tagged yeast collection and tested each for kinase activity (17). Of the 40 proteins examined, only the purified TAP-tagged Vip1 protein showed IP₆ kinase activity (Fig. 1A). We inserted the entire coding sequence of Vip1 into a glutathione S-transferase (GST) expression plasmid and produced the protein in bacteria (which lack endogenous IP₆ kinase activity). Purified recombinant GST-Vip1 also had IP₆ kinase activity (Fig. 1A). These data indicate that Vip1 functions as an intrinsic inositol pyrophosphate synthase or IP₆ kinase.

The protein information annotation for Vip1 (*Saccharomyces Genome Database*), and its *Schizosaccharomyces pombe* ortholog Asp1 (18), identified two regions with relevance to inositol signaling enzymes (Fig. 1B): a “rimK” or adenosine triphosphate (ATP)-grasp superfamily domain SSF56059 (residues 200 to 525) and a histidine acid-phosphatase or phytase PF00328 domain (residues 530 to 1025). The ATP-grasp fold is present in certain inositol signaling kinases (19), and the acid-phosphatase fold is present in microbial and fungal phytase enzymes that hydrolyze IP₆ to release inorganic phosphate (P_i) and IPs (20). Sequence alignments of Vip1 or Asp1 genes revealed that orthologs having both amino- and carboxyl-terminal domains were present in all eukaryotic genomes from yeast to man (figs. S1 and S2). Thus, the Vip1 and Asp1 proteins define a distinct class of IP₆ kinase with a conserved dual-domain structure.

Our analyses indicated that the kinase domain of Vip1 might reside within the amino-terminal portion of the protein. Therefore we expressed a deletion mutant GST-Vip1^{1–535} (residues 1 to 535) and performed kinase reactions. GST-Vip1^{1–535} had IP₆ kinase activity that

equaled or exceeded that of full-length Vip1 (fig. S3A). With full-length or truncated Vip1 proteins, we observed that IP₆ kinase activity was pH dependent, with optimum activity occurring at pH 6.2 (fig. S3B). These data demonstrate that the ATP-grasp domain of Vip1 is sufficient to encode the IP₆ kinase activity.

To determine whether Vip1 functioned to produce IP₇ in cells, we analyzed IP production in yeast mutants. The predominant IPs observed in *kes1 ddp1* null cells (*kΔ dΔ*) are IP₆ and PP-IP₅ (Fig. 1C) (16). Deletion of Vip1 in this background (*vip1 kes1 ddp1* triple null, *kΔ dΔ vΔ*) resulted in the ablation of PP-IP₅ synthesis and increased the amount of IP₆ (Fig. 1C). Production of PP-IP₅ could be restored by introduction of a plasmid encoding the *VIP1* promoter and coding sequence (Fig. 1C). We also identified that Vip1 was required to synthesize PP-IP_{4β} in cells (fig. S3C). These observations are consistent with Vip1 functioning as a cellular inositol pyrophosphate synthase that phosphorylates both IP₆ and I(1,2,3,4,5)P₅ and indicate that Vip1 encodes activities previously designated as *Ids1* (16) and *Ips1* (15).

To identify catalytic residues in the kinase domain of Vip1, we used structure-based threading software [Protein Homology/analogy Recognition Engine (PHYRE) server, www.sbg.bio.ic.ac.uk/phyre]. Within the ATP-grasp domain, we identified aspartate 487 as a putative active-site catalytic residue (fig. S1B) and, indeed, substitution with alanine (Vip1^{D487A}) rendered the mutant kinase defective in vivo (Fig. 1C) and in vitro. Similar analysis of the acid-phosphatase domain identified histidine 548 and 993 as invariant residues (fig. S2B). Substitution of H548 in Vip1 with alanine (Vip1^{H548A}) did not appear to alter IP₆ kinase activity in vitro (fig. S3A). Reintroduction of Vip1^{H548A} into *kes1 ddp1 vip1* mutant yeast cells restored PP-IP₅ and IP₆ levels to those observed in *kes1 ddp1* mutant cells (Fig. 1C). These data identify a key catalytic residue for kinase activity and are consistent with Vip1 functioning as a regulator of IP₆ and PP-IP₅ levels in cells.

To determine the molecular structure of the Vip1 kinase reaction product, samples were subjected to nuclear magnetic resonance (NMR) analysis. Comparison of proton-decoupled phosphorus NMR spectra of high-performance liquid chromatography (HPLC)-purified IP₆ standard (Fig. 2A) or PP-IP₅ Vip1 product (Fig. 2B) revealed the appearance of five singlet peaks of monophosphates and two upfield phosphorus-phosphorus-coupled doublets corresponding to the β- and α-phosphates of a pyrophosphate moiety. The spectrum observed for the Vip1 PP-IP₅ product is nearly identical to the reported spectrum for 4-PP-I(1,2,3,5,6)P₅ or its enantiomer 6-PP-I(1,2,3,4,5)P₅ purified from *Dictyostelium* (21). Two-dimensional ¹H-³¹P-NMR correlation analysis was reported, allowing for unequivocal assignment of the pyrophosphate (21). We performed NMR analysis on the PP-IP₅ product of

¹Howard Hughes Medical Institute, Department of Pharmacology and Cancer Biology, Duke University Medical Center, DUMC 3813, Durham, NC 27710, USA. ²Department of Pharmacology and Cancer Biology, Duke University Medical Center, Durham, NC 27710, USA. ³Department of Biochemistry, NMR Center, Duke University Medical Center, Durham, NC 27710, USA.

*Present address: Bharathidasan University, Tiruchirappalli, 620 024, India.

†To whom correspondence should be addressed. E-mail: yorkj@duke.edu

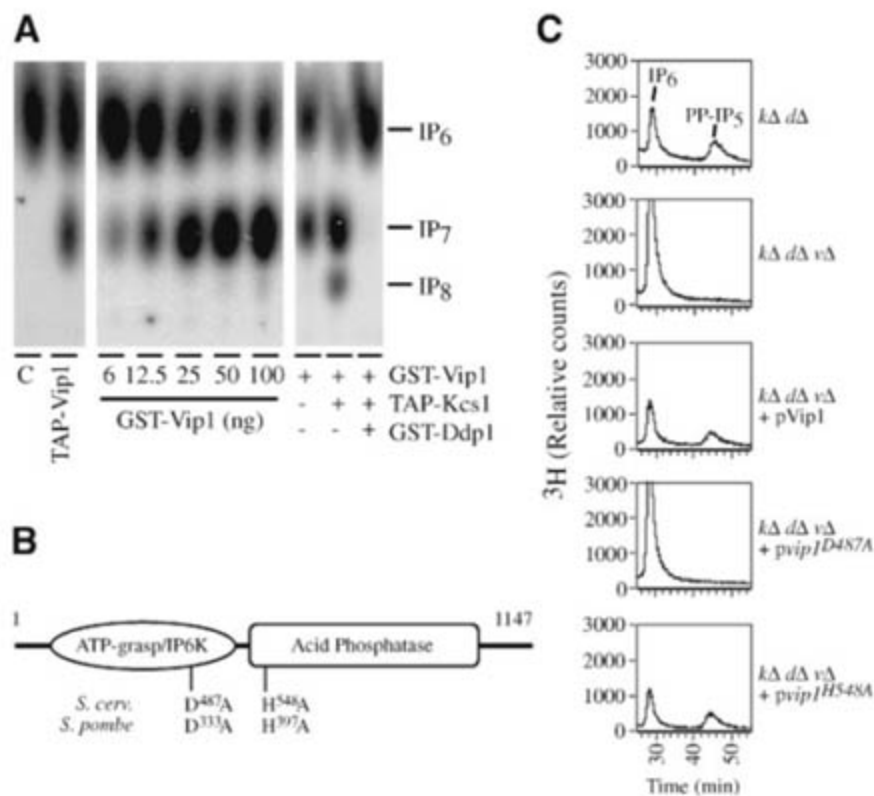


Fig. 1. Characterization of inositol hexakisphosphate IP₆ kinase enzyme, Vip1. **(A)** IP₆ kinase activity of purified yeast TAP-Vip1 and the production of IP₇ (left). Dose-dependent (ng of protein added) activity of recombinant GST-Vip1 (middle) and sensitivity of IP₇ and IP₈ products of TAP-Kcs1 and GST-Vip1 to the diphospho-inositol phosphatase GST-Ddp1 (right). **(B)** Schematic of the dual-domain structure of Vip1 and Asp1. Evolutionarily conserved residues from the ATP-grasp (IP6K) and putative acid phosphatase domains from either budding or fission yeast proteins are shown. **(C)** Function of Vip1 to regulate PP-IP₅ and IP₆ levels in cells. Loss of *vip1* in *kcs1 ddp1*-null yeast ablated PP-IP₅ production and increased IP₆ by a factor of 2, as monitored by HPLC analysis of ³H-inositol-labeled mutant yeast strains (10 mM AP increased linearly to 1.7 M AP over 12 min, followed by an isocratic flow at 1.7 M AP for 48 min) and in-line radioactivity detection. Synthesis of PP-IP₅ was restored in cells expressing either GFP-tagged full-length Vip1 (*kΔ dΔ vΔ* + pVip1) or kinase-only (*kΔ dΔ vΔ* + pvip1^{H548A}), but not kinase-deficient protein (*kΔ dΔ vΔ* + pvip1^{D487A}).

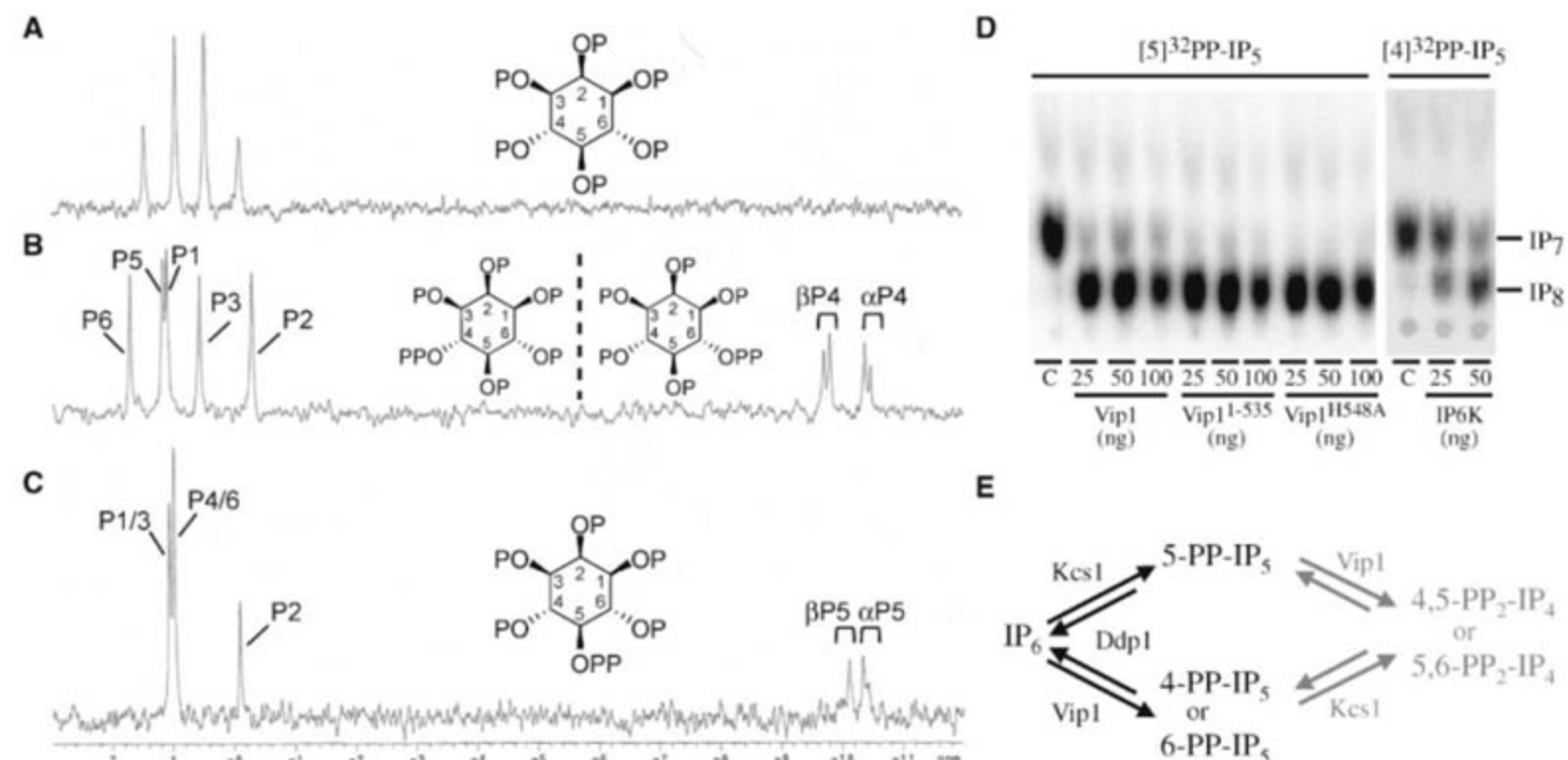


Fig. 2. Identification of Vip1 PP-IP₅ product by ³¹P NMR analysis and inositol heptakisphosphate kinase activity. Proton-decoupled phosphorus NMR spectrum of 2 mg of purified **(A)** IP₆ standard, **(B)** Vip1 product PP-IP₅, or **(C)** human IP6K1 PP-IP₅ product. All analyses were performed on HPLC-purified samples at pH 5.8. Structures of relevant IP₆ and IP₇ species are shown: 4-PP-I(1,2,3,5,6)P₅ and 6-PP-I(1,2,3,4,5)P₅ are non-superimposable mirror images (enantiomers). Resonances have been assigned based on similarity to previous reports (21, 23). P, phosphate; PP, pyrophosphate. **(D)** Characterization of Vip1 and human IP6K IP₇ kinase activity. Purified recombinant GST-Vip1 fusion proteins (ng of protein added are shown) were incubated with radiolabeled ³²PP-IPs, ATP at pH 6.2, and reactants were visualized after separation by polyethyleneimine cellulose-thin-layer chromatography (left). All three

kinase active forms of Vip1 showed robust activity and were able to convert 5-PP-I(1,2,3,4,6)P₅ to 4,5-PP₂-IP₄ (IP₈) at neutral pH. Recombinant human GST IP6K fusion protein was also examined and was found to phosphorylate 4-PP-IP₅ to 4,5-PP₂-IP₄ (right). For simplicity, we have assigned the product of the Vip1 reactions to be the D-4 species. Given our analysis, we cannot exclude that these may also be the enantiomer species harboring a D-6 pyrophosphate. **(E)** Schematic diagram of IP₆ metabolism pathway in *Saccharomyces cerevisiae* and production of IP₇ and IP₈ through the actions of Vip1 and Kcs1. Kcs1 functions as a D-5 kinase that may phosphorylate IP₆ and 4-PP-IP₅ substrates. Vip1 functions as an IP₆ kinase to generate 4- or 6-PP-IP₅ and phosphorylates the IP₇ product of Kcs1 to form IP₈. Ddp1 is an inositol pyrophosphate phosphatase that dephosphorylates IP₇ or IP₈ to IP₆.

human IP6K, which is reported to have a similar activity to that of Kcs1 (14, 16, 22). The spectrum of IP₇ produced from an HPLC-purified IP6K reaction was distinct from Vip1 product (Fig. 2C). Tentative assignment was again made based on this spectrum's appearing to be similar to that reported for 5-PP-I(1,2,3,4,6)P₅ (23). Overall, our NMR analysis confirms that the IP₇ produced by Vip1 is structurally distinct from that produced by the IP6K class of proteins, and that Vip1 appears to harbor D-4 or D-6 kinase activity, or both (fig. S3A).

Given the specificities of the Vip1 and IP6K (Kcs1) kinases, we sought to examine their roles as IP₇ kinases capable of generating IP₈ (PP₂-IP₄), which has been reported in various eukaryotic cells (7, 8, 21, 24, 25). In IP₆ kinase reactions with both GST-Vip1 and purified TAP-Kcs1, we observed the formation of IP₇ and IP₈, which were hydrolyzed to IP₆ in the presence of the inositol pyrophosphatase Ddp1 (Fig. 1A). Incubation of 5-PP-IP₅ along with ATP and recombinant GST-Vip1, GST-Vip1¹⁻⁵³⁵, or GST-Vip1^{H548A} protein, resulted in the production of PP₂-IP₄, consistent with Vip1 functioning as a 5-PP-IP₅ kinase capable of generating

4,5-PP₂-I(1,2,3,6)P₄ or 5,6-PP₂-I(1,2,3,4)P₄, or both (Fig. 2D). Similarly, when we incubated radiolabeled 4-PP-IP₅ or 6-PP-IP₅, ATP and recombinant human GST-IP6K, we observed conversion to PP₂-IP₄ product (Fig. 2D). These data indicate that Vip1 and IP6K (Kcs1) are the enzymes required for the synthesis of IP₈ or PP₂-IP₄ from IP₆ (Fig. 2E).

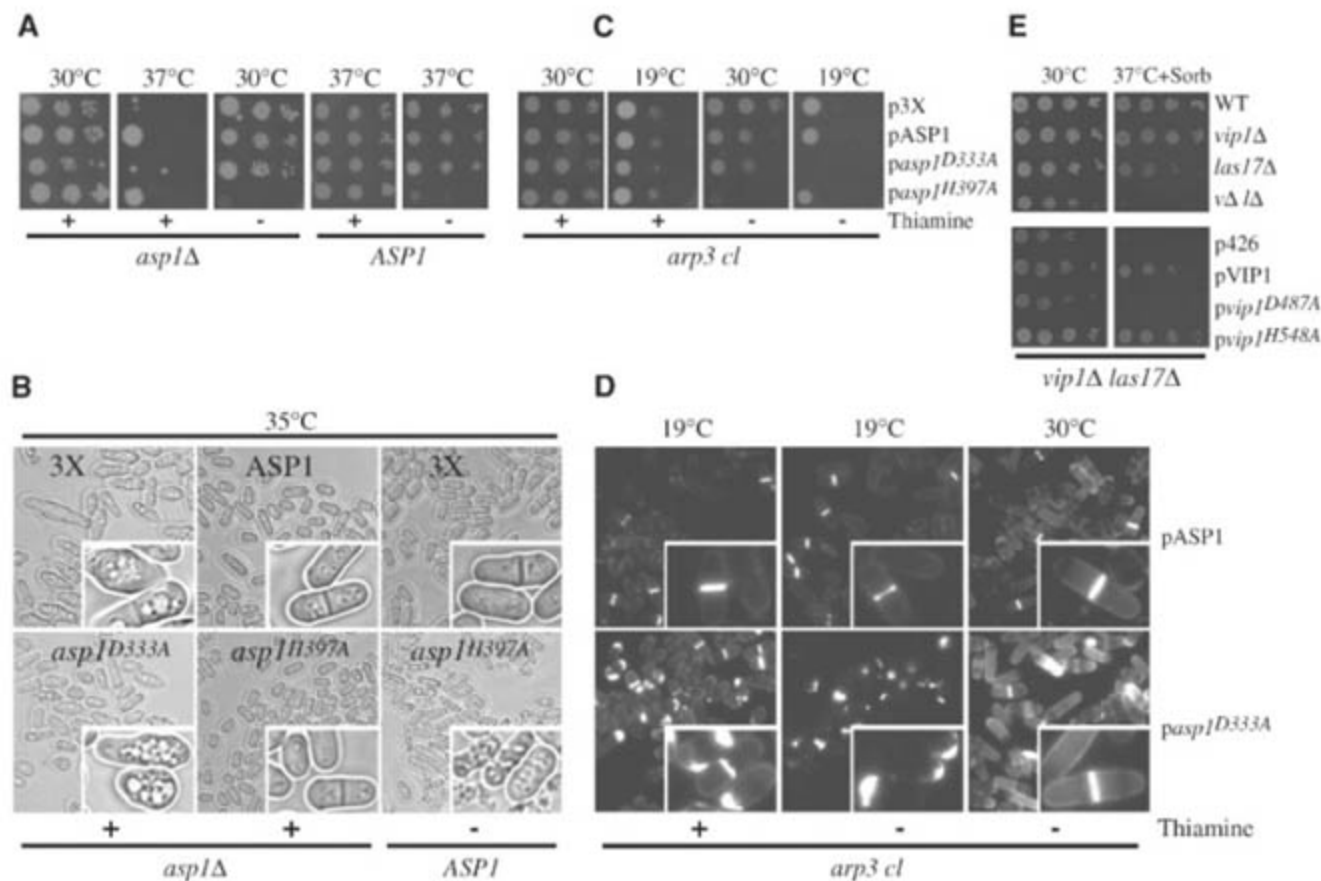
Clues into possible functional roles for the IP₆ kinase activity of Vip1 came from studies of the *S. pombe* ortholog, Asp1, which may participate in actin cytoskeleton and cellular morphology through the regulation of actin-related protein (Arp) complexes (18). Arp2/3 multiprotein complexes are involved in cellular signaling-dependent control of nucleation of branched-actin-filament networks required for regulating cell motility and endocytosis (26, 27). Activation of Arp2/3 requires additional nucleation-promoting factors such as Wiskott-Aldrich syndrome protein (WASP) (28, 29).

We therefore examined whether these phenotypes depended on IP₆ kinase activity. Wild-type and *asp1* null strains were transformed with thiamine-regulated (*nmt1* promoter) GFP-tagged expression plasmids encoding empty vector con-

trol (p3X), full-length protein (pASP1), or proteins with mutations in the kinase (*paspl*^{D333A}) or putative acid-phosphatase (*paspl*^{H397A}) domains. The temperature-sensitive growth and morphological defects exhibited by *asp1* null cells were rescued by low-level expression (medium with thiamine) of either pASP1 or *paspl*^{H397A}, consistent with a role for IP₆ kinase in mediating these phenotypes (Fig. 3, A and B). When these strains were induced to high-level expression (medium lacking thiamine), the kinase-only protein, *paspl*^{H397A}, prevented cell growth at both normal and high temperatures (Fig. 3, A and B). Cells overexpressing kinase-only protein underwent rapid lysis when analyzed by light microscopy (Fig. 3B). These data indicate that loss of IP₆ kinase activity accounts for *asp1* temperature sensitivity and morphological defects and that too much IP₆ kinase is cytotoxic.

To probe whether ARP complex function was required for the observed effects, we examined the expression of wild-type or mutant ASP1 proteins in a cold-sensitive mutant Arp3 strain (*arp3 cl*). The toxicity induced by overexpression of IP₆ kinase-only activity (*paspl*^{H397A}) was dependent on a functional Arp3 protein, as

Fig. 3. A role for IP₆ kinase activity in regulating cell morphology, growth, and ARP complex function. **(A)** Asp1 IP₆ kinase activity regulates cell growth of fission yeast. Loss of IP₆ kinase inhibited growth at increased temperatures (left two panels). Overproduction of Asp1 IP₆ kinase-only (*paspl*^{H397A}) protein (without thiamine) was toxic to cell growth at normal and elevated temperatures (middle and right two panels). Appropriate strains were serially diluted, spotted onto solid medium, and grown at the indicated temperature. **(B)** IP₆ kinase activity regulates cell morphology, vacuole biogenesis, and cell lysis. Cells lacking Asp1 kinase activity (*asp1* Δ + 3X or *asp1* Δ + *asp*^{D333A}) had rounded, vacuolated, and irregular cell morphology as compared with kinase-competent cells (*asp1* Δ + ASP1, *asp1* Δ + *asp*^{H397A}). Overproduction of IP₆ kinase-only protein (without thiamine) resulted in the inhibition of cell growth and promoted cellular lysis (ASP1 + *paspl*^{H397A}). (Insets) Zoomed images. **(C)** Toxicity induced by IP₆ kinase-only overexpression and suppression by loss of *arp3*. Cells overproducing *asp1*^{H397A} fail to grow at 30°C (Arp3⁺); however, they were able to grow when shifted to a cold temperature (*arp3*⁻). In contrast, when *arp3* function is lost (19°C), cells overexpressing Asp1 IP₆ kinase-dead protein (*paspl*^{D333A}) were unable to grow, and this defect is rescued by restoring Arp3 function (30°C). **(D)**



Expression of Asp1 IP₆ kinase-dead protein (*paspl*^{D333A}) results in Arp3-dependent defects in cell-wall deposition, as shown by microscopic analysis of cells stained by calcofluor white. Staining of cells overexpressing full-length Asp1 show normal cell wall synthesis regardless of Arp3 function. **(E)** Requirement of Vip1 IP₆ kinase activity for genetic interactions with ARP complex member, Las17. A temperature-induced growth defect was observed upon loss of both Vip1 and Las17 (*vΔΔ*, top), the WASP component of the ARP complex. This synthetic growth defect was rescued in the *vip1 las17* double-mutant strain by restoring Vip1 IP₆ kinase activity (bottom).

judged by growth at 19°C (*arp3⁻*) versus death at 30°C (*Arp3⁺*) (Fig. 3C). Furthermore, when *Arp3* function was lost, the overexpression of kinase-deficient *Asp1* was now lethal, as determined by a failure of *pas1^{D333A}*-transformed cells to grow under induced conditions at 19°C (Fig. 3C). Analysis of these cells using the cell-wall stain calcofluor white (CFW) revealed that overproduction of kinase-deficient *Asp1* resulted in aberrant appearance of cell-wall material at the growing ends rather than at the septum midline (Fig. 3D). We also examined interactions between *Vip1* and *Las17* (the yeast WASP protein) in budding yeast cell growth. Deletion of *vip1* alone did not cause temperature sensitivity; however, when combined with a loss in *las17*, the double mutant was growth-compromised at high temperatures (Fig. 3E). The temperature-sensitive growth was rescued by restoring *Vip1* IP₆ kinase activity (Fig. 3E). Overall, our functional analyses indicate that IP₆ kinase activity of *Asp1* and *Vip1* is required for maintaining cellular integrity, temperature-dependent growth, rod-shape morphology, and genetic interactions with ARP complex components.

We identified *Vip1* and *Asp1* as members of a class of IP₆ kinase that is responsible for producing signaling molecules 4-PP-IP₅ or 6-PP-IP₅, or both, that regulate cell function and yeast phosphate-responsive signaling (30). We show that the *Vip1* and *Kcs1* (IP6K) kinases generate distinct inositol pyrophosphate products and that both can function as IP₇ kinases, together capable of converting IP₆ to IP₈ (PP₂-IP₄). The

dual-domain structure of the *Vip1* class of enzymes is evolutionarily conserved, raising the possibility that there may be interplay between these two regions of the proteins to control intracellular signaling pathways.

References and Notes

- R. F. Irvine, M. J. Schell, *Nat. Rev. Mol. Cell Biol.* **2**, 327 (2001).
- P. W. Majerus, *Annu. Rev. Biochem.* **61**, 225 (1992).
- S. B. Shears, *Biochim. Biophys. Acta* **1436**, 49 (1998).
- M. J. Berridge, R. F. Irvine, *Nature* **341**, 197 (1989).
- J. D. York, *Biochim. Biophys. Acta Mol. Cell Biol. Lipids* **1761**, 552 (2006).
- G. N. Europe-Finner, B. Gammon, P. C. Newell, *Biochem. Biophys. Res. Commun.* **181**, 191 (1991).
- F. S. Menniti, R. N. Miller, J. W. Putney Jr., S. B. Shears, *J. Biol. Chem.* **268**, 3850 (1993).
- L. Stephens et al., *J. Biol. Chem.* **268**, 4009 (1993).
- A. Saiardi, H. Erdjument-Bromage, A. M. Snowman, P. Tempst, S. H. Snyder, *Curr. Biol.* **9**, 1323 (1999).
- A. Saiardi, R. Bhandari, A. C. Resnick, A. M. Snowman, S. H. Snyder, *Science* **306**, 2101 (2004).
- A. R. Odom, A. Stahlberg, S. R. Wente, J. D. York, *Science* **287**, 2026 (2000).
- A. Saiardi, J. J. Caffrey, S. H. Snyder, S. B. Shears, *FEBS Lett.* **468**, 28 (2000).
- J. D. York, A. R. Odom, R. Murphy, E. B. Ives, S. R. Wente, *Science* **285**, 96 (1999).
- M. Bennett, S. M. Onnebo, C. Azevedo, A. Saiardi, *Cell. Mol. Life Sci.* **63**, 552 (2006).
- A. M. Seeds, R. J. Bastidas, J. D. York, *J. Biol. Chem.* **280**, 27654 (2005).
- S. J. York, B. N. Armbruster, P. Greenwell, T. D. Petes, J. D. York, *J. Biol. Chem.* **280**, 4264 (2005).
- S. Ghaemmaghami et al., *Nature* **425**, 737 (2003).
- A. Feoktistova, D. McCollum, R. Ohi, K. L. Gould, *Genetics* **152**, 895 (1999).
- N. V. Grishin, *J. Mol. Biol.* **291**, 239 (1999).

- E. J. Mullaney, A. H. Ullah, *Biochem. Biophys. Res. Commun.* **312**, 179 (2003).
- T. Laussmann, R. Eujen, C. M. Weisshuhn, U. Thiel, G. Vogel, *Biochem. J.* **315**, 715 (1996).
- A. Saiardi, C. Sciambi, J. M. McCaffery, B. Wendland, S. H. Snyder, *Proc. Natl. Acad. Sci. U.S.A.* **99**, 14206 (2002).
- T. Laussmann et al., *FEBS Lett.* **426**, 145 (1998).
- M. C. Glennon, S. B. Shears, *Biochem. J.* **293**, 583 (1993).
- S. B. Shears, N. Ali, A. Craxton, M. E. Bembenek, *J. Biol. Chem.* **270**, 10489 (1995).
- E. D. Goley, M. D. Welch, *Nat. Rev. Mol. Cell Biol.* **7**, 713 (2006).
- T. D. Pollard, G. G. Borisy, *Cell* **112**, 453 (2003).
- H. N. Higgs, T. D. Pollard, *J. Cell Biol.* **150**, 1311 (2000).
- R. Rohatgi et al., *Cell* **97**, 221 (1999).
- Y.-S. Lee, S. Mulugu, J. D. York, E. K. O'Shea, *Science* **316**, 109 (2007).
- We thank members of the York laboratory for helpful discussions; J. Rudolph for assistance with kinetic analysis; K. Gould (Vanderbilt University) for published strains; M. Tsieh (Cell Signals, OH) for IP standards for NMR; and E. O'Shea and Y.-S. Lee (Harvard University) for sharing unpublished data, helpful discussions, and comments on the manuscript. This work was supported by funds from the Howard Hughes Medical Institute (J.D.Y.), and from NIH grants R01-HL-55672 (J.D.Y.), R33-DK-070272 (J.D.Y.), 2-P30-CA14236-3 (T.A.H.), and NCI P30-CA-14236 (A.A.R.). Instrumentation in Duke NMR Center was funded by NSF, NIH, the North Carolina Biotechnology Center, and Duke University. The authors have no conflicting financial interests.

Supporting Online Material

www.sciencemag.org/cgi/content/full/316/5821/106/DC1
Materials and Methods
Figs. S1 to S3
Tables S1 and S2
References

20 December 2006; accepted 5 March 2007
10.1126/science.1139099

Regulation of a Cyclin-CDK-CDK Inhibitor Complex by Inositol Pyrophosphates

Young-Sam Lee,¹ Sashidhar Mulugu,² John D. York,² Erin K. O'Shea^{1*}

In budding yeast, phosphate starvation triggers inhibition of the Pho80-Pho85 cyclin-cyclin-dependent kinase (CDK) complex by the CDK inhibitor Pho81, leading to expression of genes involved in nutrient homeostasis. We isolated *myo*-D-inositol heptakisphosphate (IP₇) as a cellular component that stimulates Pho81-dependent inhibition of Pho80-Pho85. IP₇ is necessary for Pho81-dependent inhibition of Pho80-Pho85 in vitro. Moreover, intracellular concentrations of IP₇ increased upon phosphate starvation, and yeast mutants defective in IP₇ production failed to inhibit Pho80-Pho85 in response to phosphate starvation. These observations reveal regulation of a cyclin-CDK complex by a metabolite and suggest that a complex metabolite network mediates signaling of phosphate availability.

In response to nutrient limitation, cells increase transcription of starvation response genes. Many proteins that function in nutrient response systems have been identified, but the molecular details of their regulation are not well understood (1). The *Saccharomyces cerevisiae* Pho80-Pho85 cyclin-CDK complex is a key regulator in the phosphate (*P_i*)-responsive (PHO) signaling pathway (2, 3). When cells are

grown in medium that is rich in *P_i*, Pho80-Pho85 is active and phosphorylates the transcription factor Pho4 (4), resulting in its export from the nucleus (5). Upon *P_i* starvation, Pho80-Pho85 kinase activity is decreased, leading to nuclear accumulation of Pho4 and transcription of PHO genes. In vivo, the Pho81 CDK inhibitor (CKI) is bound to Pho80-Pho85 regardless of *P_i* conditions and is required for the inhibition

of Pho80-Pho85 activity in response to *P_i*-limitation (6).

We used a biochemical strategy to identify cellular components that influence Pho80-Pho85-Pho81 activity. The Pho80-Pho85-Pho81 complex immunopurified from cells grown in *P_i*-rich conditions actively phosphorylated Pho4 in vitro, whereas the complex isolated from *P_i*-starved cells was less active (6) (Fig. 1A). To identify regulators of Pho80-Pho85-Pho81, we added extracts from cells grown in *P_i*-rich and *P_i*-starved conditions to active (from *P_i*-rich) and inactive (from *P_i*-starved) immunopurified Pho80-Pho85-Pho81 complexes and performed kinase assays with recombinant Pho4 serving as the substrate. Extracts from *P_i*-starved cells efficiently inactivated Pho80-Pho85-Pho81, whereas the *P_i*-rich cell extract had little effect (Fig. 1B). When the extract of *P_i*-starved cells was fractionated into fractions of large (>3 kD) and

¹Howard Hughes Medical Institute, Faculty of Arts and Sciences Center for Systems Biology, Department of Molecular and Cellular Biology, Harvard University, 7 Divinity Avenue, Cambridge, MA 02138, USA. ²Howard Hughes Medical Institute, Department of Pharmacology and Cancer Biology, Duke University Medical Center, Durham, NC 27710, USA.

*To whom correspondence should be addressed. E-mail: erin_oshea@harvard.edu

small (<3 kD) molecular size, most inhibitory activity was found in the fractions of small molecular size. This activity had little effect on Pho80-Pho85 purified from *pho81Δ* cells (Fig. 1C), indicating that, as is true in vivo (6), the inhibitory activity requires Pho81 for its function.

To determine the identity of the inhibitory activity, we enriched it through several fractionation steps and characterized its properties (fig. S1) (7). The low-molecular weight inhibitor contained acid-labile P_i (8), and characterization by nuclear magnetic resonance and mass spectrometry suggested that it was inositol heptakisphosphate (9), also known as diphospho-*myo*-D-inositol pentakisphosphate, PP-InsP₅, PP-IP₅, InsP₇, or IP₇ (Fig. 1D).

Inositol polyphosphates are signaling molecules found in all eukaryotic cells. They are produced through the action of a conserved set of inositol polyphosphate kinases from inositol 1,4,5-trisphosphate (IP₃) (9). IP₃, which regulates Ca^{2+} release from the endoplasmic reticulum (10), can be sequentially phosphorylated to generate IP₄, IP₅, inositol hexakisphosphate (IP₆), and inositol pyrophosphates such as IP₇. Loss-of-function studies have implicated IP₇ in recombination (11), vacuole function (12), gene expression, endo- and exocytosis (13, 14), osmotic stress (12), and telomere length control (15, 16), but it is unclear whether IP₇ directly regulates these processes. One well-characterized role for IP₇ is the regulation of chemotaxis in *Dictyostelium*, in which intracellular concentrations of IP₇ increase upon chemoattractant addition and IP₇ competes with phosphatidylinositol 3,4,5-trisphosphate (PIP₃) to bind to proteins containing a pleckstrin homology domain (17).

To test whether the inhibitory activity was IP₇, we synthesized IP₇ by a nonenzymatic

method (8) and tested its effect on the Pho80-Pho85 complex. When the Pho80-Pho85-Pho81 complex that had been immunopurified from P_i -rich cells was treated with synthetic IP₇, kinase activity was inhibited with an apparent median inhibitory concentration (IC₅₀) of ~50 μM (Fig. 2A). IP₇ had little or no effect on the kinase purified from *pho81Δ* cells, suggesting that IP₇-mediated inactivation of Pho80-Pho85 requires Pho81. Inactivation of Pho80-Pho85-Pho81 by IP₇ appears to be specific, given that inositol and several inositol derivatives did not affect kinase activity (Fig. 2B).

We next tested whether IP₇-mediated inactivation of Pho80-Pho85-Pho81 is direct or whether it requires other factors from yeast. Neither synthetic IP₇ nor the activity from P_i -starved cell extract could inactivate recombinant Pho80-Pho85 purified from *Escherichia coli* (Fig. 2C). Similarly, addition of recombinant Pho81 minimum domain (Pho81-MD) (18), a fragment that functionally substitutes for full-length Pho81 in vivo, did not cause inhibition of recombinant Pho80-Pho85 in vitro, even in two- to threefold molar excess (Fig. 2C). Because Pho81-MD binds to Pho80-Pho85 (apparent dissociation constant K_d ~ 170 nM, fig. S2), we concluded that neither Pho81-MD nor IP₇ is sufficient for the inactivation of Pho80-Pho85. However, when both IP₇ and Pho81-MD were added, Pho80-Pho85-Pho81-MD was inactivated (Fig. 2C). Therefore, IP₇ directly inactivates Pho80-Pho85-Pho81 and this inactivation requires Pho81.

To test whether the cellular concentration of IP₇ increases when cells are starved of P_i , we monitored inositol polyphosphate levels in cells labeled with [³H]-inositol and grown in P_i -rich or P_i -limiting conditions (12). In P_i -rich conditions, the IP₇ concentration was approxi-

mately 3% or less of the IP₆ concentration (Fig. 3) (12). However, upon P_i limitation, IP₇ levels increased to more than 20% of the levels of IP₆ (Fig. 3). This increase in abundance of IP₇ is not due to Pho4-dependent transcriptional activation (fig. S3) (7), and the time course and dependence of the IP₇ increase on extracellular P_i are comparable to those observed for PHO pathway regulation (fig. S3). Assuming that the IP₆ concentration is ~100 μM in cells (9) and that the IP₆ concentration does not change in response to P_i limitation, the concentration of IP₇ may reach ~30 μM during P_i limitation (fig. S3), a value similar to the apparent IC₅₀ measured in vitro (Fig. 2).

Many gene products involved in yeast inositol polyphosphate metabolism are known (Fig. 4A) (9). Kcs1 is a homolog of IP₆ kinases in other organisms (19) and is a major IP₆ kinase in yeast (12). However, IP₇ is still observable in *kcs1Δ* cells (16, 20), suggesting that another IP₆ kinase exists. A second yeast IP₆ kinase, Vip1, generates an isomer of IP₇ distinct from that

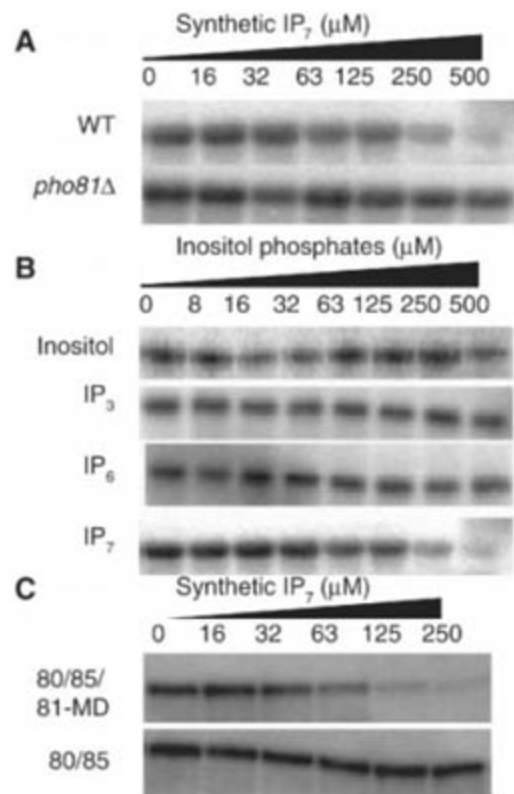


Fig. 2. Inhibition of Pho80-Pho85-Pho81 by synthetic IP₇. (A) Synthetic IP₇ was serially diluted and added to immunopurified Pho80-Pho85 isolated from wild-type (WT) or *pho81Δ* cells that had been grown in P_i -rich medium (Fig. 1C). Kinase activity was then measured. (B) Serial dilutions of inositol, *myo*-D-inositol 1,4,5-trisphosphate (IP₃), IP₆, or IP₇ were added to Pho80-Pho85-Pho81 immunopurified from wild-type cells grown in P_i -rich medium, and kinase activity was measured. (C) Synthetic IP₇ was added to recombinant Pho80-Pho85 or Pho80-Pho85-Pho81-MD complex (50 nM Pho80-Pho85 and 250 nM Pho81-MD) and incubated 20 min at room temperature. Kinase activity was then measured.

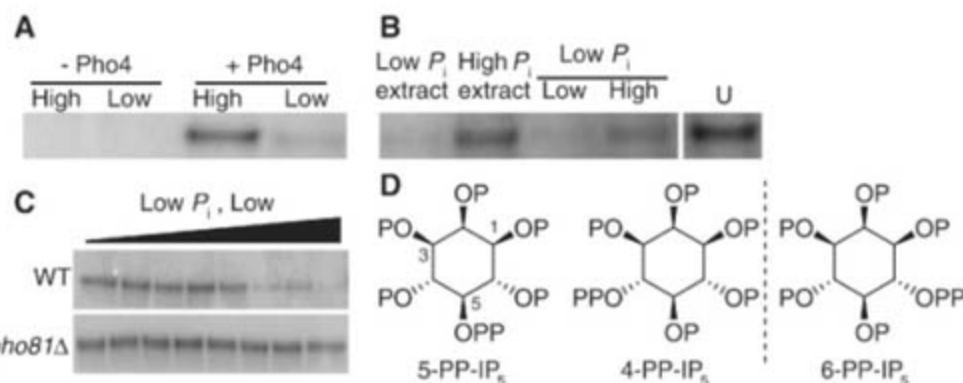


Fig. 1. Purification of a cellular component that inactivates Pho80-Pho85 in a Pho81-dependent manner. (A) Phosphorylation of recombinant Pho4 by Pho80-Pho85-Pho81 immunopurified from P_i -rich (High) and P_i -starved (Low) cells expressing Pho80-hemagglutinin tag (3HA). (B) Effects of cell fractions on Pho80-Pho85 activity. Extracts from cells (3×10^9 cells per ml extract) grown in high- P_i medium (High P_i extract) or starved for phosphate (Low P_i extract) were added either directly or after filtration (molecular weight cut-off 3 kD; Low and High indicate low- and high-molecular weight fractions, respectively) to Pho80-Pho85-Pho81 immunopurified from P_i -rich cells, and kinase assays were done as in (A). U, untreated Pho80-Pho85-Pho81 from the same gel. (C) The low- P_i low-molecular weight fraction in (B) was serially diluted and added to Pho80-Pho85 immunopurified from wild-type (WT) and *pho81Δ* cells that had been grown in P_i -rich medium. Kinase assays were then performed using recombinant Pho4 as a substrate. (D) Structures of relevant IP₇ isomers. 4-PP-IP₅ and 6-PP-IP₅ are mirror images of each other. P, phosphate; PP, pyrophosphate.

produced by the mammalian IP₆ kinase and likely distinct from that produced by Kcs1 (21). To determine which IP₆ kinase is involved in the PHO pathway, we assayed the ability of cellular extracts from P_i-starved wild-type, *kcs1Δ*, and *vip1Δ* cells to inactivate Pho80-Pho85-Pho81 in vitro (Fig. 4B). The extract from *kcs1Δ* cells inactivated Pho80-Pho85 in a Pho81-dependent

manner, whereas extract from *vip1Δ* cells did not, suggesting that Vip1 mediates synthesis of IP₇ relevant to the PHO system.

To further assess the physiological role of Vip1-generated IP₇ in P_i signaling in vivo, we determined whether yeast strains with mutations in enzymes involved in inositol polyphosphate metabolism (Fig. 4A) (9) had defects in the

regulation of Pho80-Pho85-Pho81. We monitored the activity of Pho80-Pho85 by measuring the subcellular localization of its substrate, Pho4 (Fig. 4C). In the *ipk1Δ* and *vip1Δ* strains, Pho4 was localized to the cytoplasm even in conditions of P_i starvation, suggesting that the kinase cannot be inactivated. In the *kcs1Δ* strain, Pho4 became localized to the nucleus upon P_i starvation, consistent with the model that Kcs1 does not generate the IP₇ that inhibits Pho80-Pho85-Pho81. A fraction of the *kcs1Δ* cells grown in high-P_i medium exhibited nuclear localization of Pho4; the cause of this phenotype is not understood (22, 23). Pho4 was constitutively nuclear in *ddp1Δ* cells (16), which have high levels of IP₇, but was constitutively cytoplasmic in *kcs1Δvip1Δddp1Δ* and *arg82Δ* cells, which cannot produce IP₇ and IP₅, respectively (fig. S4A). Pho4 was constitutively nuclear in a *vip1Δpho80Δ* strain and was constitutively cytoplasmic in *ddp1Δpho81Δ* cells, suggesting that IP₇ acts upstream of Pho80-Pho85-Pho81 (fig. S4B). Additionally, IP₇ enzymatically synthesized by recombinant Vip1 inhibited Pho80-Pho85-Pho81-MD in a manner dependent on Pho81-MD, but IP₇ enzymatically synthesized by the human homolog of Kcs1, hIP6K1, did not (Fig. 4D; apparent IC₅₀ ~ 50 μM; fig. S4C) (21).

We conclude that IP₇ produced by Vip1 acts as a signaling molecule that controls the yeast PHO signaling pathway: IP₇ concentrations increase in response to P_i limitation, and IP₇ is required for inhibition of Pho80-Pho85-Pho81 in vivo and in vitro. This work illuminates the molecular mechanisms underlying previously reported genetic interactions between inositol polyphosphate metabolism and the phosphate-responsive signaling pathway (22, 24). Our work reveals regulation of a cyclin-CDK-CDK inhibitor complex by a small molecule, IP₇. It is unclear whether IP₇ acts by allosterically regulating Pho80-Pho85-Pho81 or by covalently modifying one or more of these components, as it has been demonstrated to do for other yeast and mammalian proteins (25). IP₇ may be a more general signal for nutrient limitation given that P_i starvation of budding yeast and nutrient limitation of *Dictyostelium* (17) leads to elevation of IP₇ levels. In addition, considering that a mammalian IP₆ kinase is known to stimulate P_i uptake (26), a phenotype similar to P_i-starved yeast cells, it is possible that connections between phosphate metabolism and inositol polyphosphate are conserved in other organisms.

References and Notes

1. W. A. Wilson, P. J. Roach, *Cell* **111**, 155 (2002).
2. M. E. Lenburg, E. K. O'Shea, *Trends Biochem. Sci.* **21**, 383 (1996).
3. A. S. Carroll, E. K. O'Shea, *Trends Biochem. Sci.* **27**, 87 (2002).
4. A. Kaffman, I. Herskowitz, R. Tjian, E. K. O'Shea, *Science* **263**, 1153 (1994).
5. E. M. O'Neill, A. Kaffman, E. R. Jolly, E. K. O'Shea, *Science* **271**, 209 (1996).
6. K. R. Schneider, R. L. Smith, E. K. O'Shea, *Science* **266**, 122 (1994).
7. Materials and methods are available as supporting material on Science Online.

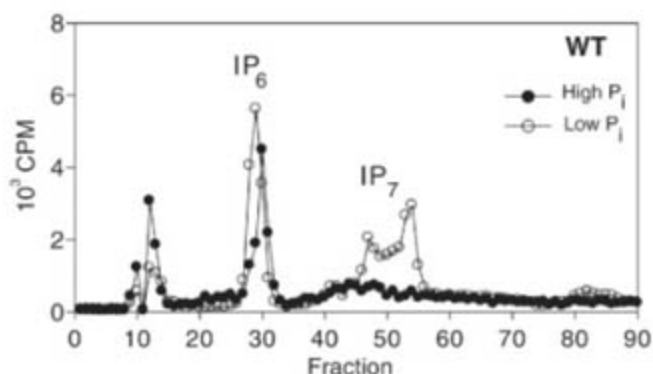


Fig. 3. Increase in IP₇ upon P_i starvation. Strong anion exchange chromatograms of extracts derived from wild-type (WT) cells labeled with [³H]-inositol grown in medium containing high P_i (10 mM) or low P_i (5 μM). Cells were starved for 2 hours at 30°C before lysis and analysis. CPM, counts per minute.

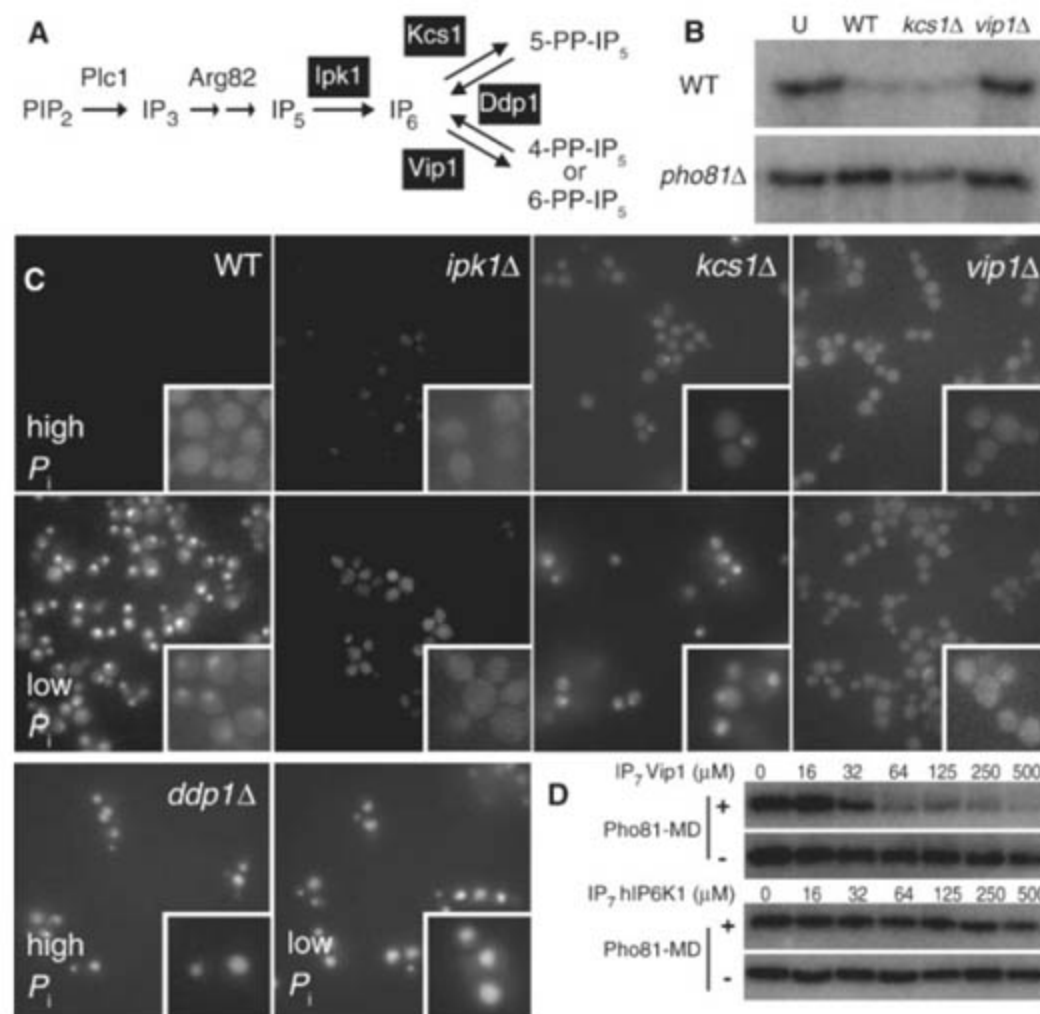


Fig. 4. Effect of disrupted inositol polyphosphate metabolism on Pho80-Pho85 activity, monitored by Pho4 localization. (A) Schematic diagram showing inositol polyphosphate metabolism in *S. cerevisiae*. (B) Wild-type (WT), *kcs1Δ*, or *vip1Δ* cell extracts from P_i-starved cells were added to immunopurified Pho80-Pho85 from P_i-rich wild-type (top) or *pho81Δ* (bottom) cells, and kinase activity was measured. U, untreated. (C) Fluorescence microscopic (100× magnification) analysis of wild-type, *ipk1Δ*, *kcs1Δ*, *vip1Δ*, or *ddp1Δ* cells expressing Pho4-green fluorescent protein, grown in medium containing high (top) or low (bottom) concentrations of P_i. (D) Isomer specificity of the IP₇-mediated Pho80-Pho85 inactivation. Pho80-Pho85 (8 nM) in the presence (top) and the absence (bottom) of His₆-Pho81-MD (250 nM) was incubated with IP₇ isomers synthesized with recombinant Vip1 (top) and human IP₆ kinase 1 (bottom), and kinase activity was measured.

8. G. W. Mayr, T. Radenberg, U. Thiel, G. Vogel, L. R. Stephens, *Carbohydr. Res.* **234**, 247 (1992).
9. R. F. Irvine, M. J. Schell, *Nat. Rev. Mol. Cell Biol.* **2**, 327 (2001).
10. H. Streb, R. F. Irvine, M. J. Berridge, I. Schulz, *Nature* **306**, 67 (1983).
11. H. R. Luo *et al.*, *Biochemistry* **41**, 2509 (2002).
12. E. Dubois *et al.*, *J. Biol. Chem.* **277**, 23755 (2002).
13. W. Ye, N. Ali, M. E. Bembek, S. B. Shears, E. M. Lafer, *J. Biol. Chem.* **270**, 1564 (1995).
14. B. Fleischer *et al.*, *J. Biol. Chem.* **269**, 17826 (1994).
15. A. Saiardi, A. C. Resnick, A. M. Snowman, B. Wendland, S. H. Snyder, *Proc. Natl. Acad. Sci. U.S.A.* **102**, 1911 (2005).
16. S. J. York, B. N. Armbruster, P. Greenwell, T. D. Petes, J. D. York, *J. Biol. Chem.* **280**, 4264 (2005).
17. H. R. Luo *et al.*, *Cell* **114**, 559 (2003).
18. S. Huang, D. A. Jeffery, M. D. Anthony, E. K. O'Shea, *Mol. Cell. Biol.* **21**, 6695 (2001).
19. A. Saiardi, H. Erdjument-Bromage, A. M. Snowman, P. Tempst, S. H. Snyder, *Curr. Biol.* **9**, 1323 (1999).
20. A. M. Seeds, R. J. Bastidas, J. D. York, *J. Biol. Chem.* **280**, 27654 (2005).
21. S. Mulugu *et al.*, *Science* **316**, 106 (2007).
22. C. Auesukaree, H. Tochio, M. Shirakawa, Y. Kaneko, S. Harashima, *J. Biol. Chem.* **280**, 25127 (2005).
23. S. Huang, E. K. O'Shea, *Genetics* **169**, 1859 (2005).
24. J. S. Flick, J. Thorner, *Genetics* **148**, 33 (1998).
25. A. Saiardi, R. Bhandari, A. C. Resnick, A. M. Snowman, S. H. Snyder, *Science* **306**, 2101 (2004).
26. M. J. Schell *et al.*, *FEBS Lett.* **461**, 169 (1999).
27. We thank Y. Liu for preparation of strains; P. Fridy for reagents; B. Stern, H. Kim, C. Leimkuhler, and D. Schwarz for comments on the manuscript; members of the J.D.Y. laboratory for unpublished data, helpful discussions, and

comments on the manuscript; and D. Kahne and his laboratory members for access to equipment. This work was supported by NIH R01 GM051377 (E.K.O.), DK070272 (J.D.Y.), and HL055672 (J.D.Y.); the David and Lucile Packard Foundation (E.K.O.); and the Howard Hughes Medical Institute (E.K.O. and J.D.Y.). The authors have no conflicting financial interest.

Supporting Online Material

www.sciencemag.org/cgi/content/full/316/5821/109/DC1
Materials and Methods

SOM Text

Figs. S1 to S5

Tables S1 and S2

References

19 December 2006; accepted 22 February 2007
10.1126/science.1139080

A Single *IGF1* Allele Is a Major Determinant of Small Size in Dogs

Nathan B. Sutter,¹ Carlos D. Bustamante,² Kevin Chase,³ Melissa M. Gray,⁴ Keyan Zhao,⁵ Lan Zhu,² Badri Padhukasahasram,² Eric Karlins,¹ Sean Davis,¹ Paul G. Jones,⁶ Pascale Quignon,¹ Gary S. Johnson,⁷ Heidi G. Parker,¹ Neale Fretwell,⁶ Dana S. Mosher,¹ Dennis F. Lawler,⁸ Ebenezer Satyaraj,⁸ Magnus Nordborg,⁵ K. Gordon Lark,³ Robert K. Wayne,⁴ Elaine A. Ostrander^{1*}

The domestic dog exhibits greater diversity in body size than any other terrestrial vertebrate. We used a strategy that exploits the breed structure of dogs to investigate the genetic basis of size. First, through a genome-wide scan, we identified a major quantitative trait locus (QTL) on chromosome 15 influencing size variation within a single breed. Second, we examined genetic variation in the 15-megabase interval surrounding the QTL in small and giant breeds and found marked evidence for a selective sweep spanning a single gene (*IGF1*), encoding insulin-like growth factor 1. A single *IGF1* single-nucleotide polymorphism haplotype is common to all small breeds and nearly absent from giant breeds, suggesting that the same causal sequence variant is a major contributor to body size in all small dogs.

Size variation in the domestic dog is extreme and surpasses that of all other living and extinct species in the dog family, Canidae (1, 2). However, the genetic origin of this diversity is obscure. Explanations include increased recombination or mutation rates (3, 4), a unique role of short repeat loci near genes (3), expansion of specific short interspersed nuclear elements (5), regulatory gene variation (6, 7), or a readily altered developmental program (1, 6). The domestic dog descended from the gray wolf at least 15,000 years ago (8–10), but the vast

majority of dog breeds originated over the past few hundred years (11). Understanding the genetic basis for the rapid generation of extreme size variability in the dog would provide critical tests of alternative genetic mechanisms and insight into how evolutionary diversification in size could occur rapidly during adaptive radiations (12).

To investigate the genetic basis for size variation in dogs and understand how change in size might occur rapidly in dogs and other canids, we first initiated sequence-based marker discovery across a 15-megabase (Mb) interval on chromosome 15 in the Portuguese water dog (PWD), a breed that is allowed large variation in skeletal size by the American Kennel Club (13). Previously, based on 92 radiographic skeletal measurements for size and shape, we found that two QTL (FH2017 at 37.9 Mb and FH2295 at 43.5 Mb) within this region were strongly associated with body size in 463 PWDs from a well-characterized extended pedigree (13, 14). We discovered 302 single-nucleotide polymorphisms (SNPs) and 34 insertion/deletion polymorphisms by sequencing 338 polymerase chain reaction (PCR) amplicons in four large

and four small PWDs and in nine dogs from small and giant breeds (<9 and >30 kg average breed mass, respectively). We then measured the association between 116 SNPs and skeletal size in a sample of 463 PWDs and identified a single peak within 300 kb of the insulin-like growth factor 1 gene (*IGF1*) (Fig. 1A), confirming the FH2295 QTL. *IGF1* is an excellent candidate gene known to influence body size in both mice and humans (15–17).

Haplotype analysis of 20 SNPs spanning *IGF1* further supported a role for the locus in determining body size. We observed that 889 of the 926 (96%) PWD chromosomes carry one of just two haplotypes, termed B and I. Dogs homozygous for haplotype B have a smaller median skeletal size [Fig. 1B; $P < 3.27 \times 10^{-7}$, analysis of variance (ANOVA)] and mass (fig. S1) than dogs homozygous for I and a lower level of IGF1 protein in blood serum (Fig. 1C; $P < 9.34 \times 10^{-4}$, ANOVA). In PWDs, 15% of the variance in skeletal size is explained by the *IGF1* haplotype. Linkage disequilibrium around *IGF1* in PWDs is too extensive to allow fine mapping, presumably because of the breed's recent origin and small population size (18, 19). However, if a mutation at *IGF1* in general underlies genetic differences in size among dog breeds, comparison of breeds of different sizes that have distinct genealogical histories may allow fine mapping of the mutation. Moreover, because size has been the target of strong selection by dog breeders, we would expect to find a signature of selection surrounding the QTL in breeds of extreme small or giant size.

To test these predictions, we surveyed genetic variation for the same 116 SNPs in 526 dogs from 23 small (<9 kg) and 20 giant (>30 kg) breeds. To obtain an empirical distribution of our association mapping test statistics, we also surveyed variation in 83 SNPs with no known association to body size on canine chromosomes 1, 2, 3, 34, and 37. These data were analyzed first to determine if intense artificial selection on body size has resulted in a "selective sweep" (20), reducing variability and increasing allele frequency divergence near *IGF1*. We found a marked reduction in marker heterozygosity and

¹National Human Genome Research Institute, Building 50, Room 5349, 50 South Drive MSC 8000, Bethesda, MD 20892–8000, USA. ²Department of Biological Statistics and Computational Biology, Cornell University, Ithaca, NY 14850, USA. ³Department of Biology, University of Utah, Salt Lake City, UT 84112, USA. ⁴Department of Ecology and Environmental Biology, University of California, Los Angeles, CA 90095, USA. ⁵Department of Molecular and Computational Biology, University of Southern California, Los Angeles, CA 90089, USA. ⁶The WALTHAM Centre for Pet Nutrition, Waltham on the Wolds, Leicestershire, LE14 4RT, UK. ⁷Department of Veterinary Pathobiology, University of Missouri, Columbia, MO 65211, USA. ⁸Nestlé Research Center (NRC-STL), St. Louis, MO 63164, USA.

*To whom correspondence should be addressed. E-mail: eostrand@mail.nih.gov

Fig. 1. Relationships of skeletal size, SNP markers, *IGF1* haplotype, and serum levels of the IGF1 protein in PWDs. (A) A mixed-model test for association between size and genotype. The association of three genotype categories (A_1A_1 , A_1A_2 , and A_2A_2) with skeletal size measurements was calculated with the use of all pairwise coefficients of consanguinity for 376 dogs. Each point represents a single SNP position on canine chromosome 15 and negative log P value for the association statistic. (B) PWD *IGF1* haplotypes and mean skeletal size. Haplotypes were inferred for 20 markers spanning the *IGF1* gene (chromosome 15: 44,212,792 to 44,278,140, CanFam1). Out of the 720 chromosomes with successful inference, 96% carry one of just two haplotypes, B and I, identical to haplotypes inferred for small and giant dogs, respectively (Fig. 3). Data are graphed as a histogram for each genotype: B/B (closed triangle, black line), B/I (open square, dashed line), and I/I (closed circle, gray line). (C) Serum levels of IGF1 protein (ng/ml) as a function of haplotype. Serum levels of IGF1 protein were assayed in 31 PWDs carrying haplotypes B and I. Box plots show the median (center line in box), first and third quartile (box ends), and maximum and minimum values (whiskers) obtained for each category: homozygous B/B ($n = 15$), heterozygous B/I ($n = 7$), and homozygous I/I ($n = 9$).

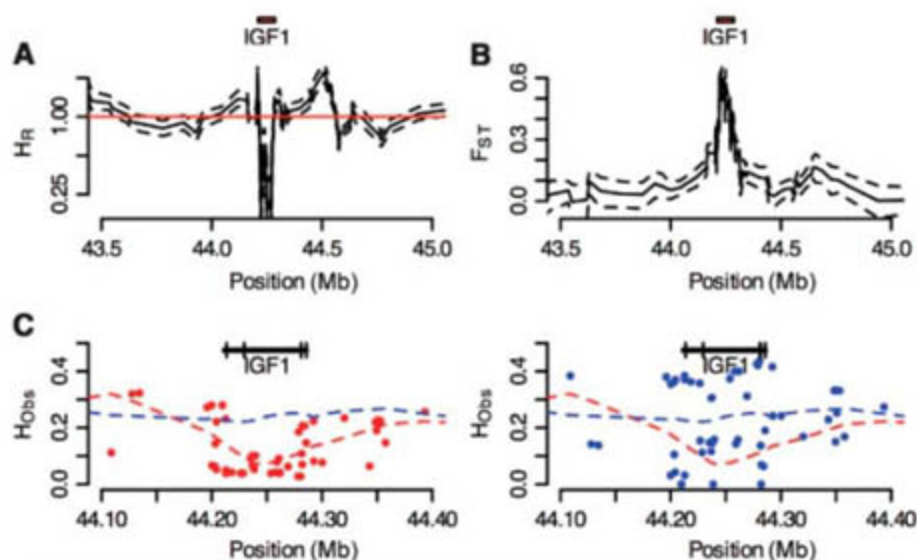
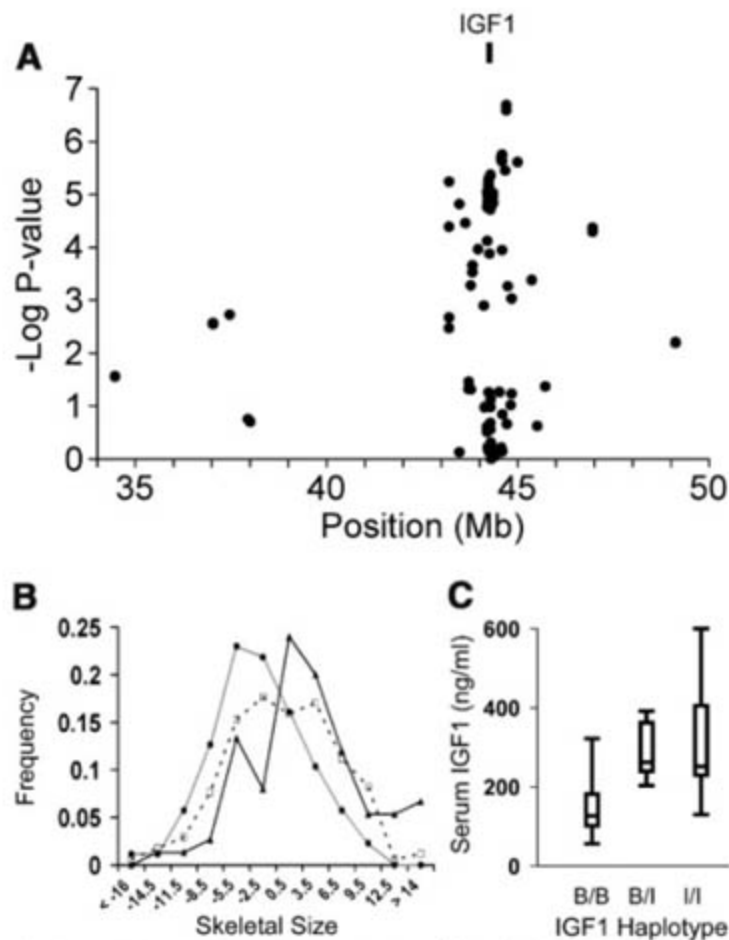


Fig. 2. Signatures of recent selection on the *IGF1* locus across 22 small and giant dog breeds. (A) Heterozygosity ratio (H_r) for small versus giant dogs. (B) Genetic differentiation (F_{ST}) for small versus giant dogs. For both (A) and (B), a sliding 10-SNP window across *IGF1* was used. Dashed lines delimit the 95% confidence intervals based on nonparametric bootstrap resampling. The *IGF1* gene interval is indicated above the graphs as a red box drawn to scale. (C) Observed heterozygosity (H_{Obs}) of SNPs near *IGF1* typed in small breeds (<9 kg) and giant breeds (>30 kg). Small breeds have a reduction in observed heterozygosity compared with that of giant breeds. Red and blue points are average observed heterozygosity in small and giant breeds, respectively. Dashed lines are locally weighted scatterplot smoothing (LOWESS) best fit to the data. The *IGF1* gene is shown as a black bar with exons indicated by vertical lines.

increased genetic differentiation between small and giant dogs centered on *IGF1* (Fig. 2). Specifically, near *IGF1*, average heterozygosity in small dogs is only 25% of that in large dogs, genetic differentiation (F_{ST} , where ST represents subpopulation) peaks significantly at 0.6, and overall heterozygosity is sharply reduced (Fig. 2B) (figs. S2 to S5). Together, these results suggest that a narrow and precisely defined genomic region holds the variant (or variants) responsible for small size in a disparate set of small dog breeds.

We next tested for association between each SNP and average breed size (Fig. 3A). The null hypothesis of no association between body size and marker frequency across breeds is rejected (Bonferroni-correct P value < 0.05) for 25 contiguous SNPs defining an 84-kb interval spanning the same region that shows evidence of a selective sweep (chromosome 15 base pairs 44,199,850 to 44,284,186) (Figs. 2 and 3A). The Mann-Whitney U statistic provides a uniform distribution of P values for 83 genomic control markers (fig. S6). Similarly, P values from Fisher's exact test of association across individuals were smaller than 10^{-100} in the 84-kb interval; although these P values are clearly biased by confounding population structure (fig. S6), as evidenced by the 83 genomic control markers [for which the minimum P value was 10^{-20} (fig. S7)], the result is significant.

Analysis of specific breed haplotypes shows that a 20-SNP haplotype spanning *IGF1* is shared by all 14 sampled small dog breeds (Fig. 3, B and C) and is identical to haplotype B in small PWDs. This haplotype was observed in only three of the nine giant breeds because most giant dogs carry one or both of two distinct haplotypes: F and I. SNP 5, located at base pair position 44,228,468 (Fig. 3B), is the best candidate for being proximate to the causative mutation for the following reasons: (i) It distinguishes haplotypes A, B, and C, associated with small body size, from haplotypes D to L, which are common in large breeds; (ii) an ancestral recombination graph suggests an absence of recombination between SNPs 4 and 5 (fig. S8); and (iii) marker analysis in the golden jackal and gray wolf indicates that the SNP 5 A allele of small breeds is the derived condition (fig. S9) (table S1). To further assess the association between body size and the SNP 5 A allele, we genotyped six tagging SNPs that distinguish all major *IGF1* haplotypes in a set of 3241 dogs from 143 breeds (Fig. 4) (table S2). The frequency of the SNP 5 A allele is strongly negatively correlated with breed average mass across this large sample of breeds (Fig. 4, Spearman's rank correlation coefficient $\rho = -0.773$; $P < 2.2 \times 10^{-16}$; likelihood ratio test = 2882.3, $\chi^2_{df=1} < 2 \times 10^{-16}$, logistic regression of allele frequency on body size). A strong negative correlation remains when the 22 breeds used to discover SNP 5 are removed from the analysis ($\rho = -0.729$; $P < 2.2 \times 10^{-16}$,

Speaman's rank correlation). Exceptions, such as the large Rottweiler or small whippet breeds, may carry compensatory mutations at other size QTL or recombinants that could aid fine mapping at *IGF1*. Our results show that a single *IGF1* haplotype is common to a large sample of small dogs and strongly imply that the same causal variant (or variants) is a major influence on the phenotype of diminished body size.

The *IGF1* gene is a strong genetic determinant of body size across mammals; mice genetically deficient in IGF1 are just 60% normal birth weight (15), and a human with a homozygous partial deletion of the gene was born 3.9 SD below normal length (16, 17). IGF1 binds the type I IGF receptor, a tyrosine kinase signal transducer. This interaction promotes cell growth and organismal longevity (21) and induces cellular differentiation (22). Serum levels of IGF1 protein (23) have been found to

correlate with body size in toy, miniature, and standard poodles (24). These studies did not compare *IGF1* genetic variation with differences in serum IGF1 protein concentrations; we observed that PWDs carrying the B haplotype of the *IGF1* gene have significantly lower serum levels of IGF1 (Fig. 1C).

Finally, to identify possible causative variants, we sequenced the exons of *IGF1* in a panel of nine small and giant dogs and found only one variation in coding sequence, a synonymous SNP in exon 3 [chromosome 15 base pair position 44,226,324, *Canis familiaris* genome assembly 1 (CanFam1)]. Extensive resequencing within introns and flanking genomic sequence was also undertaken (table S3). Several additional SNPs (table S4) and an antisense oriented retrotransposon (table S5) unique to small breeds were identified. Alleles of a dinucleotide CA_n microsatellite in the *IGF1* promoter were also significantly associated with body size

in the PWDs ($P < 1.4 \times 10^{-6}$, ANOVA) and the small and giant breeds ($P < 2.2 \times 10^{-14}$, chi-square test; table S6). All of these variations were in strong linkage disequilibrium and therefore a causative variant could not be definitively identified by this approach. Given the difficulty of developing inbred dog lines segregating small size, future studies will focus on using knock-in mice to explore the effect of these variants on phenotypes.

Our findings suggest that a single *IGF1* haplotype substantially contributes to size variation in the domestic dog. Because our sample includes small breeds that are distantly related (25) and reproductively isolated, and because the extent of haplotype sharing at *IGF1* is relatively small, the sequence variant or variants probably predate the common origin of the breeds and likely evolved early in the history of dogs. The early appearance of this allele may have facilitated the rapid genesis of size diversity in the domestic dog. The first archaeological record of dogs, beginning about 12,000 to 15,000 years ago (9, 26), shows that size diversity was present early in the history of domestication. For example, dog remains from eastern Russia dated to 14,000 to 15,000 years ago are similar in size and conformation to great Danes, whereas slightly younger dog remains from the Middle East and Europe (10,000 to 12,000 years ago) are similar in size to small terriers (9, 26, 27). The early and widespread appearance of small size suggests that an ancestral small dog *IGF1* haplotype was readily spread over a large geographic area by trade and human migration and was maintained in local gene pools by selection. Such early selection on dogs may have been manifest as intentional artificial selection exercised by early humans or as an adaptive trait for coexistence with humans in the more crowded confines of developing villages and cities (28).

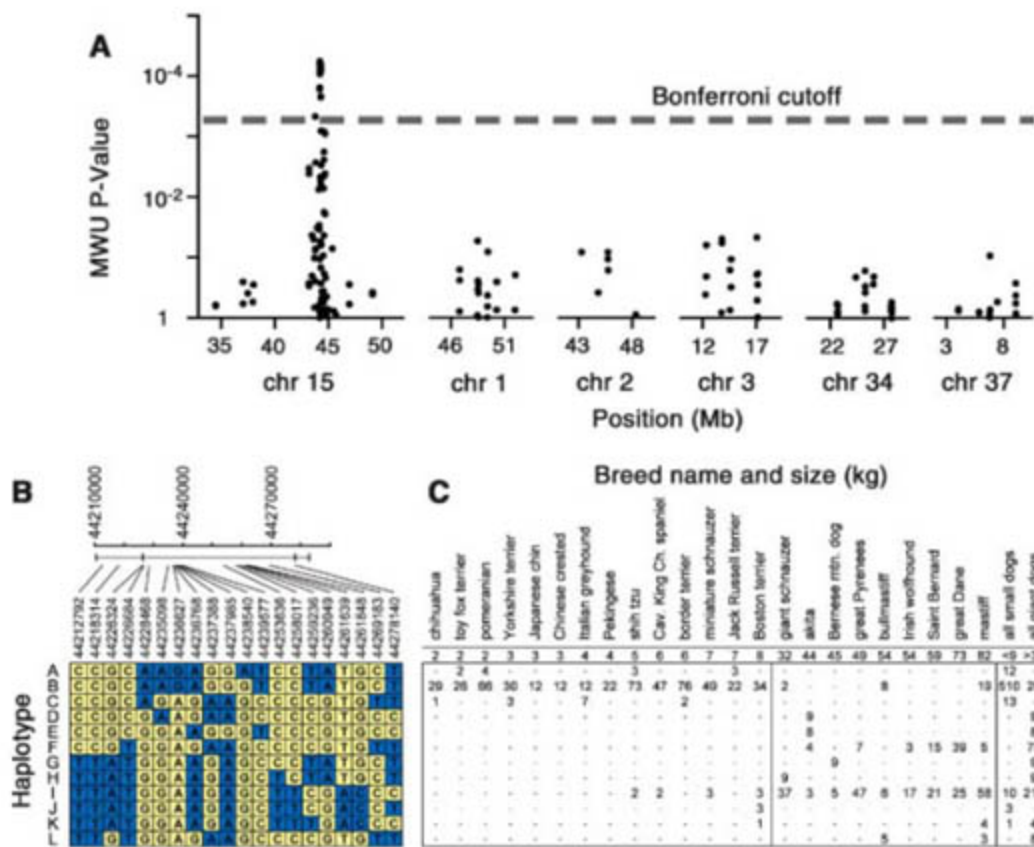


Fig. 3. Evidence of association and *IGF1* haplotypes for 14 small and 9 giant breeds. (A) Mann-Whitney U (MWU) *P* values for tests of association between individual SNPs and body size (small versus giant) for 116 SNPs on chromosome 15 and 83 SNPs on five control chromosomes. The dashed line indicates Bonferroni correction for multiple tests. Only breeds with data for at least 10 chromosomes were included (14 small and 9 giant breeds). (B) Haplotypes for the 20 markers spanning the small breed sweep interval near *IGF1*. The haplotypes were inferred independently in each breed. For each individual, fractional chromosome counts were summed for all haplotypes with at least 5% probability according to the haplotype inference software program PHASE. Chromosome sums for each breed were rounded to integer values; several breeds have odd numbers of chromosomes due to rounding error. Only inferred haplotypes carried by at least three dog chromosomes total (i.e., >0.5% frequency overall) are shown. Sequence reads collected from golden jackal (*Canis aureus*) were used to determine the ancestral allele for each SNP. The haplotypes are rows labeled A to L, and marker alleles are colored yellow for ancestral state (matching the nucleotide observed in the golden jackal) and blue for derived state. SNP positions within *IGF1* are shown at the top with *IGF1* introns (horizontal line) and exons (vertical bars) indicated. (C) Breed name and the average size of adult males in kilograms are provided. Small breeds less than 9 kg and giant breeds greater than 30 kg are grouped for totals shown at the far right.

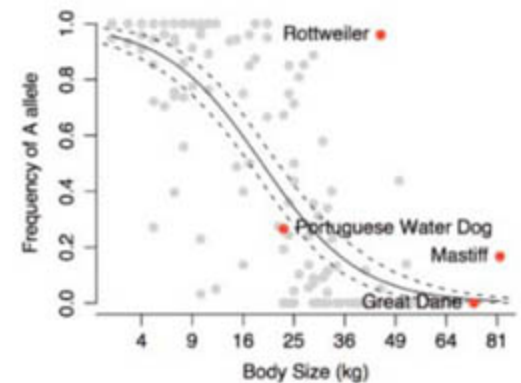


Fig. 4. Association of body size and frequency of the SNP 5 A allele. Binomial regression of allele frequency on square root of mean breed mass. Dashed lines indicate the 95% confidence interval on the predicted equation line as estimated from nonparametric bootstrap resampling. Between 5 and 109 (median = 22) dogs were genotyped for each of 143 breeds. The PWD is highlighted in red along with three giant breeds that have larger breed average masses than is predicted by their SNP 5 allele frequency.

The ubiquitous occurrence of the *IGF1* B haplotype in a diverse panel of small breeds clearly does not support unorthodox explanations of phenotypic diversity in the dog such as elevated mutation or recombination rates. Rather, we show that a single *IGF1* allele is a major determinant of small size in dogs and that intense artificial selection has left a signature in the proximity of *IGF1* that can readily be found by genomic scans of breeds sharing a common phenotype. The ability to identify a gene contributing to morphology without doing a genetic cross, but instead by using centuries of dog breeding, highlights the contribution that the study of canine genetics can make to an understanding of mammalian morphogenesis. These results provide a precedent for future studies aimed at identifying the genetic basis for complex traits such as behavior and skeletal morphology in dogs and other species with small populations that have experienced strong artificial or natural selection.

References and Notes

1. R. K. Wayne, *Evolution* **40**, 243 (1986).
2. R. K. Wayne, *J. Morphol.* **187**, 301 (1986).
3. J. W. Fondon 3rd, H. R. Garner, *Proc. Natl. Acad. Sci. U.S.A.* **101**, 18058 (2004).
4. C. Webber, C. P. Ponting, *Genome Res.* **15**, 1787 (2005).
5. W. Wang, E. F. Kirkness, *Genome Res.* **15**, 1798 (2005).
6. R. K. Wayne, *J. Zool.* **210**, 381 (1986).
7. P. Saetre et al., *Brain Res. Mol. Brain Res.* **126**, 198 (2004).
8. P. Savolainen, Y. P. Zhang, J. Luo, J. Lundeberg, T. Leitner, *Science* **298**, 1610 (2002).
9. S. J. Olsen, *Origins of the Domestic Dog* (Univ. of Arizona Press, Tucson, AZ, 1985).
10. C. Vila et al., *Science* **276**, 1687 (1997).
11. J. Sampson, M. M. Binns, in *The Dog and Its Genome*, E. A. Ostrander, K. Lindblad-Toh, U. Giger, Eds. (Cold Spring Harbor Laboratory Press, Cold Spring Harbor, NY, 2006), vol. 44, pp. 19–30.
12. B. Van Valkenburgh, X. Wang, J. Damuth, *Science* **306**, 101 (2004).
13. K. Chase et al., *Proc. Natl. Acad. Sci. U.S.A.* **99**, 9930 (2002).
14. K. Chase, D. R. Carrier, F. R. Adler, E. A. Ostrander, K. G. Lark, *Genome Res.* **15**, 1820 (2005).
15. J. Baker, J. P. Liu, E. J. Robertson, A. Efstratiadis, *Cell* **75**, 73 (1993).
16. K. A. Woods, C. Camacho-Hubner, D. Barter, A. J. Clark, M. O. Savage, *Acta Paediatr. Suppl.* **423**, 39 (1997).
17. K. A. Woods, C. Camacho-Hubner, M. O. Savage, A. J. Clark, *N. Engl. J. Med.* **335**, 1363 (1996).
18. N. B. Sutter et al., *Genome Res.* **14**, 2388 (2004).
19. K. Lindblad-Toh et al., *Nature* **438**, 803 (2005).
20. J. P. Pollinger et al., *Genome Res.* **15**, 1809 (2005).
21. R. Kooijman, *Cytokine Growth Factor Rev.* **17**, 305 (2006).
22. P. Cohen, *Horm. Res.* **65**, 3 (2006).
23. R. P. Favier, J. A. Mol, H. S. Kooistra, A. Rijnberk, *J. Endocrinol.* **170**, 479 (2001).
24. J. E. Eigenmann, D. F. Patterson, E. R. Froesch, *Acta Endocrinol. (Copenh.)* **106**, 448 (1984).
25. H. G. Parker et al., *Science* **304**, 1160 (2004).
26. H. Epstein, *The Origin of the Domestic Animals of Africa* (Africana Publishing, New York, 1971).
27. M. V. Sablin, G. A. Khlopachev, *Curr. Anthropol.* **43**, 795 (2002).
28. E. Tchernov, L. K. Harwitz, *J. Anthropol. Archaeol.* **10**, 54 (1991).
29. We thank the hundreds of dog owners who contributed samples; the AKC Canine Health Foundation; S. Hoogstraten-Miller and I. Ginty for assistance at dog shows; P. Cruz for assistance with automated PCR primer designs; S. Kim for analytical assistance, and R. Pelker for assistance with blood serum assays of IGF1. Funded by the National Human Genome Research Institute (E.A.O., N.B.S., E.K., S.D., P.Q., H.G.P., and D.S.M.), the NSF (R.K.W.), NIH grant no. 5 T32 HG002536 (M.M.G.), NSF grant 0516310 (C.D.B. and L.Z.), NSF grant DBI 0606461 (B.P.), NIH grant P50 HG002790 (K.Z. and M.N.), and the National Institute of General Medical Sciences 063056, the Judith Chiara Charitable Trust, and the Nestle Purina Company (K.G.L.).

Supporting Online Material

www.sciencemag.org/cgi/content/full/316/5821/112/DC1

Materials and Methods

Figs. S1 to S9

Tables S1 to S6

References

1 November 2006; accepted 8 March 2007

10.1126/science.1137045

Binding of the Human Prp31 Nop Domain to a Composite RNA-Protein Platform in U4 snRNP

Sunbin Liu,^{1*} Ping Li,^{1,2*} Olexandr Dybkov,¹ Stephanie Nottrott,¹ Klaus Hartmuth,¹ Reinhard Lührmann,^{1†} Teresa Carlomagno,^{2†} Markus C. Wahl^{3†}

Although highly homologous, the spliceosomal hPrp31 and the nucleolar Nop56 and Nop58 (Nop56/58) proteins recognize different ribonucleoprotein (RNP) particles. hPrp31 interacts with complexes containing the 15.5K protein and U4 or U4atac small nuclear RNA (snRNA), whereas Nop56/58 associate with 15.5K-box C/D small nucleolar RNA complexes. We present structural and biochemical analyses of hPrp31-15.5K-U4 snRNA complexes that show how the conserved Nop domain in hPrp31 maintains high RNP binding selectivity despite relaxed RNA sequence requirements. The Nop domain is a genuine RNP binding module, exhibiting RNA and protein binding surfaces. Yeast two-hybrid analyses suggest a link between retinitis pigmentosa and an aberrant hPrp31-hPrp6 interaction that blocks U4/U6-U5 tri-snRNP formation.

Most eukaryotic pre-mRNAs contain introns that are removed before translation by a multi-megadalton ribonucleoprotein (RNP) enzyme, the spliceosome (1–3). A spliceosome is assembled anew on each intron from small nuclear (sn) RNPs and non-snRNP splice factors (4, 5). The RNP network of the spliceosome is extensively restructured during its maturation (2, 6, 7), reflected by changing RNA interactions. The U6 snRNA is delivered to the pre-mRNA in a repressed state, in which catalytically important regions are base-paired to the U4 snRNA (8, 9). During

spliceosome activation, the U4-U6 interaction is disrupted, U4 snRNA is released, and U6 snRNA forms short duplexes with U2 snRNA and the pre-mRNA substrate (6). Understanding this catalytic activation of the spliceosome requires detailed structural information on the snRNPs.

As for other complex RNPs (10), the U4/U6 di-snRNP is built in a hierarchical manner. A U4 5' stem loop (U4 5'-SL) between two base-paired stems of U4/U6 serves as a binding site for the highly conserved U4/U6-15.5K protein (11). 15.5K binds to and stabilizes a kink turn (K turn)

in the U4 5'-SL (12) and is required for subsequent recruitment of the human (h) Prp31 protein to the U4/U6 di-snRNP (13). hPrp31 does not interact with either the 15.5K or the RNA alone (13, 14), but it is not known whether 15.5K merely prestructures the RNA for subsequent binding of hPrp31 or whether 15.5K provides part of the hPrp31 binding site. hPrp31 is essential for pre-mRNA splicing (15) and is a component of both major and minor spliceosomes. In the latter, the U4 snRNA is replaced by the U4atac snRNA (Fig. 1A). Nevertheless, both snRNAs bind 15.5K, and both primary RNPs incorporate hPrp31 in a strictly hierarchical manner (13, 16).

The 15.5K protein also binds to a K turn in box C/D small nucleolar (sno) RNAs (17, 18), but subsequently Nop56 and Nop58 (Nop56/58; Nop5p in archaea) are recruited to the snoRNPs (Fig. 1A) (17, 19). Stem II of the snRNAs and snoRNAs (Fig. 1A) encompasses crucial identity elements for secondary protein binding. In the box C/D snoRNAs, stem II is longer by one base

¹Abteilung Zelluläre Biochemie, Max-Planck-Institut für Biophysikalische Chemie, Am Faßberg 11, D-37077 Göttingen, Germany. ²AG Flüssig-NMR Spektroskopie, Max-Planck-Institut für Biophysikalische Chemie, Am Faßberg 11, D-37077 Göttingen, Germany. ³AG Makromolekulare Röntgenkristallographie, Max-Planck-Institut für Biophysikalische Chemie, Am Faßberg 11, D-37077 Göttingen, Germany.

*These authors contributed equally to this work.

†To whom correspondence should be addressed. E-mail: Reinhard.Luehrmann@mpi-bpc.mpg.de (R.L.); taco@nrm.mpi-bpc.mpg.de (T.C.); mwahl@gwdg.de (M.C.W.)

pair, and no sequence deviation is tolerated (19–21). Somewhat paradoxically, both hPrp31 and Nop56/58 contain a conserved, ~120-residue Nop domain (hPrp31^{215–333}) (15, 22, 23) (fig. S1), which seems to mediate binding to the different primary RNPs (24).

To delineate the structural basis for the ordered and selective binding of hPrp31, we first probed whether hPrp31 engages in direct contacts with 15.5K in the context of the U4 snRNP by using nuclear magnetic resonance (NMR) spectroscopy (25). [¹⁵N]15.5K protein was bound to an RNA representing the entire U4 5'-SL [residues 20 to 52 of U4 snRNA (Fig. 1A)], and NMR chemical shift changes were monitored upon addition of hPrp31. Primarily residues in helices $\alpha 2$ and $\alpha 3$ of 15.5K were affected (Fig. 1B). Saturation transfer from the aliphatic protons of hPrp31 to the amide resonances of 15.5K in a ternary complex containing [¹⁵N,²D,¹H_N]15.5K confirmed direct contacts between hPrp31 and helices $\alpha 2$ and $\alpha 3$ of 15.5K (Fig. 1B).

By using limited proteolysis, we defined fragment hPrp31^{78–333}, whose binding activity

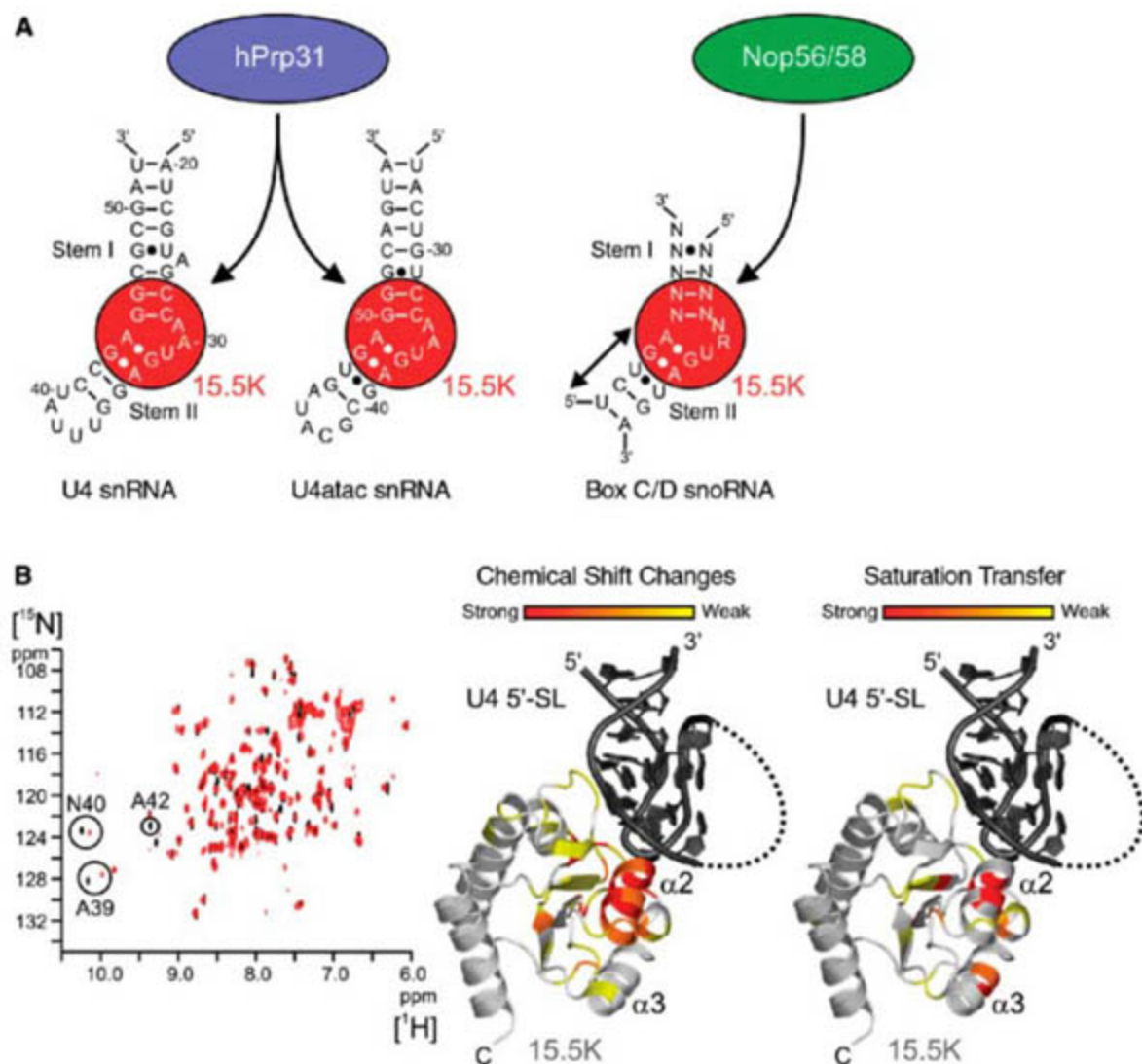
resembled that of full-length hPrp31 [Supporting Online Material (SOM) text and fig. S2]. A reconstituted hPrp31^{78–333}-15.5K-U4 5'-SL complex yielded a 2.6 Å resolution crystal structure (table S1), in which residues 4 to 128 of 15.5K and 85 to 333 of hPrp31 (excluding residues 256 to 265 that form the tip of a flexible loop) and all RNA residues (nucleotides 20 to 52 of U4 snRNA) could be traced (fig. S3). The hPrp31^{78–333}-15.5K-U4 5'-SL complex is triangular, with one subunit at each vertex of the triangle and each subunit contacting the other two (Fig. 2A). The negatively charged RNA is sandwiched between positively charged areas on hPrp31^{78–333} and 15.5K (fig. S4). The region of hPrp31^{78–333} interacting with 15.5K exhibits alternating positively and negatively charged surface patches matched by a complementary set of patches on the 15.5K protein (fig. S4).

hPrp31^{78–333} exhibits an all-helical fold with three domains (Fig. 2A and fig. S1). Residues 85 to 120 (helix $\alpha 1$) and 181 to 215 (helix $\alpha 6$) form two branches of an extended coiled coil, which is interrupted at the tip by a small

globular module (residues 121 to 180; helices $\alpha 2$ to $\alpha 5$). An oval-shaped Nop domain (residues 215 to 333; helices $\alpha 7$ to $\alpha 13$) follows the coiled-coil motif at the C terminus. hPrp31^{78–333} contacts the primary RNP exclusively via its Nop domain (Fig. 2A), suggesting that this element is the most crucial RNP interacting module in hPrp31.

The Nop domain of hPrp31^{78–333} exhibits a flat surface formed by helices $\alpha 9$, $\alpha 10$, $\alpha 12$, and $\alpha 13$ (Fig. 2, A and B). The lower part of this surface (helix $\alpha 9$ and the C-terminal half of helix $\alpha 12$) interacts with the $\alpha 2$ and $\alpha 3$ region of 15.5K (contact regions a and b in Fig. 2B). Details of the interactions between hPrp31^{78–333} and 15.5K (Fig. 3, A and B) agree well with full-length hPrp31-15.5K contacts mapped by NMR (Fig. 1B). The upper portion of the surface (helix $\alpha 10$ and the N-terminal half of helix $\alpha 12$) contacts the RNA on the side that is not associated with 15.5K (contact region 1 in Fig. 2B) and in the major groove of stem II (region 2). A loop following helix $\alpha 10$ interacts with the capping pentaloop (region 3). The surfaces of 15.5K and of the RNA buried upon binding of

Fig. 1. (A) Schematics of the 5'-SLs of U4 snRNA (left), U4atac snRNA (middle), and the K-turn region of box C/D snoRNAs (right). N indicates any nucleotide; R, purine. Binding of 15.5K and the secondary binding proteins is indicated. Stem II of the K turn in the box C/D snoRNAs is longer by one base pair (20), and a single additional base pair in stem II is known to interfere with hPrp31 binding (21). Box C/D snoRNPs act as sequence-specific 2'-O methyltransferases, which posttranscriptionally modify several functional RNAs. **(B)** (Left) ²H-¹⁵N heteronuclear single-quantum coherence spectra of 15.5K in the binary 15.5K-U4 5'-SL complex (black) and in the ternary complex containing full-length hPrp31 (red). Assignments of selected resonances are indicated. ppm, parts per million. (Middle) Mapping of NMR chemical shift changes elicited by the addition of hPrp31 on the structure of the 15.5K-RNA complex [coordinates from (12); PDB ID 1E7K]. Dashed line is the disordered pentaloop of the RNA; 15.5K, light gray; and RNA, dark gray. All structure figures were prepared with PyMOL (34). (Right) Mapping of saturation transfer from hPrp31 to RNA-bound 15.5K, indicating residues of 15.5K that are directly contacted by hPrp31. Apparent contacts to the central β sheet of 15.5K arise from spin diffusion. Degrees of chemical shift changes and saturation transfer are color-coded: red, strong; orange, intermediate; and yellow, weak. A similar picture is obtained when mapping the contacts of hPrp31^{78–333} on 15.5K in the framework of the 15.5K-U4 5'-SL complex (SOM text), confirming that the hPrp31^{78–333} fragment interacts with 15.5K in the same way as the full-length protein.



the Nop domain are comparable (550 to 650 Å² each) and are confluent (fig. S5). Thus, the Nop domain presents an RNP recognition motif, as opposed to pure RNA interaction domains found in other proteins (26).

On the basis of this architecture, failure of hPrp31 to bind either 15.5K or the RNA alone (13, 14) can be attributed to 15.5K and the RNA, each contributing about half of the hPrp31 interaction surface, so that neither of the components alone is able to supply a sufficiently large interface. In addition, 15.5K stabilizes the RNA K-turn region in a conformation favorable for hPrp31 binding and thus pays the entropic cost for immobilizing part of the RNA structure (SOM text).

The conformation of the core 15.5K-RNA complex is unaffected by the addition of hPrp31⁷⁸⁻³³³ (Fig. 2A). Furthermore, the Nop domain of hPrp31⁷⁸⁻³³³ closely resembles the corresponding domain of the archaeal Nop5p protein in the absence of a primary RNP (24) (table S2). Therefore, binding of the hPrp31 Nop domain to 15.5K and the K turn resembles a lock-and-key-type interaction. hPrp31⁷⁸⁻³³³ binds to one side of the bulged U31 of the K-turn via water-mediated interactions, van der Waals contacts, and hydrogen bonds to the backbone (Fig. 3C and contact region 1 in Fig. 2B). This situation is reminiscent of protein-DNA interactions, where the DNA-bound water structure provides important latching points for proteins

(27). In addition, the short helix α 10 of the Nop domain lines the major groove of stem II of the RNA where C247 (28) engages in hydrogen bonds to the bases of C41 and G43, representing the only sequence-specific contact of hPrp31⁷⁸⁻³³³ to the RNA (Fig. 3D; contact region 2 in Fig. 2B).

Major structural changes in the RNA upon formation of the ternary complex are confined to the RNA pentaloop (nucleotides 36 to 40), which becomes ordered on addition of hPrp31⁷⁸⁻³³³ (Fig. 2A). hPrp31⁷⁸⁻³³³ stabilizes the pentaloop by direct contacts and by reinforcing intramolecular interactions. H270 (28), from a flexible loop of hPrp31⁷⁸⁻³³³, stacks on the penultimate residue of the pentaloop, A39, which in turn stacks on the terminal base pair of stem II and forms a hydrogen bond across the loop (Fig. 3E and contact region 3 in Fig. 2B). The apparent malleability of the RNA pentaloop allows its remaining part to wrap around and engage in hydrogen bonds with H270 (Fig. 3E). The terminal U40 of the pentaloop stacks on a hydrophobic surface patch of the Nop domain (Fig. 3F). Because the above contacts ensue between flexible elements of the protein and the RNA, we conclude that hPrp31⁷⁸⁻³³³ recognizes and stabilizes the RNA pentaloop by induced fit interactions (SOM text).

Although the entire pentaloop of the U4 5'-SL can be removed without completely disrupting the binding of hPrp31, it becomes protected from hydroxyl radical cleavage upon binding of hPrp31 (21) or hPrp31⁷⁸⁻³³³ (Fig. 4A). Our structure reconciles this apparent discrepancy. Even though large portions of the pentaloop are exposed, the C4' atoms, which are the primary sites of hydroxyl radical attack (29), are partially or entirely buried for residues 36, 39, and 40 (Fig. 4B). The flexible loop of hPrp31⁷⁸⁻³³³ (residues 256 to 265) is suspended next to the C4' atoms of residues 37 and 38 (Fig. 4B), where it can scavenge radicals and protect the RNA even in the absence of direct contacts.

hPrp31 recognizes complexes of 15.5K with U4 or U4atac snRNA, whose sequences differ markedly in the hPrp31 contact regions defined by the crystal structure (Fig. 1A). In the U4 structure, hPrp31⁷⁸⁻³³³ avoids sequence-specific interactions with the RNA bases and instead maintains water-mediated interactions, contacts to the backbone, or stacking interactions with the bases (Fig. 3, C to F). With the exception of a single hydrogen bond from C247 of hPrp31⁷⁸⁻³³³ to C41 of the U4 snRNA, all contacts could be maintained in a complex containing the U4atac 5'-SL. Consistent with a similar interaction, H270 of hPrp31 has been ultraviolet light (UV)-cross-linked to U44 of the U4atac snRNA (13, 30), implying an identical stacking arrangement as seen with the corresponding A39 of U4 snRNA (Fig. 3E).

The largely sequence-independent RNA contacts of hPrp31⁷⁸⁻³³³ suggest that structural rather than sequence differences preclude bind-

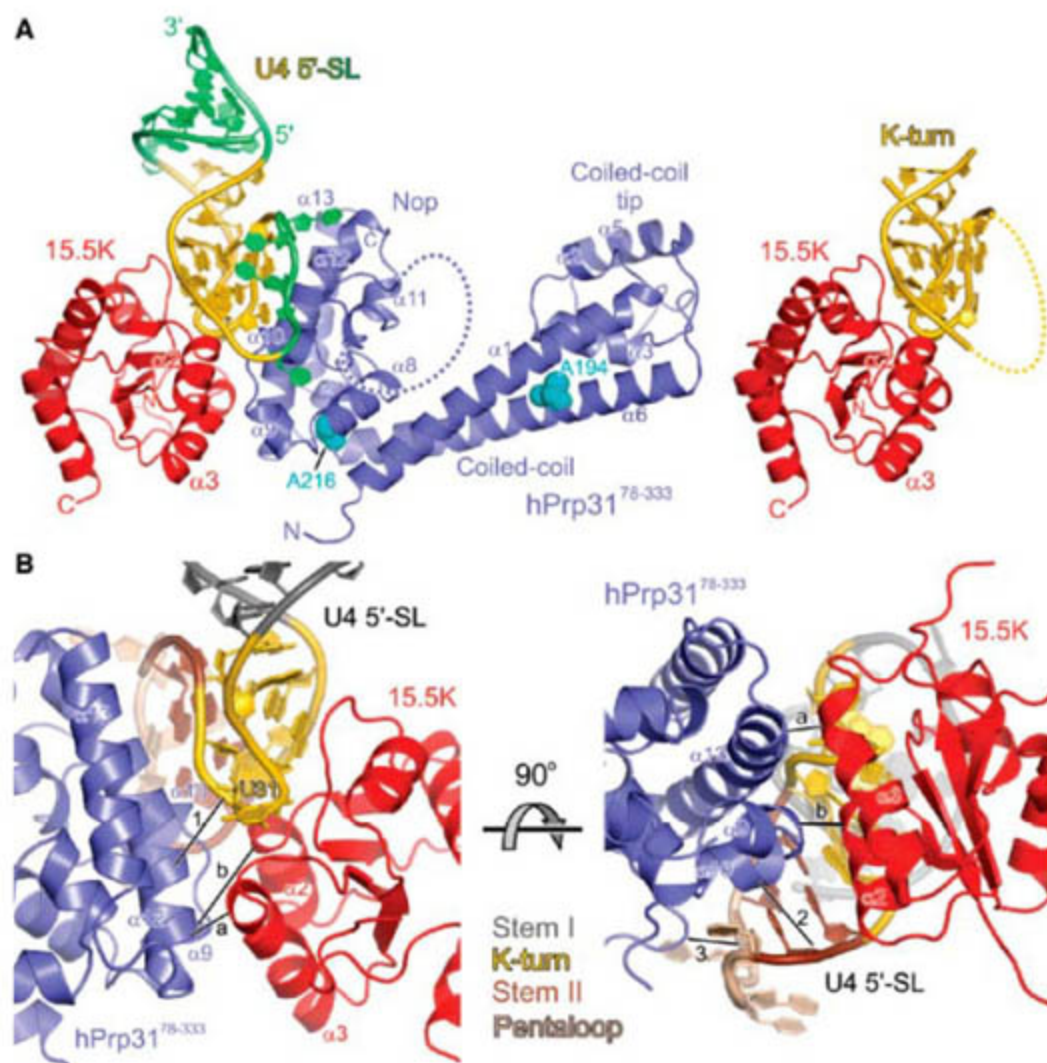


Fig. 2. (A) Overview of the hPrp31⁷⁸⁻³³³-15.5K-U4 5'-SL complex (left). hPrp31⁷⁸⁻³³³, blue; 15.5K, red; RNA, gold. RNA elements not seen in the binary 15.5K-22-mer RNA complex with a shorter stem I [right (12); PDB ID 1E7K] are in green. Positions A194 and A216, at which missense mutations have been linked to the RP11 form of retinitis pigmentosa, are shown as space-filling models and colored cyan. Dashed line in hPrp31⁷⁸⁻³³³, disordered loop. Dashed line in the binary complex, unstructured pentaloop. Although induced-fit interactions are the hallmark of most RNA-protein complexes (32), the structuring of the RNA pentaloop upon hPrp31⁷⁸⁻³³³ binding observed here is particularly pronounced. The crystal structure contains two crystallographically independent ternary complexes per asymmetric unit that are largely identical (table S2). (B) Close-up views of the complex from the back (left) and from the bottom (right). Main contact regions between hPrp31⁷⁸⁻³³³ and 15.5K and between hPrp31⁷⁸⁻³³³ and the RNA are indicated by connecting lines and are labeled by letters and numbers, respectively. Regions of the RNA are color-coded: distal portion of stem I, gray; K-turn region, gold; distal portion of stem II, brown; and pentaloop, beige. The bulged-out U31 denotes the tip of the K turn and is shown in sticks.

ing to box C/D-like RNAs. In our structure, all hPrp31 contacts with the RNA are mediated by the Nop domain, suggesting that this motif alone is able to discriminate against an extended stem II. To verify this hypothesis, we conducted gel mobility shift assays by using wild-type (WT) and mutant U4 5'-SLs and a Nop-domain fusion protein [maltose binding protein (MBP)-hPrp31²¹⁵⁻³³³]. Like full-length hPrp31, the Nop domain did not bind to RNPs, in which stem II of the RNA was extended by a noncanonical U-U (Fig. 4C, lanes 7 to 9) or by a canonical C-G base pair (lanes 10 to 12). These data confirm that the Nop domain is both required and sufficient for binding to the primary RNP and for decoding its structural specificity determinants.

An elongated stem II would reposition the pentaloop and thus the stacking platform for H270 (Fig. 3E). Loss of hPrp31 affinity to 15.5K complexes with elongated stem II RNAs could, therefore, arise due to the disruption of H270-A39 stacking. We tested this possibility by converting H270 to an alanine or to a lysine (as found in Nop56/58). Loss or alteration of the H270 side chain resulted in reduced affinity of hPrp31^{H270A} and hPrp31^{H270K} to the 15.5K-RNA 5'-SL complexes (Fig. 4D, lanes 1 to 5). However, the mutants retained significant binding activity and discriminated strongly against long stem II constructs (Fig. 4D, lanes 6 to 10), indicating that H270 is not required for measuring the length of stem II.

Next, we modeled an extended stem II A-form duplex into the present structure. The additional base pair would lie in the stacking level occupied by A39 in the WT complex. Although A39 fits snugly next to helix $\alpha 10$ of the Nop domain, the helical twist would lead to a severe clash between an additional Watson-Crick base pair and helix $\alpha 10$ (fig. S6). In contrast, in a tetraloop RNA, to which hPrp31 (21) and hPrp31²¹⁵⁻³³³ (Fig. 4C, lanes 4 to 6) still bind, the nucleotides would be turned away from helix $\alpha 10$. Thus, we conclude that helix $\alpha 10$ acts as a ruler for measuring the length of stem II by presenting a physical barrier to additional base pairs. A different recognition mechanism must be at work in Nop56/58, in which the Nop domain is compatible with elongated stem II RNAs.

The hPrp31⁷⁸⁻³³³ fragment encompasses both A194 and A216 (28) that have been linked to the RP11 form of retinitis pigmentosa (23). A194 maps to the second helix of the coiled coil, whereas A216 lies in a short loop connecting the coiled coil to the Nop domain (Fig. 2A and fig. S7). Thus, neither of the two residues interacts directly with 15.5K or the U4 5'-SL in the present structure (Fig. 2A). The Ala¹⁹⁴→Glu¹⁹⁴ (A194E) substitution most likely disturbs the local structure and/or the surface properties of the coiled coil, because the A194 side chain is embedded in a hydrophobic environment (fig. S7A). The Ala²¹⁶→Pro²¹⁶ (A216P) replacement (fig. S7A) potentially

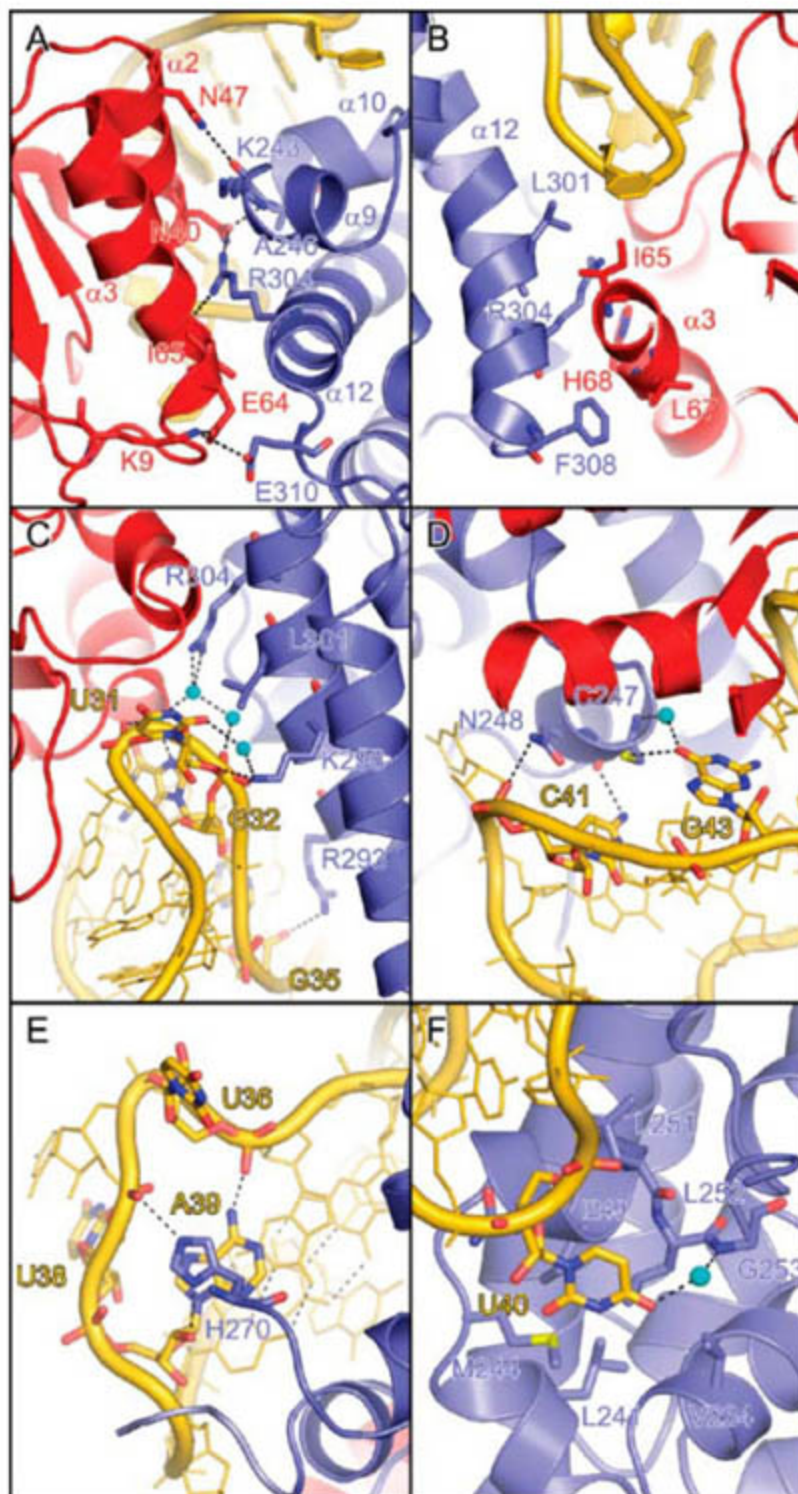


Fig. 3. Detailed interactions in the ternary complex. Selected interface residues (sticks) are labeled and color-coded by atom type (carbon and phosphorus, as the respective molecule; oxygen, red; nitrogen, blue; sulfur, yellow; bridging waters, cyan spheres). (A) Hydrogen bonds and salt bridges (dashed lines) involving helices $\alpha 2$ and $\alpha 3$ of 15.5K and the hPrp31⁷⁸⁻³³³ Nop domain (view from bottom of Fig. 2A). A network of alternating residues from 15.5K and hPrp31⁷⁸⁻³³³ extends from the backbone carbonyl of I65 (15.5K) over the side chain of R304 (hPrp31⁷⁸⁻³³³) and the side chain of N40 (15.5K) to the backbone nitrogen of A246 (hPrp31⁷⁸⁻³³³). (B) Hydrophobic contacts between the N terminus of helix $\alpha 3$ of 15.5K and the C terminus of helix $\alpha 12$ of hPrp31 (view as in Fig. 2A). Our crystal structure and NMR analysis show that residues 74 to 77 of 15.5K, which upon joint mutation inhibited the binding of hPrp31 (33), are not involved in contacts to hPrp31⁷⁸⁻³³³ or full-length hPrp31, respectively, and elicit their effect indirectly, for example, by influencing the structure of 15.5K. (C to F) Details of the interaction of hPrp31⁷⁸⁻³³³ with the K turn (C), with the major groove of stem II (D), with the 5' portion of the pentaloop (E) and with the 3' portion of the pentaloop (F). The central lock-and-key interaction region around the K turn [(C) and (D)] is of paramount importance for the stability of the ternary complex, because the RNA pentaloop can be removed without completely disrupting the binding of hPrp31 (21). The induction of a stable structure in the RNA pentaloop by hPrp31⁷⁸⁻³³³ [(E) and (F)] is reminiscent of the way some primary binding ribosomal proteins induce novel binding sites for secondary binding proteins (10). Here, three of the five pentaloop bases are turned outward (E) and conceivably provide a binding platform for another spliceosomal component.

alters the structure and flexibility of a protein loop, which may affect the relative orientation of the Nop and the coiled-coil domains. Either of the above mutations could influence other interactions of hPrp31, for example, with hPrp6 of the U5 snRNP. To test this hypothesis, we conducted a targeted yeast two-hybrid analysis using pGADT7-hPrp6 as prey and pGBKT7-hPrp31, pGBKT7-hPrp31^{A194E}, and pGBKT7-hPrp31^{A216P} as bait under stringent conditions.

Whereas introduction of proline at position 216 had no effect on the interaction with hPrp6, a glutamate at position 194 significantly weakened the interaction (fig. S7B). This result supports the idea that the hPrp31 coiled coil is an interaction site for hPrp6 and links a retinitis pigmentosa mutation in a spliceosomal protein to an aberrant molecular communication.

By interacting concomitantly with both 15.5K and the RNA, the Nop domain rein-

forces the 15.5K-RNA interaction. The latter interaction is crucial for the transition from the spliceosomal B complex to the C complex (11), during which spliceosome activation occurs. Thus, on the one side hPrp31 may regulate the RNA-protein network at the U4 5'-SL and thereby facilitate disruption of the U4/U6 snRNA duplex. Our work also suggests that hPrp31 stabilizes the U4/U6-U5 tri-snRNP by concomitantly interacting with hPrp6 via a separate coiled-coil domain. Intriguingly, hPrp6 links hPrp31 to hBrr2 and hSnu114 (14), which have been shown to be the DEAD-box protein and regulatory guanosine triphosphatase (GTPase), respectively, that are crucial for both spliceosome activation and disassembly (31). Therefore, our structural data are in line with the previous hypothesis (14) that hPrp31 may represent one of the ultimate targets of the helicase and GTPase machinery of the U5 snRNP that acts during spliceosome activation.

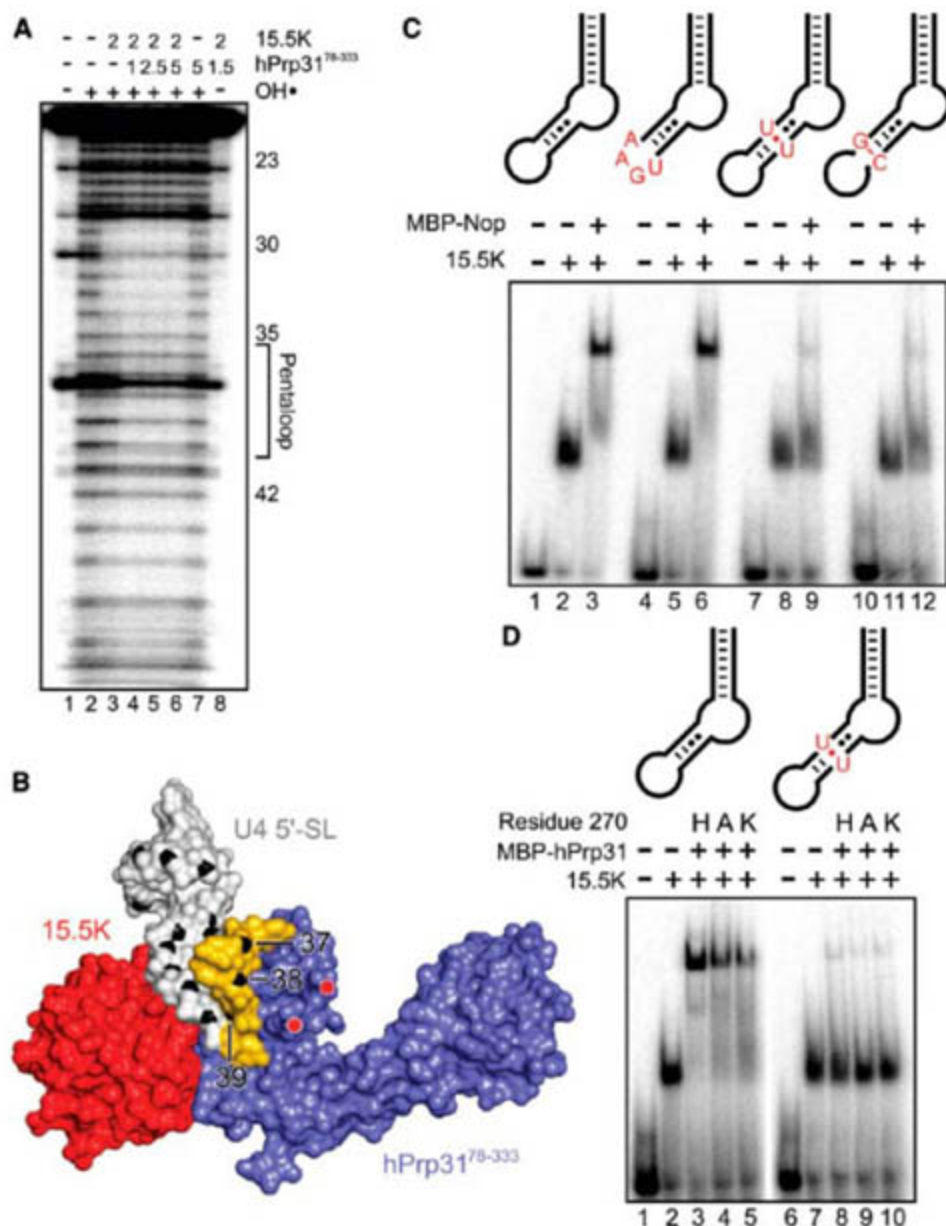


Fig. 4. (A) Hydroxyl radical footprinting of the U4 5'-SL in the absence of protein (lane 2), in the presence of only 15.5K (lane 3) and in the presence of 15.5K and increasing amounts of hPrp31⁷⁸⁻³³³ (lanes 4 to 6). Numbers indicate the protein concentration in $\mu\text{mol/L}$. Numbers on the right indicate positions in the U4 5'-SL. The location of the pentaloop is indicated. (B) Surface of the hPrp31⁷⁸⁻³³³-15.5K-U4 5'-SL complex (RNA, gray; pentaloop, gold). Sugar C4' atoms are highlighted in black and labeled for residues 37 to 39. Red dots, beginning (lower dot) and end (upper dot) of a flexible loop in the protein that is suspended next to the sugars of the pentaloop. (C) Gel mobility shift assays monitoring the binding of a Nop domain fusion protein (MBP-hPrp31²¹⁵⁻³³³) to U4 5'-SL constructs. Lanes 1 to 3, WT RNA sequence; lanes 4 to 6, replacement of the pentaloop by a UGAA tetraloop; lanes 7 to 9, addition of a U-U base pair to stem II following the sheared G-A pairs; and lanes 10 to 12, addition of a C-G base pair at the terminus of stem II. (D) Gel mobility shift assays monitoring the effects of converting H270 into an alanine (A) or a lysine (K). Mutant hPrp31 proteins bind less strongly to a WT U4 5'-SL (lanes 1 to 5) but still discriminate against RNAs with a longer stem II (lanes 6 to 10).

References and Notes

- C. B. Burge, T. Tuschl, P. A. Sharp, in *The RNA World*, R. F. Gesteland, T. Cech, J. F. Atkins, Eds. (Cold Spring Harbor Laboratory Press, Cold Spring Harbor, NY, 1999), pp. 525-560.
- T. W. Nilsen, *Bioessays* **25**, 1147 (2003).
- C. L. Will, R. Lührmann, in *The RNA World*, R. F. Gesteland, T. Cech, J. F. Atkins, Eds. (Cold Spring Harbor Laboratory Press, Cold Spring Harbor, NY, 2006), pp. 369-400.
- R. Reed, L. Palandjian, in *Eukaryotic mRNA Processing*, A. R. Krainer, Ed. (IRL Press, Oxford, 1997), pp. 103-129.
- J. Gornemann, K. M. Kotovic, K. Hujer, K. M. Neugebauer, *Mol. Cell* **19**, 53 (2005).
- J. P. Staley, C. Guthrie, *Cell* **92**, 315 (1998).
- D. A. Brow, *Annu. Rev. Genet.* **36**, 333 (2002).
- P. Bringmann et al., *EMBO J.* **3**, 1357 (1984).
- C. Hashimoto, J. A. Steitz, *Nucleic Acids Res.* **12**, 3283 (1984).
- S. C. Agalarov, G. S. Prasad, P. M. Funke, C. D. Stout, J. R. Williamson, *Science* **288**, 107 (2000).
- S. Nottrott et al., *EMBO J.* **18**, 6119 (1999).
- I. Vidovic, S. Nottrott, K. Hartmuth, R. Lührmann, R. Ficner, *Mol. Cell* **6**, 1331 (2000).
- S. Nottrott, H. Urlaub, R. Lührmann, *EMBO J.* **21**, 5527 (2002).
- S. Liu, R. Rauhut, H. P. Vornlocher, R. Lührmann, *RNA* **12**, 1418 (2006).
- O. V. Makarova, E. M. Makarov, S. Liu, H. P. Vornlocher, R. Lührmann, *EMBO J.* **21**, 1148 (2002).
- C. Schneider, C. L. Will, O. V. Makarova, E. M. Makarov, R. Lührmann, *Mol. Cell Biol.* **22**, 3219 (2002).
- N. J. Watkins et al., *Cell* **103**, 457 (2000).
- L. B. Szewczak, J. S. Gabrielsen, S. J. Degregorio, S. A. Strobel, J. A. Steitz, *RNA* **11**, 1407 (2005).
- N. J. Watkins, A. Dickmanns, R. Lührmann, *Mol. Cell Biol.* **22**, 8342 (2002).
- T. Moore, Y. Zhang, M. O. Fenley, H. Li, *Structure* **12**, 807 (2004).
- A. Schultz, S. Nottrott, K. Hartmuth, R. Lührmann, *J. Biol. Chem.* **281**, 28278 (2006).
- T. Gautier, T. Berges, D. Tollervey, E. Hurt, *Mol. Cell Biol.* **17**, 7088 (1997).
- E. N. Vithana et al., *Mol. Cell* **8**, 375 (2001).
- M. Aittaleb et al., *Nat. Struct. Biol.* **10**, 256 (2003).
- Materials and methods are available as supporting material on Science Online.
- C. G. Burd, G. Dreyfuss, *Science* **265**, 615 (1994).
- Z. Shakked et al., *Nature* **368**, 469 (1994).
- Single-letter abbreviations for the amino acid residues are as follows: A, Ala; C, Cys; D, Asp; E, Glu; F, Phe; G, Gly; H, His; I, Ile; K, Lys; L, Leu; M, Met; N, Asn; P, Pro; Q, Gln; R, Arg; S, Ser; T, Thr; V, Val; W, Trp; and Y, Tyr.

29. J. C. Wu, J. W. Kozarich, J. Stubbe, *J. Biol. Chem.* **258**, 4694 (1983).
30. E. Kühn-Hölsken, C. Lenz, B. Sander, R. Lührmann, H. Urlaub, *RNA* **11**, 1915 (2005).
31. E. C. Small, S. R. Leggett, A. A. Winans, J. P. Staley, *Mol. Cell* **23**, 389 (2006).
32. J. R. Williamson, *Nat. Struct. Biol.* **7**, 834 (2000).
33. A. Schultz, S. Nottrott, N. J. Watkins, R. Lührmann, *Mol. Cell. Biol.* **26**, 5146 (2006).
34. PyMOL, <http://pymol.sourceforge.net/>.
35. We thank S. Bhattacharya (University College London, UK) for supplying pTriEx-hPrp31, H. Urlaub for mass

spectrometric analyses, G. Bourenkov (European Molecular Biology Laboratory, Hamburg, Germany) and the group of H. Bartunik (beamline BW6, Deutsches Elektronen Synchrotron, Hamburg, Germany) for beamline support, and C. Will for fruitful discussions and critical reading of the manuscript. This work was supported by the Max-Planck-Gesellschaft (to R.L., T.C., and M.C.W.), the Deutsche Forschungsgemeinschaft (LU294/12-3), the Fonds der Chemischen Industrie (to R.L.), and the Ernst-Jung-Stiftung (to R.L.). Coordinates and structure factors have been deposited with the RCSB Protein Data Bank (www.rcsb.org/pdb/) under accession code 2OZB and will

be released upon publication. The authors declare that they have no competing financial interests.

Supporting Online Material

www.sciencemag.org/cgi/content/full/316/5821/115/DC1

Materials and Methods

SOM Text

Figs. S1 to S7

Tables S1 and S2

References

22 November 2006; accepted 1 March 2007

10.1126/science.1137924

An ATP Gate Controls Tubulin Binding by the Tethered Head of Kinesin-1

Maria C. Alonso,¹ Douglas R. Drummond,¹ Susan Kain,¹ Julia Hoeng,² Linda Amos,² Robert A. Cross^{1*}

Kinesin-1 is a two-headed molecular motor that walks along microtubules, with each step gated by adenosine triphosphate (ATP) binding. Existing models for the gating mechanism propose a role for the microtubule lattice. We show that unpolymerized tubulin binds to kinesin-1, causing tubulin-activated release of adenosine diphosphate (ADP). With no added nucleotide, each kinesin-1 dimer binds one tubulin heterodimer. In adenylyl-imidodiphosphate (AMP-PNP), a nonhydrolyzable ATP analog, each kinesin-1 dimer binds two tubulin heterodimers. The data reveal an ATP gate that operates independently of the microtubule lattice, by ATP-dependent release of a steric or allosteric block on the tubulin binding site of the tethered kinesin-ADP head.

Kinesin-1 molecular motors are adenosine triphosphate (ATP)-driven walking machines that move in 8-nm steps toward the plus ends of microtubules, turning over one ATP molecule per step under a range of loads (1–5). Even at very high backward loads, when the motor can be forced to step processively backward (6), stepping remains coupled to ATP binding (6, 7). Between steps, the motor pauses stably in a dwell state. It is clear that ATP binding triggers exit from this dwell state, but the structural mechanism is controversial (8).

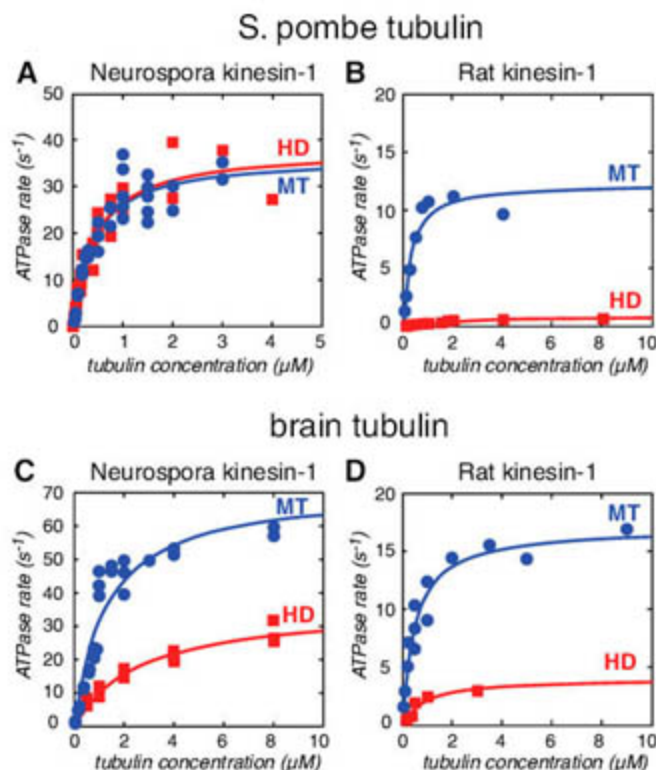
Two general types of model for this ATP gate have been proposed. In the first, kinesin dimers are proposed to dwell between steps with only one head attached to the microtubule, whereas the other diffuses to some extent on its tether but cannot access its next binding site along the microtubule because the site is too far away. ATP binding to the microtubule-attached head drives a conformational change that shifts the tethered head along the microtubule, biasing and focusing its diffusional search for its next binding site (9, 10). In the second type of model, kinesin is proposed to dwell with both heads attached to the microtubule (5), and

gating is ascribed to the effects of the resulting intramolecular strain, together with any external strain, on nucleotide exchange (11, 12). These two types of model are not mutually exclusive; the influential Rice *et al.* model (9), for example, proposes that the first step in each run of steps uses the first type of gate and that subsequent steps use the second type. Both

types of model require the microtubule lattice for their operation, either to set a prohibitive distance between binding sites or to apply strain to the kinesin heads. Here, we report an ATP gate that operates independently of the microtubule lattice.

We have found that kinesin-1 binds to free tubulin heterodimers in solution, causing tubulin-activated release of adenosine diphosphate (ADP). This shows that tubulin activation of the kinesin adenosine triphosphatase (ATPase) is not unique, as had previously been thought, to the depolymerizing kinesins (13). The degree of activation of the kinesin-1 ATPase by unpolymerized tubulin varies according to the source of kinesin-1 and tubulin, but clearly activation of the kinesin-1 ATPase does not require the interheterodimer interfaces that arise in the microtubule lattice. For a fungal kinesin-1 and a fungal tubulin, maximal activation by unpolymerized tubulin heterodimers is equivalent to that produced by assembled microtubules (Fig. 1A). For brain tubulin and brain kinesin, tubulin activation of the kinesin ATPase is modest compared with microtubule activation (Fig. 1, B to D).

Fig. 1. Activation of kinesin dimers by tubulin and microtubules. The microtubule- or tubulin heterodimer-stimulated steady state ATPase activity of kinesin was measured at 25°C with an enzyme-linked assay in 20 mM Pipes, pH 6.9, 5 mM MgCl₂, 1 mM dithiothreitol (22). Values for V_{max} (the projected maximum ATPase rate) and K_m (the tubulin concentration giving half-maximal ATPase) were obtained by least-squares fitting to plots of ATPase versus tubulin heterodimer concentration, using Kaleidagraph 3.6.4 (Synergy Software, Reading, PA, USA). MT, microtubule; HD, heterodimer. (A) V_{max} 38.1 s⁻¹, K_m 0.44 μM for HD, V_{max} 36.4 s⁻¹, K_m 0.39 μM for MT. (B) V_{max} 0.9 s⁻¹, K_m 2.03 μM for HD, V_{max} 12.2 s⁻¹, K_m 0.28 μM for MT. (C) V_{max} 35.9 s⁻¹, K_m 1.29 μM for HD, V_{max} 71.1 s⁻¹, K_m 0.62 μM for MT. (D) V_{max} 4.0 s⁻¹, K_m 0.86 μM for HD, V_{max} 17.0 s⁻¹, K_m 0.49 μM for MT.



¹Molecular Motors Group, Marie Curie Research Institute, The Chart, Oxted, Surrey RH8 0TL, UK. ²Medical Research Council Laboratory of Molecular Biology, Hills Road, Cambridge CB2 2QH, UK.

*To whom correspondence should be addressed. E-mail: r.cross@mcri.ac.uk

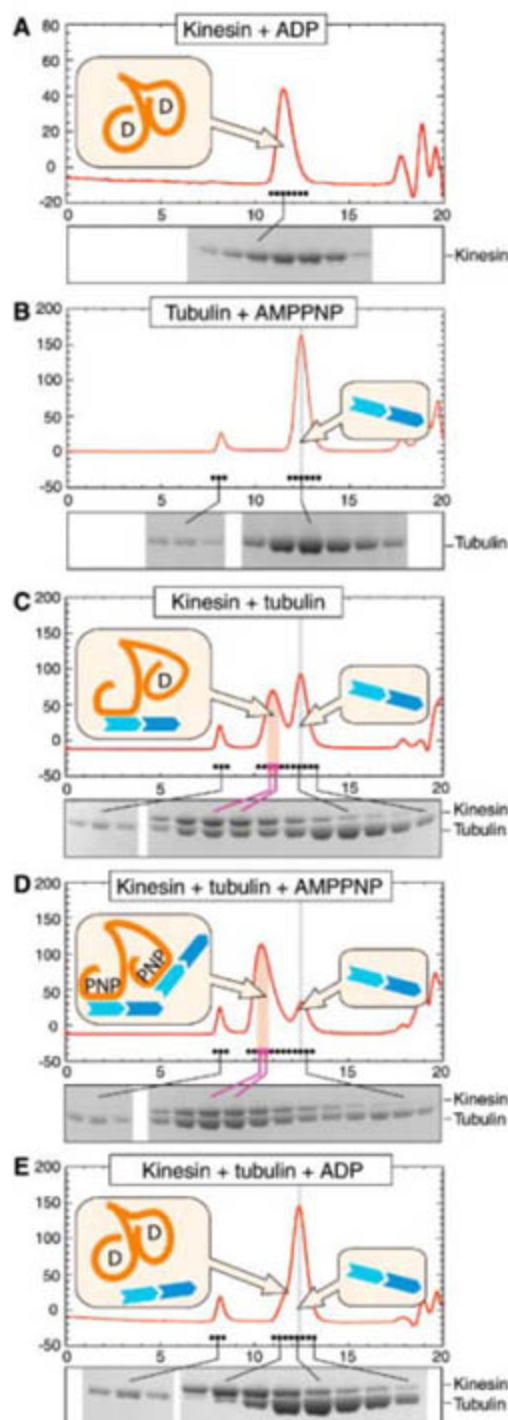


Fig. 2. Superose 12 column chromatography of kinesin-tubulin complexes. (A) 6.5 μM rK430 rat kinesin in ADP. (B) 13 μM pig-brain tubulin in AMP-PNP. (C) 13 μM tubulin + 6.5 μM kinesin; no added nucleotide. (D) 13 μM tubulin + 6.5 μM kinesin in 0.2 mM AMP-PNP. (E) 13 μM tubulin + 6.5 μM kinesin in 2 mM ADP. Y-axis marks are in mAU at 290 nm. X-axis marks are at intervals of 1 ml. The included volume of the column was 20.0 ml, and the void volume was 8.1 ml. Samples (240 μl) were run at 0.5 ml min^{-1} in 50 mM Pipes pH 6.9, 2 mM MgCl_2 , 1 mM EGTA with or without 2 mM ADP or 0.2 mM AMP-PNP. The gray vertical line indicates the tubulin elution position. The elution profiles of tubulin alone and kinesin alone were the same in ADP or AMP-PNP. Binding stoichiometry was measured for the shaded fractions.

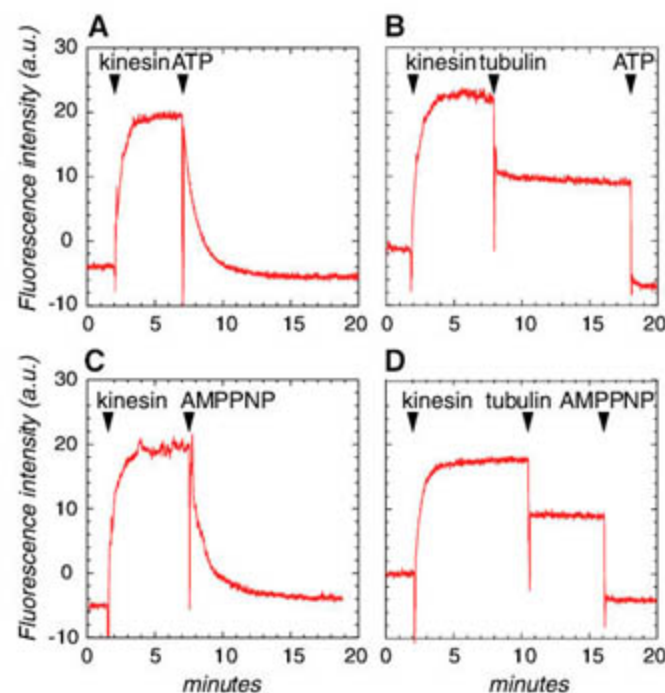
Gel-filtration experiments (Fig. 2) revealed that the stoichiometry and affinity for kinesin-1 binding to unpolymerized tubulin depends on the bound nucleotide. With no added nucleotide, kinesin dimers bind tightly to tubulin heterodimers, and the two proteins elute together from a fast protein liquid chromatography gel-filtration column as a complex in which each kinesin dimer binds 1.01 ± 0.06 SD ($n = 4$) tubulin heterodimers (Fig. 2C). By contrast, in the presence of the nonhydrolyzable ATP analog adenylyl-imidodiphosphate (AMP-PNP), each kinesin dimer binds 1.83 ± 0.08 SD ($n = 4$) tubulin heterodimers (Fig. 2D). In the presence of ADP, the binding is weakened, although some interaction is still apparent (Fig. 2E). Kinesin binding does not deplete the total amount of tubulin included by the column, even in AMP-PNP, which indicates that kinesin binding does not cause tubulin to aggregate. Furthermore, addition of guanosine monophosphate-cooxypiperazin-4-yl-propyl-1-phosphonic acid (GMP-CPP) or taxol to AMP-PNP-kinesin-tubulin complex did not cause microtubule assembly, as judged by video-enhanced differential interference contrast microscopy, suggesting that the two tubulin heterodimers in the AMP-PNP-kinesin-tubulin complex are held in an arrangement that prohibits their assembly into a microtubule.

Tubulin activation of the kinesin ATPase occurs, as for microtubule activation, by acceleration of the ADP release step of the kinetic cycle (Fig. 3). Using kinesin in which both heads are primed with the fluorescent analog 2'(3')-O-(N-methylanthraniloyl)-ADP (mantADP), we find that half of the fluorescence signal corresponding to bound mantADP decays on initial mixing with an excess of tubulin heterodimers, whereas the remainder decays only on addition of an AMP-PNP or

ATP "chase" (Fig. 3B and 3D). This shows that only one head releases mantADP immediately and that tubulin-activated mantADP release from the second kinesin head requires that AMP-PNP or ATP bind to the first head. This two-step tubulin-activated release of ADP from kinesin is likely to be related to the half-site ADP release for kinesin binding to microtubules first reported by Hackney (14, 15), in which microtubule-activated ADP release occurs from only the microtubule-bound head, whereas ADP release from the tethered head is dependent on the binding of AMP-PNP or ATP to the microtubule-bound head (16–18). A similar structural mechanism may underlie both behaviors.

How might ATP binding to the microtubule-bound head convert the tethered head from a refractory state in which it traps ADP (19) and cannot bind tubulin into a state in which it binds tubulin and releases ADP? Strain-based mechanisms are ruled out, because ATP gating occurs with unpolymerized tubulin. There are then two broad possibilities: a steric mechanism, in which the tubulin binding site in the tethered ADP head is physically masked, or an allosteric mechanism, in which the tubulin binding site on the tethered ADP head undergoes a conformational change that is triggered by ATP binding to the tubulin-attached, nucleotide-free head. To try to distinguish these possibilities, we fitted 3KIN, the only available kinesin dimer crystal structure, into an existing cryogenic electron microscopy (cryo-EM) reconstruction of the complex of kinesin dimers with helical (15 protofilament) microtubules (20, 21), obtained in the absence of added nucleotide. Fitting was only possible by docking each head separately into the cryo-EM density. In the resulting fit, the second kinesin head sits slightly ahead and to the

Fig. 3. Two-step tubulin-activated ADP release from kinesin. (A and C) Fluorescence transients corresponding to slow binding of 1 μM mantATP to 1 μM rat kinesin, followed by slow release of mantADP from both kinesin heads induced by a chase of nonfluorescent 1 mM ATP or 1 mM AMP-PNP. (B and D) The same experiment, but with 2 μM tubulin heterodimers added before the addition of the chasing nucleotide. Buffer 20 mM Pipes, pH 6.9, 2 mM MgCl_2 .



left of the attached head (Fig. 4) (22), suggesting that the tethered head is positioned so as to mask its microtubule binding site. Further work will be required to test this preliminary interpretation.

Existing data indicates that ATP binding has profound effects on the kinesin head, reconfiguring the active site and shifting the conformation of the microtubule binding loops L8 and L12 and the neck linker. The neck linker is a 13-residue sequence that connects the coiled-coil tail of kinesin-1 to the C terminus of the alpha-6 helix in the head domain. Mutating the neck linker or cross-linking it to the main part of the head inhibits kinesin-driven motility (23–25). Rice and colleagues (9) first proposed that ATP binding to the kinesin head drives an undocked-to-docked transition of its neck linker, and that this event drives stepping of two-headed molecules by shifting the leading head closer to its next binding site along the microtubule. EM evidence from gold-labeled kinesin monomers (9), electron paramagnetic resonance studies (9, 26), and a variety of subsequent evidence from fluorescently labeled kinesin dimers (27–29) is consistent with ATP-dependent neck-linker docking. Our own data show that ATP binding to a tubulin-attached head releases the other head from a sterically or allosterically blocked state. Apparently, ATP binding drives both neck-linker docking and escape of the tethered kinesin head from a blocked state. Further work will be necessary to determine whether these two events are coupled.

In the one-head-blocked kinesin dimer state that we have identified, one head binds tubulin and the other has its tubulin binding site blocked. It is not clear whether this functional asymmetry is due to a preexisting structural asymmetry or whether blocking of one head results from tubulin binding to the other head. In

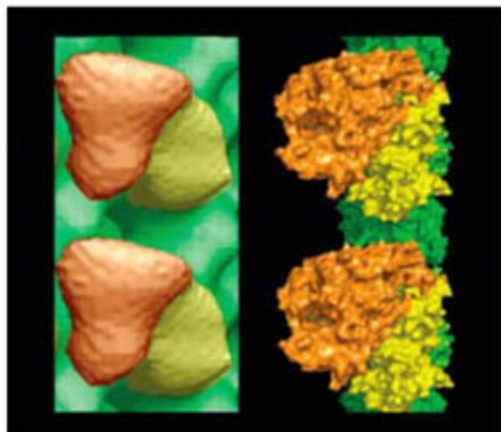


Fig. 4. Fitting of cryo-EM maps of the apo state of kinesin dimers attached to microtubules. The microtubule plus end is toward the top of the page. (Left) Cryo-EM map (20). (Right) Fitted orientation of two heads of rat kinesin. One head (yellow) is attached to the underlying microtubule protofilament, whereas the other head (orange) is parked in a forward-biased position that masks its tubulin binding site.

3KIN, there is already an asymmetry, but modeling indicates that both tubulin binding sites in 3KIN could be occupied without producing a steric clash (22). Notwithstanding this issue, and whether the blocking mechanism

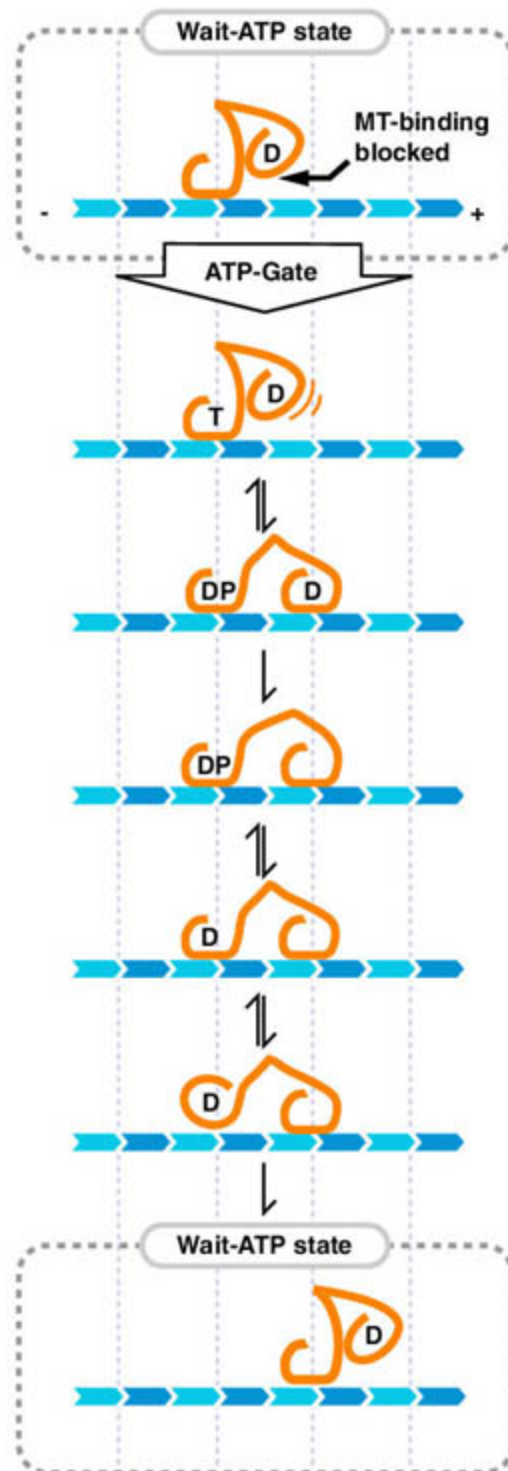


Fig. 5. Gating scheme. The cycle begins with ATP-gated exit of the tethered head from a refractory dwell state (dotted box) in which the tubulin binding site of the tethered head is blocked. After ATP binding to the attached head, the block is released and the tethered head is then free to diffuse to its next site along the microtubule. Hydrolysis and phosphate release on the trailing head return it to a weak-binding K.ADP state, which then detaches, diffuses to a forward-biased position, and reverts to a blocked state.

is steric or allosteric, our data identify an ATP gate that operates independently of the microtubule lattice, by a mechanism that is not based on the strain developed between two attached heads, or on a step-change in the diffusional distance to the next binding site along the microtubule. What role might this gate play in the kinesin walking mechanism?

Our data show that in the absence of ATP, only one head binds tubulin and that ATP binding to this tubulin-attached head is required to unblock the tubulin binding site on the other head. On this basis, we predict the scheme shown in Fig. 5, in which whenever the trailing kinesin head cycles through to the K.ADP intermediate, it detaches and reverts to a state in which its tubulin binding site is blocked. Exit from this blocked state requires ATP binding and is expected to be rate limiting at low ATP concentrations and/or high loads. At high ATP concentrations and low loads, ATP will bind rapidly, and exit from the blocked state will be correspondingly fast. In these circumstances, it is possible that the two-heads-attached configuration will have the longest lifetime in the cycle. Nonetheless, we emphasize that the ATP gate will still operate, requiring that ATP must bind to sanction stepping, and fulfilling its function of checking and adjusting the phasing of the kinetic cycles on the two heads.

At least one current model proposes that the gate controlling kinesin's first step is different from that controlling subsequent steps (9). In our model, the same gate controls the first and all subsequent steps. Our model is consistent with recent single-molecule work showing that ATP binding under load is necessary to escape a cycle of repeated futile back-stepping induced by a slowly releasing phosphate analog (12) and with earlier work showing that ATP binding is necessary for both foresteps and backsteps (6, 7). Our model is, however, inconsistent with proposals that in the ATP-waiting dwell state, both kinesin heads attach stably to the microtubule (30).

A key point of controversy in the kinesin mechanism is the question of which biochemical step or steps generate force. In our model, ATP binding generates force, but indirectly, by sanctioning binding of the ADP-containing lead head to its next site, which in turn triggers microtubule-activated ADP release from the lead head and stabilizes it in a force-holding state (6, 8). The requirement that ATP must bind to allow exit from this state then serves to coordinate lead-head attachment and trail-head detachment and to maintain tight coupling by ensuring a consistent phase lag between the kinetic cycles of the two heads (16). An emerging general theme for mechanochemical nucleotidases such as kinesin and myosin is the amplification of local, nucleotide-dependent conformational changes by causing them to gate larger-scale diffusional motions (8).

References and Notes

1. J. Howard, A. J. Hudspeth, R. D. Vale, *Nature* **342**, 154 (1989).
2. W. Hua, E. C. Young, M. L. Fleming, J. Gelles, *Nature* **388**, 390 (1997).
3. K. Kaseda, H. Higuchi, K. Hirose, *Nat. Cell Biol.* **5**, 1079 (2003).
4. C. L. Asbury, A. N. Fehr, S. M. Block, *Science* **302**, 2130 (2003).
5. A. Yildiz, M. Tomishige, R. D. Vale, P. R. Selvin, *Science* **303**, 676 (2004).
6. N. J. Carter, R. A. Cross, *Nature* **435**, 308 (2005).
7. M. Nishiyama, H. Higuchi, T. Yanagida, *Nat. Cell Biol.* **4**, 790 (2002).
8. N. J. Carter, R. A. Cross, *Curr. Opin. Cell Biol.* **18**, 61 (2006).
9. S. Rice *et al.*, *Nature* **402**, 778 (1999).
10. W. H. Mather, R. F. Fox, *Biophys. J.* **91**, 2416 (2006).
11. S. S. Rosenfeld, P. M. Fordyce, G. M. Jefferson, P. H. King, S. M. Block, *J. Biol. Chem.* **278**, 18550 (2003).
12. N. R. Guydosh, S. M. Block, *Proc. Natl. Acad. Sci. U.S.A.* **103**, 8054 (2006).
13. C. E. Walczak, *Nat. Cell Biol.* **8**, 903 (2006).
14. D. D. Hackney, *Proc. Natl. Acad. Sci. U.S.A.* **91**, 6865 (1994).
15. D. D. Hackney, *Biochemistry* **41**, 4437 (2002).
16. Y. Z. Ma, E. W. Taylor, *J. Biol. Chem.* **272**, 724 (1997).
17. S. P. Gilbert, M. L. Moyer, K. A. Johnson, *Biochemistry* **37**, 792 (1998).
18. I. Crevel, N. Carter, M. Schliwa, R. Cross, *EMBO J.* **18**, 5863 (1999).
19. R. A. Cross, *Trends Biochem. Sci.* **29**, 301 (2004).
20. K. Hirose, J. Lowe, M. Alonso, R. A. Cross, L. A. Amos, *Mol. Biol. Cell* **10**, 2063 (1999).
21. R. A. Cross *et al.*, *Philos. Trans. R. Soc. London B Biol. Sci.* **355**, 459 (2000).
22. Materials and methods are available as supporting material on Science Online.
23. M. Tomishige, R. D. Vale, *J. Cell Biol.* **151**, 1081 (2000).
24. R. B. Case, S. Rice, C. L. Hart, B. Ly, R. D. Vale, *Curr. Biol.* **10**, 157 (2000).
25. K. Hahlen *et al.*, *J. Biol. Chem.* **281**, 18868 (2006).
26. S. Rice *et al.*, *Biophys. J.* **84**, 1844 (2003).
27. S. S. Rosenfeld, G. M. Jefferson, P. H. King, *J. Biol. Chem.* **276**, 40167 (2001).
28. K. Sugata, M. Nakamura, S. Ueki, P. G. Fajer, T. Arata, *Biochem. Biophys. Res. Commun.* **314**, 447 (2004).
29. A. B. Asenjo, Y. Weinberg, H. Sosa, *Nat. Struct. Mol. Biol.* **13**, 648 (2006).
30. A. Yildiz, P. R. Selvin, *Trends Cell Biol.* **15**, 112 (2005).
31. We thank our colleagues at the Medical Research Council (MRC) Laboratory of Molecular Biology and the Marie Curie Research Institute for discussions, the MRC for strategic funding for our *S. pombe* tubulin project, and the Marie Curie Foundation for continuing support. The first author dedicates this paper to Graham Currie.

Supporting Online Material

www.sciencemag.org/cgi/content/full/316/5821/120/DC1

Materials and Methods

SOM Text

Figs. S1 to S4

References

31 October 2006; accepted 2 February 2007

10.1126/science.1136985



Protein Crystal Services

ProXyChem™ provides cost effective and timely crystallographic structure determination services using state-of-the-art synchrotron facilities and a highly experienced team of scientists. Our ever-expanding portfolio of catalog proteins is one of the most extensive in the industry, allowing for the rapid structure determination of ligands bound to their target proteins.

Catalog Proteins include

AurA	GSK3 β	PTP1b
CK2 α	KDR	PDE4B, 4D, 5A
CDK4	JNK 1, 2, 3	PPAR α , γ
Erk2	MAPKAP2	Cathepsin B

Future Catalog Proteins include

p38 α , γ	CDK5, 6, 7	MEK1, 2
cMET	PDK1	Tie2

• Other proteins available upon request

For information about our full portfolio of catalog proteins visit our website at www.proxychem.com

Phone: 1-617-395-4266

E-mail: info@proxychem.com

Portland Press » publishing innovation

cell signallingbiology

- an essential online resource by one of the world's leading experts
Professor Sir Michael J Berridge

Contents

1. Introduction
2. Cell signalling pathways
3. Ion channels
4. Sensors and effectors
5. Off mechanisms
6. Spatial and temporal aspects of signalling
7. Cellular processes
8. Development
9. Cell cycle and proliferation
10. Neuronal signalling
11. Cell stress, inflammatory responses and cell death
12. Signalling defects and disease

"Valuable to investigators as well as teachers and students who can tour cell signalling pathways online or even download materials for courses. Highly recommended."

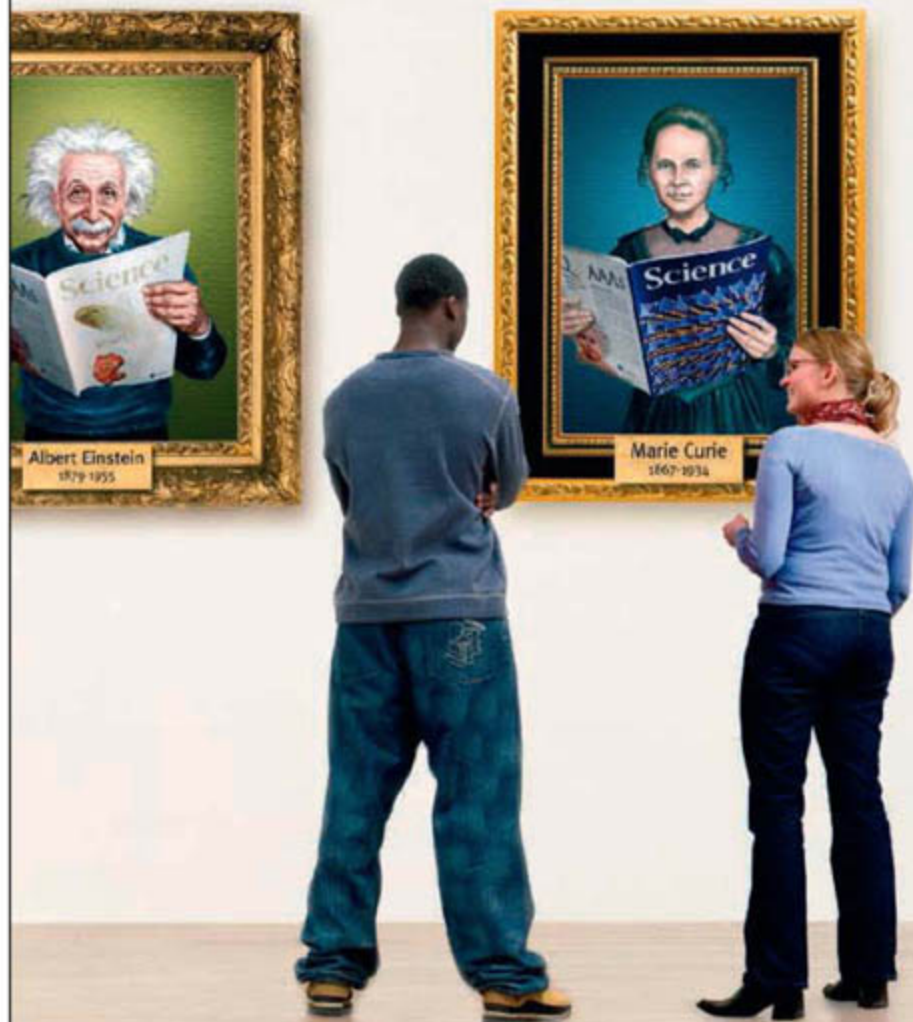
James T. Stull, UT Southwestern Medical Center

Updates coming soon - including coverage of additional cell types, cellular processes and diseases, plus animated figures!

Subscribe today or register for further information on updates at www.cellsignallingbiology.org

Career advice, insight and tools.

Turn to the experts for the big picture.
Visit www.ScienceCareers.org



Your career is too important to leave to chance. So to find the right job or get career advice, turn to the experts. At ScienceCareers.org we know science. And we are committed to helping take your career forward. Our knowledge is firmly founded on the expertise of *Science*, the premier scientific journal, and the long experience of AAAS in advancing science around the world. Put yourself in the picture with the experts in science. Visit www.ScienceCareers.org.

ALBERT EINSTEIN and related rights ™/© of The Hebrew University of Jerusalem, used under license. Represented by The Roger Richman Agency, Inc., www.albert-einstein.net.

ScienceCareers.org

We know science



CELL SIGNALING PHOSPHORYLATION, KINASES, AND KINASE INHIBITORS

Cell signaling is a broad and frequently confusing field. This overview describes some of the exciting new technologies that promise to drive research via more specific, user-friendly assays, reagents, and services, and the development of new inhibitors. **By Lynne Lederman**

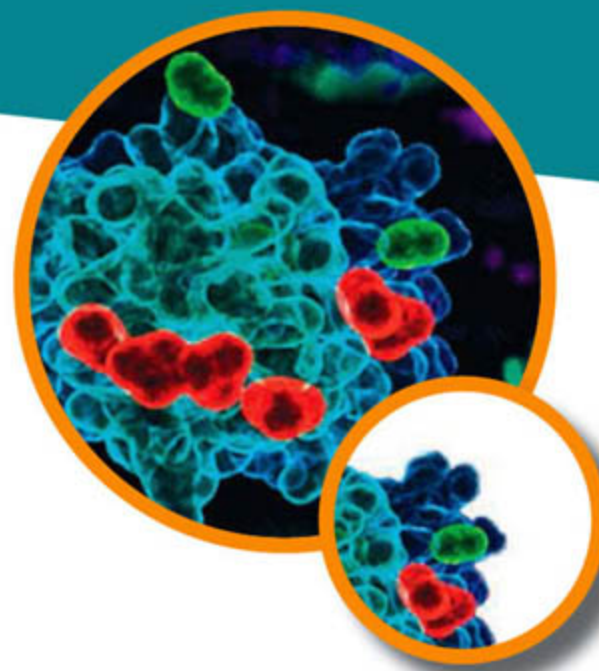
Understanding the signaling pathways, networks, and interactions that cells require to function is a major scientific challenge. Kinases are involved in the many signaling pathways cells use for growth proliferation, differentiation, and death. Assays to elucidate kinase-related components of signaling pathways may rely on “classic” methods using radioactive phosphates to detect kinase activity (phosphorylation), inhibition, or dephosphorylation, or they may rely on more recently developed fluorescent or colorimetric technologies. Antibodies specific to phosphotyrosine, phosphoserine, and phosphothreonine and to specific target sequences are also useful for assay development. Companies with an interest in cell signaling provide a variety of products that are driving basic research, including enzymes, substrates, inhibitors, antibodies, and off-the-shelf or custom assay kits.

Keeping Track

PhosphoSite is a unique online resource developed at **Cell Signaling Technology (CST)**, to provide information about all in vivo mammalian phosphorylation sites. Funded by both the company and three grants from the US National Institutes of Health (NIH), it identifies over 15,000 unique sites from the literature and over 8,000 previously unpublished sites discovered by scientists at CST and elsewhere. PhosphoSite identifies sites of phosphorylation, and contains extensive information curated from the literature about the regulation and biological consequences of protein phosphorylation. By mid 2007, an enhanced version of PhosphoSite is expected to be launched. Roberto D. Polakiewicz, chief scientific officer, expects that the site will be freely accessible by the academic world, and that there will probably be a subscriber’s fee for other users. “We need the funds to keep adding information,” Polakiewicz says, “so the database won’t become obsolete.”

Huda Shubeita, technical service scientist, **EMD Biosciences**, an affiliate of **Merck KGaA**, which includes the Calbiochem brand, notes that a big focus of the company is signal transduction. Calbiochem’s Interactive Pathway Resource provides over 20 interactive signaling pathways, including Akt and PI3 kinases, and mTOR signaling. There are also disease-specific pathways, including ones for diabetes and inflammation. Users select a target within a pathway to obtain lists of available assay kits, antibodies, enzymes, substrates, inhibitors, and other products. “Kinases are involved in every cell signaling pathway you can think of, and, directly or indirectly, in most disease processes,” Shubeita says. “The differential regulation of molecules dictates the characteristics of cells, whether they remain normal or become pathological.”

Ambion, an **Applied Biosystems** business, has a website where customers will be able to search about 300 pathways for their protein of interest to see what is up- and downstream and whether its activity is associated with the cell [continued](#) >



“Kinases are involved in every cell signaling pathway you can think of, and, directly or indirectly, in most disease processes.”

Look for these Upcoming Articles

Stem Cells — April 20

RNAi — June 1

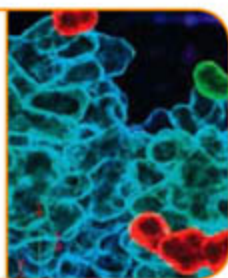
Cell Signaling 2 — June 22

Microarray Technologies — August 24

Inclusion of companies in this article does not indicate endorsement by either AAAS or Science, nor is it meant to imply that their products or services are superior to those of other companies.

Cell Signaling

"In an ideal situation, patients' blood could be monitored for the drug's effect on signaling pathways."



surface, nucleus, or cytoplasm. *Science's* own **Signal Transduction Knowledge Environment (STKE)** provides tools and approaches to allow users to acquire, understand, and use the vast array of cell regulatory information that is available, through a database, virtual journal discussion groups, and other formats.

Antibody-Based Tools in Combination Technologies

Polakiewicz believes Cell Signaling Technology "leads the pack in terms of tools to study signal transduction, having developed [as part of New England Biolabs] the first commercially available antibodies specifically to phosphoproteins in their activation state. More recently," he says, "we have been developing antibodies capable of detecting phosphorylation in the context of fixed amino acid residues corresponding to kinase recognition motifs, which help to identify and detect multiple novel kinase substrate proteins in a biological sample." These and other tools like general phosphotyrosine antibodies, Polakiewicz observes, are becoming useful to study the phosphorylation of proteins using CST's PhosphoScan technology." PhosphoScan can identify hundreds of phosphotyrosine sites in a single analysis. It uses an immunoaffinity step to isolate phosphopeptides from protease-digested cellular or tissue extracts. The peptides are then identified using tandem mass spectrometry. "If you want to globally interrogate the phosphotyrosine proteome in a cell type or tissue in one shot, it's a robust and powerful method," Polakiewicz concludes.

According to Roberto Campos-Gonzalez, director, cell signaling research, **BD Biosciences**, "One of the most exciting recent developments in the phosphorylation field for BD Biosciences is the development of BD Phosflow, a unique way to monitor protein phosphorylation states in kinase signaling pathways." The technology is based on phospho-specific, fluorochrome-labeled antibodies that are detected using flow cytometry. "It has a unique appeal to the pharmaceutical segment where it could be used to monitor the effectiveness of a compound in clinical trials," he observes. "In an ideal situation, patients' blood could be monitored for the drug's effect on signaling pathways, for example, the Akt or MAP kinase pathways, in specific cell types because flow cytometry allows discrimination between different cell immunophenotypes, such as different subtypes of B or T cells." Experiments have been done with up to 11 different colors of labels, and Campos believes that this is not the upper limit. "It's a powerful way to monitor in vivo studies where primary cells are not as abundant as are cell lines used for in vitro studies, and are present in mixed cell-type populations," he says.

Circumventing the Use of Antibodies

According to Annegret Boge, director for reagent and assay R&D, **Molecular Devices**, her company's IMAP TR-FRET (time-resolved

fluorescent resonant energy transfer) detection system is helping drive drug discovery in cancer research, among other areas. IMAP uses a high-affinity reagent, trivalent metal complex immobilized on nanoparticles bound via a linker to a terbium (Tb) donor, to bind phosphate. When a fluorescent peptide substrate containing tyrosine, serine, or threonine is phosphorylated by a kinase, the fluorescent phosphopeptide product binds to the IMAP reagent, bringing it closer to the Tb-donor complex, resulting in resonance energy transfer from the donor to the acceptor (peptide substrate) and emission of a stable signal as measurable light. In addition to TR-FRET, IMAP can be performed using fluorescence polarization (FP) readout. This assay circumvents the need for highly specific antibodies as well as the effort and cost required to generate them.

Another advantage of antibody independence is the ability to test lipid kinases and phosphodiesterases. "IMAP fits very well in the cell signaling field. We have a portfolio of over 150 fluorescently labeled substrates for tyrosine, serine, and threonine kinases. Our products are geared toward research where there is pressure to quickly validate a high quality assay for high throughput screening." Boge says the assay also allows testing the activity of potential kinase inhibitors. Molecular Devices sells substrates, buffers, and the IMAP binding system primarily to users who "don't need us to tell them how to design an assay. We provide a modular approach with dedicated support," Boge notes.

Inhibit and Protect

"A product we're really excited about for 2007 is PhosSTOP," says Jeffrey Emch, product manager, **Roche Applied Science**. "These phosphatase inhibitor cocktail tablets greatly increase convenience, stability, and reliability, allowing users to make a preoptimized inhibitor solution as needed." PhosSTOP is designed to inhibit the broad spectrum of phosphatases that are released when cells are lysed, and to protect the phosphorylation state of proteins from being altered, which can affect the detection and isolation of functional proteins of interest. This should allow researchers to capture more accurately the phosphorylation state of their protein at a particular moment in time.

At Your Service

Those who don't have the time, resources, or inclination to perform their own kinase assays can turn to companies who will perform them as a service. Jeff Till, group product manager, drug discovery, **Millipore**, observes that, as Upstate, the company was the first to sell recombinant kinases, and today kinases are still big targets in cancer therapeutics. Millipore has a portfolio of over 250 recombinant, disease-relevant kinases which form the basis of KinaseProfiler, a direct radiometric kinase inhibitor profiling service for the evaluation of candidate pharmaceutical compounds. Till refers to the assay, which was introduced about five years ago, as the "tried and true gold standard." The service, performed in Dundee, Scotland, allows clients to avoid the use of radioactive isotopes. Till says, "Most of our clients are looking for kinase inhibitors, primarily in the oncology setting." The company also has a specificity testing service for PI3-kinases, called PIProfiler. Because PI3 kinase is a lipid kinase, it is not as amenable to direct radiometric-formatted testing as are the protein kinases. PIProfiler uses HTRF (homogeneous time-resolved fluorescence), the company's copyrighted name for its [continued](#)

TR-FRET-based technology, for lead identification and evaluation against the human PI3 kinases beta, gamma, and delta.

Biomol International, in partnership with **Innova Biosciences**, launched SpeedLead-P in July 2005, according to Mark Engleka, technical marketing specialist. SpeedLead-P is a service for selectivity screening against a panel of 19 highly active phosphatases. The turnaround is two weeks, and compounds can be screened against the entire panel or a subset of the enzymes for percent inhibition or IC50. "Our service allows researchers to determine the inhibition profile of a given molecule against a panel of phosphatases without having to clone and express many phosphatases and develop assays in house," says Engleka. Biomol also has a large collection of assay kits, recombinant kinases and phosphatases, kinase inhibitors, including a kinase inhibitor library, phosphospecific antibodies, and peptide substrates.

Disease-Specific Applications

At **Pfizer's** Research Technology Center, the kinase platform has a mandate to identify members of the kinase gene family as drug discovery targets, according to Jessie M. English, director of the Kinase Center of Emphasis. The platform partners with Pfizer scientists, determining where roadblocks in the discovery process may occur, and looking for approaches to address needs within the company. "Pfizer is a drug discovery company," English says. "Our primary goal is to identify novel, effective, and safe therapeutics for human disease. There is a substantial need to better understand the molecular events underlying efficacy and safety as well as more clearly delineate the implications of inhibiting specific kinase targets. There sometimes is a gap between what is seen in in vitro kinase assays and what happens in cells."

James Christensen, associate research fellow, PGRD (Pfizer Global Research and Development), is working in the oncology therapeutic area in drug discovery and clinical development. His projects include researching kinase inhibitors in early clinical development. Of interest is determining the subtypes of patients whose disease will be most likely to respond to kinase inhibitors. "We are looking at kinase pharmacogenomics—targeting polymorphisms, gene amplifications, mutations and other molecular profile analyses, and determining

their relationship to patient clinical benefit from kinase targeted therapies," he says. This information could be used to analyze clinical trial results retrospectively to define the molecular profiles of patients whose disease would respond favorably to a treatment; it could eventually be applied as a prospective diagnostic. "Another area of interest is to better define the molecular events downstream of kinase signaling, utilizing genomic and proteomic approaches in nonclinical models to identify biomarkers that are predictive of clinical response, and ultimately to apply the most robust biomarker approaches for clinical use," Christensen says.

Express and Silence

Another approach to dissecting cell signaling pathways is to use small or short interfering RNA (siRNA) to silence the expression of genes of interest in viable cells. A number of well-known companies offer kits and reagents for kinase-related gene silencing studies relying on RNA interference (RNAi). **Ambion** Silencer siRNA libraries have three individual siRNAs per target, and include human kinase, phosphatase, and druggable genome libraries, which comprise transcription factors and other sequences that may be of therapeutic relevance. Kathy Latham, Ambion's senior product manager, RNAi, says the company also makes custom siRNA libraries. "RNAi as a technology has revolutionized how people think of target validation. Instead of finding inhibitors to figure out the role of kinases in a particular biologic event, RNAi allows you to knock down expression if you know the sequence of the gene," she observes. David Dorris, senior director and general manager, cell biology and RNAi, agrees. "It's a great tool. Pharmaceutical companies have adopted the technology most quickly, particularly in the kinase field. RNAi can be used to see how specific the mechanism of action of a drug is. RNAi can knock down a target in a signal transduction pathway, and the effects on the pathway up- and downstream of the target can be seen." As part of Applied Biosystems, the company has field-based scientists worldwide, who provide technical support.

Sigma-Aldrich has design services for customized siRNA oligonucleotide sequences that are analyzed to reduce nontarget binding. It also provides a wide range of kinase and phosphatase reagents and kits as well as the individual enzymes, substrates, activators, and inhibitors. Similarly, **Qiagen** offers a portfolio of high throughput–tested siRNA sets in addition to providing custom siRNAs and controls. In addition to human and mouse sets against the whole genomes, druggable genes, and phosphatase and phosphatase-associated genes and kinases, Qiagen's newest products include siRNA against rat kinases, phosphatases, and phosphatase-associated genes. Its new FlexiPlate siRNA system allows custom selection of siRNAs targeting human and mouse genes along with controls, scales, and plate layout for efficient, economical screening with minimum off-target effects and maximal knockdown efficiency.

Driving Forces

As more information accumulates about cell signaling pathways, it will be crucial for researchers to be able to access databases and interactive pathways to see where their kinase of interest fits in the big picture. Combination technologies, too, will continue to drive research and development.

Lynne Lederman, Ph.D., is a freelance medical and science writer based in New York.

Featured Participants

Ambion

www.ambion.com

Applied Biosystems

www.appliedbiosystems.com

BD Biosciences

www.bdbiosciences.com

Biomol International

www.biomol.com

Cell Signaling Technology

www.cellsignal.com

EMD Biosciences

www.emdbiosciences.com

Innova Biosciences

www.innovabiosciences.com

Merck KGaA

www.merck.de

Millipore Corporation

www.millipore.com

Molecular Devices Corporation

www.moleculardevices.com

Pfizer

www.pfizer.com

Qiagen

www.qiagen.com

Roche Applied Science

www.roche-applied-science.com

Sigma-Aldrich

www.sigmaaldrich.com

Signal Transduction Knowledge Environment

www.stke.org

New Products

**Next-Generation Coulter Counter**

The Multisizer 4 Coulter Counter, the latest advancement in a long line of particle counting and sizing instruments, is designed to deliver an increased dynamic range. Its unique digital pulse processing provides size analysis results in real time. Originally developed to count blood cells, the Coulter Counter has a broad range of applications, from cells and bacteria to food and hydraulic fluids. The Multisizer 4 features new sample management technology to ensure reproducibility. The EZAccess fluid management system, software wizards, and automated functions improve ease of use and increase productivity. Software functions include an automated time stamp for real-time sample tracking and electronic blockage detection. The digital pulse processing scans and stores data for additional analyses and reporting.

Beckman Coulter

For information 714-993-8955

www.coultercounter.com

Cell-Based ERK1/2 ELISA

The dual-fluorescence PhosPho-ERK1/2 Cell-Based ELISA (enzyme-linked immunosorbent assay) is the first to measure total and phosphorylated proteins simultaneously in the same well, without the need for specialized equipment. Sample preparation is simple: Cells are grown, permeabilized, and blocked in the same 96-well plate. Primary antibodies against phosphorylated ERK1/2 or total ERK1/2, combined with species-specific horseradish peroxidase-conjugated or alkaline phosphatase-conjugated secondary antibodies and specific fluorogenic substrates allow for measurement using a standard fluorescence plate reader. Normalizing the fluorescence of phosphorylated ERK1/2 to total ERK1/2 makes it easy to account for well-to-well variations such as cell number.

R&D Systems

For information 800-343-7475

www.RnDSystems.com/go/CellBasedELISA

Protection from Phosphatases and Proteases

The combination of PhosSTOP Phosphatase Inhibitor Cocktail Tablets and cOMplete Protease Inhibitor Tablets can protect proteins from both phosphatases and proteases. PhosSTOP is a proprietary blend of phosphatase inhibitors that acts on a broad spectrum of acid and alkaline phosphatases, serine/threonine phosphatases, and tyrosine protein phosphatases. The cOMplete Protease Inhibitor Tablets inhibit serine, cysteine, and metalloprotease activity, and are available in tablets for either 10 ml or 50 ml of lysate, with or without ethylenediaminetetraacetic acid (EDTA). Both products are nontoxic and effective across a wide range of sample materials, including animals, plants, yeast, and bacteria.

Roche Applied Science

For information 317-521-2000

www.roche-diagnostics.us

Multiplexed Phosphorylation Analysis in Single Cells

BD Phosflow is an innovative flow cytometry-based technology that enables activation-state analysis of multiple proteins at single-cell levels. BD Phosflow reagents used in combination with cell surface markers make it possible to study phosphorylation events directly in small subpopulations of complex primary samples. The reagent line includes close to 100 directly conjugated phosphorylation-site-specific antibodies. A proprietary buffer system enables Phosflow analysis directly in whole blood samples. This technology not only boosts cell-signaling network analysis and high content secondary screening for drug discovery and

development, but also enables the identification of signaling pathway-dependent biosignatures for disease.

BD Biosciences

For information 877-232-8995

www.bdphosflow.com

Protein Interaction Analysis

Biacore X100 is a system for label-free protein interaction for multiproject life science research laboratories. This general purpose system, designed to be readily accessible to multiple users, includes state-of-the-art software that leads the user from preparation to result within a day. The Biacore X100 enables scientists to draw conclusions based on comprehensive characterization of how proteins interact with other molecules in real time. This single instrument can determine affinity and rate constants, binding specificity, concentration, and thermodynamic parameters of the interaction. It provides deeper understanding of molecular mechanisms and interaction pathways to determine protein functionality and elucidate disease mechanisms.

Biacore/GE Healthcare

For information +44 (0) 79 710 8311

www.biacore.com

Tyrosine Phosphorylation Discovery Tool

The PhosphoScan (P-Tyr-100) Kit features patented technology that enables investigators to identify hundreds of thousands of phosphorylated sequences and observe the state of protein tyrosine phosphorylation in cells and tissues. The PhosphoScan technology was recently used in the discovery of a novel activating mutation in the JAK3 kinase in acute myeloid leukemia cells. The method underlying the kit involves the specific enrichment of phosphotyrosine-containing peptides from protease-digested cell extracts using Phospho-Tyrosine Mouse mAb (P-Tyr-100) #9411 coupled to protein G agarose beads. Phosphopeptides eluted from the beads are subsequently identified by liquid chromatography/tandem mass spectrometry. Typically, several hundred phosphotyrosine sites from one sample can be identified in a single analysis, depending on the sample's phosphorylation level and the sensitivity of the mass spectrometer. Researchers at Cell Signaling Technology have used PhosphoScan to determine cellular phosphorylation profiles in hundreds of cell lines, xenografts, and primary human tumors.

Cell Signaling Technology

For information 978-867-2300

www.cellsignal.com

Classified Advertising



From life on Mars to life sciences

For full advertising details, go to www.sciencecareers.org and click on **For Advertisers**, or call one of our representatives.

United States & Canada

E-mail: advertise@sciencecareers.org
 Fax: 202-289-6742

IAN KING Sales Manager/Industry
 Phone: 202-326-6528

NICHOLAS HINTIBIDZE West
 Phone: 202-326-6533

DARYL ANDERSON Midwest/Canada
 Phone: 202-326-6543

ALLISON MILLAR Northeast/Southeast
 Phone: 202-326-6572

Europe & International

E-mail: ads@science-int.co.uk
 Fax: +44 (0) 1223 326532

TRACY HOLMES Sales Manager
 Phone: +44 (0) 1223 326525

CHRISTINA HARRISON
 Phone: +44 (0) 1223 326510

LOUISE MOORE
 Phone: +44 (0) 1223 326528

Japan

JASON HANNAFORD
 Phone: +81 (0) 52-757-5360
 E-mail: jhannaford@sciencemag.jp
 Fax: +81 (0) 52-757-5361

To subscribe to Science:
 In U.S./Canada call 202-326-6417 or 1-800-731-4939
 In the rest of the world call +44 (0) 1223-326-515

Science makes every effort to screen its ads for offensive and/or discriminatory language in accordance with U.S. and non-U.S. law. Since we are an international journal, you may see ads from non-U.S. countries that request applications from specific demographic groups. Since U.S. law does not apply to other countries we try to accommodate recruiting practices of other countries. However, we encourage our readers to alert us to any ads that they feel are discriminatory or offensive.



POSITIONS OPEN

DIRECTOR

The University of Southern Mississippi School of Ocean and Earth Sciences

The College of Science and Technology at the University of Southern Mississippi seeks a **DIRECTOR** for the School of Ocean and Earth Sciences (SOES).

The University of Southern Mississippi (USM), a Carnegie Doctoral/Research Extensive and a Southern Regional Education Board (SREB) Category 1 institution, is the only comprehensive university in the state that has dual-campus status (Hattiesburg and Long Beach). USM has several other teaching and research sites on the Mississippi Gulf Coast. The SOES was established in 2005, and comprises the academic Departments of Coastal Sciences (Ocean Springs), Geography and Geology (Hattiesburg), and Marine Science (Stennis Space Center) as well as the Gulf Coast Research Laboratory (Ocean Springs). For more information, see **websites:** <http://www.usm.edu/colleges/cost/> and <http://www.usm.edu/cost/soes.htm>.

The Director will guide development of a shared vision and a strategic plan for the future of ocean and earth sciences at USM that facilitates interactions among the diverse units of SOES. The Director will be an advocate for the School at local, regional, and national levels, including fundraising, and will promote diversity and interdisciplinary expertise. The Director will coordinate an integrated program of research, teaching, outreach, and service in support of the School's mission.

The successful candidate will have a Ph.D. and will be eligible for tenure in one of the academic disciplines within SOES and will demonstrate a record of achievement in research, extramural funding, and teaching, and will have strong administrative and supervisory skills. Qualified persons should submit a letter of intent, current curriculum vitae, and the names of three references who will be contacted only with the explicit permission of the candidate. Nominations are welcomed. Review of applications and nominations will begin May 1, 2007, and will continue until the position is filled. All correspondence will be held in confidence and should be mailed or e-mailed to: **Dr. Rex Gandy, Dean, College of Science and Technology, The University of Southern Mississippi, 118 College Drive, Number 5165, Hattiesburg, MS 39406-0001. E-mail: rex.gandy@usm.edu, telephone: 601-266-4883. Visit the USM website: <http://www.usm.edu>.**

The University of Southern Mississippi is an Equal Opportunity Employer; diversity is highly valued. Minorities and women are encouraged to apply. Affirmative Action/Equal Opportunity Employer/ADA.

FACULTY POSITIONS
 Pathology Research

The Department of Pathology at the University of Illinois at Chicago (UIC) College of Medicine is searching for candidates to fill two mid-senior level tenure-track/tenured positions at the **ASSISTANT, ASSOCIATE, or FULL PROFESSOR** level in its Research Division. Desirable candidates will have a Ph.D. in a biomedical field (or an M.D. with equivalent research experience), and a record of at least three years of productive research as an independent investigator. Hiring of two individuals who have worked together or have linked programs in the same area is possible. The Department has a research focus in cancer prevention and molecular epidemiology; however, investigators with interests outside of cancer will be considered. Preference will be given to individuals conducting research that involves human samples, or that has obvious near-term translational potential. Excellent new laboratory facilities, tissue resources, clinical collaborations, and infrastructure support are available. Rank and salary will be commensurate with qualifications. For fullest consideration, submit curriculum vitae and list of three references by May 1, 2007, to: **Dr. Peter Gann (e-mail: pgann@uic.edu), University of Illinois at Chicago, Department of Pathology, 840 S. Wood Street, Room 113 CSN, MC847, Chicago, IL 60612. UIC is an Affirmative Action/Equal Opportunity Employer.**

POSITIONS OPEN



FACULTY POSITION

Northwestern Feinberg School of Medicine Department of Neurology and Neuroscience

The Neuromuscular Disorders Program of the Department of Neurology announces a new search to recruit outstanding individuals for full-time, tenure-track appointments at the level of **ASSISTANT PROFESSOR**, depending upon prior experience and research accomplishments.

Applications will be considered in the areas of novel therapeutic applications to amyotrophic lateral sclerosis (ALS) or study of the biology of motor neurons.

The Ph.D. or M.D. appointees are expected to have demonstrated exceptional potential in either therapeutic approaches to ALS research or study of motor neurons. Responsibilities of the positions are to develop dynamic, independently funded research programs and to participate in medical, graduate, and postgraduate teaching. High-quality laboratory space and excellent startup support will be provided. Salary will be negotiable depending upon experience.

The appointees will have access to new state-of-the-art animal facilities and to shared facilities for tissue culture, cell imaging, transgenic and knockout projects, monoclonal antibodies, gene and protein micro-arrays, structural biology, and biotechnology.

Additional information about the Neuromuscular Disorders Program can be found on our web pages (**website:** <http://www.neurogenetics.northwestern.edu>). Applicants must include the following materials: (1) current curriculum vitae and list of publications, (2) brief statement of research interests (three pages or less), and (3) three letters of reference sent on their behalf to either: **John A. Kessler, M.D. (e-mail: jakessler@northwestern.edu)** or **Teepu Siddique, M.D. (e-mail: t-siddique@northwestern.edu)**, Co-Chairs, Amyotrophic Lateral Sclerosis Search Committee, Northwestern University, Feinberg School of Medicine, Ward 10-185, 303 E. Chicago Avenue, Chicago, IL 60611.

Please refer to academic search number P-128-06. Completed applications must be received by July 1, 2007. Appointments will commence on or after October 1, 2007.

Northwestern University is an Equal Opportunity/Affirmative Action Educator and Employer and invites applications from all qualified individuals. Applications from women and minorities are especially sought. Hiring is contingent upon eligibility to work in the United States.

CARDIOVASCULAR PHARMACOLOGIST

The Department of Veterinary Physiology and Pharmacology, College of Veterinary Medicine and Biomedical Sciences, Texas A&M University announces the availability of a tenure-track position for **ASSISTANT/ASSOCIATE PROFESSOR** in the area of pharmacology. A strong research program in cardiovascular science is desirable. A proven record in teaching is required. The successful candidate will be expected to contribute to a team-taught pharmacology course in the professional curriculum. Departmental faculty and their interests can be identified at **website:** <http://www.cvm.tamu.edu/vtpp>. Review of applications will begin immediately and continue until the position is filled. Candidates should send curriculum vitae, letter of application, and names and addresses of three references to: **Randolph H. Stewart, D.V.M., Ph.D., Department of Veterinary Physiology and Pharmacology, TAMU 4466 Texas A&M University, College Station, TX 77843-4466. Telephone: 979-862-7764, fax: 979-845-6544. E-mail: rstewart@cvm.tamu.edu.**

Texas A&M University is an Equal Opportunity Employer/Educator.

The Gerstner Sloan-Kettering Graduate School of Biomedical Sciences offers the next generation of basic scientists a program to study the biological sciences through the lens of cancer — while giving students the tools they will need to put them in the vanguard of research that can be applied in any area of human disease.

PhD Program

An Internationally Recognized Research Faculty in:

- Cancer genetics
- Genomic integrity
- Cell signaling and regulation
- Structural biology
- Immunology
- Chemical biology
- Developmental biology
- Computational biology
- Experimental therapeutics
- Experimental pathology
- Imaging and radiation sciences
- Oncology
- Genomics
- Animal models of disease

An Innovative, Integrated Curriculum Provides a Fundamental Understanding of:

- The nature of genes and gene expression
- Cellular organization
- Tissue and organ formation
- Cell-cell interactions
- Cellular response to the environment
- Enzyme activity

Student Support and Services:

Students receive a fellowship package that includes a stipend, tuition, textbook allowance, and health insurance. Students also have access to affordable housing within easy reach of the school.

Please visit our Web site to learn how to apply, for application deadlines, and for more information about our PhD program.

www.sloankettering.edu

gradstudies@sloankettering.edu | 646.888.6639



Gerstner Sloan-Kettering
Graduate School of Biomedical Sciences

New York City

MANY PATHS TO CHOOSE

Ask a cross-section of scientists how they got into cancer research, and you'll hear about a dizzying variety of routes from fields as diverse as biology, pharmacology, mathematics, and medicine. And with certain attributes – an inquiring mind, self-discipline, and a dash of ambition – it seems that there's no limit to what can be achieved.

By Julie Clayton

Cancer research has moved with the times, embracing new technologies enabling scientists to pursue more varied research goals than ever. Cancer researchers can find themselves in various settings linked to either academia or industry, working in many areas, from tackling basic questions in the laboratory to testing new drugs and vaccines in the clinic.

Many young scientists at the basic research end of the spectrum will admit that they were initially attracted more by the desire to investigate fundamental questions in biology than to work specifically on cancer. But they often then realize the importance and applicability of their work to understanding the underlying biological processes leading to cancer. From such understanding, new treatments can arise.

Laura Buttitta, for example, is a postdoctoral fellow at the Fred Hutchinson Cancer Research Center in Seattle. Armed with a Ph.D. in mouse embryology she was drawn by the center's top-class reputation for basic research. She is investigating the molecular switches that govern cell division – using fruit flies as a model system.

"I have to confess that I was more interested in how our cells work at the molecular level than in cancer research. But since coming to the Hutch, I've been able to attend [clinical research] seminars and have become more interested in that."

"The Hutch" is one of 39 comprehensive cancer centers across the United States designated as such by the National Cancer Institute at the National Institutes of Health (NIH). It brings together, under one roof, basic research into cancer at the cellular level, clinical research, and epidemiology – for studying the cause and prevention of cancer at the population level. It offers various research training and support initiatives, including internal postdoctoral awards, interdisciplinary training programs, and pilot startup initiatives that enable researchers to embark upon new projects that are too speculative initially to win short-term awards.

Cancer Research Competition Increases

In fiscal year 2005, The Hutch received more than \$10 million in funding from the National Institutes of Health – the world's largest cancer research funder. This is typical of the favorable status of cancer centers; their portion of NIH funds has risen by around 30 per cent in the past five years. On the surface, NIH spending appears to have increased significantly all-round over the past decade. The agency's total spending on cancer research rose from just over \$2 billion in fiscal year 1995 to almost \$5 billion in FY 2005. But taking inflation into account, actual spending by NIH on research has flattened over the past five years, including on cancer research. "Obviously, this has negatively impacted cancer research," comments The Hutch's chief financial officer Randy Main.

At the same time, competition has intensified: Since 1996, the number of grant applicants to the NIH has more than doubled, leading to a fall in the proportion of grants awarded, from 27 percent in 1996 to 19 percent in 2005. Researchers are turning instead to smaller funders. The Susan G. Komen Breast Cancer Foundation, for example, received more than four times its usual number of applications owing to cuts in NIH spending on breast cancer research, according to **Paula Witt-Enderby**, a researcher at Duquesne University in Pittsburgh and a member of the charity's grant review panel.

In Europe, spending on cancer research is highly variable from one **continued »**



©iStockphoto.com/Andreas

“You look down the microscope at the diversity of cancer and it makes you want to understand more.”



Paula Witt-Enderby

UPCOMING FEATURES

Careers for Postdoc Scientists: Transferable Careers — April 20

Biotech and Pharma — April 27

Interdisciplinary Research — May 4



Cancer Research Center of Hawai'i
UNIVERSITY OF HAWAII

The Cancer Research Center of Hawai'i, an NCI-designated cancer center, is embarking on a major expansion of its research programs. With dedicated funding from the State of Hawai'i through a tax on cigarette sales, the center is about to construct a state of the art 320,000 sq. ft. research and clinical care facility on the Honolulu waterfront. We plan to recruit tenure track faculty at the Assistant, Associate and Full Professor ranks in the following areas:

- **Associate Center Director for Clinical Affairs and Director of the Clinical Research Program.** This position requires an MD degree with board certification in an area of oncology. The successful candidate will have an extensive track record of extramural research funding, scholarly and scientific accomplishments, administrative responsibilities, and experience in clinical trials.
- **Clinical Sciences.** Multiple positions are available for clinical scientists at all ranks and in all areas of oncology.
- **Director of Cancer Prevention and Control.** An individual with national funding is sought to lead a program of behavioral research related to cancer prevention, detection and control. Candidates with an interest in tobacco control are particularly encouraged to apply but other areas will be favorably considered.
- **Cancer Prevention and Control.** Multiple faculty positions at all ranks are available for scientists with research interests in any area of cancer prevention and control.
- **Thoracic Oncology.** We are seeking several basic research or clinical scientists with nationally funded research in lung cancer, asbestos, mesothelioma or other thoracic malignancies. Individuals with research interests in environmental carcinogenesis and viral oncology are also strongly encouraged to apply.
- **Cancer Epidemiology.** We are seeking several individuals with a background in clinical or molecular aspects of cancer epidemiology to complement ongoing population research which takes advantage of the unique ethnic diversity of Hawai'i. Individuals at all ranks are encouraged to apply.
- **Biostatistics.** Multiple positions are available at all ranks for biostatisticians to support research projects and to conduct related methodological research.
- **Natural Products and Cancer Biology.** We are seeking scientists with research interests in fundamental molecular mechanisms of cancer cell biology and/or with an interest in the identification and development of novel anti-cancer agents.

Applicants should hold an MD and/or PhD or other doctoral degree. Strong preference will be given to applicants with nationally funded cancer research grants. We offer a highly interactive and multidisciplinary research environment, excellent startup packages and competitive salaries. For more information please see our website at www.crch.org or contact Alan McClelland PhD, Associate Director for Scientific Administration, at amcclelland@crch.hawaii.edu. Applications including a curriculum vitae and a statement of current and future research interests should be sent to facultyjobs@crch.hawaii.edu or Search Committee, Cancer Research Center of Hawai'i, 1236 Lauhala Street, Suite 510, Honolulu, HI 96813.

An Affirmative Action/Equal Opportunity Employer.

Ludwig Institute for Cancer Research
the global cancer institute

Group Leaders in Cancer Biology

The establishment of a new Branch of the Ludwig Institute for Cancer Research (LICR) in Oxford University will focus its research endeavours on cancer biology including suppressing tumour growth and preventing cancer metastasis. We are actively recruiting Research Group Leaders at the Assistant Member (Assistant Professor/Lecturer), Associate Member (Associate Professor/Senior Lecturer/Reader) and Member (Professor) levels.

The LICR Oxford Branch will be housed in a new state of the art building in the Institute of Cancer Medicine and be affiliated to the Nuffield Department of Clinical Medicine (NDM); part of the Medical Sciences Division, University of Oxford. The LICR is a global non-profit organization with nine Branches and numerous Affiliates worldwide.

As an LICR faculty member, you will enjoy the benefits of being a distinctive part of a dynamic local environment at a world-class university, and also of belonging to an internationally recognized Institute that is actively pursuing the translation of its research discoveries into applications for human benefit.

For further details about these positions and how to apply, please email Sarah Barnsley, sbarnsley@ludwig.ucl.ac.uk, quoting ref – oxf-sci. The closing date is Monday 30th April 2007.



www.licr.org

The Ludwig Institute for Cancer Research is an Equal Opportunity Employer. All qualified applicants will receive consideration for employment without regard to race, color, religion, sex or national origin.

Vice Chair for Clinical Research Substance Dependence

An open-rank research faculty position is now available at Montefiore Medical Center, The University Hospital for the Albert Einstein College of Medicine.

We seek an M.D. with the ability to maintain an active, extramurally funded program in medications development for substance dependence disorders; build a Research Division; and, ultimately, establish a Center. Our hospital network oversees treatment of some 5,000 patients with substance dependence disorders.

The successful candidate will have an appointment in the Department of Psychiatry and Behavioral Sciences.

A highly competitive salary and a generous start-up package will be available. Send curriculum vitae and statement of research interests to: **T. Byram Karasu, M.D., Silverman Professor & the University Chairman, Department of Psychiatry & Behavioral Sciences;** e-mail: karasu@aecom.yu.edu. We are an equal opportunity employer.

MONTEFIORE

Better. Believe it.
www.montefiore.org/careers

MONTEFIORE
Medical Center
The University Hospital for the
Albert Einstein College of Medicine

country to another. The UK spends the most, and has seen around a 9 percent growth in cancer research funding over the past five years – supported mainly by charities – with £343 million spent in 2005 by the partners of the UK's National Cancer Research Institute. According to **Michael Stratton**, director of the Cancer Genome Project at the Wellcome Trust Sanger Institute in Cambridge, UK, Europe has a lot to offer, and it is “to be expected” that postdoctoral researchers will move from one country to another to gain experience. Stratton arrived at his position originally from a clinical background. He made such a leap after specializing in pathology at the Hammersmith Hospital in London. “It brought me closer to the scientific basis of disease – you look down the microscope at the diversity of cancer and it makes you want to understand more. I always wanted to do research, but it was a rude shock not to go back to medicine.”

Top-level cancer research institutes around Europe are now thriving, including The Netherlands Cancer Institute (NKI), Amsterdam; CNIO in Madrid; the Radium Institute, Oslo; The Karolinska Institute, Stockholm; the Marie Curie and Gustav Russett Institutes in Paris; the World Health Organization-funded IARC in Lyon; and the German National Cancer Institute (DKFZ) in Heidelberg. Each of these institutes has something unique to offer, drawing excellent local researchers as well as exceptional international scientists.

Translational Potential

Rather than focus on basic cancer research, many investigators are moving into the burgeoning area of translational research, taking basic developments toward the clinic. Witt-Enderby at Duquesne is using her expertise in molecular pharmacology to study the effects of melatonin on a mouse breast cancer model. She is now in discussions with the University of Pittsburgh about starting a small clinical trial. “It’s a very big therapeutic strategy, and I just love it that all this research on signaling and how a cell works is finally paying off,” she says.

Witt-Enderby enjoys the academic setting as well as her mentoring role toward graduate students. She notices, too, that increasing numbers of graduate students show a specific interest in cancer research. “They read about it or they know someone who has had cancer. They want to know how drugs work and how to apply that to cancer.”

Witt-Enderby is on the grant review panel for the Susan G. Komen Breast Cancer charity, which is placing greater emphasis on translational research, and a corresponding increase in suitable bids. “We’re starting to see that bridging. I’ve read so many grants where you see M.D.s teamed up with Ph.D.s.” Other fund-holders are also encouraging the trend, including the biggest of them all, the U.S. National Cancer Institute.

In Europe, a similar boon is occurring, with increasing numbers of scientists becoming involved in running clinical trials. **Fran Balkwill**, head of the London-based Translational Oncology Laboratory of Cancer Research-UK, sums up the mood: “We’ve learned so much in the past 25 years but



“It’s the only way forward – to have tight collaboration and mutual respect between clinicians and scientists.”

—Fran Balkwill

we can’t just spend the next 25 years finding out more. We can and should tackle the big divide between what we know and what we can do for those patients on the ward.”

Balkwill’s first clinical trial starts later this year, based on developments in her laboratory. She will be using therapeutic antibodies to dampen the inflammation around ovarian tumors. This, she hopes, will enable “the good guys” – cells of the immune system – to specifically attack and destroy tumors.

Her lab is embedded within a cancer center, which allows closer contact between scientists and clinicians, and which offers several advantages, including an improved flow and quality of tissue samples from clinic to laboratory and greater commitment from doctors. “It’s the only way forward – to have tight collaboration and mutual respect between clinicians and scientists,” she says.

Back in the US, and further along the translational pipeline is **Doug Lowy**, of the NIH in Bethesda, Maryland, who has already experienced the potential of harnessing basic research for clinical use. He has devoted the past 20 years to studying human papilloma viruses (HPV), including their ability to cause cancer of the cervix. This includes the development of the HPV-based vaccines now licensed to GlaxoSmithKline and Merck for the protection of women against this disease. Lowy’s next goal is to develop a second generation of vaccines that can be produced more easily and cheaply, making them more available for use in developing countries, and active against a broader range of HPV strains than the currently approved versions.

Many of Lowy’s former graduate students, postdocs, and clinical fellows have moved on to prominent cancer research positions in academia and industry. He attributes their success to a combination of skills and qualities, including initiative, curiosity, technical and

intellectual abilities, and last but not least, self-discipline. “There are many brilliant people who are not successful as scientists because they don’t focus, or are not innovative, or do not have sufficient technical skills. And you need patience, because it takes a long time to achieve anything meaningful.”

Industry Beckons

Biotechnology companies are eagerly promoting translational cancer research. Two years ago, **Keith Luhrs** moved to Peregrine Pharmaceuticals after completing his first postdoc at nearby University of California, Irvine. He is now developing antibody-based therapeutics for cancer and other diseases. “I was looking for something a bit more applied. Having that goal of **continued** »

Cancer Research UK
www.cancerresearchuk.org

Duquesne University
www.duq.edu

Exelixis, Inc.
www.exelixis.com

Fred Hutchinson Cancer Research Center
www.fhcrc.org

National Cancer Institute
www.cancer.gov

Peregrine Pharmaceuticals
www.peregrineinc.com

The Wellcome Trust Sanger Institute
www.wellcome.ac.uk

Cancer Research UK Career Development Fellowship and Senior Cancer Research Fellowship

Would you like to work with one of the world's leading cancer research organisations? Can your research be relevant to preventing, diagnosing or treating cancer? Are you aiming to become a leader in your field? Cancer Research UK is committed to developing the next generation of leaders in all areas of cancer research. If this is the opportunity you are looking for then our fellowship schemes can help you achieve your goals.

Career Development Fellowship

We will provide:

- 6 years support
- Salaries for you, a post-doctoral researcher and a technician
- Consumables costs and equipment

About you:

- You are a promising post-doctoral scientist who wishes to achieve independence in your research for the first time
- You have developed a strong track-record of research
- You have between 3 and 6 years of postdoctoral research experience
- You will not have previously run your own research group. However, you are now ready to step up and direct a small programme of work

Senior Cancer Research Fellowship

We will provide:

- 6 years support
- Salaries for you, 2 post-doctoral researchers, a technician and a student
- Consumables costs and equipment

About you:

- You are an outstanding scientist who wishes to develop your independence
- You have shown exceptional ability in your previous work
- You have between 6 and 10 years of postdoctoral research experience
- You may already be running your own research group. You may even hold a tenured position. We would still be interested in hearing from you, as long as you have been doing this for no more than six years

Cancer Research UK is also keen to support the broader development of its fellows, through opportunities for training and regular fellows' meetings.

You must check your eligibility for these awards on our website at: fellowships.cancerresearchuk.org You will also find the application forms and information about recently appointed fellows here.

The deadline for preliminary applications is Friday 8 June 2007.

If you would like to discuss your application for any of these fellowships, or have any other questions, please contact Dr Matthew Wakelin at matthew.wakelin@cancer.org.uk or call 020 7438 5333.

Charity no: 1089464

CANCER RESEARCH UK



Harold M. Weintraub Graduate Student Awards – 2007

The Fred Hutchinson Cancer Research Center congratulates the following recipients of the 2007 Harold M. Weintraub Graduate Student Award in recognition of outstanding achievement during Graduate Studies in the Biological Sciences.

Sung Hee Ahn-Upton
Rockefeller University

Michael A. Crickmore
Columbia University

Ellen Ezratty
Columbia University

Douglas Fowler
Scripps Research Institute

Goarav Gupta
Cornell University Medical College

Gianna Hammer
University of California, Berkeley

Seyun Kim
Johns Hopkins University School of Medicine

Carolyn Phillips
University of California, Berkeley

Zachary Pincus
Stanford University

Scott Tomlins
University of Michigan

Omer Yilmaz
University of Michigan

Hui Zhu
Case Western Reserve University

The recipients will participate in a Symposium this spring honoring Hal Weintraub and his commitment to innovative science. More information on this award can be found at: <http://www.fhcr.org/science/basic/weintraub>



The Leukemia & Lymphoma Society
Fighting Blood Cancers

The Leukemia & Lymphoma Society's Research Grant Program is based on the belief that scientifically sound research toward the cure or control of leukemia, lymphoma, and myeloma should be encouraged on a worldwide basis. The Society supports basic laboratory research and its application in clinical settings. The Society's Research Grant Programs include:

Career Development Program: Stipend support for basic and clinical investigators at the level of Scholar, Special Fellow and Fellow.
Deadlines: Preliminary Application (submit via website) - **September 15**; Full Application - **October 1**

Specialized Center of Research Program: Support for team-based projects that are interdisciplinary, cohesive, and sharply focused.
Deadlines: Preliminary Application (submitted via website and hard copy) - **November 1**; Full Application (by invitation only) - **March 15**

Translational Research Program: Funding for projects that translate laboratory findings to clinical application.
Deadlines: Preliminary Application (submitted via website) - **March 1**; Full Application - **March 15**

Guidelines are available at: www.LLS.org



Cell and Molecular Biology

Postdoctoral Fellowship Award from the Francis Golet Charitable Lead Trust, at the Sidney Kimmel Cancer Center in San Diego

We are pleased to offer a 3-year Francis Golet Postdoctoral Fellowship in the laboratories of **Drs. Robert Margolis and Rati Fotodar** at the Sidney Kimmel Cancer Center. SKCC is one of the few centers nationwide to have been honored to offer this prestigious award. The applicant will have the opportunity to study mechanisms of mitotic exit and cell cycle checkpoints in mammalian cells. The Golet Fellowship is intended for outstanding candidates with exceptional profiles and leadership qualities. The candidates will receive generous remuneration and will work in the newly constructed research facility on the 10-acre SKCC campus in the middle of the densest concentration of health science research institutes and companies in the United States. The Francis Golet Fellow will have available state-of-the-art techniques and equipment in cell and molecular biology and of the Drug Development Core at the SKCC.

Please send c.v. with recommendations to: **Dr. Albert Deisseroth, Chair, Golet Fellow Search Committee, Sidney Kimmel Cancer Center-PDGS, 10905 Road to the Cure, San Diego, CA 92121; humanresources@skcc.org.**

EOE

Keith Luhrs, Missag Parsaghian

“If you step into the right small company you will end up having to sharpen your skills in a wide variety of the life sciences.”
—Missag Parsaghian



something that is useful for human disease is definitely a driving force. I wanted to get things done at a faster pace, and make something beneficial.”

What also attracted Luhrs was the prospect of honing many skills. “In a given week I’ll do cell culture, protein chemistry, molecular biology, microscopy, and structural biology on the computer,” adds Luhrs.

“If you step into the right small company you will end up having to sharpen your skills in a wide variety of the life sciences,” adds **Missag Parsaghian**, Peregrine’s director of research and development.

New technologies have enabled a whole slew of biotech companies to form in recent years. Lexicon Genetics of Houston, Texas, for example, grew from the use of mouse embryonic stem cell technology to create mouse models of disease. Its founder, **Allan Bradley**, was at the time based at the M.D. Anderson Cancer Research Center in Houston, Texas, and now heads the world’s largest mouse genetics program at the Wellcome Trust Sanger Institute, which has a strong cancer component. Many of his original team took up positions with Lexicon Genetics.

“There has been a significant trickle of people who’ve gone to industry from my lab,” Bradley said. “They had unique skills that industry did not have and they could get very lucrative salaries. I’ve had people who’ve gone to Merck, Pfizer, either into the laboratory or into management and business.”

Bradley himself resisted the lure of industry, preferring instead the academic freedom of his current position. This enables him to make his resources – embryonic stem cell lines and mouse models – freely available to researchers outside the institute. He also prefers the idea of having greater control of his research. “In a company you’re not in charge of your own destiny. Projects come and go. If the company decides it, a project ends,” he says.

Such sudden changes of direction in industry are something that **Steve Gendreau**, a cell biologist and project leader at Exelixis in South San Francisco, has experienced five times in the past nine years. But rather than give up, he supports the change as necessary for keeping his company’s R&D portfolio moving toward a successful product. “These projects can feel like your own children. It’s sometimes difficult to say goodbye. But the pragmatic view is that the ability to remain flexible is absolutely key – we have to move people from one project to another,” he says.

One of the trade-offs, he adds, is avoiding what some see as the hang-ups of academia. “I am not required to teach classes, write grants, or oversee graduate committees. I am paid to do what I love: discover life-changing cancer therapeutics.”

Part of this involves developing assays for assessing the activ-

ity of new anticancer compounds. These are aimed specifically at pathways involved in either the initiation and progression of cancer or its resistance to conventional drugs. One successful compound, named Exel 647, that targets nonsmall-cell lung cancer in previously untreated patients is now in a phase 2 clinical trial.

Right Person for the Job?

As for personal qualities, it is perhaps no surprise that cancer researchers have much in common with other scientists. Bradley emphasizes the importance of academic knowledge. “You need a deep and broad knowledge, very good molecular biology skills, and the ability to generate ideas.” He also emphasizes the need for speed in translating ideas into results by being technically competent so as to be able to perform experiments “quickly and efficiently ahead of someone else who’s going to compete with you on that idea.”

Witt-Enderby prizes students and postdocs with an open mind and a willingness to read about topics as diverse as molecular biology, endocrinology, drug mechanisms, pharmacology, and biostatistics. “Because mine is a very interdisciplinary lab you have to learn so much. You have to know a lot because out of that will come a very good answer to a research question.”

Stratton often recruits graduate students and postdocs with an inclination toward bioinformatics, who can organize and process data from genomewide screens, and improve high throughput DNA sequencing and analysis. On top of this, he values the involvement of trained bioinformaticians to be “roaming wild and free through all our data to find something interesting, not constrained by goals and targets.”

The Future of Cancer Research

Looking ahead, cancer research looks set to thrive – particularly in the translational research arena and the development of new therapeutics.

“This is one of the most exciting times in cancer research. I believe that the next 10 years is going to be a golden age,” says Gendreau. This is partly due to what he describes as “a more sophisticated view that these cancers are similar in their molecular footprint – in the pathways that have caused them to become tumorigenic.” New drugs targeting these pathways may be useful against a variety of different cancers.

In turn, Parsaghian of Peregrine Pharmaceuticals predicts that antibody-based therapeutics – and diagnostics – will continue to be a growth area in cancer research, together with other protein-based biological agents and stem cell technology.

The excitement over translational research is tempered, however, by the need to maintain “a balanced portfolio” between blue-sky research and clinical studies, according to Balkwill. “You still need the basic research, because there’s still a lot to learn, and you need clinical trials. But you also need this not-so-well-developed in-between world,” says Balkwill.

“It’s just as important that people do basic science,” agrees Witt-Enderby. “If you have to show that everything has translational potential within a short space of time, then you would lose out.”

Julie Clayton, a freelance science writer and journalist, works out of Bristol, UK.



Abraham A. Mitchell

Distinguished Clinical Cancer Investigator Awards

The USA Mitchell Cancer Institute (USAMCI) at the University of South Alabama (USA) invites nominations and applications of highly qualified, clinically active physician-scientists for senior faculty positions in oncologic sciences and interdisciplinary clinical oncology within the USAMCI. A successful candidate will bring to the USAMCI an established, well-funded research program, and will receive from the USAMCI a research expansion funding award in the aggregate total of \$1,000,000 over a 3-5 year time period, with the goal of further growing the individual's and the institution's research grant funding base and enhancing translational research links both within and external to the USAMCI. Funds from the award may be used for partial salary support for the awardee (research time only) and/or member(s) of his/her research team, materials and supplies, other operational expenses and/or equipment. Awardees will be expected to participate in the Institute's interdisciplinary clinical services not to exceed 2 days/week, with the balance of time devoted to research. Preference may be given to candidates whose research and/or clinical specialty interests are most complementary to existing or planned future USAMCI programs. Appointees to these positions will receive highly competitive salary and benefits, and academic rank commensurate with training, experience and accomplishments.

Faculty Positions in Cancer Research

The University of South Alabama Mitchell Cancer Institute (USAMCI) is seeking highly qualified candidates for cancer research faculty positions at all ranks. Preference may be given to candidates whose research background and expertise complement current or future thematic areas of emphasis within the USAMCI including genomics and gene expression, proteomics, developmental therapeutics, molecular pathology and diagnostics, metastasis research and molecular oncology. The positions will be filled with researchers capable of establishing cutting-edge, core technologies and independent research projects in the respective fields, providing collaborative core research support for other investigators within the USAMCI, and achieving/maintaining self-sufficiency through peer-reviewed external funding. The USAMCI is being organized and developed to facilitate highly interactive research involving laboratory and clinical investigators, and unique collaborative opportunities between experts in different fields. Appointees to these positions will have attractive start-up resources and compensation, and academic rank commensurate with training, experience and accomplishments. Appointees will have dedicated space within a new state-of-the-art interdisciplinary basic/translational research and clinical facility scheduled for completion in 2007.

The USAMCI is ideally located in Mobile, AL, a progressive, mid-sized port city of rich cultural history, in the beautiful upper Gulf coastal region. Moderate climate, abundant outdoor recreational opportunities, low cost-of-living and a "college-town" atmosphere all contribute to a high "quality-of-life" opportunity.

Applicants please send letter of interest and curriculum vitae to: **Office of the Director - USAMCI, 307 N. University Blvd., MSB 2015, Mobile, AL 36688** or e-mail sallen@usouthal.edu.

The University of South Alabama is an Affirmative Action and Equal Opportunity Employer.

COME SEE US AT AACR BOOTH 845

(osi) pharmaceuticals

Shaping Medicine, Changing Lives

OSI scientists have turned early research opportunities into medical advances that focus on the needs of patients. If you are a bench scientist with excellent communication skills and strong knowledge of cell biology, join our Cancer Biology group and work in our fast-paced team oriented environment.

Research Scientist

Scientists with excellent molecular biology skills are sought to generate clones and stable cell lines for EMT models. Candidates must possess a Ph.D. with 0-3 years post-doc experience, or an MS with 10+ years of relevant industry experience in cell and molecular biology. An understanding of different methods of cell line generation, gateway cloning and lentiviral systems are required. Must have working knowledge of Vector NTL. **Ref # FA00129**

Research Scientist

Scientists with strong cell biology and microscopy skills are invited to design, develop and implement cell-based 2D and 3D EMT models used to study the impact of small molecule inhibitors on the epithelial to mesenchymal transition. A Ph.D. with 0-3 years post-doc experience in EMT biology, confocal microscopy along with an excellent publication record and proven ability to engage in collaborative research efforts are required. Knowledge of cell signaling pathways as it relates to oncology is a plus. **Ref # ME00190**

OSI offers excellent salaries and benefits including 401K, vacation, stock and much more. **Interested candidates, please apply online at <http://careers.osip.com>.** Please include ref#. EOE M/F/D/V.

POSITIONS OPEN

The Weizmann Institute of science

will award a limited number of

Distinguished Postdoctoral Fellowships

Known as

Koshland Scholars

The fellowships are available in all the fields of scientific research that are pursued at The Weizmann Institute in the following areas:

**Biology, Chemistry, Computer Science, Physics,
Mathematics, Biochemistry**

All courses and seminars at the Institute are conducted in English.

Applications may be submitted at any time, but the awards will be made shortly after the usual deadlines for the submission of Fellowship applications: January 5 and May 15 of each year. Candidates for Koshland fellowships must be sponsored by a Faculty Member of the Weizmann Institute. Interested candidates are advised to contact prospective sponsors directly.

For additional information and application forms, consult the Feinberg Home Page at <http://www.weizmann.ac.il/feinberg> or write to: Postdoctoral Fellowship Program, The Feinberg Graduate School, The Weizmann Institute of Science, Rehovot 76100, Israel; Fax: 972-8-934-4114; e-mail: postdoc@weizmann.ac.il

The Weizmann Institute of Science invites outstanding Ph.D. students at universities abroad who are nearing graduation (or who have recently completed their Ph.D. studies) to visit the Institute for a few days, meet its scientists, explore postdoctoral research opportunities, and experience its warm and relaxed atmosphere. A limited number of such visits are subsidized by the Institute on a competitive basis. Those who are invited are under no obligation to the Institute to continue their postdoctoral studies here. For more details, see http://www.weizmann.ac.il/feinberg/student_visit



Science For A Better Life



HealthCare

www.myBayerjob.com

Lucia Rosano wants to make the world a better place - for everyone. As a bioscientist at Bayer, Lucia knows she is doing just that. Searching for solutions and never giving up. That is the passion that unites all of us at Bayer. We call it the Bayer Spirit. If you feel it, too, then it is high time we had a chance to talk about a career at Bayer.

Postdoctoral Research Scientist (m / f)

Responsibilities The Target Discovery group at Bayer HealthCare in Wuppertal, Germany offers a three year Postdoctoral Research Scientist position funded by the Marie Curie Research Training Network.

The project is to identify changes in chromatin plasticity during heart failure.

Qualification The candidate will have a PhD and be highly motivated with qualifications in molecular/cellular biology and in vivo pharmacology. A good knowledge in the area of expression profiling using chip technology, primary cell cultures, RNAi gene knock down and cardiovascular pharmacology would be desirable. Good communication and organizational skills are also essential, along with the ability of writing reports and publications for international journals, present and disseminate project results in national and international meetings.

Your application If you are interested in the above position, please apply online, quoting box number 0000000480 and attaching the relevant documents. Please also indicate your salary expectations and the earliest possible date on which you could take up employment. Visit the website www.chromatin-plasticity.org for more information on the Marie Curie Research Training Network and www.bayerhealthcare.com for information on Bayer HealthCare.

www.myBayerjob.com

Phone +49 214 30 99 777



NIEHS
National Institute of
Environmental Health Sciences
National Institutes of Health

Senior Investigator in Bioinformatics Research Triangle Park, North Carolina

Biostatistics Branch – The NIEHS in Research Triangle Park, North Carolina, is seeking a senior investigator in Bioinformatics/Computational Biology to assume directorship of a Bioinformatics Section in the Biostatistics Branch, Environmental Diseases and Medicine Program, Division of Intramural Research. NIEHS is one of the National Institutes of Health. The incumbent will develop and direct a strong research group to carry out independent and collaborative research in the general area of bioinformatic and computational biology, particularly as related to biological networks, analysis of high-dimensional data, proteomics, comparative and functional genomics, gene expression, and epigenetics. This work will provide a bioinformatic infrastructure and innovative data mining approaches to advance intramural research aimed at understanding biological responses to environmental stressors, in the context of cell biology, animal experimentation, clinical research and epidemiology.

A Ph.D. or equivalent degree is mandatory. The ideal candidate is a senior investigator with an international reputation in a specific area within the broad context of bioinformatics and a genuine passion for science. Possible research backgrounds include but are not limited to mathematics, computational biology, physics, statistics, genetics, biochemistry, bioinformatics, bioengineering and molecular biology. The successful candidate will have an outstanding

publication record and proven history of research leadership. Salary is commensurate with experience and level of accomplishments.

Applications from women and members of minority groups are particularly welcome. To apply, submit a curriculum vitae, bibliography, brief statement of research interests and arrange for three letters of recommendation to be sent by **June 15, 2007**, to the below address. Applications received after that date will be considered as needed.

Ms. Barbara Curtis (DIR07-03)
National Institutes of Health
National Institute of Environmental Health Sciences
P.O. Box 12233, Maildrop A2-06
111 T.W. Alexander Drive, Room A235
Research Triangle Park, NC 27709
E-mail: dir-appls@niehs.nih.gov

<http://www.niehs.nih.gov>

DHHS and NIH are
Equal Opportunity Employers



U.S. Department of Health and Human Services
National Institutes of Health

Postdoctoral, Research and Clinical Fellowships at the National Institutes of Health

www.training.nih.gov/pdopenings

www.training.nih.gov/clinopenings

Train at the bench, the bedside, or both

Office of Intramural Training and Education
Bethesda, Maryland 20892-0240
800.445.8283



HEALTH SCIENTIST ADMINISTRATOR National Institute of General Medical Sciences Cell Biology and Biophysics Division

The National Institute of General Medical Sciences (NIGMS), a major research component of the National Institutes of Health (NIH) and the Department of Health and Human Services (DHHS), is seeking applications from exceptional scientists to serve as **Chief of the Biophysics Branch in the Division of Cell Biology and Biophysics Division**. The Biophysics Branch supports major research grant programs in such areas as physical and chemical studies of proteins and nucleic acids, structural analyses of macromolecules, development of physical techniques for the analysis of molecular structure and function, and theoretical approaches to molecular biophysics. The Institute is seeking an individual with scientific, administrative, and leadership credentials who can manage individual grant programs in biophysics as well as serve as Chief of the Biophysics Branch. Information about the Division of Cell Biology and Biophysics can be found at: <http://www.nigms.nih.gov/About/Overview/CBB.htm>

Qualifications: The successful individual will possess a Ph.D., M.D. or equivalent degree in a field relevant to the position, have research experience in biophysics, biochemistry or related fields, an in-depth knowledge of biological processes, leadership and managerial skills, and strong oral and written communication skills. Applicants must be U.S. citizens.

Salary: The current salary range is \$110,363 – 143,471, depending on experience and accomplishments; a full Civil Service package of benefits (including retirement, health, life and long term care insurance, Thrift Savings Plan participation, etc.) is available. Recruitment or relocation incentive may be awarded and moving expenses will be paid.

How to Apply: Position requirements and detailed application procedures are provided in vacancy announcement NIGMS-07-172576, which can be obtained by accessing the NIGMS website at <http://www.nigms.nih.gov>. All applications and supplemental information must be received no later than **April 16, 2007**. For additional information, contact **Ms. Eric Bandak at (301) 594-2035**.



Help Us Help Millions

Are you ready for an exciting career that could help improve millions of lives around the world?

Then consider joining the scientific and medical forces at the National Institute of Allergy and Infectious Diseases (NIAID). NIAID supports and conducts basic, applied and clinical research to better understand, treat, and prevent some of the world's most deadly diseases. The Division of Microbiology and Infectious Diseases (DMID), an extramural research division of NIAID, supports extramural research related to the control and prevention of diseases caused by virtually all human infectious agents (over 250 pathogens) except HIV. DMID has the following scientific opportunities available:

Chief, Office of Clinical Research Affairs (OCRA)

As the Chief of OCRA, DMID, the selected candidate will provide scientific/medical leadership and direction for the planning, implementation, management, and evaluation of a broad, coordinated national/international program that deals with critical biomedical research issues. In this capacity, has oversight, provides medical information and resolves critical medical issues related to the study design, safety/efficacy, monitoring and data analysis of clinical trials. The Chief of OCRA determines the programmatic structure of the Branch; establishes priorities for new clinical trials program initiatives; oversees medical/scientific liaison with the FDA, other government agencies and pharmaceutical companies. Candidates must have a Doctor of Medicine or Doctor of Osteopathy. The selected candidate will have experience in the methodology, design, implementation, monitoring and assessment of clinical research trials, providing scientific/medical leadership and direction for the planning and management of a national/international program and demonstrated expertise in oral and written communication. Experience in Regulatory Affairs, Vaccine Development, and International Studies is desirable.

This vacancy is being advertised under the Title 5 and Title 42 hiring authorities. Salary is commensurate with experience and accomplishments.

Title 5 vacancy: Applicants must be a U.S. citizen. To apply for this vacancy, please visit <http://usajobs.opm.gov>. Vacancy number: NIAID-07-170767-DH. Specific application procedures apply and applications must be submitted to a Human Resource Specialist.

Title 42 vacancy: Non-citizens may apply. Please submit curriculum vitae/bibliography and three letters of reference to Denise Blackwell, 6610 Rockledge Drive, Room 6015, Bethesda, MD 20892 or electronically to dblackwell@niaid.nih.gov. You may direct inquire to Denise Blackwell at dblackwell@niaid.nih.gov or 301-402-5598.

Deadline for receipt of all applications is **April 27, 2007**.

Program Officer

As part of DMID, the Parasitology and International Programs Branch (PIPB) is responsible for planning and conducting programs of extramural research aimed at understanding the biology of protozoan and helminth parasites and their interaction with the human host as well as their vectors and intermediate hosts. As a Program Officer for PIPB, the selected candidate will provide leadership and scientific/medical expertise and guidance in the planning, development, implementation and evaluation of basic and clinical research concepts, projects and initiatives to appropriate advisory groups; identify opportunities and problem areas, research gaps and relevant program needs and make recommendations for and facilitate new research efforts, clinical studies, clinical trials or other initiatives; and communicate with grantees/contractors, cooperative group members/representatives and others on policy interpretation, merit review and evaluation processes and procedures, and on decisions, concerns or other issues/matters of a medical/scientific nature. In order to be considered for this position, applicants should have experience in basic and/or clinical research to examine the causes, diagnosis, treatment and prevention of infectious diseases; research experience in bacteriology, mycology, virology, or parasitic and other tropical diseases, is required. Candidates with a Ph.D. and relevant experience are highly desired.

To apply for this vacancy, please visit <http://usajobs.opm.gov>. Vacancy number: NIAID-07-170616-DE and NIAID-07-170616-MP. Salary: \$79,397-\$121,967. Specific application procedures apply. Applications must be submitted to a Human Resource Specialist by **May 4, 2007**.

A full Civil Service package of benefits (including retirement, health, life and long-term care insurance, Thrift Savings Plan participation, etc.) is available for both positions.

We invite you to explore our Institute and other available opportunities at <http://healthresearch.niaid.nih.gov/dms>



Department of Health and Human Services
National Institutes of Health
National Institute of Allergy and Infectious Diseases

Proud to be Equal Opportunity Employers

A*STAR INVESTI

in **BIOMEDICAL SCIENCES** and



Prestigious research award for outstanding

Biomedical Sciences

Candidates are invited to apply in the following areas: **molecular and cell biology, genetics and genomics relevant to human diseases and health.**

The **A*STAR Investigatorship Selection Panel** is composed of:

Professor Tadataka Yamada, President, Global Health Program, Bill and Melinda Gates Foundation

Professor Edward Holmes, Executive Deputy Chairman, Translational and Clinical Sciences, Biomedical Research Council, A*STAR; Executive Chairman, National Medical Research Council, Singapore

Professor Sir David Lane, Executive Deputy Chairman, Biomedical Sciences and Technology, Biomedical Research Council, A*STAR; Executive Director, Institute of Molecular & Cell Biology, A*STAR

Professor Alex Matter, Director, Novartis Institute for Tropical Diseases

Professor Axel Ullrich, Programme Director, Singapore OncoGenome Laboratory, Institute of Medical Biology, A*STAR; and Managing Director, Max Planck Institute of Biochemistry

Singapore's Agency for Science, Technology and Research (A*STAR) invites applications for the **A*STAR Investigatorships** which will support and promote the early independent career development of potential leaders in biomedical science, physical science and engineering research. Interested applicants should have obtained their PhD or MD within 24 months (not more than 48 months) of the application date, and should have demonstrated strong ability and creativity in research.

The award supports **independent** research for a duration of 3 years and is renewable for a further 3 years. The **Investigatorships** will be tenable at A*STAR's prestigious biomedical research institutes or physical science and engineering research institutes depending on the field of specialization. **A*STAR Investigators** may select a mentor from A*STAR research institutes



A*STAR INVESTIGATORSHIPS (Biomedical Research Council)

Agency for Science, Technology & Research,
20 Biopolis Way, #08-01, Centros Singapore 138668
Email: A-STAR_ADMIN_BMRC@a-star.edu.sg
www.a-star.edu.sg/astar_investigators

GATORSHIPS

PHYSICAL SCIENCES & ENGINEERING



young scientists and engineers

but will conduct and publish their research independently.

A*STAR Investigators will receive attractive remuneration, support for set-up costs, research funding, research staff and have access to state-of-the-art scientific equipment and facilities. Each **A*STAR Investigator's** laboratory would be funded up to US\$500K per annum.

Applications will close on **31 May 2007**. Up to 10 shortlisted candidates will be invited to Singapore for interviews and review based on a scientific presentation, expected to be held in **August 2007**.

Applicants are requested to submit their CVs, including 3 academic referees, and a 5-page research proposal (1 hard copy & 1 soft copy) to the respective research council:

Physical Sciences & Engineering

Candidates are invited to apply in the following areas:
• nanoscience and quantum-based systems • organic electronics • clean energy technologies

The **A*STAR Investigatorship Selection Panel** is composed of:

Professor Charles Zukoski, Chairman, SERC, A*STAR and Vice Chancellor for Research, University of Illinois at Urbana Champaign

Lord Ronald Oxburgh, member of the UK House of Lords Select Committee on Science & Technology and former Chairman, Shell

Dr Christian Joachim, CNRS, France

Professor Mark Kryder, Carnegie Mellon University and former CTO, Seagate

Professor Richard Syme, Microsystems Technology, EEE Department, Imperial College

A*STAR INVESTIGATORSHIPS (Science and Engineering Research Council)

Agency for Science, Technology & Research,
30 Biopolis Street, #09-01, Matrix Singapore 138671
Email: A-STAR_ADMIN_SERC@a-star.edu.sg
www.a-star.edu.sg/astar_investigators





**Chair, Department of Neurosciences
College of Medicine
The University of Toledo
Health Science Campus**

The University of Toledo College of Medicine seeks an internationally-recognized neuroscientist as Professor and Chair of the Department of Neurosciences. The recent merger of the University of Toledo with the former Medical University of Ohio has created dramatic growth opportunities, and neuroscience research has been targeted for significant development. Substantial resources including new research space and faculty positions are available to create a nationally recognized department, complementing current departmental research strengths (<http://hsc.utoledo.edu/depts/neurosciences/index.html>) including developmental sensory physiology, neurodevelopment, neuroendocrine synaptic physiology, and related areas in structural anatomy and intravital imaging. State-of-the-art imaging, proteomics/genomics and flow cytometry cores as well as AAALAC-accredited animal facilities are available on the modern Health Science Campus. The new Chair must have a distinguished record of extramural funding, strong leadership and administrative skills, and should promote alliances with clinical neuroscientists to stimulate research with translational implications in such areas as drug abuse, developmental neurobiology, stroke, epilepsy, neurooncology, neuroimmunology, functional brain imaging, Parkinson's disease or neurodegeneration. The successful candidate must also be committed to medical and graduate education, supporting the use of innovative educational technologies in gross and microscopic anatomy, and fostering development of the Neurosciences and Neurological Disorders Ph.D. training program. The University of Toledo is a state supported institution in the vibrant port city of Toledo (<http://www.toledo.com>).

Candidates should send a *curriculum vitae* and a cover letter summarizing research, educational and administrative background to: **Chair, Neurosciences Search Committee, c/o Shirley Joseph, COM Dean's Office, 3045 Arlington Avenue, University of Toledo Health Science Campus, Toledo, OH 43614;** or e-mail: shirley.joseph@utoledo.edu (PDF format).

The University of Toledo is committed to diversity and equal opportunity. Applications from women and minority candidates are strongly encouraged.



**Postdoctoral Research Associate/ Senior
Research Associate Position in Drosophila
or Yeast Genetics/Molecular Biology**

The Stowers Institute for Medical Research has an immediate opening for a Postdoctoral Research Associate or Senior Research Associate with interest in the field of transcription biology, in the laboratory of Ali Shilatifard, Ph.D., Investigator.

Responsibilities

The successful candidate will design and conduct experiments that will contribute to our understanding of the molecular machinery required for proper transcriptional regulation by RNA polymerase II in yeast (either *S. cerevisiae* or *S. pombe*), or in *Drosophila melanogaster*; and have the skills and desire to supervise and train other individuals in the laboratory.

Minimum Requirements

Applicants must have a Ph.D. in molecular biology, biochemistry, or a related field and experience in genetics, molecular cloning, and protein engineering in either yeast or *Drosophila*. Experience in DNA-microarray analyses and enzyme assays is desired.

How to Apply

Applicants should send a current curriculum vitae, including a list of publications, a description of present research activity, and two reference letters to mcu@stowers-institute.org or:

Maura Cullinan
Shilatifard Lab
Stowers Institute for Medical Research
1000 East 50th Street
Kansas City, MO 64110

**For more information visit
www.stowers-institute.org**

The Stowers Institute is committed to equal opportunity in all of our programs.



**Director – Imaging Core Facility
University of Maryland Baltimore
School of Medicine
Position #03-305-45**

The University of Maryland School of Medicine is seeking a Director of The University of Maryland, Baltimore Core Imaging Facility <http://medschool.umaryland.edu/confocal/>. The Core Imaging Facility was established in 1994 and serves over 250 users from 28 Departments. We are now looking for a highly motivated individual at the Assistant Professor level who desires to manage the facility as we enter a period of rapid expansion. The successful candidate will be committed to the continued development of a multi-disciplinary Core facility that contains cutting edge imaging technologies not available elsewhere on campus. In collaboration with faculty and other Programs of the University, the Director will play a key role in obtaining extramural funding for the support of the facility. Day-to-day responsibilities will include business management of the facility, training of users, and oversight of maintenance. Candidates should have a PhD or equivalent degree, experience in fluorescence, confocal and multi-photon microscopy, and/or other imaging modalities, and should possess strong managerial and inter-personal skills.

Please submit before **April 30, 2007** your curriculum vitae, a brief description of your career goals, and the names, addresses, telephone numbers, and e-mail addresses of three potential references by e-mail to **W. Gil Wier Ph.D., Chair, Core Imaging Facility Search Committee** at physiologydirector@som.umaryland.edu.

The University of Maryland, Baltimore is an Equal Opportunity, Affirmative Action Employer. Minorities, women, veterans and individuals with disabilities are encouraged to apply.

**Dean of Multicultural Affairs
Tufts University School of Medicine**

Tufts University School of Medicine is seeking nominations and applications for the position of Dean of Multicultural Affairs. The School of Medicine embraces the philosophy of providing a workplace that emphasizes a diverse faculty, staff and student body, and multicultural competence in its curriculum. This is a dynamic, highly visible, new opportunity for someone who is seeking to make a demonstrable difference and have a major impact on the Medical School.

Responsibilities: Reporting to the Dean of the School, the successful candidate will develop and manage programs to promote a diverse faculty, staff and student body; develop strategies for enhancing the school's environment and curriculum with respect to cultural sensitivity and competence; and serve as the school's principal representative to the University and external groups addressing diversity.

Qualifications: Applicants should have at least five years of experience related to increasing diversity and/or multicultural competence within an academic institution. M.D. and/or a Ph.D. and a record of academic accomplishment consistent with a senior faculty level appointment are required. Prior supervisory experience is desirable. The successful candidate will be an active faculty member in their particular specialty area in the Medical School. Interested candidates should apply online via www.tufts.edu.

Nominations/Applications may be sent to:

Jeff Glassroth, M.D.
Vice Dean
Tufts University School of Medicine
136 Harrison Avenue
Boston, MA 02111
or electronically to jeff.glassroth@tufts.edu.

Applicants should provide a letter addressing their qualifications and a copy of their curriculum vitae. Tufts University is an equal opportunity/ affirmative action employer.

www.tufts.edu/hr/jobs/





**Scientist Positions within the
Advanced Study Group
of the Max Planck Society at the Centre of Free
Electron Laser Science in Hamburg**

The "Advanced Study Group" (ASG) funded by the Max-Planck-Society (MPG) is part of the newly founded "Centre for Free Electron Laser Science" (CFEL) (http://hasylab.desy.de/science/cfel/index_eng.html). The ASG shall support research activities of the Max-Planck-Society at 4th generation Free Electron Laser (FEL) light sources such as FLASH in Hamburg and LCLS in Stanford.

Applications are invited for two scientist positions, located at DESY/SLAC, to establish in Hamburg a fast-laser and pulsed x-ray laboratory for the preparation of MPG-FEL experiments, supported by two technicians and students. Specifically, we are looking for scientists experienced in

- (1) **time-resolved diffraction methods.** The successful candidate should have a strong background in physics, chemistry or biophysics. Experience in FEL, SPPS or ESRF experiments or, alternatively, in ultra-fast x-ray science based on table top pulsed x-ray sources, are of advantage
- (2) **ultra-fast pump-probe laser physics** and technologies for the preparation and assistance of time-resolved spectroscopic and imaging experiments with FELs, mainly in atomic, molecular and soft-matter physics. Again, VUV-FEL experience is appreciated.

We expect the successful candidates to interact collaboratively among a variety of disciplines. Apart from supporting experiments actively pursued within the ASG, independent research is encouraged.

Remunerations are according to TVöD (German civil service scale). The initial appointment will be for three years, with the possibility for a two-year extension. It is intended to have a long term perspective, given excellent performance and the continuation of funding by MPG within the CFEL.

As an equal opportunity employer, the Max-Planck-Society seeks to increase the percentage of female employees in areas where they are under-represented. Qualified women are therefore strongly encouraged to apply. The Max-Planck-Society is also committed to employing more individuals with disabilities. We therefore actively encourage individuals with disabilities to apply.

To apply, please send your CV including a brief description of your research / scientific interests, a list of publications, a copy of the most relevant publication, and names and email addresses of two referees either as email attachments or hard copy to:

Prof. Dr. Joachim Ullrich
Max-Planck-Institut für Kernphysik
Saupfercheckweg 1
D-69117 Heidelberg
joachim.ullrich@mpi-hd.mpg.de

Informal enquiries may be sent to Dr. Simone Techert (Simone.Techert@mpi-bpc.mpg.de) and Dr. Robert Moshhammer (moshamme@mpi-hd.mpg.de) for position 1 and 2, respectively. Deadline for applications is May 31st 2007, desired starting date is July, 2007.

Skirball Institute of Biomolecular Medicine



Faculty Positions

The Skirball Institute and the Kimmel Center of Biology and Medicine at New York University School of Medicine invite applicants for tenure-track positions at the assistant, associate or full professor level. We seek applicants with an exceptional record of achievement to join our existing programs in Molecular Neurobiology, Developmental Genetics, Structural Biology and Molecular Pathogenesis. These programs are interdisciplinary and reflect strengths at NYU's School of Medicine and College of Arts and Sciences. Special priority will be given to applicants with broad interests working at the cutting edge of mammalian genetics, stem cell research, neurobiology or molecular cell biology.

NYU School of Medicine offers excellent resources to support new faculty, including generous start-up packages and core facilities for cell sorting, imaging, proteomics, mouse molecular genetics, genomics and structural biology.

Successful candidates are expected to initiate and maintain vigorous independent research programs that will enrich and be enriched by the highly collaborative environment at the Skirball Institute and throughout the NYU research community.

This is an electronic application process. No mail applications will be accepted. Create your application packet by formatting it as a single PDF document. Use the following page order: (1) Cover Letter - **indicating Program preference**, (2) Curriculum Vitae, (3) Research Statement.

Email application packet to
skirballsearch@saturn.med.nyu.edu.

Three letters of reference should be sent independently to: skirballsearch@saturn.med.nyu.edu

New York University School of Medicine was founded in 1841 and is an equal opportunity affirmative action employer. Women and minority candidates are encouraged to apply.

<http://saturn.med.nyu.edu>

From life on Mars to life sciences

For careers in science,
turn to *Science*



If you want your career to skyrocket, visit ScienceCareers.org. We know science. We are committed to helping you find the right job, and to delivering the useful advice you need. Our knowledge is firmly founded on the expertise

of *Science*, the premier scientific journal, and the long experience of AAAS in advancing science around the world. ScienceCareers.org is the natural selection.

www.sciencecareers.org

Features include:

- Thousands of job postings
- Career tools from Next Wave
- Grant information
- Resume/CV Database
- Career Forum

ScienceCareers.org

We know science





MAX-PLANCK-GESELLSCHAFT

PhD Scholarships

within the International Max Planck Research School for Quantum Dynamics in Physics, Chemistry and Biology

The International Max Planck Research School (IMPRS) for Quantum Dynamics in Physics, Chemistry and Biology is a graduate school offering a doctoral degree program in these disciplines. The IMPRS is a joint initiative of the Max Planck Institute for Nuclear Physics, Ruprecht-Karls University, the German Cancer Research Center (DKFZ), the Max Planck Institute for Medical research (all in Heidelberg) and the Heavy Ion Research Center (GSI) in Darmstadt. Membership in the Heidelberg Graduate School of Fundamental Physics is envisaged. Further information may be found on the school's website <http://www.mpi-hd.mpg.de/imprs-qd/>.

Applications of students from all countries are welcome. To be eligible for PhD studies at the University of Heidelberg, applicants should have a Master of Science degree (or equivalent). Applicants who do not have a Master thesis may be accepted if they can prove their ability to carry out independent research projects. International applicants whose mother-tongue is not English or German are advised to provide a proof of English proficiency.

At equal level of qualification, candidates with disabilities are given preference. Women are encouraged to apply.

Applications for the academic program starting in September 2007 must be received by May 15, 2007. Each applicant has to initiate his/her application by registering online at <http://www.mpi-hd.mpg.de/imprs-qd/> and following the steps outlined there.



DEUTSCHES
KREBSFORSCHUNGSZENTRUM
IN DER HELMHOLTZ-GEMEINSCHAFT



Max-Planck Institut
für medizinische Forschung



THE CHINESE UNIVERSITY OF HONG KONG

Applications are invited for:-

School of Chinese Medicine

Professor / Associate Professor / Assistant Professor

(Ref. 07/052(665)/2) (Closing date: April 27, 2007)

Applicants should have (i) a PhD degree in life science, preferably in Chinese medicine or related areas; (ii) established scholarship with a track record of high-quality publications and award of competitive research grants; preferably (iii) teaching and clinical experience in Chinese medicine; and (iv) qualifications for practising Chinese medicine in Hong Kong. Applicants for Professorship should also have extensive teaching experience and an outstanding publication record in related fields. Duties include (a) teaching undergraduate and postgraduate courses; (b) supervising research projects; (c) conducting research in own field(s) of specialization; and (d) assisting in administration of the School and curriculum development. Appointment will normally be made on contract basis for up to three years initially, leading to longer-term appointment or substantiation later subject to mutual agreement. [Note: Those who have responded to the previous advertisement for Associate Professorship/Assistant Professorship (under Ref. no. 07/013/2) need not re-apply on this occasion.]

Salary and Fringe Benefits

Salary will be highly competitive, commensurate with qualifications and experience. The University offers a comprehensive fringe benefit package, including medical care, plus a contract-end gratuity for an appointment of two years or longer, and housing benefits for eligible appointees.

Further information about the University and the general terms of service for appointments is available at <http://www.cuhk.edu.hk/personnel>. The terms mentioned herein are for reference only and are subject to revision by the University.

Application Procedure

Please send full resume, copies of academic credentials, a publication list and/or abstracts of selected published papers, together with names, addresses and fax numbers/e-mail addresses of three referees to whom the applicants' consent has been given for their providing references (unless otherwise specified), to the Personnel Office, The Chinese University of Hong Kong, Shatin, N.T., Hong Kong (Fax: (852) 2603 6852). The Personal Information Collection Statement will be provided upon request. Please quote the reference number and mark 'Application - Confidential' on cover.

ASSISTANT PROFESSOR NEUROSCIENCE AND CELL BIOLOGY

Developmental Neurobiology, Molecular and Cellular Neuroscience, and Structural Neurobiology Assistant Professor Positions

The Department of Neuroscience and Cell Biology at the University of Texas Medical Branch at Galveston (UTMB) seeks applicants for full-time tenure-track positions at the Assistant Professor level. The candidates should hold an M.D. and/or Ph.D. within the following preferred areas of specialty: developmental neurobiology, molecular and cellular neuroscience, neurogenomics and neuroinformatics, or neuroproteomics and structural neurobiology. Candidates should have an established level of expertise in one of these areas as evidenced by postdoctoral research work, publications, external funding, and relevant national and international reputation.

The successful applicants are expected to establish vigorous, externally funded research programs at UTMB. Teaching and service contributions to the School of Medicine and the Graduate School for Biomedical Sciences will be expected. Levels of appointment will be commensurate with experience and accomplishments.

The positions offer a competitive salary and benefits package and generous start-up funds. Applications should include curriculum vitae, summary of research interests and goals, and the name and contact information (including e-mail) of three references. Applications and references should be addressed to: **Dr. Henry F. Epstein, Cecil H. and Ida M. Green Distinguished University Chair in Neuroscience and Cell Biology, Department of Neuroscience and Cell Biology, The University of Texas Medical Branch, 301 University Boulevard, Galveston, TX 77555-0625; E-mail: hepstein@utmb.edu.**

UTMB is an Equal Opportunity, Affirmative Action Institution which proudly values diversity. Candidates of all backgrounds are encouraged to apply.



From physics to nutrition

For careers in science,
turn to *Science*



If you want your career to bear fruit, don't leave it to chance. At ScienceCareers.org we know science. We are committed to helping you find the right job, and to delivering the useful advice you need. Our knowledge is

firmly founded on the expertise of *Science*, the premier scientific journal, and the long experience of AAAS in advancing science around the world. ScienceCareers.org is the natural selection. www.sciencecareers.org

Features include:

- Thousands of job postings
- Career tools from Next Wave
- Grant information
- Resume/CV Database
- Career Forum

ScienceCareers.org

We know science



OTOLARYNGOLOGIST

The Section of Otolaryngology - Head and Neck Surgery at Dartmouth-Hitchcock Medical Center seeks a board certified or board eligible Otolaryngologist for a full-time faculty position. The candidate should possess an interest in an academic career and in the education of medical students and residents. This position will combine a general otolaryngology with a subspecialty practice in otology or pediatric otolaryngology. Fellowship training in otology/ neurotology or pediatric otolaryngology is desirable. Research interests will be encouraged. Academic rank will be commensurate with qualifications and experience.

Interested applicants are encouraged to send letters of inquiry and CV to:

Daniel Morrison, MD, Chairman
Section of Otolaryngology - Head & Neck Surgery
Dartmouth-Hitchcock Medical Center
One Medical Center Drive
Lebanon, NH 03756
Telephone: 603-650-8123



Dartmouth-Hitchcock Medical Center is an affirmative action/equal opportunity employer and is especially interested in identifying female and minority candidates.

www.DHMC.org

DUKE NUS

GRADUATE MEDICAL SCHOOL SINGAPORE

Director, Program in Emerging Infectious Diseases

The Duke-NUS Graduate Medical School Singapore (GMS) is unique in bringing post-baccalaureate, research-intensive medical education to Asia, and represents a truly global partnership between two leading universities: National University of Singapore and Duke University. The GMS shares a modern campus with Singapore's largest hospital and several national research centers. The GMS is creating a world-class, academically based Program in Emerging Infectious Diseases that will both enhance health care in Singapore and serve as a national and international resource of excellence in emerging infectious diseases. The mission of the Program faculty will be to conduct high-level basic and applied research, and to train graduate students, post-doctoral fellows, and physician scientists in the disciplines relevant to emerging infectious diseases.

We are seeking an individual with exceptional scientific credentials and leadership skills to head the Program. The position of founding Director will include full salary, a very generous start-up and five years of annual research funding. The Director will be provided with the space and resources necessary to recruit 6-8 outstanding faculty members at all academic ranks. The packages for these faculty recruits would include full salary, generous start-up, and five years of annual research funding of up to \$500K/p.a., assuring a stable base of support that can be supplemented by competitive grant awards, which are expanding rapidly in Singapore. The director and the faculty members he/she recruits will join the pioneering Duke and Singapore investigators already affiliated with the GMS (see www.gms.edu.sg).

Interested candidates should send a CV and the names of three references to: **Mariano A. Garcia-Blanco, M.D., Ph.D., Chair, Search Committee on Emerging Infections, Duke-NUS Graduate Medical School, Singapore** by email to: director.id@gms.edu.sg

The GMS is a collaboration of the Duke University School of Medicine and the National University of Singapore.

FULL TIME ASSISTANT RESEARCH ANATOMIST POSITION

UNIVERSITY OF CALIFORNIA
SAN FRANCISCO
DEPARTMENT OF ANATOMY

The candidate will study the transmission and control of pain messages as well as the neuronal circuits that underlie the production of pain. The candidate will oversee the work of students and technicians, and work directly on bench research involving transgenic mice (ZW mice) to investigate the CNS circuitry implicated in pain transmission. In addition, he/she will work with the Principal Investigator and other scientists in the laboratory to develop overall experimental strategies, to design specific experiments and controls, and to interpret experimental results.

Applicants must have a Ph.D. in biology and at least four years postdoctoral research experience (foreign training/experience acceptable). The candidate must have demonstrated experience in use of viruses to introduce new genes into the CNS, "in vitro" and "in vivo" approaches, immunohistochemistry, western blot, cell culture, DNA constructs for knock-ins, genetics (including the generation of transgenic mice) and mouse behavior. This candidate will also have a track record of publishing in highly regarded peer-reviewed journals.

Send curriculum vitae and names of references prior to **May 4, 2007** to:

Yvonne Dea, Analyst
Department of Anatomy
513 Parnassus Ave, Box 0452
San Francisco, CA 94143

UCSF seeks candidates whose expertise, teaching, research, or community service has prepared them to contribute to our commitment to diversity and excellence. UCSF is an affirmative action/equal opportunity employer. The University undertakes affirmative action to assure equal employment opportunity for underutilized minorities and women, for persons with disabilities, and for covered veterans. All qualified applicants are encouraged to apply, including minorities and women.

LANCASTER
UNIVERSITY



Lancaster Environment Centre
Department of Environmental Science

Professor or Reader Atmospheric Science

£41,544 - £46,758 p.a.
Professor min £50,565 (negotiable)

We invite applications for the post of Professor or Reader in Atmospheric Science in this research-led Department (which is an integral part of the Lancaster Environment Centre).

The anticipated start date is on or before 1 September 2007.

Informal enquiries may be addressed to n.hewitt@lancaster.ac.uk or a.binley@lancaster.ac.uk

To apply or receive further information online, please visit <http://www.personnel.lancs.ac.uk/> or telephone Personnel Services, quoting reference **A763R**, on answerphone +44 (0)1524 846549.

Closing date: 9 May 2007.

Interviews: 5 June 2007.



Aiming for Greater
Diversity

University of Cincinnati

Post Doc Fellow - Ophthalmology

(27UC3488) The University of Cincinnati (UC) is pleased to announce availability of endowed funding for research in macular degeneration or other visual disorders of the elderly and invites application for a **Crawley Postdoctoral Scholar Award** as part of the **Edith J. Crawley Memorial Scholars Program**. An award of this type will fund up to three years of mentored vision neuroscience research at UC.

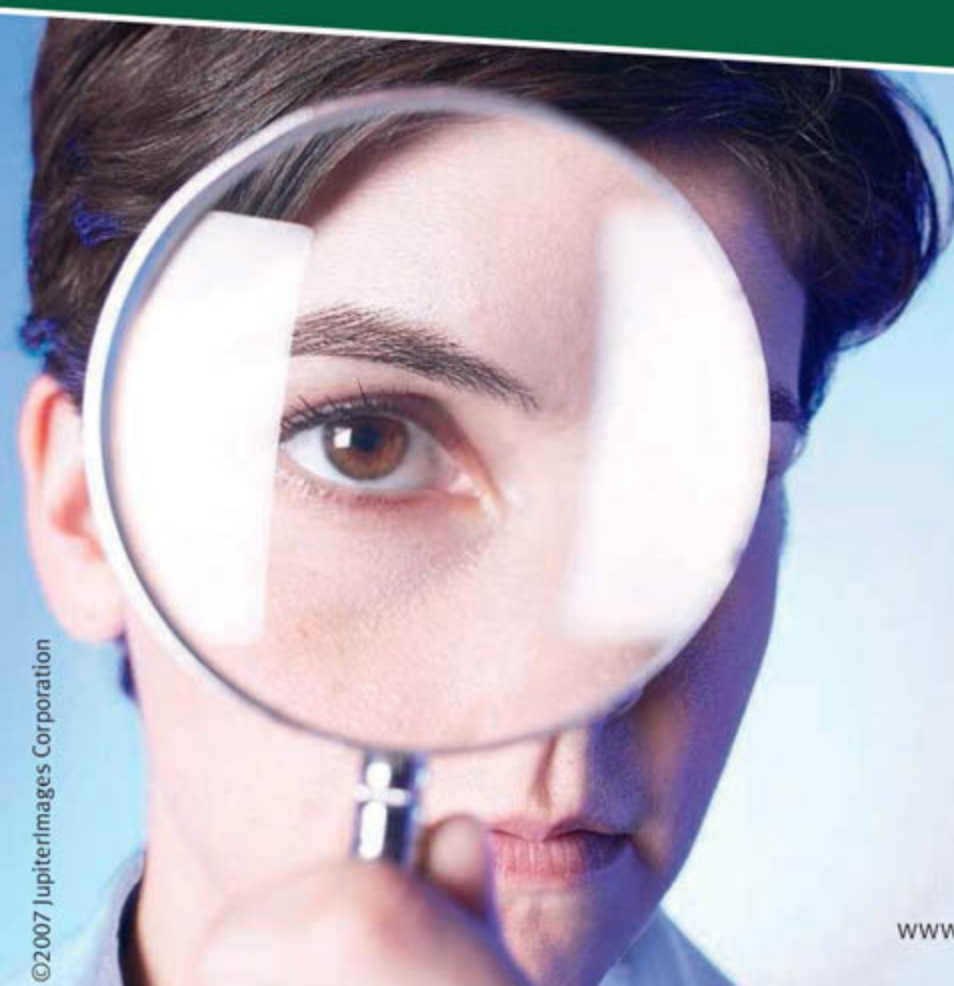
Qualified applicants should hold a doctoral degree in life sciences (i.e., M.D., Ph.D. and/or equivalent degree) and be committed to a career in vision neuroscience research. Successful candidates may either participate in ongoing projects in vision-neuroscience or new projects or avenues of research approved by the mentor. The awardee will be expected to develop one or more independent research projects worthy of extramural support upon completion of training.

Interested individuals should submit a curriculum vitae, statement of research interest, and three references to Winston W.-Y. Kao, Ph.D., Ben and Louise Tate Professor and Director, Ophthalmic Research, Department of Ophthalmology, Health Professions Building, Suite 350, University of Cincinnati College of Medicine, 3233 Eden Avenue, Cincinnati, OH 45267-0527 (Phone: 513-558-2802, Fax: 513-558-3108, Winston.Kao@uc.edu) For additional information about the position #27UC0988, please see www.jobsatuc.com.

The University of Cincinnati is an affirmative action/equal opportunity employer.
UC is a smoke-free work environment.



©2007 Jupiterimages Corporation



Looking for Career Advice?

Find a wealth of information relevant to your current career and future employment decisions in the *Science Career Features*.

UPCOMING FEATURES:

April 20: Postdoctoral Careers: Transferable Skills

April 27: Biotech and Pharma

May 4: Interdisciplinary Research

Also available online at:

www.sciencecareers.org/businessfeatures

ScienceCareers.org

We know science



TENURE TRACK FACULTY POSITIONS DEPARTMENT OF BIOCHEMISTRY AND MOLECULAR BIOLOGY VIRGINIA COMMONWEALTH UNIVERSITY SCHOOL OF MEDICINE

As part of an ongoing major expansion in biomedical research at Virginia Commonwealth University Medical Center, we invite applications from outstanding individuals with expertise and interest in cellular and molecular signaling for tenure-track positions. We welcome candidates in all areas of biochemistry and biomolecular sciences. Candidates should have an active research program with a record of sustained research productivity. More senior candidates should have current extramural funding. Applicants should have a M.D., Ph.D. or equivalent degree and will be expected to contribute to the Department's teaching mission as well as develop vigorous collaborative efforts with other VCU researchers. The Department's and VCU's research expertise is spread across several programs having national prominence in terms of NIH-funded research ranking. More information about the School of Medicine and the Department, and this open position can be found at www.medschool.vcu.edu/ and www.pubinfo.vcu.edu/facjobs/. Applicants should submit by email a CV with names and e-mail addresses of three references to: **Dr. Robert F. Diegelmann (rdiegelm@vcu.edu)**, Department of Biochemistry & Molecular Biology, Virginia Commonwealth University School of Medicine, Richmond, VA 23298-0614.

Virginia Commonwealth University is an Equal Opportunity/Affirmative Action Employer. Women, persons with disabilities, and minorities are encouraged to apply.

THE METHODIST HOSPITAL RESEARCH INSTITUTE

The Methodist Hospital Research Institute of The Methodist Hospital, Houston, Texas, seeks an exceptional physician scientist to lead its effort in clinical research. The Methodist Hospital System consists of 1,450 beds, including 1,000 located in the Texas Medical Center in Houston. With our partners at Weill Cornell Medical College and New York-Presbyterian Hospital in New York City, there are 3,500 beds available for clinical investigation and clinical trials. The successful candidate will be responsible for organizing and leading the Institute's clinical research in Houston and collaborating with our Cornell and NYP colleagues. We encourage applications from individuals who currently lead substantial funded programs conducting clinical research. The hospital has entered an unprecedented expansion phase that includes construction of a 420,000 SF state-of-the-art research building and a 750,000 SF ambulatory care building, both designed to foster interdisciplinary collaboration. The successful applicant will receive a generous salary, fringe benefits, and a relocation package, and may be eligible for an endowed chair.

Individuals interested in this unique career opportunity should send via e-mail a curriculum vitae, including grant funding information to: **James M. Musser, M.D., Ph.D., c/o Ms. Ginny Gittemeier, Co-Director and Executive Vice President, The Methodist Hospital Research Institute; gittemeier@grantcooper.com; Phone: 636-240-2090; Fax: 314-726-5294.**



ASSISTANT PROFESSOR, IMMUNOLOGY

The University of Idaho is seeking a talented educator and researcher to join our faculties in the Department of Microbiology, Molecular Biology & Biochemistry in the area of immunology.

The individual selected will be expected to contribute to the overall research, teaching, and service mission of the department, college and university by serving on committees, advising students, participating in seminars and interacting with faculty and students.

Requires M.D., Ph.D. or equivalent in Molecular Life Sciences or a related field with at least two years of postdoctoral research experience; strong record of accomplishments in research as demonstrated by publications in peer-reviewed journals; teaching experience at the undergraduate and/or graduate level.

For a full description and application materials, visit

<http://www.hr.uidaho.edu/>

Review of applications
begins 4/30/07.

University of Idaho

Open Space. Open Minds.

To enrich education through diversity, the University of Idaho is an Equal Opportunity/Affirmative Action Employer.



Dave Jensen
Industry
Recruiter



Science Careers Forum

- How can you write a resume that stands out in a crowd?
- What do you need to transition from academia to industry?
- Should you do a postdoc in academia or in industry?

Let ScienceCareers.org help you answer these questions. ScienceCareers.org has partnered with moderator Dave Jensen and four well-respected advisers who, along with your peers, will field career-related questions.

Visit ScienceCareers.org and start an online dialogue.

ScienceCareers.org

We know science



IF YOU THINK OUR
PIPELINE IS IMPRESSIVE,
YOU SHOULD SEE

THE SCIENCE BEHIND IT!

Every day, your work has the ability to impact lives. Many of GSK Consumer Healthcare's well-known products are global brands, and offer people a new lease on life. Whether smoking cessation, weight loss, pain management or even restoring a quiet night's sleep, our products make life better for millions.

Recently named the 2006 Pharmaceutical Company of the Year by *Med Ad News*, GSK is no stranger to the power of exceptional science and global product marketing. As we expand our portfolio of consumer products, which already include such market leaders as: Nicoderm, Breathe Right, Panadol, Abreva, Polident, and Alli, the first FDA approved OTC weight loss product, GSK Consumer Healthcare is eager to attract the most passionate scientific talent in the marketplace.

Our New Product Development and New Product Research departments, located in **Parsippany, New Jersey**, currently have the following opportunities available for exceptional professionals:

- **Principal Development Scientists, NPD**
(Req. ID: 38859 & 39590)
- **Principal Scientists, NPR**
(Req. ID: 40776, 40204, & 41512)

We also have a Principal Scientist, Oral Healthcare (Req. ID: 41875) position available on our Aquafresh team at our London Innovation Centre. Company provided relocation available.

To learn more about these positions and to apply online, please visit www.gsk.com/careers. Indicating Req. ID is essential to search.



Together we can make life better.

gsk.com/careers

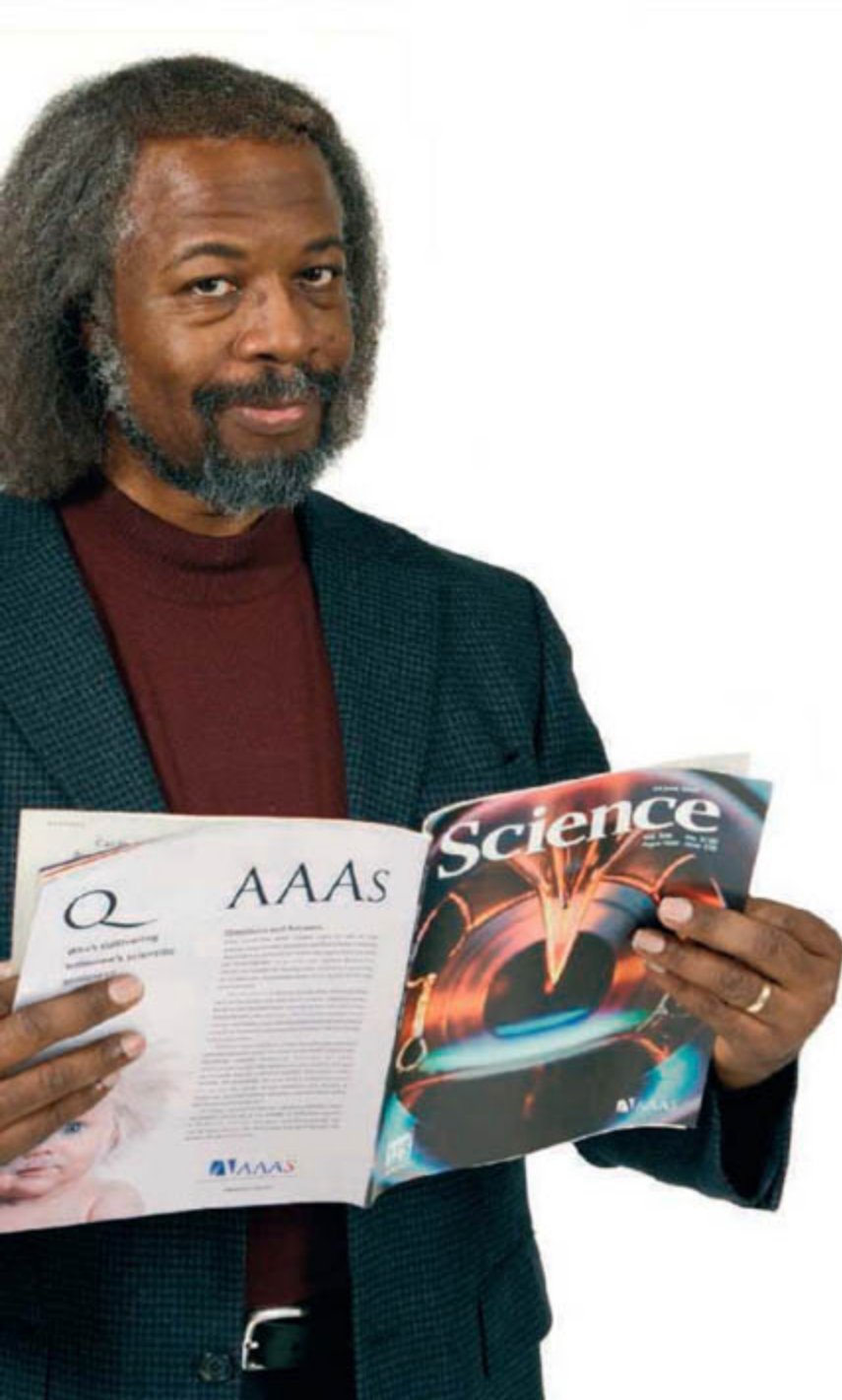
GlaxoSmithKline is dedicated to supporting you with career-long opportunities and learning. We offer a competitive benefits and compensation package designed to attract and retain the very best. We are proud to be an equal opportunity employer.



GlaxoSmithKline
Consumer Healthcare

Q

Who's helping bring
the gift of science
to everyone?



AAAS

“ As a child I got very interested in space travel. When I was six my father gave me some books on rockets and stars. And my universe suddenly exploded in size because I realized those lights in the sky I was looking at were actually places.



I wanted to go there. And I discovered that science and technology was a gift that made this possible. The thrill of most Christmas presents can quickly wear off. But I've found that physics is a gift that is ALWAYS exciting.

I've been a member of AAAS for a number of years. I think it's important to join because AAAS represents scientists in government, to the corporate sector, and to the public. This is very vital because so much of today's science is not widely understood.

I also appreciate getting *Science* because of the breadth of topics it covers. It gives me a great grounding for many activities in my professional life, such as advising government agencies and private corporations. ”

Jim Gates is a theoretical physicist and professor at the University of Maryland. He's also a member of AAAS.

See video clips of this story and others at www.aaas.org/stories

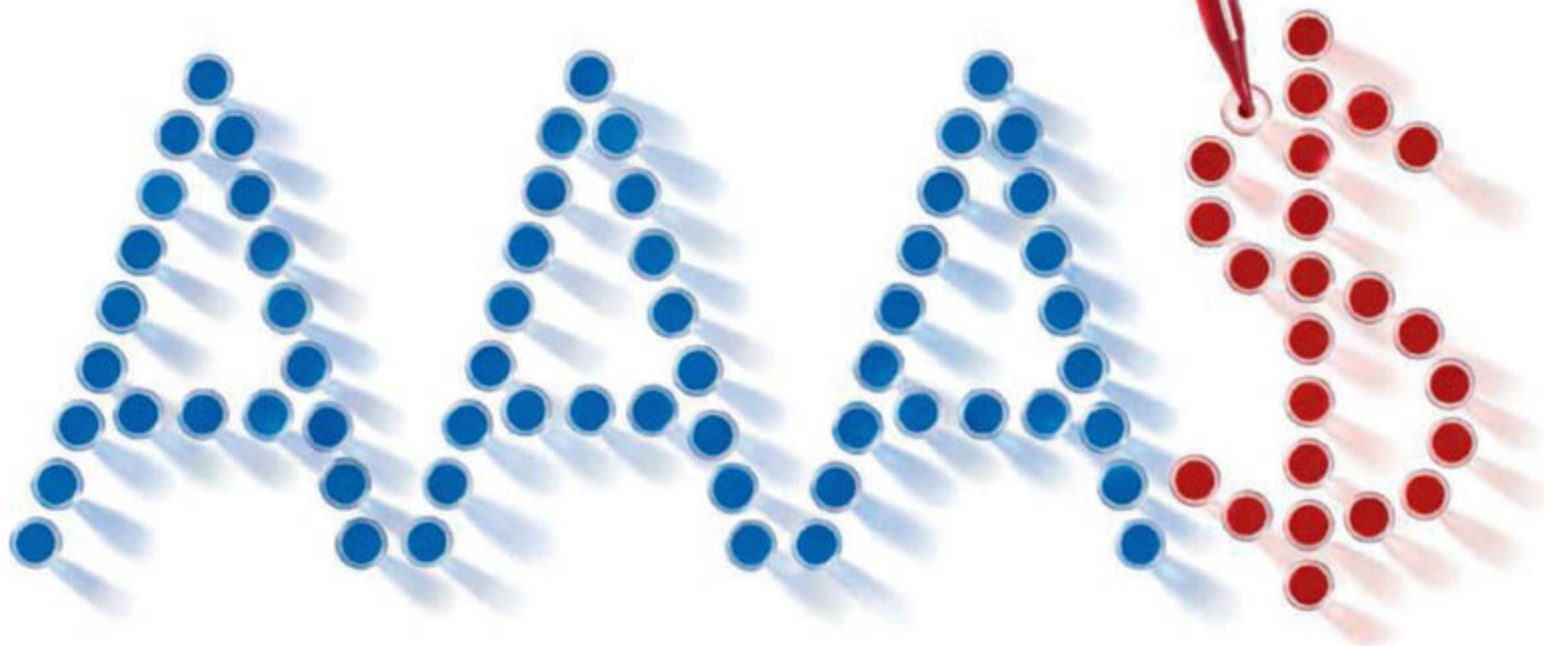
S. James Gates Jr., Ph.D.
Theoretical physicist
and AAAS member



ADVANCING SCIENCE, SERVING SOCIETY

Q

Who's working
to increase support
for science?



Top quality research depends on comprehensive support. AAAS is present at every stage of the process – from advising on funding policy initiatives to tracking the US Federal R&D budgeting process. As the experts, we brief Congressional staffers and representatives from

governments around the world. And only AAAS Funding Updates – sent out monthly – provide continual coverage of R&D appropriations. By actively working to increase support for research, AAAS advances science. To see how, go to www.aaas.org/support



ADVANCING SCIENCE. SERVING SOCIETY

POSITIONS OPEN

UNIVERSITY OF MINNESOTA

Cancer Center

ASSISTANT/ASSOCIATE PROFESSOR

The University of Minnesota Cancer Center, the Department of Laboratory Medicine and Pathology, and the Department of Urologic Surgery are expanding the Cancer Center Research Program in Prostate Cancer Research and invite applications for a Tenure-Track Faculty Position. We are interested in candidates with specific research interests, experience, publication, and external funding in prostate biology, prostate cancer, and the cellular and molecular mechanisms associated with prostate cancer genesis, invasion and metastasis, and experimental therapeutics. The goal of this search is to attract faculty members that will enhance ongoing research programs in the following areas: (1) Genesis and development of neoplastic changes in the prostate. Tumor microenvironment with a specific focus on musculoskeletal tumor growth, the bone/tumor microenvironment, tumor metastasis to bone, animal models of bone metastases and/or emerging therapies for bone cancer; (2) Progression associated changes in signal transduction pathways associated with alterations in the structure/function of plasma membrane microdomains, signalosome assembly/function, or other tumor associated changes in cell growth/survival signal transduction pathways; (3) Proteomic, genomic, and tumor/stromal changes associated with primary tumor growth/progression of prostate tumors. Preference will be given to individuals who use novel three dimensional and/or co-culture systems to model progression in vitro and in vivo.

Successful candidates will be expected to develop projects that have translational potential in pre-clinical models, with a long-term goal of developing novel clinical approaches for the diagnosis/treatment of prostate cancer in patients. The candidate must hold a Ph.D. or M.D./Ph.D. degree and preference will be given to candidates with external funding, established research programs, and training in prostate biology. Academic rank and salary are commensurate with training and experience.

Submit curriculum vitae, a brief research statement, and contact information of three references online to requisition #145924 at website: <http://employment.umn.edu>. Information about the Cancer Center is available at website: <http://www.cancer.umn.edu>. The University of Minnesota is an Equal Opportunity Employer and Educator.

POSTDOCTORAL ASSOCIATE

A Postdoctoral Associate position for a Ph.D., M.D., or M.D./Ph.D. is available immediately in the Division of Hematology, Oncology, and Transplantation, Department of Medicine. The duties and responsibilities of this position will be to study the effects of cytochrome P450 enzymes on breast cancer cell proliferation in vitro and in vivo. Studies will involve analysis of eicosanoids and other lipids by mass spectrometry, using tumor xenograft models. The job duties will include, but not be restricted to, performing the isolation of cell lines expressing recombinant signaling proteins, performing cell growth inhibition assays and soft agar colony formation assays, performing tumor xenograft assays and the use of mass spectrometry assays for eicosanoids. The successful applicant must have the ability to work independently, analyze and report research results. Writing and figure production skills necessary for drafting manuscripts is essential, as well as familiarity with statistical analysis of biochemical and pharmacological data. Working experience with eicosanoid biochemistry, experimental pharmacology, mass spectrometry, enzymology, and breast cancer xenograft models will be helpful.

Apply online at website: <http://employment.umn.edu>. Applications should consist of curriculum vitae and names of three references.

The University of Minnesota is an Equal Opportunity Employer and Educator.

POSITIONS OPEN

The University of California, San Diego (UCSD) Center for Human Genetics and Genomics (website: <http://chgg.ucsd.edu/>) in conjunction with the Departments of Pediatrics and Medicine at the UCSD School of Medicine invites applications for several **TENURE-TRACK/TENURED POSITIONS** from outstanding individuals to develop a vigorous research program in any area of contemporary human genetics and genomics. The appointments will be at any academic level, and will involve teaching at both the graduate and medical school levels. There are openings for both junior and senior faculty, including **DIVISION CHIEF** positions in medical genetics in both the Departments of Pediatrics and Medicine. Candidates must possess a doctoral degree and be well trained in any area of contemporary human genetics and genomics with a demonstrated track record of outstanding peer-reviewed research. For the Division Chief positions, Board certification in any area of medical genetics is desirable. Space will be provided in the Center for Human Genetics and Genomics on the fourth floor of the new Skaggs School of Pharmacy and Pharmaceutical Sciences building or other sites within the UCSD Health Sciences campus. In addition, an attractive and competitive startup package will be provided. The goal of the Center is to galvanize already existing genetics and genomics efforts throughout the School of Medicine and UCSD campus, and these recruitments will play a major role in this exciting effort.

Applicants should e-mail their curriculum vitae and names and addresses of three references to e-mail: coffey@ucsd.edu or mail to: **Christine Coffey, Assistant to Anthony Wynshaw-Boris, M.D., Ph.D., Director, Center for Human Genetics and Genomics University of California, San Diego School of Medicine, 9500 Gilman Drive, 0627 La Jolla, CA 92093-0627.**

Review of applications will begin on April 1, 2007, and will continue until positions are filled. UCSD is an Equal Opportunity/Affirmative Action Employer committed to excellence through diversity.

TENURE-TRACK POSITIONS in ANATOMY, PHYSIOLOGY, and GENETICS
F. Edward Hebert School of Medicine
Uniformed Services University of the Health Sciences

The Department of Anatomy, Physiology and Genetics, Uniformed Services University School of Medicine, Bethesda, Maryland, chaired by **Harvey B. Pollard, M.D., Ph.D.**, invites applications for tenure-track positions at the **ASSISTANT/ASSOCIATE PROFESSOR** level. The Department has strong commitments to medical education and biomedical research and is located in an interactive scientific environment adjacent to the National Institutes of Health and National Library of Medicine. Outstanding core facilities are available to support medical education and biomedical research in cell biology, genomics, and proteomics. The successful applicant will have a Ph.D. and/or M.D. degree and will be expected to: (i) contribute to the Department's interdisciplinary anatomy and physiology curriculum for first-year medical students and (ii) establish an independent and extramurally funded research program. Teaching experience in physiology is desirable. Research interest in regenerative biology and stem cell research is an asset. Candidates should submit curriculum vitae, an outline of their proposed research program, and have three letters of reference sent to: **Gregory P. Mueller, Ph.D., Search Committee Chair, Department of Anatomy, Physiology, and Genetics, Uniformed Services University of the Health Sciences, 4301 Jones Bridge Road, Bethesda, MD 20814-4799 (e-mail: gmueller@usuhs.edu).** Positions open until filled. *Foreign nationals will be considered if qualified United States citizens are not available. USUHS is an Equal Opportunity Employer with a strong commitment to racial, cultural, and ethnic diversity.*

What's your next career move?

Get help from the experts.

www.sciencecareers.org

- Job Postings
- Job Alerts
- Resume/CV Database
- Career Advice from Next Wave
- Career Forum
- Graduate Programs
- Meetings and Announcements

ScienceCareers.org

We know science

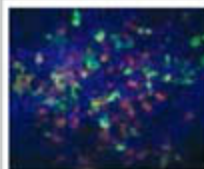
AAAS

Conferences organised at the Institut Pasteur, Paris, France in 2007



FROM MOLECULES TO COGNITION: A TRIBUTE TO JEAN-PIERRE CHANGEUX
September 17-19, 2007

Website: http://www.pasteur.fr/infosci/conf/sb/neuroscience_pasteur
 Information: neuroscience@pasteur.fr - Fax: +33 1 40 61 37 21



EARLY STEPS OF THE VIRUS LIFE CYCLE: MOLECULAR AND CELLULAR INSIGHTS
October 4-5, 2007

Website: http://www.pasteur.fr/infosci/conf/sb/virus_cell/
 Information: virus-cell@pasteur.fr - Fax: +33 1 40 61 37 21



GENETICS AND MECHANISMS OF SUSCEPTIBILITY TO INFECTIOUS DISEASES
November 21-24, 2007

Website: http://www.pasteur.fr/infosci/conf/sb/host_genetics
 Information: conference-ip@pasteur.fr - Fax: +33 1 40 61 37 21



VIBRIO 2007

November 28-December 1, 2007

Website: <http://www.pasteur.fr/infosci/conf/sb/vibrio2007>
 Information: vibrio-2007@pasteur.fr - Fax: +33 1 40 61 37 21

Science Alerts in Your Inbox

Get daily and weekly E-alerts on the latest breaking news and research!

Science News This Week
Brief summaries of the journal's news content

ScienceNOW Weekly Alert
Weekly headline summary

Science Express Notification
Articles published in advance of print

Science Posting Notification
Alert when weekly issue is posted

ScienceNOW Daily Alert*
Daily headline summary

Science Magazine TOC
Weekly table of contents

STKE TOC
Weekly table of contents

Editors' Choice
Highlights of the recent literature

This Week in Science
Summaries of research content

Get the latest news and research from *Science* as soon as it is published. Sign up for our e-alert services and you can know when the latest issue of *Science* or *Science Express* has been posted, peruse the latest table of contents for *Science* or *Science's* Signal Transduction Knowledge Environment, and read summaries of the journal's research, news content, or Editors' Choice column, all from your e-mail inbox. To start receiving e-mail updates, go to:

<http://www.sciencemag.org/ema>



POSITIONS OPEN


FACULTY POSITIONS
Academia Sinica, Taiwan

Applications are invited for faculty positions to participate in the Summit Project at Academia Sinica. Through this project, we plan to make several strategic appointments in research programs of (1) stem cell, (2) infectious disease, and (3) drug discovery. We are seeking for outstanding scholars at **ALL FACULTY LEVELS** in the following areas.

Stem cell (code: SC): Functional genomics, cellular and molecular biology of stem cells, including cancer stem cells.

Infectious disease (code: ID): Development of antiviral and antibacterial strategy, drug resistance, vaccine and disease models.

Drug discovery (code: DD): Synthetic organic chemistry and medicinal chemistry, drug design and synthesis.

The funding for the Summit Project is substantial and long-term. In addition, Academia Sinica has established several national core facilities, including mouse mutagenesis and disease models, genotyping, microarrays, RNAi, mass spectrometry and proteomics, X-ray, nuclear magnetic resonance, magnetic resonance imaging, nanotechnology and bioinformatics, and recently has established two P3-level laboratories and an ultra-high throughput screening (uHTS) system. Familiarity with the operation of such environment and equipment would be an advantage.

Qualification: Candidates with doctoral degrees and strong track records in the above areas are encouraged to apply. Please indicate the code on your cover letter describing your research experience and interest, and send a copy of curriculum vitae, including a list of publications along with name and contact information of three references to: **Vice President, Dr. Andrew H.J. Wang, Academia Sinica, 128 Academia Road, Section 2, Nankang, Taipei 115, Taiwan. Telephone: +886-2-2789-9407; fax: +886-2-2788-2043. E-mail: searchvp@gate.sinica.edu.tw. Website: <http://www.sinica.edu.tw/>.**

ASSISTANT PROFESSOR
Histology/Cell Biology
Mercer University, Macon, Georgia

Mercer University School of Medicine invites applications for a 12-month salaried, tenure-track position in histology/cell biology at the rank of Assistant Professor. The successful candidate must have a strong commitment to medical education excellence in a multidisciplinary, case-based curriculum, and will be expected to develop an independent, externally funded research program. Applicants should have a doctoral degree with an expertise in human histology and cell biology, and three years of postdoctoral training. Review of applications will continue until the position is filled. For online submission of applications, visit **website: <https://www.mercerjobs.com>**. *Affirmative Action/Equal Opportunity Employer/Americans with Disabilities Act.*

POSTDOCTORAL POSITIONS
Available at Sloan-Kettering Institute

Seeking **RESEARCH SCIENTISTS**, with or without postdoctoral experience, who wish to join a laboratory focused on defining the molecular events underlying normal or leukemic hematopoiesis. Applicants should have considerable interest and expertise in the use of mouse models to study hematopoietic stem cell biology, mechanisms of transformation, or therapeutic approaches to hematologic malignancies. Send a description of your research interests, curriculum vitae, and the names and telephone numbers of three references to: **Dr. Stephen D. Nimer, Memorial Sloan-Kettering Cancer Center, 1275 York Avenue, P.O. Box 575, New York, NY 10021. Memorial Sloan-Kettering is an Affirmative Action/Equal Opportunity Employer.**

POSITIONS OPEN

FACULTY POSITIONS in PHYSIOLOGY

The Department of Physiology at the Medical College of Wisconsin (MCW) invites applications for two tenure-track faculty positions at the **ASSISTANT or ASSOCIATE** level with research interests in the physiological function of the cardiovascular system, the kidney, or pulmonary system. Favored candidates will be those that: (a) complement the Department's strengths in connecting genes to complex functional pathways; (b) are highly focused on endothelial or epithelial ion channels and cell signaling; (c) are capable of extending their research to more integrated level; (d) are interested in developing translational collaborative projects with clinical scientists. The overall goal of the Department is to sustain a breadth of scientific expertise and research spanning from genome and cell to the whole organism. Superb opportunities exist for collaborative research and our faculty are closely affiliated with the MCW Human and Molecular Genetic Center (housing the National Heart, Lung, and Blood Institute Program of Genomic Applications), the Cardiovascular Center (housing the National Institute of Neurological Disorders and Stroke-Program Project Grant in stroke), the Biotechnology and Bioengineering Center (housing the NHLBI Center of Proteomics), and the Center of Kidney Research. Candidates will be expected to participate in both the graduate and medical curriculums. The candidate must hold a Ph.D. and/or M.D. degree, and demonstrate clear evidence of research independence such as current or imminent grant support. The positions will remain open until filled and applicants should send their curriculum vitae, statement of interest, and three letters of recommendation to: **Allen W. Cowley, Jr., Ph.D., Chairman, Department of Physiology. E-mail: cowley@mcw.edu. Website: <http://www.phys.mcw.edu/index.htm>.**

PENN STATE UNIVERSITY

Penn State York invites applications for an **INSTRUCTOR** in biology (multi-year appointment, 36 weeks) starting August 2007, or as negotiated. Teach freshman biology with laboratory sections and advanced courses in area of expertise; prefer interest in operating a small greenhouse. Participate in course, curriculum, and program development and advise students. Qualifications: Ph.D. in biology (or related discipline). Prefer background in botany, plant pathology, plant physiology, or entomology.

To learn more about the campus and Penn State, visit **website: <http://www.psu.edu/ur/cmpcoll.html>**.

To learn more about the position and how to apply, visit **website: <http://www.psu.jobs/Opportunities/Opportunities.html>** and select location: Penn State York.

Affirmative Action/Equal Opportunity.
POSTDOCTORAL FELLOWSHIPS
in the Epigenetics of Disease
Johns Hopkins University School of Medicine

Postdoctoral Fellowships are available for the study of the epigenetic basis of human cancer and other human disease. Studies include the epigenetic progenitor origin of cancer (*Nat. Rev. Genet.* 7:21-33, 2006), and development of high throughput epigenomic technology, through a Center of Excellence in Genome Sciences, extending epigenetics to common disease, such as bipolar disorder and autism. The candidate should be a prospective or recent recipient of a Ph.D. or M.D./Ph.D. with good publication(s) in genetics or genomics. Please e-mail **Dr. Andrew P. Feinberg** curriculum vitae and names and e-mail addresses of three references, but no other attachments, to **e-mail: afeinberg@jhu.edu**. *Johns Hopkins University is an Equal Opportunity/Affirmative Action Employer.*

POSITIONS OPEN


WOODS HOLE OCEANOGRAPHIC INSTITUTION
**ECOLOGIST and ENVIRONMENTAL/
 RESOURCE ECONOMIST**
Woods Hole Research Center

The Woods Hole Research Center (WHRC) seeks: an Ecologist who will work on the relation between the condition of forest ecosystems and the "ecosystem services" they deliver; and an Environmental/Resource Economist who will focus on the economic valuation of the products and services derivable from forest ecosystems and mechanisms for reflecting the value of these products and services.

For more information, go to **website: http://whrc.org/about_us/jobs.htm**

WHRC is an Equal Opportunity Employer and actively seeks a diverse pool of candidates in this search.

ASSISTANT PROFESSOR of PHYSIOLOGY
Department of Pharmacology and Physiology

The Department of Pharmacology and Physiology at Oklahoma State University-Center for Health Sciences invites applications for one tenure-track physiology faculty position at the level of **ASSISTANT PROFESSOR**. For all applicants, a Ph.D. is required with at least two years of postdoctoral experience. The successful applicant is expected to develop an extramurally funded research program and contribute to medical and graduate teaching. Individuals with interests in neurobiology of social behavior are invited to apply. Applicants must apply online at **website: <https://jobs.okstate.edu>**, job # 02963.

Affirmative Action/Equal Opportunity Employer.

MEETINGS

MEETING ANNOUNCEMENT

The University of Georgia will host an international conference on the "Immunobiology of Influenza Virus Infection: Approaches for an Emerging Zoonotic Disease" from July 29 through 31, 2007.

This meeting will assemble influenza experts from academia, government, and industry to foster effective translation of new findings in basic influenza research into effective vaccines and therapies. It is intended for students, scientists, and others who need to be informed about the latest scientific developments in the influenza field. A keynote address by 1996 Nobel Laureate Peter C. Doherty will precede presentations by eminent leaders in the field of viral immunity, and poster sessions will provide cutting-edge research on virus biology, vaccines, therapeutics, detection, diagnostic procedures, and other topics of interest. For further information refer to the following **website: <http://www.virus-EID.org>**.

MARKETPLACE

 Widely
 Recognized
 Original &
 Guaranteed

KlenTaq 1

 8¢/u
 Truncated
 Taq DNA
 Polymerase
 Withstand 99°C

 US Pat #5,436,149 **e-mail: abpeps@msn.com**
 Call: **Ab Peptides** 1-800-383-3362
 Fax: 314-968-8988 **www.abpeps.com**
Oligo Synthesis Reagents

↓ Specialty CPG Supports

↓ Linkers, Spacers, & Modifiers

↓ Bulk Reagent Pricing Available

**BIOSEARCH
 TECHNOLOGIES**
Advancing Nucleic Acid Technology™

 +1.800.GENOME.1
 www.btisynthesis.com

The power of small **x8**

1 μ l analysis — increased throughput

The NanoDrop® ND-8000
8-Sample Spectrophotometer

1 μ l samples. No cuvettes. No dilutions.



Revolutionary technology. **8 readings in under 30 seconds.** The NEW NanoDrop® ND-8000 8-Sample Spectrophotometer is powerful — eight 1 μ l samples at once.

Full spectrum UV/Vis analysis of 1 μ l samples for quantitation, purity assessments and more: nucleic acids, microarrays, proteins and general spectrophotometry.

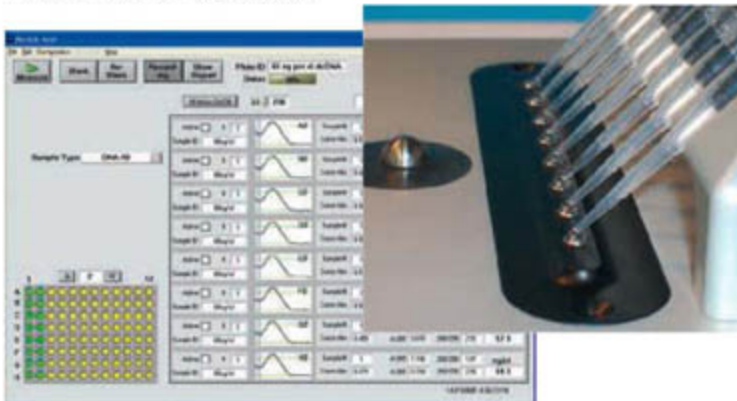
Measurement is quick and easy — pipette up to eight samples and measure. Each sample is read using two path lengths to achieve an extensive

dynamic range (e.g., 2-3700 ng/ μ l dsDNA), virtually eliminating the need for dilutions. Then just a quick wipe clean and you're ready for your next samples. What could be easier — or more powerful?

And for the power of small in single-sample absorbance or fluorescent measurements, check out the NanoDrop® ND-1000 Spectrophotometer or the NanoDrop® ND-3300 Fluorespectrometer (ultra low fluorescent detection limit of sample mass — e.g., 2 pg dsDNA).

Ready to experience the power of small x8? **Test a NanoDrop® ND-8000 8-Sample Spectrophotometer in your own lab.**

FREE one-week evaluation www.nanodrop.com
302.479.7707



 **NanoDrop**



Surveyor IC Analytes:

Phospho-Akt
(S473) Pan SpecificPhospho-ERK1/
ERK2Phospho-ERK2
(T185/Y187)

Total HIF-1 alpha

Total HSP70

Phospho-p38
alpha (T180/Y182)

Total Survivin

Phospho-TOR
(S2448)

R&D Systems Surveyor™ IC Immunoassays

The ease of ELISA applied to intracellular factors.

R&D Systems Surveyor IC ELISA kits simplify the detection and quantification of intracellular factors important for cell signaling. These kits provide all of the components necessary to run a successful sandwich ELISA with a clear, easy-to-follow protocol.

ASSAY FEATURES

High specificity

Quantitative

Rapid

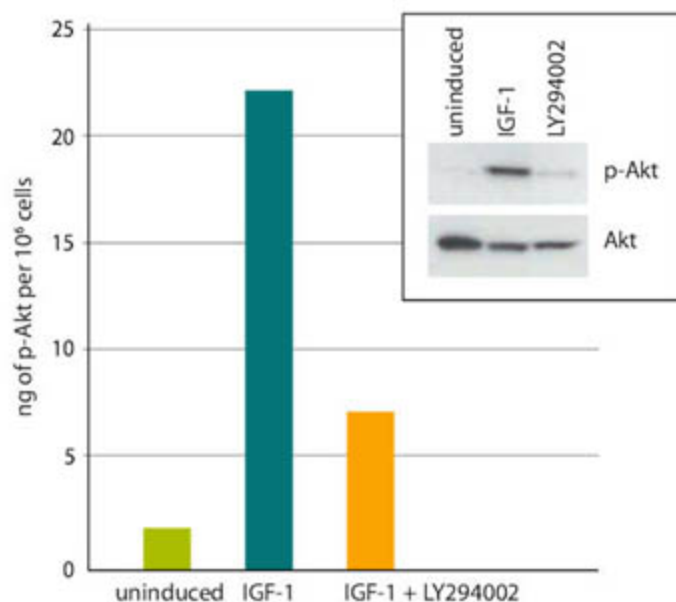
Colorimetric detection

Validated for a variety of cell lysates

Superb alternative to Western blot



For more information visit our website at www.RnDSystems.com/go/SurveyorIC



MCF-7 cells were incubated with or without IGF-1 and the PI3 Kinase inhibitor LY294002. Cells were lysed and phosphorylated Akt was quantified with phospho-Akt Surveyor IC (Catalog # SUV887). The same lysates were also immunoblotted (inset) with either anti-phospho-Akt (S473) (p-Akt) or anti-Akt antibodies. The Surveyor IC Immunoassay results correlate well with the amounts of phosphorylated Akt detected by Western blot.

For research use only. Not for use in diagnostic procedures.

U.S. & Canada
R&D Systems, Inc.
Tel: (800) 343-7475
info@RnDSystems.com

Europe
R&D Systems Europe Ltd.
Tel: +44 (0)1235 529449
info@RnDSystems.co.uk

R&D Systems is a registered trademark of TECHNE Corporation.

Selection expanding weekly—visit www.RnDSystems.com to sign up for weekly new product updates.

R&D
SYSTEMS®